A GIS based analysis of meandering channel evolution focussing on channel curvature, meander cut-off events and bank erosion rate interactions over a 125-year time period

Thesis submitted in accordance with the requirements of the University of Liverpool for the degree of Doctor in Philosophy

by Siôn Edward Regan

September 2019

Abstract

The development and evolution of meandering channels has long held a fascination for scientists of many disciplines. Researchers have used field, archival and modelling sources to investigate the dynamics and long-term behaviour of meandering channels to help understand and predict future changes. There is still a great deal of uncertainty about why different meander bends are active and why similar bends are stable. Questions also remain about how the impact of change on one part of the river is propagated upstream and downstream. These questions are important as dynamic rivers can be challenging for human settlements, but also provide an opportunity to increase biodiversity and habitat opportunity in the riparian zone.

The aims of this thesis are to explore the variability of meander migration in space and time for two actively meandering rivers in the UK. The long-term evolutionary behaviour of individual bends is explored using historic Ordnance Survey maps. Finally, a data modelling approach is used to predict channel change within a large dataset, with rivers from a third catchment, the River Ribble included, with a view to predicting future channel change.

It is shown a high degree of variability exists both along channel reaches and between different periods. The mean annual migration rate for a reach varied from a minimum of 0.04ma^{-1} and 0.15ma^{-1} in the Lugg and Till catchments respectively to a maximum 1.29ma^{-1} and 0.92ma^{-1} for the catchments. The River Migration Toolbox is used to measure the migration rate of individual bends for each reach and rates of up to 3ma^{-1} were measured, which represent some of the most active rivers in the UK. There appears to be a strong relationship between the rate of migration and length of period between two map dates as the shortest time between the map dates tended to have the highest migration rates. The implications for management of this phenomenon is discussed.

The evolutionary behaviour of meander bends is then investigated and the relationship between channel radius of curvature and migration rate quantified. It is shown that the migration rate tends to increase as the radius of curvature decreased, although there was a high amount of scatter present in the results. The trajectories of individual bends in a bend curvature-migration rate phase space were analysed to help understand the behaviour of different types of bends. The changes of the curvature profile of individual bends was measured and showed bends would develop a long section with a low radius of curvature, before becoming compound or double-headed.

The final section of the research uses a machine learning approach to understand the importance of the different factors on the migration rate of individual bends and to predict channel change. The approach showed human infrastructure has an important control on migration rate, along with channel curvature and riparian vegetation. The machine learning approach was able to predict the location of active meandering channels but had a worse performance when predicting the rate of erosion. The potential future applications of the approach are discussed.

Acknowledgements

"It has been said that everything everywhere affects everything else. This may be true. Or perhaps the world is just full of patterns" Terry Pratchett – Wings (1990).

I would like to thank Professor Janet Hooke, Dr Hugh Smith, Dr Edoardo Patelli and Dr Neil MacDonald for their supervisory support during my research. Special thanks have to be given to Janet, who kindly agreed to take over primary supervision halfway through the project and provided invaluable discussion and advice while I completed my research. Thank you also to Hugh who supported me at the start of the research and provided invaluable advice and direction for the project. I would also like to thank Dr Barbara Mauz who encouraged me to apply for a research grant during my undergraduate studies and provided me the opportunity to join her on a field visit to Oman. That journey inspired me to continue into academia after my undergraduate studies and I've taken that experience with me throughout my time at Liverpool. The funding was provided by the Royal Geographical Society through their Learning and Leading Fieldwork Apprenticeship, and I am eternally grateful for the opportunity provided by the grant. Finally, I would like to thank Dr Yuichi Onda who provided the opportunity and support for me to travel to Japan to experience fieldwork and research culture in a completely different environment from the United Kingdom.

I am grateful to The University of Liverpool who have provided me with countless opportunities throughout my undergraduate and post graduate studies to develop as a person and a scientist. The Geography department has been my home for the last eight years and I am sad to be leaving the many wonderful members of staff that make up the department.

I would also like to thank the fantastic River Ribble Trust, who provided an insight into the practical needs of river managers and gave me the opportunity to present my work to many different stakeholders and allowed me to develop my communication skills.

I would not have been able to complete this project without the support and discussion with friends and colleagues throughout the project. Special thanks have to be given to Peter Hristov and Rachel Gong who helped coding in MatLab and to Simon Clarke and Maria Mendoza Puchades, with whom I have travelled on this journey and share the highs and the lows. I would like to thank the postgraduate demonstrator team who were

happy to listen to the complaints about PhD struggles and helped give a sense of perspective throughout my time at Liverpool.

To my family, your support and belief during my thesis has kept me going when times have gotten tough. I am especially grateful to my Mum, who provided a home and support during the last part of my thesis, without which I would have never been able to complete the research. Finally, but certainly not least, Julie. You have been there for me throughout my time at Liverpool and supported me even when we were apart. I promise I am finished being a student now and I am looking forward to the next stage in our life together.

Table of Contents

List of Figures

List of Tables

1. Introduction

1.1. Justification

Meandering river channels have long fascinated researchers from a wide range of backgrounds, including geomorphology, engineering, ecology and mathematics. They are ubiquitous on Earth and occur in many different landscapes, not just in alluvial systems but also on bedrock channels and on glaciers. Meanders are an example of nature producing patterns with highly regular forms (Seminara, 2006). Many meandering channels are active, migrating both downstream and across the floodplain, producing significant landscape change within the floodplain (Hooke, 2013). Where the rate of change is fast, there can be practical problems for human infrastructure located close to the river channel and the riverbanks can supply high amounts of sediment to the river channel (Kessler et al., 2012), which is a frequent cause of water impairment. The high sediment load can also reduce the carrying capacity of channels further downstream and increase the risk of flooding. In some instances, rivers are actively eroding into contaminated floodplains and adding considerable pollution to the watercourse (O'Neal and Pizzuto, 2011; Rhoades et al., 2009). The practical need to understand the patterns, processes and rates of river channel migration has driven much of the research in this field and the development of many models to attempt to predict meander bend behaviour. Alongside the practical problems caused by meandering channels, there are benefits, especially for ecology and biodiversity where active rivers can create a wide range of habitats. Meandering channels can also reduce the speed of flood peaks compared to artificially straightened channels. A recent trend in conservation has been to restore meandering channels, recognising that the meandering is an inherent behaviour of river channels.

Meandering rivers can be considered as a dynamical system far from equilibrium, which are continuously evolving around some statistical stationarity (Camporeale et al., 2007). Both morphological processes and fluid dynamic processes drive river evolution, which, in combination, can cause lateral migration and cutoffs when two parts of the river channel intersect. These dynamics are forced by different system inputs, mainly hydrological and vegetation processes, alongside anthropogenic and geological constraints. The river system is therefore sensitive to different types of environmental change including climate change, sediment supply and anthropogenic factors. The need to understand both the morphological processes and the fluid dynamic processes has led to two interrelated

approaches to researching meander dynamics. These approaches have been completed using observational techniques and theoretical modelling.

Geomorphology is the investigation of the processes that produce the Earth's landforms. The main approach has been through field and laboratory studies, which attempt to extract general behaviours from the complexity observed. Geomorphological approaches have a longer history of study from the initial laboratory studies by Friedkin (1945) and the field studies of Fisk (1944), which were investigating problems associated with the actively migrating Mississippi River. A major era of fluvial geomorphological research began in the 1950s with the pioneering work of Leopold and Wolman (1957, 1960), Langbein and Leopold (1966), and Schumm (1960, 1963). The initial researchers believed that meander evolution occurred over long-time scales and that meanders produced a form with minimum variance, gradually becoming stable. However, during the 1970s attention began to focus on shorter term processes through increased use of field and historical evidence. Research by Brice (1974), Hickin (1974, 1978), Hickin and Nanson (1975), Hooke (1977, 1979), and Thorne and Lewin (1979) occurred simultaneously in North America and the United Kingdom showing that change could be detectable over short timescale, over a few years and that meanders could continuously evolve. The occurrence of asymmetrical and compound bends was analysed and considered part of the evolutionary development of a river bend and not just a response to variations in floodplain resistance.

As the amount of field studies declined in the 1980s, research into theoretical and computational modelling began. Ikeda et al. (1981) proposed a model relating the erosion rate to the flow field. Parker et al. (1982) studied nonlinear effects on bend growth and found downstream migration decreased as amplitude increased, causing the characteristic asymmetry noted by the geomorphological researchers. Blondeaux and Seminara (1985) found that a resonance phenomenon could occur at a critical curvature value and controlled bend growth. They related the resonance to bar instability. Johannesson and Parker (1989) studied the effect of secondary flows in mildly sinuous channels and found there was a downstream phase lag between the channel curvature and magnitude of the secondary flow. Cooperation between geomorphologists and fluid dynamicists has created a new branch of fluid dynamics, geomorphological fluid dynamics, according to Seminara (2006). A rational framework for the quantitative understanding of fluvial dynamics has been developed, focusing on features that develop from the interaction between a sediment-carrying fluid and an erodible boundary. He proposed that most geomorphological patterns are caused by

fundamental instability mechanisms and that “any small random perturbation of channel alignment eventually grows, leading to a meandering pattern.”

Research on meandering channels has seen a resurgence in the past decade as remote sensing techniques have become more widely available. Improvements in satellite and LiDAR (Light Detection and Ranging) technology have allowed for large databases of channel change to be created. De Rose and Basher (2011), combined sequential LiDAR and historic aerial photographs to determine migration rates and sediment supply, Dewan et al. (2017) used a combination of Landsat data and hydrological data to study planform changes on the Ganges-Padma river system in Bangladesh and O’Neal and Pizzuto (2011) used terrestrial LiDAR to measure the annual river bank erosion in Virginia. There is still a need to combine the results of long-term monitoring approaches with meander models to determine how well the computer models can represent actual channel behaviour, although Güneralp and Rhoads (2010) and Luppi et al. (2009) have combined models with monitoring to examine the performance of the modelling approaches.

One of the fundamental questions relating to meandering is why do rivers meander. A number of different reasons and theories have been suggested relating to either flow properties or sediment dynamics, but no individual reason appears to be able to explain the behaviour seen in all environments, including other fluid flows such as the Gulf Stream (Seminara, 2006; Hooke, 2013). There are further questions about the nature of change and the drivers behind the change. Are the changes to river pattern autogenic, i.e. produced internally within the system, or allogenic - driven by changes to the environment from either natural or anthropogenic causes, or a combination of autogenic and allogenic processes that vary depending on the conditions? Other questions are why and how do compound forms develop within the bend pattern (Brice, 1974).

Scale is a major issue within geomorphology, as processes often look different at different spatial and temporal scales (Couper, 2004). This means that ideas and understanding that are developed at one scale may not be applicable to all or any other scale. This is especially important in studies of riverbank erosion and meander evolution as investigations have taken place at numerous different time and spatial scales, ranging from individual bends to larger catchment scale approaches. There has been a predominance of shorter studies at a reach scale, which influences the perception of riverbank erosion. Lawler (1993) showed the range of temporal scales that have been studied, which can range from daily measurements to decadal or century scale investigations.

There are two main processes involved in the development of meandering channels. The first is the gradual migration of the channel, usually driven by erosion on the outer concave bank, which increases the complexity of the channel form. Alongside the erosion on the concave bank, deposition of sediments occurs on the inner convex bank, further forcing the fastest flowing water (thalweg) towards the outer bank. Deposition tends to balance the erosion over time, unless there is a change in the hydrological characteristics of the system, which will lead to a widening or narrowing of the channel. There has been some debate as to whether meander evolution is erosion driven or deposition driven, i.e. bank pull, where rapid erosion on the outer bank leads to deposition on the inner bank (e.g. Hooke, 1979; Hickin and Nanson, 1975, 1984, Sylvester et al., 2019), or bar push, where sediment is deposited on the inner bank and forces erosion on the outer bank (e.g. Parker et al., 2011; Eke et al., 2014; Czuba and Foufoula-Georgiou, 2015; Ahmed et al., 2019). The elongation of bends can provide a spatial memory within the floodplain (Camporeale et al., 2005), which makes unstable systems sensitive to the initial conditions. The opposing process occurs when the river channel experiences a cutoff, either as a chute cutoff removing a short section of the river channel or a neck cutoff, which occurs when two separate parts of the meander chain interact (Camporeale et al., 2007). A chute cutoff occurs when overflow scour creates a new channel in the floodplain, possibly occupying a previous channel position and a neck cutoff occurs when the river can cross the thin neck between two meander bends. Cutoffs tend to be sporadic, causing sudden reductions in the channel length and complexity. The occurrence of these cutoffs places an upper limit on the overall complexity of a river channel. Stolum (1996, 1998) proposed that this threshold can be identified when measuring the sinuosity of a channel (i.e. the ratio of the channel length to the valley length) and that for freely migrating rivers the threshold would be 3.14. If the river channel is at a critical value of sinuosity then a single cutoff can trigger a cluster of cutoffs in the local area (Stolum, 1996; Hooke, 2004) causing the river channel to rapidly adjust. The oxbow lake left behind during a cutoff event will have a different sedimentary profile to the surrounding floodplain as it infills, which will potentially influence the rate of meander migration if the river channel starts to erode into a previously abandoned channel (Constantine and Dunne, 2008).

There are numerous factors that affect the rate of channel migration (Henshaw et al., 2013), both hydrologically and physically in the environment. The interaction between these different factors is complex, non-linear and often not well defined. Factors can also both increase and decrease the rate of migration at different stages of development. For

example, riparian vegetation can help reinforce the strength of the bank through root cohesion and by deflecting the flow away from the riverbank. However, when vegetation fails, large amount of sediment can be delivered to the river channel and large woody debris in the channel can deflect flow towards the bank in unexpected locations causing high erosion rates. Different types of bank material are also vulnerable to different hydrological processes (Julian and Torres, 2006). Riverbanks with a high silt-clay content are more vulnerable to repeated wetting and drying and frost action, while sandy and gravelly banks are more vulnerable to high local flow velocities. There is also a seasonal component to these factors, with vegetation coverage lowest during the winter months, a high incidence of frost action and more frequent high flow events in many climates.

Up to the 1990s the prevailing management response to meandering and mobility was to install hard engineering approaches to reduce the amount of erosion. However, there was a paradigm shift away from these approaches (Gilvear, 1999) as they tend to be expensive to install and maintain, fossilise the rivers and limit the connectivity with the surrounding floodplain. There has been a drive recently to restore rivers back to a more natural state, but this leads to questions about what the actual natural state of a river is, as many have experienced human intervention, and restoration has to be balanced with the need to protect people and settlements on the floodplain (Church and Ferguson, 2015). Church and Ferguson (2015) note there are a number of concerns around the changes that occur during major flood events, the impact of climate change and producing viable methods of restoration. Kondolf (2006) suggests that restoration projects often attempt to create meandering river channels, even on sections of river that would not naturally meander, which are at risk of being washed out as they respond to the sediment flux and hydrological regime. These sections of river will require heavy armouring if they are to remain stable. Piégay et al. (2005) and Biron et al. (2014) both proposed a quantified method of river management that would create space for rivers to natural evolve through time, promoting a sustainable approach to channel management and increasing the resilience to climate change and land use changes. Biron et al. (2014) found the average minimum mobility space required for rivers was around 1.7 times the average channel width, but this was highly variable and cannot be predicted from the average. A second, larger level was created for larger floods and more mobile rivers over a longer period of time. While it remains necessary to protect infrastructure in urban areas, rivers should be given space to migrate. Chone and Biron (2016) assessed the relationship between river mobility and habitat and found there

was a strong relationship between geomorphological activity and biodiversity. Allowing rivers to actively migrate across the floodplain creates new habitats and provides valuable ecosystem services.

1.2. Hypotheses

Three different hypotheses were tested for this thesis. The first hypothesis will test whether there are measurable differences in the migration rate of river bends between different time periods and explore whether the "Sadler" effect can be identified. Sadler (1981) recognised that there are problems with making comparisons between annual rates over dissimilar time periods, with a trend showing a decreasing rate in sediment accumulation rates as a function of increasing time period. The first chapter will explore whether this effect can be found in river migration rates when comparing dissimilar time periods. The second hypothesis that will be tested focuses on the development of individual bends over time. Three related theoretical models of meander bend evolution have been proposed in the literature (Brice, 1974; Hickin and Nanson, 1975; Hooke, 2003) that suggest that meandering river bends will follow a defined evolutionary path from a simple form to a complex form. The second chapter will test the applicability of these models to previously actively meandering channels in the River Lugg and River Till catchment. The final hypothesis tested in this study examines whether machine learning techniques can be used to understand and predict river bend migration rates based on a set of physical characteristics.

1.3. Aims

There are a number of aims that will be explored in order to test the hypotheses described above. The first results chapter explores the variations in migration rate between different reaches and dissimilar time periods. The aims associated with this chapter are:

- Identify novel active reaches in the United Kingdom, with migration rates high enough to be captured on historic Ordnance Survey maps.
- Develop a new automated method of measuring channel migration rates at an individual bend scale so a large dataset of bends can be generated.
- Investigate whether the "Sadler" effect can be identified for the different time periods between the historic Ordnance survey maps and explore other potential reasons for any differences measured.

- Investigate how cutoffs affect the migration rate upstream and downstream of the location of the cutoff, and the importance of the type of cutoff. Discuss the importance of thresholds in cutoff dynamics.

The aims associated with the second hypothesis are:

- Explore the relationship between channel curvature and migration rate for individual bends and identify whether bends follow the trajectories suggested by Hooke (2003) for rapidly migrating and stable bends.
- Classify individual bends based on the Brice (1974) classification and quantify how the bends develop over time through the classification from simple symmetric bends through to compound asymmetric bends.
- Explore how the shape of individual bends evolve through time, relating the minimum radius of curvature to the magnitude and location of migration.

The aims for the final chapter are:

- Identify any physical characteristics that may influence the rate of migration based on the literature review and can be readily measured for remote data sources.
- Create a large dataset of the physical characteristics and the migration rate of individual bends.
- Apply a type of machine learning (Boosted Regression Trees) to examine the influence of the different physical characteristics on channel migration rate, the first use of boosted regression trees to explore river channel migration.
- Use the boosted regression tree models to predict the migration rate on a subset of bends not included in the model to test the accuracy of the method.

1.4. Thesis Outline

Chapter 2 will examine the existing literature on migrating river channels, the processes driving the change, the different controls on the rates and mechanisms, and the different approaches to investigating the behaviour. Chapter 3 will introduce the study areas, the data sources used for the investigation and the method of analysing the different channel variables. Chapter 4 investigates the rates of lateral channel migration between the different reaches and different periods and discusses the potential causes of the differences found in the catchments. Numerous neck and chute cutoffs occurred in the study catchments,

allowing the relationship between sinuosity and the different types of cutoff to be investigated in Chapter 4 also, exploring whether different thresholds in channel sinuosity exist. Chapter 5 investigates the relationship between channel curvature and channel migration rate in relation to the three conceptual models proposed by Hickin (1974, 1978), Brice (1974) and Hooke (1995, 2003). Chapter 6 applies a machine learning technique, boosted regression trees (Elith et al., 2008) to develop insights into the relationship between different variables and the migration rate of river bends, and to produce a model capable of predicting the location and rate of riverbank erosion on a large spatial scale. Chapter 7 provides a synthesis of the preceding chapters and the potential implications of the research, especially for management purposes and final conclusions.

2. Literature Review

2.1. Introduction

Meandering rivers have been studied from a wide range of perspectives, including geomorphology, mathematics, engineering, biology and ecology. Meandering rivers are a key component of the landscape, reworking floodplain sediments, transporting material through the river network, creating new habitats, and helping to improve biodiversity. Mobile rivers can, however, cause issues by undermining important floodplain infrastructure, such as bridges and roads, and lead to excess sediment in rivers derived from riverbanks, increasing the turbidity of the water and damaging fish species (Owens et al., 2005). Understanding the processes of channel movement, and the rates and patterns of channel changes has therefore been a priority for many researchers. Many management approaches in the 19th and 20th centuries have focused on controlling river movement through the installation of hard engineering structures, but a more recent trend has acknowledged that many rivers are active and need to be given space in which to develop naturally (Piegay et al., 2005; Biron et al., 2014).

The initial drivers of research into meandering rivers were practical problems associated with erosion on the Mississippi River, with some of the first quantitative research performed by Fisk (1944) and Friedkin (1945). Fisk (1944) studied the relationship between meander morphology and floodplain materials and other geomorphological controls for the lower Mississippi River, while Friedkin (1945) performed some of the first experimental modelling of meander dynamics. Quantitative research into river behaviour developed in the 1950s and 1960s, with seminal work by Leopold and Wolman (1957), Wolman (1957), Wolman and Miller (1960), Leopold and Langbein (1966) and Schumm (1960, 1963), which started to develop relationships between channel form and input variables. These relationships appear to hold regardless of scale. It was originally assumed that meandering rivers develop over long timescales and that meanders developed towards an equilibrium state and become stable as they develop. However, once the relations between meander planform and different input characteristics were understood, researchers began to explore longer term dynamics using a combination of fieldwork and historic evidence. Researchers in North America (Brice, 1974, 1977; Hickin, 1974, 1978; Hickin and Nanson, 1975) and the UK (Lewin, 1972, 1976, 1978; Hooke, 1977, 1979; Thorne and Lewin, 1979) showed that changes could be measured over a short time period and that some meanders will continuously

evolve through time into more complex forms. It was initially assumed that asymmetry in river form was due to difference in floodplain resistance, but Brice (1974) showed that the asymmetry was part of an evolutionary sequence of meander bends. Research also started to understand the processes of erosion and deposition on riverbanks (Hooke, 1979), and different modes of riverbank collapse were presented by Thorne and Tovey (1981) and Osman and Thorne (1988).

Alongside the development of field studies of meander evolution, increasing computer power allowed for the development of complex computer models that could help understand the process of river channel change over longer time periods. They can be necessary in many cases as direct observation is usually on the scale of years to decades, while long-term processes and patterns can take centuries to millennia to fully evolve (Coulthard and Van de Wiel, 2012). Modelling provides an opportunity to study long-term processes or high magnitude, rare events that would otherwise be unobservable in the field. Many computer models are based on a linear model developed independently by Hasegawa (1977) and Ikeda et al. (1981), where the excess near-bank velocity and a dimensionless coefficient determine the rate of channel migration. Despite the models only strictly applying to river bends with low curvature values, the agreement with observed river pattern has led to this approach being used for theoretical investigations of meander evolution (e.g. Howard, 1984; Stolum, 1996, 1998; Sun et al., 1996; Camporeale et al., 2005). Fully non-linear models have been developed, such as Mosselman (1991, 1998) and Darby et al. (2002), which can resolve flow dynamics better, but require much higher computational time. There have been attempts to model riverbank behaviour using 3-D models, but due to the high computational demands, the models have only focused on simple geometry bends (Campeoreale et al., 2007).

There is a wide range of characteristics that can be applied to meandering rivers, which are shown in Figure 2.1. The concave bank refers to the riverbank on the outer side of a river bend and usually experiences erosion and lateral migration. The convex bank is on the inside of the bend, where deposition often occurs leading to the formation of a point bar. The sinuosity (S) of a channel is the ratio of the channel length to the valley length (between A and B in Figure 2.1) and quantitatively defines the meander planform. The meander amplitude (2A) is the distance across the floodplain between two consecutive bends or twice the distance from the valley centreline to the apex of the bend. The meander wavelength (λ) is the distance between the apexes of successive bends on the same side of the valley.

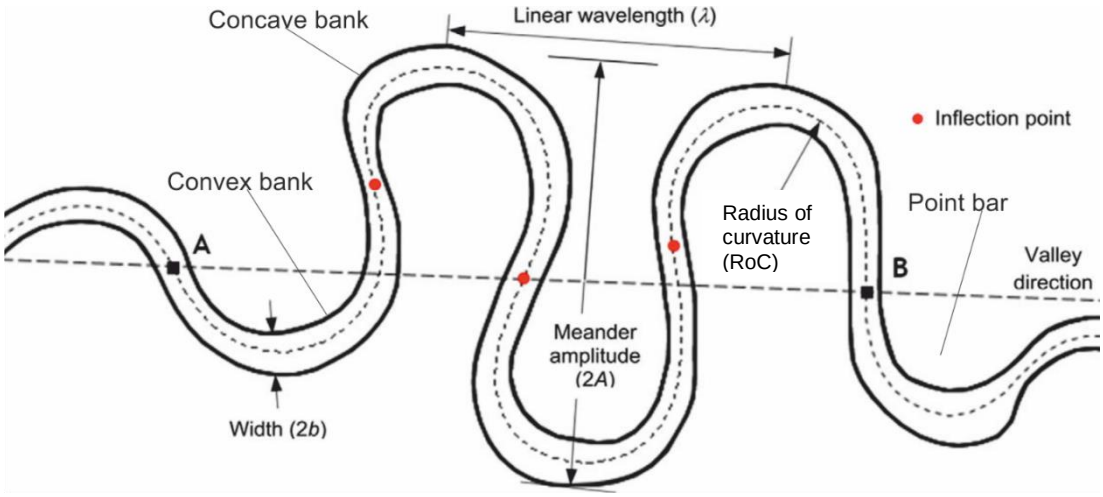

Figure 2.1. The different terms commonly applied to meandering channels, adapted from Guneralp and Marston (2012)

Channel curvature (C) measures the change in direction of the channel centreline along the streamwise axis and the inflection point indicates a point at which the sign of the curvature changes. The inflection points indicate the beginning of a new bend for simple bend forms. The radius of curvature (RoC) is the radius of a circle that fits the channel centreline. The channel planform is rarely as smooth as shown in Figure 2.1, so often the mean or minimum radius of curvature is used to represent the RoC of a bend (Hickin and Nanson, 1984).The apex of the bend is defined at the point of minimum radius of curvature within the bend.

2.2. Meander Processes

2.2.1. Bank erosion processes

Meander evolution is the combination and interaction between gradual lateral migration, which increases the channel length, and the sudden shortening of the channel through a neck or chute cutoff (Stolum, 1996, 1998). There is a consistent channel planform pattern that appears to repeat irrespective of the pattern or the scale of the investigation, which suggests there is a higher level of self-organisation than from the erosion and deposition processes occurring at a local scale. These emergent properties occur in a variety of environments, from polar to temperate to tropical rivers.

There are three main types of erosion processes that occur on meandering channels: sub-aerial processes, fluvial entrainment and mass failure (Lawler, 1995). Lawler suggested that the different processes would dominate at different scales and locations from the source areas to the downstream areas of the river, although overall riverbank erosion rates would be a combination of all three processes (Darby et al., 2007). Sub-aerial processes were

initially thought to be preparatory processes, which would loosen bank material, prior to being removed through fluvial entrainment. However, Couper and Maddock (2001) found that sub-aerial processes were the main cause of erosion on the River Arrow in Warwickshire, although the rates were relatively low. There are a number of different sub-aerial processes that occur on riverbanks, all of which can contribute to migration rates and are all related to the moisture within the riverbank. Freeze-thaw processes occur in humid and sub-arctic conditions (Lawler, 1995), when moisture within the riverbank freeze and expands, loosening the bonds between individual particles (Couper and Maddock, 2001; Thorne, 1990). Freeze-thaw is thought to be most effective on fine-grained soils, with a silt-clay content of over 20 per cent required before frost action will have a major impact (Matsuoka, 1996). Desiccation occurs through the drying of a cohesive soil mass, shrinking the overall volume of the soil and creating cracks, which are a weakness within the bank that can be exploited when exposed to flowing water (Thorne and Osman, 1988). Alternatively, an increase in soil moisture can decrease the cohesive forces between individual particles, making them more susceptible to erosion during high flow events. Hooke (1979) and Simon et al. (1999) found the highest rates of erosion occurred after a longer wet period, rather than just related to the highest flow period. The final sub-aerial process is slaking, which occurs when dry material is rapidly soaked, causing positive pore water pressures and detachment of individual particles from the riverbank (Couper and Maddock, 2001).

Fluvial entrainment or scour is the direct removal of material from the bank due to shear stresses caused by water flowing next to the bank (Lawler, 1992, 1995). Lawler related the local shear stress to the stream power and then calculated theoretical maxima for the stream power based on both linear and power/exponential functions of discharge and slope. The stream power would form a curve, which would peak in the middle reaches of the river system. Darby et al. (2010) used an excess shear stress formulation to estimate the bank retreat rates on the Mekong River, which is based on the excess shear created by the drag component of boundary shear stress over a critical shear stress. Predicting the different components of the excess shear formula is difficult as the parameters are highly variable over small spatial scales and can help explain why rates of erosion can vary over several orders of magnitude (Hooke, 1980; Darby et al., 2007). The relationship will also depend on the type of material being eroded, with non-cohesive sediments following the same relationship as bed sediments, with some modifications for the bank angle (Lane, 1955). However, cohesive sediments have bonds between the individual particles that are affected by the clay and

organic content and the relationship is not easily determined. Theoretically, the maximum shear stress should occur at the base of the water column (Richards, 1982). Thorne (1982) and Darby et al. (2007) suggest that hydraulic erosion is the dominant factor controlling long-term erosion rates due to removal of material at the toe of the bank, causing undermining of the riverbank and eventually leading to the bank collapsing through a mass failure event. Rates of fluvial entrainment can also be increased through sub-aerial processes weakening the bank material and lowering the critical shear stress required to remove particles (Lawler, 1995; Grove et al., 2013).

Mass failure of riverbanks occur when the weight of the bank overcomes the resistant shear forces and causes large portions of the riverbank to collapse (Lawler, 1995; Simon et al., 2000). The weight of the bank depends on the height of the bank, and the density and wetness of the bank material. The latter factor can vary greatly during flood events (Simon et al., 2000) and depends on the antecedent conditions. Thorne and Tovey (1981) identified three different types of mass failure mechanism: circular slip on a high bank, toppling failure on a low bank and cantilever failure on undermined banks. A factor of safety is often used to describe the point at which a bend will become unstable (Osman and Thorne, 1988) and is the ratio of the resisting force to the driving force. The resisting force is

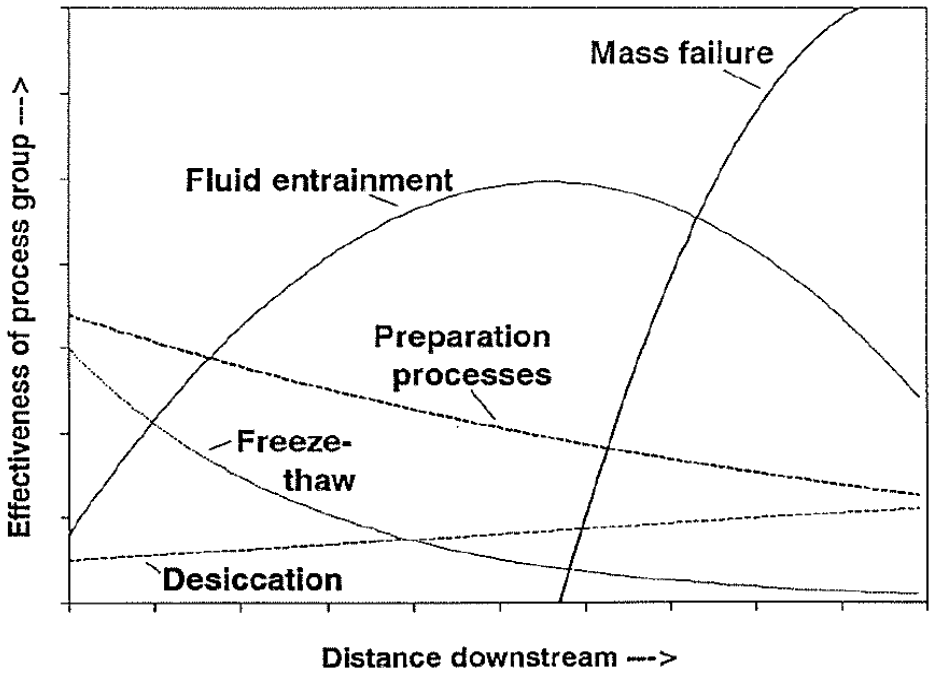

Figure 2.2. The different process domains and the theoretical changes in effectiveness as a function of distance downstream. From Lawler (1995)

proportional to the effective cohesion and the angle of friction and the driving force is the weight of the bank and the angle of the bank. Material deposited at the toe of the bank can remain in situ until removed by competent high flow events (Thorne and Tovey, 1981). These blocks can become stable if the river is unable to remove them and become part of the lower bank.

For riverbanks that are composite, i.e. a non-cohesive layer at the base of the bank and a cohesive layer sitting on top, the erosion process is a combination of fluvial entrainment and mass failure. Composite riverbanks are common, especially in areas with a gravel bed and a laterally active river. These banks tend to form in the most active middle reaches of a river profile, where gravel-bed rivers migrate across the floodplain and riverbanks form on previously abandoned bars. Although the non-cohesive layers are usually coarse grained, they tend to be more susceptible to erosion through fluvial entrainment (Thorne, 1978; Thorne and Tovey, 1981). The more cohesive bank which sits on top of the gravel layer is more resistant to erosion. The flow velocities also appear to be lower at the top of the bank during high flow events (Bathurst et al., 1979). The difference in the erodibility between the two parts of the bank means that the top part is often undercut and will fail through cantilever failure, before removal of the failed block. Thorne and Tovey (1981) related the rate of undercutting to the flow during controlled releases from a reservoir in Wales and found the rate of undercutting was 50mm per day, while the observed overhangs ranged from 400 to 500mm, suggesting that there is a cycle of erosion, failure and removal and that there is no simple relationship between flood magnitude and erosion rate. Daly et al. (2015) used the Bank Stability and Toe Erosion Model (BSTEM) to investigate the impact of the nature of the retreat of composite banks. They found banks protected by root cohesion had lower retreat rates in both the model and the real world and were able to accurately predict retreat rates. They suggest that process-based models can be used to help in the design of stabilisation projects.

Lawler (1995) suggested that the different processes of riverbank erosion would dominate in different domains along the river channel (Figure 2.2). In the upstream sections of the river channel, the stream power and the bank heights are low, leading to a dominance of the sub-aerial processes, namely freeze-thaw as these sections tend to have higher altitudes. Further downstream, fluvial entrainment beings to dominate as stream power reaches a maximum and the floodplain width increases allowing the river to migrate across the valley floor. In the lower reaches, the stream power is reduced as the gradient of the

channel declines and the bank material becomes more cohesive, leading to mass failure being the dominant process. The processes would overlap, but each would be the greatest influence in its domain (see Figure 2.2).

2.2.2. Factors affecting the rate of riverbank erosion

There is a wide variety of factors that affect the rate of riverbank erosion, that are broadly split into driving processes (described above) and controls on the effectiveness of those driving processes (Henshaw et al., 2013). Camporeale et al. (2007) produced a schematic of the main processes involved in meandering dynamics (see Figure 2.3).

One of the main controls for all three processes is the type of bank material and whether the material is cohesive or not (Thorne, 1982; Parker et al., 2008). There have been numerous studies that have shown the importance of internal soil strength in bank and slope stability (Thorne et al., 1981; Simon and Darby, 1997; Simon et al., 2000; Darby et al., 2000; Parker et al., 2008). Simon et al. (2000) developed a factor of safety for riverbanks based on the ratio between the resisting and driving forces. When the ratio is around 1.0 or less then the bank is at risk of failure. The mechanical soil properties are highly variable over single river bends (Guneralp and Rhoads, 2011; Konsoer et al., 2016) making predicting bank failures difficult. Closely related to the composition of the bank material is the moisture

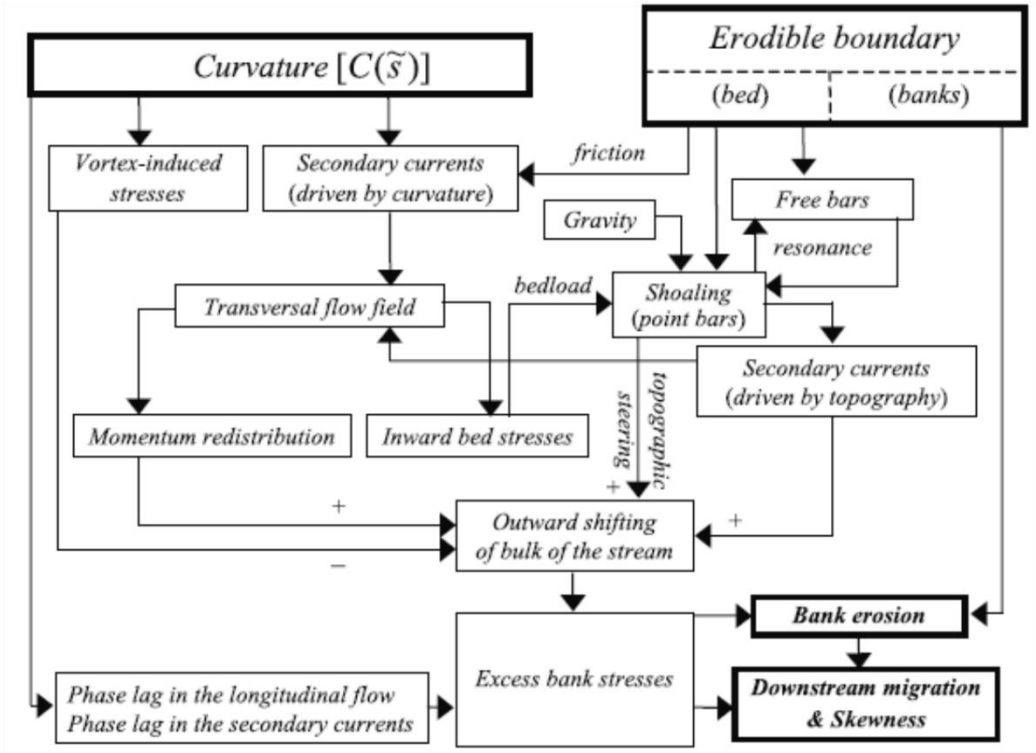

Figure 2.3. The main processes occurring on meandering rivers, with curvature driven flow dynamics. From Camporeale et al. (2007)

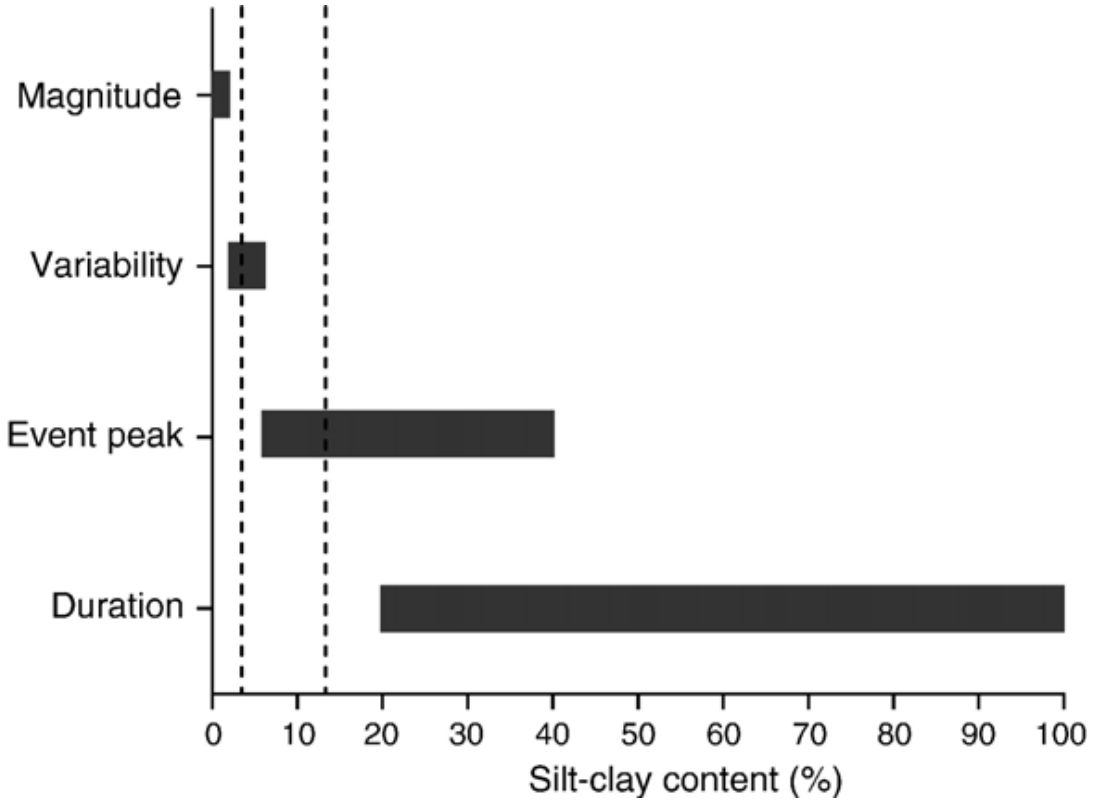

Figure 2.4. Theoretical domains for different percentage of silt-clay content in riverbanks and the type of flow event that will cause the highest amount of erosion. From Julian and Torres (2006)

within the bank. The effect of positive water pressures has been identified as an important contributor to streambank instability (Simon et al., 2000), as the positive pressures in the bank are not counteracted by the force of water on the bank, once the recessional stage of the hydrograph has begun. One factor that was not included in the earlier work was the effect of negative pore-water pressures on the riverbank stability (Parker et al., 2008). When a bank has both saturated and unsaturated zones, the negative water pressure between the unsaturated and the saturated zone help increase the strength of the bank.

The type of material and cohesiveness of the particles also affect the direct fluvial entrainment of bank material (Julian and Torres, 2006). For non-cohesive particles, the entrainment of sediment is quantified by the magnitude of the shear stress and the size of the particle (Shields, 1936); while for cohesive sediments, material is removed through the entrainment of aggregates and needs to overcome the electrochemical forces between the aggregates (Thorne, 1982; Simon and Collison, 2001). Cohesive banks are also more susceptible to sub-aerial processes such as positive pore water pressures, desiccation and freeze-thaw as the aggregates adjust to the varying levels of water within the riverbank.

Arulanandan et al. (1980) developed the model most often used to predict hydraulic erosion rates by using flume studies:

$$E = k(\tau-\tau_c) \quad (1)$$

where E is the lateral erosion rate, k is an erodibility coefficient, τ is the shear stress from the flow and τ_c is the critical shear stress required for entrainment. The model assumes the total amount of erosion is related to the magnitude of the excess shear stress, but other studies have found the total amount of erosion is also related to the duration of the flow (Wolman, 1959; Knighton, 1973), the event peak (Hooke, 1979), the variability in the flood peaks (Knighton, 1973) and the flood history of the system (Mao, 2012). Julian and Torres (2006) related the strength of the bank to the silt-clay content of the material and found an exponential relationship between the strength of the bank and the erosion rate recorded during the study. They suggested that the silt-clay content could be a predictor for which of the different types of hydrological event will be the most effective at eroding the riverbank (see Figure 2.4). This relationship built on the previous work by Schumm (1968) and Hooke (1980) who investigated the relationship between silt-clay percentage and erosion rates.

Further downstream, where, according to Lawler (1992, 1995), the stream power decreases and the main cause of bank erosion changes from fluvial entrainment to mass failure, the height of the riverbank becomes a controlling factor in the rates of retreat (Michelli and Kirchner, 2002; Walling, 2005). As the height of the bank increases, the weight of the bank and (hence the shear stresses acting upon the bank) also increase, meaning the bank is more liable to fail. However, Kessler et al. (2013) used a number of different physical characteristics such as face area, length, height, aspect, slope and inclined slope area to extrapolate from individual bend measurements to an entire river channel. They found there was no statistical relationship between any of the individual factors and bank erosion rates.

Vegetation has a complicated influence on the stability of the riverbank, but the exact nature of this impact has been difficult to quantify (Hickin, 1984). Hickin suggests there are five important mechanisms through which vegetation controls fluvial processes: “resistance to flow (due to increased roughness on the riverbank), bank strength, nucleus for bar sedimentation, construction and breaching of log-jams, and concave bank bench deposition.” Beeson and Doyle (1995) found vegetated banks were five times less likely to experience detectable erosion during major floods in 1990, and major bank erosion was 30 times more likely on non-vegetated banks. Micheli et al. (2004) studied migration rates on

the Sacramento River and found migration rates were higher through agricultural land compared to riparian forest areas. When riparian forest was removed the erodibility of the banks increased by between 80% and 150%. Stott (1997) found bank erosion was correlated with incidence of frost on upland streams in Scotland and that minimum temperatures in the forested areas were 3.7°C warmer than those outside of the forest and the incidence of frost was half as frequent within the forest areas. Gurnell (2014) reviewed the research that has occurred since the 1950s on the influence of riparian vegetation on fluvial processes, including field and laboratory research. Riparian vegetation can have a fundamental role on the river planform, influencing whether a river is single thread or multi-thread and causing feedbacks between flow-vegetation-sediment dynamics.

It has been established that tree roots can help stabilise banks by increasing the shear strength of the bank, reducing the chance of mass failure (Abernathy and Rutherford, 1998, 2000a) and are more resistant to fluvial entrainment. Vegetation can also help stabilise point bar surfaces on the inner bank leading to channel narrowing and deepening (Kiss and Blanka, 2012). There have been some suggestions the increased weight from trees on the riverbank can decrease the stability of the bank, however Abernethy and Rutherfurd (2000b) found the trees only contributed 4.1% of the total mass of the slumped blocked and it was not possible to determine whether the addition of the trees helped cause the failure. The roots help bind the bank material together through tractive forces between the fibres and soil, and by transferring load between regions of high stress and low stress (Abernathy and Rutherford, 2001). Abernathy and Rutherford (2000a) found the inclusion of root reinforcement from native riparian vegetation increased the factor of safety of unstable banks from 1.0 to 1.6. This effect occurred even under the highest flow conditions and occurs, with varying effectiveness, for a range of vegetation locations. The study was the first to attempt to model and quantify the effect of riparian vegetation on riverbank strength using a physically based slope stability model. The most effective location for riparian vegetation was located at the point where the failure plane intersects with the floodplain but increases in effective bank strength were predicted even when the tree was located 15m away from the edge of the bank. Van de Wiel and Darby (2007) combined a bank stability model with a model to represent the root distribution of vegetation in the soil and found the highest increase in stability occurred when the vegetation was located at point where the failure plain intersected with the floodplain. However, they found the effect was limited and only increased the factor of safety by less than 5%. They suggest there must be alternative

processes occurring that help reduce the rate of erosion, such as vegetation interacting with the river flow. Pizzuto et al. (2010) studied the retreat rates in forested, cohesive catchments. They found a scalloped bank morphology would develop where the erosion rate in between trees was higher. The sections of the bank with trees on would eventually become undercut and the toppling of the trees would produce a large retreat and sediment input into the channel. They suggested a cycle of erosion and planform evolution based on the location of the trees, occurring on a timescale of 5-15 years.

Many of the studies concentrated on either analogues for different species in flume studies or case studies of one or two species (e.g. Abernathy and Rutherfurd, 2001). Polvi et al. (2014) used the vegetation root component of the BSTEM model (Simon et al., 2000) to test a range of different vegetation types. Woody and non-woody species were modelled along with different sizes from trees, shrubs and forbs. They found trees roots added significantly more to bank stability than smaller forb roots.

While most native riparian vegetation helps to reinforce the riverbank and increase stability, there are examples of non-perennial vegetation that may increase soil erosion and decrease the stability of banks (Greenwood and Kuhn, 2013, 2015). Greenwood and Kuhn note the example of Himalayan Balsam (*Imaptiens glandulifera*), which is a highly invasive species with an annual growth pattern. The species favours damp fertile soils and can eject its seeds over 3m meaning that it is able colonise quickly and effectively along river channels. Once they have matured the Himalayan Balsam quickly crowd out natural vegetation but are rapidly killed once the temperature drops and the first frost of the year occurs. Banks that were previously protected by perennial vegetation become susceptible to erosion during the winter, when higher flows are more common.

Channel slope has also been considered as a major control on river channel pattern (Eaton et al., 2010) and can mark a threshold between stable single-thread channels, stable multi-thread channels and unstable braided channels. Leopold and Wolman (1957) performed the first empirical analysis of river channel patterns based on discharge of the channel, which was later expanded upon to include median grain size of the bed material and critical slope (Henderson, 1963; Van Den Berg, 1995). Stream power has been used as a measure of the relationship between discharge and energy slope (Lawler, 1992, 1995; Knighton, 1999; Bizzi and Lerner, 2015), and is a measure of driving forces acting on a channel and is defined by:

$$\Omega = \gamma Q s \quad (2)$$

where γ is the specific weight of water (9810Nm^{-3}), Q is the water discharge (m^{3}s^{-1}) and s is the energy slope (m m^{-1}). This term has shown to be important for channel pattern (Knighton and Nanson, 1993) and channel migration (Nanson and Hickin, 1986). It is thought to have important implications for both generating the channel pattern and transporting sediment (Bizzi and Lerner, 2015). Lawler (1992, 1995) proposed that stream power would peak in the middle reaches of the catchment, due to a combination of the slope and discharge as shown

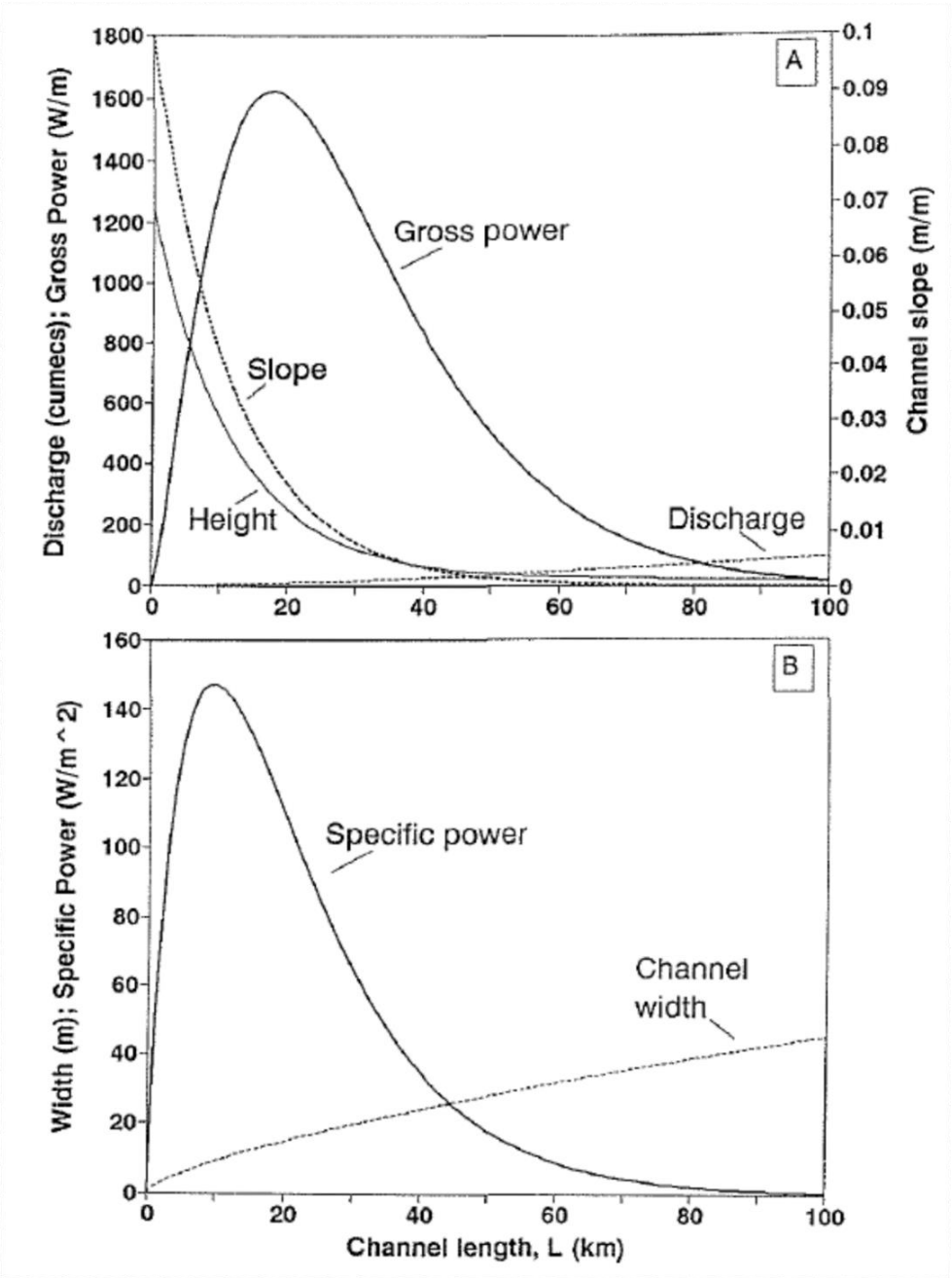

Figure 2.5. Variations in streampower as a function of distance downstream. From Lawler (1995)

in Figure 2.5. The specific stream power is calculated as the stream power divided by the channel width, hence the decline in the power as the distance downstream increases.

Channel planform has an important role in determining rates of erosion. Hickin (1974) and Hickin and Nanson (1975) were the first to recognise the influence of channel curvature of lateral migration rates with a non-linear increase in the migration rate of river bends as the radius of curvature to width ratio (r_m/w) approached 3.0. This relationship will be discussed in more detail later in this chapter. Hickin (1978) examined the flow structures on nine consecutive bends and found the strength of the secondary flows increased as the r_m/w decreased from 4.0. Once the r_m/w decreased below 2.0 the highest secondary flow velocities were measured on the inner bank and a reduction in migration rate was measured. While early work concentrated on local bend curvatures, it became apparent that meander bends would only increase in amplitude and not migrate downstream if only local bend curvature were used (Guneralp and Rhoads, 2009). Theoretical models of meander bend evolution have used a weighted aggregate of local, upstream and downstream curvature to express migration rates at any point along the meander chain (Ikeda et al., 1981; Parker and Andrews, 1986; Camporeale et al., 2007; Guneralp and Rhoads, 2010). The maximum near-bank flow velocity is often measured just downstream of the maximum channel curvature. The lag between the highest curvature and fastest migration rate leads to the downstream skewness in the shape of the loop and the downstream migration seen on many rivers (Camporeale et al., 2007). The lag is expected to be on the order of a channel width. There is a secondary phase lag introduced due to variations in the curvature, which affects the secondary flow currents and has a spatial scale on the order of the channel depth.

Tooth et al. (2002) studied the geological controls on meandering channels in South Africa and found the meandering bends located in weakly cemented sandstone had a higher sinuosity and gradient and a wider floodplain than the channel located just downstream that was located in a more resistant dolerite material. The different types of geology meant the erosion processes were different between the two types of geology. In the more resistant dolerite, erosion was along fracture lines in the rock and was mainly through incision. In the sandstone floodplains the rivers were able to migrate laterally through both the bedrock and the alluvium deposited by the river. Nicoll and Hickin (2010) discussed the impact of confinement of the behaviour of meandering channels on the Canadian prairies. These channels had a greater ratio of channel wavelength to channel width and a higher r_m/w than freely migrating river. The channels tended to migrate downstream as a coherent waveform

and not develop towards cutoffs. Lewin and Brindle (1977) identified three different types of confinement, based on the relation between the channel width and the valley width. The first type of confinement was infrequent, with a wide valley floor and little contact between the channel and the valley side. The second type occurs in narrow valleys, where the amplitude of the meanders is greater than the valley width and the channel is in contact with the valley side for nearly all bends. The final type of confinement is fully confined, where free meander bends are unable to develop due to the position of the valley walls. Hall et al. (2007) defined a channel as confined if the floodplain to channel width ratio was ≤ 3.8 and unconfined if the ratio was > 3.8. Rapp and Abbe (2003) defined a channel as confined if the valley width was less than two channel widths, semi-confined if the valley width was between two and four channel widths and unconfined if the valley width was greater than four channel widths.

Anthropogenic effects have also been known to influence bank erosion processes, over the last 5000 years (Gregory, 2006) and have produced channels that are extensively modified. The impacts can both accelerate and decrease the rates of erosion depending on what type of anthropogenic effect is occurring. There have been changes in the shape, size and composition of channels, with increases and decreases of up to ten times the initial size of the channel (Gregory, 2006). Gregory lists 35 different human influences that affect river channels at different scales. The different scales include cross-section/point effects, reach scale effects, network scale effects and wider spatial impacts. Kondolf (1997) studied the impacts of gravel mining and dams causing sediment starvation in channels. Sediment-starved water is prone to incision and lateral erosion as the balance between sediment erosion, deposition and transport is altered and the bed slope is increased. The incision will increase the bank height and potentially undercut the riverbank. The increased incision can cause sediment to be transported downstream, aggrading the channel and causing instability. This knickpoint can migrate upstream, further destabilising the channel and potential undermining human structures in the river channel like bridge piers and buried pipelines. While the introduction of dams can reduce the amount of sediment available, they can also regulate the flow and reduce the amount of mobility downstream of the dam, especially if the riverbanks are created from a resistant material or when bed armouring occurs rapidly (Gilvear, 2004). Brewer and Lewin (1998) showed that flow regulation on the River Severn partly froze the braided planform further downstream, on a previously active section of channel.

Another human intervention has been the installation of bank stabilisation structures, which can aim to completely halt any planform mobility to protect human structures (Erskine, 1992; Surian, 1999; Kiss et al., 2008; Depret et al., 2017). Depret et al. (2017) studied three reaches on the Cher River in France to investigate whether the lateral stability has been caused by ancient bank stabilisation works or due to changes in the frequency and/or magnitude of flood events after the end of the Little Ice Age period. They demonstrated that the high density of engineering structures was the primary cause of the stability on the river channels and the channels did have the capacity to laterally erode once the structures were removed or decayed. While the immediate local impacts of bank protection works and embankments may decrease the amount of erosion, it will increase the amount of water being carried in the channel (Gregory, 2006). This can have unexpected downstream impacts with increased flow velocities occurring in areas without bank protection work and increasing the rate of erosion.

Another human installation that has affected the hydraulics and sediment transport of river systems has been the construction of in-channel weirs. Weirs have a long history of controlling water levels and helping to divert water for practical purposes (Candel et al., 2018; Lewin and Macklin, 2010), with the relic anastomosing patterns still present along many English rivers. Depret et al. (2017) found the influence of the Boutet weir on Cher River extended 5.5km downstream of the weir with an absence of lateral erosion, bars and riffles along this section of the river channel. There are also upstream effects of weirs, with raised water levels reducing flow velocity and turbulence and helping fine sediment deposition (Anderson et al., 2015). Dixon et al. (2018) suggest that the high number of weirs (over 3600) on the Murray-Darling River explain the stability of the confluence between the Murray and Darling Rivers. The removal of weirs can have significant impacts on the river system. Thomas et al. (2015) studied the impacts of the removal of a low-head weir in Wales and found rapid channel widening due to the wave of bed material that had been trapped behind the weir for at least a century. The material was finer than the typical bed material and all the particles were mobilised during bankfull flows. The material was deposited in the centre of the channel, forcing the flows closer to the bank and increasing the channel width by over 20% of the original size.

2.2.3. Deposition processes

Acting in tandem to the erosion processes on the outer bank are the deposition processes occurring, usually on the inner bank or in the middle of the channel. The most

characteristic depositional landform is the point bar (Hooke, 2015), which forms on the inner part of meander bends and is attached to the floodplain. These bars tend to be fixed in their location and do not migrate downstream within the channel and only adjust as the planform migrates. These point bars will grow through lateral accretion. Bars can also exist separated from the floodplain and are termed as free bars. These bars can migrate downstream. Mid-channel bars can be a common occurrence in actively meandering channels (Hooke and Yorke, 2010), where shallowing occurs in the middle of the river channel until the bed is exposed at medium and low flows. Vegetation can establish on the bar, further stabilising the bar and increasing the rate of deposition. Usually one of the channels will become the main channel and deposition will occur in the secondary channel until it eventually forms part of the floodplain. Hooke and Yorke (2010, 2011) found that the life cycle of the mid channel bars is between seven and nine years. Church and Rice (2009) found that point bars have a longer life cycle of around 100 years, during which the gravel bar forms quickly and approaches an equilibrium length. They showed there is a constraint on the vertical height of bars as they are only able to grow to the height that the main sediment size can be lifted by the given flow conditions.

2.2.4. Flow and sediment transport patterns

The flow patterns within meander bends were first characterised by Leliavsky (1955) and subsequently by Hooke (1975) and Dietrich et al. (1979), which showed a periodically reversing helical motion. Any small flow deviation causes a centrifugal force towards one side of the bend, developing a transverse flow. The existence of a well-developed cell next to the outer bank was measured in the field by Bathurst et al. (1977), and Thorne and Hey (1979). Figure 2.6 shows the classic characteristics of flow patterns within a meander bend. The water surface becomes super-elevated around river bends, with the height difference increasing as the bend curvature increases. The flow pattern has outward flow at the surface of the water column and inward flow at the base. The greater the curvature of the bend, the higher the velocities of these secondary flows. There is, however, a limit on the increase in curvature. Bagnold (1960) identified that flow separation can occur on very tight bends on

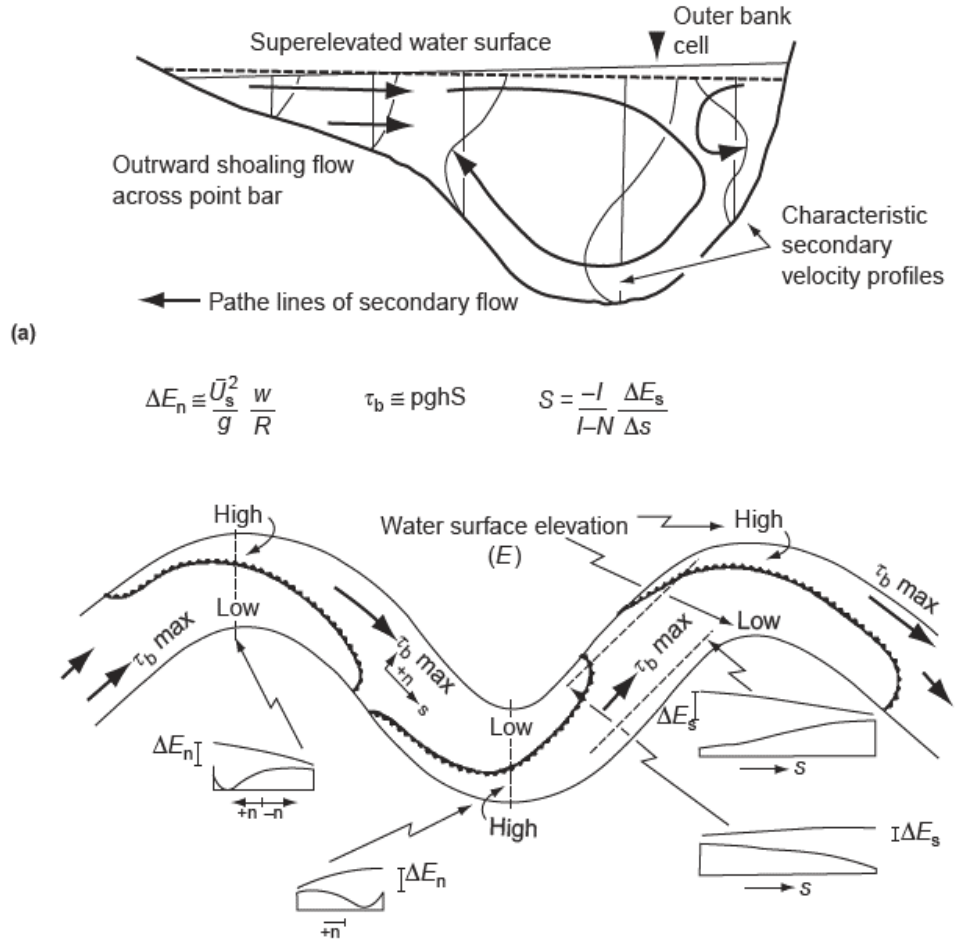

Figure 2.6. Typical flow characteristics in meandering channels. Note the secondary flows, which direct flows towards the inner bank. From Makram and Thorne, 1992

both the inner and outer bank, reducing the velocity of the flow and reducing the effectiveness of the secondary flows. The fastest flow starts at the inner bank at the entrance to the bend and crosses to the outer bank around the zone of maximum curvature. In simple bends, the maximum shear stresses occur just downstream of the apex (point of maximum curvature). The maximum rates of bank erosion usually occur near the apex of the bend, where the impingement of the flow on the outer bank is highest. In compound (multi-lobe) bends, the maximum rates of erosion will differ for the upstream and downstream lobes, increasing the asymmetry between the bends as they develop.

2.2.5. Cutoffs

Cutoffs are a well-known meandering process, where a sudden shortening of the channel length occurs (Gay et al., 1988; Hooke, 1995, 2004), although the processes occurring are less known due to the infrequent nature of cutoffs (Guneralp and Marston, 2012). Cutoffs and the associated formation of an oxbow lake are important for floodplain construction and can influence the subsequent rate of meander migration as often more resistant fine material is deposited in oxbow lakes and has implications for engineering (Hooke, 1995, 2004; Constantine and Dunne, 2008). Cutoffs become inevitable as the meander sinuosity increases and therefore can be considered as a process that is intrinsically related to the internal mechanisms of the system (Stolum, 1996, 1998; Frascati and Lanzoni, 2010).

There are two different types of cutoff, chute and neck, which occur at different scales and potentially have different impacts on the surrounding channel. Chute cutoffs usually occur during high flow events, when the flow goes overbank and erodes into the floodplain, reactivating an old channel across the point bar or incising a new channel in the floodplain. Neck cutoffs occur mainly due to the geometry of the channel, when two separate parts of the channel come into contact with each other, removing a large section of the river channel (Camporeale et al., 2008). The actual breakthrough can occur during moderately low flow events and can lead to rapid adjustment in the surrounding channel. Lewis and Lewin (1983) found that chute cutoffs tended to occur on higher gradient reaches and neck cutoffs occurred on lower gradient floodplains. Harrison et al. (2015) investigated the hydraulic and sedimentological processes occurring along a section of reconstructed river and interpreted the implications for chute cutoffs. The controls they found on the development of chute cutoffs included flood magnitude, floodplain gradient, river curvature, sediment erodibility and the resistance to flow due to riparian vegetation. Hooke (1995) recorded the river channel adjustment to meander cutoffs of the River Dane and River Bollin and found that

rapid widening and sedimentation occurring immediately after the cutoff. For one cutoff there was progressive steepening of local channel slope and accelerated erosion upstream, but for the other cutoff the erosion was localised. Multiple riffles and bars formed in the first 2-4 years after the cutoff, before becoming more regular and stabilising within eight years. The oxbow lakes persisted in the abandoned channels for much longer than time taken for the channel to adjust.

Stolum (1996, 1998) used a combination of simulations and empirical data to show that meandering rivers can form to a critical state in which the river can oscillate between an ordered and chaotic state. When the river transitions between the two states then clusters of cutoffs tend to occur. Stolum proposed that two different domains exist, a high sinuosity domain with a planform sinuosity ~3.5 and a low sinuosity domain with a sinuosity ~2.7. If a cutoff occurred on a channel in the low sinuosity domain then it would likely introduce chaos in the long-term, while if a cutoff occurred in the high sinuosity domain then a cutoff will most likely lead to a cluster of cutoffs occurring, resulting in a more ordered state being the outcome. The models that Stolum used found the mean value of sinuosity of 3.14 for the transition between the ordered and chaotic states, but this was lower if chute cutoffs or valley confinement was included in the model. Hooke (2003) proposed a framework for analysing river instability, considering that instability is inherent within meandering channels. The occurrence of multiple cutoffs along a river channel could be linked to self-organised criticality within the meandering system. Multiple cutoffs were originally associated with changes in hydrologic or climatic conditions, but Hooke (2004) proposed that a series of cutoffs that occurred over the winter of 2000-01 on the River Bollin were caused by the river being in a critical state and adjusting rapidly to a relatively low magnitude flood event.

Cutoffs tends to eliminate the most mature meander loops (Camporeale et al., 2005), placing a limit on the planform complexity and they generate intermittent noise that can influence the dynamics of the whole river system (Perucca et al., 2005; Camporeale et al., 2008; Frascati and Lanzoni, 2010). The cutoffs also provide a type of self-confinement for the meander belt, limiting the ability of the river to meander across the floodplain. Cutoffs stabilise the mean river geometry around a statistically steady state, while a single event can trigger the propagation of noise through the whole river system. The impact can be dramatic if multiple cutoffs occur simultaneously, with large sections of the river channel removed. Perucca et al. (2005) investigated the presence of non-linearity within the geometry of meandering channels and found that no relevant nonlinearities were detected. They suggest

that the occurrence of cutoffs prevent nonlinear processes from influencing the long-term dynamics of meandering rivers.

Constantine and Dunne (2008) noted that evolution models of meander cutoff only allow cutoffs to occur under a narrow set of conditions and the associated planforms often have a much higher sinuosity that is seen in nature. Introducing randomly occurring chute cutoffs reduced the overall sinuosity and produced more realistic meander planforms.

2.3. Monitoring and Modelling Approaches

2.3.1. Empirical approaches to recording river channel change

There are numerous different approaches to investigating river channel change that vary depending on the spatial and temporal scale of interest. Each of the approaches have advantages and disadvantages depending on the process and behaviour being studied. Lawler (1993) reviewed the different approaches available to study bank erosion at the time and produced Figure 2.7, which considered the resolution of the different approaches and timescales of interest. It is difficult to measure a truly continuous rate of riverbank erosion, and the researcher must select the approach most suitable to the aim and questions of the study. At short timescales, constant measurement of the bank has allowed for detailed study of the processing occurring but is only available at short timescales and with a small spatial coverage. Historic sources and sedimentological evidence allow a much longer period to be studied, as well as a larger spatial scale with historic sources, but the data tends to be more sporadic and incomplete, meaning that missing data needs to be interpreted. Since the review was published, other techniques have become more widely available, namely widespread high-resolution satellite imagery and terrestrial and airborne Light Detection and Ranging (LiDAR) (e.g. De Rose and Basher, 2011) and unmanned aerial vehicles, which allow for lower and multiple flights (Cook, 2017).

The diverse approaches have developed due to: i) the different emphases of the particular researcher, whether the study concerns processes, mechanisms or river behaviour; ii) the different disciplinary back ground of the researchers or research groups; iii) the different riverine conditions in terms of the geometry and sediment size of the river itself and the differing hydrological and climatic conditions; and iv) the timescale of interest for the researcher. Lawler's (1993) paper was, in part, an attempt to help standardise the diverse techniques and to help facilitate the comparison between the different studies.

The different techniques can be split into long, intermediate and short timescales. Generally, as the temporal scale of the method increases, the spatial scale of the investigation can increase. Methods that can be used at short timescales, such as erosion pins, photo-electric erosion pins, terrestrial LiDAR scanning and terrestrial photogrammetry tend to be completed at a bend scale (e.g. Lawler, 1994) with repeat measurements completed on a daily to monthly scale. The method can be labour intensive and there is the possibility of missing data if the erosion pins are completely eroded out of the bank or covered by deposited material, but it allows for detailed investigation of the rates and location of erosion and deposition on the riverbank. More recently, the invention of terrestrial laser scanning stations has allowed for the rapid profiling of the riverbank and for repeat surveys to be completed (O'Neal and Pizzuto, 2011). This has increased the amount of data that can be collected and the area that can be covered from this approach.

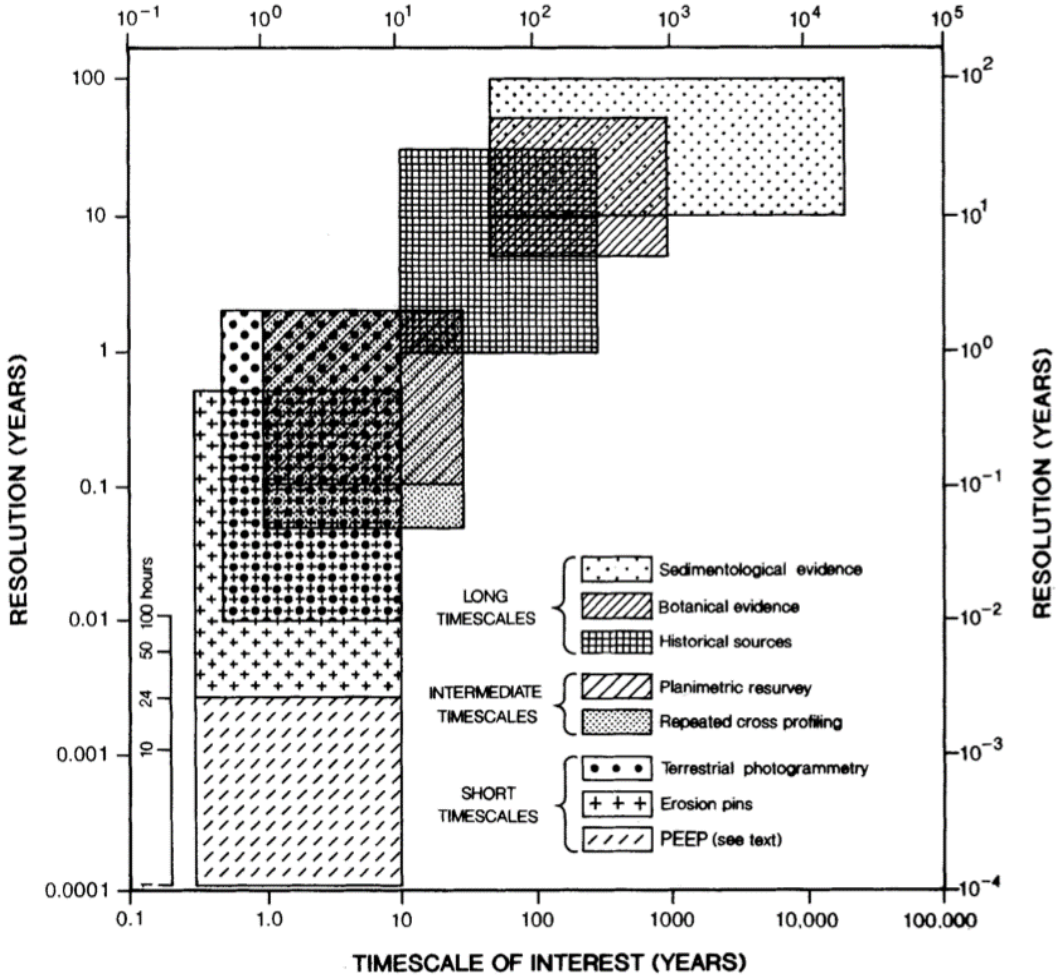

Figure 2.7. The different types of approaches to investigating river channel change, based on the temporal scale of interest. From Lawler (1993)

At the intermediate timescales, approaches such as planimetric resurvey and repeated cross profiling have been used to measure either the 2D horizontal planform or the 2D cross-sectional profile of the river channel. During planimetric resurvey, the position of the channel bank is mapped and repeated at a certain time interval (ranging from monthly to yearly) to measure where changes have been occurring. Originally the measure would use electronic distance measuring techniques (e.g. Pugh, 1975), while recent developments in global positioning satellite technology has allowed for the accuracy of the measurement to be increased to centimetre scale. There are some limitations associated with this approach: there is difficulty in accurately defining the channel bank, especially when the vegetation is abundant and the position of the inner bank is not as well defined as the outer bank and there maybe inconsistencies between different sites and researchers; and the approach can only measure the top of the riverbank and does not take into account bank material that has been removed due to undercutting. Abundant vegetation can also affect the GPS signal, reducing the accuracy of the recording. This type of erosion will only be recorded by this method once the bank has failed and may not be related to the flow event that caused the erosion. Repeated cross profiling can be used to overcome some of these limitations, by measuring the changes to the riverbank and riverbed position at fixed cross sections across the river channel. The profile should be orthogonal to the channel edge, but this may need to be adjusted if the channel is active.

At the longer timescales, a range of approaches are available to investigate the long-term evolution of the channel and floodplain. Sedimentological evidence can be used to identify the position of the river channel by identifying fluvial deposits within the floodplain. If the deposit can be accurately dated, then changes to the river channel can be reconstructed. This approach is limited by the availability of datable material, the complexity of fluvial deposits and subsequent destruction by geomorphological processes. Botanical evidence can also be used in a similar way, with the age of vegetation along ridge-and-swale features being measured and used to reconstruct the channel position (Hickin and Nanson, 1975). This approach is limited by an unknown rate of colonisation of vegetation on the point bar and changes in climate over the longer period. If large trees are present, then trees rings can be used to date the floodplain. Lichenometry has also been used to date floodplain material, e.g. Harvey et al. (1984), but relies on rocky material being present. However, the approach allows estimating the channel position for a longer period that is available from archival sources and allows longer-term evolution of river channels to be investigated. The

last approach at the longer timescale is the use of historic sources, namely maps, and more recently aerial photography and satellite data. The channel bank line is usually digitised and the changes between the different available dates is recorded and analysed (e.g. Hooke and Kain, 1982; Hooke and Redmond, 1989; Brewer and Lewin, 1998). The rate of change can then be measured as the total distance between the channel position and the number of years between the two maps. A standardised area change can also be used if the planform changes are complex (Lewin, 1987). The earliest accurate maps in the United Kingdom are available as the Tithe maps of the 1840s and the first Ordnance Surveys were completed in the 1870s and 1880s (Mosley, 1975; Hooke, 1977), which gives between 150 and 180 years of recorded channel activity. The minimum gap between different maps dates is around 10 years for Great Britain but can be much longer depending on the coverage available. This varies regionally within the UK and internationally. Aerial photographs can be used to fill in missing gaps within the map coverage, but the coverage starts at a later date compared to the historic maps and is available mainly from the 1940s. Aerial photography brings an additional advantage with more detail on the floodplain including scroll bars, cutoffs and abandoned channels. The amount of riparian vegetation can also be determined from aerial photography, although vegetation close to the riverbank can obscure the exact position of the riverbank and make determining the bank position less accurate. More recently, satellite imagery has become available, with increasing accuracy and resolution as satellite technology has improved. However, while satellite imagery has been widely applied to many of the world's largest rivers (e.g. Deb and Ferreira, 2015; Dixon et al., 2018; Kummu et al., 2008), the resolution is still too low to be useful for the smaller rivers in the UK.

The wide spatial availability of the historic maps, aerial photographs and satellite data means that larger areas can be studied compared to the short and intermediate timescales and over much longer timescales than is available for monitoring approaches, meaning that the long-term behaviour of the rivers can be explored. Hooke and Redmond (1989) used comparison of erosion rates between 1870 and 1950 Ordnance Survey maps and found the rates and extent of channel change in England was higher than previously considered. They found that 35% of rivers draining upland areas had shown pattern instability during that period, although the extent varied between different rivers and even along individual rivers.

However, there are some limitations to using this approach using historic maps and aerial photographs (Lawler, 1993). There is an assumption that the change between the two

dates has been regular and the channel has moved in a simple way. Whereas in reality the change in the channel in usually complex and episodic, meaning that the peak rates of migration can be smoothed out when an average migration rate is calculated between the two dates. Assumptions of stability, increasing erosion or decreasing erosion rates could be identified from data sources, depending on the temporal sampling. Figure 2.8 shows a theoretical change in sinuosity over time with four sample points. If the maps dates available were at t_1 and t_2 then the river would appear to have increased its sinuosity during the study period, while if the sample period was between t_3 and t_4 then the river would appear to have decreased its sinuosity. The same issue can occur when calculating a mean annual migration rate for a period (see Figure 2.8). The mean annual migration rate (calculated as the total distance between bank positions divided by the length of time) can vary greatly depending on which maps dates are available. Sadler (1981) found that sediment accumulation rates could vary greatly between different time spans, with a systematic trend of decreasing accumulation rate with increasing time span due to unsteady and discontinuous sedimentation, and the same effect can occur when measuring erosion rates using the historic map and aerial photograph approach (Hooke, 1980; Kessler et al., 2013).

There are also errors associated with the data sources, particularly in the early maps such as the Tithe maps (Hooke and Kain, 1982). The Ordnance Survey County Series of the late nineteenth century had increased accuracy with errors of between 1 and 2m reported on the River Bollin (Mosley, 1975). There can also be issues with the scale of the available maps. Maps with a scale above 1:25000 can exaggerate the channel width and the accuracy between the different scales will change. Where possible, the highest resolution maps should

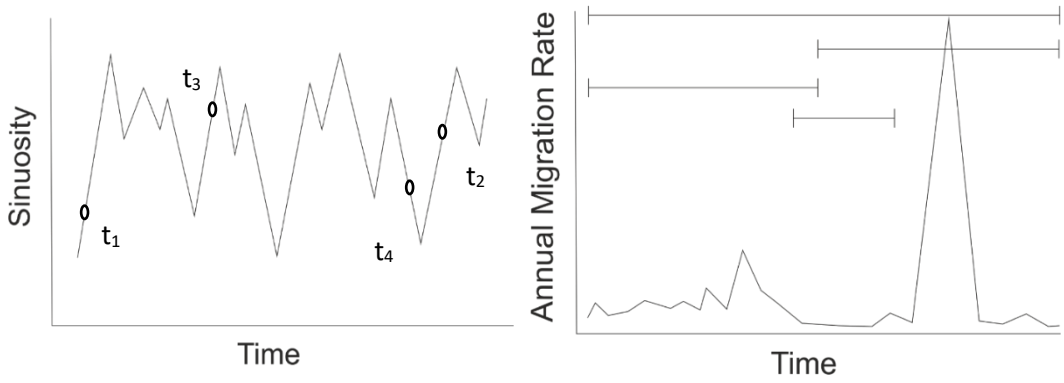

Figure 2.8. Potential difficulties related to temporal sampling using historical sources. The different length time periods will give contrasting results that may not be representative of the system

be used. There can also be some confusion over the definition of a channel bank. Usually on Ordnance Survey maps the bank line is defined as the 'normal winter level' (Harley, 1965), but other surveyors have used bank top. The identification of the bank top can be difficult, especially on the inside of a bank and there have been repeated efforts to define a bankfull stage (Lawler, 1993).

2.3.2. Modelling Approaches

There have been a large number of different numerical models developed for understanding river behaviour and evolution (Coulthard and Van De Wiel, 2012), which reflect the wide range of backgrounds and interests of the researchers involved. The different model types include landscape evolution models, meander models, cellular models, alluvial architecture models and computational fluid dynamics models. There are some similarities between the models, but also notable differences in terms of the scale (spatial and temporal), data requirements, assumptions and computational cost. All the different approaches are a simplified abstraction of river systems, with different levels of complexity. Although the simplification of the processes has limitations and relies on assumptions, there are several advantages to using modelling approaches over field-based research (Coulthard and Van De Wiel, 2012). They can provide a controlled environment of river evolution, in which the different input variables can be altered and the effects studied. They also provide the opportunity to study the long-term evolution of river systems, which is not possible based on field approaches, and at more regular intervals than archival sources, which depend on the date of the survey and are often incomplete. However, all models need to be validated to confirm their accuracy.

Coulthard and Van De Wiel (2012) defined three broad categories for the different types of modelling approaches: black box models, stochastic models and process-based models. In the black box model outputs are related to the inputs with no prior knowledge of the system or how it operates and are usually regression or statistical models based on empirical data. Stochastic models try to reproduce the natural variability and chaos found in natural systems by including a random element into the model, such as sampling the results from a probability distribution. Process-based models try to simulate the physical processes occurring in the river system, which may be split into different components and the interactions between the different components modelled. Each of the different approaches has advantages and disadvantages. The black box approaches can work well on the data with which they are developed, but the results may not be applicable to different environments

and give little information on the processes occurring within the system. The process-based models can inform researchers about interactions between the different processes in a dynamic system but are difficult to validate with field-based studies. All the approaches contain some level of generalisation, with even the most complex computational fluid dynamic models containing some empirical relationships.

All the different approaches will have to discretise the time and space component of the processes to a defined temporal and spatial scale. The initial meander models (e.g. Ikeda et al., 1981) represented the channel as a single line, with calculations performed at a defined position along the channel. Later models developed a two-dimensional representation of the channel, with cell elevations able to rise and fall as sediment is transported (e.g. Coulthard et al., 2002, Coulthard et al., 2007). Finally, three-dimensional models have been constructed that can represent flow and sediment transport in all directions. As the detail of the models increases, the complexity of the calculations and the data required also increases, adding to the computational requirements of the model (e.g. Kasvi et al., 2015). Coulthard and Van De Wiel (2012) provide a good overview of the different types of river evolution models, while the rest of this section will focus on the models developed specifically for meander migration.

Meander models have a long history of use in trying to understand meander evolution. Many of the meander models have built on the initial numerical modelling of Ikeda et al. (1981) and Parker et al. (1982). They used fluid dynamical models to explore the behaviour of channels with an erodible bank, with a constant channel width and a large radius of curvature at the bend apex. Near-bank velocities and a function of upstream channel curvature were used to evaluate bank erosion at a point, with the amount of erosion on the outer bank balanced by deposition on the inner bank. The initial 1981 paper concerned the linear instability of bends, while the 1982 paper further developed the analysis by including non-linear migration of bends. A non-linear stability analysis is used to explain the skewing of bends, a process seen in many naturally migrating rivers. The non-linear effects reduce the migration rate of bends at the meander length with the highest linear instability and leads to the development of skewing as the bends continue to migrate.

The initial models were time invariant, but Parker and Andrews (1986) applied a two-time expansion to the original bend equation to study the time development of meander bends. They found many bends are unstable, with long wavelength bends growing until they cutoff and short wavelength bends returning to a straight planform. Hasegawa (1989) added a bank erosion coefficient to the Ikeda et al. (1981) model based on a penetration test of the

bank material. Hasegawa tested three rivers in Hokkaido and found the highest erosion rates occurred on rivers with sand and gravel banks, while clayey banks had lower erosion rates. Furbish (1991) used the spatial convolution of upstream curvature based on the approach by Ikeda et al. (1981) to produce an autoregressive form of the model, which is equivalent to a stochastic linear-difference equation. Bend curvature is then treated as a random process within the model. The model suggests that large bends will tend to grow rather than small bends, but there is no tendency for intermediate bend sizes, and also predicts the downstream shift in migration. Furbish showed that the meandering process is sensitive to the initial geometry of the channel, and that the diverse bend shapes seen in freely migrating rivers is independent of unsteady flow and non-uniform erodibility.

Sun et al. (1996, 2001a, b) used the Ikeda model to investigate the dynamics between a meandering river and sediment flux by altering the erodibility of the floodplain to mimic floodplain features such as point bars and oxbow lake deposits. They found the heterogeneity in floodplain material was important for the development of different river geometries but had no impact on the meander wavelength. Within the model, they found rivers could form their own meander belt, with cutoffs producing a self-confinement process, but this process depended on the properties of the floodplain material and the erodibility of the different size sediments. Abad and Garcia (2005, 2006) created the RVR Meander model, which was based on the Ikeda approach to estimating lateral erosion but could be applied using a GIS. This allowed for statistical analysis of migration rates in both the transverse and longitudinal direction. The model was later combined with the stream bank erosion sub-model of CONCEPTS (Langendoen and Alonso, 2008; Langendoen and Simon, 2008; Motta et al., 2012a, b) to investigate the impact of floodplain heterogeneity on meander shape. The research showed that floodplain complexity could contribute to the complex planform often seen in natural rivers, such as elongated and compound bends, and could produce downstream skewed bends, which did not occur in homogenous floodplains.

Blondeaux and Seminara (1985) noted there were limitations with the Ikeda approach and attempted to unify the bar theory of meander initiation with the bend theory of meander growth developed by Ikeda et al. (1981). They discovered a ‘resonance’ phenomenon when certain critical values are reached for the parameters in the model and this resonance controls the bend growth. Zolezzi and Seminara (2001) and Seminara et al. (2001) further investigated these resonance conditions to explore the upstream and downstream influences on bend form and planform evolution. They used a three-

dimensional form of the continuity and momentum equations for fluids, coupled with an evolution model for bed topography to derive a two-dimensional model of river morphodynamics. In the sub-resonance conditions the maximum scour is located downstream of the apex of the bend but moves to upstream of the apex in super-resonance conditions, meaning that meander bends can be skewed either upstream or downstream depending on which type of resonance is encountered. When applied to meander geometry, the sub-resonant conditions produce meanders of the Kinoshita type in which the downstream migration rate decreases as the transverse migration increases to a maximum, before eventually decaying. Seminara et al. (2001) found two distinct phases of growth in the sub-resonant conditions: a linear growth initially, followed by slower non-linear growth, which leads to the fattening and skewing of the meander shape. In the super-resonant conditions, the meanders were found to migrate upstream and skew in the downstream direction. As these meanders develop, the average channel slope and width to depth ratio decrease and the meander bend will pass back into sub-resonant behaviour in the later stages of evolution.

Darby et al. (2002) developed a new model, combining a mechanistic model of bank erosion, with a two-dimensional depth-averaged flow model from Delft University of Technology and Delft Hydraulics (Mosselman, 1991, 1992). The model improved on previous approaches by including deposition and removal of material on the failed bank and allowing the riverbanks to be moveable boundaries, which can adjust as material is eroded and deposited. When the model was tested against field data, the performance for flow was encouraging, but limitations in resolving flow when the bed topography varied rapidly meant the model under-predicted scour and was not able to produce the multiple pools observed on longer bends. Darby et al. (2007, 2010) further developed this model by coupling hydraulic erosion, finite element seepage and stability models. The model was tested on eroding banks on the Mekong River, with in situ jet testing to help determine the bank properties. Rinaldi et al. (2008) applied this approach to a high curvature bend on the Cecina River and found bank failures are caused by a combination of pore water pressures and hydrostatic pressures during the drawdown and rising phases of multi-peaked flood events. Rinaldi and Nardi (2013) reviewed the advances in modelling the interaction between river hydrology and mass failures and noted the need to improve the parameterization of soil properties and the need to improve the modelling of seepage and fluvial erosion. These types of studies, however,

are usually only applied to individual banks and there are issues scaling up to meander belt scales.

2.4. Meander Bend Behaviour

One fundamental question is why do meander bends form on river channels (Seminara, 2006). Leopold and Wolman (1957) suggested the formation of alternate bars leads to flow being forced to one side of the riverbank and initiate erosion. However, if alternate bars were the driver of meandering channels, the wavelength of the developed bars fall in the stable range of bend stability and the bends would not grow across the floodplain (Seminara, 2006). The original quantification of meander behaviour focused on the equations and relationships between different meander parameters and inputs. The researchers found a consistency in the relationship between discharge and meander wavelength for example (Langbein and Leopold, 1966) and suggested that the river planform is caused by the river minimizing the sum of the squares of changes in direction. Meandering channels achieve the minimum variance, and Langbein and Leopold suggest that: "meandering is the most probable form of channel geometry and thus is more stable geometry than a straight or non-meandering alignment". Leopold and Wolman (1960) found a near constant ratio of radius of curvature to bend width and ratio of radius of curvature to bend length, which leads to an apparent similarity between bends, regardless of the scale of observation. Langbein and Leopold suggested that meandering river channels could be approximated as a "sine-generated curve" as the changes in direction of the channel are a sinusoidal function of distance downstream. Seminara (2006) suggested that any perturbation on an initially straight channel would eventually grow and develop into a meandering pattern. Zolezzi and Seminara (2001) and Seminara et al. (2001) used mathematical theory to show that meandering is inherent on river channels that are free to migrate. Using the classical approach of Langbein and Leopold, Seminara shows that if bank erosion is in phase with the local channel curvature then the bends will grow indefinitely across the floodplain and not migrate downstream. If there was a lag between the local channel curvature and the migration rate, then the meanders will both grow and migrate either upstream or downstream. Several other explanations have been put forward, including the Coriolis force, meandering being an inherent property of turbulent flow, and the minimisation of energy in the system (Hooke, 2013).

The theory of equilibrium and adjustment has been applied widely to fluvial geomorphology (Hooke, 2007; Nanson and Qing Huang, 2016) and assumes that channel

form is adjusted to the discharge and sediment load in the river. When there are changes to these external controls, through climate change or land use changes for example, the channel form will adjust to form a new equilibrium stage. Once the equilibrium state is achieved the meander bends will still be mobile, but mainly through downstream migration and they will not change their overall morphology. In this scenario, variations in migration rate will be caused mainly by heterogeneities in floodplain material or constrictions due to valley width. These variations in migration rate are the main driver of cutoffs. Large flood events can cause a shift between different types of planform, between meandering and braided (Brewer and Lewin, 1998). In extreme cases, the flood can cause a permanent metamorphosis in channel pattern. Camporeale et al. (2005) believe that the opposing mechanisms of meander migration and cutoff help rivers achieve a long-term equilibrium, which proved to be universal and not affect by short-term river behaviour.

However, researchers in the 1970s began to produce evidence of non-equilibrium development of meander bends and non-linear behaviour in the migration rate of meanders (e.g. Brice, 1974; Hickin, 1974; Hickin and Nanson, 1975; Hooke and Harvey, 1983; Nanson and Hickin; 1983), which will be discussed below. There were still questions about the causes of the instability and whether changes to external factors were causing the change (Hickin, 1983) or whether the changes were caused by intrinsic relationships within the meandering system (Hooke and Harvey, 1983).

Ideas of chaos and self-organised criticality have been applied to geomorphology (e.g. Stolum, 1996, 1998; Hooke, 2003, 2004, 2007; Fonstad and Marcus, 2003; Frascati and Lanzoni, 2010; Croke et al., 2015) to varying degrees of success. The idea of self-organised criticality was first developed by Bak et al. (1987) and shown to occur in earthquakes (Bak and Tang, 1989) and in sand piles (Bak and Chen, 1991). It was shown that many complex systems could evolve to a critical state at which a small event can have large impacts on the whole system. It cannot be explained by analysing the separate parts and requires a holistic view of the system. Hooke (2007) understood self-organisation to mean "the formation and maintenance of patterns of structures attributable to the internal dynamics of the systems, independent of external controls" and criticality in the system occurs when there is a sudden readjustment and the system regains order.

Stolum (1996, 1998) applied this idea to river meander cutoffs and suggested that a straight channel represents the most ordered state and a highly sinuous channel represents a chaotic state. The system evolves through lateral channel migration, until a critical

threshold is reached, at which cutoffs occur to maintain the critical sinuosity of the channel. A super-critical state also exists, in which a single cutoff can cause a cluster of cutoffs to occur and the reorganisation of the river system. Hooke (2004) applied this to a series of cutoffs on the River Bollin and suggested that self-organised criticality could explain the unusual number of cutoffs that occurred on a reach over a single winter.

Fonstad and Marcus (2003) applied the idea of self-organised criticality to riverbank systems to attempt to understand where and when a natural river becomes unstable. They found a power law relationship exists for the number of bank failures and the magnitude of the failures. The relationship suggests that lower gradient streams are more susceptible to large bank failures. While it is not possible to predict a specific failure event, the probability distribution for the magnitude and spatial frequency of the events should be possible. They further suggest that if riverbanks are part of a critical system, then long-term or widespread stability is not possible. Reducing the number of small-scale failures will increase the number of low frequencies, widespread large-scale failures and local work to increase stability will transfer that instability into another part of the system. Croke et al. (2015) used an extreme flood event in Queensland to investigate the existence of self-organised criticality and found the data to support the idea of a self-organised critical state was variable. The data did not fit an inverse power law and it was difficult to identify a single critical state due to the feedback and multiple types of adjustment. Frascati and Lanzoni (2010) used a physics-based simulation to produce a long temporal scale record of meandering river channel. They examined the spatial series of channel curvature and time series of sinuosity using nonlinear methodologies from time series analysis to determine whether chaotic behaviour or self-organised criticality could be identified. They conclude that neither channel curvature nor sinuosity changes can be explained using chaotic dynamics alone. They found no evidence of clustering in meander cutoffs and a lack of a temporal power-law scaling, which argues against the idea of self-organised criticality in meandering systems.

2.4.1. Brice (1974) model of bend evolution

Brice (1974) proposed a scheme for classifying the shape of river meander bends and suggested an evolutionary trend for individual bends. Bend loops were classified as either simple symmetric, simple asymmetric, compound symmetric or compound asymmetric. A loop was defined once the length of the bend exceeded the radius and would initially be symmetrical with a roughly constant curvature throughout the loop. The loop becomes asymmetrical when a second arc begins to form on either the upstream or downstream side of the bend and becomes compound when the arc has developed far enough to be considered a loop. Figure 2.9 shows the different types of meander loop proposed by Brice and the sixteen different forms based on studies of aerial photographs and topographic maps from the United States. Brice found that simple arcs would start as a section of constant curvature with a large radius of curvature, similar to Bend A in Figure 2.9. Bends would increase in height and decrease in radius as they develop (bend B and C). Loops may develop towards bend D if the height increases and the curvature remains consistent when the loop is closely connected to the surrounding bends. If there are straight segments between loops then the bends would develop in a similar form to bends E and G, although this elongation of the river bend does not continue indefinitely. Asymmetry in bends is very common and

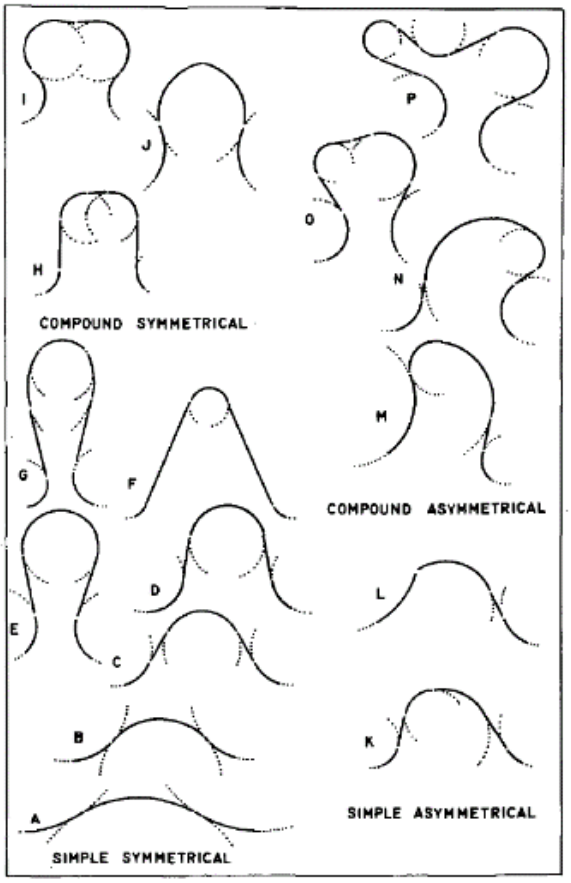

Figure 2.9. The different theoretical bend forms from Brice (1974)

caused when a secondary arc forms on the original loop and becomes compound when the secondary arc has passed the definition of a loop, with the length of the bend greater than the radius of curvature. Brice found that the asymmetry in the simple loops was not dependant on the flow direction, although the smaller arc was more common on the upstream side of the bend.

Brice suggests that the compound development of the bends is a gradual process with the development of the secondary arc into a loop. The compound bends can contain more than two simple loops, either tangential to each other or connected by straight sections of channel. Compound asymmetrical bends were more common in the channels studied by Brice, but compound symmetrical bends could be identified, especially bends H and I in the classification above. Brice suggested there was a general evolution of meander loops, from a simple arc/loop, which increases in amplitude through lateral migration. Once the secondary arc develops, the bend will have become asymmetrical and finally compound once that simple arc has developed into a secondary loop.

2.4.2. Hickin (1974) model of bend evolution

Hickin (1974) investigated the relationship between the ratio of radius of channel curvature to channel width (r_m/w) and meander bend behaviour using aerial photographs, and ridge and swale features left in the floodplain on an actively migrating river system. Erosion pathlines of downstream and cross-valley migration were created for individual point bars and compared to create a true migration rate measurement. Hickin identified a critical value for r_m/w, which once reached tended to control the development of the meander bend. The critical value of r_m/w on the Beatton River was 2.11. Leopold and Wolman (1960) showed that a large proportion of bends had r_m/w ratio between 1.5 and 4.3, suggesting that in natural channels an equilibrium condition exists. In the early stages of meander bend evolution, the r_m/w values are high but there is an increasing transverse acceleration of the flow, leading to a deepening of the channel near the outer bank and an increase in the local

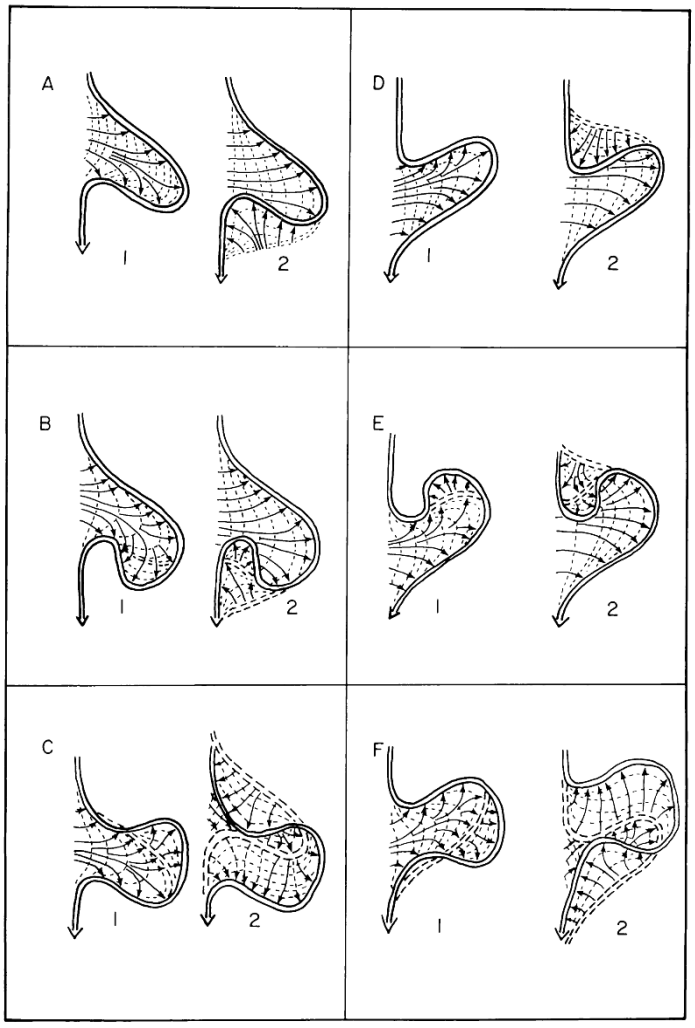

Figure 2.10. Theoretical development of meander bends, produced from erosion pathlines on the River Beatton. From Hickin (1974)

flow velocities. Leopold et al. (1960) found there was an increase in the resistance to flow as curvature increased; this was negligible for r_m/w values above 5.0, but increased rapidly once r_m/w dropped below 5.0. Experimental studies in pipes found the minimum flow resistance to curvature occurs when r_m/w approaches 2.0 (Hofmann, 1929), while Bagnold (1960) found that for values below 2.0 the separation zone created on the convex bank begins to break down and there is an increase in the resistance to flow. Taken together these findings suggest that bends will rapidly become meandering from a straight channel and decrease the r_m/w ratio to a value below 5.0. Once this value is reached, the resistance to flow will begin to increase, counteracting the increase in near-bank flow velocities. Once the r_m/w ratio approaches 2.0, the resistance to flow increases dramatically and the erosion rate drops. Hickin (1978a) studied the flow structures on the Squamish River and found the fastest velocities would move towards the outer bank as the bend began to develop, becoming the closest to the outer bank as the r_m/w ratio approached 3.0. As the ratio continued to decrease, the separation zone was created on the outer bank and the highest flow velocities were pushed back towards the inner bank.

Hickin (1974) also suggested a pattern of change for meandering bends on the Beatton River (see Figure 2.10) based on the erosion pathlines from the meander scrolls. Bends would start as type A, with the dominant mode of erosion across the floodplain and some erosion on the downstream limb in the upstream direction (A2). The bends could then develop towards either type B or type C, with type B being the most common. Type B occurs when there is deposition on the downstream limb and radius of channel curvature increases, leading to a compound form in the bend. Type C occurs when there is deposition on the upstream limb and what was the secondary erosional axis becomes the primary axis. Types D, E and F have the same evolution as A, B and C, just oriented in the upstream direction.

Hickin and Nanson (1975, 1984) and Nanson and Hickin (1983) further analysed the relationship between r_m/w and lateral migration rate. They showed there was a rapid increase in migration rate to around $r_m/w = 3.0$ and declined either side of this value. It was suggested the absence of data near $r_m/w = 3$ was caused by the rapid adjustment of the channels at this ratio. A non-linear relationship between channel curvature and migration was proposed (Hickin, 1978b), with an initiation stage at high values r_m/w values (> 5.0) before a rapid growth phase as r_m/w approached 3.0. Tighter bends ($r_m/w < 3$) would enter a termination phase, where the migration would decrease rapidly before reaching a minimum

at $r_m/w = 2$. Figure 2.12 represents the conceptual model for this behaviour, with the line representing an envelope curve for the fastest migrating bends on the river.

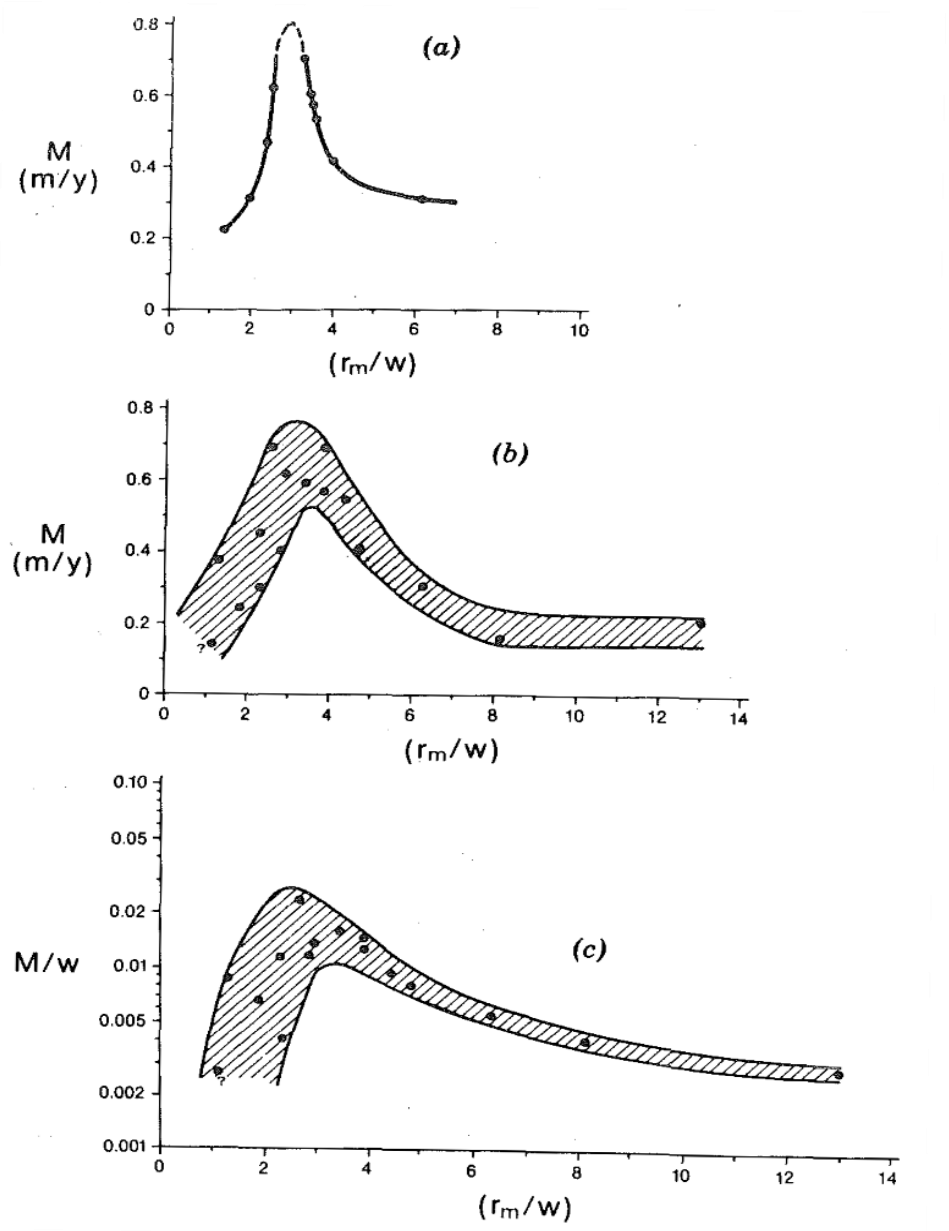

Figure 2.11. Measurements of migration rate against the channel curvature (r_m/w) measured on the Beatton River. From Nanson and Hickin (1983)

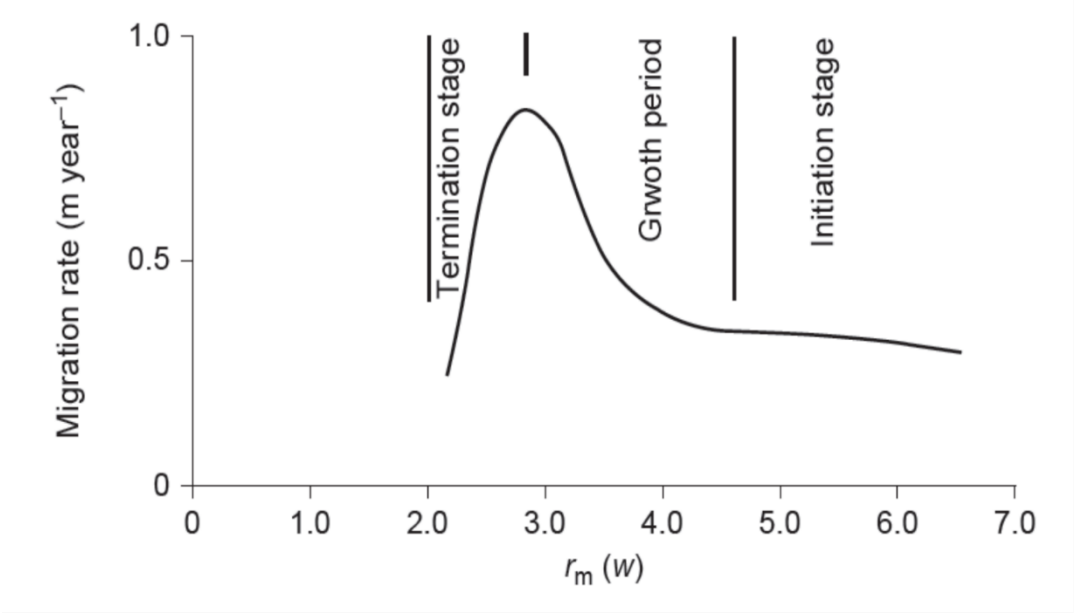

Figure 2.12. Conceptual model of behaviour for active river bends, with an acceleration in growth rate as r_m/w decreases, before a termination phase reduces the migration rate. From Hickin (1978)

2.4.3. Hooke (1995, 2003) model of bend evolution

Hooke (1995) created a qualitative model for meander evolution based on a sequence from initiation, downstream migration, growth, double-heading (or compound) behaviour and finally cutoff (see Figure 2.13), with meander bends showing a progressive, dynamic style of change and not an equilibrium form that had been suggested in earlier work. This was based on observations on the River Dane from maps, aerial photographs and field survey (Hooke and Harvey, 1983). Hooke and Harvey identified three main types of movement: migration, growth and lobing (bends becoming compound). They also noted the importance of the pool-riffle relationship within bends and suggested that beyond a critical combination of path length and curvature secondary flows breakdown and new riffles are produced at the apex of the river bend. The long-term record of the bends showed that many bends increased their complexity through time. Once a bend become double-headed the individual lobes tended to develop as separate bends, independent of each other. They ascribed the changes to intrinsic thresholds within the system, rather than any specific extrinsic change within the catchment or the river system. These ideas were in contrast to conventional theory that suggested meanders evolve to an equilibrium form in balance with the discharge and sediment fluxes present (Leopold and Wolman, 1960; Hooke, 2007).

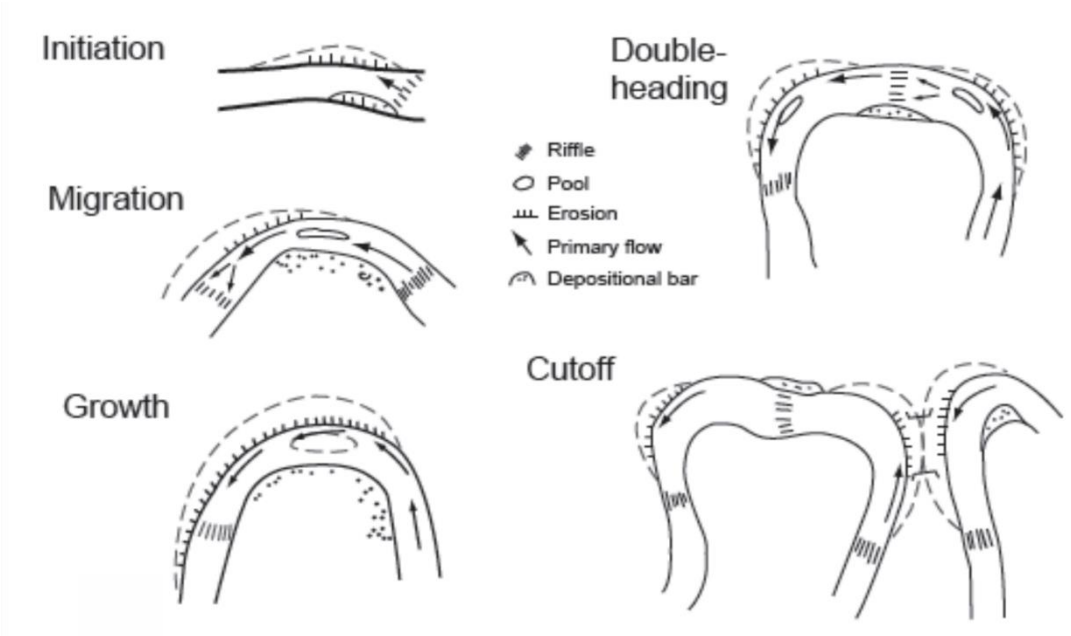

Figure 2.13. Qualitative model for highly active meandering bends, including the pool-riffle sequence and the development of an extra riffle as the bend becomes double-headed. From Hooke (1995)

Hooke (2003) used the qualitative model to produce a quantitative framework, in which meander behaviour and instability could be analysed. Theoretical work suggests that instability in river systems can be inherent and that behaviour in river bends can range from stable to chaotic. These ideas were developed from the self-organised criticality shown by Bak et al. (1987) and developed for meander bends by Stolum (1996, 1998).

A range of behaviour has been identified, with some bends showing instability and constantly readjusting, while other bends show long-term stability (Hooke, 2003). As discussed in the previous section, Hickin (1974) and Hickin and Nanson (1975) found a non-linear relationship between channel curvature and meander migration rate with phases of behaviour as the bend reached a certain curvature. One of the frameworks for analysis suggested by Hooke used a phase space from the ratio of radius of curvature to channel width ratio (r_m/w) and migration rate. The r_m/w value and rate of movement use a width-averaged measurement so that rivers of different sizes can be compared. If it is possible to follow the evolution of a single bend through time then it may follow the different trajectories proposed in the model (see Figure 2.14). Trajectory A represents the most active bends that develop towards neck cutoff. They start from a straight channel, with a small initial kink in the flow

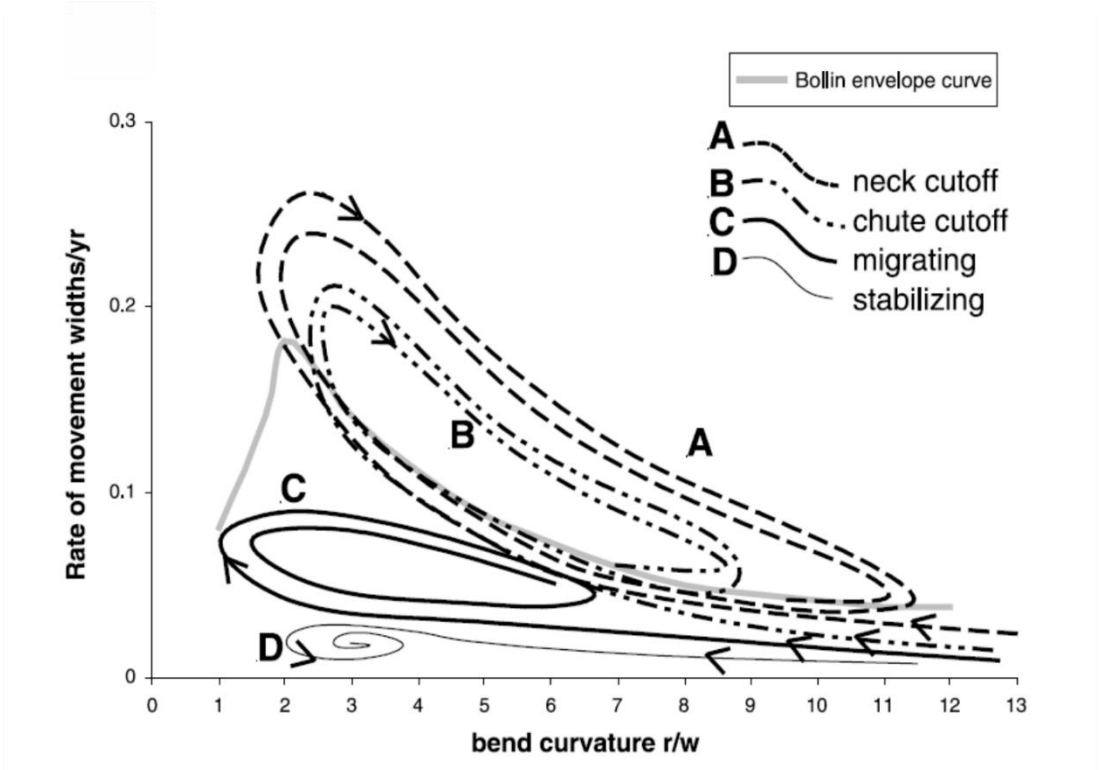

Figure 2.14. Hypothetical trajectories for different types of meander bend behaviour in a curvature-migration rate phase space. From Hooke (2003)

before migrating downstream as the bend curvature decreases. Once the r_m/w value approaches 5.0, it can switch from the migrating downstream to rapidly growing across the floodplain, as suggested by Hickin and Nanson. Once a critical bend length has been reached and the secondary flow circulation breaks down, the migration rate begins to drop, and the r_m/w value increases as the bend becomes double-headed. The evolution of these bends will finish through the occurrence of a neck cutoff and start the process again as a simple bend with high r_m/w value. Trajectory B is for bends that experience chute cutoffs. These bends follow a similar trajectory to neck cutoffs but tend to cutoff earlier and therefore the increase in r_m/w value is not as great when the cutoff occurs. Some bends can develop low r_m/w values but do not experience the growth across the floodplain and simply migrate downstream as a consistent rate. These bends would track as trajectory C. Finally, some loops have developed to have low r_m/w values, but are now stable or evolving slowly, and these bends would follow trajectory D.

Current records of actual meander development are not long enough to follow multiple trajectories around the different attractors, but the meanders should be able to redevelop and plot around the loops multiple times if the record is long enough. The trajectories will rarely be as smooth as produced in the model as meander migration is episodic and requires flows over a certain threshold for erosion to occur. Within this type of analysis, it is possible to examine bends with different types of behaviour and search for reasons why a bend might swap between the different types of trajectories, possibly through changes in effective discharge or riparian vegetation coverage helping to stabilise the riverbanks.

2.5. Implications for management and restoration of river systems

During the 1990s, there was increasing scrutiny of the hard engineering approach to managing rivers after a series of failures to prevent flooding and increasing economic and environmental costs (Gilvear, 1999). The move towards more applicable timescales during the 1980s and 1990s by geomorphologists allowed for more discussion with engineers. Gilvear proposed four key components that fluvial geomorphologists could use to help complement engineering approaches to river management:

- To promote the importance of lateral, vertical and downstream connectivity in fluvial systems and how they relate to each other.
- Stress the importance of fluvial history and chronology over different timescales, and using palaeo and active landforms to determine the stability of the landscape.

- Highlight how sensitive geomorphic systems can be to disturbance, especially when close to intrinsic thresholds
- Show how important landforms and processes are in creating diverse habitats and increasing the biodiversity along the river system.

The challenges required to gain acceptance from engineers include using the most recent technology, developing deterministic equations that can be used to predict bed and bank instability, developing an understanding of the importance of geomorphology for biodiversity; and developing catchment scale approaches.

Connectivity within the fluvial system is important as changes upstream can affect functions downstream (Gilvear, 1999). Kondolf (1997) developed the concept of "hungry water" where rivers starved of sediment, for example downstream of a dam, would have higher energy and more erosive ability. Reducing the lateral mobility of rivers can also increase the unit stream power as overbank flooding helps to dissipate the energy of the river (Gilvear, 1999). Often inappropriate defences were constructed on rivers and there was no consideration of other potential solutions.

River restoration projects have become an important activity to help improve water quality, enhance the habitat and facilitate human uses (Downs and Kondolf, 2002; Kondolf, 2006; Wharton and Gilvear, 2010). The early approaches usually had the objective of creating a stable, single-thread meandering channel, even when these rivers would not historically be meandering or have a sediment and discharge regime that would not suit meandering channels (Kondolf, 2006) and could quickly become washed out. In the UK, early projects were often opportunistic and small scale, with limited impact (Wharton and Gilvear, 2010; Gilvear et al., 2011). Gilvear et al. (2013) presented a conceptual framework and methodology to help optimise catchment-scale river rehabilitation projects. The approach focussed on providing ecosystem services at the river network scale and explored the linkages between different rehabilitation measures, fluvial processes and long-term ecosystem services. The potential of different restoration projects could be scored using the method proposed in the paper. Gurnell et al. (2016) proposed a multi-scale hierarchical framework based on a process-based understanding of geomorphological processes to deliver sustainable management practices. The REFORM framework was developed for the European context, with nested spatial units starting at the catchment scale as the largest spatial scale, down to geomorphic units and finer scales.

A concept has been developed known as the “erodible river corridor” approach (Piegay et al., 2005) or “freedom space for rivers” (Biron et al., 2014), which propose creating space for rivers to behave naturally within a certain planned zone. The approaches use a combination of flood modelling and historical mapping to estimate the area required by a river over planning timescales (30-50 years) to be able to behave naturally. Appropriate management and planning strategies can then be implemented within this area, allowing the river to perform economic and ecosystem services. An understanding of how the river planforms change is important to help protect engineering structures and to help understand the diversity of habitats on meandering channels (Gilvear et al., 2000).

2.6. Summary

From this review, it is apparent that the evolution and behaviour of meandering channels is a complex phenomenon, combining many different fluvial, sediment transport and biological processes. There are numerous factors affecting the rates and distribution of channel planform migration, which are still not fully understood. Approaches to investigate fluvial geomorphology and river channel change have developed over the last 60 years, since the seminal paper by Leopold and Wolman (1957). An understanding of meandering rivers as dynamic and unstable systems developed during the 1970s and 1980s with papers by Brice (1974), Hickin (1974) and Hooke and Harvey (1983) recognising a pattern of change in river planform and attempting to develop conceptual models of the behaviour. To fully investigate and understand the behaviour of meandering channels, a long-term approach to measuring channel change is required.

The prediction of the location and rates of migration rates remains a difficult task, especially at the scale most useful for river managers – catchment scale. There are numerous computer models available, which attempt to predict future channel behaviour. The complexity can range from one-dimensional models with simple relationship between channel curvature and migration rate applied at reach scale, to three-dimensional models, which combine hydraulic and sediment transport equations, but are only applied at a bend scale.

This thesis will apply the conceptual models described in the literature review to rivers in the United Kingdom. In this thesis, a long-term data source – historical maps - will be used and a method developed to semi-automatically measure the rates and location of migration of individual bends in three rural catchments in the United Kingdom in Chapter 5.

Using the bends measured in Chapter 5, the evolution of the meandering river channels will be analysed in Chapter 6 and compared to the conceptual models developed to understand meander behaviour. A novel method of measuring the curvature profile of individual bends will be used to investigate the evolution of individual bends. In the Chapter 7, a predictive model will be developed using the boosted regression tree approach and evaluated on channel changes between the 1970s and 2010s. This will be the first use of a machine learning approach to try and predict the location and rates of migration for individual river bends.

3. Study Areas and Data Collection

3.1. Introduction

This chapter introduces the three river catchments used in this study, along with details on the study sites used for the detailed investigation in this thesis. The physical characteristics of the catchments will be discussed, alongside the dominant land use and any human intervention affecting the river channel. The catchments were chosen as they have shown measurable change during the last 150 years, the period available for historic mapping. The most active sections were chosen so that as much of the evolution of the river bends was captured as possible in the available timescales. The following section will discuss

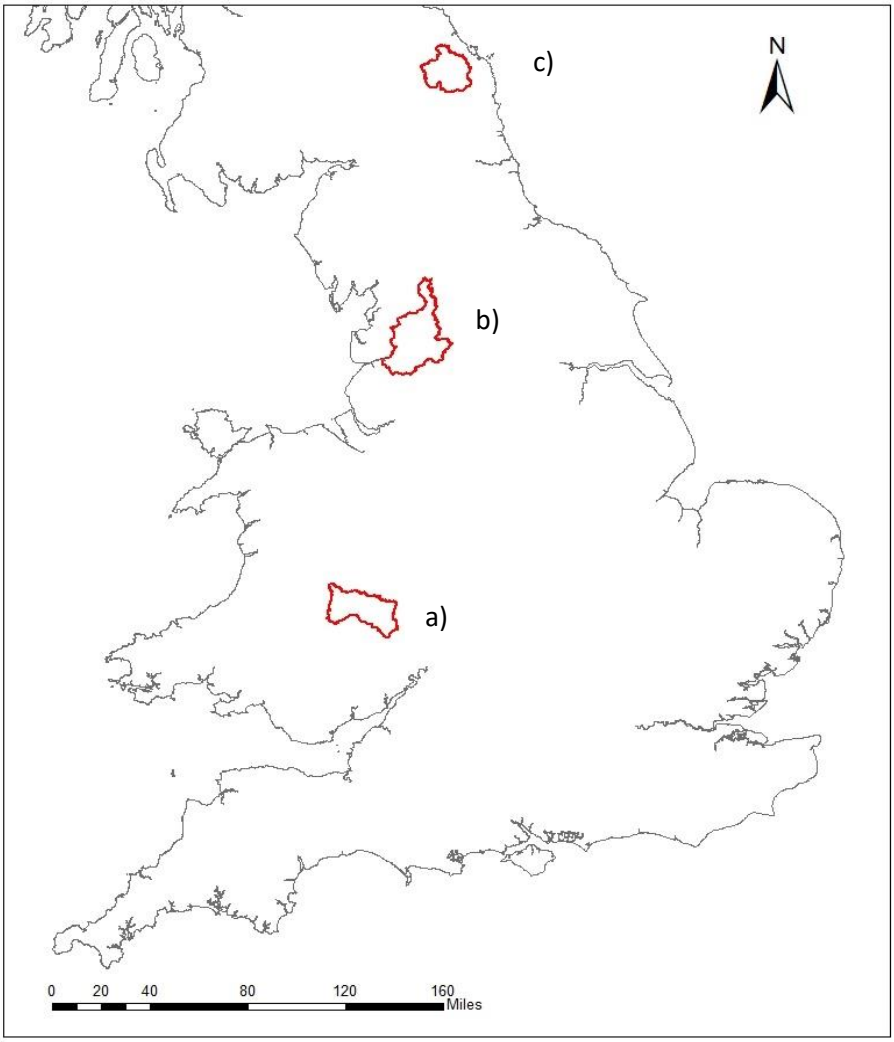

Figure 3.1. Location of the three catchments within the United Kingdom. a) River Lugg; b) River Ribble; c) River Till

how the main datasets were generated for this study, using historic Ordnance Survey maps and aerial photographs. The historic maps were used to provide the complete spatial picture for the longest time possible, allowing the full long-term behaviour of the channels to be investigated.

3.2. Study Catchments

The three river catchments used in this study were the River Lugg, River Till and River Ribble catchments. These are three medium size river catchments in United Kingdom (1077km^2, 950km^2 and 1351km^2 respectively). The main land use in each catchment was grassland (56.1%, 50.0% and 71.1% respectively), followed by arable/horticultural for the River Lugg and River Till catchment and woodland in the River Ribble catchment. The total urbanisation in each catchment was low (1.9%, 1.0% and 6.8% respectively). The rivers in the River Lugg and River Till catchments were used in the first two chapters to explore the evolutionary behaviour of individual meander bends, including the differences in rates of migration and the relationship between channel curvature and migration rate. Rivers from the River Ribble catchment were included in the final chapter, "Multivariate modelling of riverbank erosion rates using Boosted Regression Trees", to include different types of river The reaches included in the thesis are summarised in Table 3.1 and Table 3.2 including the number of bends in the earliest dataset and the dates for each study.

Table 3.1. The number of bends for each reach studied in chapters 4 and 5 to explore the relationship between channel curvature and migration rate

Catchment	River	Reach	Number of bends in earliest dataset	Periods studied
Lugg	Lugg	1	47	1889-1903, 1903-1928, 1928-1963, 1963-1975, 1975-2012
Lugg	Lugg	2	38	1886-1903, 1903-1928, 1928-1963, 1963-1976, 1976-2012
Lugg	Lugg	3	42	1886-1903, 1903-1963, 1963-1975, 1975-2012
Lugg	Lugg	4	31	1886-1903, 1903-1928, 1928-1963, 1963-1974, 1974-2012
Lugg	Lugg	5	24	1886-1903, 1903-1928, 1928-1963, 1963-1973, 1973-2012
Lugg	Arrow	1	48	1886-1904, 1904-1928, 1928-1964, 1964-1974, 1974-2012
Lugg	Arrow	2	52	1886-1904, 1904-1928, 1928-1964, 1964-1971, 1971-2013
Lugg	Arrow	3	38	1886-1904, 1904-1928, 1928-1964, 1964-1971, 1971-2014
Till	Till	3	88	1866-1897, 1897-1924, 1924-1957, 1957-1970, 1970-2012
Till	Glen	1	57	1866-1897, 1897-1924, 1924-1957, 1957-1965, 1965-2013

Table 3.2. The additional reaches used to create the dataset for the machine learning approach used in Chapter 6

Catchment	River	Reach	Number of bends in earliest dataset	Periods studied
Ribble	Calder	1	18	1970-2012
Ribble	Holden Beck	1	23	1970-2012
Ribble	Loud	1	120	1970-2012
Ribble	Skirden Beck	1	18	1970-2012
Till	Till	1	34	1970-2012
Till	Till	2	123	1970-2012

3.2.1. River Lugg and River Arrow

The River Lugg catchment is located in the west of the England, on the border between England and Wales (Figure 1). The main River Lugg channel and major tributary, the River Arrow were used for this study. The sections of both rivers used are highlighted in Figure 1. All the sections were located upstream of the confluence between the River Arrow and the River Lugg. Further downstream of the confluence the River Lugg was stable during the last 150 years due to a combination of low slope, channel confinement and human intervention. The reaches used in Chapters 4 and 5 to investigate the dynamics of meandering rivers focused on the most active sections of the river, while the sections used to develop the statistically based modelling in Chapter 6 used the sections in the previous chapters and more stable bends upstream and downstream, based on the availability of historic aerial photographs.

The sources of the River Lugg and River Arrow are found in the west of the catchment, before travelling in south-easterly direction to the confluence with the River Wye at Mordiford. The maximum elevation in the catchment is 659.7m before falling to 46.7m at the confluence with the River Wye. The mean discharge at the Butt's Bridge gauge on the River Lugg (see Figure 1) is 5.88m^3s^{-1} and the mean annual flood is 45.51 m^3s^{-1}. The gauging station is located just before the confluence of the River Arrow. The mean discharge at Titley Mill on the River Arrow is 2.36m^3s^{-1} and the mean annual flood is 27.25 m^3s^{-1}. This gauge is located upstream of the study reaches on the River Arrow. The long-term mean annual precipitation ranged from 1041mm in the west of the catchment to 847mm in the south east of the catchment. The geology of the catchment is Silurian sandstones in the headwaters of the catchment and Old Red Sandstone in the lower sections of the catchment. The sandstones moderate the high flows in the catchment, with a base flow index of 0.66 (Lazar

et al., 2010) indicating the dominance of groundwater. Wade et al. (2007) and Lazar et al. (2010) chose the River Lugg for a study on phosphorus routing due to the high concentrations found in the river channel, especially in the lower part of the catchment.

The reaches on the River Lugg have a range of glacial histories that may affect the meander channel dynamics. Reaches 1 and 2 are located in a former glacial lake basin with a high clay content found on the floodplain, while reach 3 is located in a narrow glacial spillway that restricts confines the river and restricts the ability of the river to laterally migrate. Reaches 4 and 5 are located outside of the limit of the last glacial maximum and the floodplain becomes much wider for these reaches giving more space for the river to laterally migrate. Reach 5 was designated as a geomorphological Site of Special Scientific Interest due to the classical meander evolution. However, there was substantial human modification of this section of the river during the construction of the flood alleviation scheme for Leominster in the 1960s and 1970s. There was channel widening and realignment, flood embankment and weir construction, and dredging.

The River Arrow appears to have had less direct human intervention on the channels themselves, especially for reach 1 and 2. At reach 3 the River Arrow splits into the Little Arrow and the main River Arrow channel, and the mean channel width is reduced at this point. All of the reaches are located on a wide floodplain.

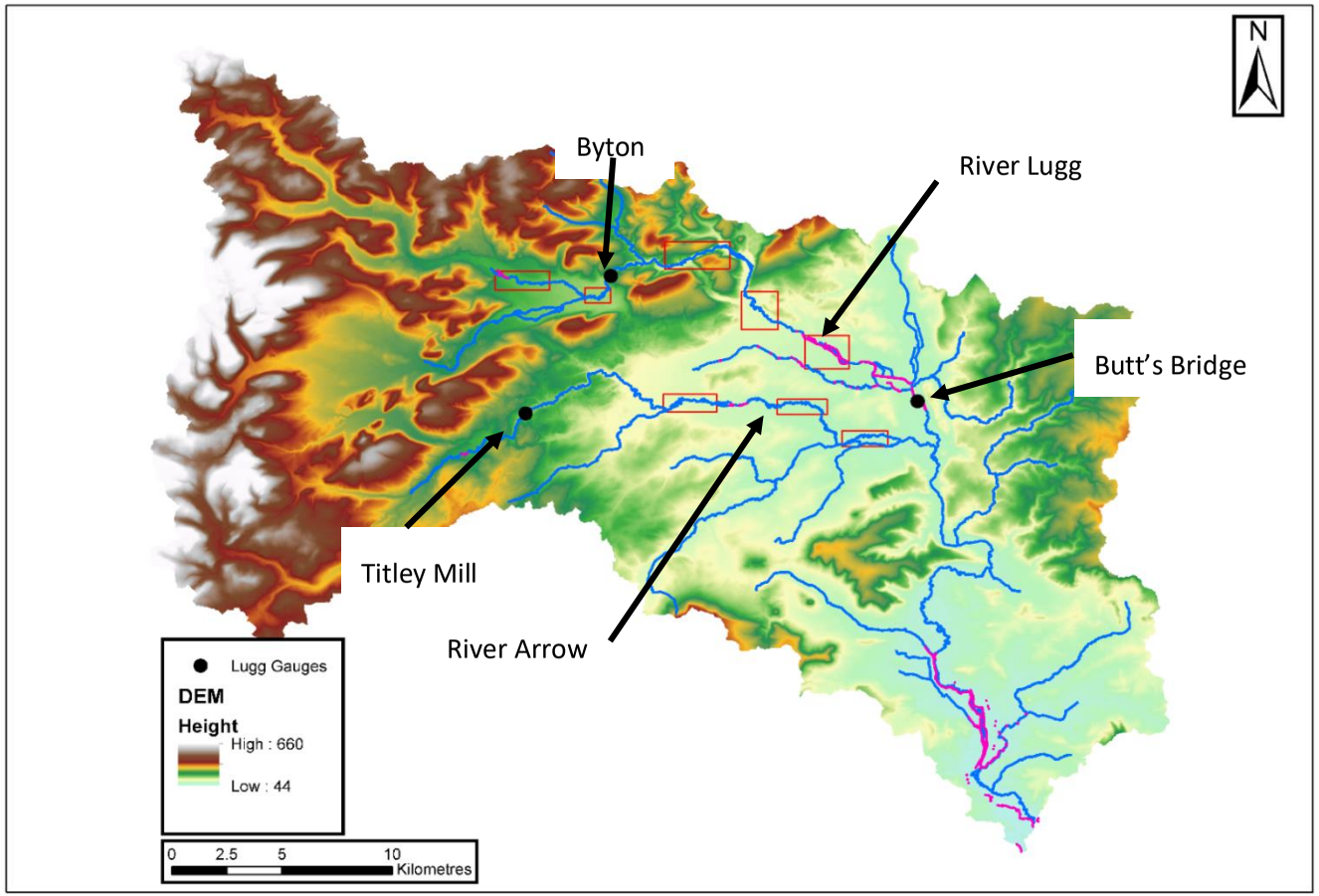

Figure 3.2. Location of the River Lugg and River Arrow study reaches. The pink lines represent the sections of the river channel with artificial flood defences. Downstream of the flow gauge at Butt's Bridge the channel was stable during the historic period. The reaches, highlighted in red, were numbered sequentially downstream.

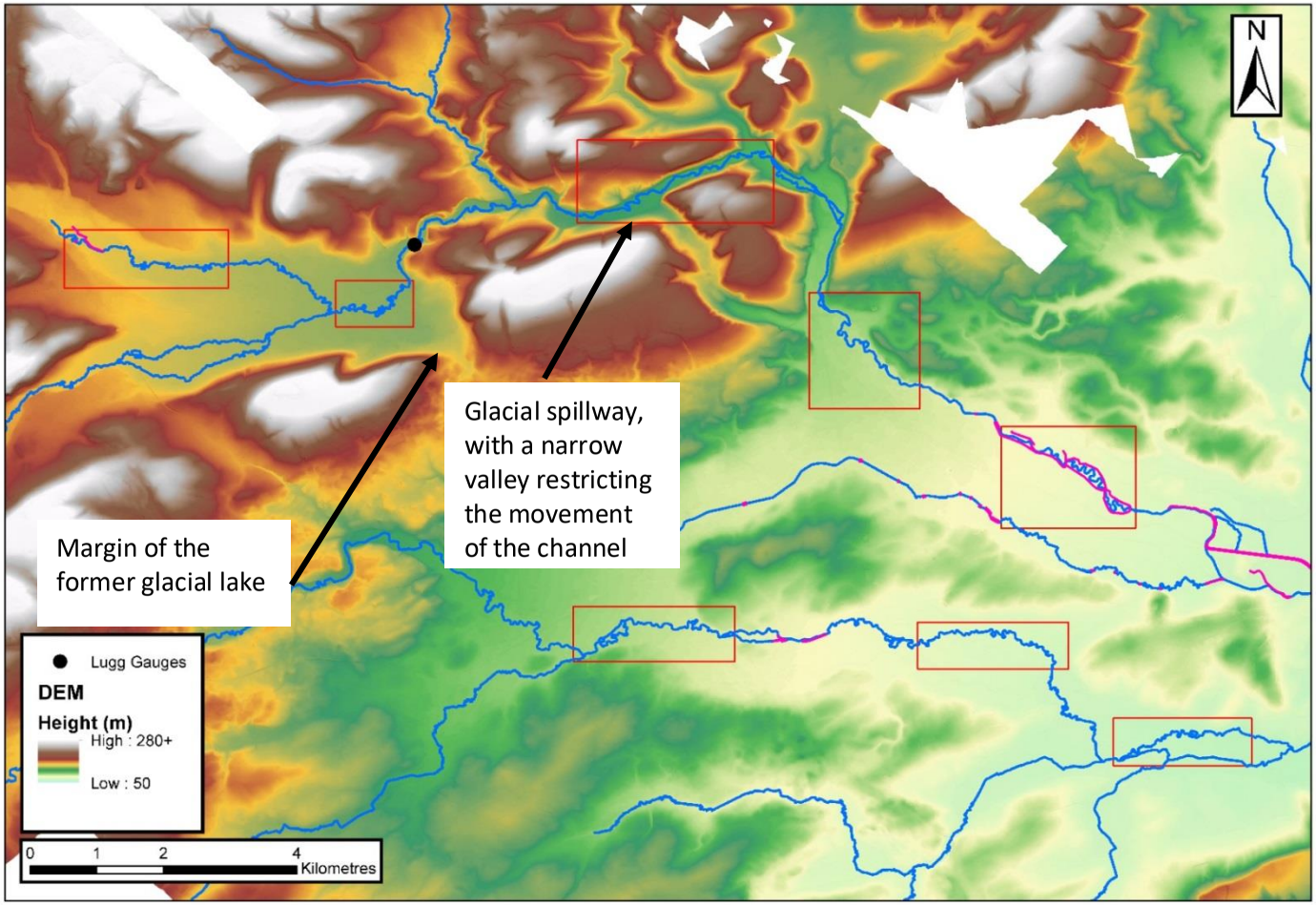

Figure 3.3. There is a strong glacial legacy affecting Reach 1-3 on the River Lugg. Reaches 1 and 2 are located in former glacial lake basin, while Reach 3 is located in a spillway and has a much narrower floodplain compared to the other reaches

3.2.2. River Till and River Glen

The River Till catchment is located in the north-east of England and is a major tributary of the River Tweed. The River Till and the lower section of its main tributary, the River Glen. The source of the river is located in the Cheviot Hills and it travels in a north-west direction until meeting the River Tweed. The catchment elevation ranges from 814m in the Cheviot Hills to 15m at the tributary with the River Tweed. The selected reaches are highlighted in Figure 2. The lower sections of the River Till and River Glen were used in Chapters 4 and 5 where the floodplain was wide and continuous sections of the river were freely laterally migrate. Two reaches further upstream on the River Till were used for Chapter 6, where erosion tended to be restricted to individual bends. Three discharge gauges are available in the catchment at Etal and Heaton Mill on the River Till and Kirknewton on the River Glen. The mean discharge at Etal is 8.48m^3s^{-1} and 2.93 m^3s^{-1} at Kirknewton. The mean annual flood is 82.90m^3s^{-1} at Etal and 44.45m^3s^{-1} at Kirknewton. There is no mean discharge data available at Heaton Mill, only peak flow data is available from the National River Flow Archive (CEH). The region was extensively modified by glacial action and meltwater dynamics during Marine Isotope Stage 2 with large deposits of glacial till found across the catchment (Passmore et al., 2006). There are substantial deposits of alluvium close to the river channel, especially in the Milfield Basin, where the River Glen joins the River Till. The region has been noted internationally for its archaeological record, including a henge complex located on the extensive river terraces (Passmore et al., 2006).

There has been a history of human activity within the catchment, with extensive gravel mining occurring in the upper part of the catchment. In the lower catchment, large parts of the floodplain have had artificial levees constructed. The data of construction is not known but are present on the original Ordnance Survey maps from the 1860s. These levees confine the river channel and prevent the river from growing across the floodplain. The flood defences have led to the loss of wetland habitat (Northumberland Biodiversity Partnership, 2007).

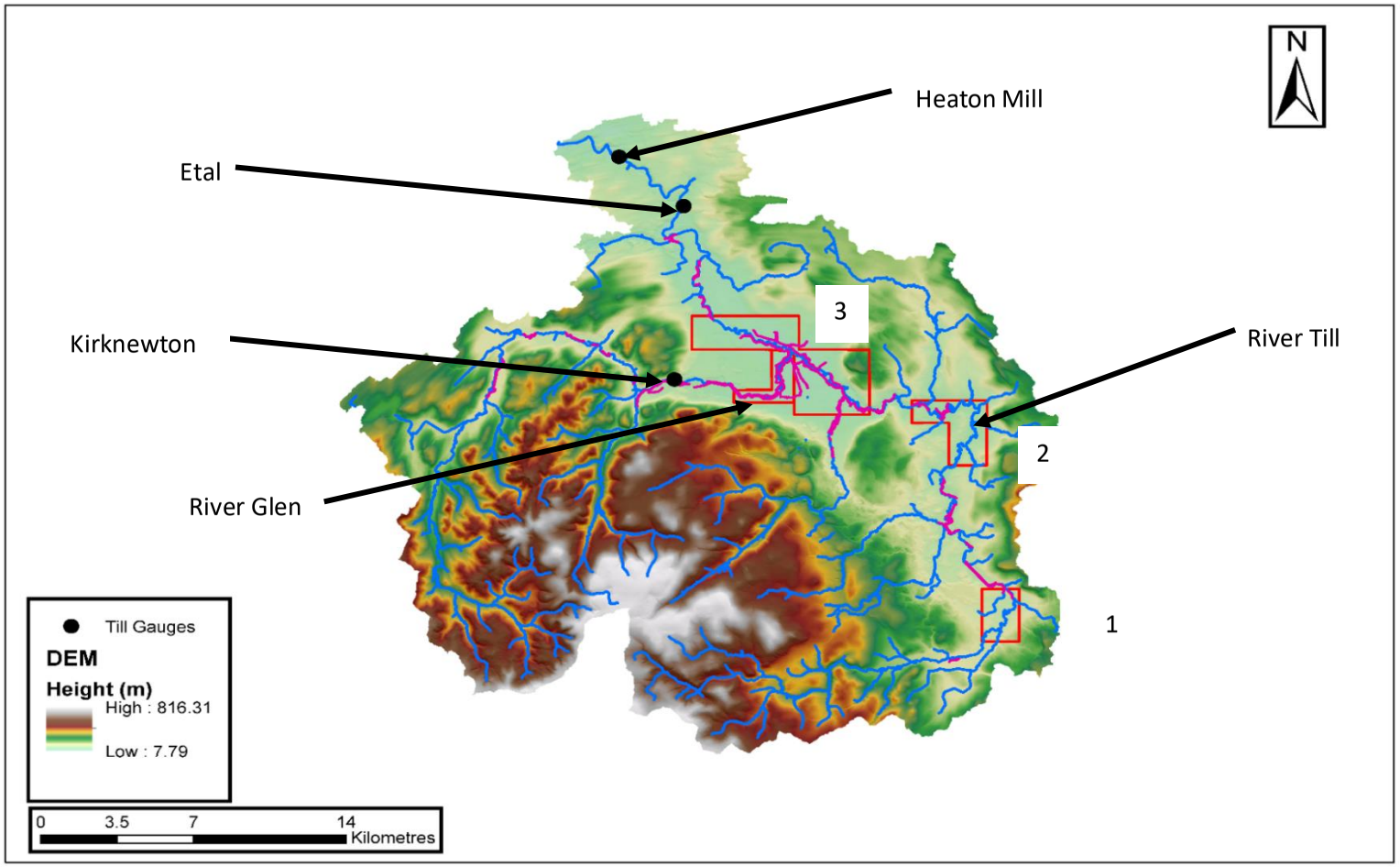

Figure 3.4. Location of the River Till and Glen study reaches. The pink lines indicate the flood defences located in the catchment, which were present from the beginning of the study period. The rivers were still active within the flood defences.

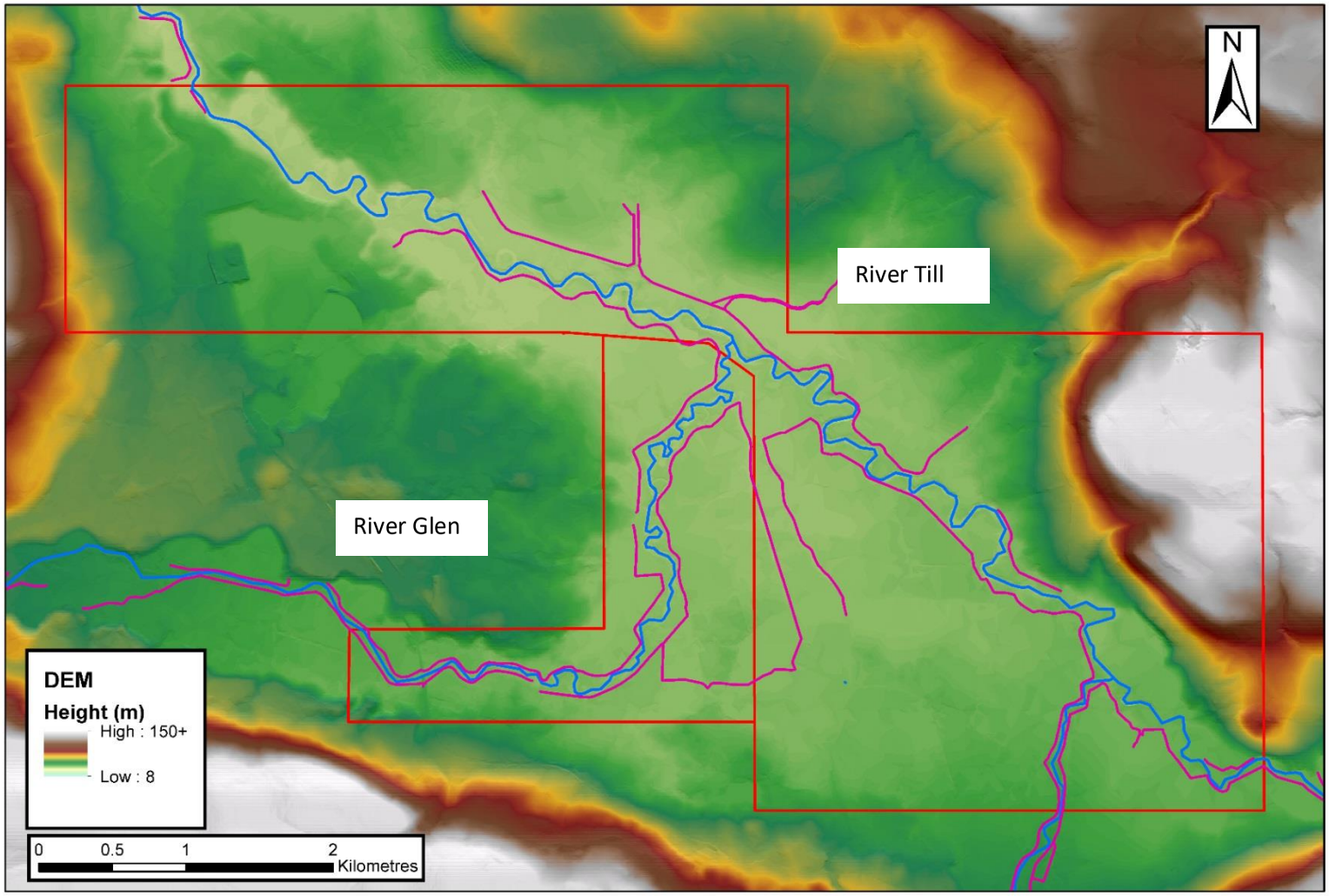

Figure 3.5. Detailed view of the confluence between the River Till and the River Glen, used in Chapter 4 and Chapter 5

3.2.3. River Ribble Catchment

The River Ribble is the largest catchment in Lancashire, with a catchment area of 1351km^2 to the tidal limit at Preston and a further tributary, the River Douglas, joining the catchment in the estuary. The main River Ribble channel appeared to the stable during the historic map period, often confined against the edge of the valley. The lower section of the River Calder, upstream from Whalley was included in the study as it was actively eroding throughout the study period and was included in Chapter 6. There is a flow gauge available at Whalley on the River Calder and has a mean daily discharge of 8.7m^{3}s^{-1}. Three smaller catchments, with issues of excess sedimentation and bank erosion were identified in partnership with the River Ribble Trust and included in the study. The River Loud is a tributary of the River Hodder and travels in a north east direction and has a catchment area of 55km^2 at the end of the study reach. Skirden Beck and Holden Beck are two small, gravel-bed upstream catchments, which were highly active during the study period. Thompson (1986) examined the surface flow patterns and bed morphology of Skirden Beck and investigated the changes to an individual bend between 1892 and 1979.

There are three main tributaries upstream of Preston, the River Calder, the River Hodder and the River Darwen. The source of the River Ribble is found in the western Yorkshire Dales; the River Hodder drains from the Forest of Bowland, and the River Calder starts in the west Pennine Moors. The drainage network is a reflection of the deglaciation at the end of the last glaciation. It is thought that extensive erosion lead to the capture of the

Figure 3.6. Terraces within the River Ribble catchment can act as a large supply of sediment when rivers are actively eroding at the base of the slope. This picture was taken on Holden Beck, and the location is marked on **Error! Reference source not found.**

Hodder and Ribble headwaters driven by glacial meltwaters (Harvey, 1985, 1997), with extensive terracing identified in the catchment (Foster et al., 2009; Chiverrell et al., 2010). The geology of the Ribble catchment is mainly limestone, shale and grit from the carboniferous period. Deforestation during the late Holocene caused an increase in the sediment supply from hillslopes, and combined with an increase in the instability in the riverbanks and floodplains led to formation of several different terraces in the Ribble catchment (Foster et al., 2009; Chiverrell et al., 2010). A terrace is located in between Skirden Beck and Holden Beck and can be a significant source of sediment to the river channel (see Figure 3.6).

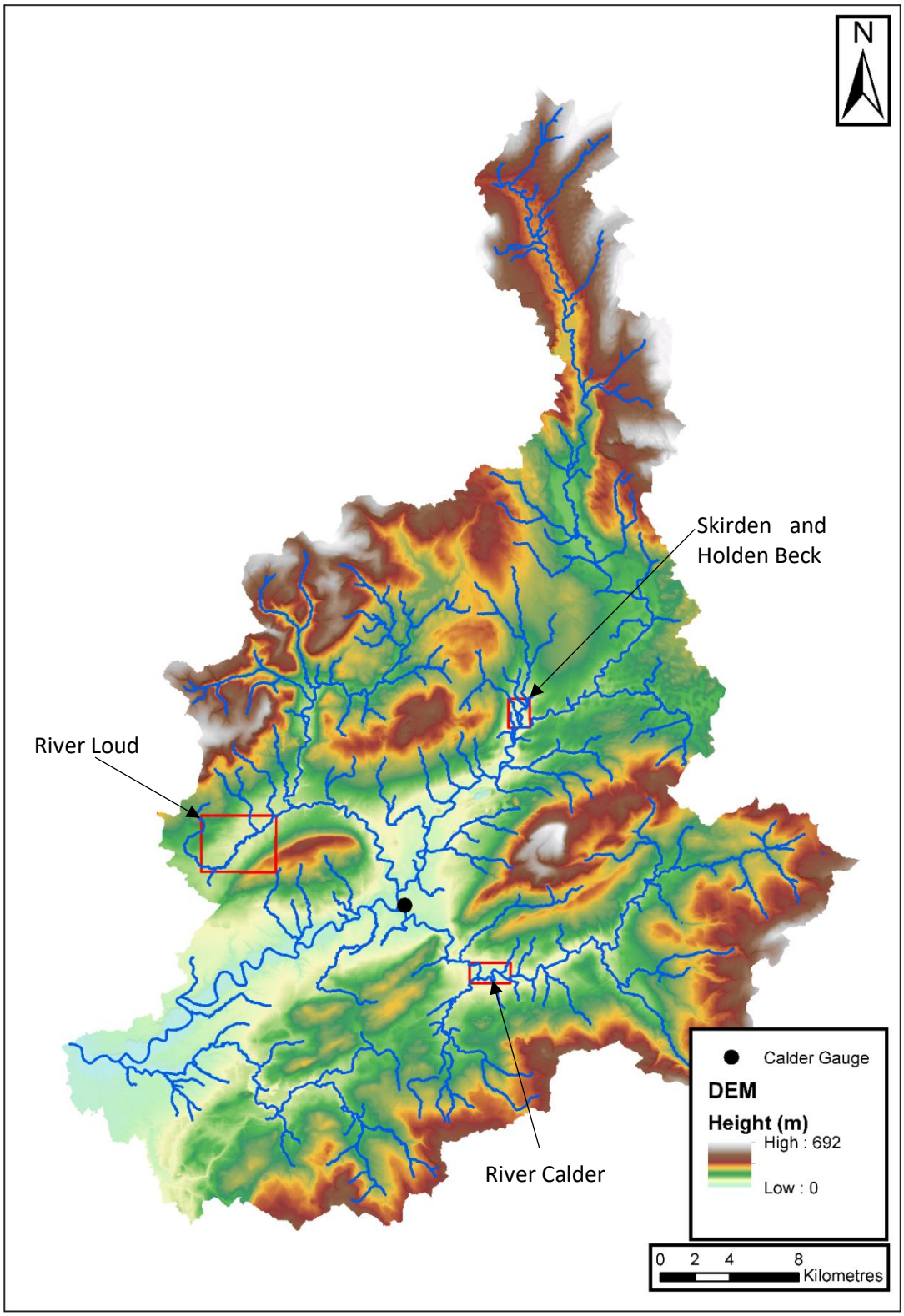

Figure 3.7. Location of the study reaches in the River Ribble catchment. Large areas of the catchment were stable during the study period and it was not possible identify eroding banks from the historical maps.

3.3. Data Sources and Collection

The aim of this thesis was to develop an understanding of dynamics of meandering river channels and a long-term approach is required to fully capture the evolution of channels. The main data source for this study was historic Ordnance Survey maps. The data is available at Digimap (Edina, 2019) and is already geo-rectified, meaning that ground control points are not required. The first edition county series Ordnance Survey maps were initially started in the 1870s using accurate trigonometrical survey (Harley, 1965) and have been updated regularly since, with a conversion to national grid coordinate system in the 1970s. The spatial coverage of the revisions varied for different parts of the country, but widespread revisions occurred in the 1900s, 1950s and 1970s. The Ordnance Survey maintains revisions and the most recent map is also available from Digimap. The available maps for each river are shown in Table 4.1, along with the scale used in the study. Where possible the highest resolution maps were used to define the channel bank lines, which was usually the 1:2500 scale maps. The accuracy of Ordnance Survey mapping is generally thought to be good with less than 1m error in the location of fixed features in the floodplain (Harley, 1965; Hooke, 1980). However, there are some sources of uncertainty when using maps to define the channel position. Normal winter flow is usually used to define the channel position, and this required some interpretation from the surveyor, especially on the inner bank of river bends or where an edge is not well defined. Another source of uncertainty was caused by the scale differences between the majority of the maps at 1:2500 scale and the 1:10560 maps used to map the 1960s river position. These maps are at a lower resolution and increase the uncertainty of the position of the channel bank line. The channel centreline is commonly used to define the channel position and helps to reduce the uncertainty by representing the average of two lines rather than using two single lines to represent the channel position.

The channel bank lines were digitised for each map date in ArcMap (ESRI, 2019) with a maximum of 20m between individual points, and a much higher concentration around bends. Any mid-channel bars that appeared on the maps were also digitised. A channel centreline was produced by collapsing the two bank lines to a single line using the Collapse Dual Lines to Centreline in the Cartography toolbox. Errors in the tool were created when the channel planform was complex and were corrected manually by redrawing the centreline between the channel banks. The centreline was then smoothed using the Smooth Line tool using the PAEK smoothing algorithm and the smoothing tolerance of 25m in the Cartography Toolbox to remove small perturbations. The final step in the initial data processing was to

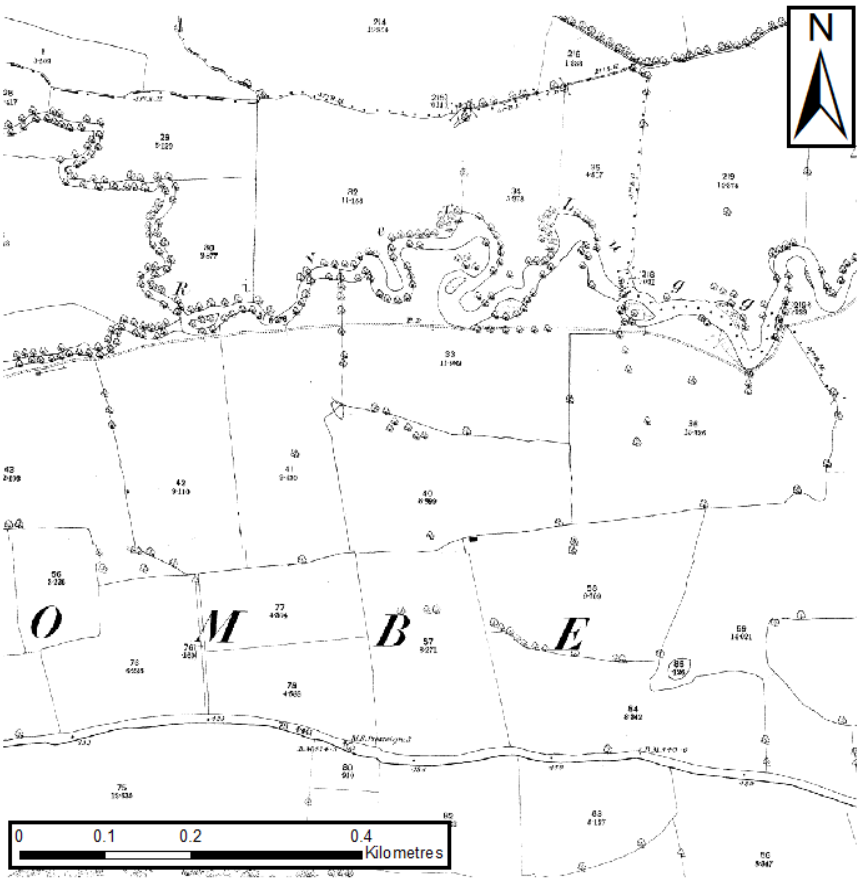

Figure 3.8. An example of the historic Ordnance Survey maps from 1886 used for the study. This part of the channel is from the River Lugg, Reach 2. The banklines were digitised at a maximum of 10m intervals, and much less through complex parts of the channel.

generate points at 10m intervals along the channel centreline, and a new line is created from the points so that the vertexes are equally spaced along the centreline for analysis in subsequent chapters.

The second main data source used in this thesis was obtained from aerial photographs from the 1970s and 2010s. The aerial photographs from the most recent decade were available from Digimap and were provided geo-rectified. The 1970s aerial photographs were obtained from the Historic England archive in Swindon. Polygons were created of the study reaches and the aerial photographs in this area were made available by Historic England. During visits to the facilities in Swindon, the aerial photographs with the river present were identified and checked for quality. Due to cost and quality considerations, it was decided to focus on the 1970s aerial photographs which had the best spatial coverage and highest quality of the historic aerial photographs. High quality scans were obtained of the photographs for the study reaches. The photographs were geo-rectified in ArcMap with

a minimum of ten ground control points per photograph. Fixed structures, such as bridges and buildings were used to reference the photograph based on the 2010s photographs.

A 33m buffer was created around the channels from the 1970s and 2010s, and polygons were drawn around any vegetation within the buffer. A 33m buffer will capture the capture any woody vegetation that is potentially influencing the failure plane of the riverbank. It was not possible to distinguish between different types of vegetation as the 1970s photographs were black and white, and the 2010s photographs had thick vegetation

Figure 3.9. The historic aerial photograph for Reach 2 on the River Lugg. The photograph was geo-rectified using fixed ground control points and a 1st order polynomial transformation. Vegetation in the 33m buffer zone was manually digitised in ArcMap 10.6.

coverage and it was not possible to identify different species of vegetation. The total vegetation coverage in the riparian zone was calculated for both the 1970s and 2010s. The proportion of each bend with vegetation coverage on the outer bank was also calculated by classifying the sections of the bend as either vegetated or unvegetated based on the absence or presence of a vegetation polygon. For the River Lugg and River Till catchments the entire record of historic Ordnance Survey maps were used. For the River Lugg catchment, the six

dates were available for each reach: 1886-1889, 1903-1904, 1928, 1963-1964, 1971-1976 and 2012. In the River Till catchment the map dates were: 1866, 1897, 1924, 1957, 1965-1970 and 2012. There were some differences in publishing date as the updates were completed at different times for the different reaches. For the River Ribble catchment, only the 1970 and 2012 dates were used in the machine learning approach. The aerial photographs were all taken from Ordnance Survey flyovers in the 1970s and 2012-2013 period.

4. Bend scale analysis of two actively meandering rivers in the United Kingdom: The River Lugg and River Till.

4.1. Introduction

Meandering channels have long held a fascination for researchers from many different backgrounds, including fluvial geomorphology, river engineering and fluid mechanics. Meandering channels can be mobile, migrating both downstream and across the floodplain and contributing to landscape change within the floodplain. Although original work focused on the regularity and stability of meanders (Langbein and Leopold, 1966), attention began to shift to the inherent instability of complexity that many meander forms take (Brice, 1974; Hickin, 1974; Hooke and Harvey, 1983; Hooke, 1984). The rates of movement can vary across and between different river systems and between different sections along a single river. While channel bank erosion and migration are important processes that help maintain the conveyance capacity of channels (Lane et al., 2006) and help promote biodiversity in riparian zones (Salo et al., 1986), high rates of channel movement can cause problems for infrastructure close to the river and excess bank erosion can be a major source of sediment in rivers (Henshaw et al., 2012). Therefore, understanding the nature of meander morphology and the historic rates of riverbank erosion is important not just from an academic viewpoint, but also in practical terms for stakeholders managing within the floodplain.

The study of meanders over long periods has allowed for several conceptual models to be developed for the evolution of meander bends. These models show that active meander bends can develop from simple forms into more complex, compound forms autogenically, i.e. without any changes of input, and simplify through neck or chute cutoffs (Brice, 1974; Hickin, 1974; Hooke and Harvey, 1983; Hooke, 1995). Brice (1974) studied the evolution of meanders on ten alluvial streams in the United States using aerial photographs and suggested that four different meander forms can be identified: simple symmetrical, compound symmetrical, simple asymmetric and compound asymmetric. Hickin (1974) also used aerial photographs to identify ridge and swale patterns in floodplains, which were then used to plot erosion pathlines for the meander bends. Hickin identified a critical value of channel curvature to width ratio of 2.11, at which channel curvature strongly controls the subsequent meander evolution. Hickin proposed a non-linear increase in migration rate as

curvature increases and demonstrated the results for Canadian rivers (Nanson and Hickin, 1983). This relationship was further confirmed for rivers in the UK (Hooke, 1997, 2003) and USA (Hudson and Kesel, 2000). Hooke (1995) proposed a qualitative model for compound meander bend development from initiation to cutoff based on work by Hooke and Harvey (1983) and Hooke and Redmond (1992). In this model meander bends or loops would develop from small perturbations within a channel, with a riffle forming just upstream of a depositional bar, and erosion occurring on the opposite side. This initially small amount of erosion would develop as secondary flows forced the fastest flowing water against the outside bank leading to increased migration downstream and a deep pool developing close to the outer bank. The fastest migrating bends would develop a tight apex and start growing across the floodplain. After growing rapidly across the floodplain, these bends would start to show double-heading or compound growth and a new riffle would form between the two lobes. The two lobes could either develop into new separate bends if given enough space or cutoff if they encounter channels upstream or downstream.

The purpose of this chapter is to investigate the channel changes on two active rivers in the United Kingdom over a period of 150 years using historic Ordnance Survey maps. The chapter will investigate the patterns and rates of changes at both individual bend scale and reach scale. This chapter will also investigate the relationship between channel sinuosity and cutoff events for a total of 52 cutoffs that occurred during the study period in the two catchments. There are major questions about the nature and patterns of meander evolution, and reasons for meanders migrating at different rates. The two catchments in this section of the study provide the opportunity to study active rivers in the United Kingdom, with the River Lugg catchment mainly able to migrate freely across the floodplain and the River Till catchment restricted by human intervention, but still active within the confined valley.

4.2. Study Areas

Two catchments with active bank erosion were selected in England and Wales, which had been previously identified by Hooke and Redmond (1989). They are both mainly agricultural catchments with less than 2% urbanisation and limited urban development during the study period. There has also been no major river impoundment in the form of dams or reservoirs during the study period so impoundment will not have impact on the flow in the river.

4.2.1. River Lugg

The River Lugg is a major tributary of the River Wye, with a total catchment area of 1077km^2. It is characterised by both upland and lowland areas. The major land uses in the catchment are agriculture, with cattle and sheep production dominating, and woodland areas (Lazar et al., 2010). Sandstones are the dominant geology of the catchment, with Silurian sandstones in the headwaters of the catchment and Old Red Sandstone and extensive gravel deposits in the lower reaches. The geology helps to moderate the peak flows in the Lugg catchment, with a base flow index of 0.66 (Wade et al., 2007). The precipitation in the catchment varies, with the highest rainfall in the west of the catchment at Butts Bridge (1048mm per year) and the lowest average annual rainfall in the south-east of the catchment near the confluence with the River Wye (850mm per year). The waterbody condition of the River Lugg was considered moderate to poor under the Water Framework Directive (EU, 2000) due to poor fish status and excessive sedimentation (Lazar et al., 2010; Jacobs, 2015). The River Lugg catchment also contains a major tributary, the River Arrow that is included in this study. Reaches were selected from within the catchments that show the highest amounts of activity during the study period, which are located in the middle sections of the river. The

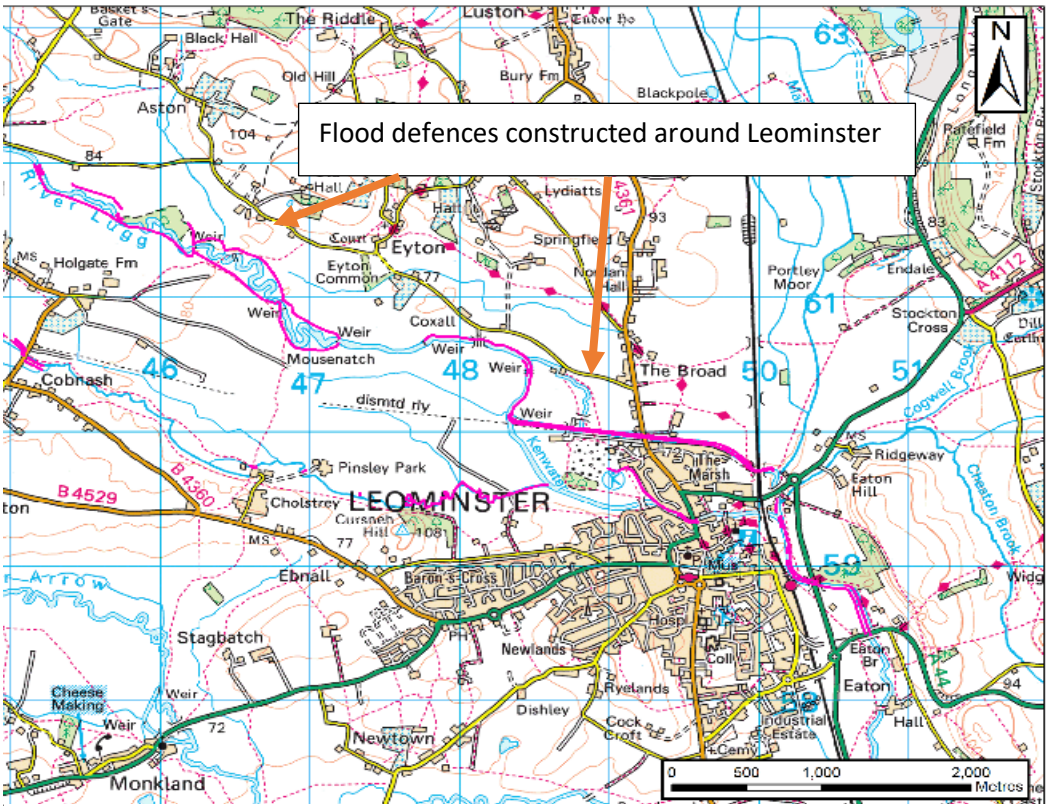

Figure 4.1. Flood defences constructed in the 1970s to protect Leominster

upstream catchment areas are 263km^2 and 279km^2 respectively. The average channel width for the River Lugg reaches is 12.8m and 11.6m for the River Arrow. Although the selection of these reaches will bias the results towards the most dynamic sections, these can provide the best information for how meanders evolve and behave over long periods of time (Hooke, 2007b). Accurate records are not available to record the full evolution of slowly migrating rivers, and therefore the most active sections provide the most information of the temporal sequences. The most active reaches are also most likely to impact on the floodplain and are of interest to stakeholders and managers working in the riparian zone. The total length of channel studied in the Lugg catchment is 27.9km across eight reaches. Most of the channel is free from human intervention in the form of flood defences or bank reinforcement with the exception of the Reach 5 on the River Lugg. A flood alleviation scheme was completed in the 1970s to protect Leominster. This involved channel widening, flood embankment construction and weir construction. The reach was still included within the results as there was no intervention for the majority of the study period and it offers the opportunity to study the impacts of the flood defences on the activity of the river.

4.2.2. River Till

The River Till is located in Northumbria and drains northwards from the Cheviot Hills to the River Tweed. The total catchment area to the confluence with the River Tweed is 671km^2. The River Glen is a major tributary to the River Till and the lower sections have been included within this study. The total channel length studied is 18.9km, and the average channel widths are 17.1m for the River Till and 12.4m for the River Glen. The main land use is rural, with rough pasture and moorland in the upper catchment, and arable crops and improved pasture in the lower catchment. The landscape was modified by the retreat of the ice sheets at the end of MIS2 and is covered with glacial till. There are extensive areas of outwash sands and gravels on the valley floor and the underlying geology is mainly an igneous intrusion in the upper areas and sandstones in the lower catchment (Passmore et al., 2006). There are flood defences along multiple sections of the River Till, which appear to have been in place throughout the study period. These banks are currently maintained by the Environment Agency but there appears to be no direct reinforcement of the riverbank. The rivers are still active within the restricted floodplain and provide the opportunity to contrast the freely migrating river bends in the River Lugg catchment to bends that are constrained in their movement in the River Till.

4.3. Data and Methods

The main source of data for this analysis is historical evidence from maps. The use of historical maps to analyse planform changes over longer timescales were first used by Hooke (1977) and have become much more widespread with developments in GIS making the collection and measurement of changes much easier. This approach has been used in China (Zhou et al., 2017), Australia (Rhoads et al., 2016) and across Europe (Depret et al., 2017; Quik and Wallinga, 2018; Ziliani and Surian, 2016). For this project, historic maps were collected from an online data source (Edina Digimap, 2018) for each catchment and at all available dates. Table 4.1 shows the dates of map available for each river and the scale. The highest resolution map was selected for each available date. More recently, satellite data and aerial photographs have become more widely available but were not included in this study for a number of reasons. The rivers used in this study are relatively small on an international scale (11m-19m wide) and the channel would only be defined by one or two pixels from satellite data, making them unsuitable for these rivers. Aerial photographs provide much higher resolution imagery, however for the River Lugg catchment many of the photos have been taken during the spring or summer when vegetation has a high leaf coverage and it is impossible to determine the location of the banks. Using historic maps allows means that the banklines have been drawn consistently through time and allows for the best comparison between different dates. LiDAR data was not used in this study to ensure consistency of the definition of the bankline between the different time periods.

Channel banklines were manually digitised using ArcGIS 10.5.1 (ESRI, 2017) at a scale of 1:800 or higher and smoothed centrelines were produced for each reach and date using tools within the ArcGIS toolbox. The majority of the channels were single thread and the

Table 4.1. The different catchments and rivers within those catchments chosen for this study, with the available map dates for each area. The map scale is 1:2500 unless indicated by [1] were the scale was 1:10560

Catchment	River	Available Map Dates	Source
Lugg	Lugg	1886-1889, 1903, 1928, 1963[1], 1973-1976, 2012	County Series 1st Edition, County Series 1st Revision, County Series, 2nd Revision, National Grid 1st Imperial Edition, National Grid 1st Edition, OS Street View
	Arrow	1886, 1904, 1928, 1964, 1971-1974, 2012	
Till	Till	1866[1], 1897, 1924, 1957[1], 1970, 2012	
	Glen	1866[1]. 1897, 1924, 1957[1], 1965, 2012	

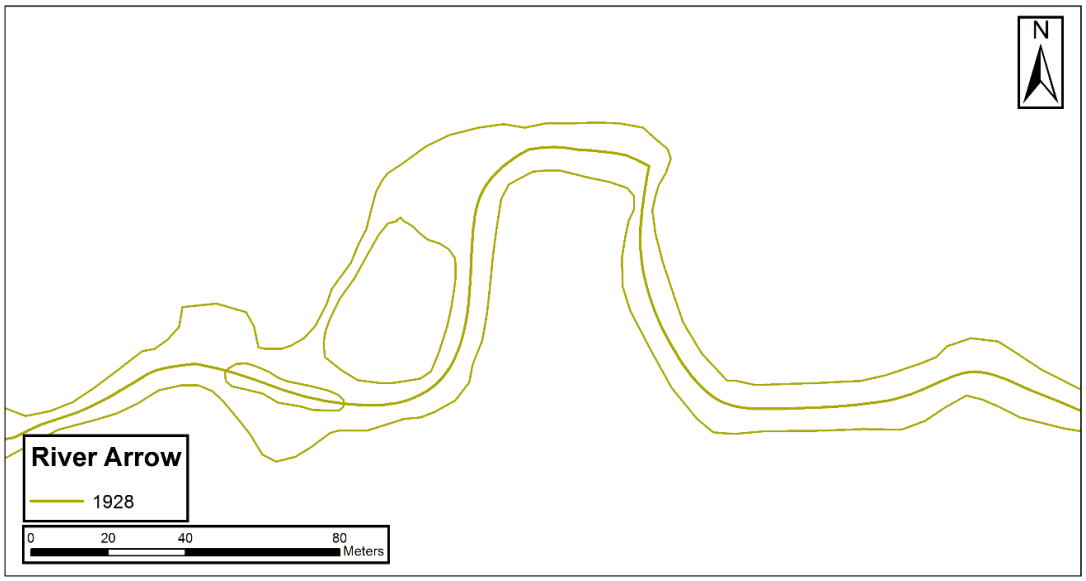

Figure 4.2. The centreline for each map date was produced by collapsing the banklines to a single line. If a mid-channel bar split the channel evenly then the centreline was drawn through the centre of the two bank lines. If one channel was larger than the other was, the larger channel was used.

centrelines were easy to produce. However, certain sections of the river channel contained multiple sections from either a middle channel bar or anabranched channels. For these sections of the channel it can be difficult to determine how best to represent the channel as a single centreline. For the purpose of this research, the centreline was placed in the channel that was dominant, i.e. at least twice the width of the other channel. If neither channel was dominant then the centreline was drawn in the middle of the two banks, regardless of the position of the mid channel bar. Once the centreline was produced it was smoothed to remove small variations in the centreline. The PAEK smoothing algorithm was used with a tolerance of 25m.

Once the centreline had been created for each reach and each date, the migration rate and channel width of meander bends was measured using the Channel Migration Toolbox (Legg et al., 2014), which measures the change between two centrelines at defined intervals. A polygon was first created between two consecutive centrelines, representing the lateral migration of the centreline and transects were automatically generated perpendicular to the initial centreline at a defined distance. The transects were edited in highly sinuous sections of the river to ensure that each transect only passed through the lateral migration polygon once. The distance between current centreline and the following centreline was then measured. The measurement was performed for each available map period, with new

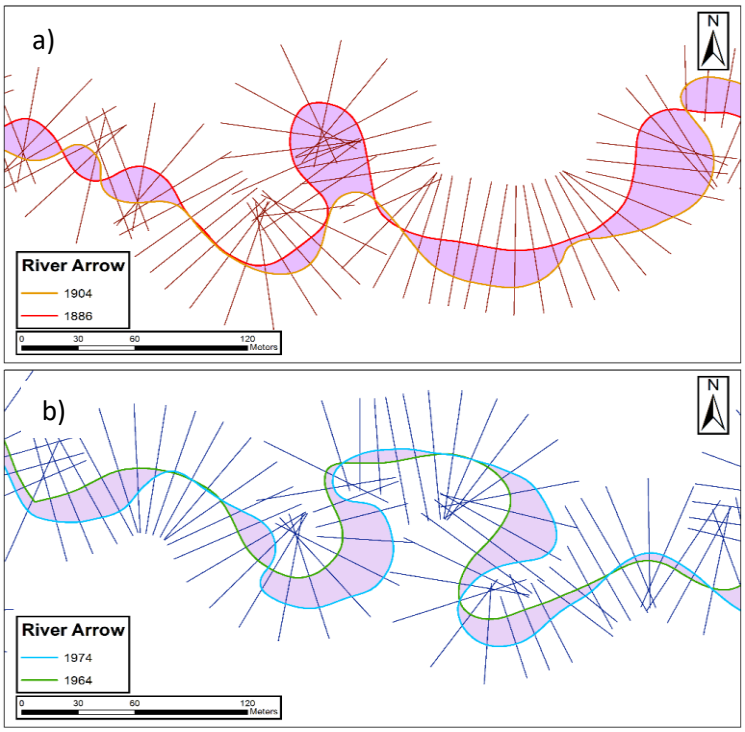

Figure 4.3. An example of the transects drawn to measure the migration between consecutive centrelines. If a cutoff occurred as in a) then the migration rate was considered to be $0ma^{-1}$. The transects were edited to ensure they only crossed through the migration polygon once, as shown in b).

transects developed for each map period. Measurements were performed every 10m, equivalent to just less than one channel width and the same distance used by Hooke and Harvey (1983) on a similar sized river. If a section of the river experienced a cutoff during the study period, the migration distance between the two channels was considered 0m as a new channel had been formed and the channel had not laterally migrated to the new position. The same procedure was used to measure the channel width using a polygon representing the channel. Each transect therefore had a migration distance and channel width measurement, along with the number of channels for sections that contained mid channel bars.

The inflection points of the centrelines were then created using the polyline disaggregation tool in the Fluvial Corridor Toolbox (Roux et al., 2013). The tool generates the points of inflection based on changes in the sign of the angle along the centreline. The inflection points were removed for small variations in angle and a minimum bend length of 30m was used as recommended by Hooke and Harvey (1983). The centreline was then split based on the location of the inflection points. A script was written in MATLAB R2016a, which places individual transects into bends based on the inflection points generated. Each

Table 4.2. Conceptual approach to group individual transects into bends. As the distance downstream of each transect and of each inflection point is known, the transects can be grouped together into bends

Transect distance downstream	Cumulative bend distance downstream	Bend number
0	0	1
10		1
20		1
30	35	1
40		2
50		2
60		2
70	72	2
80		3
90		3
100		3
110		3
120		3
130	134	3
140		4
150		4
160		4
170		4
180		4
190		4
200	200	4

measurement of channel width, channel curvature and migration rate is located at a known distance from the start of each reach. The distance of each inflection point from the start of the centreline is also known, which allows each measurement to be assigned to an individual bend. Table 4.2 shows the conceptual approach to grouping the individual transect measurements into bends. Grouping the individual transects into bends allows statistics such as mean channel width, and maximum and mean channel migration to be measured for each bend. Each bend was numbered sequentially downstream and the changes to each bend were measured through time. The bend number for each reach was recalculated for the different time periods and so the bend number is not necessarily consistent through time, especially on the more active reaches. Individual bends were tracked through time, including the change to bend number.

The overall sinuosity for each reach was measured and the changes through time were calculated. The sinuosity around cutoffs were also calculated based on the length of the channel for three bends upstream and downstream to determine whether any thresholds in channel sinuosity can be identified for these reaches and how they compare to the theoretical maximum of 3.14 proposed by Stolum (1996, 1998).

A total of 465 bends were analysed for this chapter, covering 228km across both river catchments and the map dates.

4.4. Results

4.4.1. Variations of migration rate and channel width

The data presented in this chapter allow for a thorough investigation of the rates and location of channel changes in the River Lugg and River Till catchments. As acknowledged in the methods section this study will be biased towards the most active reaches and bends, but they are perhaps of most interest to land managers and are the most useful for investigating the evolution of meanders as they are the most likely to include the full cycle of development of a bend from initiation to cutoff.

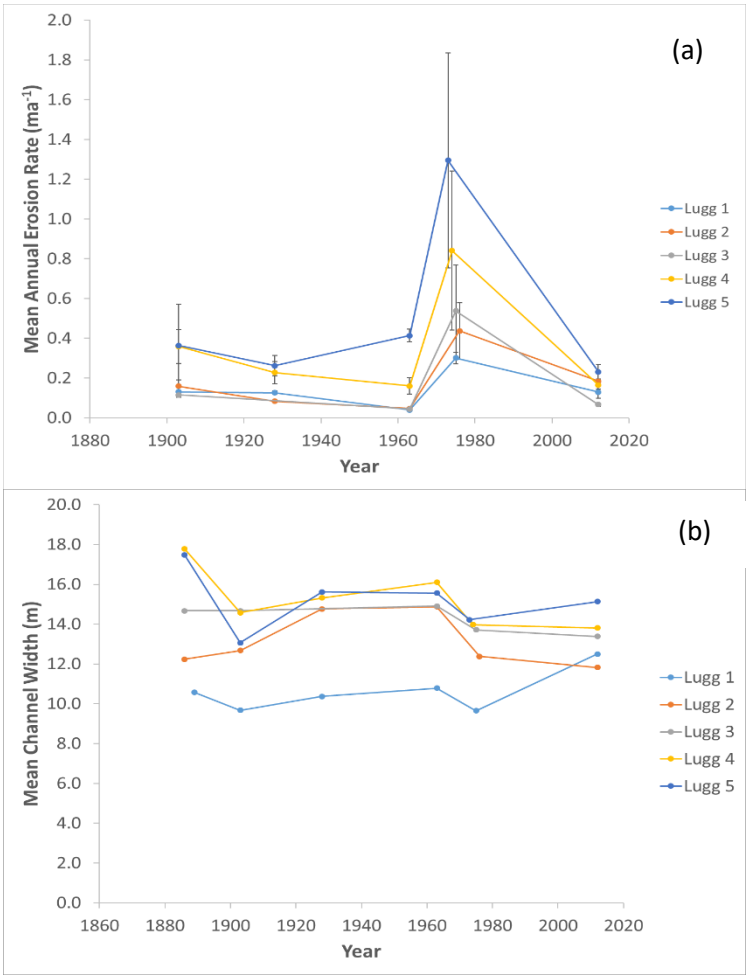

Figure 4.4. The mean migration rate (a) and the mean channel width (b) for the River Lugg reaches. The highest rate was measured in the 1960s for each reach. This period also had the highest variance between the individual bends.

4.4.1.1. River Lugg Reaches

The data for the River Lugg contained five discontinuous reaches ranging in length from 2.5km to 4.2km. Figure 4.4a shows the mean annual erosion rate for each reach along with the variance. The mean erosion rate for all the bends in each reach varies considerably between the different dates. This highest erosion rates were measured between the 1960s and 1970s for all reaches on the River Lugg, with the highest erosion rate being 1.30ma^{-1} measured on Reach 5. The variance measured for this period was also much higher than the other periods. The lowest erosion rate was recorded between 1928 and 1963 for Reaches 1, 2 and 3, with less than 0.1ma^{-1} of lateral change during this period. The average channel width also varies between the different reaches, increasing downstream as the catchment area increases. There are variations between the different time periods, with all of the reaches showing a decrease in average channel width between 1963 and 1976. Figure 4.4b shows the changes in mean channel width for each reach on the River Lugg.

4.4.1.1.1. Reach One

Reach one passes just north of the village of Presteigne on the border between Wales and England, as seen in **Error! Reference source not found.**. Bends 7-11 are affected by flood defences, which restrict the ability of the channel to migrate through this section. Within individual reaches many of the bends were migrating at different rates. **Error! Reference source not found.** shows the most recent channel position.

1889-1903: Between 1889 and 1903 the rates of migration were generally low and most of the bends were stable during this period. The mean annual erosion rate was 0.13ma^{-1} and the maximum rate was 0.29ma^{-1}.

1903:1928: Between 1903 and 1928 the lateral migration rates were generally low again, although there was an increase in bends 28, 29, 43 and 44. The mean annual erosion rate remained constant at 0.13ma^{-1} but the maximum rate increased to 0.56ma^{-1}.

1928-1963: The reach was particularly stable between 1928 and 1963, with the exception of bends 16 and 17, which had a lateral erosion rate of 0.2ma^{-1}. A cutoff did occur at bend 29, but did not lead to an increase in erosion rate either upstream or downstream of the bend. The mean annual erosion rate was 0.04ma^{-1} during this period.

1963-1975: There is an increase in migration rate in the 1963-1975 period compared to the 1928-1963 period. The mean erosion for the reach increases from 0.04ma^{-1} to 0.30ma^{-1}, with much greater variation between the different bends. The maximum rate was 0.91ma^{-1}, which was measured towards the end of the reach on bend 45.

1975-2012: Between 1975 and 2012, a cutoff occurs between bend 20 and 21, with a slight increase in erosion rate downstream of the cutoff. Towards the end of the reach bends 36, 37, 41, 42, 45 and 46 all show an increase in migration rate. The mean annual erosion rate decreased to 0.13ma^{-1}, but the highest maximum erosion rate for a bend was measured during this period at 0.97ma^{-1} on bend 46.

Figure 4.10 shows the variation in channel width for each bend for Reach 1. There is high variation in channel width along the reach and between the different periods.

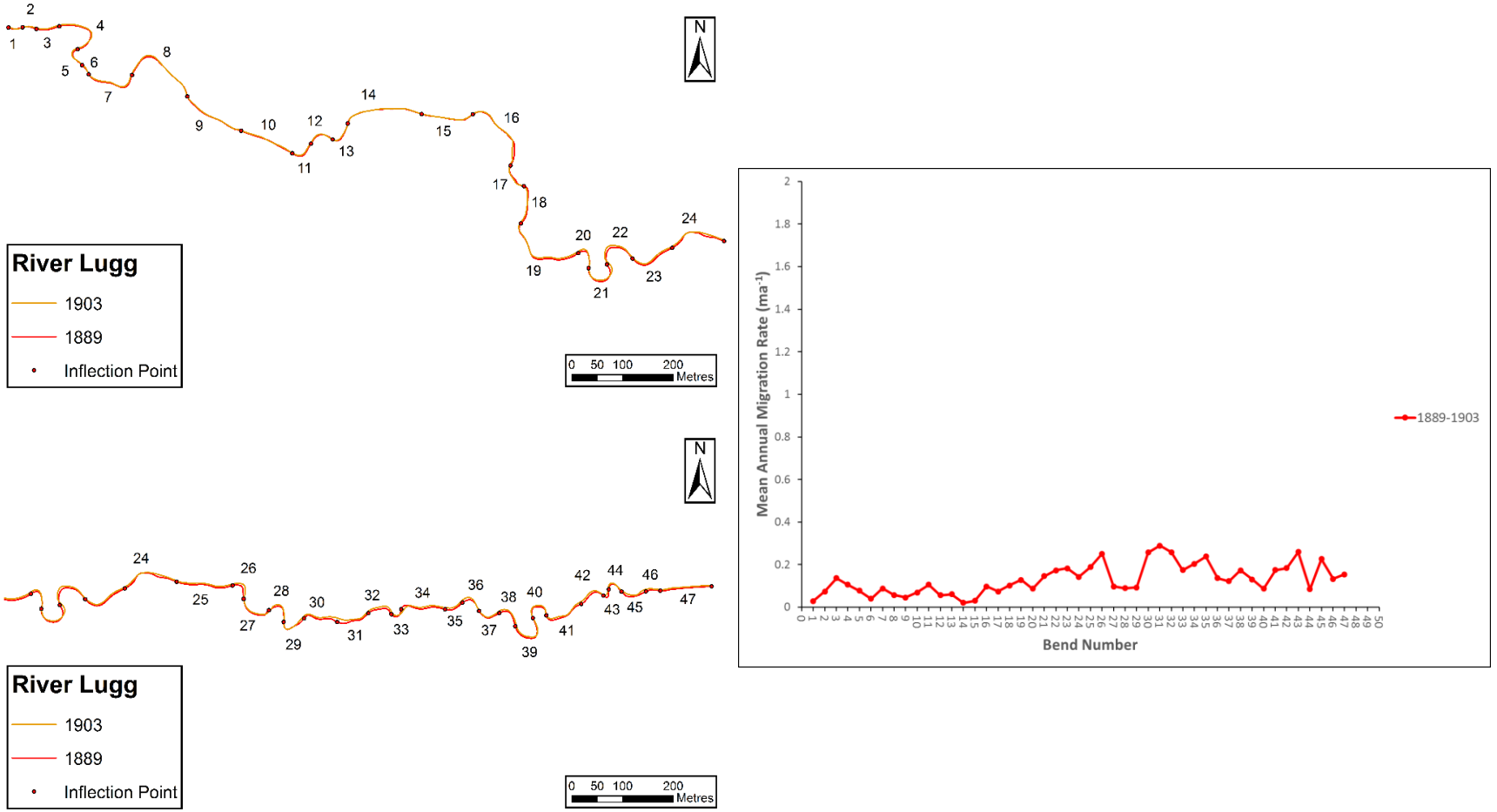

Figure 4.5. The migration rate for each individual bend on Reach 1, River Lugg, between 1889 and 1903

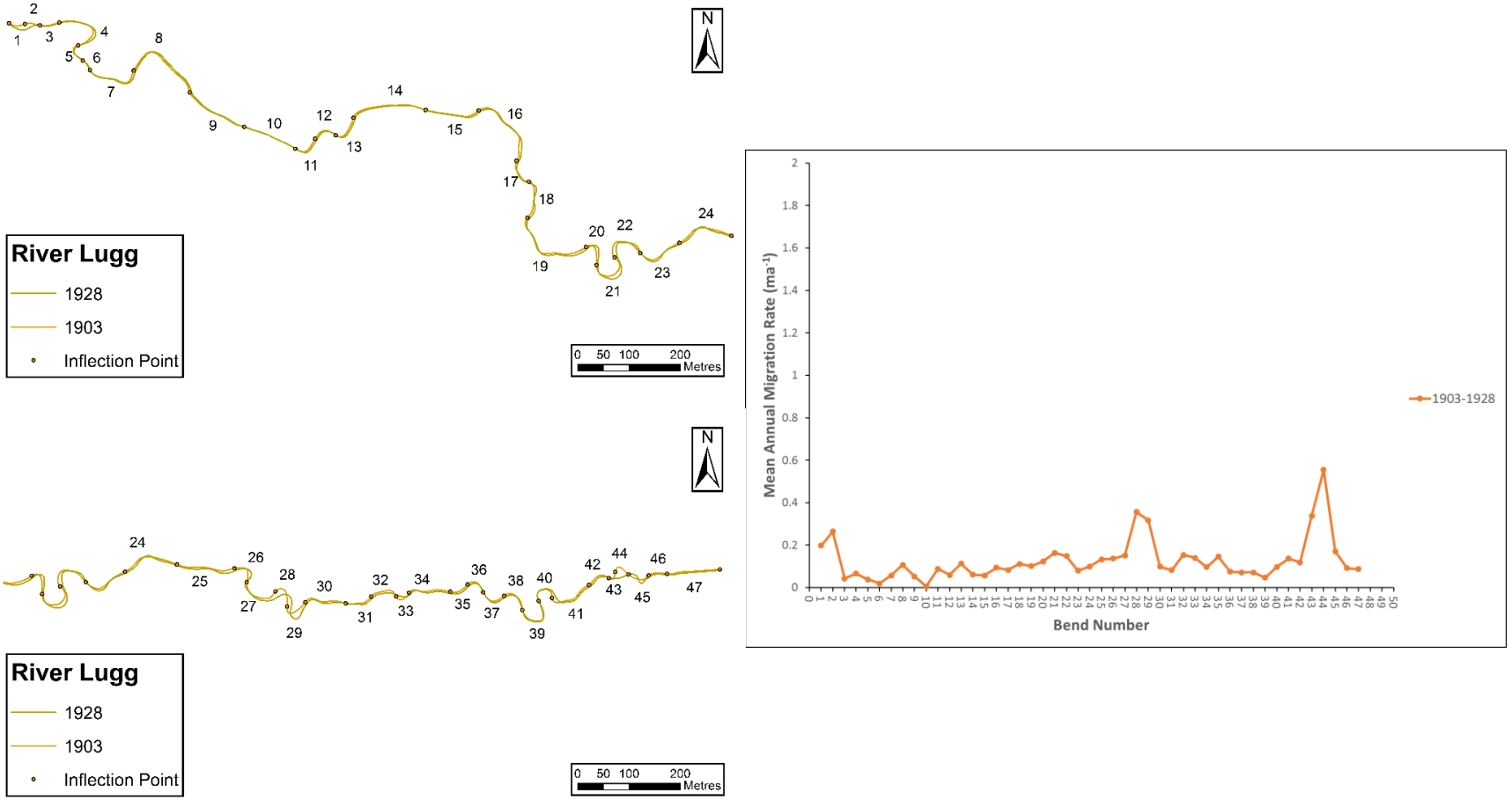

Figure 4.6. Migration rate for individual bends on Reach 1, River Lugg, between 1903 and 1928

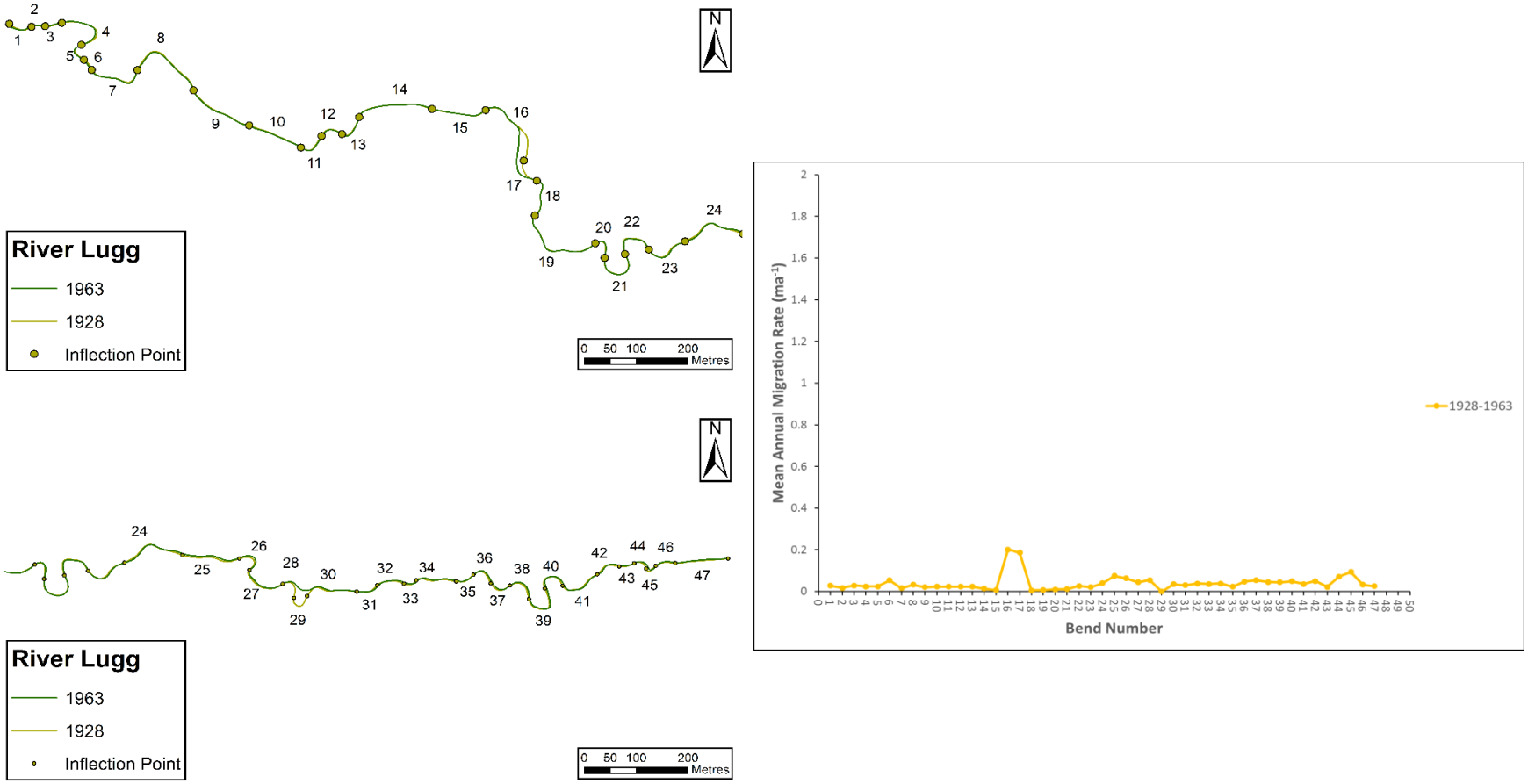

Figure 4.7. Migration rates for individual bends for Reach 1, River Lugg, between 1928 and 1963

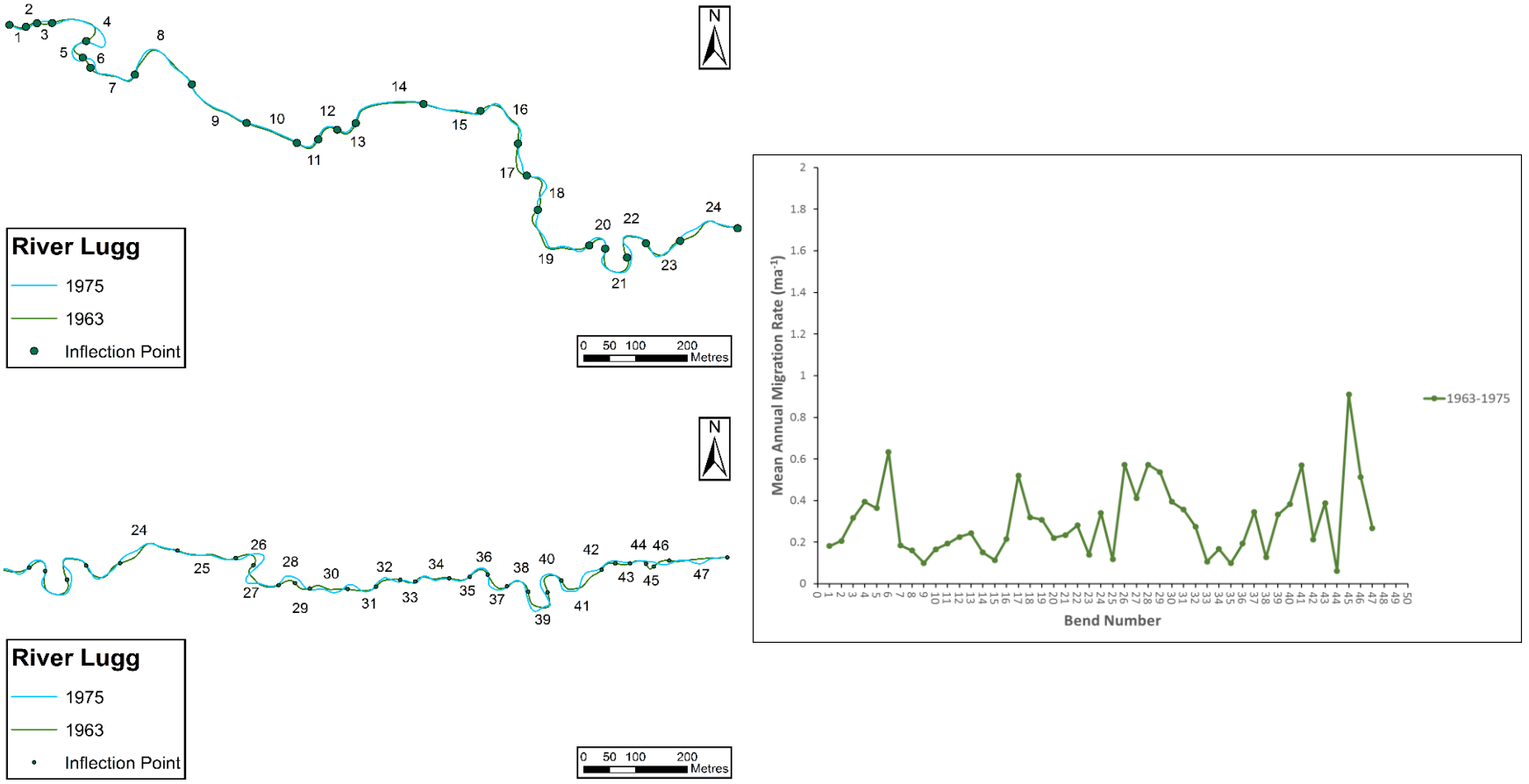

Figure 4.8. Migration rates for individual bends on Reach 1, River Lugg, between 1963 and 1975

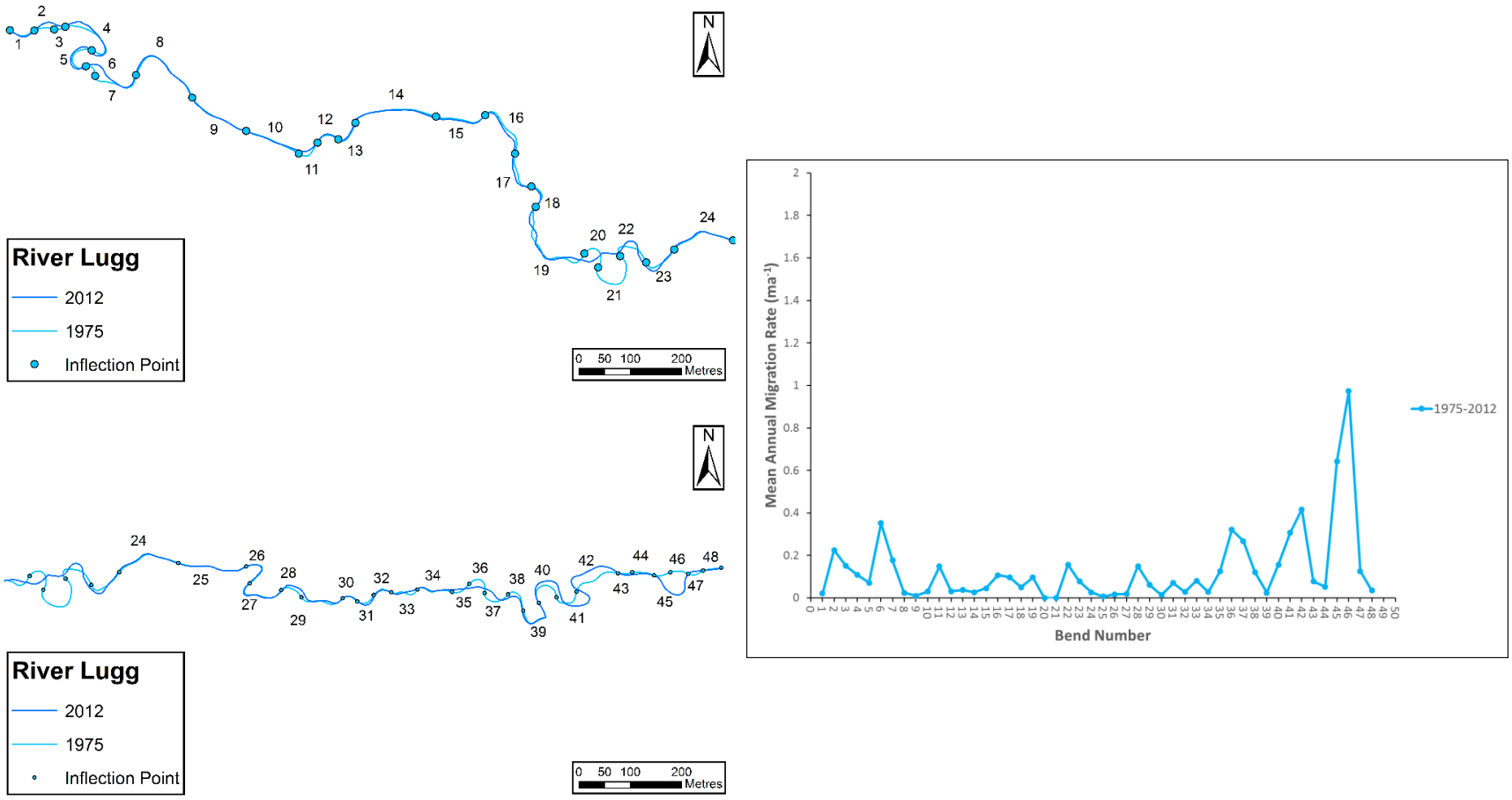

Figure 4.9. Migration rates of individual bends on Reach 1, River Lugg, between 1975 and 2012

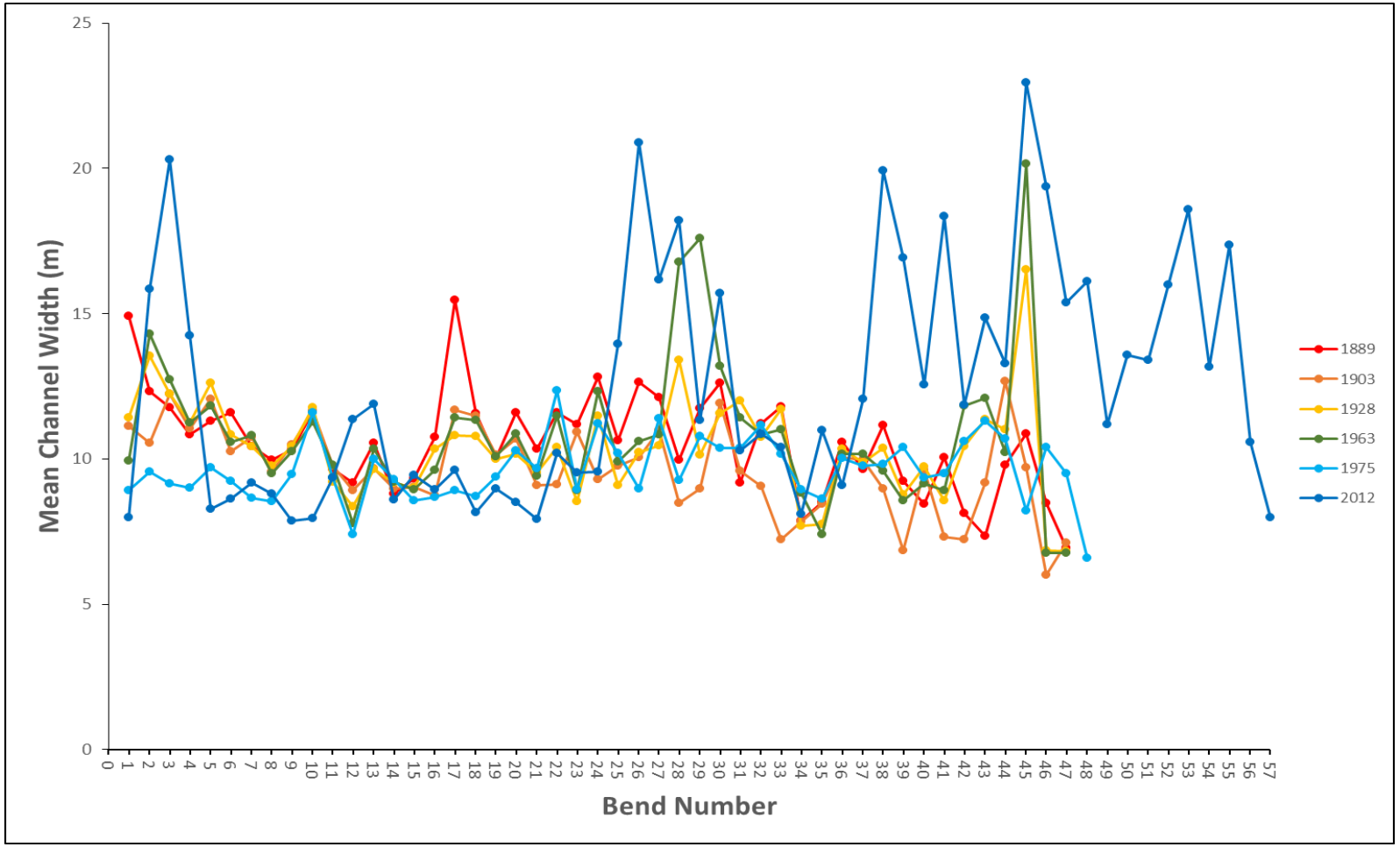

Figure 4.10. The mean channel width of each individual bend for Reach 1

4.4.1.1.2. Reach Two

Reach two is located just downstream of the confluence between the River Lugg and Hindwell Brook. There is no human infrastructure located along the banks of the reach, with the exception of light fencing installed to prevent cattle access to the river channel (see Figure 4.11). The last bend on the reach is restricted by the side of the valley, while the rest of the reach has no lateral restriction. Overall, the reach is more mobile than the previous reach.

1886-1903: The mean annual erosion rate for this period was 0.16ma^{-1}, with a maximum rate of 0.68ma^{-1} measured on bend 12 and bend 16. Most of the erosion is concentrated between bends 8 and 16, with little activity towards the end of the reach.

1903-1928: Both the mean and the maximum annual erosion rate decreased during this period to 0.08ma^{-1} and 0.27ma^{-1} respectively, with the reach remaining stable on most bends. There was some slight downstream migration on bend 15, which had the highest erosion rate for the reach.

1928-1963: Between 1928 and 1963 there is very little change on the reach, with only bend 10 growing across the floodplain. Even on this bend, the erosion is limited to the apex of the bend, while the rest of the bend remains stable. The mean erosion rate is 0.05ma^{-1} during this period and the maximum erosion rate is 0.14ma^{-1}.

1963-1976: Between 1963 and 1976, bend 10 experienced a neck cutoff, cutting off 250m of the river channel. There was an increase in migration rate immediately upstream of the

Figure 4.11. Bend 18 on the River Lugg. The fencing to prevent cattle access to the river was the only human infrastructure present.

cutoff, with 1.4ma^{-1} and 1.9ma^{-1} of lateral migration occurring on bends 4 and 8. Bend 13 downstream also experienced an increase in erosion compared to the period before 1963. There is considerable change along the whole of the reach, with nearly all bends showing an increase in migration rate. The mean migration rate was 0.44ma^{-1} for this period with a maximum rate of 1.93ma^{-1}.

1976-2012: The migration rate remained high during this period, especially on bends 4-8 (0.6ma^{-1}, 0.3ma^{-1}, 0.5ma^{-1}, 0.7ma^{-1} and 0.8ma^{-1} respectively) and bends 18-19 (0.3ma^{-1} for both bends). A cutoff occurred at bends 15 and 16, between 1976 and 2012. The mean annual erosion rate decreased to 0.18ma^{-1}, with a maximum rate of 0.80ma^{-1} measured on bend 8.

The mean channel width of each bend again varies across the whole reach and between the different dates (see Figure 4.17).

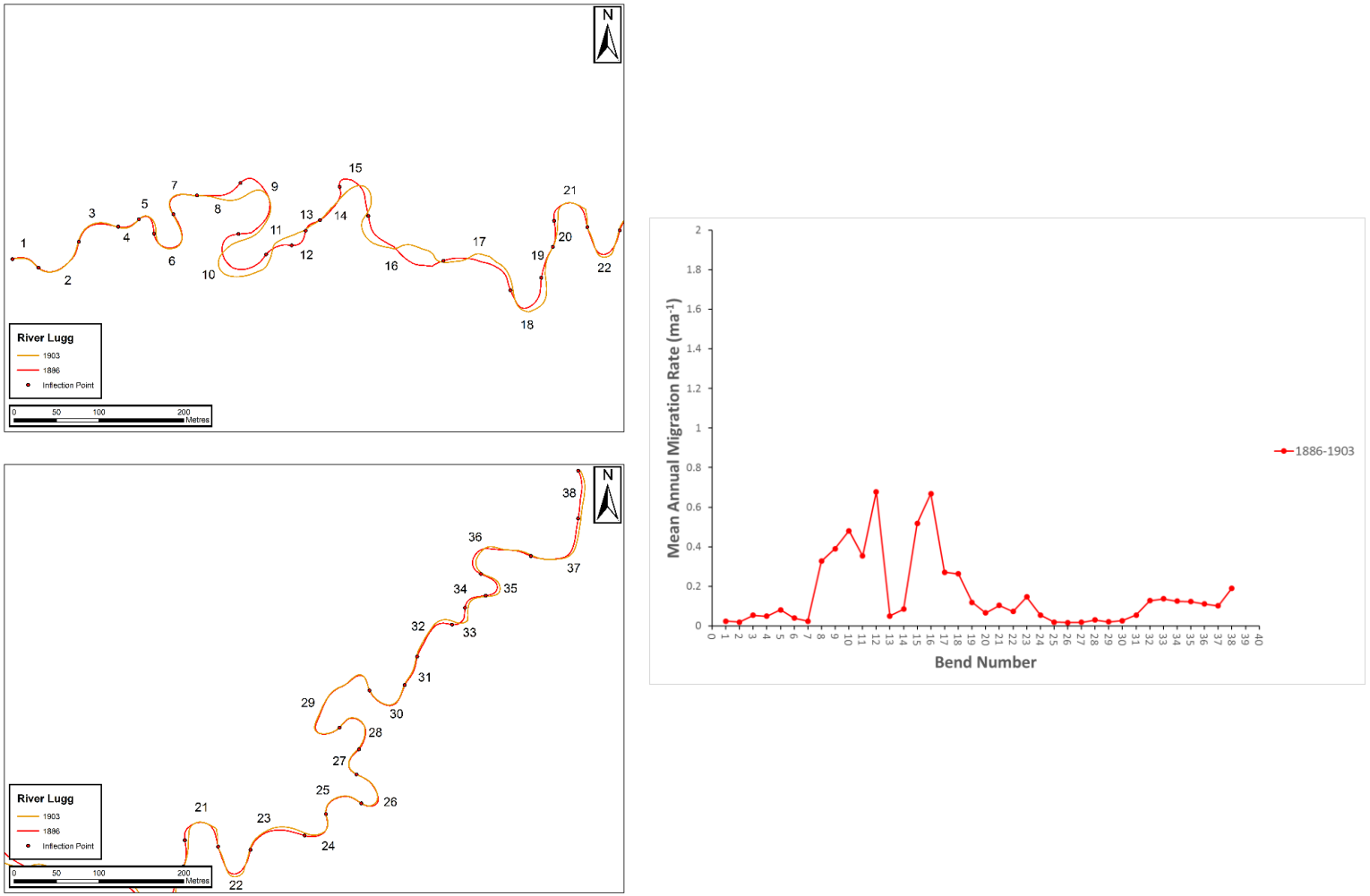

Figure 4.12. Migration rates on Reach 2 of the River Lugg between 1886 and 1903

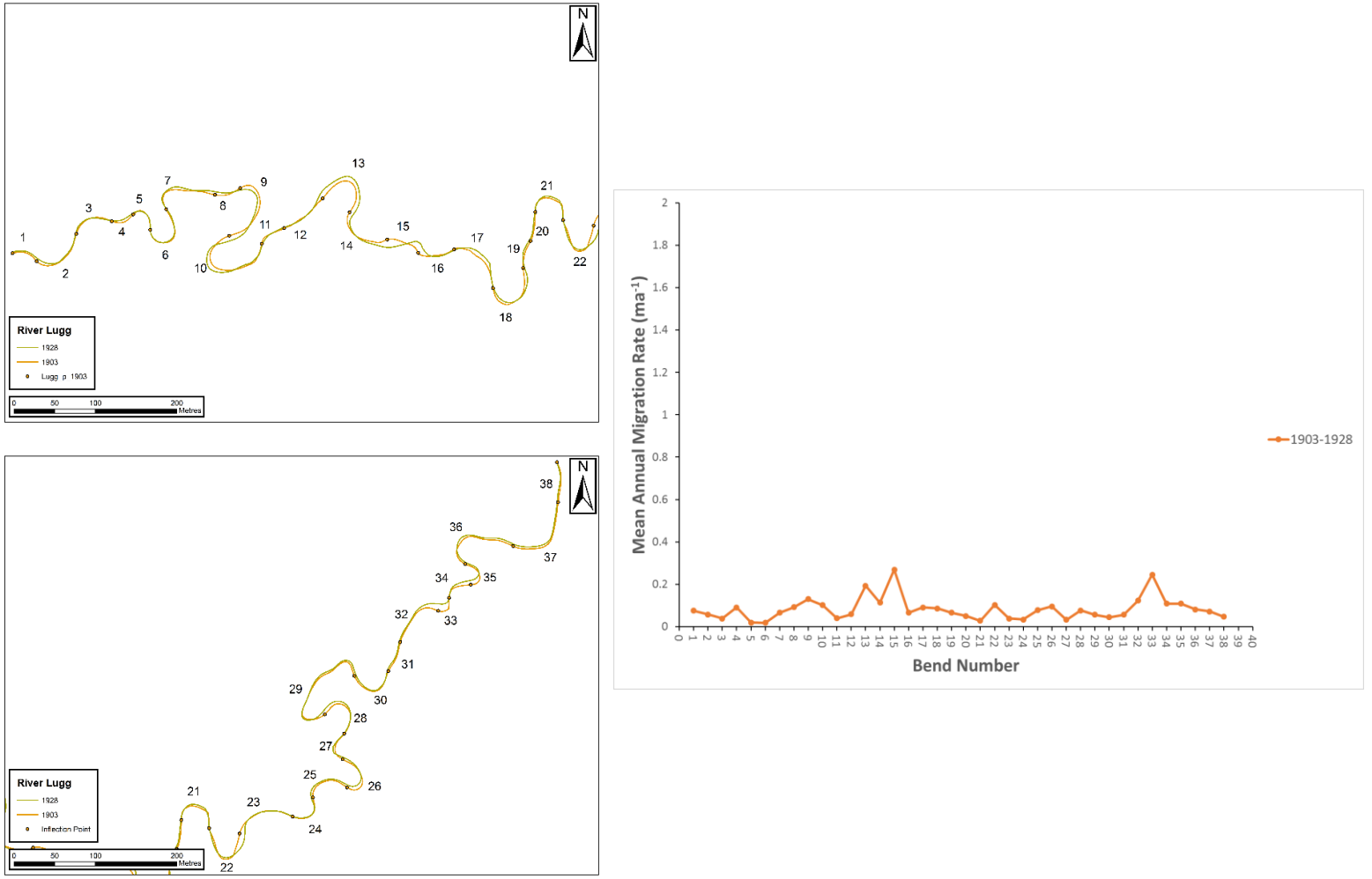

Figure 4.13. Migration rates on Reach 2 of the River Lugg between 1903 and 1928

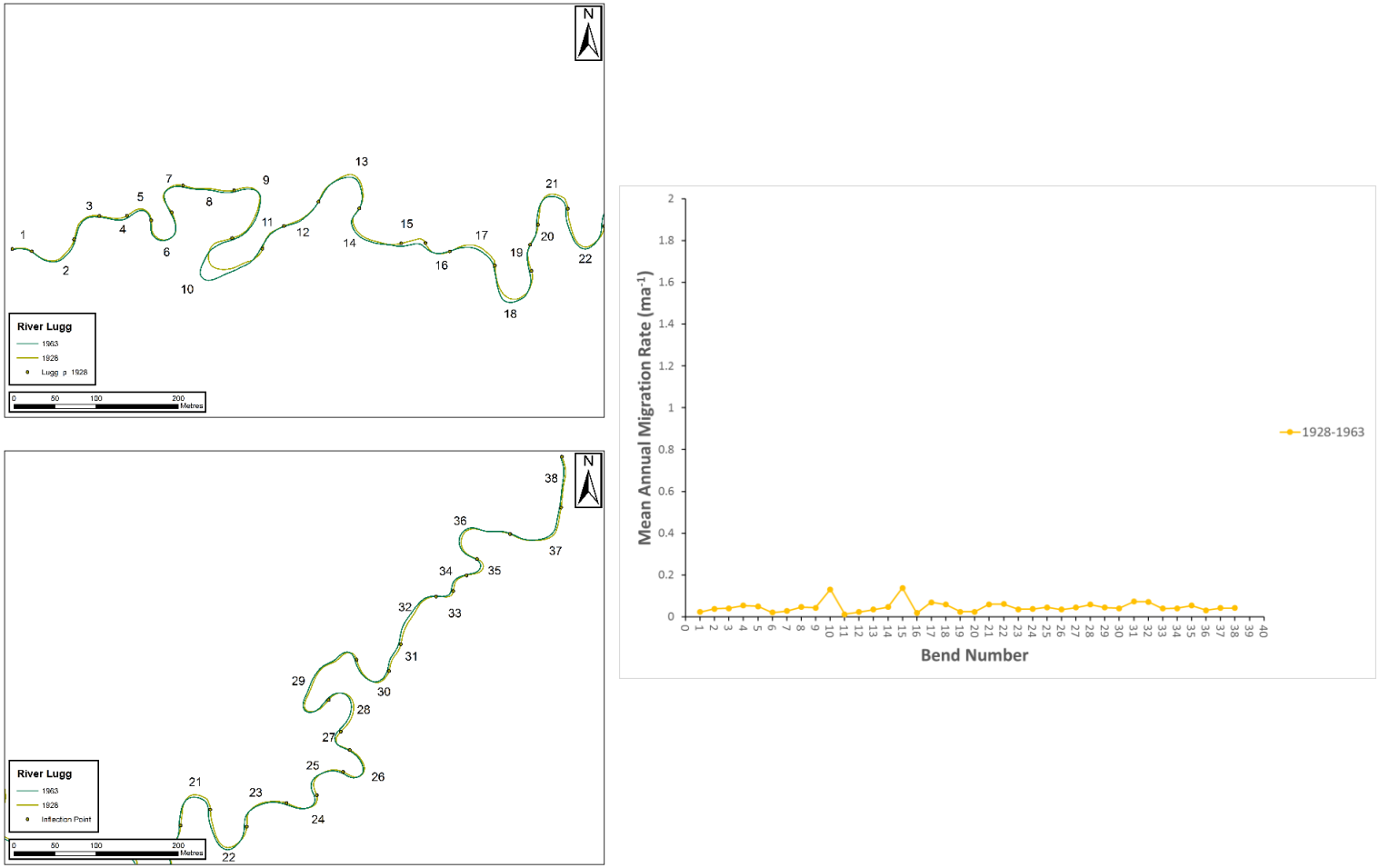

Figure 4.14. Migration rates on Reach 2 of the River Lugg between 1928 and 1963

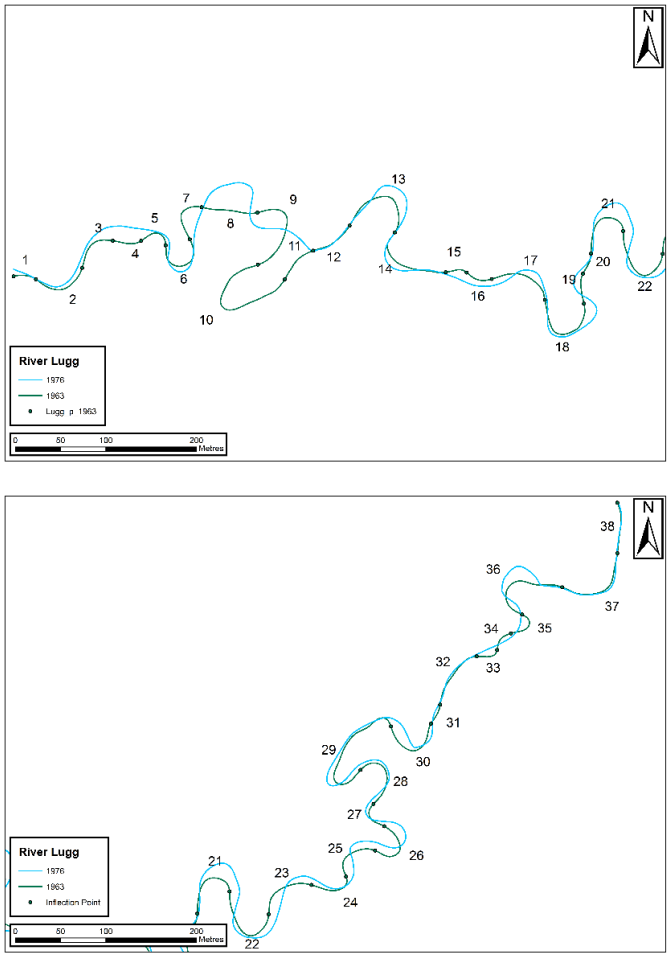

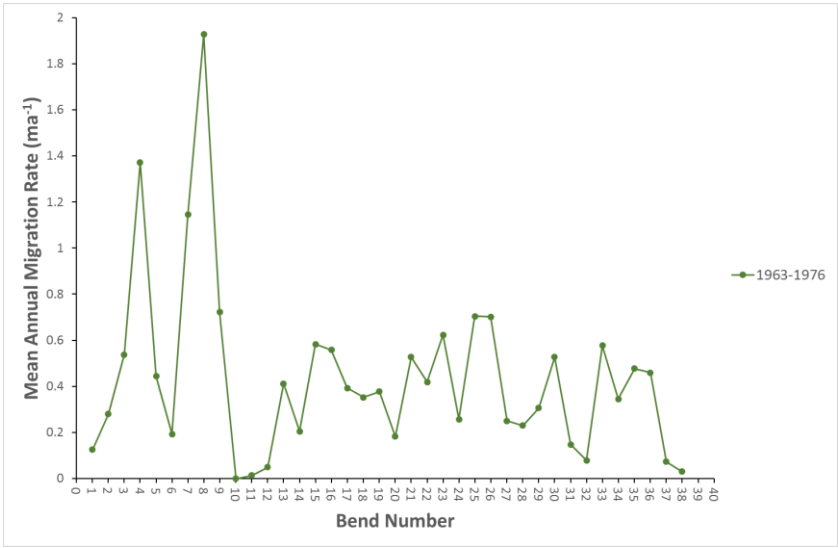

Figure 4.15. Migration rates on Reach 2 of the River Lugg between 1963 and 1976

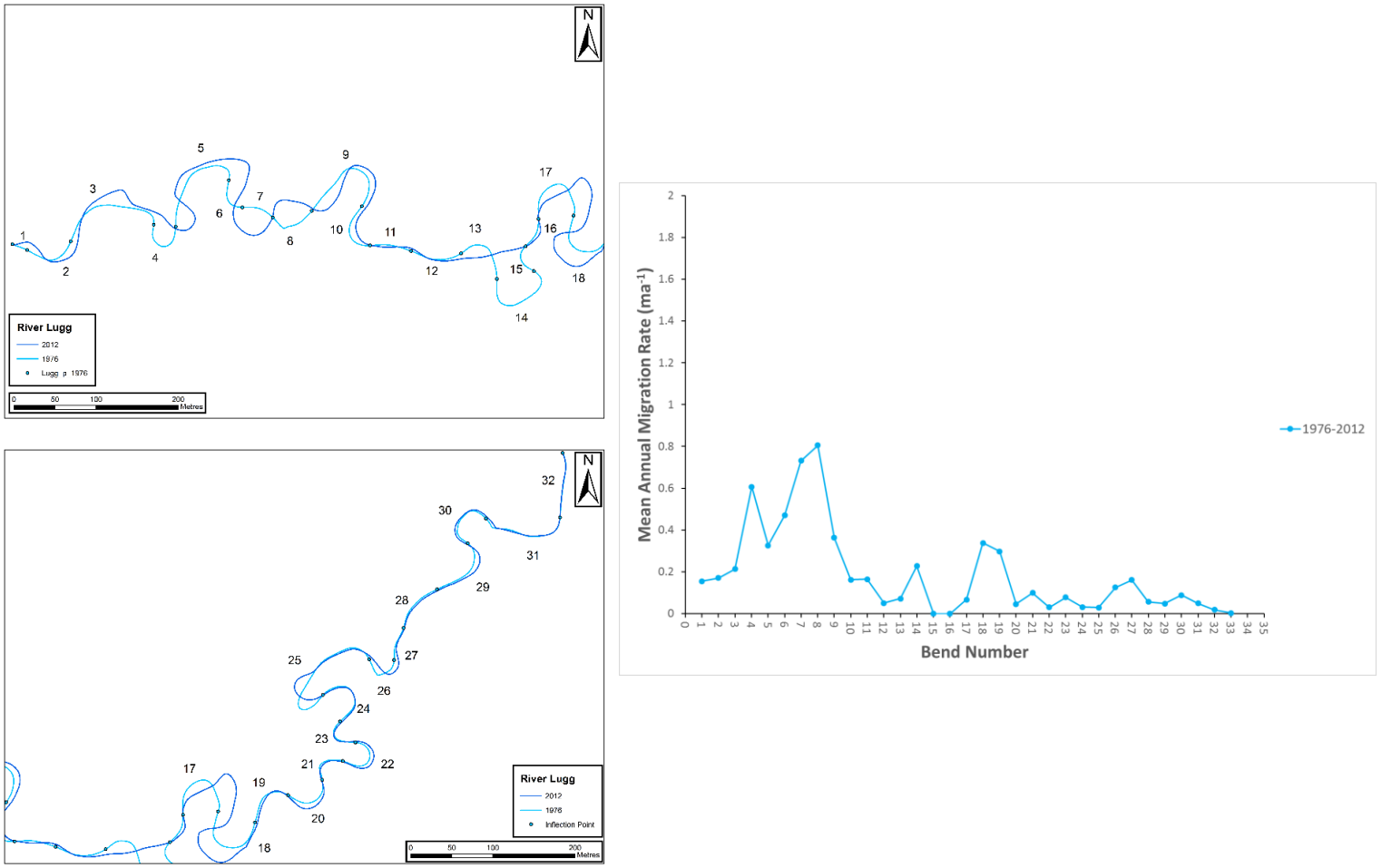

Figure 4.16. Migration rates on Reach 2 of the River Lugg between 1976 and 2012

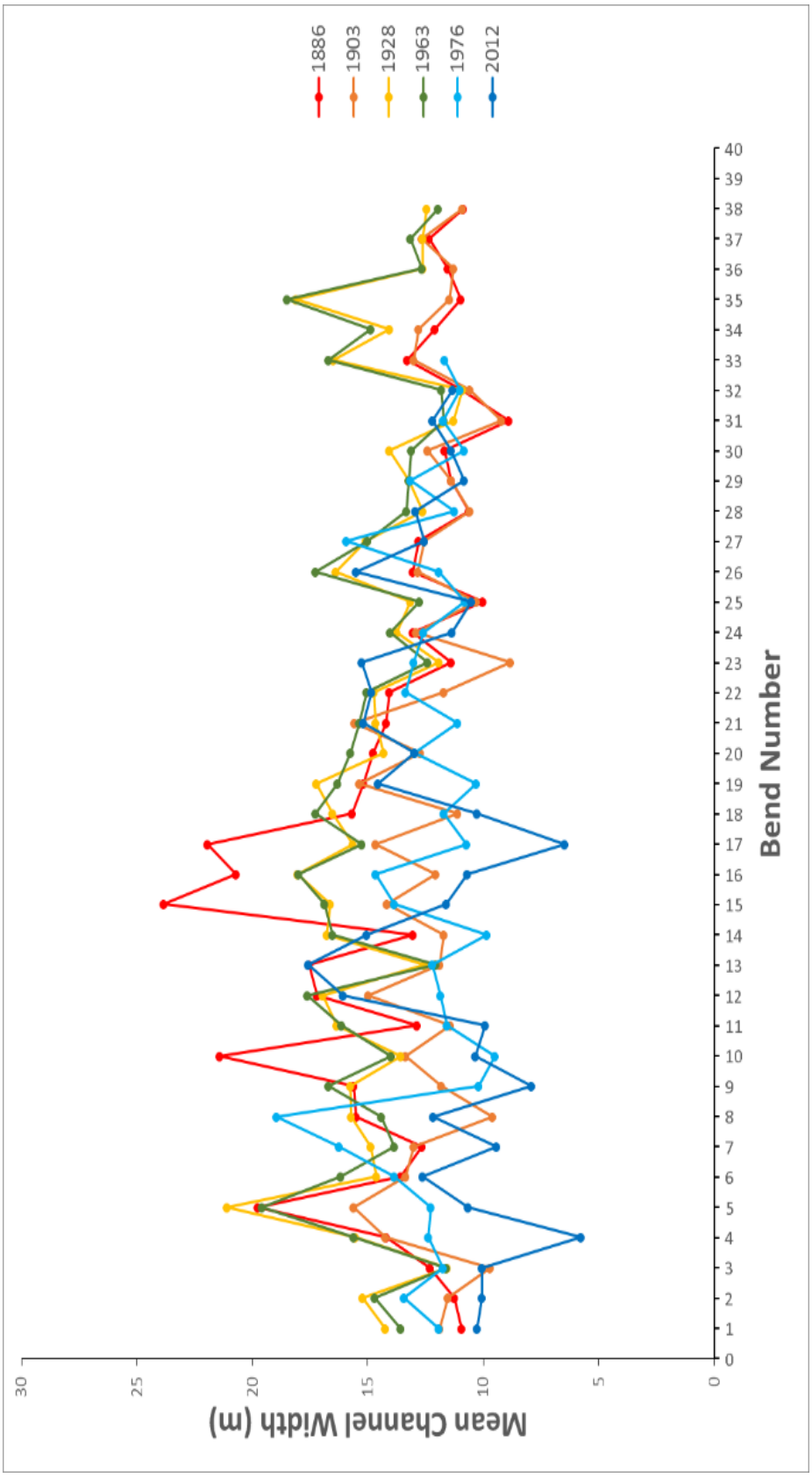

Figure 4.17. The mean channel width of each individual bend

4.4.1.1.3. Reach Three

Reach Three is located to the south of Upper Lye. For this reach, the River Lugg has entered a narrow valley formed in a former glacial spillway, which acts to confine the movement of the river channel. Most of the bends are stable in this reach, and the bends that are active tend to migrate downstream. There was no map available for 1928 for this reach and therefore a much longer period between 1903 and 1963 was used.

1886-1903: The mean migration rate for 1886-1903 was $0.12ma^{-1}$. Individual bends did migrate during this period, such as bend 11 ($0.42ma^{-1}$) and bend 34 ($0.67ma^{-1}$) but the erosion was isolated and the bends around were stable exhibiting very little change.

1903-1963: Between 1903 and 1963, the mean migration on the reach decreased from $0.12ma^{-1}$ to $0.04ma^{-1}$ and virtually all of the bends remained stable during this period. The maximum rate was $0.23ma^{-1}$ on bend 34 that migrated slightly downstream.

1963-1975: The period 1963-1975 showed a large increase in the migration rate for many of the bends across the reach. Bend 24 had the highest erosion at $2.5ma^{-1}$ as the bend migrated downstream rapidly, with high erosion rates evident on bend 28 and 32 evident as well. The mean migration rate increased to $0.54ma^{-1}$.

1975-2012: Between 1975 and 2012, the majority of bends became stable again with isolated erosion occurring on bend 2 and bend 35. A cutoff occurred on bend 24, which had experienced the very high erosion rate in the previous period, but this had very limited impact on the surrounding bends as the river channel was directly next to the valley side for the bends downstream of the cutoff. The mean migration rate decreased to $0.07ma^{-1}$ during this period.

The mean channel width for bends was more consistent through time for Reach Three compared to the previous reaches indicating increased stability.

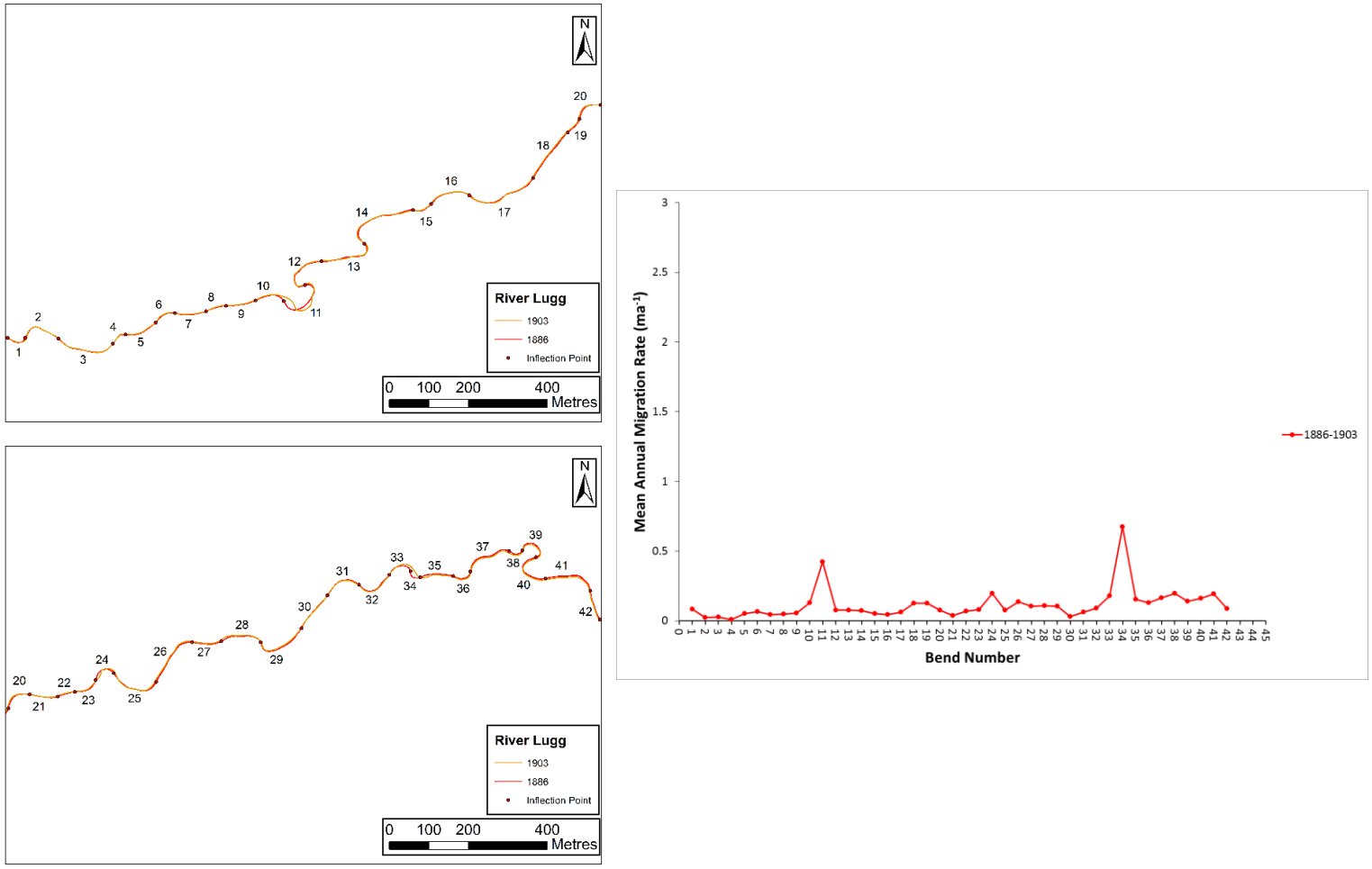

Figure 4.18. Migration rates on Reach 3 of the River Lugg between 1886 and 1903

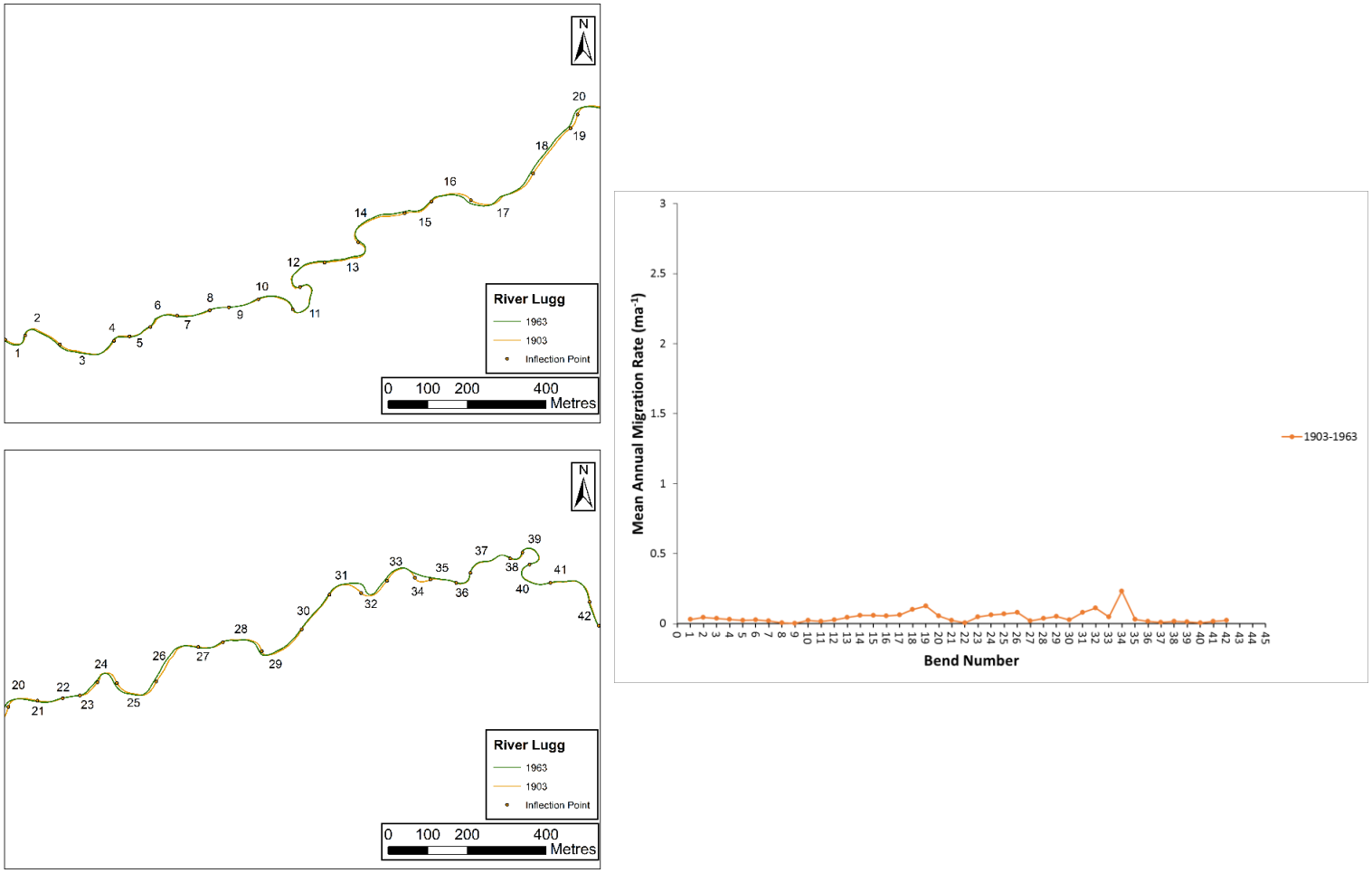

Figure 4.19. Migration rates on Reach 3 of the River Lugg between 1903 and 1963

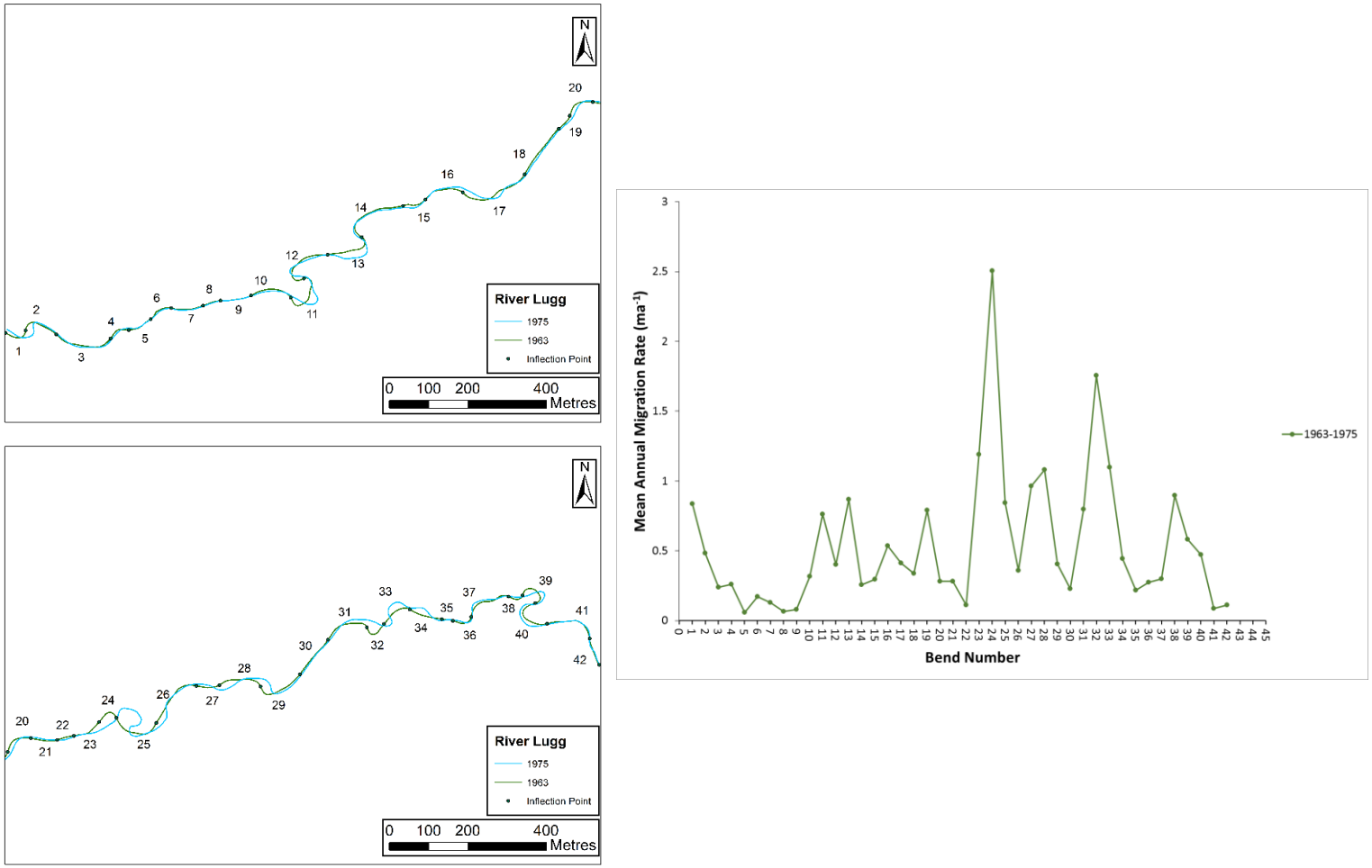

Figure 4.20. Migration rates on Reach 3 of the River Lugg between 1963 and 1975

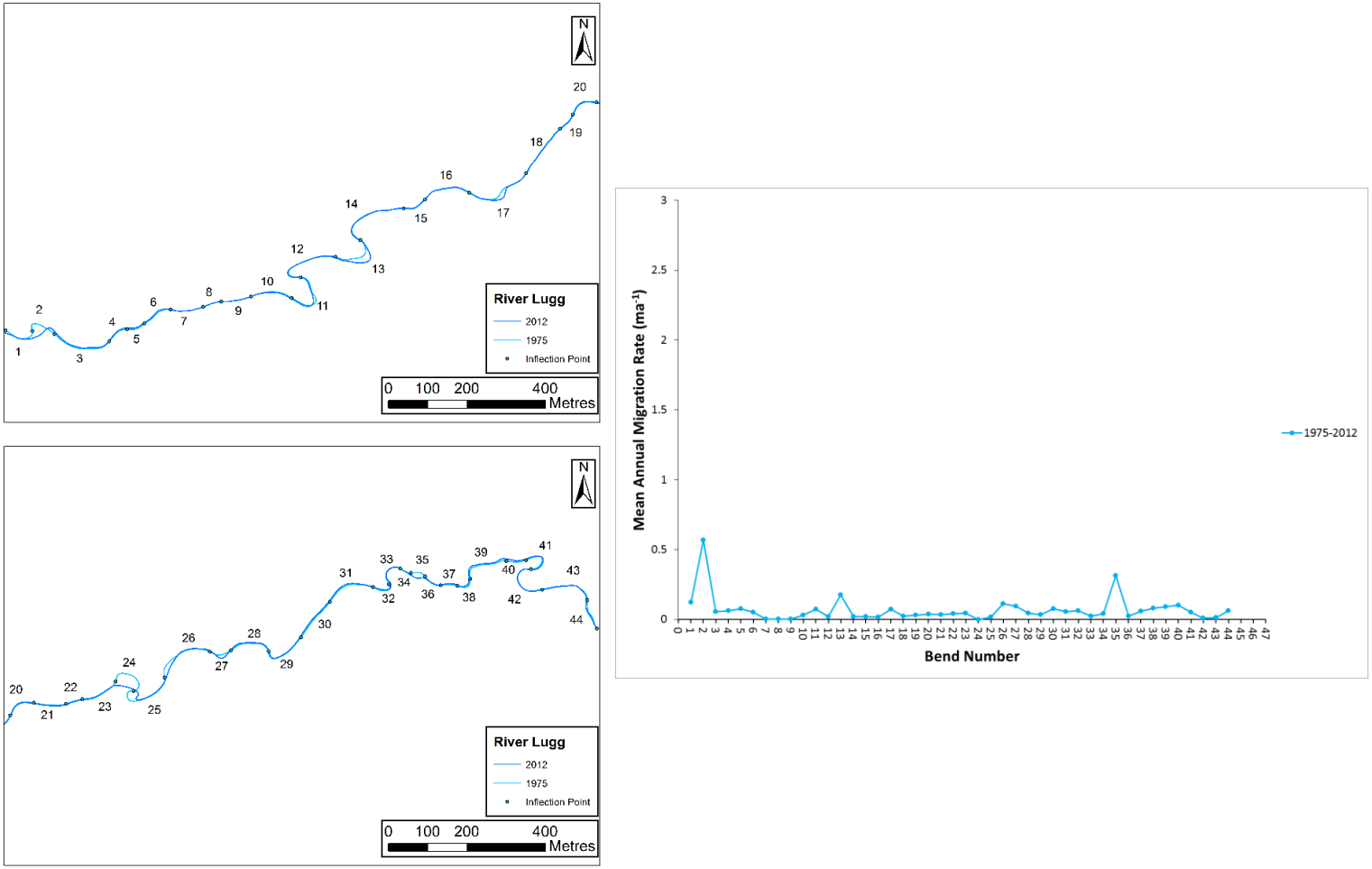

Figure 4.21. Migration rates on Reach 3 of the River Lugg between 1975 and 2012

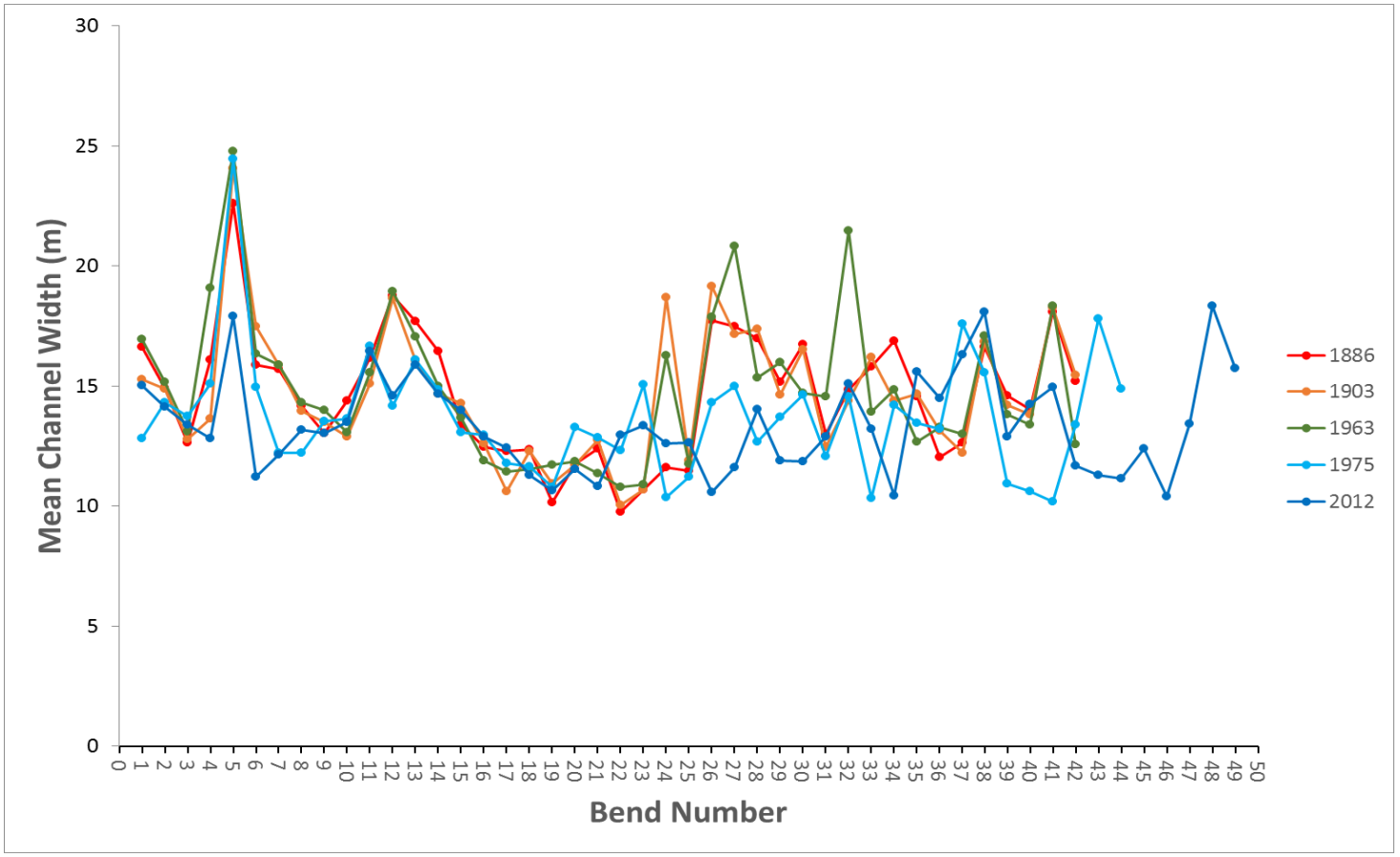

Figure 4.22. Mean channel width for individual bends on Reach 3. There was more consistency between the different periods compared to the other reaches

4.4.1.1.4. Reach Four

Reach four enters a wide floodplain just to the east of Mortimer's Cross. This section of the River Lugg is considerably more active than the previous reach, with numerous cutoffs occurring in the different periods and active erosion on many banks during each period.

1886-1903: Between 1886 and 1903, the highest rates of erosion were found on bends 9-11 and 13-16, with bend 10 migrating at the fastest rate of 1.48ma^{-1}. The mean annual erosion for this period was 0.36ma^{-1}.

1903-1928: The mean annual erosion for the reach decreases slightly for the 1903-1928 period (from 0.36ma^{-1} to 0.23ma^{-1}) and the highest rates of erosion were measured between bends 16 and 19 during this period. The maximum rate was lower, measured at 0.87ma^{-1} on bend 18. A cutoff occurs at bend 21, with an increase in erosion evident immediately downstream.

1928-1963: Between 1928 and 1963 numerous cutoffs occur, with three consecutive bends, 20-22 cutoff completely. Cutoffs also occur on bends 9 and 14, with the highest rate of erosion measured just downstream of bend 14 at 0.99ma^{-1}. Despite the number of bends cutoff and the associated steepening of the channel, the mean migration rate decreased to 0.16ma^{-1}.

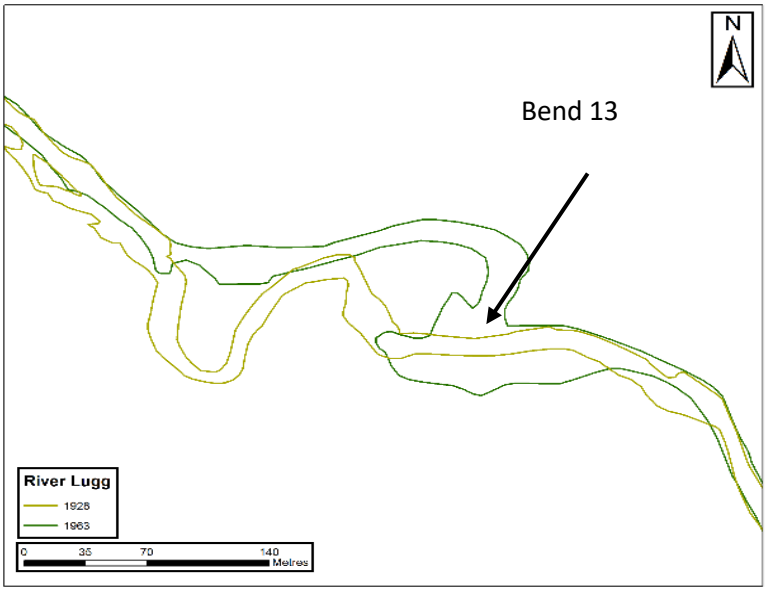

Figure 4.23. An avulsion between 1928 and 1963 left a large backwater area on bend 13, which led to the high mean channel width for this bend

1963-1974: Between 1963 and 1974, nearly all of the bends in the reach experience high levels of erosion with two further cutoffs occurring. These cutoffs occurred on bends that had not developed into compound form suggesting that the cutoffs were chute cutoffs rather than neck cutoffs. The average bend erosion during this period is $0.84ma^{-1}$. The maximum rate of $2.52ma^{-1}$ was measured on bend 8, just upstream of a cutoff that occurred in the 1928-1963 period.

1974-2012: The lateral erosion rate decreases for many of the bends between 1974 and 2012, although many of the bends continue to erode at rates between $0.2ma^{-1}$ and $0.5ma^{-1}$. Another cutoff occurs on bends 25-27, removing a complex compound set of bends to form a simple symmetric bend. The mean annual erosion rate decreased to $0.16ma^{-1}$ and the maximum rate was $0.49ma^{-1}$.

The channel width varies along the reach and between the different periods. Bend 13 in 1963 has a very high mean channel width as the channel has either avulsed or migrated downstream quickly just upstream, causing a very complicated planform at bend 13 as shown in Figure 4.23.

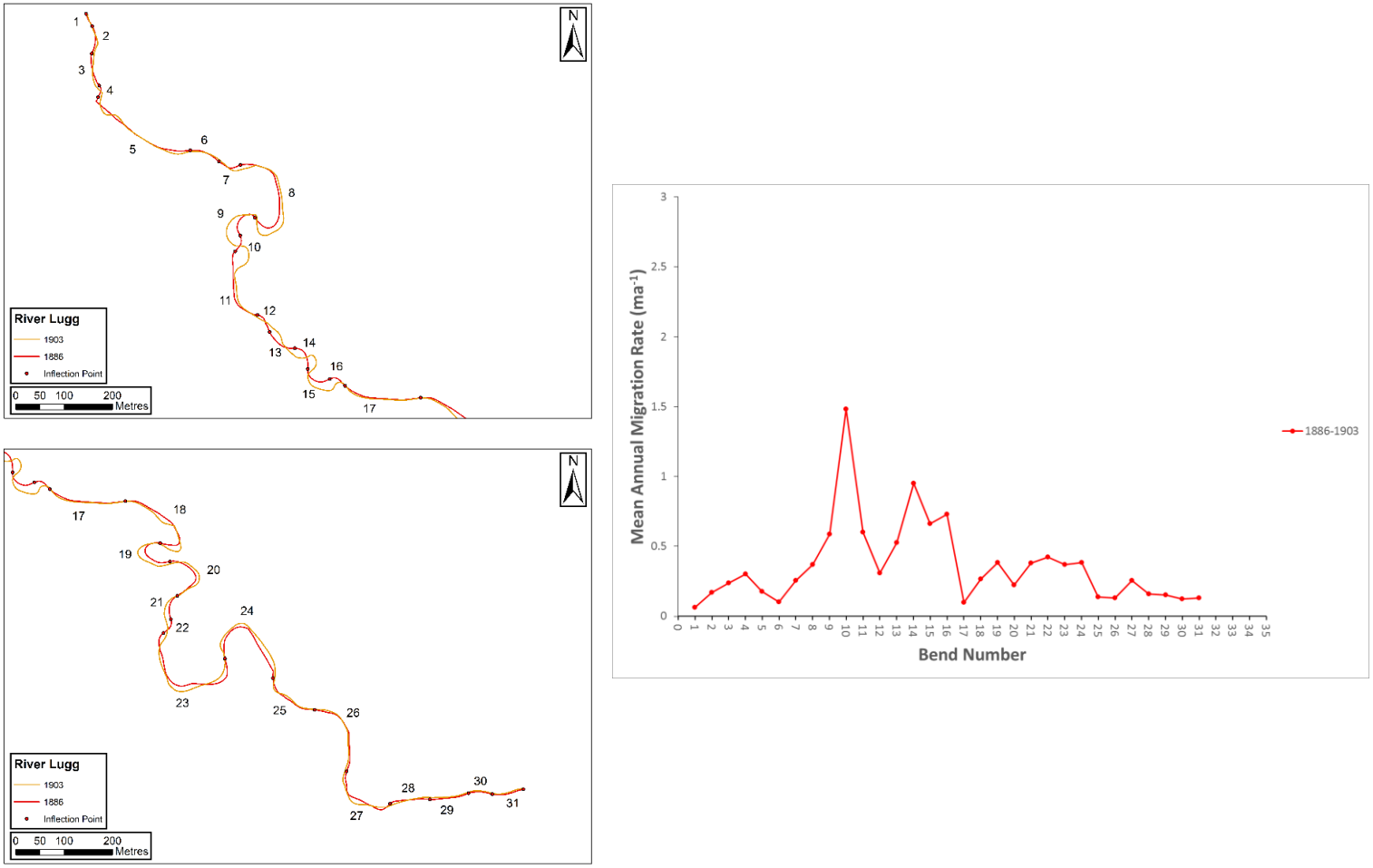

Figure 4.24. Migration rates on Reach 4 of the River Lugg between 1886 and 1903

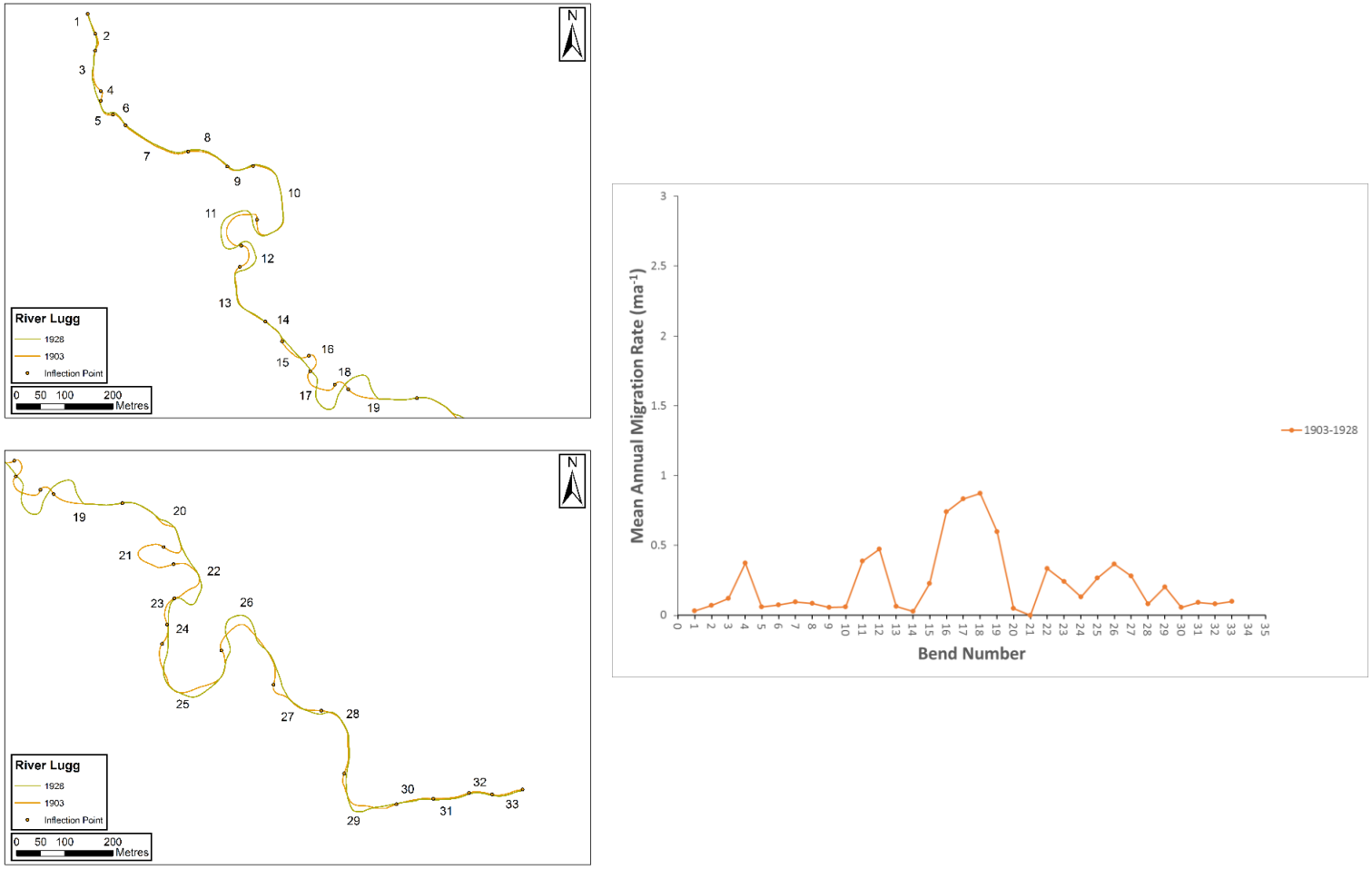

Figure 4.25. Migration rates on Reach 4 of the River Lugg between 1903 and 1928

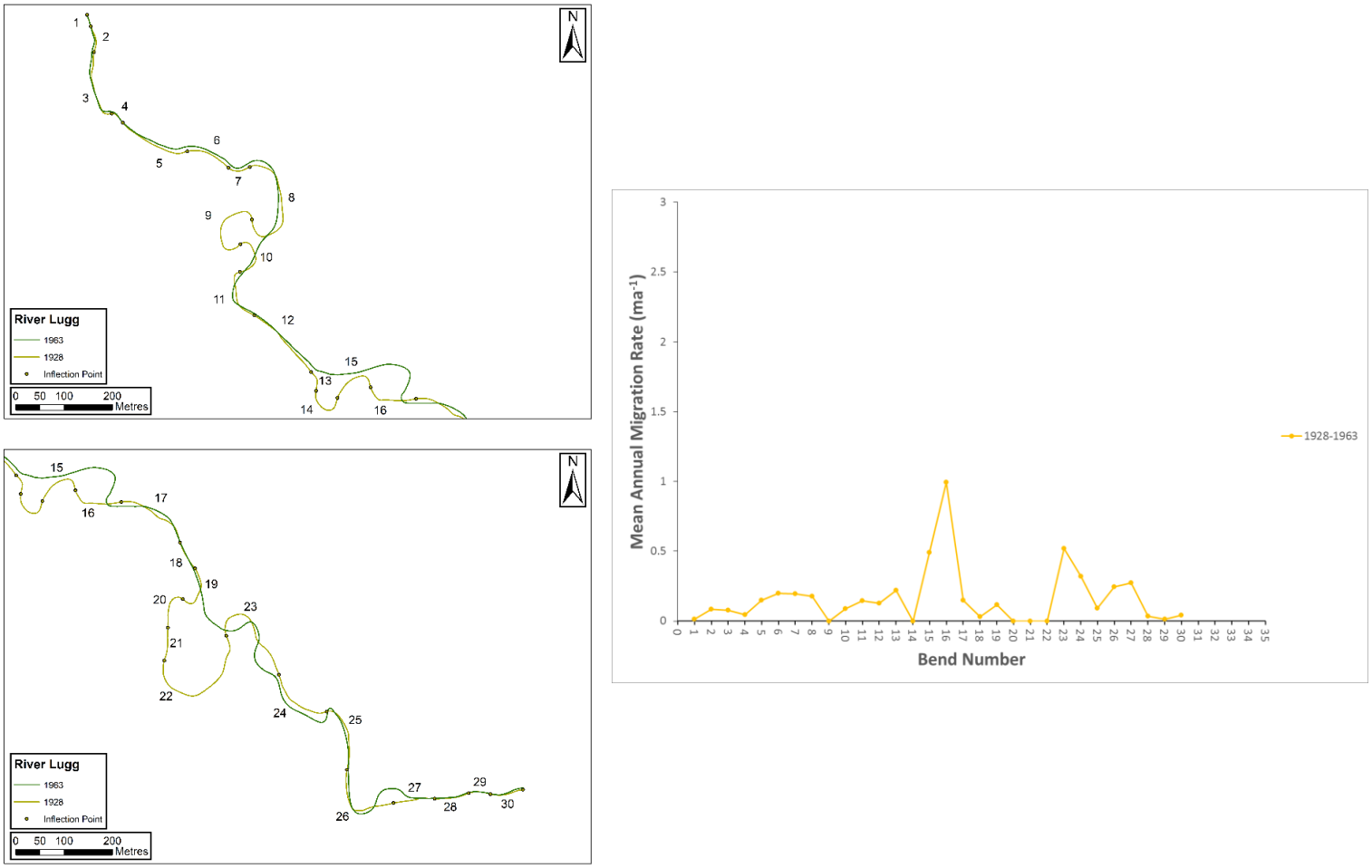

Figure 4.26. Migration rates on Reach 4 of the River Lugg between 1928 and 1963

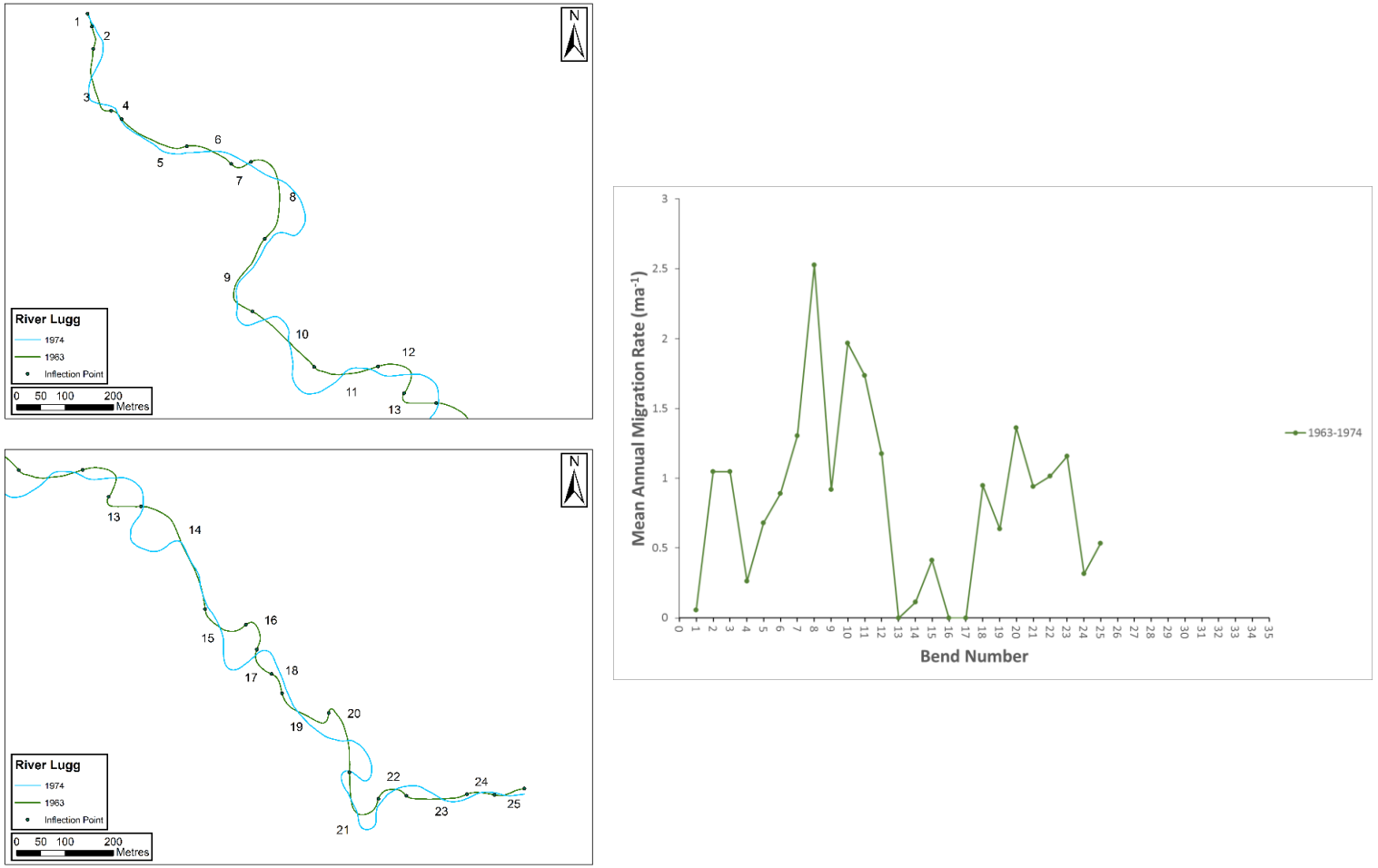

Figure 4.27. Migration rates on Reach 4 of the River Lugg between 1963 and 1974

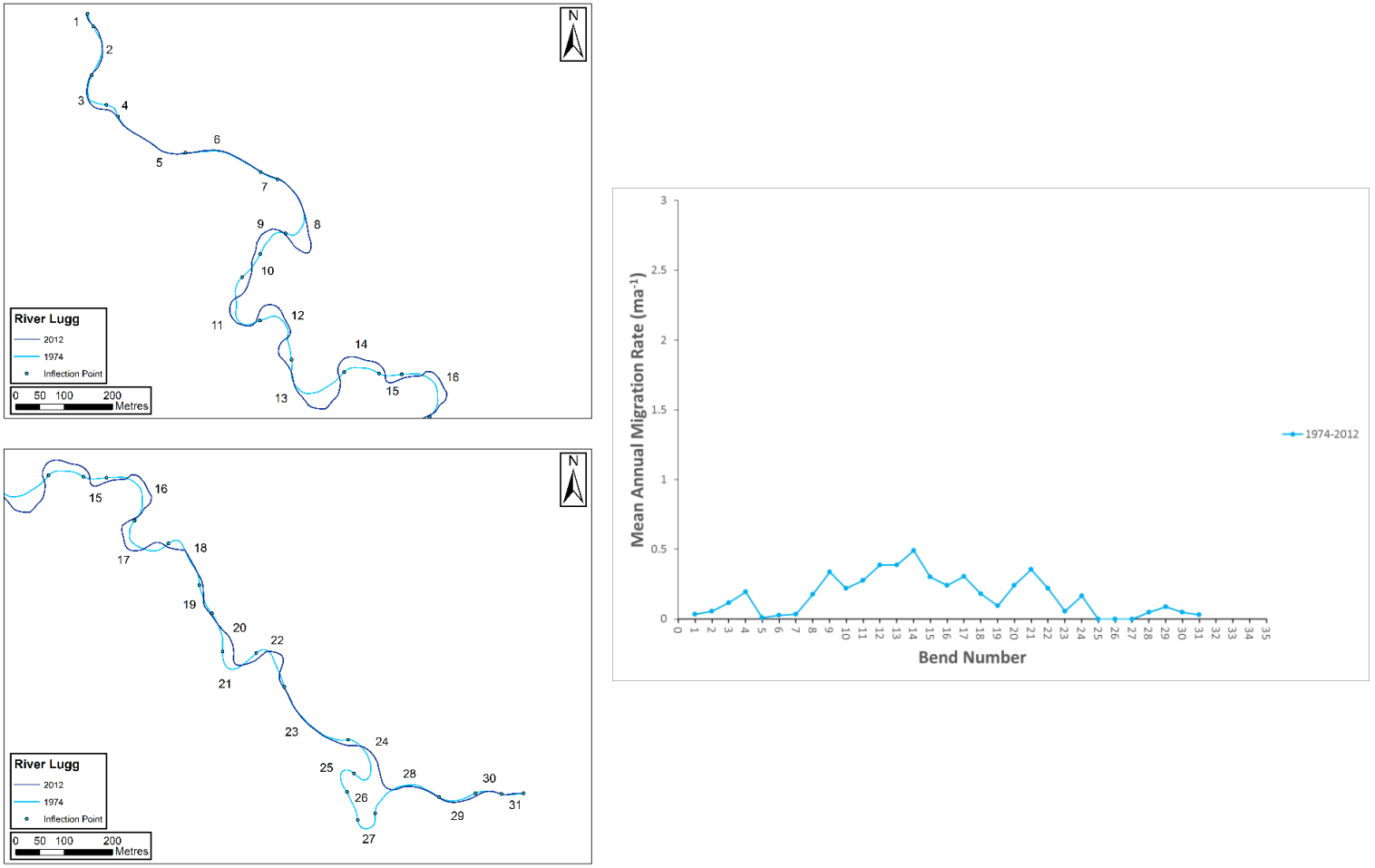

Figure 4.28. Migration rates on Reach 4 of the River Lugg between 1974 and 2012

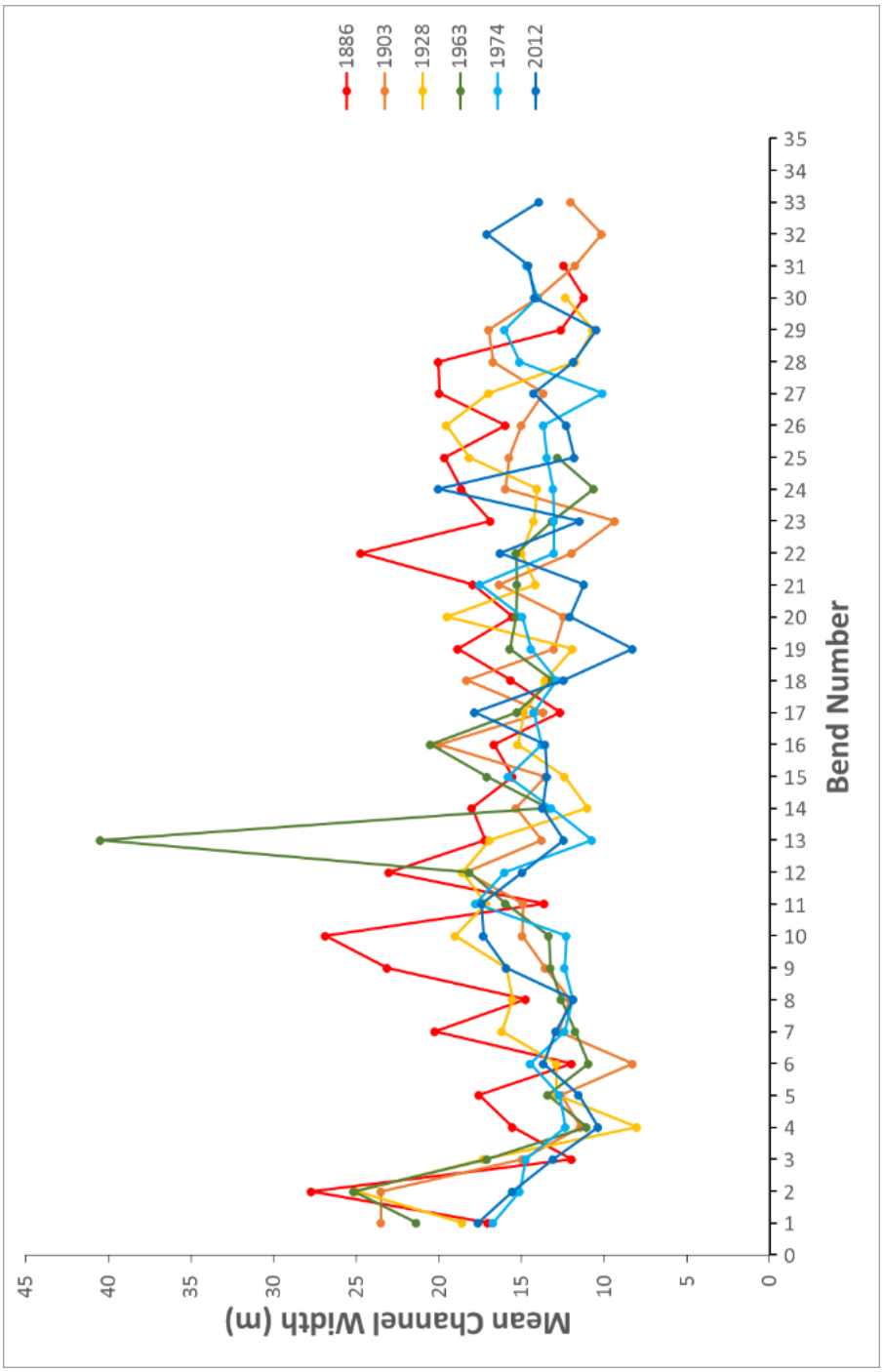

Figure 4.29. The mean channel width for Reach 4. Bend 13 has a much greater average width as described in the text

4.4.1.1.5. Reach Five

Reach Five is located just downstream of Reach Four, to the east of Kingsland. The River Lugg is still located within a wide, open floodplain with little natural constriction on the movement of the channel. The reach appeared free from human intervention for most of the study period, however, after a series of floods in the 1960s flood defences were built in the early 1970s (Jacobs, 2015). These defences took the form of embankments in the floodplain and a series of weirs. The reach was still included as it was active for most of the study period and to investigate the impact of the installation of the flood defences. The reach provides an example of planform evolution from a simple form to a complex, highly sinuous planform.

1886-1903: Between 1889 and 1903, the most active parts of the reach are located towards the start of the reach. The highest rates of lateral migration were measured in the first 10 bends of the reach. The mean annual erosion for the reach was $0.36ma^{-1}$ and the highest rate was $1.49ma^{-1}$ measured on bend 9.

1903-1928: Between 1903 and 1928, the mean annual rate of erosion was lower ($0.26ma^{-1}$ compared to $0.36ma^{-1}$), with bends 8-11 cutoff during this period. Further downstream, bends 17 to 28 started to grow across the floodplain and develop a more complex planform and the migration rate increased compared to the previous period.

1928-1963: The mean annual erosion rate increased during this period to $0.41ma^{-1}$. One cutoff did occur on bend 11, when the channel reoccupied a section of the channel that had been abandoned in 1903.

1963-1973: Between 1963 and 1973, there are major changes along the entire length of the reach. The average migration rate for the reach is $1.29ma^{-1}$, with nearly all bends showing signs of migration or experiencing a cutoff. A total of seven bends were cutoff during this period, and highest erosion rate was $3.1ma^{-1}$ measured on bend 6. There are significant changes in planform both upstream and downstream of the cutoffs.

1973-2012: Between 1973 and 2012, most of the bends become stable and experience low amounts of lateral change, especially in the previously active section on bends 20-30. Three cutoffs occur during this period, but it is not possible to determine whether these occurred naturally or were artificially performed during the construction of the flood defences. There are isolated bends that continue to migrate during this period, but the majority of the bends remain stable. The mean migration rate decreased to $0.23ma^{-1}$.

The channel width varies greatly between the different bends within the same reach. The range of channel widths for different bends on the 1963 map is over 20m (31.7m at bend 6 and 9.9m at bend 19).

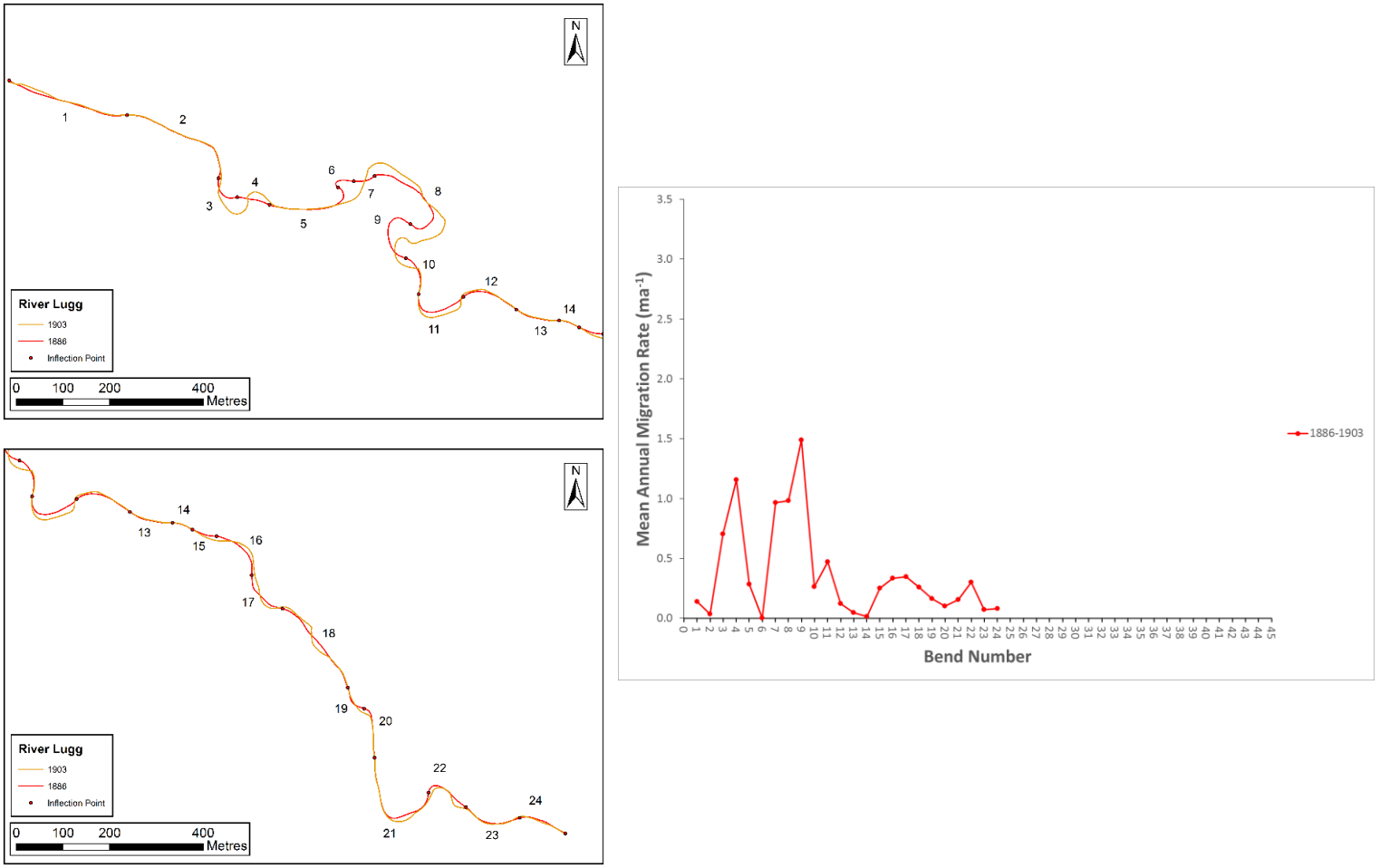

Figure 4.30. Migration rates on Reach 5 of the River Lugg between 1886 and 1903

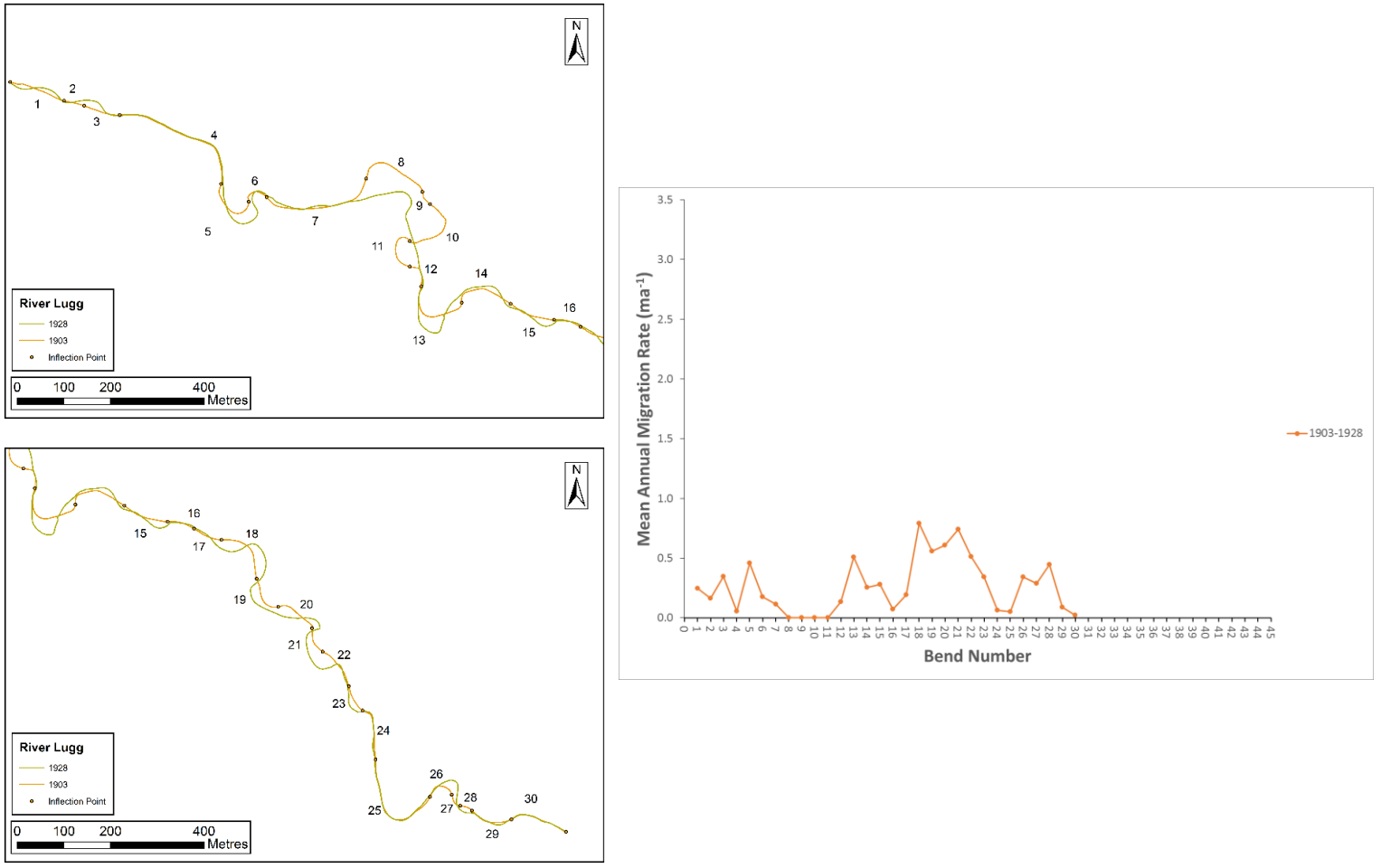

Figure 4.31. Migration rates on Reach 5 of the River Lugg between 1903 and 1928

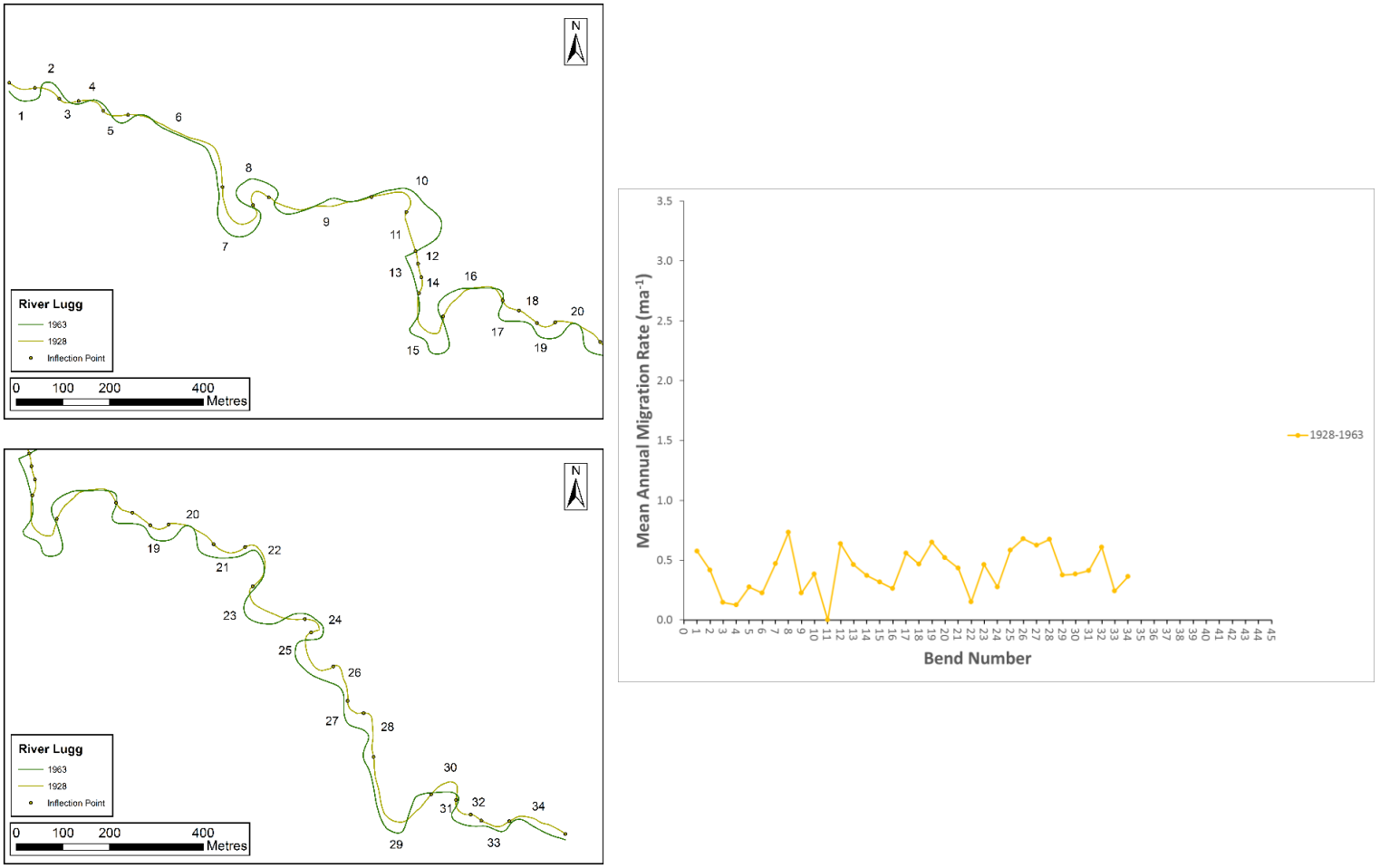

Figure 4.32. Migration rates on Reach 5 of the River Lugg between 1928 and 1963

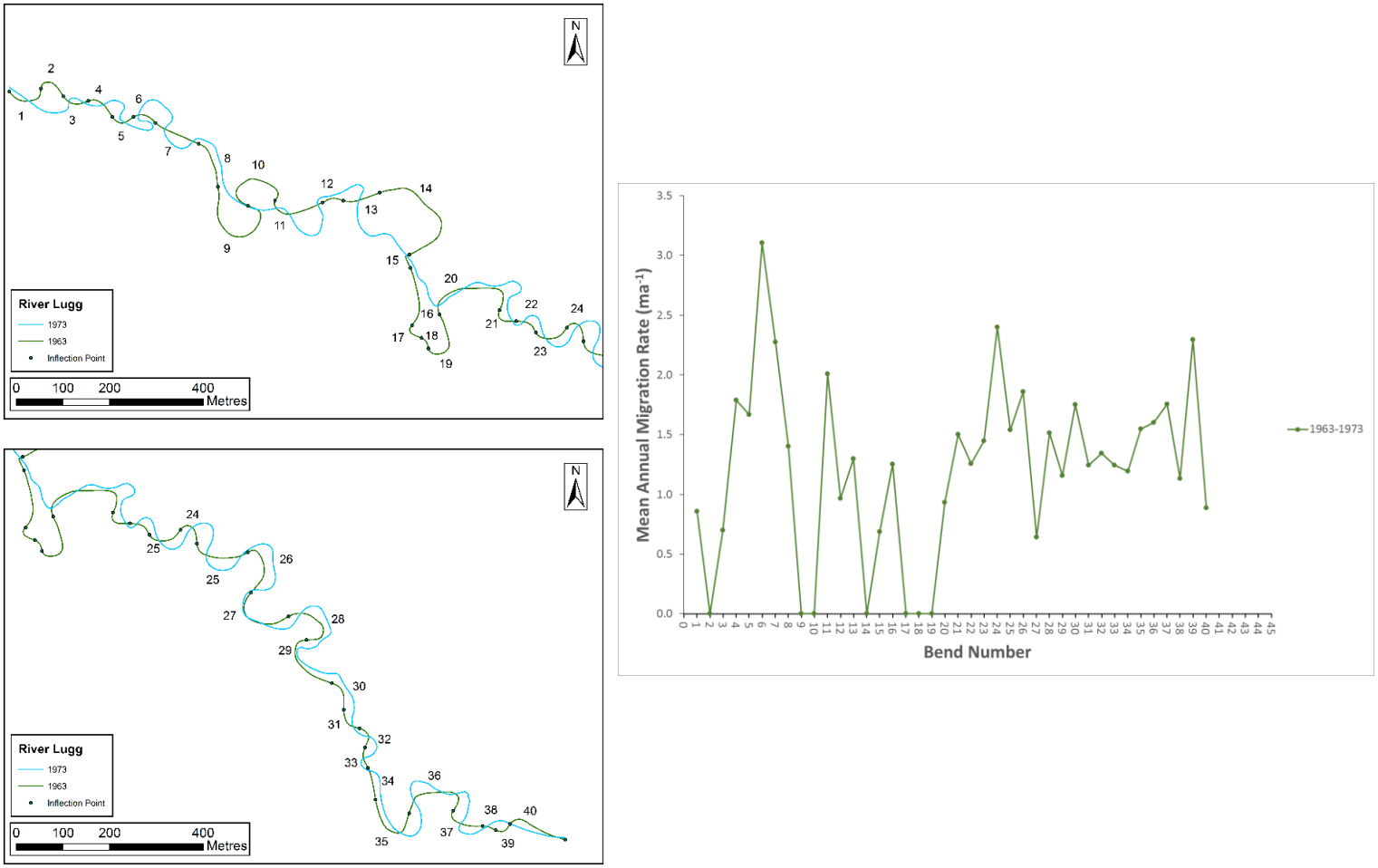

Figure 4.33. Migration rates on Reach 5 of the River Lugg between 1963 and 1973

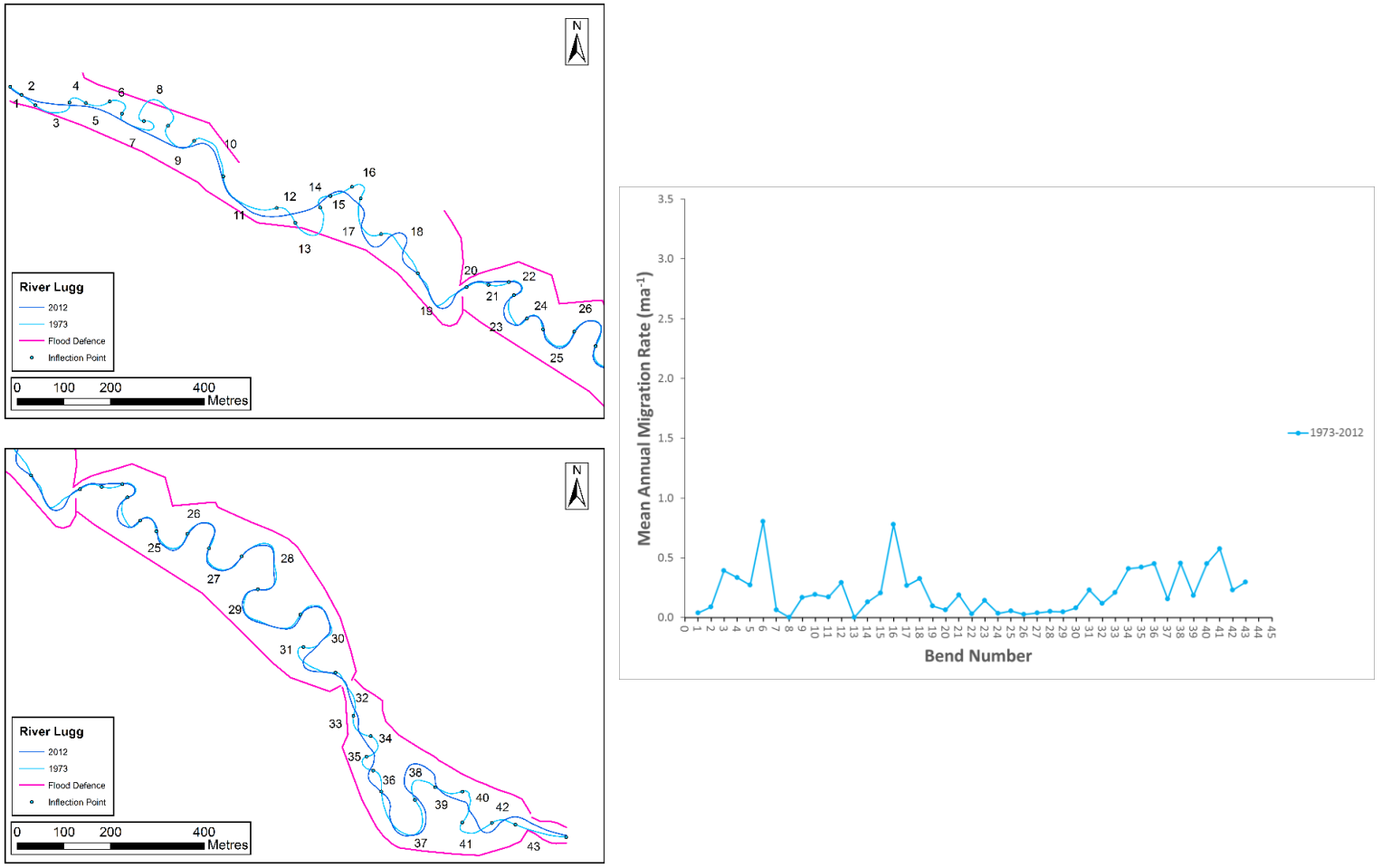

Figure 4.34. Migration rates on Reach 5 of the River Lugg between 1973 and 2012

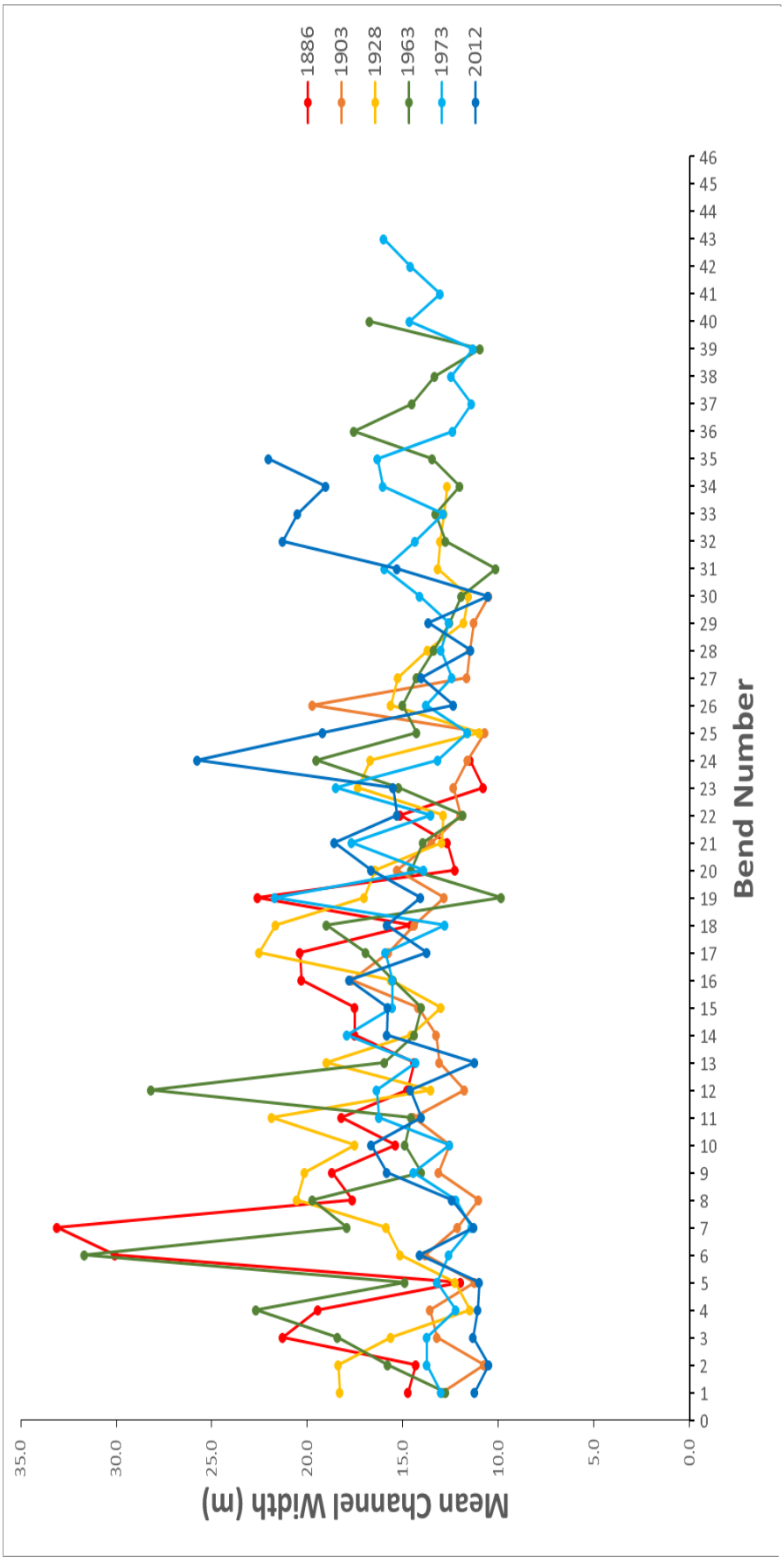

Figure 4.35. Mean channel width for each bend

4.4.1.2. River Arrow Reaches

The River Arrow was split into three separate reaches, avoiding a section of the river that travels through the large village of Eardisland and a section further downstream where the river has anabranched into three stable channels and is no longer a single thread meandering channel. The reaches range in length from 3.1km to 4.2km. The highest mean erosion rates were measured in the 1964-1974 period, which also corresponded to the highest variance between the different bends on the reach. The mean erosion rates for reaches 1, 2 and 3 during this period are $0.85ma^{-1}$, $1.44ma^{-1}$ and $0.69ma^{-1}$ respectively. The maximum erosion outside of this period is $0.27ma^{-1}$ on reach 2, between 1928 and 1964. The mean migration rate for all the periods, excluding the 1964-1974 period was $0.14ma^{-1}$, compared to $0.31ma^{-1}$ when the 1964-1974 period is included. The mean channel width for the reaches decreases downstream, decreasing from 12.2m to 10.7m. The mean channel width for reach 3 was consistent through time, while the mean channel width decreased for reach 1 and 2 between 1886 and 1904, before increasing to 1964. Reach 1 then shows a decrease of mean channel width between 1964 and 1974 from 12.8m to 10.5m, before increasing to 12.3m in 2012.

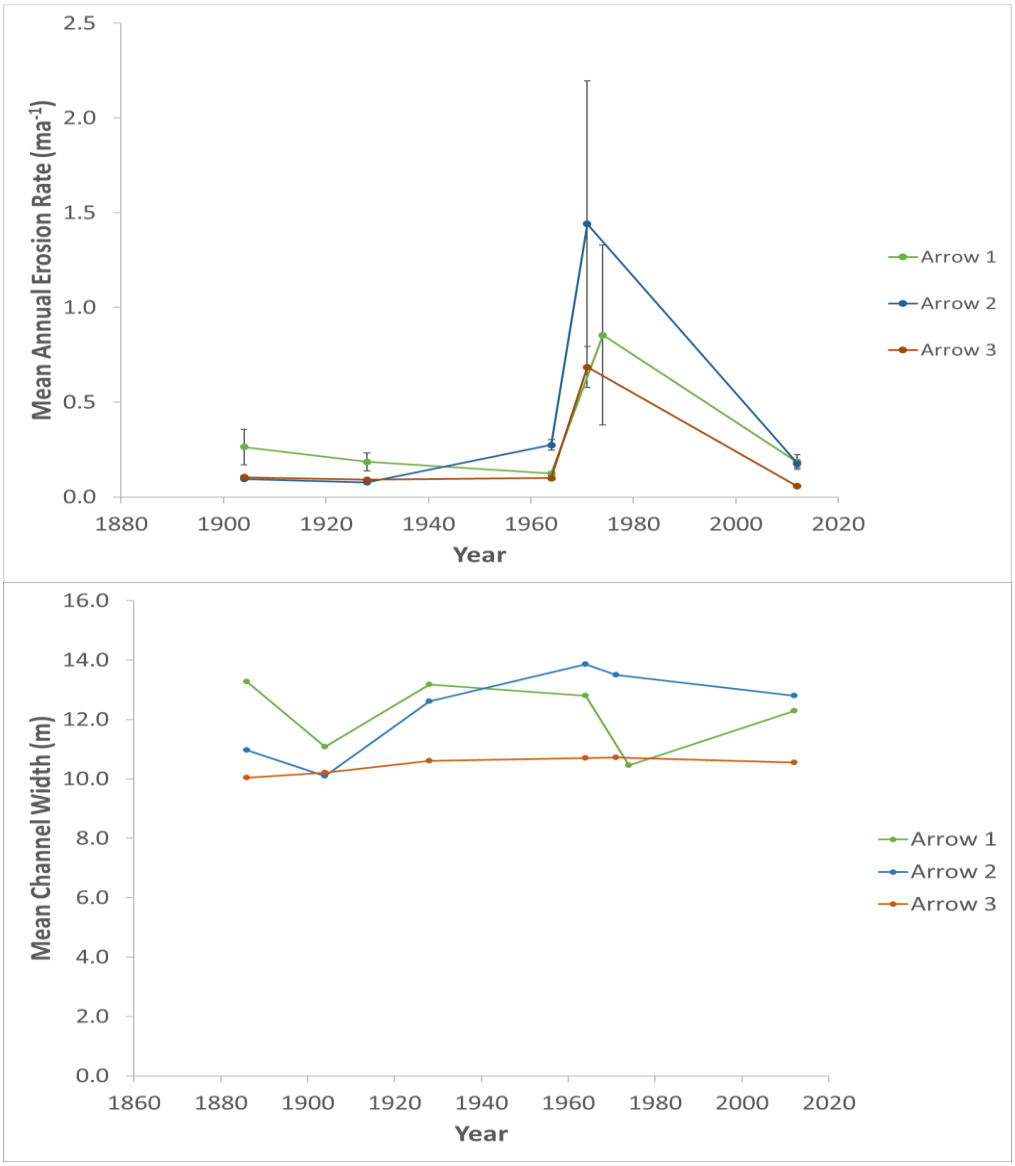

Figure 4.36. The mean migration rate and the mean channel width for the three River Arrow reaches.

4.4.1.2.1. Reach One

Reach one on **Error! Reference source not found.** is a 4.2km section of the River Arrow, located between the Pembridge and Eardisland. The floodplain is wide, and the majority of bends are free to migrate, with the exception of bends 3-5, which are restricted by the valley side.

1886-1904: The mean migration rate for 1886-1904 was 0.26ma^{-1}, with most of the change occurring towards the middle of the reach. A cutoff occurred on bend 32, and there is evidence of erosion occurring both upstream and downstream of the cutoff. Bend 33 immediately downstream became compound and split into three separate bends, with the highest rates of erosion measured on bend 34 at 1.37ma^{-1}. The upstream section of the channel remains stable during this period.

1904-1928: The mean erosion rate was 0.19ma^{-1} during this period, with a maximum rate of 0.88ma^{-1} measured on bend 24, with the bend retracting from the apex. Bend 32 experienced a further cutoff with further erosion occurring downstream on bends 33 and 34. The upstream section of the river, between bends 1 and 20, remained stable during this period. A complex series of changes occurred on bends 35 and 36, with bend 35 growing to have a very tight apex towards the channel downstream, but not cutting off in the 1904-1928 period.

1928-1964: The mean erosion rate during this period was 0.12ma^{-1} and the maximum was 0.37ma^{-1} measured on bend 36. Bend 36 and 38 both migrated upstream during this period. A large loop, bend 33, is cutoff during this period with erosion occurring downstream of the cutoff, but no major changes upstream. In this period there is erosion in the upstream section, with bends 16 and 17 migrating downstream.

1964-1974: During this period the mean annual erosion rate increased to 0.85ma^{-1} and the maximum rate was 2.97ma^{-1} measured on bend 39. During this period, five cutoffs occur including two large neck cutoffs on bends 17 and 26. Bends 21, 22 and 23 show an increased rate of erosion, changing from being mainly stable to migrating at 1.81ma^{-1}, 0.84ma^{-1} and 0.96ma^{-1} respectively. Bend 32 grows across the floodplain after the cutoff that occurred in the 1928-1964 period and has developed into three separate bends by 1974. Downstream of the cutoff at bend 32 it appears that two chute cutoffs have occurred on bends 35 and 37.

1974-2012: The mean annual erosion during this period decreases to 0.18ma^{-1} for all of the bends in the reach, with a maximum rate of 0.94ma^{-1} on bend 25. A series of cutoffs have

occurred on bends 27, 28 and 29, with three large loops experiencing a neck cutoff. Erosion occurred upstream and downstream of the cutoffs. Bend 39 had increased erosion on the upstream side of the bend and had developed into three separate bends. There was some minor erosion in the upstream part of the reach, between bends 7 and 16.

The mean channel width for each bend varies along the reach and between the different periods. The mean channel width ranged from 5.33m (Bend 37, 1974) to 23.65m (Bend 43, 1886).

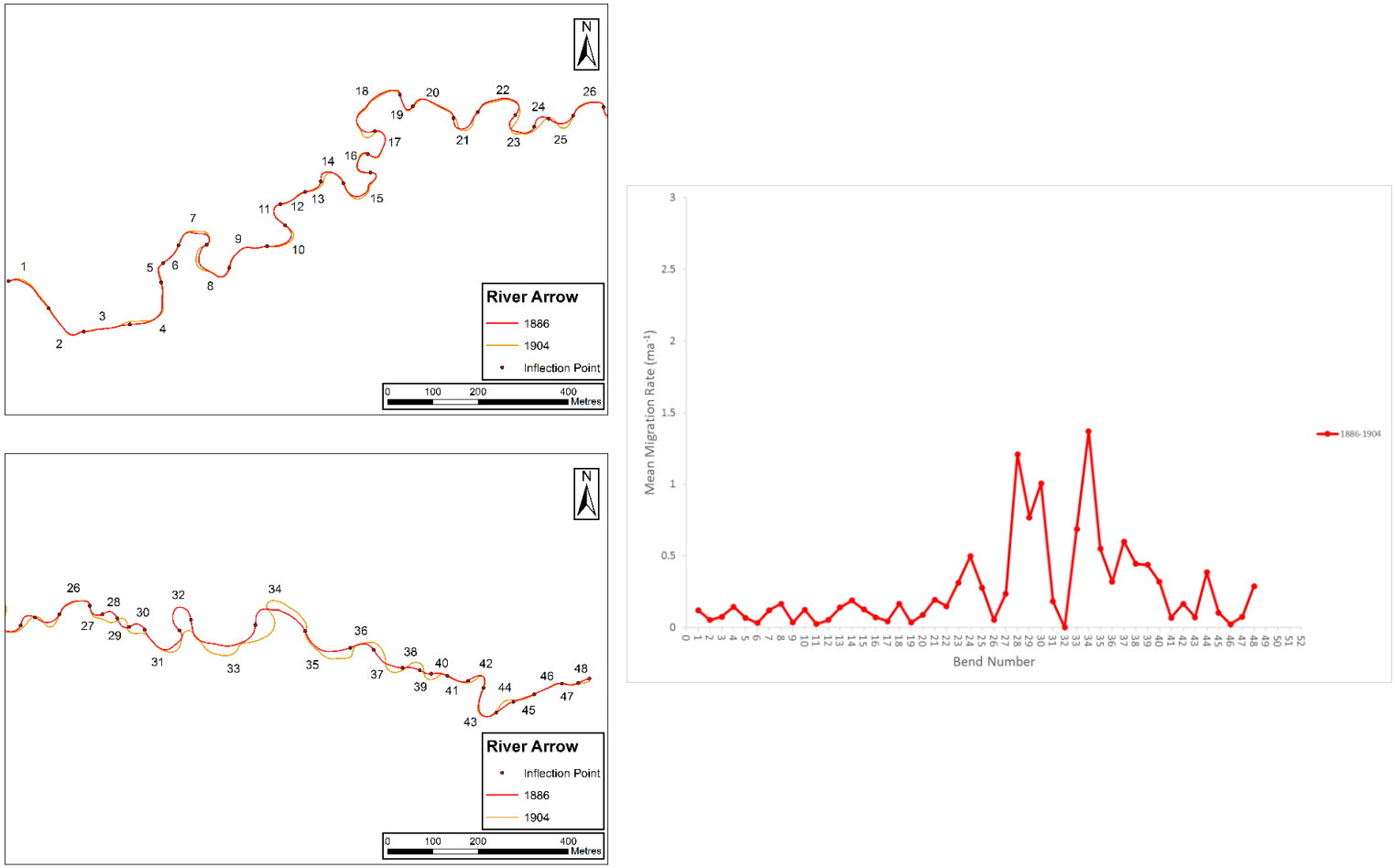

Figure 4.37. Migration rates on Reach 1 of the River Arrow between 1886 and 1904

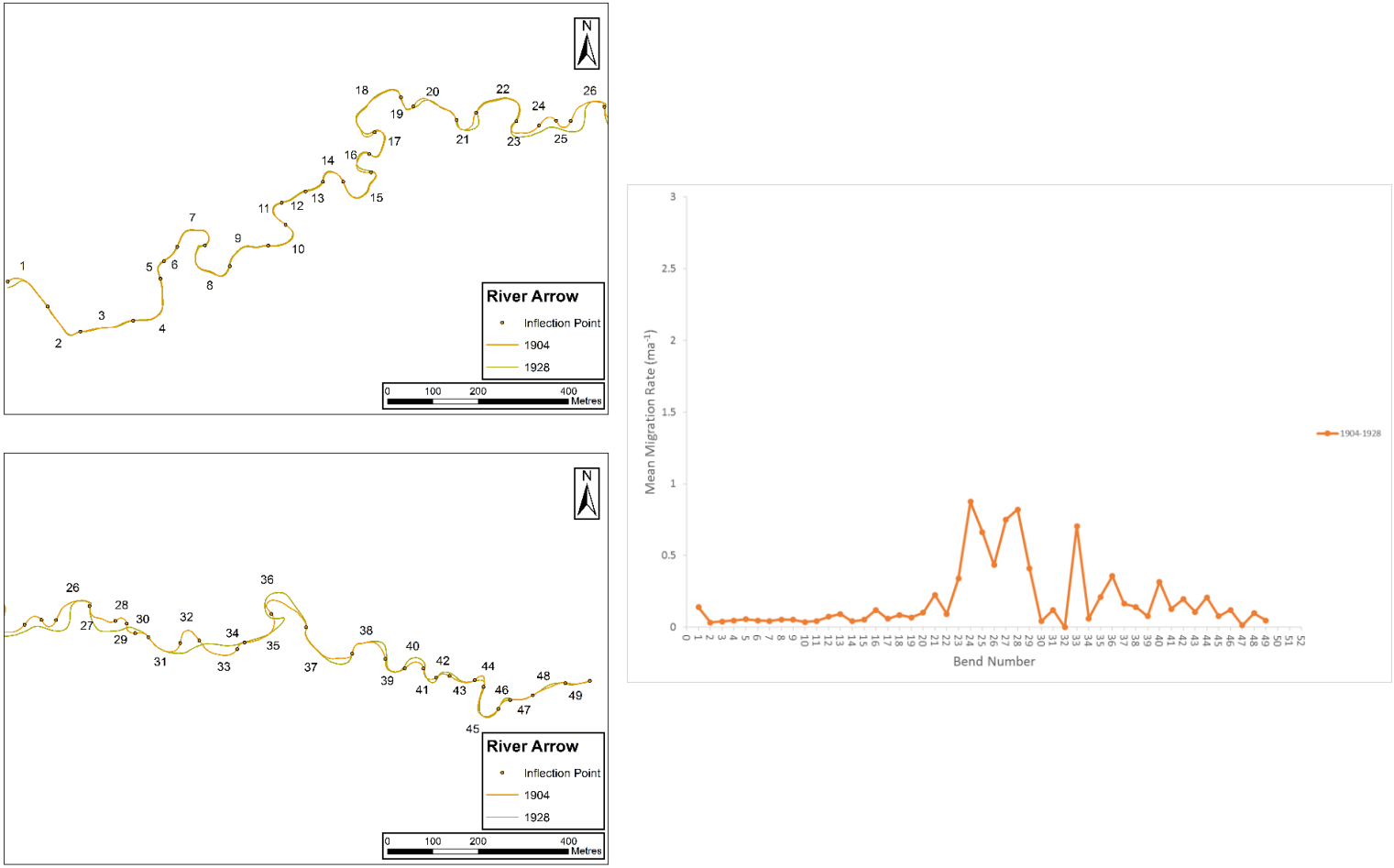

Figure 4.38. Migration rates on Reach 1 of the River Arrow between 1904 and 1928

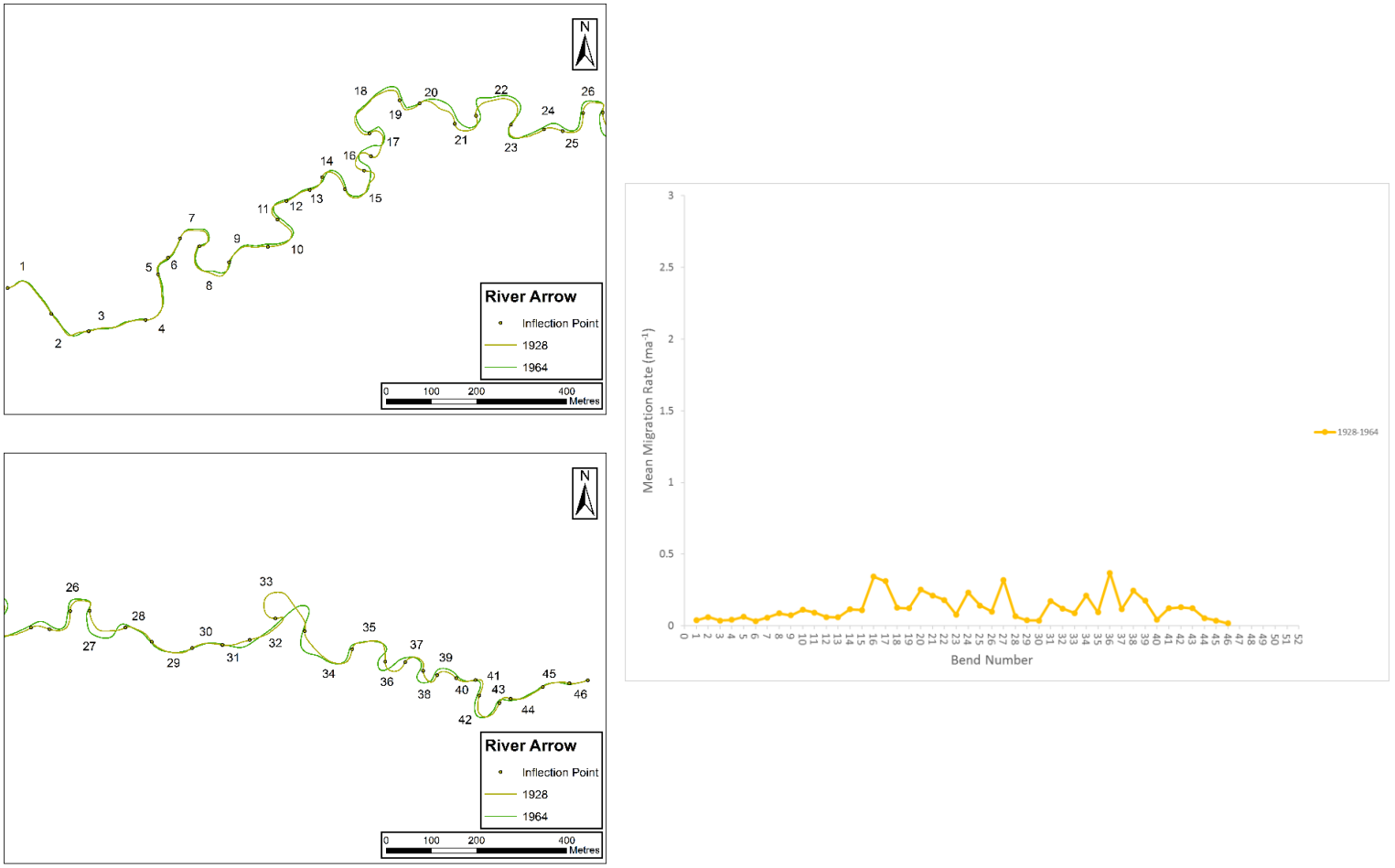

Figure 4.39. Migration rates on Reach 1 of the River Arrow between 1928 and 1964

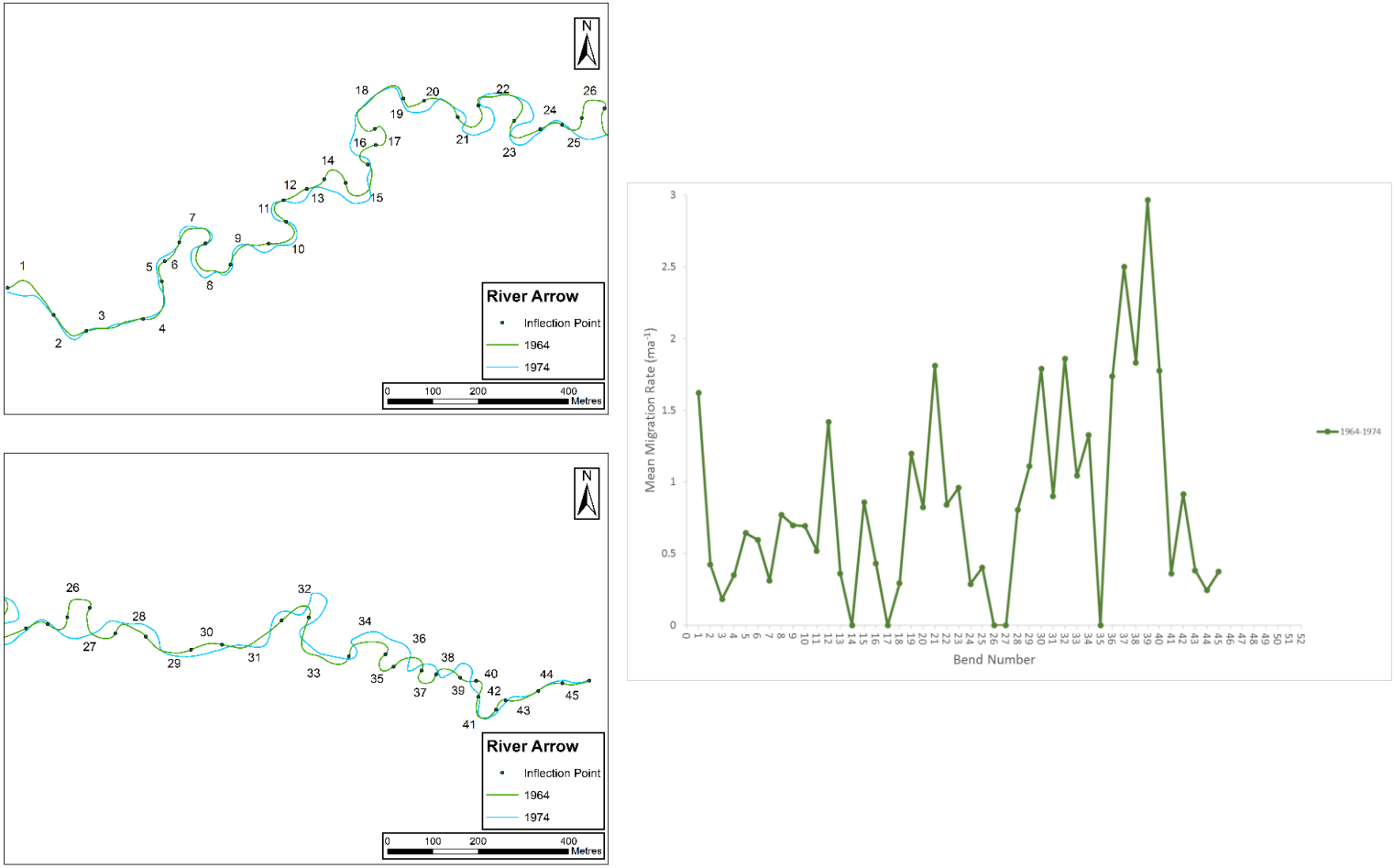

Figure 4.40. Migration rates on Reach 1 of the River Arrow between 1964 and 1974

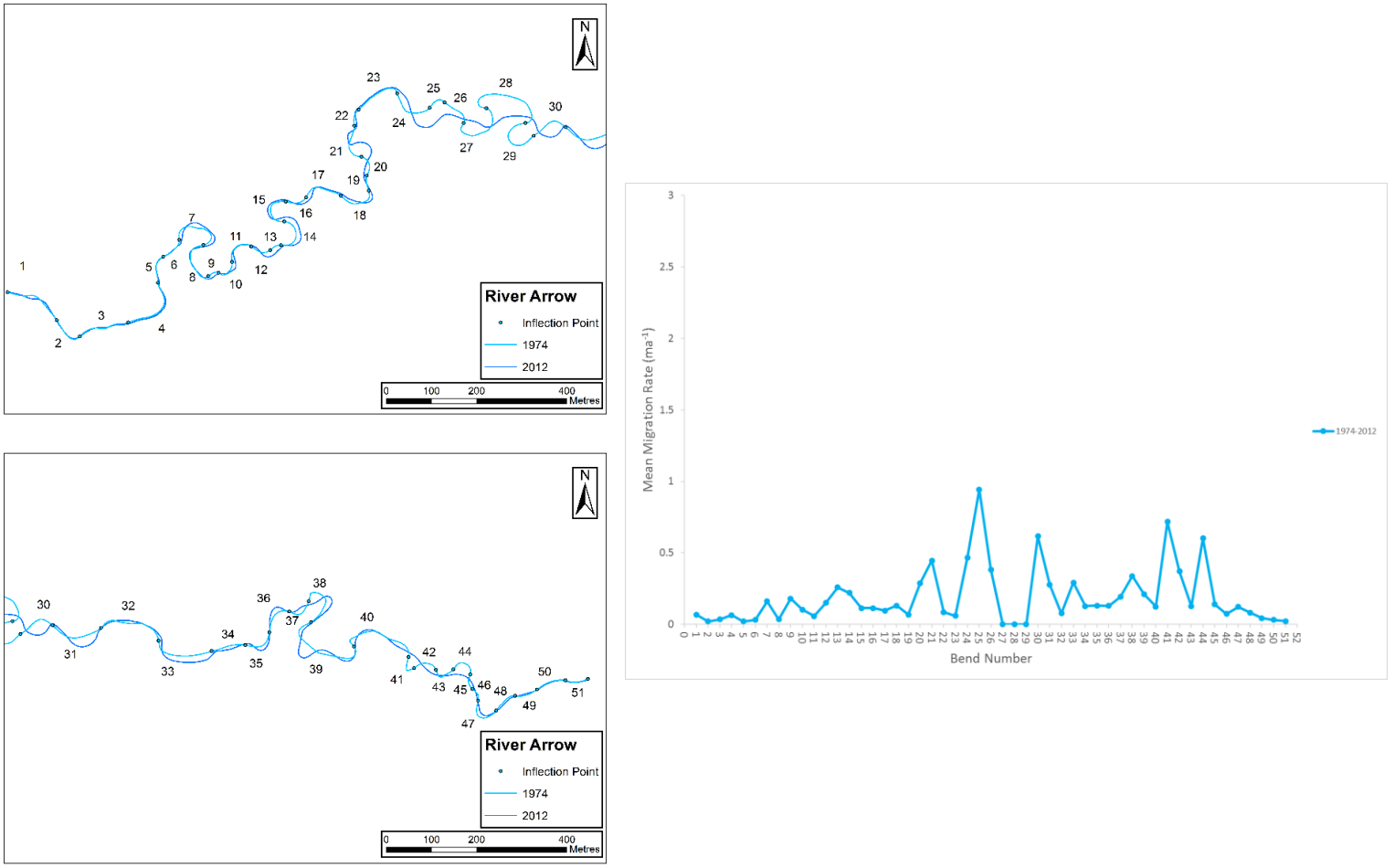

Figure 4.41. Migration rates on Reach 1 of the River Arrow between 1974 and 2012

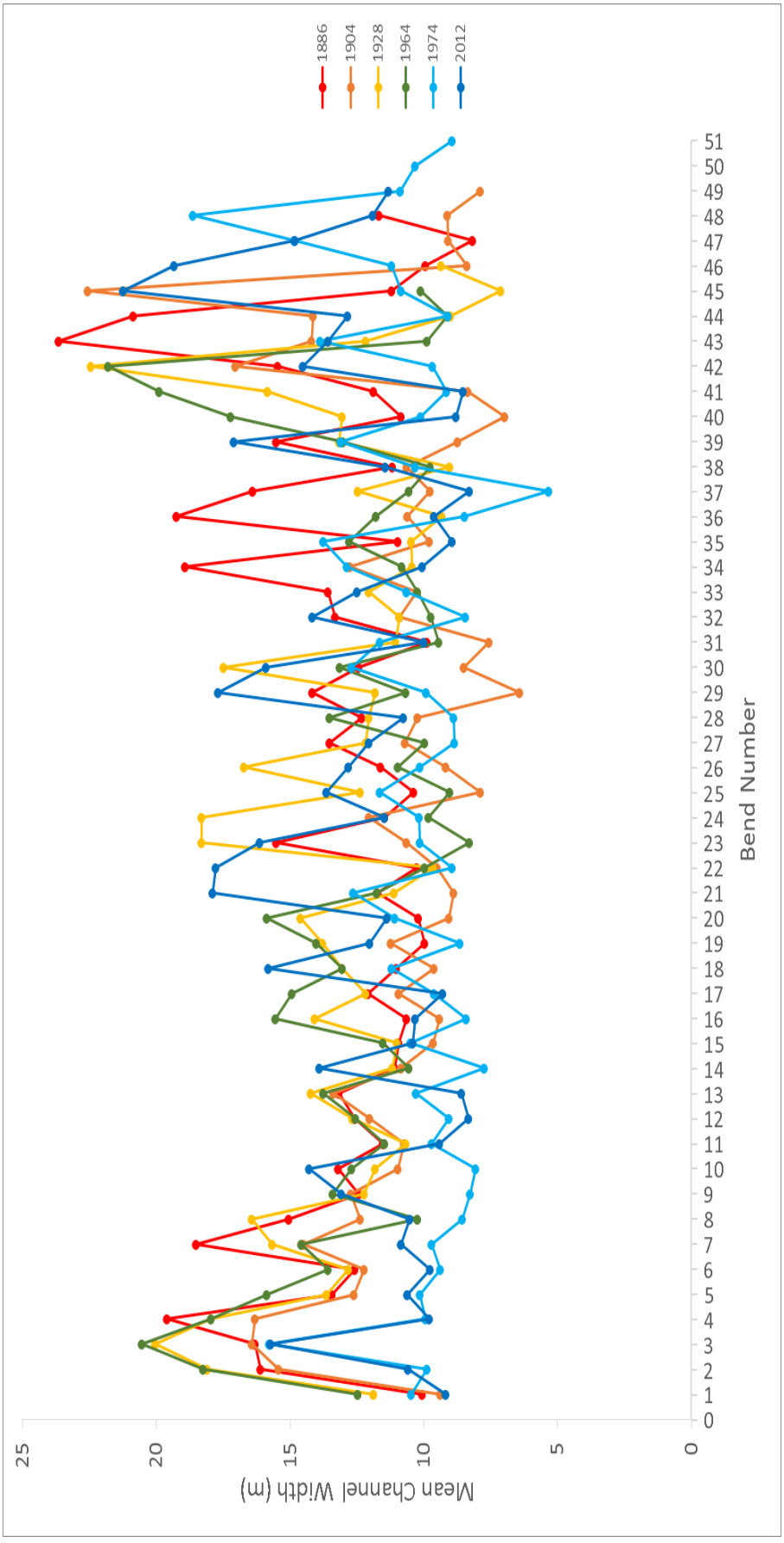

Figure 4.42. The mean channel width for each individual bend

4.4.1.2.2. Reach Two

Reach two is located between Eardisland and Monkland (see **Error! Reference source not found.**) on a section of floodplain that is wide and there is no visible human intervention preventing the movement of the channel. The channel length is 3.5km for this reach.

1886-1904: Between 1886 and 1904, there is very little change along the entire reach. The mean annual erosion rate was 0.10ma^{-1} and the maximum rate was 0.25ma^{-1}. A small chute cutoff occurred on bend 26, but the bends around the cutoff remain stable during this period.

1904-1928: The mean annual erosion rate remains low between 1904 and 1928 at 0.08ma^{-1} with a maximum rate of 0.49ma^{-1} measured for bend 1. There are no cutoffs during this period and small amounts of downstream migration on a limited number of bends such as bend 6, 13 and 39.

1928-1964: There appears to be significant morphological change occurring along the entire reach between 1928 and 1964. The mean annual erosion is 0.27ma^{-1} and the maximum rate is 0.76ma^{-1}. However, despite most of the bends appearing to migrate during this period, the shape of the bends did not change. The map used for the 1964 data was a lower scale, 1:10560 compared to 1:2500 for the other dates and the uncertainty caused by this difference appears to have a high impact for this particular reach.

1964-1971: Substantial morphological change occurred again between 1964 and 1971, with a mean annual erosion rate of 1.44ma^{-1} and a maximum rate of 4.39ma^{-1} measured for bend 8! The uncertainty associated with the different map resolutions also applied to this period and the short period between the two map dates, only seven years, exaggerated the annualised rate of erosion. There are, however, changes in the morphology of the bends, with two chute cutoffs occurring on bends 40 and 47, which indicate that there is morphological change occurring during this period and changes are not only due to the uncertainties in the source data.

1971-2012: There continues to be morphological change for most of the reach between 1971 and 2012. The mean annual erosion rate for the reach is 0.18ma^{-1} and the maximum rate is 0.71ma^{-1}. Two large neck cutoffs occurred towards the end of the reach along with two smaller chute cutoffs on bends 9 and 32.

The mean channel width for each bend varies along the reach. The maximum range between consecutive bends was nearly 15m for bends 53 and 54 in 2012.

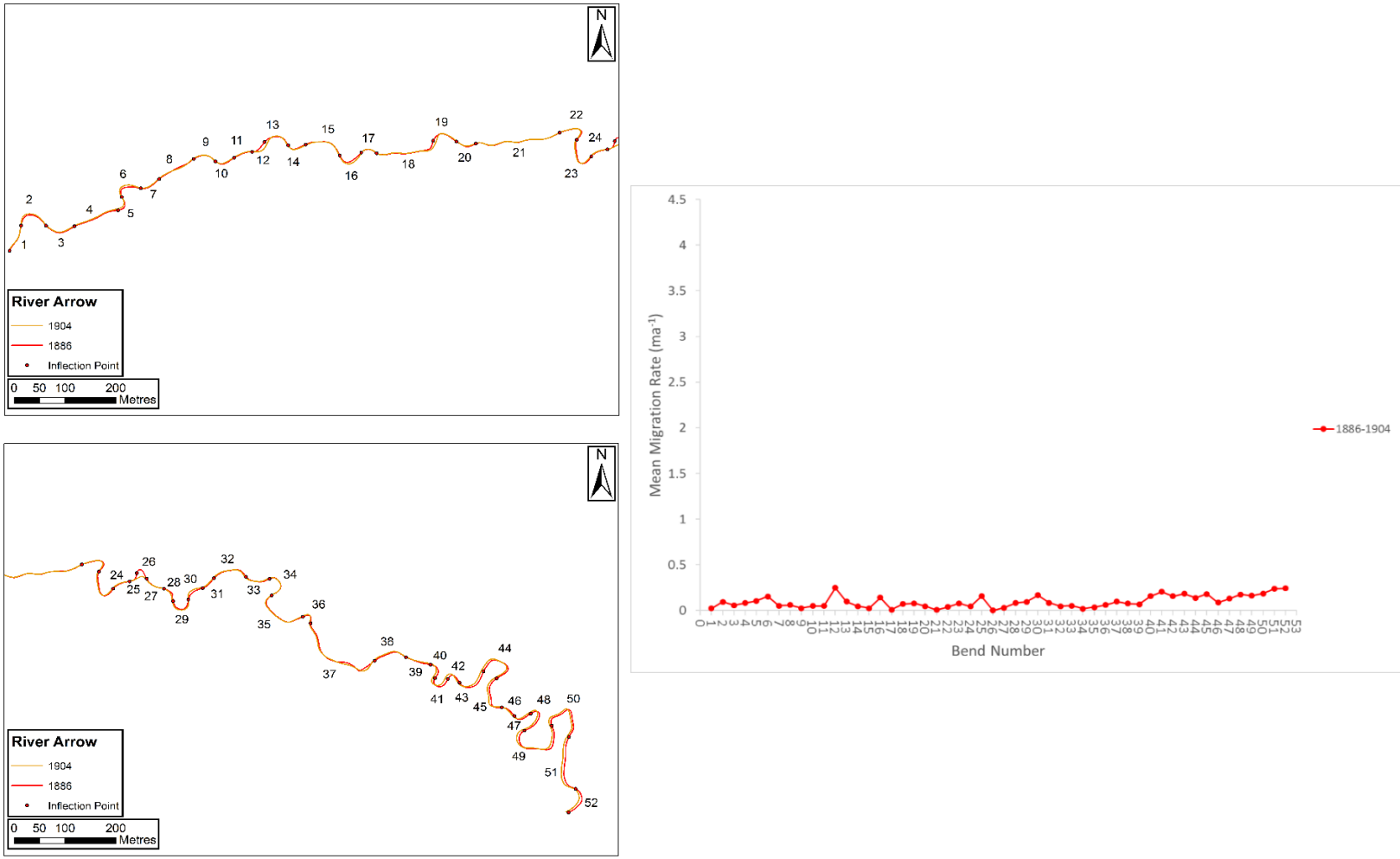

Figure 4.43. Migration rates on Reach 2 of the River Arrow between 1886 and 1904

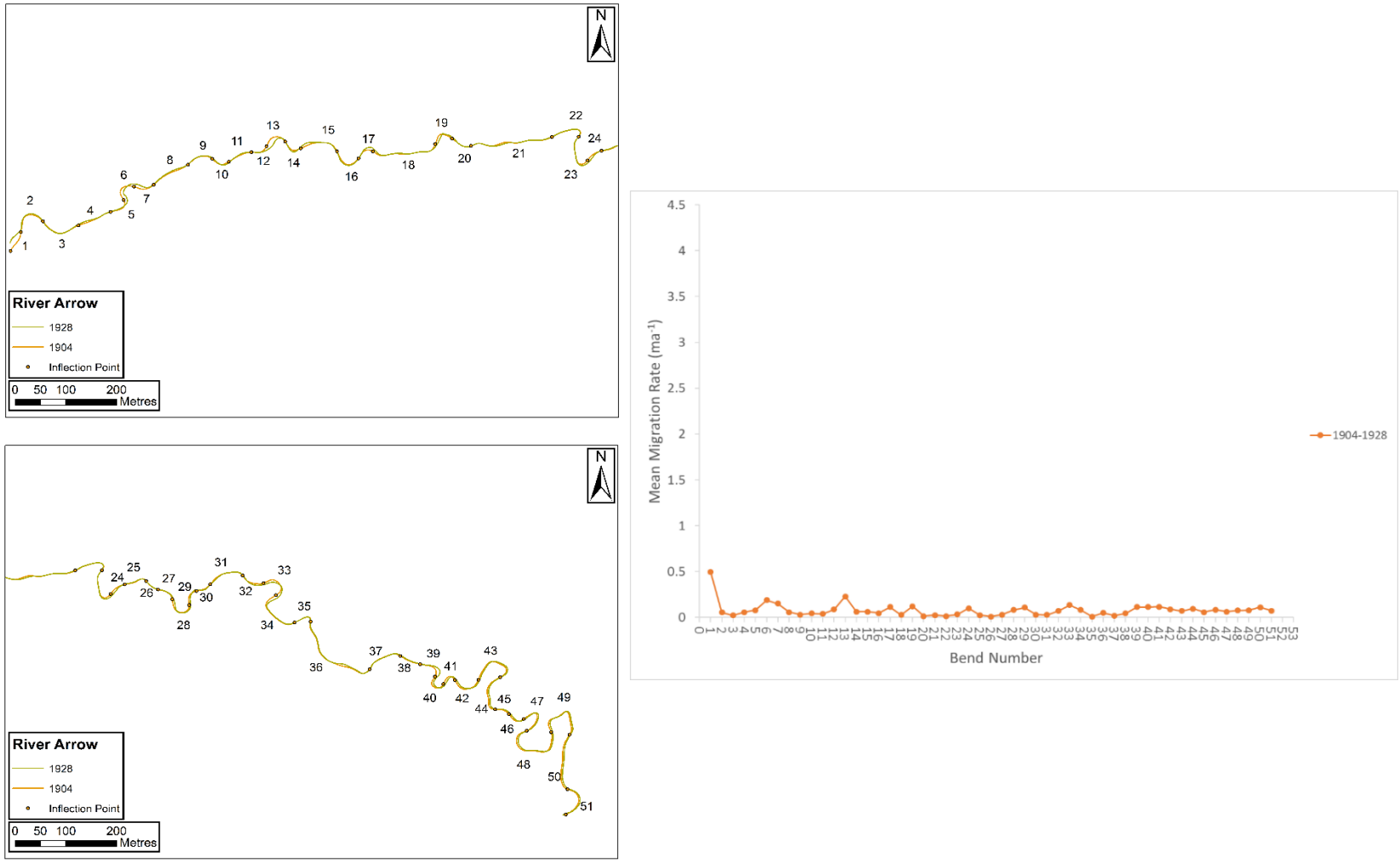

Figure 4.44. Migration rates on Reach 2 of the River Arrow between 1904 and 1928

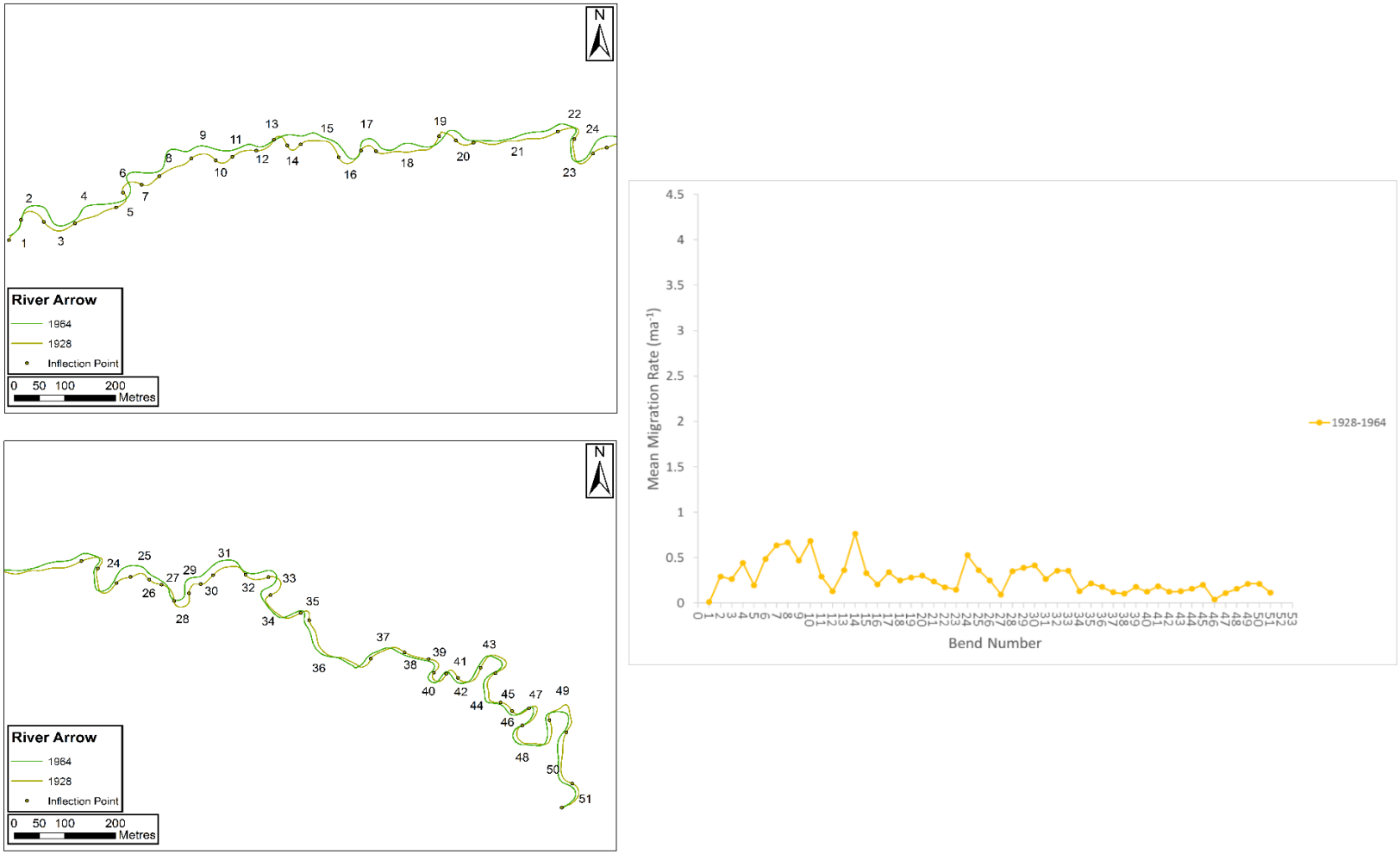

Figure 4.45. Migration rates on Reach 2 of the River Arrow between 1928 and 1964

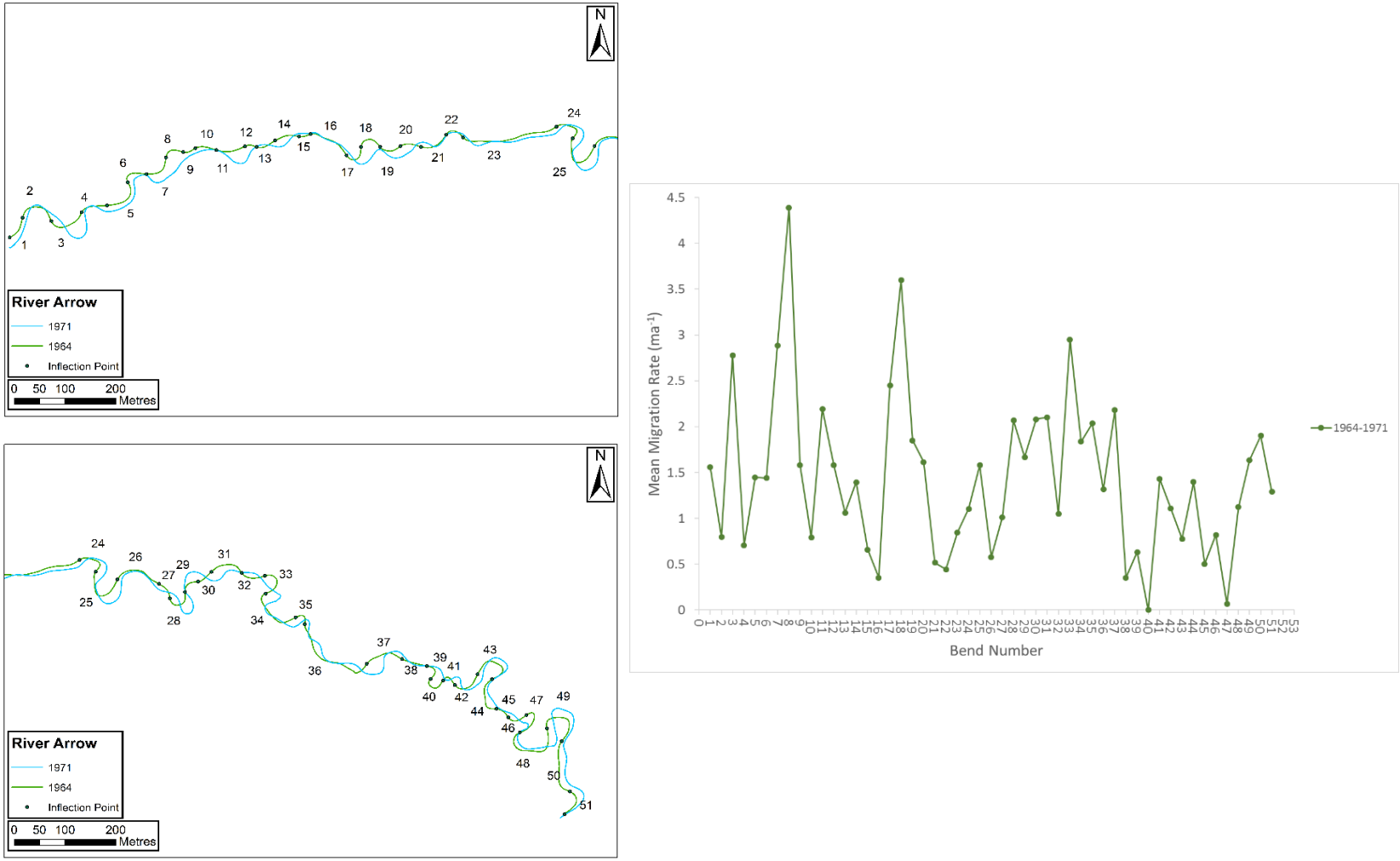

Figure 4.46. Migration rates on Reach 2 of the River Arrow between 1964 and 1971

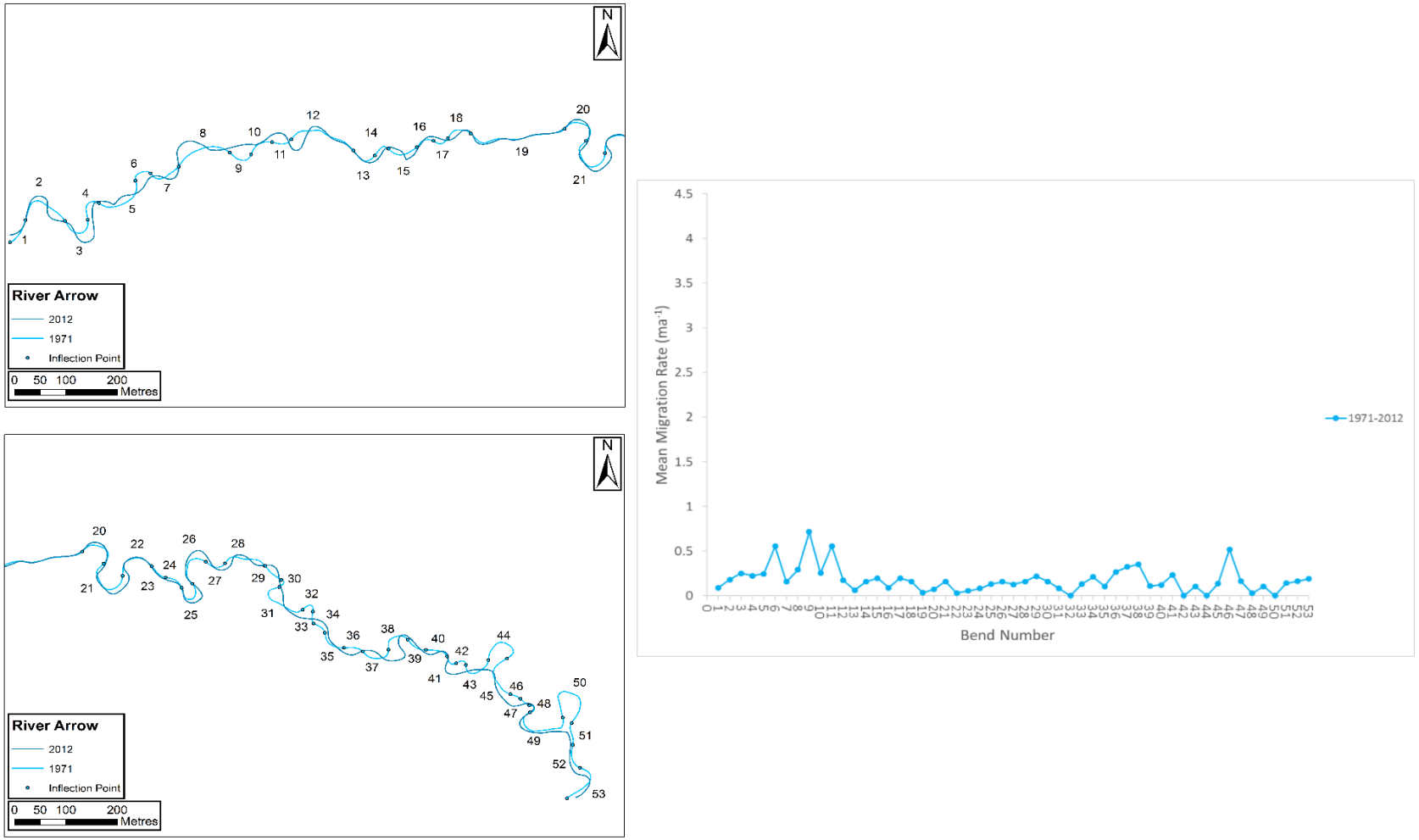

Figure 4.47. Migration rates on Reach 2 of the River Arrow between 1971 and 2012

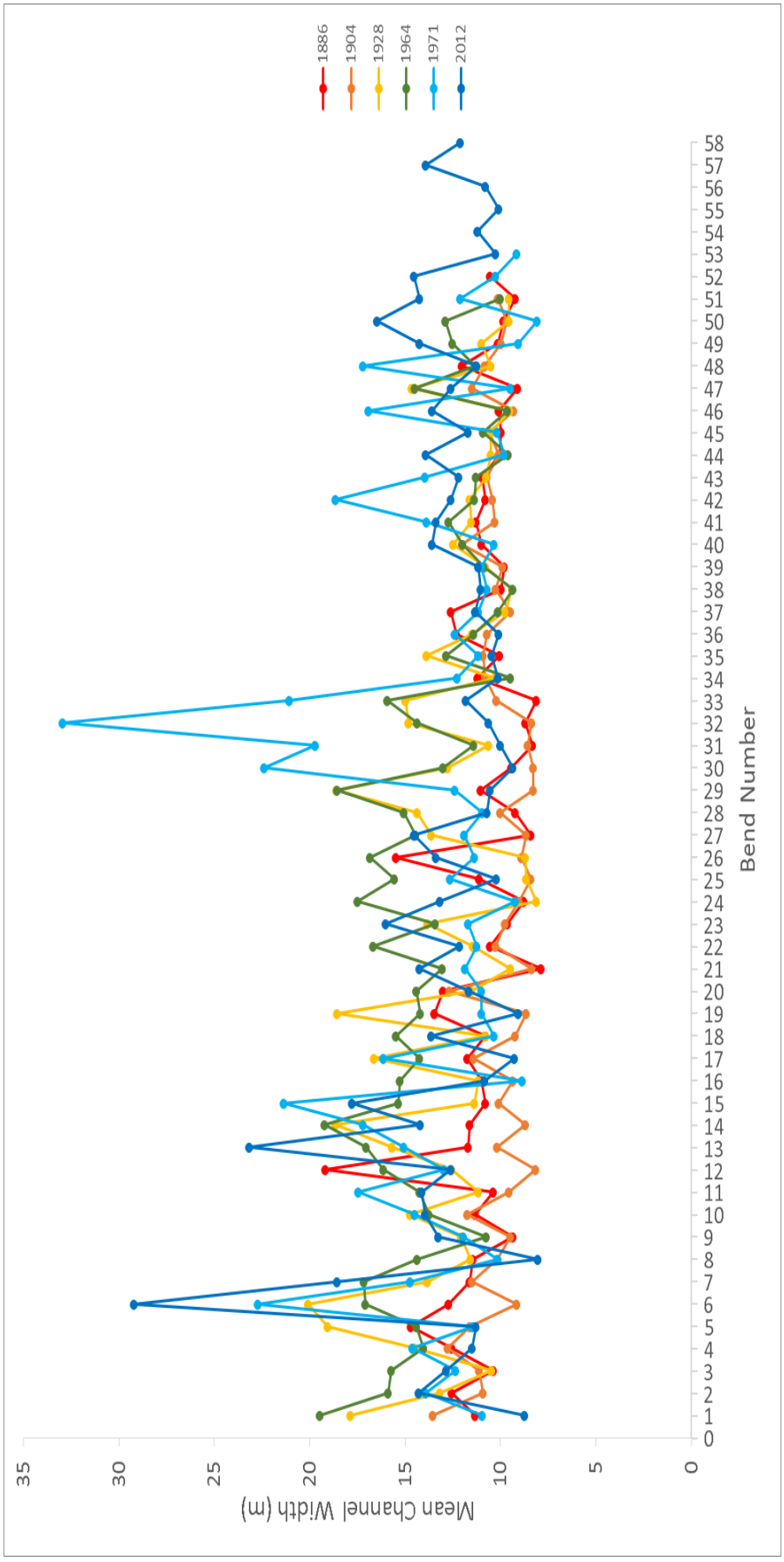

Figure 4.48. The mean channel width of each individual bend

4.4.1.2.3. Reach Three

Reach Three (see **Error! Reference source not found.**) is located between Monkland and the confluence with the River Lugg. The river is mainly unrestricted through the reach, with the exception of bend 14, which has a bridge located in the middle of the bend.

1886-1904: The mean annual erosion rate during this period was 0.10ma^{-1} and the maximum rate was 0.29ma^{-1}. All of the bends are stable during this period.

1904-1928: The mean annual erosion rate was 0.09ma^{-1} during this period and the maximum rate was 0.16ma^{-1}. The bends have remained stable and there has been very little morphological change.

1928-1964: The mean annual erosion rate for the reach remains low, at 0.10ma^{-1}, with a maximum of 0.22ma^{-1} measured. The changes in the channel position seem to be caused by the changing scale between the 1928 map and the 1964 map.

1964-1971: Between 1964 and 1971, the activity on the reach has increased. The mean annual erosion rate was 0.69ma^{-1} for all of the bends and the maximum rate was 1.96ma^{-1} measured on bend 14. A small chute cutoff occurred on bend 8. Bend 28 and 29 showed an increase in the mean annual rate of erosion, with both bends migrating downstream.

1971-2012: Between 1971 and 2012, most of the bends in the reach become stable again and the mean annual erosion rate is 0.06ma^{-1}. However, bends 26 and 27 continue to erode across the floodplain. Bend 26 has become double headed and eroded faster in the upstream direction and the highest rate of erosion, 0.24ma^{-1}, was measured on bend 27.

The mean channel width for each bend for the different periods is shown in Figure 4.54. The mean channel width is lower than the preceding reaches, despite the reach being further downstream. This is due to the channel bifurcating prior to the start of reach three and a smaller channel, known as the Little Arrow taking some of the flow from the main channel.

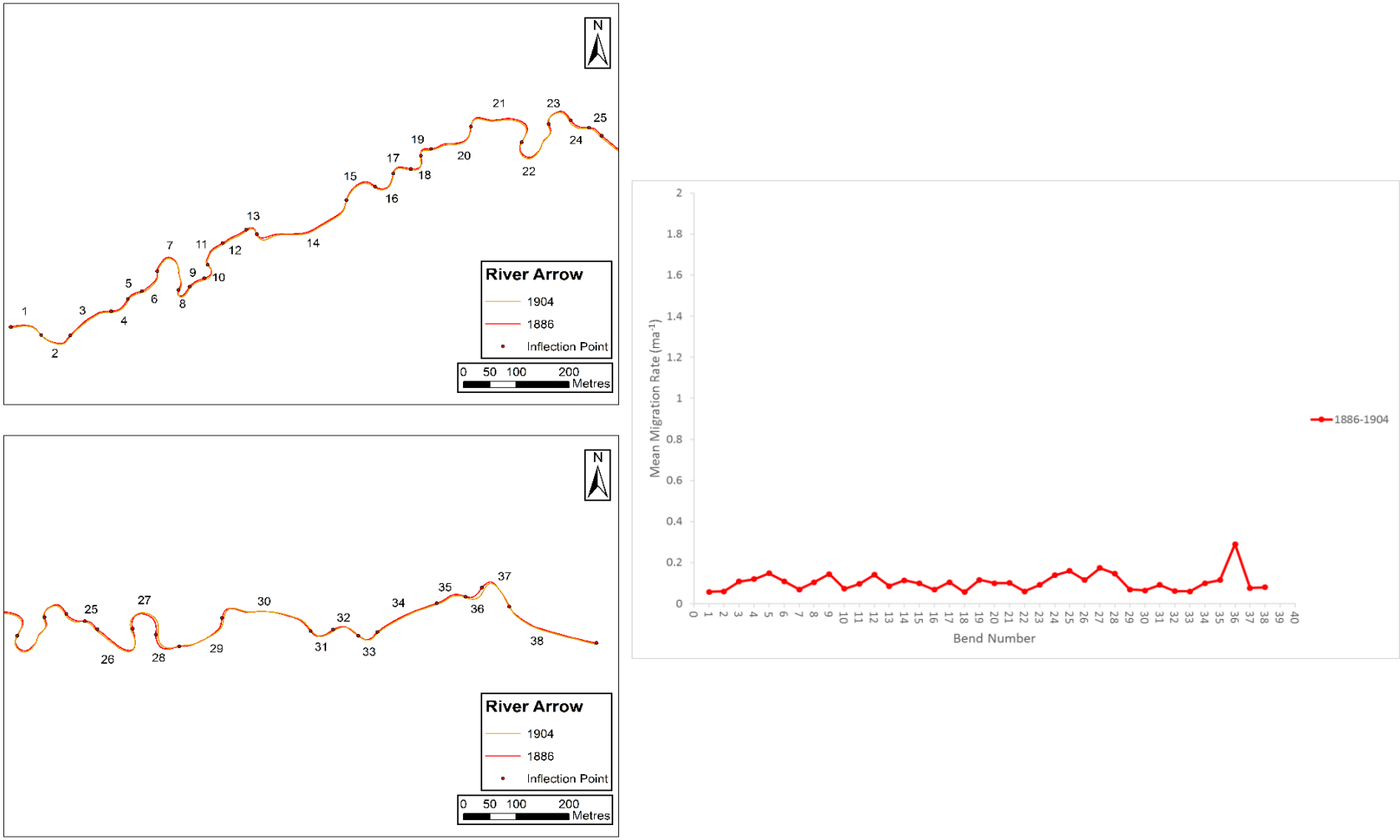

Figure 4.49. Migration rates on Reach 3 of the River Arrow between 1886 and 1904

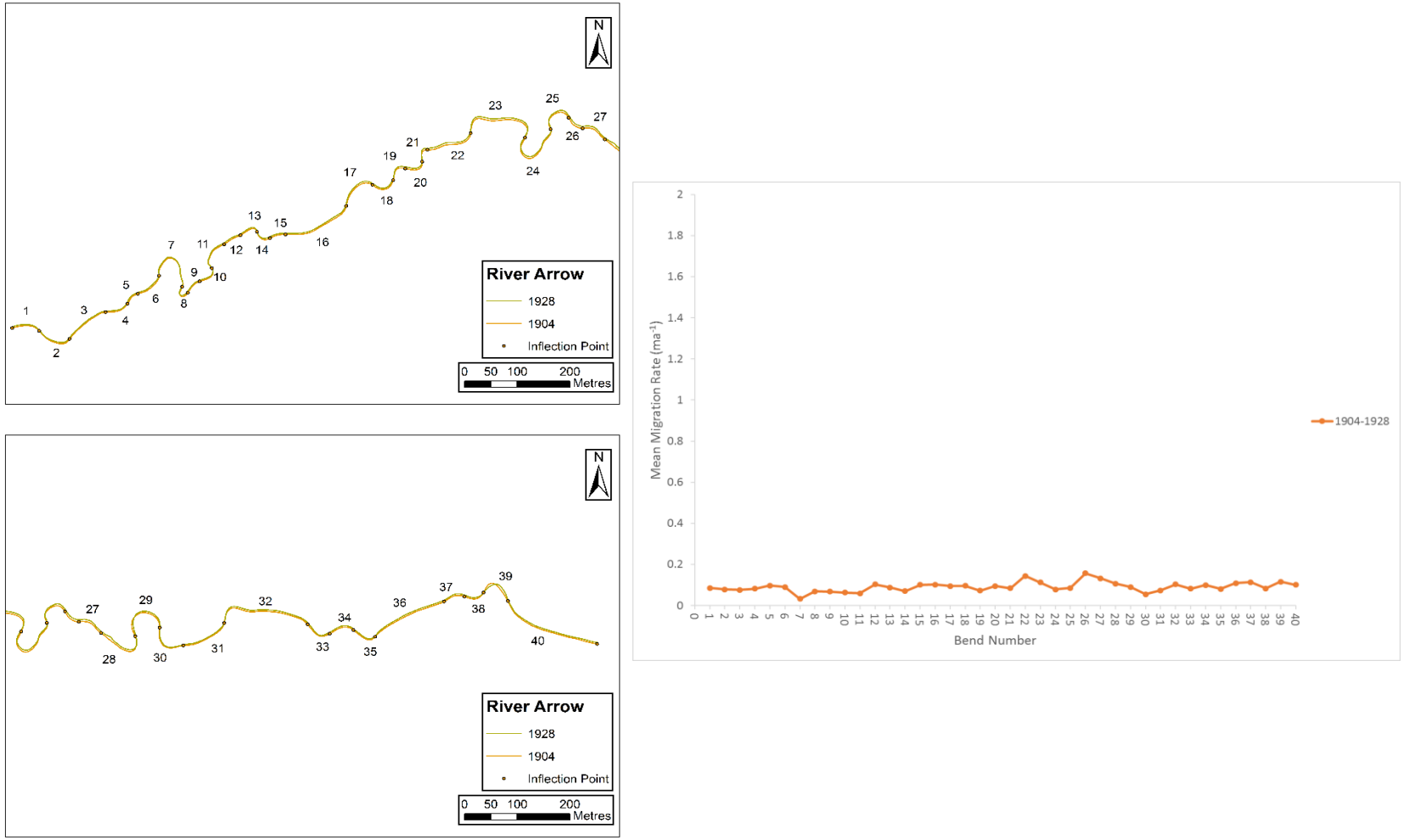

Figure 4.50. Migration rates on Reach 3 of the River Arrow between 1904 and 1928

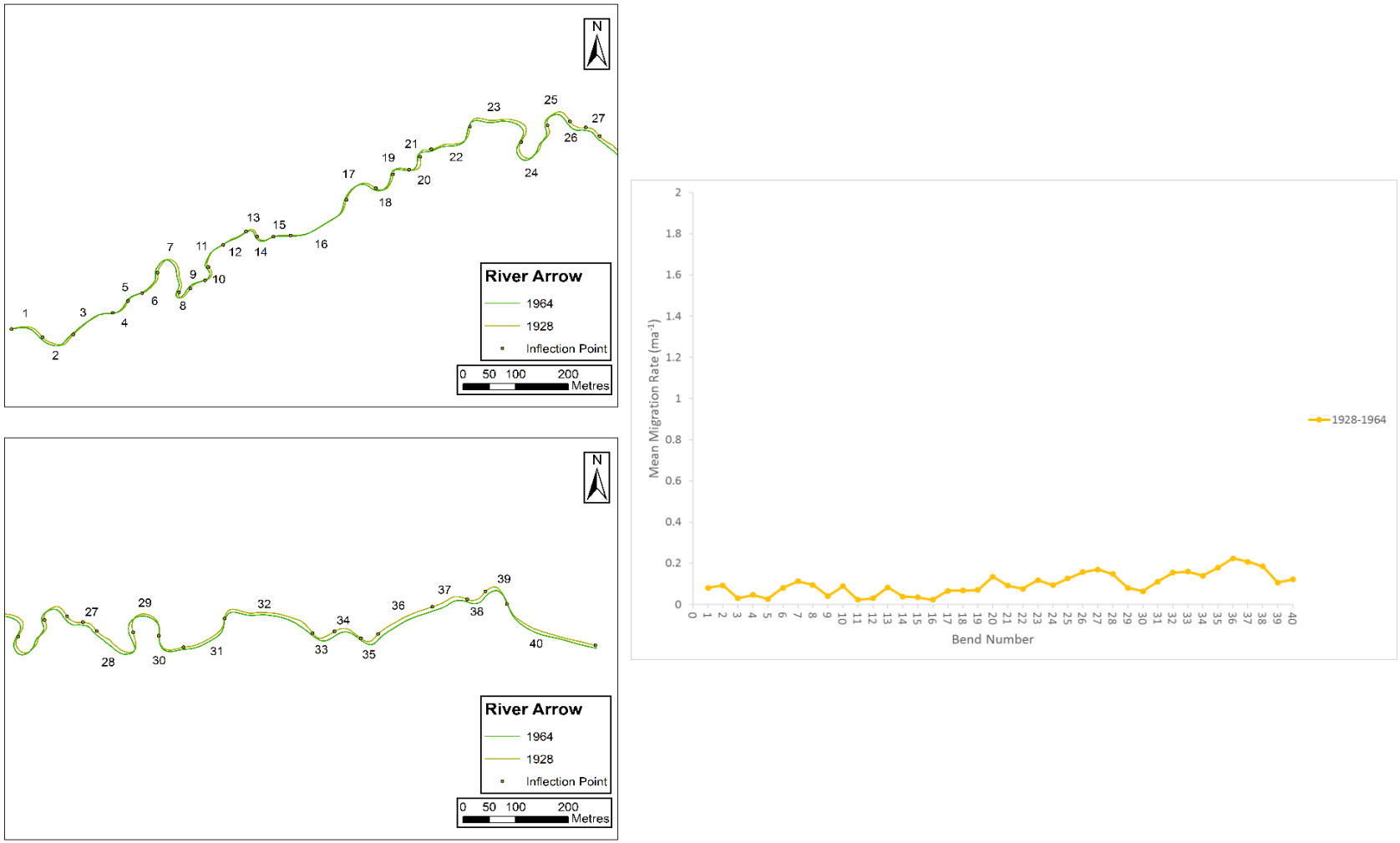

Figure 4.51. Migration rates on Reach 3 of the River Arrow between 1928 and 1964

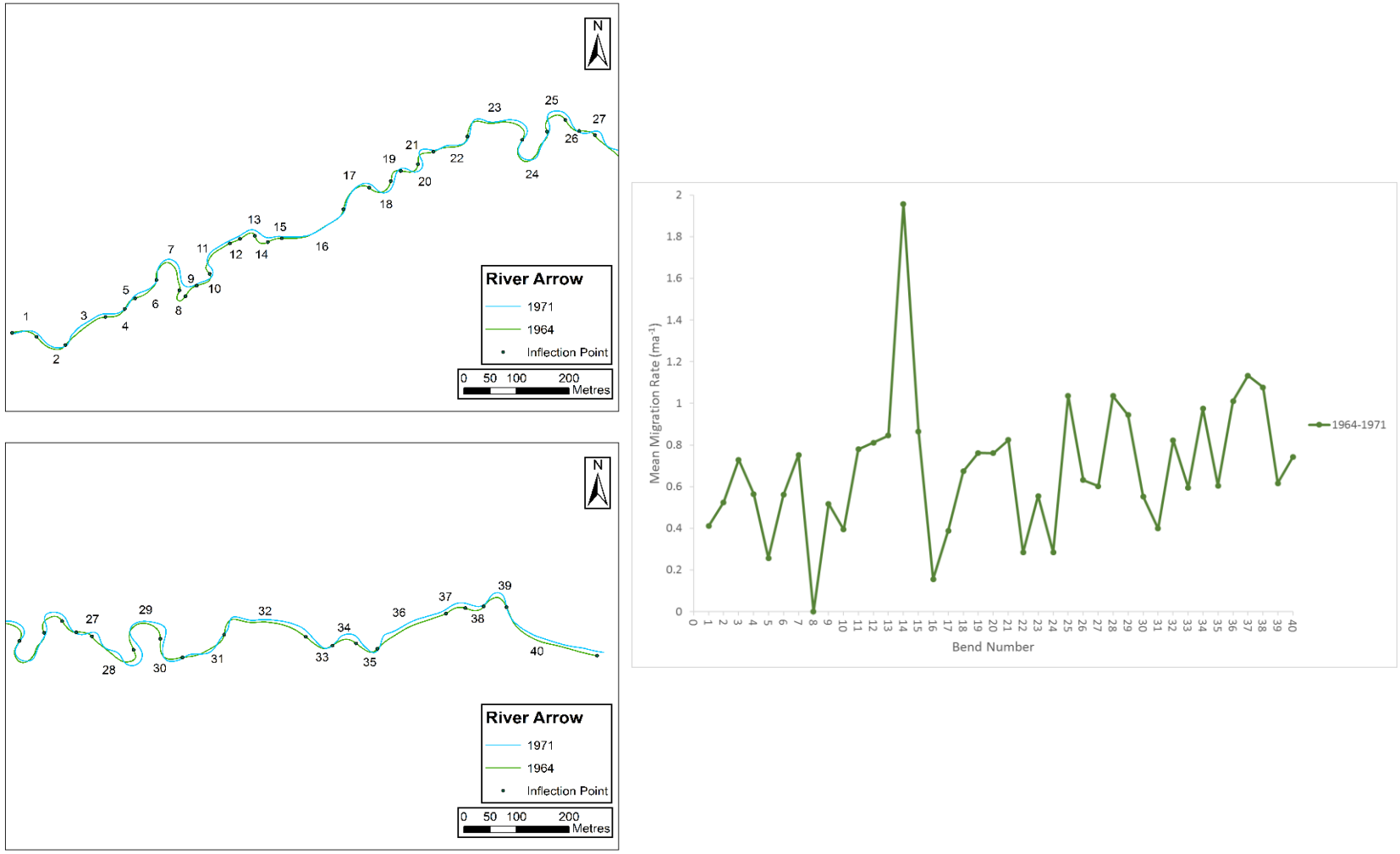

Figure 4.52. Migration rates on Reach 3 of the River Arrow between 1964 and 1971

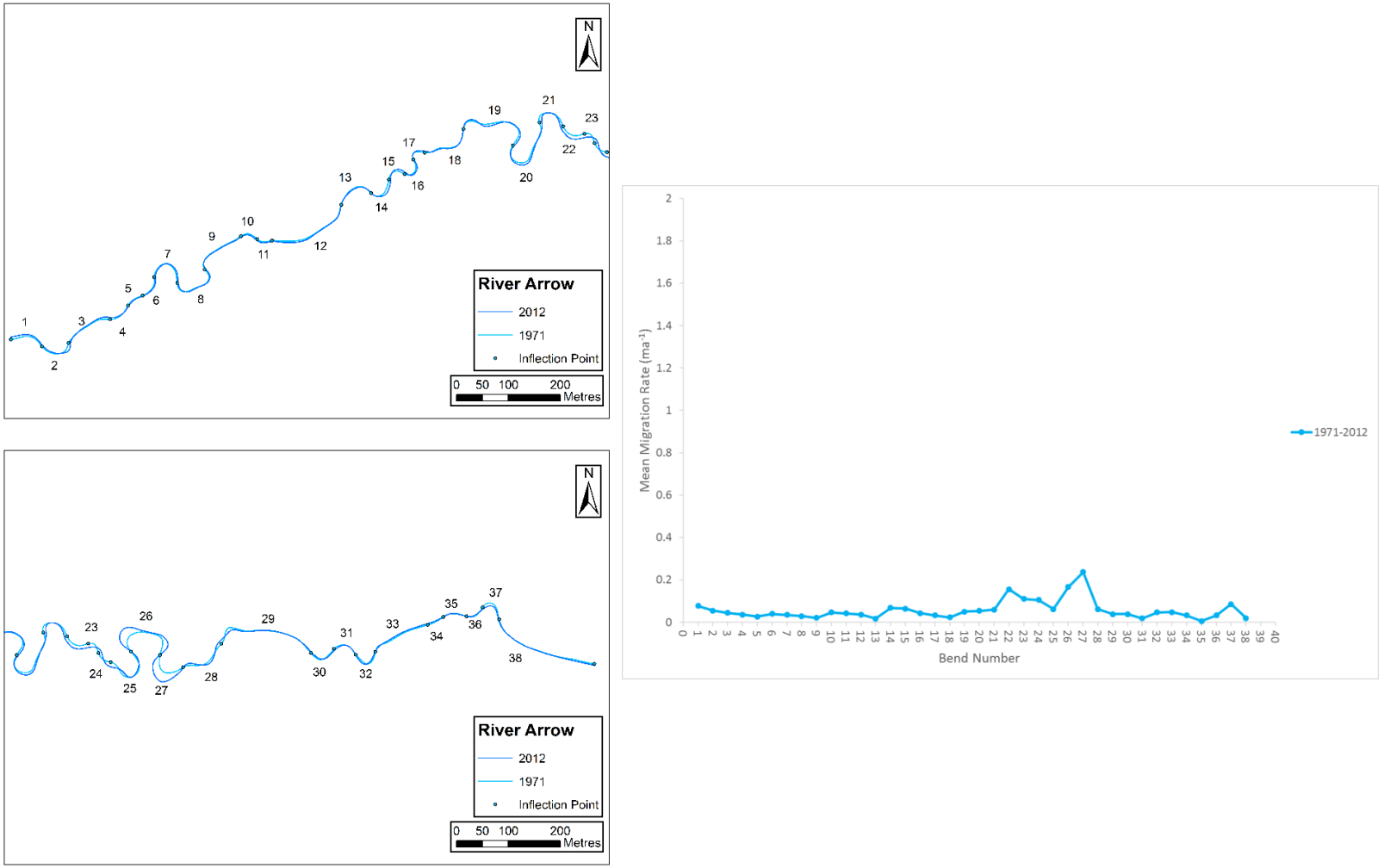

Figure 4.53. Migration rates on Reach 3 of the River Arrow between 1971 and 2012

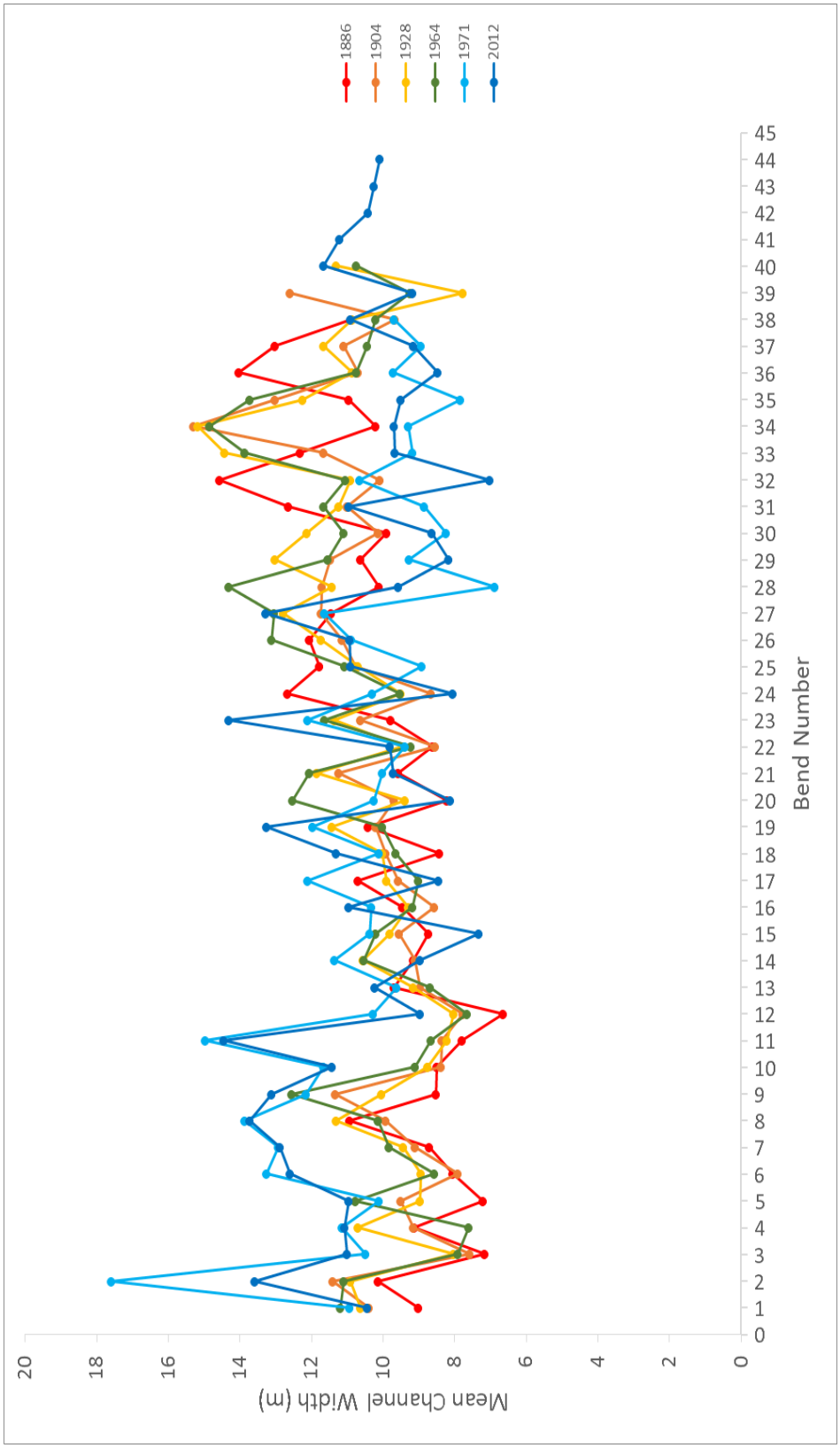

Figure 4.54. The mean channel width of each bend

4.4.1.3. River Till Reaches

The active meandering reaches in the River Till catchment are located around the confluence between the River Glen and the River Till. One of the major differences between the Lugg catchment and the Till catchment is the presence of flood defences located in the floodplain. The two reaches used for this study are the River Glen between Akeld and the confluence with the River Till (mean channel length is 5.6km) and the River Till between West Horton and Milfield (mean channel length is 13.5km) and includes the tributary with the River Glen (see **Error! Reference source not found.**). The mean annual erosion rate ranged from 0.92ma^{-1} on the River Glen between 1957 and 1965 to 0.15ma^{-1}, between 1965 and 2012. The mean annual rate on the River Till ranges from 0.21ma^{-1} to 0.63ma^{-1}. The variance in the

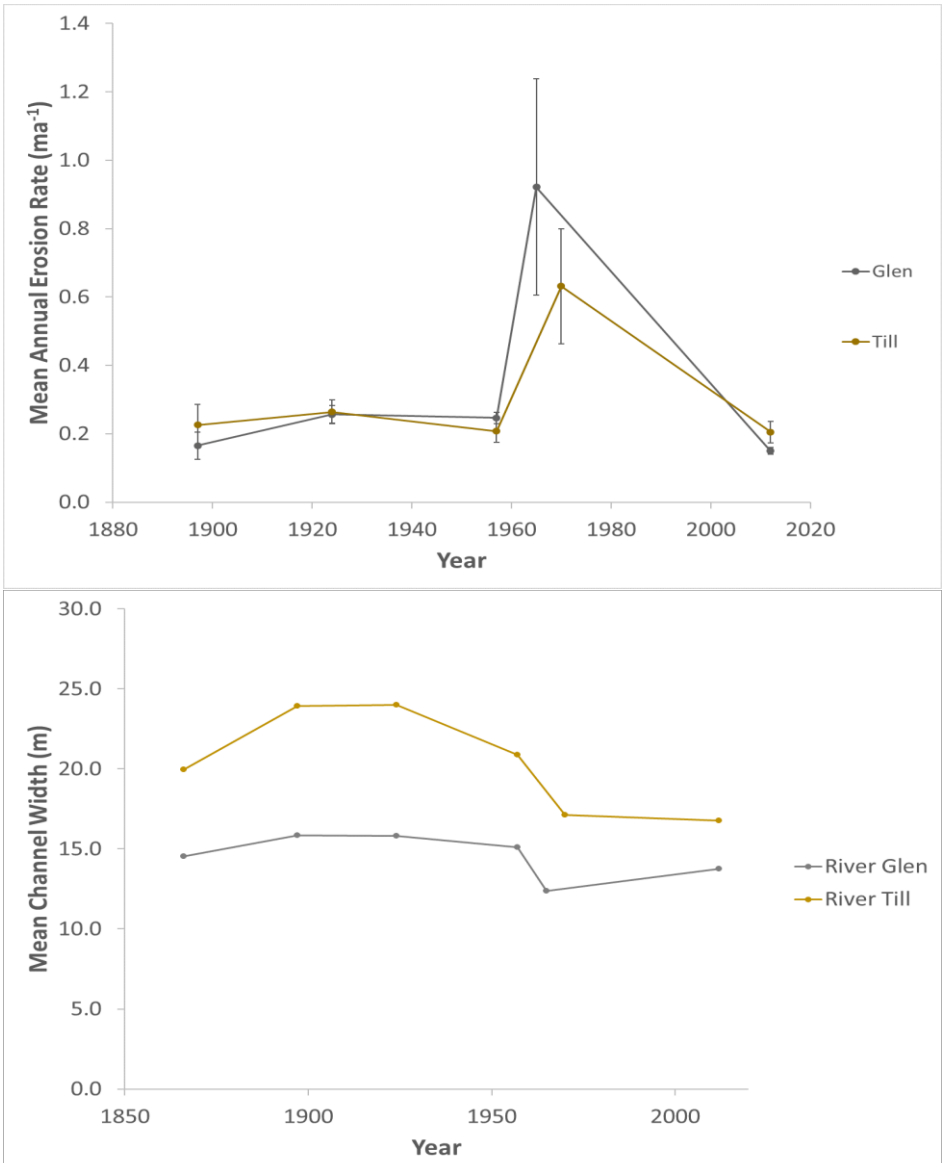

Figure 4.55. The mean migration rate and mean channel width for the River Glen and the River Till

erosion rates also differs between the different periods, with the highest variance measured between 1957 and 1970 for both reaches. The average channel width for the River Glen was 14.6m and 20.4m for the River Till across all the periods.

4.4.1.3.1. River Till

The section of the River Till is located on the wide floodplain between West Horton and Milfield. The effective floodplain width is restricted, however, by a series of flood defences that were built before 1866. Even within this restricted floodplain the river channel has still been active, with eleven cutoffs occurring during the study period and change occurring on many bends.

1866-1897: The mean annual erosion rate was 0.23ma^{-1} and the maximum annual erosion rate for a bend was 1.01ma^{-1} during this period. The highest rates were found towards the start of the reach, with two small chute cutoffs and the active bends migrating downstream. The downstream section of the reach is mainly stable with the exception of bend 72, which was changing through retraction of the bend and erosion occurring on the inside of the bend. The extension on bend 25 is followed immediately downstream by retraction on bend 26.

1897-1924: The mean annual erosion rate increased to 0.26ma^{-1} for this period, but the maximum rate of erosion decreased to 0.74ma^{-1}. The erosion was more evenly distributed throughout the reach. Two loops were cutoff during this period, bends 7 and 53. The retraction on bends 26 and 72 has continued through to this period.

1924-1957: The mean annual erosion rate decreased slightly to 0.21ma^{-1} during this period, while the maximum rate was 0.87ma^{-1}. There were two large loop cutoffs, bends 27 and 59, along with two smaller cutoffs on bends 26 and 63. The highest erosion on bends 14 and 15 led to bend 15 becoming much tighter.

1957-1970: Both the mean annual and maximum annual erosion rate increased in this period to 0.63ma^{-1} and 1.92ma^{-1} respectively. There were two small chute cutoffs. The remaining part of bend 27 was cutoff, along with bend 15, which had become much tighter in the previous period. The highest rates of annual erosion were measured between these two cutoffs.

1970-2012: During this period the mean annual erosion is 0.21ma^{-1} and the maximum rate of erosion is 0.93ma^{-1}. There are no cutoffs during this period. Most of the erosion appears to be concentrated around individual bends with bends either side remain stable.

The mean channel width shows considerable variability during the study period. The highest width was 58.7m measured on bend 25 in 1897 and 1924. This bend had experienced erosion on the inner back as the channel retracted from the outer bank.

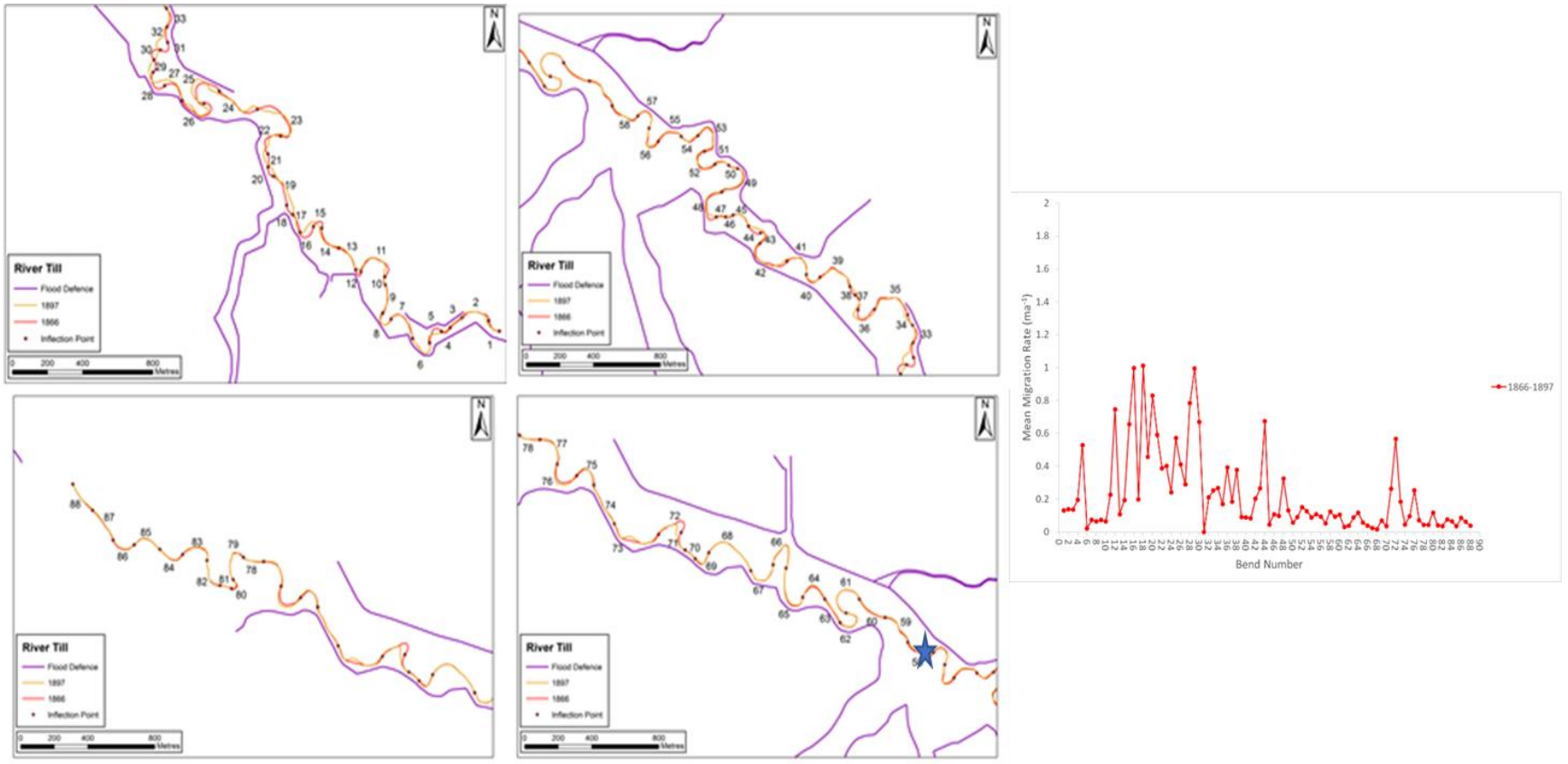

Figure 4.56. Migration rate for individual bends on the River Till, between 1866 and 1897

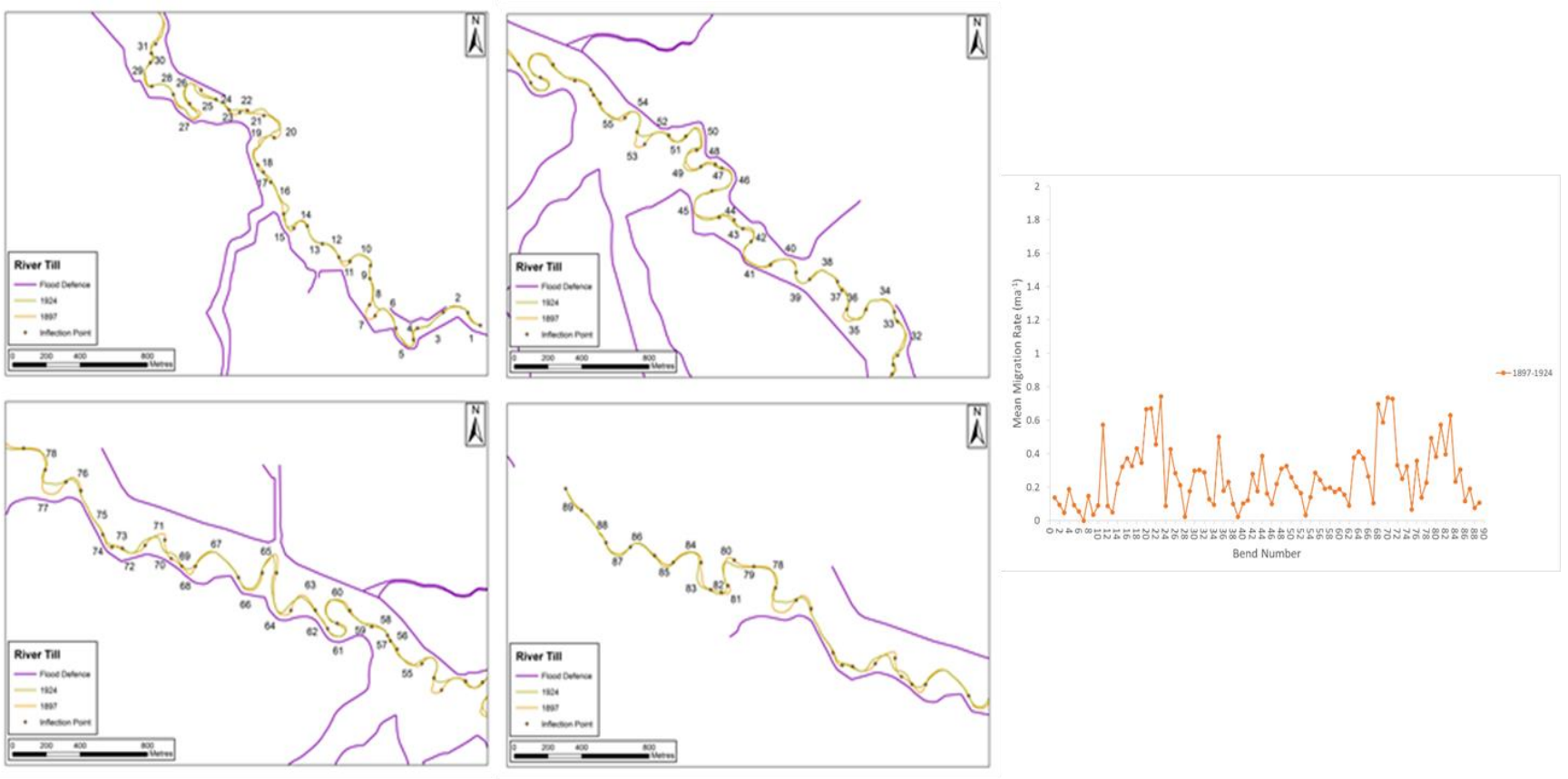

Figure 4.57. Migration rate of individual bends on the River Till between 1897 and 1924

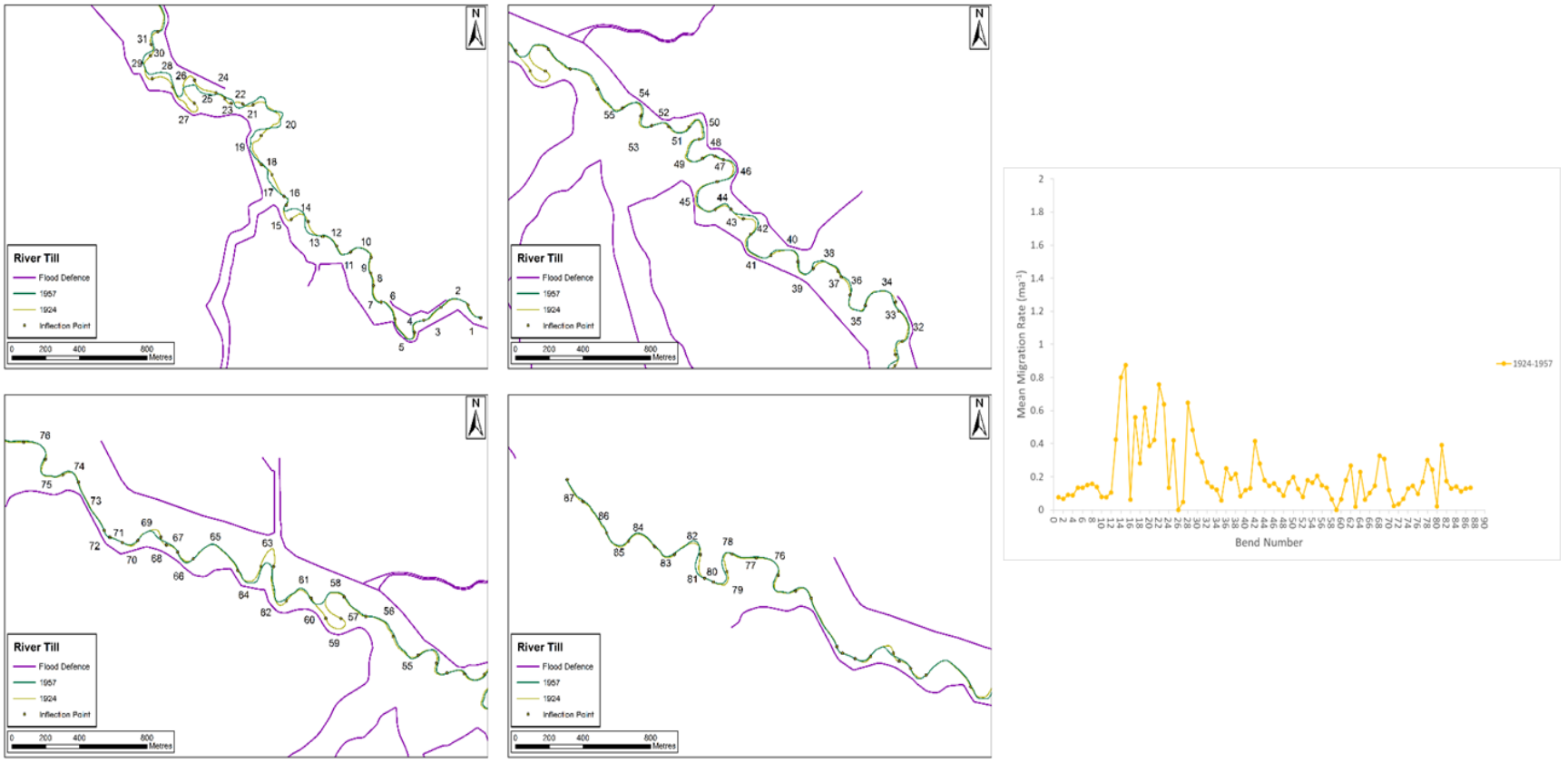

Figure 4.58. Migration rate of individual bends on the River Till, between 1924 and 1957

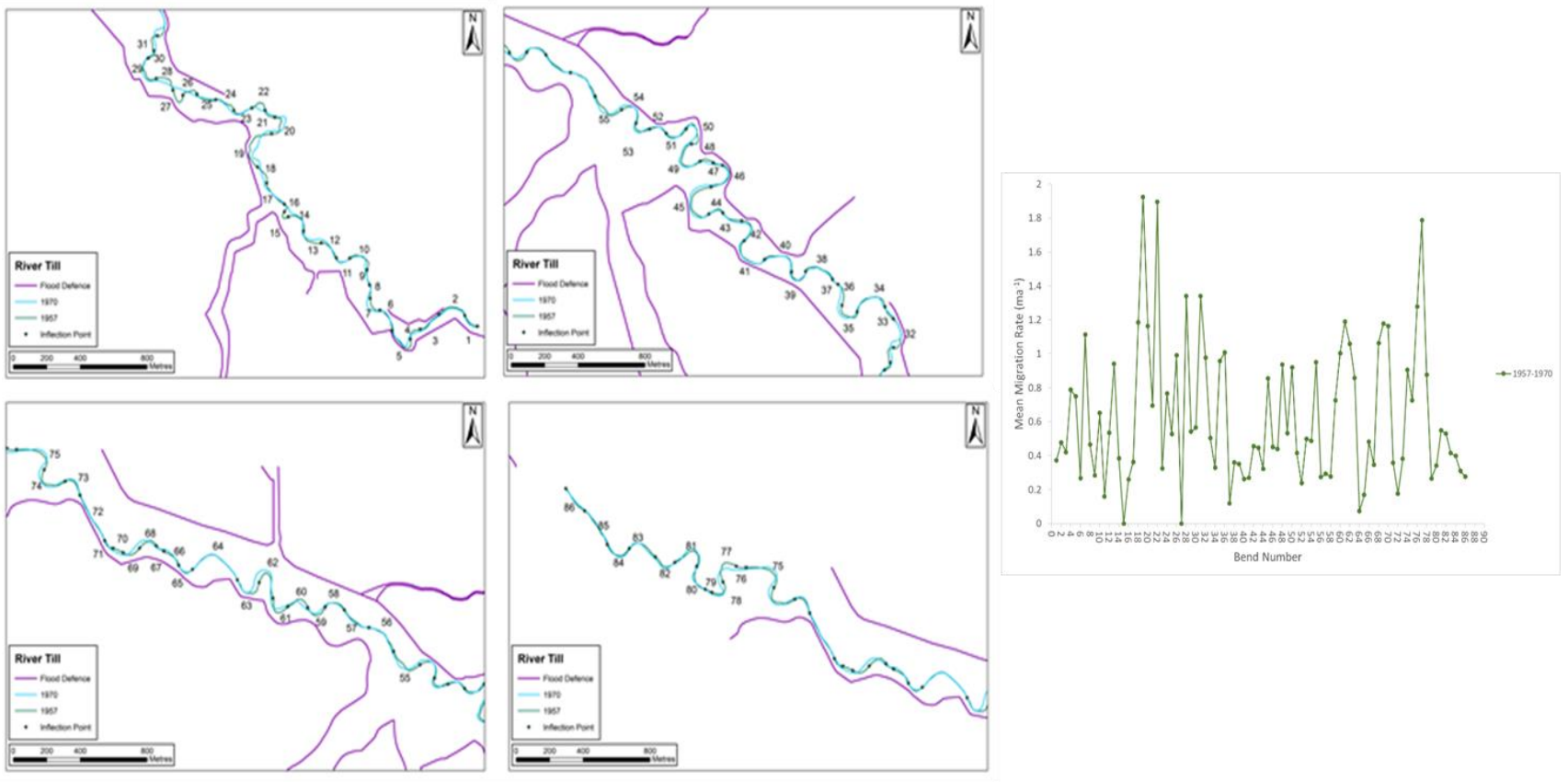

Figure 4.59. Migration rate of individual bends on the River Till, between 1957 and 1970

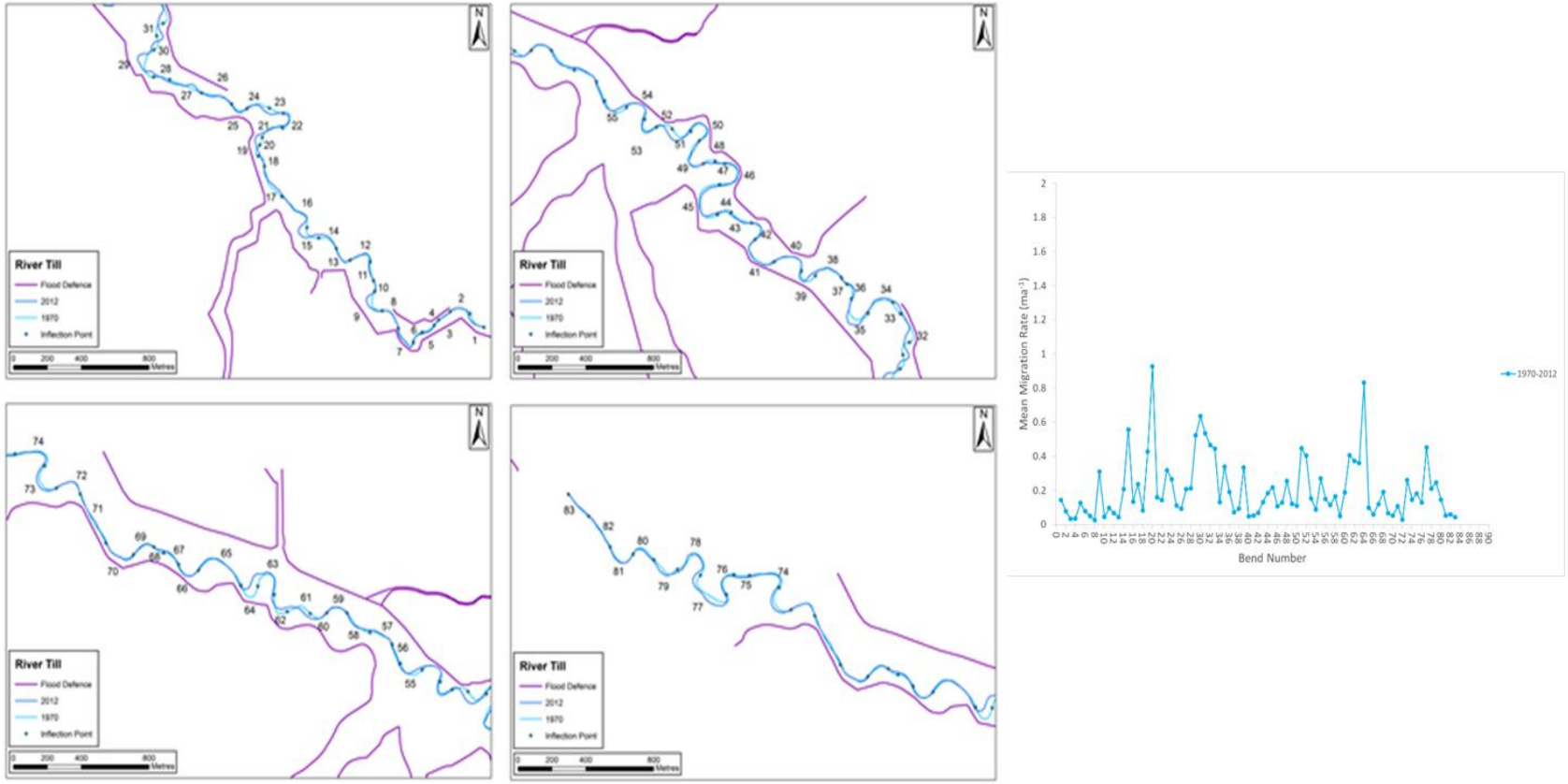

Figure 4.60. Migration rate of individual bends on the River Till, between 1970 and 2012

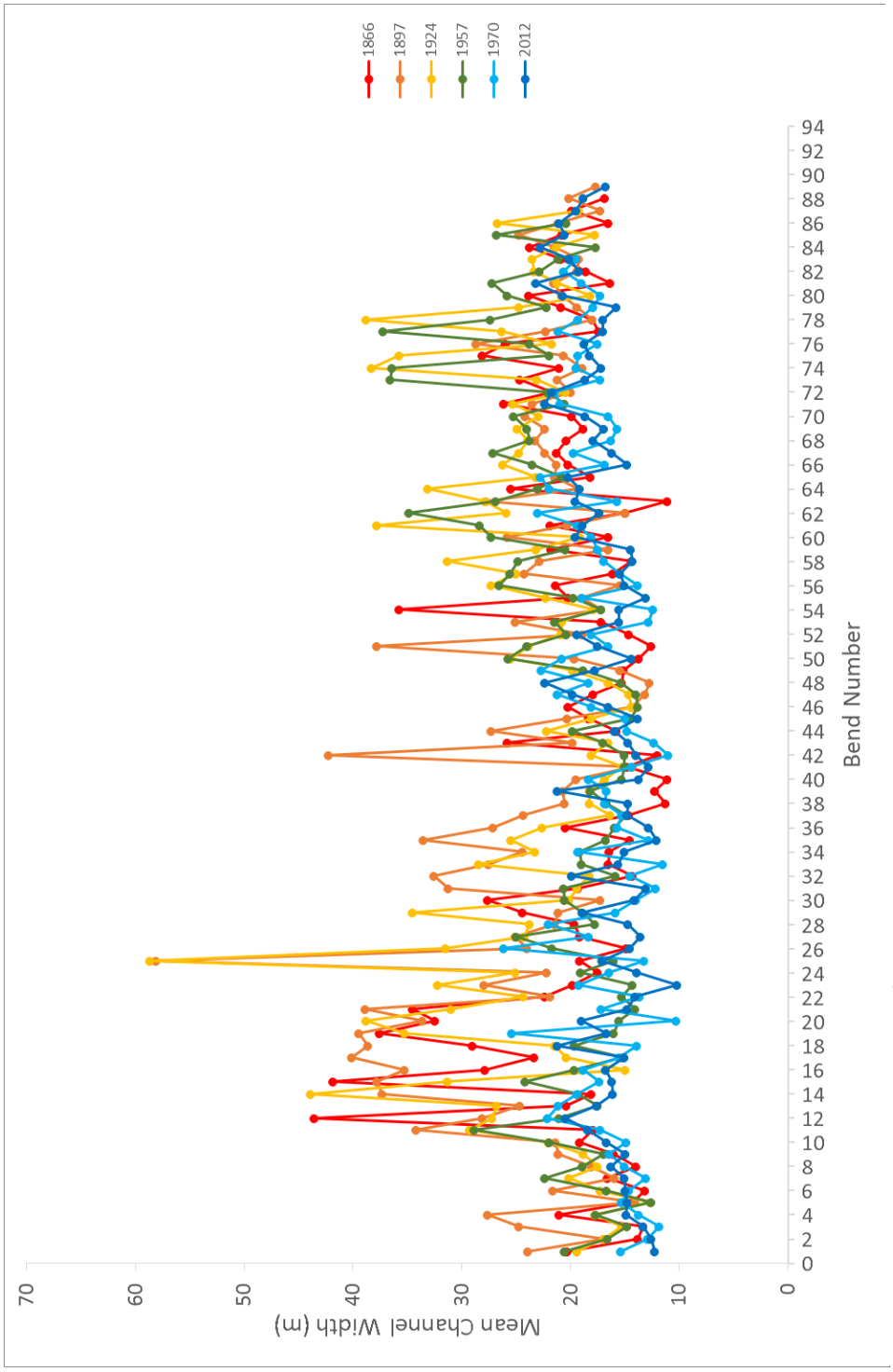

Figure 4.61. Mean channel width for individual bends on the River Till

4.4.1.3.2. River Glen

The River Glen section is located between Akeld and the confluence with the River Till. Nearly the entire reach is bounded by flood defences that restricted the ability of the channel to migrate across the floodplain. However, the river continues to be active, both cutting off and migrating downstream for numerous bends. The sections further upstream were dominated by avulsions rather than lateral migration and so were not included in this study.

1866-1897: The mean lateral erosion rate during this period was 0.16ma^{-1}, with a maximum rate of 0.96ma^{-1} measured on bends 12 and 24. The high erosion rate on bends 24 and 25 is probably associated with the cutoffs that occurred just upstream, with a neck cutoff and a chute cutoff occurring for the two preceding bends. The downstream section of the reach remained stable through the study period, with the exception of bend 38.

1897-1924: Between 1897 and 1924, a large loop is cutoff at bend 39. Downstream of the cutoff there is considerable erosion on many of the bends. The mean rate of erosion is 0.33ma^{-1} compared to 0.23ma^{-1} upstream of the cutoff. The overall mean annual erosion rate is 0.26ma^{-1}. The maximum rate of erosion was 0.85ma^{-1} measured on bend 54, which was migrating downstream.

1924-1957: The mean annual erosion rate was 0.25ma^{-1} during this period, with a maximum rate of 0.64ma^{-1}. Erosion was distributed throughout the whole reach, but the changes are minor. There was some downstream migration towards the end of the reach on bends 37, 38 and 42.

1957-1965: The shortest period between two maps also had the highest mean annual erosion rate, 0.92ma^{-1}. The maximum annual erosion rate for a bend was 2.72ma^{-1}, nearly 2ma^{-1} faster than any of the other time periods. There is some morphological change, especially on bend 42, which has migrated further downstream and bend 38, which is beginning to grow across the limited floodplain.

1965-2012: The mean annual erosion rate for the reach decreased to 0.15ma^{-1} during this period, with a maximum rate of 0.60ma^{-1} measured on bend 18. One chute cutoff occurs on bend 44. Bends 38 and 39 have been active during this period, with bend 38 migrating downstream, narrowing the neck of bend 39, which also grew across the floodplain during this period.

Figure 4.67 shows the mean channel width for each date on the River Glen. There was considerable variation between consecutive bends along the reach, although the mean channel width for the whole reach remained similar between the different dates.

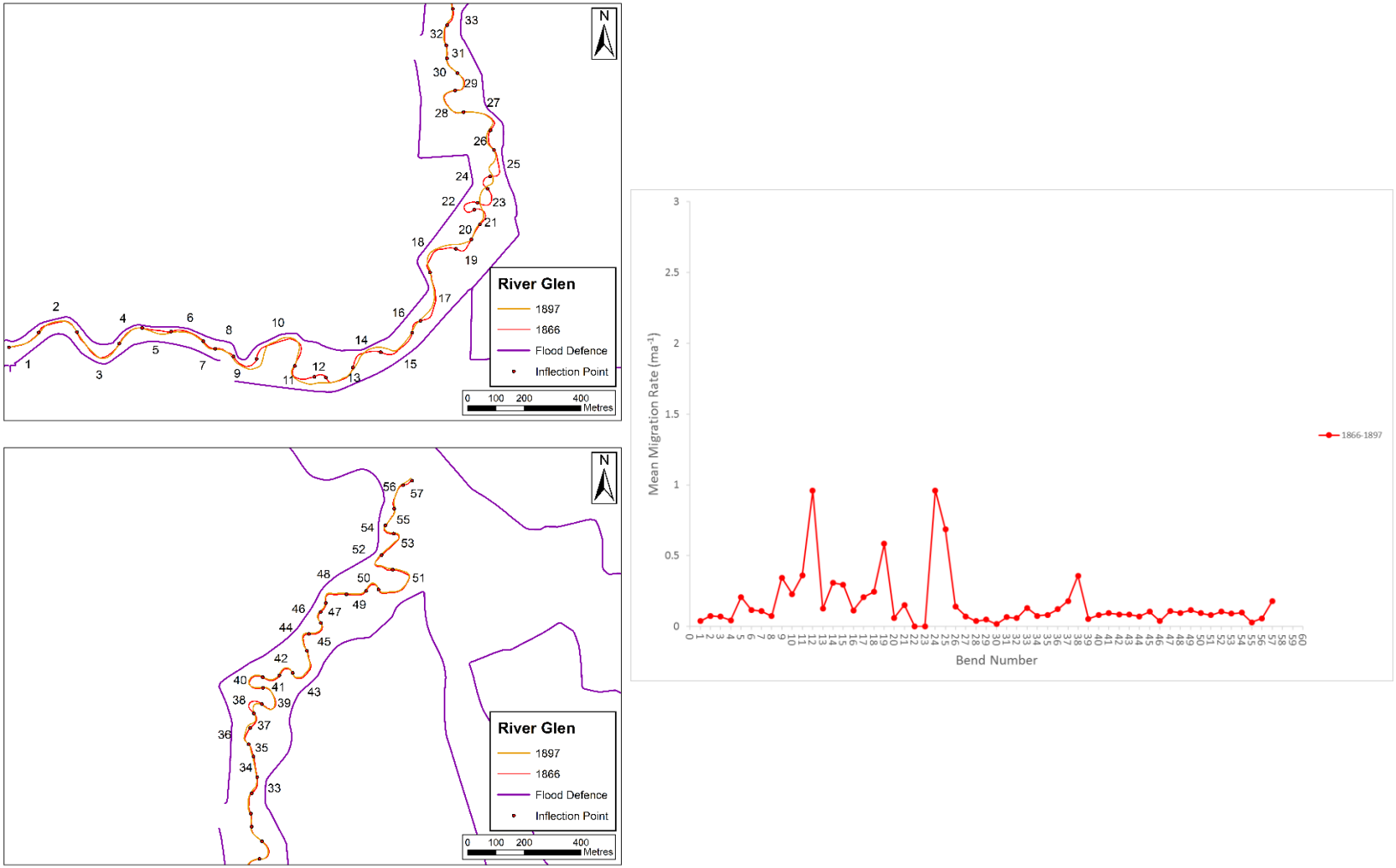

Figure 4.62. Migration rates on the River Glen between 1866 and 1897

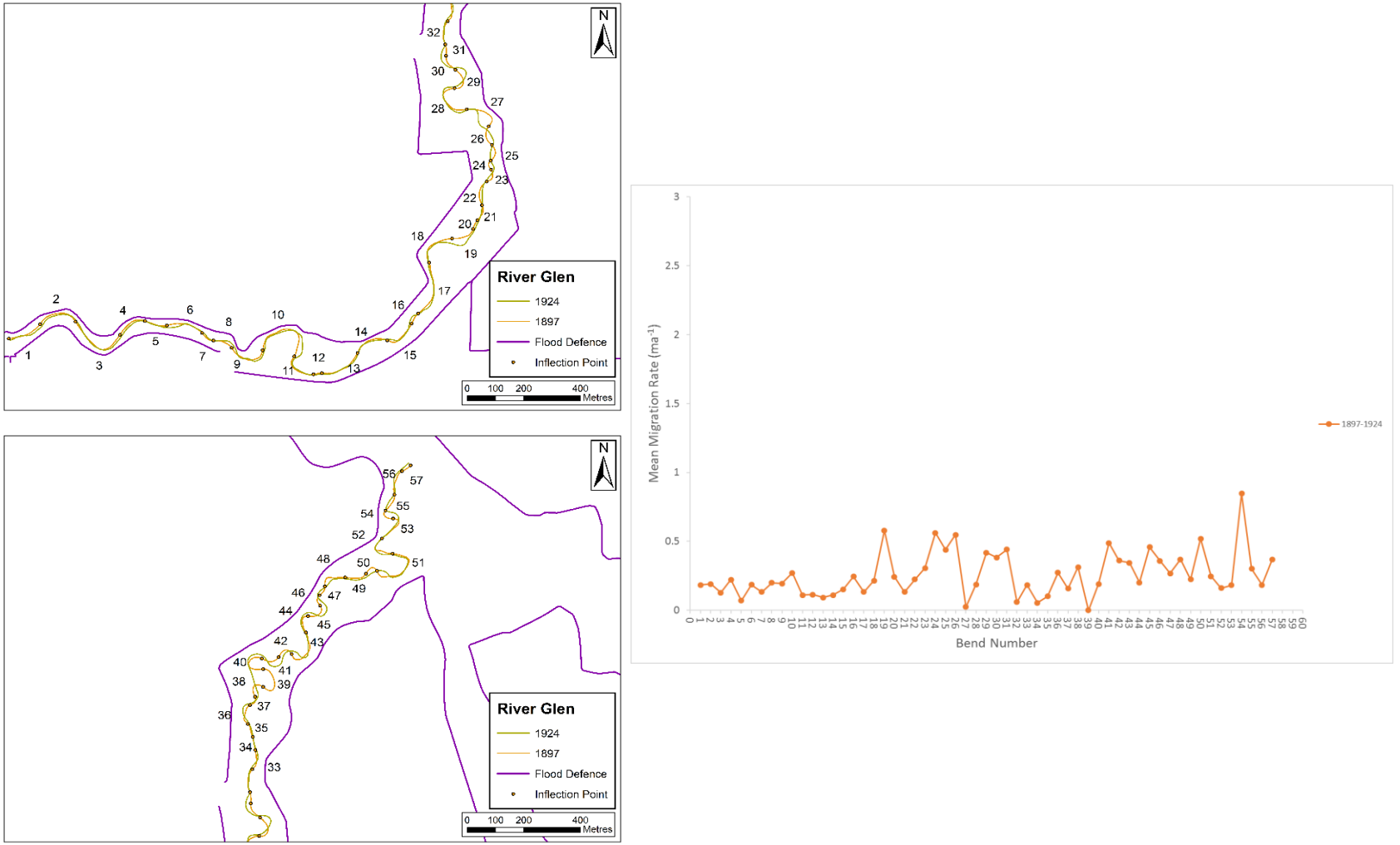

Figure 4.63. Migration rates on the River Glen between 1897 and 1924

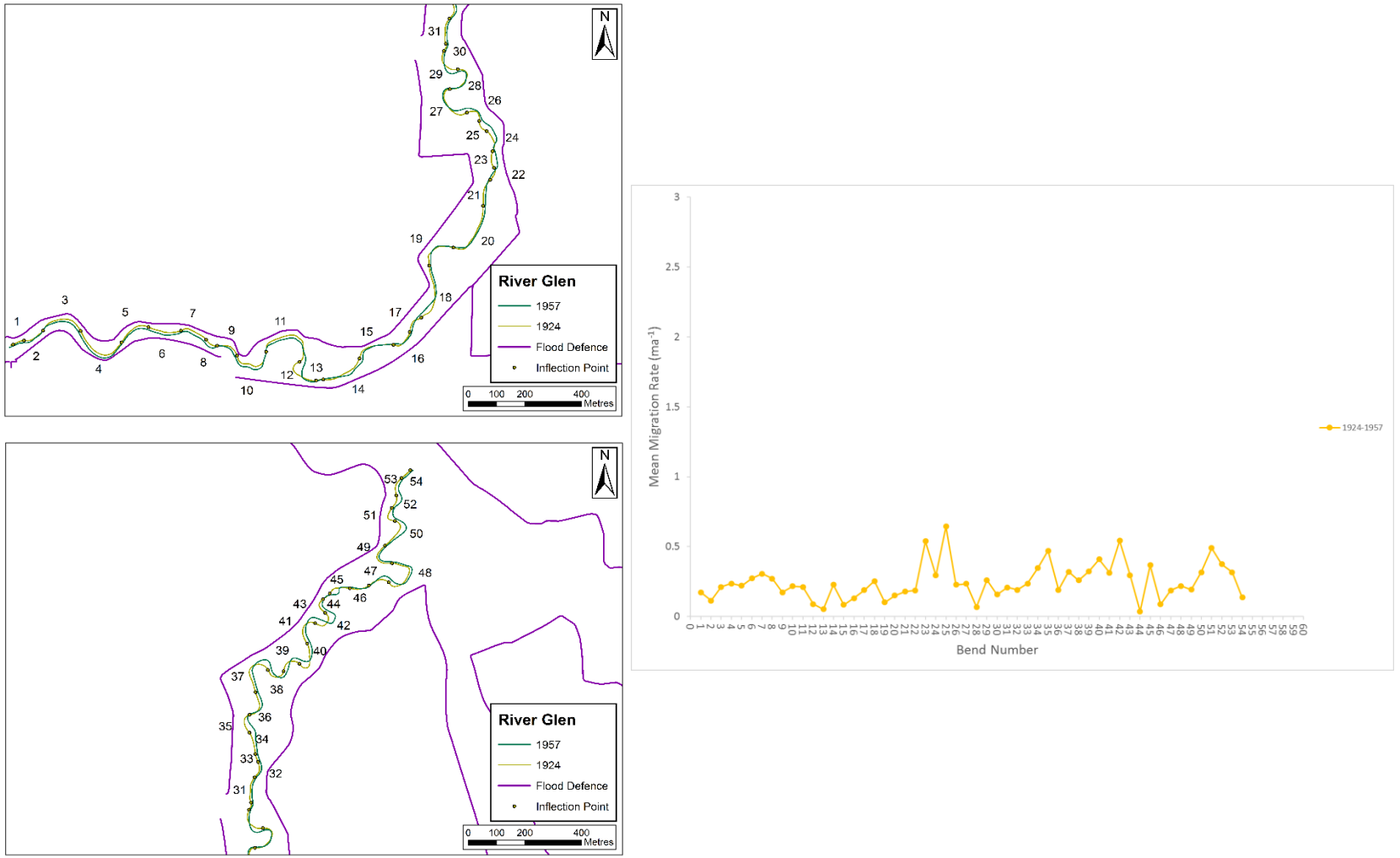

Figure 4.64. Migration rates on the River Glen between 1924 and 1957

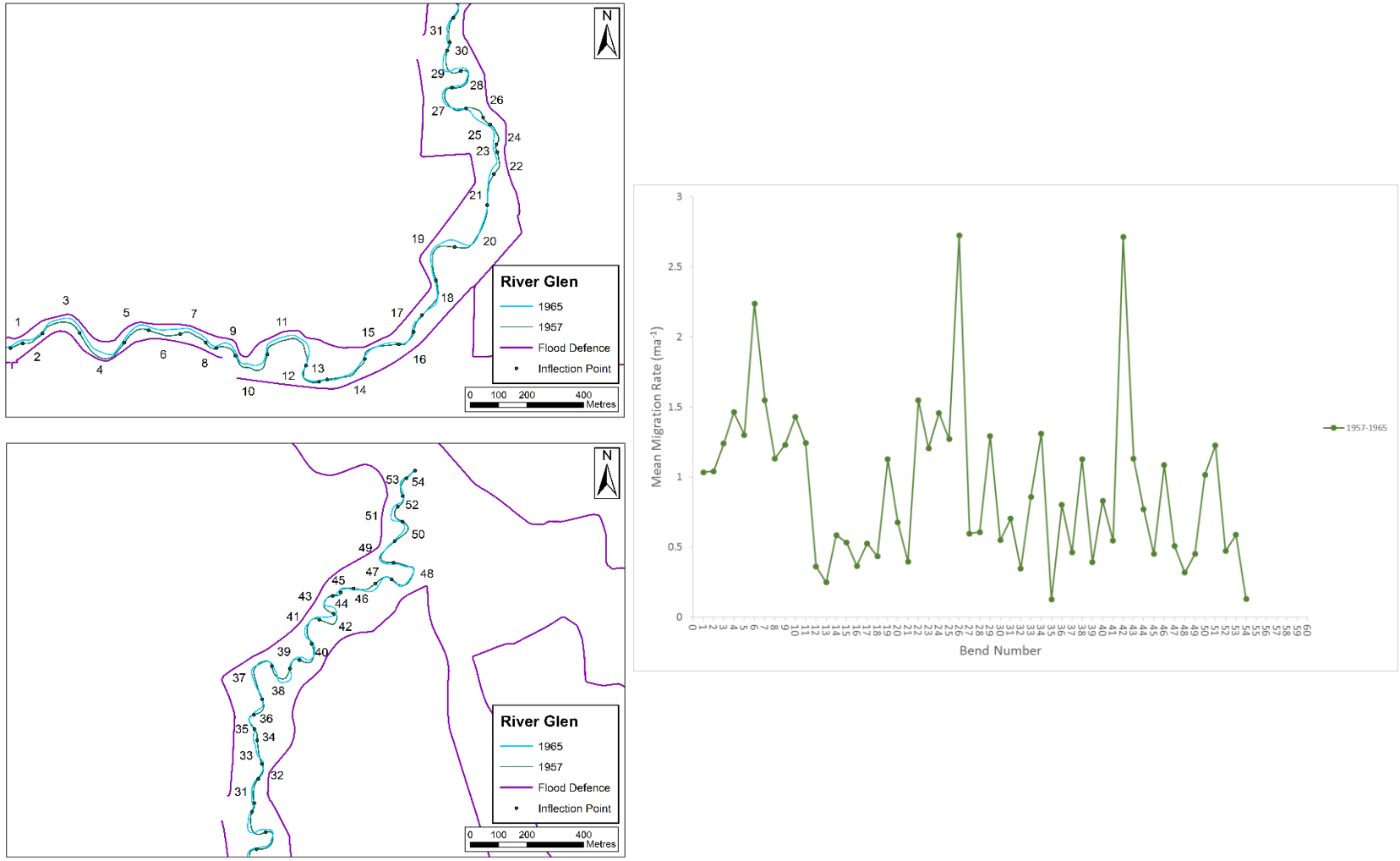

Figure 4.65. Migration rates on the River Glen between 1957 and 1965

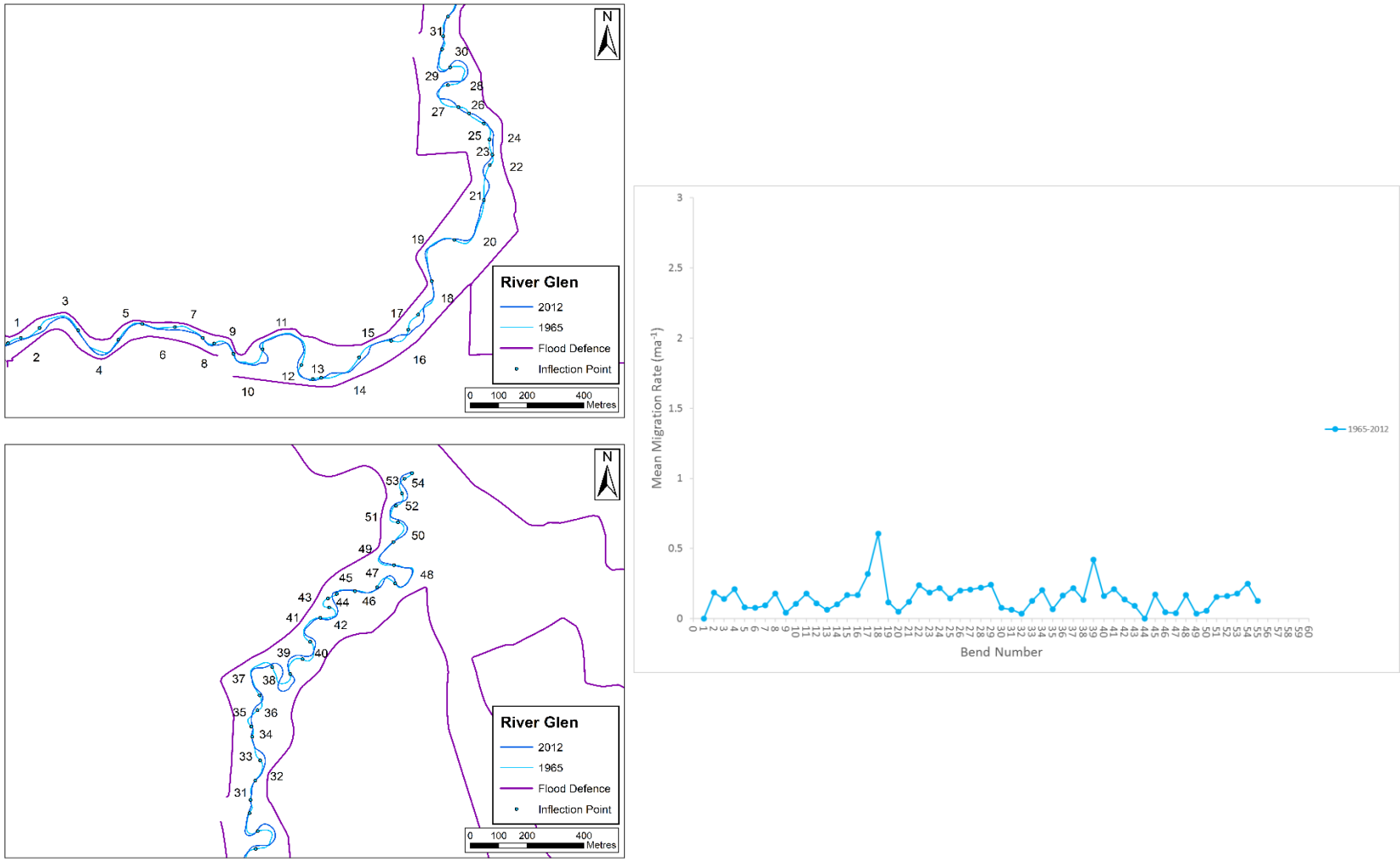

Figure 4.66. Migration rates on the River Glen between 1965 and 2012

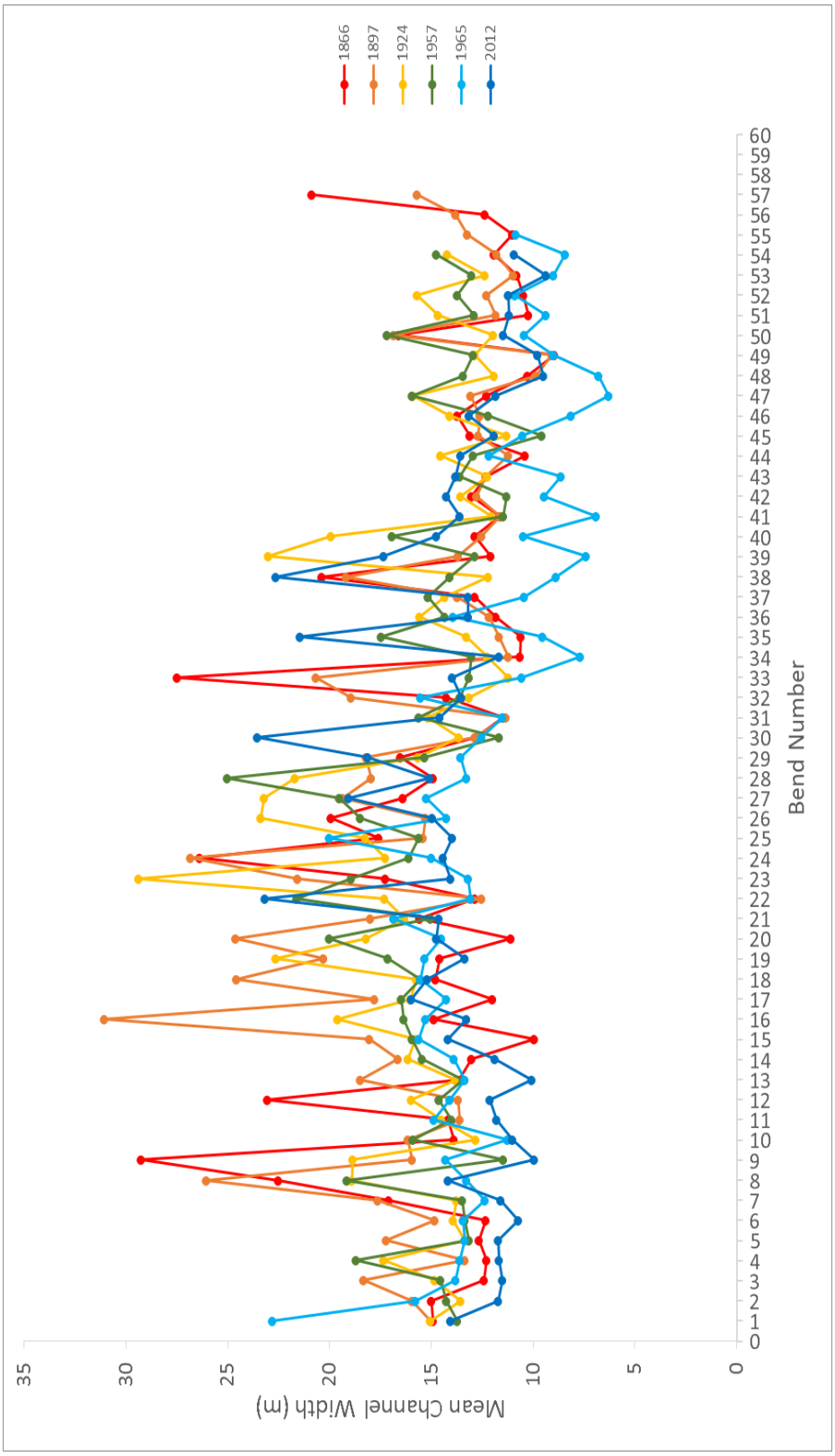

Figure 4.67. The mean channel width for each individual bend

4.4.2. Sinuosity changes – Reach Scale and Prior to a Cutoff

The length of the record in this study, both spatially and temporally, allows the sinuosity of the channel to be recorded through time, especially the changes prior to a cutoff occurring. Neck and chute cutoffs are recognised as the two main types of cutoffs that occur on single thread meandering channels and a total of 71 were identified across the study periods and reaches. This provides the opportunity to examine the relationship between channel sinuosity and cutoff occurrence and to test whether any thresholds can be identified as theorised by Stolum (1996, 1998). Changes in sinuosity can also represent the activity of the river channel. If a river channel is actively migrating and growing across the floodplain between the start and the end of the reach, and no cutoffs occur, the sinuosity of the reach will continue to increase. A sinuosity of 1.0 represents a straight line.

4.4.2.1. River Lugg Reaches

The reaches generally showed a small increase in the overall sinuosity between 1886 and 2012. Table 4.3 shows the sinuosity measured at the start of the study period and the end of the study period. Reaches 4 and 5 show considerable variability in sinuosity, with the sinuosity of reach 5 increasing between 1886 and 1973, before decreasing after the construction of the flood defences. Reach 4 experienced a large decrease in sinuosity after a large cutoff occurred between bends 20 and 22, removing over 400m of the channel.

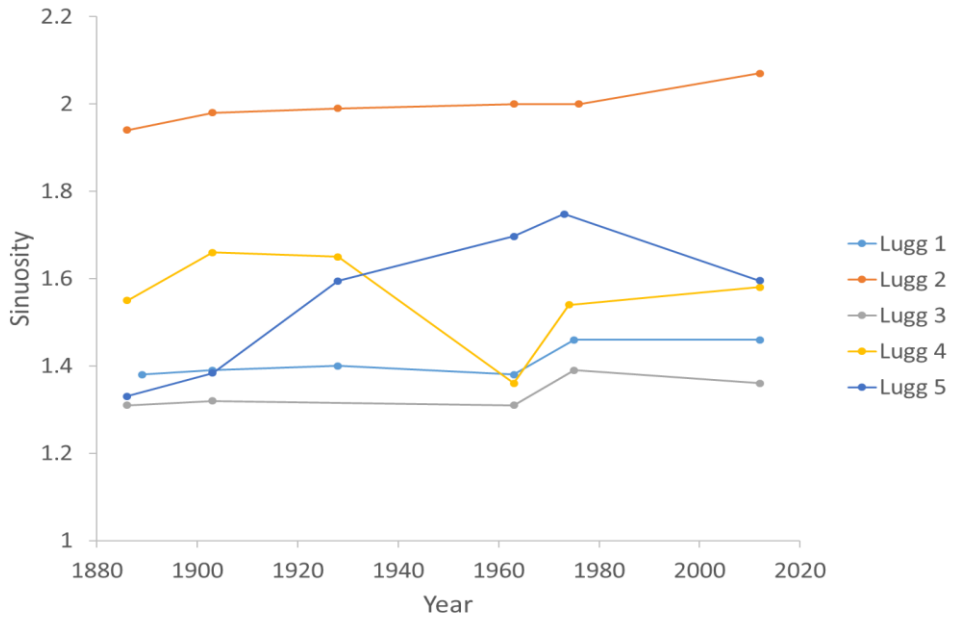

Figure 4.68. The changes in sinuosity for each reach on the River Lugg

4.4.2.1.1. River Lugg Cutoffs

A total of 26 cutoffs occurred between 1886 and 2012 across the five River Lugg reaches. The cutoffs can be described as either neck or chute cutoffs. A neck cutoff occurs when a well-developed meander loop is removed from the active channel as bends upstream and downstream of the loop intersect with each other. A chute cutoff occurs when either part of a bend is cutoff or when a less developed bend is cutoff. Chute cutoffs generally occur through avulsions. For the River Lugg, eleven of the cutoffs were classed as a chute cutoff and fifteen were classed as neck cutoffs. Table 4 gives the location, date and sinuosity of each cutoff in the Lugg catchment. The average sinuosity prior to a chute cutoff was 1.72, while the average sinuosity for a neck cutoff was 1.83. There is a range of sinuosity values apparent before a cutoff occurs, with chute cutoffs ranging from 1.24 to 2.63 and neck cutoffs ranging

Table 4.3. The sinuosity of the river channel before a cutoff occurred on the River Lugg. The sinuosity was calculated for three bends upstream and downstream of the cutoff.

River	Reach	Year	Bend Number	Sinuosity	Cutoff Type
Lugg	1	1928	29	1.24	Chute
	1	1975	21	2.11	Neck
	2	1963	7	2.09	Chute
	2	1963	9	2.18	Chute
	2	1963	10	2.20	Neck
	2	1976	15	2.16	Neck
	3	1975	24	1.31	Neck
	4	1903	21	2.01	Neck
	4	1928	9	1.69	Neck
	4	1928	20,21,22	1.69	Neck
	4	1928	14	1.65	Chute
	4	1963	16	1.34	Chute
	4	1963	20	1.40	Chute
	4	1974	26	1.59	Neck
	5	1886	6	1.46	Chute
	5	1903	9	1.64	Neck
	5	1903	11	1.67	Neck
	5	1963	9	1.73	Neck
	5	1963	10	1.80	Neck
	5	1963	14	2.38	Neck
	5	1963	18	2.03	Neck
	5	1973	8	1.64	Neck
	5	1973	13	1.61	Chute
	5	1973	16	1.48	Chute
	5	1973	31	1.86	Chute

from 1.30 to 2.50. The threshold here appears to be lower than the threshold of 3.14 suggested by Stolum (1998) for freely migrating rivers. It is not possible to know whether the cutoffs that occurred on Reach 5 during the construction of the flood defences, in the period 1963-1973, were natural or caused during the engineering works to help manage the channel. The bends were in a highly sinuous state and close to cutting off but may have been artificially cutoff to help stabilise the channel during the construction.

Due to the length of time between map periods, it is not possible to determine whether cutoffs have been clustered during one winter or storm event as recorded by Hooke (2004), but several cutoffs have occurred in close spatial proximity. On Reach 2 between 1963 and 1976, a large bend (bend 10) experienced a neck cutoff, with two chute cutoffs occurring within three bends upstream (see Figure 4.69). The sinuosity of this section of the river was 2.50 for the neck cutoff and 2.62 and 2.63 for the chute cutoffs. Apart from the changes to the three bends, the changes downstream are limited. This could indicate that the effects of the cutoff are spatially limited or that the cutoffs occurred very close to the map survey date and the river channel has not had time to adjust.

Reach 4 was highly active during the study period with a total of seven cutoffs occurring between 1886 and 2012 and cutoffs occurring in every period with the exception of 1886-1903. A particularly interesting series of cutoffs occurred towards the end of the reach, where a chute cutoff appears to have led to a neck cutoff occurring further downstream. Bends 25 and 26 were mainly stable between 1886 and 1963, with a small amount of erosion occurring on the bends. Bend 25 became tighter due to erosion in 1963, and subsequently a chute cutoff occurred between 1963 and 1974. This cutoff led to rapid erosion downstream and bend 26 becoming compound and narrowed the neck of bend 26 to 35m. Between 1974 and 2012 the bend then experienced a cutoff, reducing the sinuosity. Figure 4.70 shows the sequence of change for these bends. The sinuosity trajectory for the two bends were also measured through time from 1886 to 2012 and is plotted on Figure 4.71.

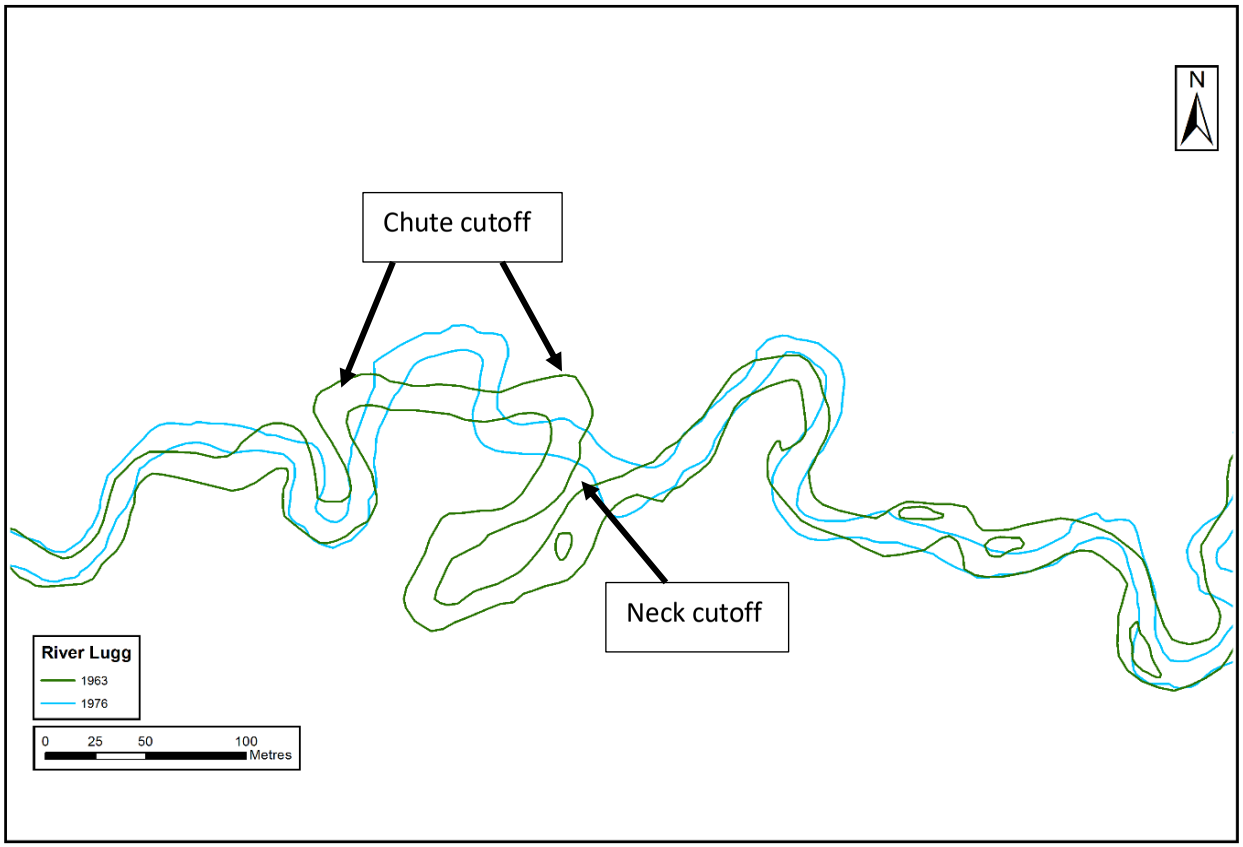

Figure 4.69. The multiple cutoffs that occurred on Reach 2. Bend 10 was cutoff through a large loop cutoff and two bends upstream had chute cutoffs.

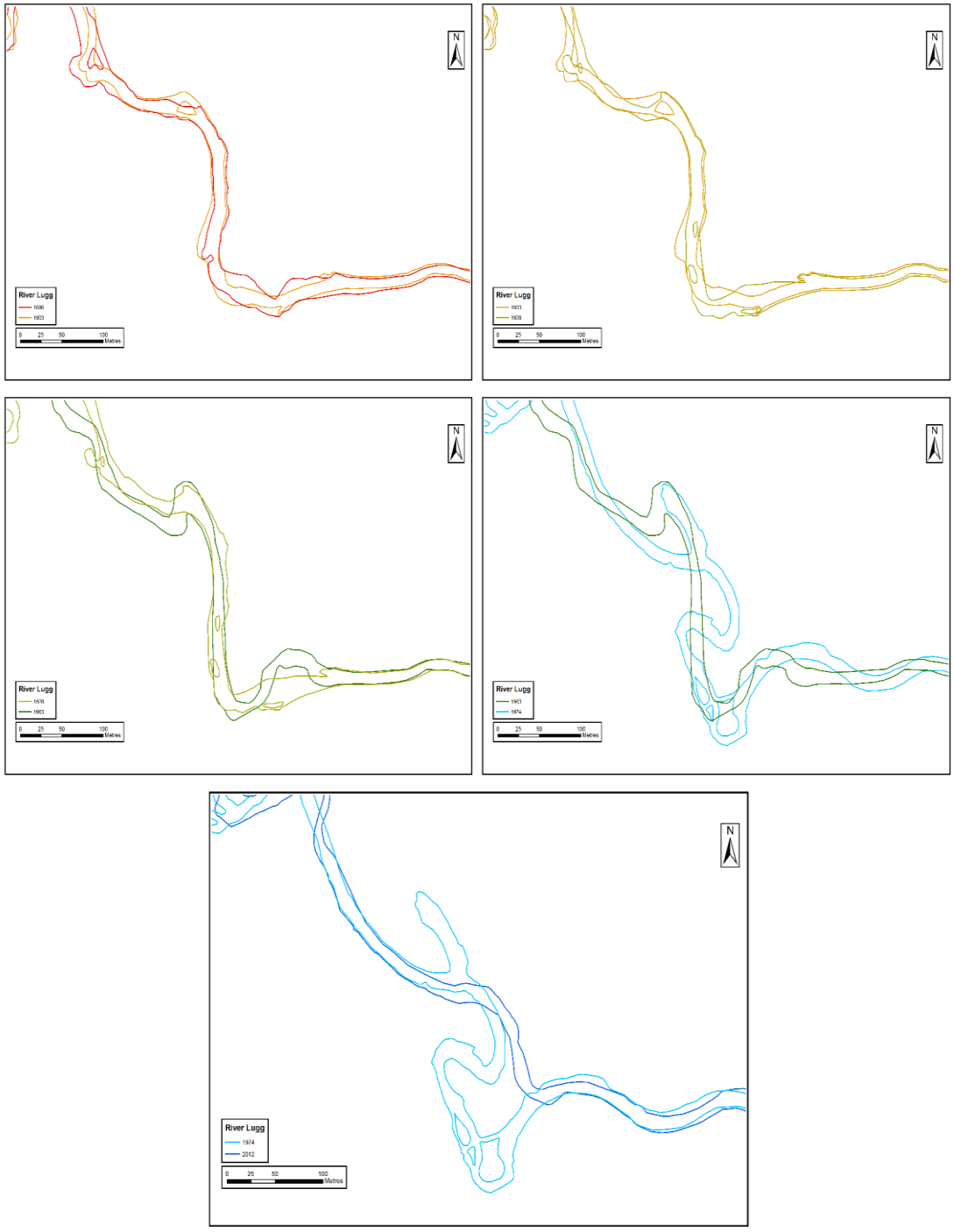

Figure 4.70. The evolution of bends 26 and 27 from a simple form to a compound form and finally cutoff.

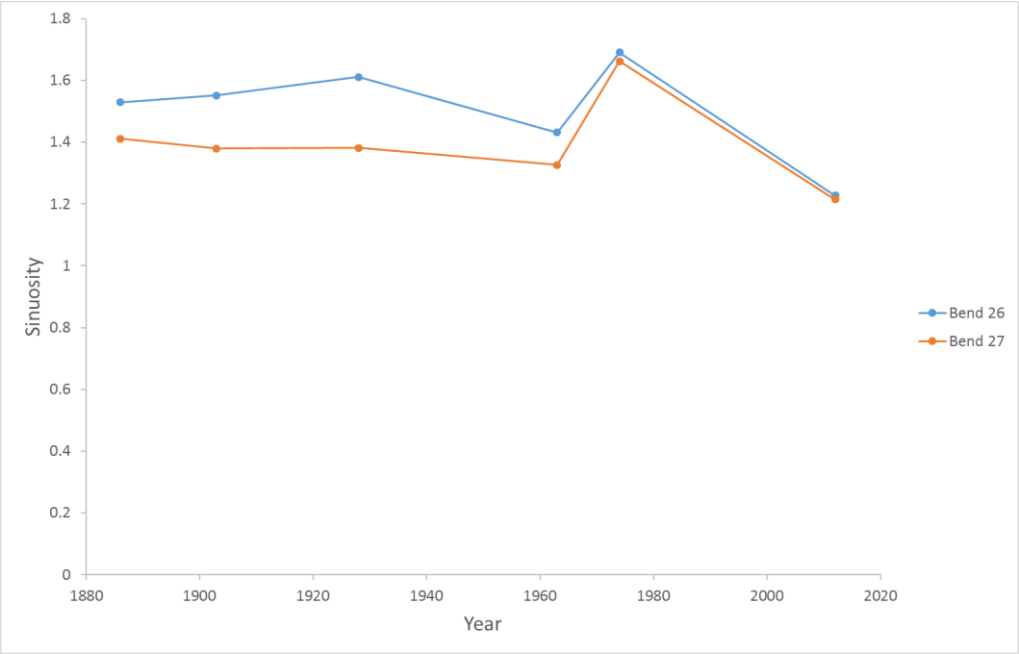

Figure 4.71. The sinuosity trajectory of bends 26 and 27. Bend 26 experienced a chute cutoff between 1963 and 1974 and bend 27 experienced a neck cutoff between 1974 and 2012.

4.4.2.2. River Arrow Reaches

The River Arrow reaches showed a slight increase through time in the overall sinuosity of the channel, as shown in the Figure 4.72. All three reaches showed the largest increase in sinuosity between 1964 and 1974, the period that also measured the highest mean annual erosion rate.

4.4.2.2.1. River Arrow Cutoffs

The River Arrow had a total of 23 cutoffs during the study period, with nine neck cutoffs and fourteen chute cutoffs. The average sinuosity for a neck cutoff was 1.86 and for a chute cutoff was 1.60. The majority of cutoffs occurred in Reach 1 (see Table 4.4 for details). At least one cutoff occurred in every time period for Reach 1, with a total of six occurring between 1964 and 1974 out of a total of 45 bends.

A series of cutoffs occurred between 1974 and 2012 on Reach 1, when three consecutive river bends were all cutoff. The reach had a maximum sinuosity of 2.01, less than the theoretical maximum of 3.14 proposed by Stolum (1996, 1998) and lower than the maximum of 2.92 measured by Hooke (2004) on the River Bollin before a series of cutoffs occurred, but it is a high sinuosity for the reaches on the River Arrow. The section of the river started in a sinuous state with bends 22, 23 and 24 having a sinuosity of 1.85, 1.52 and 1.47

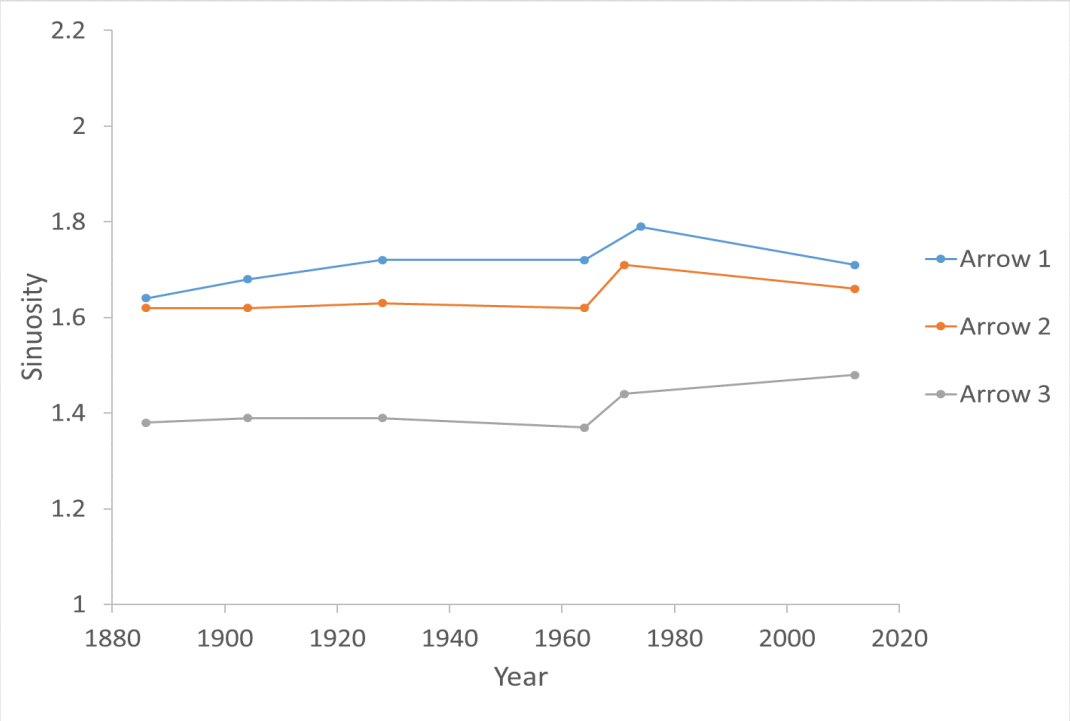

Figure 4.72. The changes in sinuosity on the River Arrow

respectively. Bend 22 showed a slight decrease between 1886 and 1928 before increasing to a maximum in 1974. For bends 23 and 24 the sinuosity was increasing steadily between 1886 and 1964, before bend 23 showed a large increase in sinuosity between 1964 and 1974 (from 1.61 to 1.91). All three bends had a peak sinuosity in 1974. Just downstream of the series of three bends there was a cutoff on bend 27 between 1964 and 1974, which potentially caused the increase in erosion measured on bends 22-24. Between 1974 and 2012 all three bends were cutoff leaving a much less sinuous channel. It is not possible to know from the data used in this study whether the bends were cutoff during one event or season but given the high local sinuosity and narrowness of the river bends it is possible that the cutoffs occurred in a short space of time. The sinuosity for the three bends was 1.25, 1.24 and 1.22 when the bends were measured in 2012.

Table 4.4. The sinuosity of the river channel before a cutoff occurred on the River Arrow

River	Reach	Year	Bend Number	Sinuosity	Cutoff Type
Arrow	1	1886	33	1.52	Neck
	1	1904	24	1.55	Chute
	1	1904	32	1.44	Chute
	1	1928	33	1.67	Neck
	1	1964	14	1.86	Chute
	1	1964	17	2.16	Neck
	1	1964	26	1.48	Neck
	1	1964	35	1.71	Chute
	1	1964	37	1.69	Chute
	1	1964	40	1.65	Chute
	1	1974	27	2.01	Neck
	1	1974	28	1.91	Neck
	1	1974	29	1.75	Neck
	1	1974	41	1.85	Chute
	1	1974	44	1.63	Chute
	2	1886	26	1.63	Chute
	2	1964	40	1.67	Chute
	2	1971	9	1.21	Chute
	2	1971	31	1.46	Chute
	2	1971	32	1.40	Chute
	2	1971	44	1.93	Neck
	2	1971	50	2.34	Neck
	3	1964	8	1.63	Chute

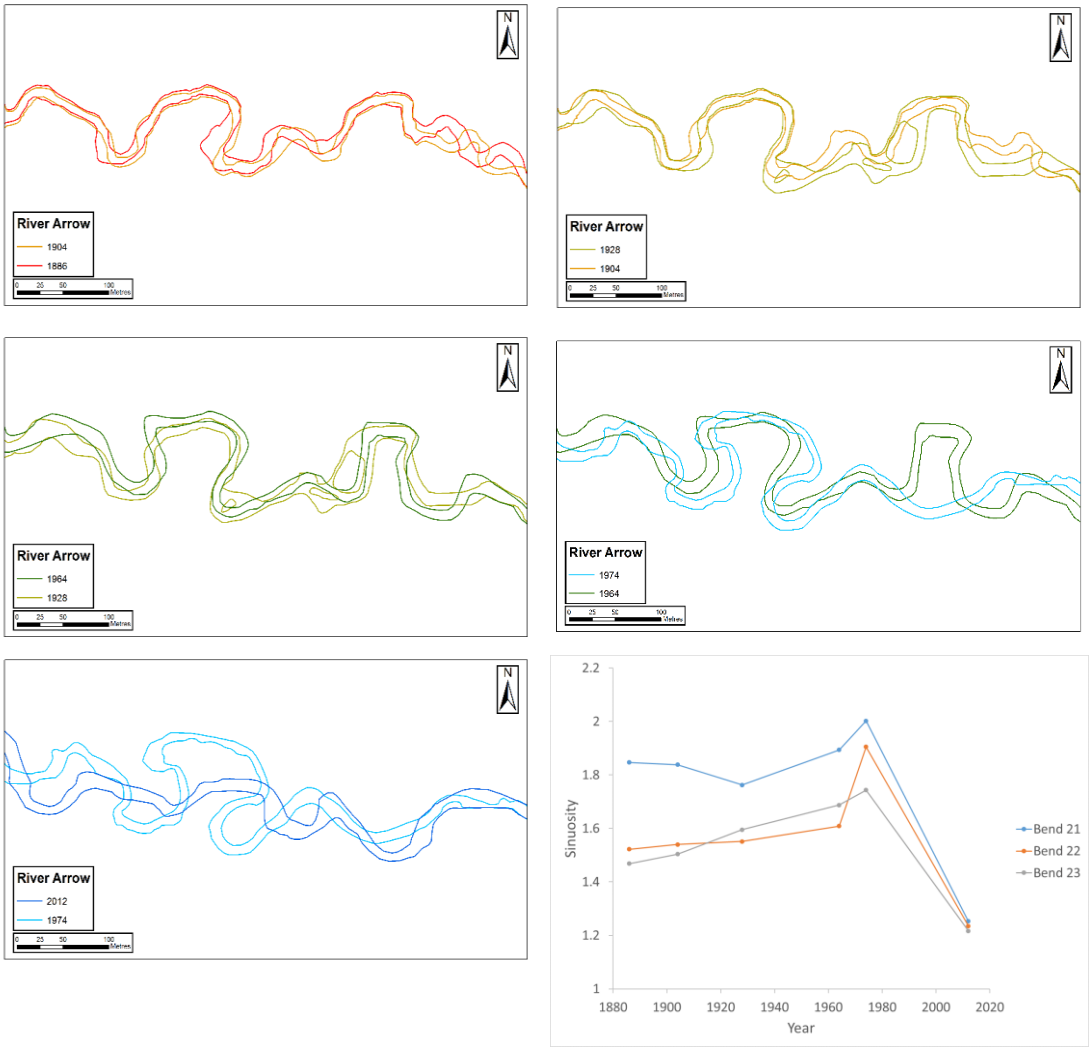

Figure 4.73. A series of bends in close proximity were cutoff between 1963 and 2012. The trajectories of the three bends are shown, with each bend increasing in sinuosity until the cutoffs occurred. A threshold of around 2 appears to occur on the River Arrow

4.4.2.3. River Till Reaches

The behaviour of the River Till and River Glen was different to the rivers in the Lugg catchment. The flood defences limited the amount of space for the rivers to freely migrate and in many bends the river is located very close to the flood defences. The sinuosity on the River Glen was very similar in 1886 (1.86) and 2012 (1.88) after having a slight decrease in between. The River Till showed a decline in sinuosity throughout, from 1.75 to 1.58. Three large loops were cutoff in the study period for the River Till and none of the bends were able to grow across the floodplain. The main type of channel planform change was either retraction or downstream migration.

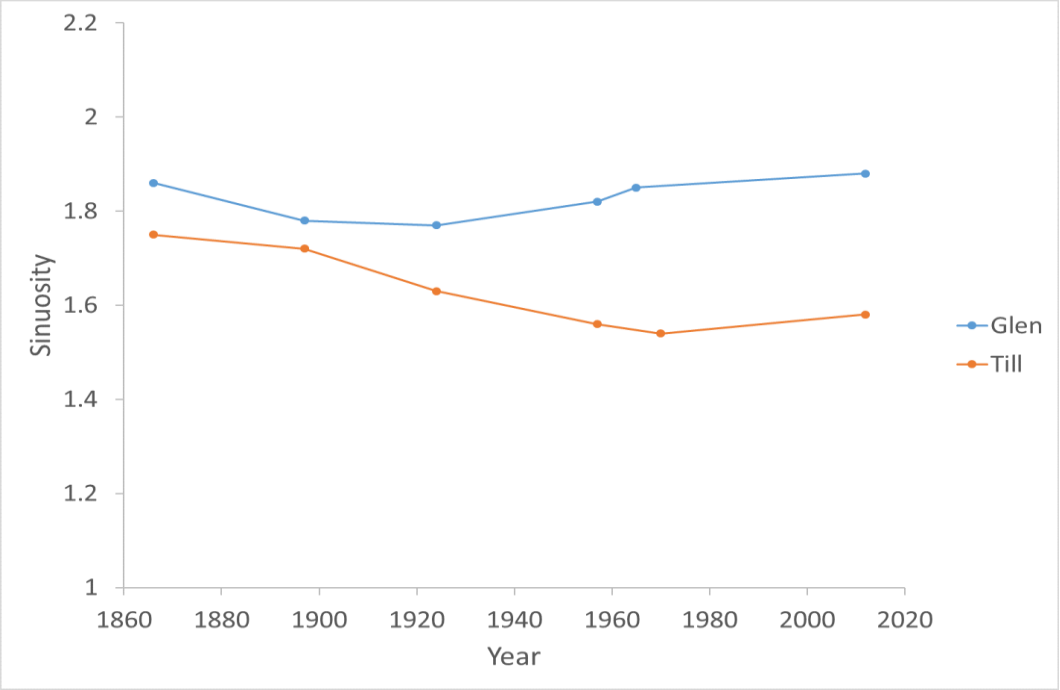

Figure 4.74. Sinuosity changes on the River Glen and River Till. The reaches are restricted and not able to grow across the floodplain.

4.4.2.3.1. River Till Cutoffs

In total 22 cutoffs occurred on the River Glen and River Till between 1866 and 2012. The majority of the cutoffs were chute cutoffs (eighteen chute cutoffs compared to three neck cutoffs) as shown in Table 4.5. The average sinuosity for a chute cutoff was 1.62 and the average sinuosity for a neck cutoff was 1.88. A particularly important cutoff occurred just downstream of Doddington Bridge on the River Till. An aerial photograph from the 1970s shows the bridge damaged and a temporary replacement bridge built in its place just upstream from a large neck cutoff. The neck cutoff occurred in two phases across two different periods. The first main neck cutoff occurred between 1924 and 1957 when a large section of the loop was cutoff. In the following period the remains of the loop were cutoff and the section of the channel was left much straighter. Subsequently the channel is starting to show evidence of initiation with new bend being formed, this time of the opposite side of the floodplain. The section of channel had a peak sinuosity of 2.01 in 1924 before the cutoffs occurred. The channel had a minimum sinuosity of 1.39 in 1970 after the two cutoffs had occurred, before starting to increase again in 2012.

Table 4.5. Sinuosity measurements on the River Glen and River Till before cutoff occurred. Most of the cutoffs were through chute cutoffs, due to the restricted floodplain width

River	Reach	Year	Bend Number	Sinuosity	Cutoff Type
Glen	1	1866	22	1.66	Neck
	1	1866	23	1.59	Chute
	1	1866	25	1.81	Chute
	1	1897	27	1.44	Chute
	1	1897	39	1.97	Neck
	1	1924	12	1.52	Chute
	1	1965	44	1.57	Chute
Till	1	1866	5	1.62	Chute
	1	1866	12	1.57	Chute
	1	1866	31	1.45	Chute
	1	1897	7	1.86	Chute
	1	1897	11	1.45	Chute
	1	1897	35	1.67	Chute
	1	1897	53	1.66	Chute
	1	1897	77	1.68	Chute
	1	1924	26	1.97	Chute
	1	1924	27	2.07	Neck
	1	1924	59	1.83	Neck
	1	1924	63	1.61	Chute
	1	1957	15	1.20	Chute
	1	1957	22	1.91	Chute
	1	1957	27	1.51	Chute

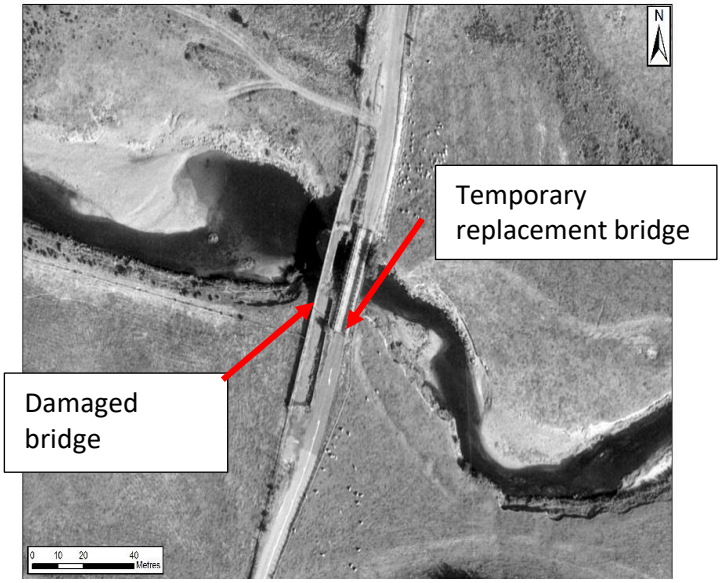

Figure 4.75. Damage caused to Doddington Bridge over the River Till from a 1970s aerial photograph, which was potentially related to the cutoff that occurred just downstream of the bridge

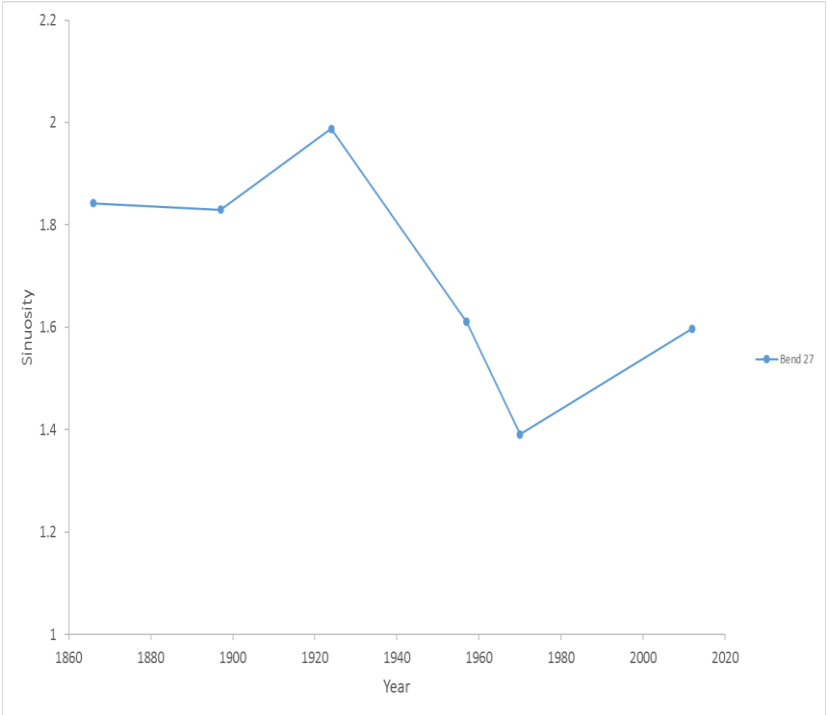

Figure 4.76. Sinuosity trajectory of bend 27. The cutoff occurred as the sinuosity approached 2 and further decreased between 1957 and 1970 to the most ordered state.

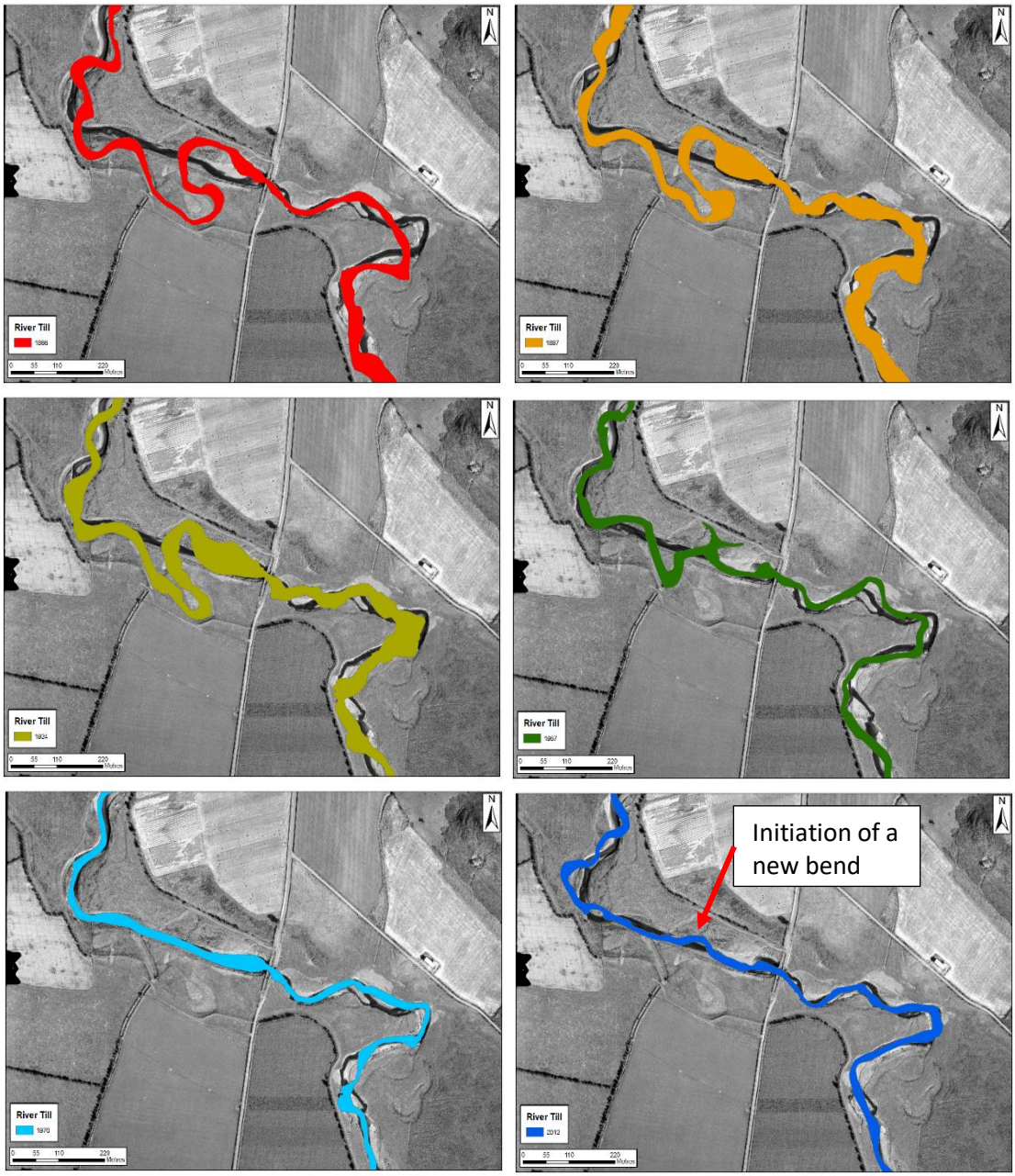

Figure 4.77. The channel changes just downstream of Doddington Bridge. The cutoff of the large loop will have increased the steepness of the channel considerably and this knickpoint could quickly move upstream. This could have destabilised the bridge and helped to cause the damage seen in the aerial photograph.

4.4.3. Flow discharge measurements

The discharge measurements in each catchment were analysed to assess whether there any obvious hydrological reasons for the increased erosion measured in the 1960s period. The increased erosion rate could possibly be explained by a series of high flow events during that period, or the erosion could have been caused by a particularly high flood compared to the rest of the flow record.

There are two gauges available close to the River Lugg reaches with a reliable daily flow record, Byton (gauge number 55014) which is located in between Reach 2 and Reach 3 and Butt's Bridge (gauge number 55021), which is located just downstream of Leominster at the end of Reach 5. The Byton gauge covers from 1966 to present day and the Butt's Bridge covers 1969 to present day. A longer record is available at near the end of the catchment at Luggwardine, however, there are multiple issues with the flow record, recent peaks are truncated at 32.1 cumecs and peak measurements between 1953 and 1965 are unreliable. Due to the distance from the study reaches and the unreliability of the measurements, this gauge was not included in the analysis. A long-term gauge is available just to the south of the Lugg catchment on the River Wye. The Belmont gauge (55002) was installed in 1908, with a reliable flow record from 1932. The correlation between the flow at Belmont and the flow at Byton and Butt's Bridge was calculated, with a R^2 value of 0.74 and 0.70 respectively. Using this regression relationship, it was possible to extend the flow record of the two River Lugg gauges back to 1935. Despite the increase in the length of the record, the flow record does not cover two map periods, 1886-1903 and 1903-1928.

The peak over threshold (POT) for Byton is 15.73m^3s^{-1} and for Butt's Bridge is 23.36m^3s^{-1}. The total number of flow events that were over the threshold (including multiple day events) was 264 for the Byton gauge and 257 for the Butt's Bridge gauge. Figure 4.78 shows the discharges of all the POT events at the Byton and Butt's Bridge gauge. The peak discharge for each gauge was measured during a high flow event on 21st July 2007, for both gauges. The peak discharge was 46.8m^3s^{-1} for the Byton gauge and 76m^3s^{-1} for the Butt's Bridge gauge. This event, which lasted for four days, is unusual as it was a summer flood event. The majority of the high flow events for this catchment occurred in the winter.

The time series was split into decadal periods based on the start of the extended flow record in 1935. The maximum and mean discharge was then calculated for both gauges for each of the periods, along with the total number of days and events that were POT, and the

maximum and average duration of these events. The mean discharge during each decadal time period varied little, with a maximum of 21.68 cumecs and minimum of 18.84 cumecs for the Byton gauge and a maximum of 35.40 cumecs and minimum of 28.94 cumecs measured at the Butt's Bridge gauge. However, there was a large increase in the number of days on which a POT event occurred, the maximum duration for a flow event and the average duration of POT events. Table 4.6 shows the changes in the different variables for each decadal period.

The flow data for the River Till catchment is sparser. There are two gauges available: the River Till at Etal, which covers from 1956 to 1980 and the River Glen at Kirknewton, which covers from 1966 to 2010, with a large break in the data between 1983 and 1989. The period covered by the Kirknewton gauge only covers the last period of mapping and so it is not possible to examine whether there have been any changes to the flow regime for the different map periods. The gauge at Etal does partially cover two different map periods, with evidence of high flow peaks in both periods. There is a period of low flow from 1971 to 1976, with the highest discharge measured at 55.49m^3s^{-1} in 1975 compared to 134.2m^3s^{-1} measured in 1965. The mean discharge in the 1970s period is 5.1m^3s^{-1} compared to 9.6m^3s^{-1} for the rest of the flow record.

Table 4.6. Both the Byton and the Butt's Bridge gauges showed an increase in the maximum discharge recorded and the number of days with a peak over threshold event between 1935 and 2015. The maximum duration of the flow events also increased during the flow record period.

Gauge	Period	Total # POT (days)	Total # POT (Events)	Max Discharge (m^3s^{-1})	Mean Discharge (m^3s^{-1})	Maximum Flow Duration (days)	Mean Flow Duration (days)
Byton	1935-1945	55	38	27.09	18.84	3	1.5
	1946-1955	65	32	40.05	20.90	9	2.0
	1956-1965	41	26	41.49	19.40	4	1.6
	1966-1975	54	26	37.95	19.24	5	2.0
	1976-1985	95	37	30.39	19.19	7	2.6
	1986-1995	146	37	33.07	20.69	16	4.0
	1996-2005	111	35	45.39	21.17	13	3.2
	2006-2015	102	31	58.69	21.68	15	3.3
Butt's Bridge	1935-1945	51	34	41.22	29.10	3	1.5
	1946-1955	63	30	60.96	32.06	9	2.1
	1956-1965	40	25	63.17	29.66	4	1.6
	1966-1975	59	28	47.20	29.51	6	2.1
	1976-1985	73	28	50.74	28.94	6	2.6
	1986-1995	97	31	57.00	31.66	11	3.1
	1996-2005	96	34	62.00	33.25	13	2.8
	2006-2015	146	45	76.00	35.40	23	3.2

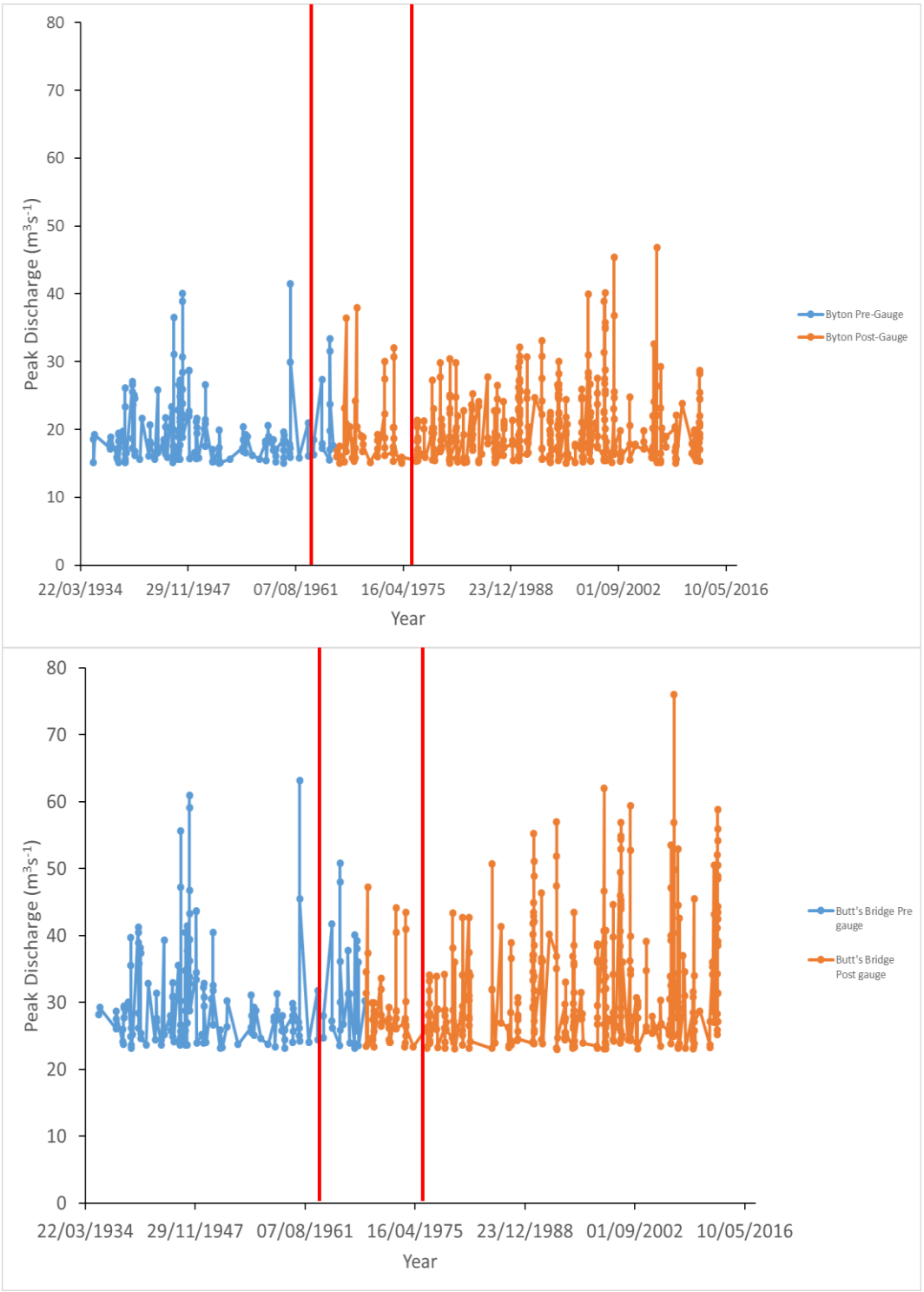

Figure 4.78. The discharge of the POT events at the Byton and Butt's Bridge gauges on the River Lugg. The red lines indicate the dates of the maps. The data coloured blue indicates the flow record derived from the relationship with the Belmont gauge on the River Wye

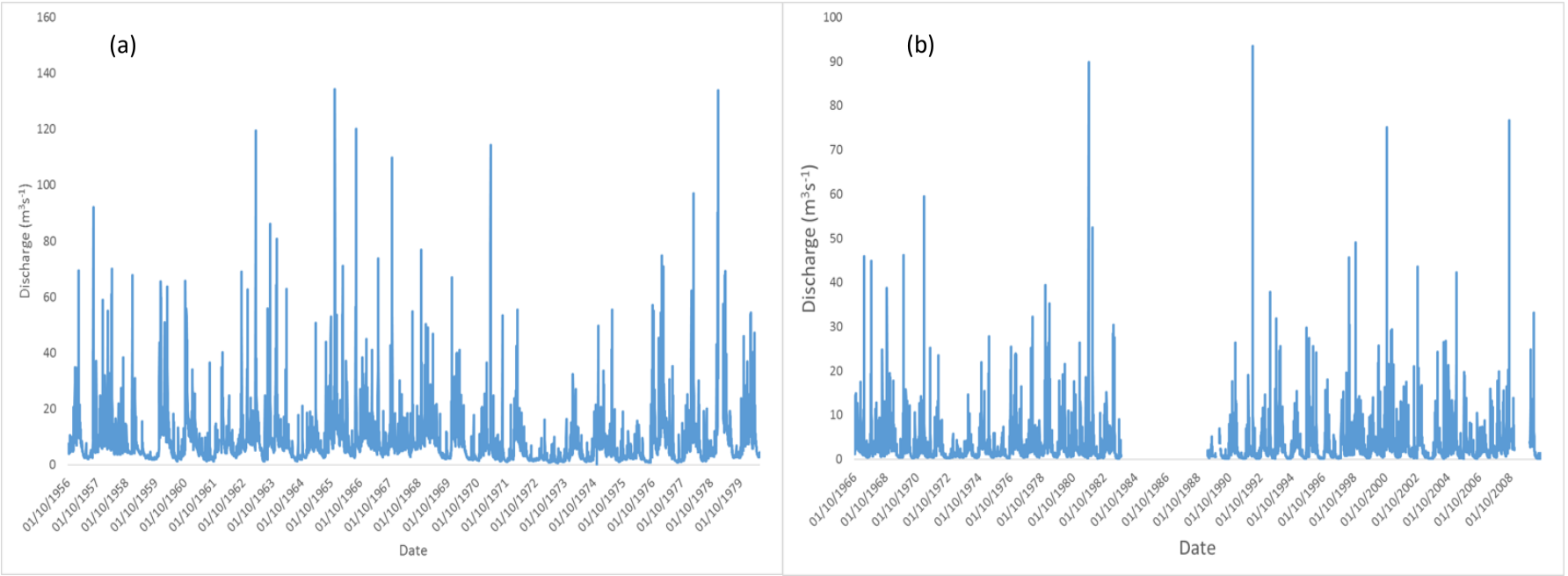

Figure 4.79. Flow record for the gauge at (a) Etal and (b) Kirknewton. The short and incomplete record makes it difficult to compare between the different map periods.

4.5. Discussion

4.5.1. Variations in erosion rate

It is expected that there would be variations in the amount of lateral migration between different years as the river channel responds to the different magnitude, frequency and duration of flow events during the year, and erosion only occurring once a certain threshold has been reached. However, this variation should be smoothed out over longer periods as a wider range of typical and higher magnitude events are incorporated.

During this study, it has been found that the highest rates of mean annual erosion were all measured during the periods with the shortest time between the two available map dates. Figure 4.80 shows the mean annual erosion rate for each reach and the period length between the two data points and the same data on a logarithmic scale. These periods represent the 1963-1976 period for the River Lugg catchment and the 1957-1970 period for the River Till catchment. Sadler (1981) studied nearly 25000 accumulation rates from 700 references and recognised that there was a systematic trend in sedimentation rates where the sedimentation rate would increase logarithmically with decreasing time period between data points. He found an inverse log-normal relationship between sedimentation rate and the length of time period and suggested that the cause of this is unsteady and discontinuous sedimentation. Hurst (1951) recognised that there was a long-term persistence in data sequences for hydrological and geophysical events, for which periods of wet and dry years could dominate for number of years. These discontinuities occur at all time scales and longer time periods between data points will incorporate more and longer hiatuses in geomorphic activity meaning that the sedimentation rate would decrease as the length between data points increased. A similar trend appears when comparing the annual erosion rate between different length periods, with a logarithmic increase in mean annual erosion rate as the period length decreases. The effect of this will be greater on rivers that have a high flow discharge threshold for erosion to occur compared to rivers with a low threshold.

There are uncertainties associated with the methodology used in this study, which need to be recognised. The impact of these uncertainties will have a greater impact on the annual erosion rate for map dates that are closer together. The first uncertainty is associated with the difference between the date the maps were published and the actual survey date. The date of publication is available for the Ordnance Survey data provided by Digimap but the actual survey date is not included. This is a systematic error as the survey date must be before the publication date and should be similar for all

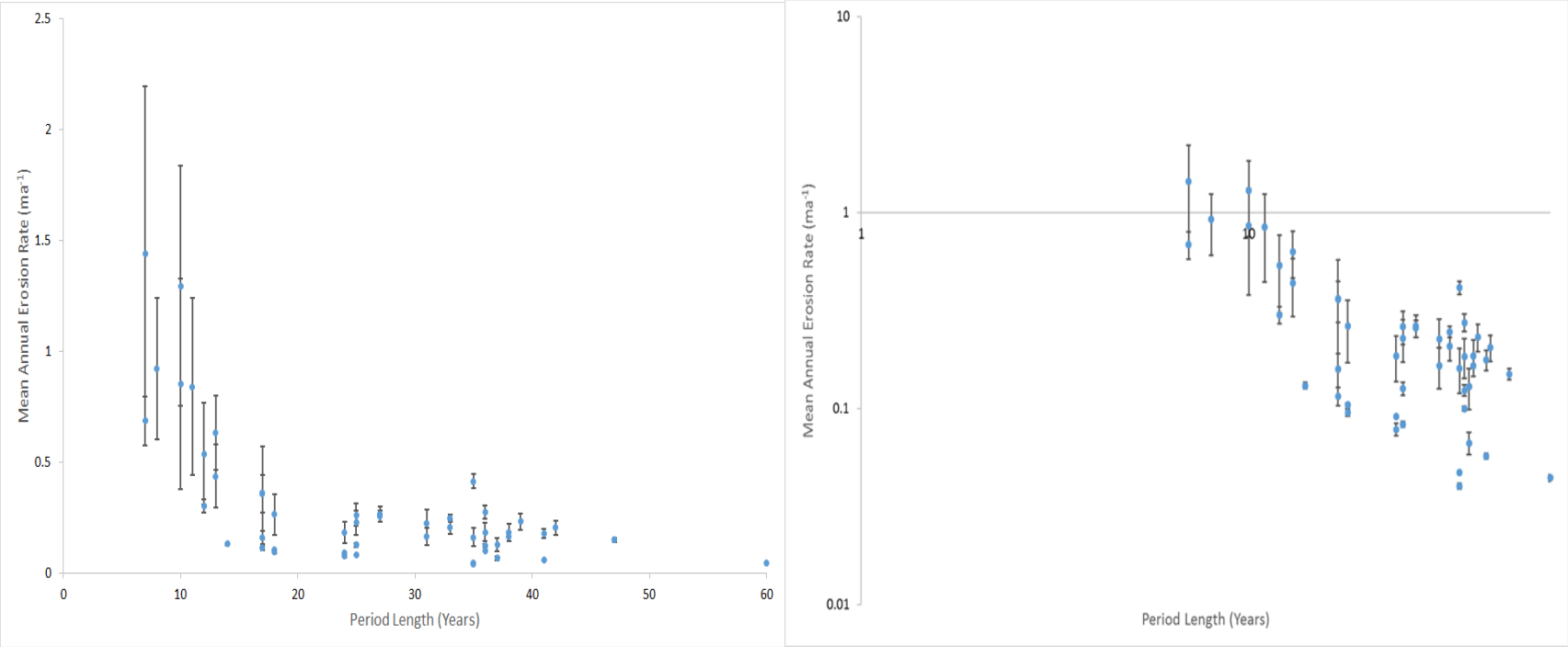

Figure 4.80. The mean annual migration rates for each period against the length of time between map dates, which showed an inverse relationship when plotted on a log-log scale.

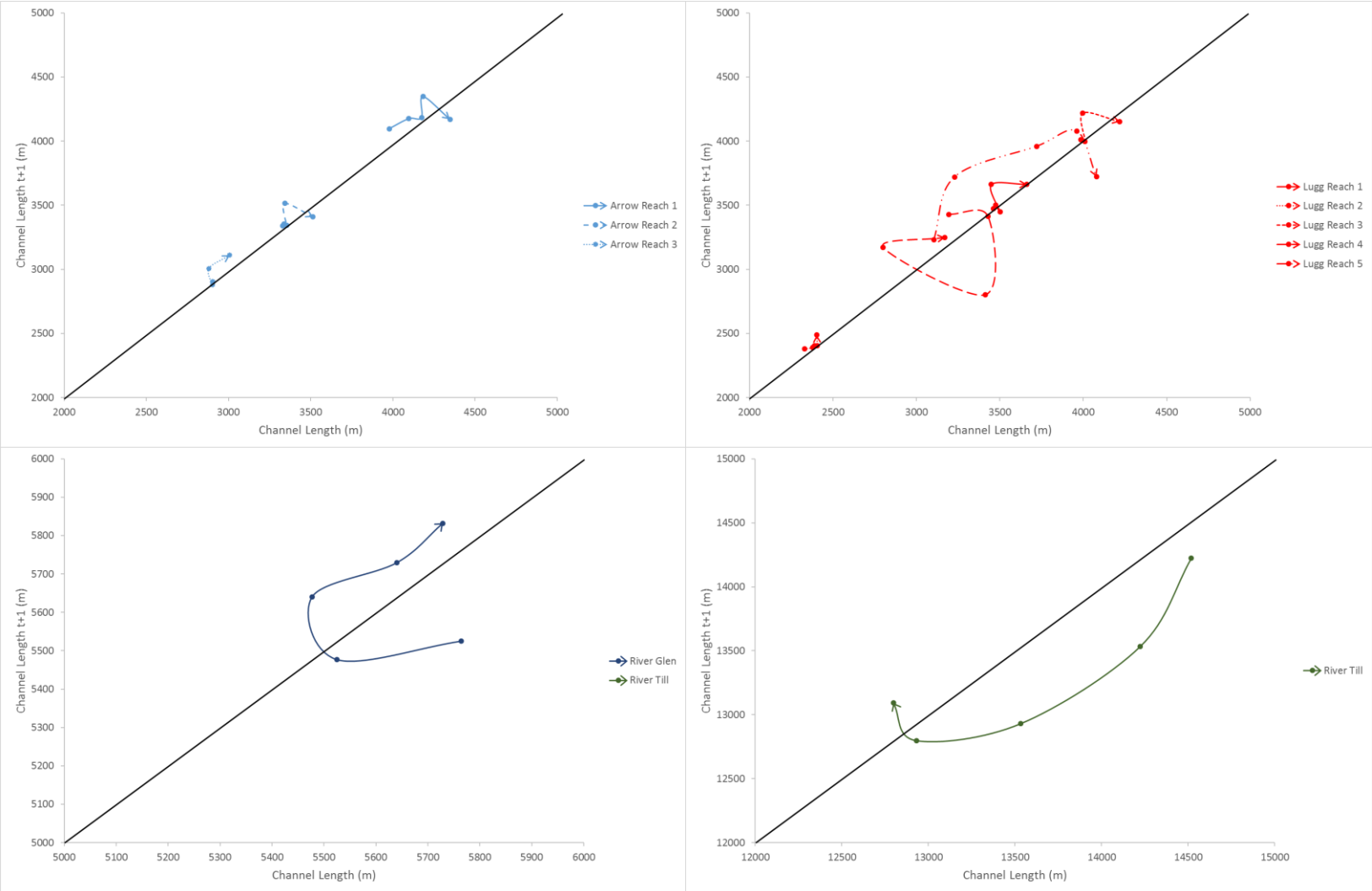

Figure 4.81. The trajectory of channel length for each of the individual reaches. The black line indicates a stable channel length

of the map dates. There are also some uncertainties associated with the definition of the bank position. The bankline is usually defined by the winter flow (Harley, 1965), but this could vary depending on the surveyor and the flood conditions at the time of the study. Using the centreline rather than the bankline reduced some of the uncertainty associated with this problem. One final source of uncertainty is from the changing map scales available for the study. While most of the map were at 1:2500 resolution, the 1960s National Grid 1st Imperial Edition was published at 1:10560 scale for the River Lugg catchment and the 1860s County Series 1st Edition was 1:10560 in the River Till catchment. The 1960s National Grid 1st Imperial Edition also coincides with shortest period between different map dates (i.e. 1960s to 1970s) for the River Lugg and may add further uncertainty to this period.

There are other potential measurements of channel activity during a period that can be used to test whether a particular period is more active than another period. By plotting the channel length against channel length for the following period it is possible to measure whether the channel length has increased or decreased. Figure 4.81 shows the changes for the River Lugg and River Till catchment. The line represents a stable channel length with no change from one period to the next, while reaches plotting above the line represent an increase in channel length and hence erosion of river bends, and reaches plotting below the line represent a decrease in channel length, mainly due to cutoffs. The further away from the line the higher the activity rate on the particular reach for that period. The 1960s period for the River Lugg plots on average further away from the no change line than any of the other periods, which suggests that the amount of lateral erosion was high during this period. Reach 2, which plots close to the no change line experienced a large cutoff during this period, with over 10% of the whole channel length being cutoff. This indicates that many of the other bends in the reach were growing across the floodplain for the overall channel length increase slightly. The River Till shows a different behaviour, with the overall channel length decreasing between different periods. This is mainly due to the flood defences present for these reaches preventing the channel from migrating across the floodplain. Many of the sections of the River Till and River Glen had a high sinuosity and loops were cutoff during this study period, reducing the overall length of the channel.

There are other potential causes of the increased migration rate in the 1960s on the River Till and River Lugg. It is possible that during these periods there were more high magnitude flow events or that they occurred more regularly. Unfortunately, the flow records do not cover the entire study period and there is no direct measure of the flow in either of

the catchments prior to 1960. A series of high magnitude flood events occurred in the 1960s in the Lugg catchment, in 1960, 1964, 1965, 1968 and 1969. However, the magnitude, frequency and duration of the events is not exceptional when compared to the later period. The duration of POT events increased towards the end of the 20th century with the highest mean duration measured in 1986-1995 period for the Byton gauge and 2006-2015 for the Butt's Bridge period. However, these higher magnitude and longer events appear to have a smaller geomorphic impact compared to the 1960s period. The period prior to 1966, for which the flow record is derived from the Belmont gauge on the River Wye, shows a relatively low flow period between 1950 and 1960 with fewer peak flows and lower maximum discharges. There are, however, a series of high discharge events recorded for the 1940s (9/2/1946, 19/3/1947 and 13/1/1948), with the 1947 flood recorded as notable within the Lugg catchment (Jacobs, 2015). These flow events in the 1940s appear to have had limited impact for reaches 1, 2 and 3 on the River Lugg and all three of the Arrow reaches, but there was high erosion on reaches 4 and 5 on the River Lugg during this period.

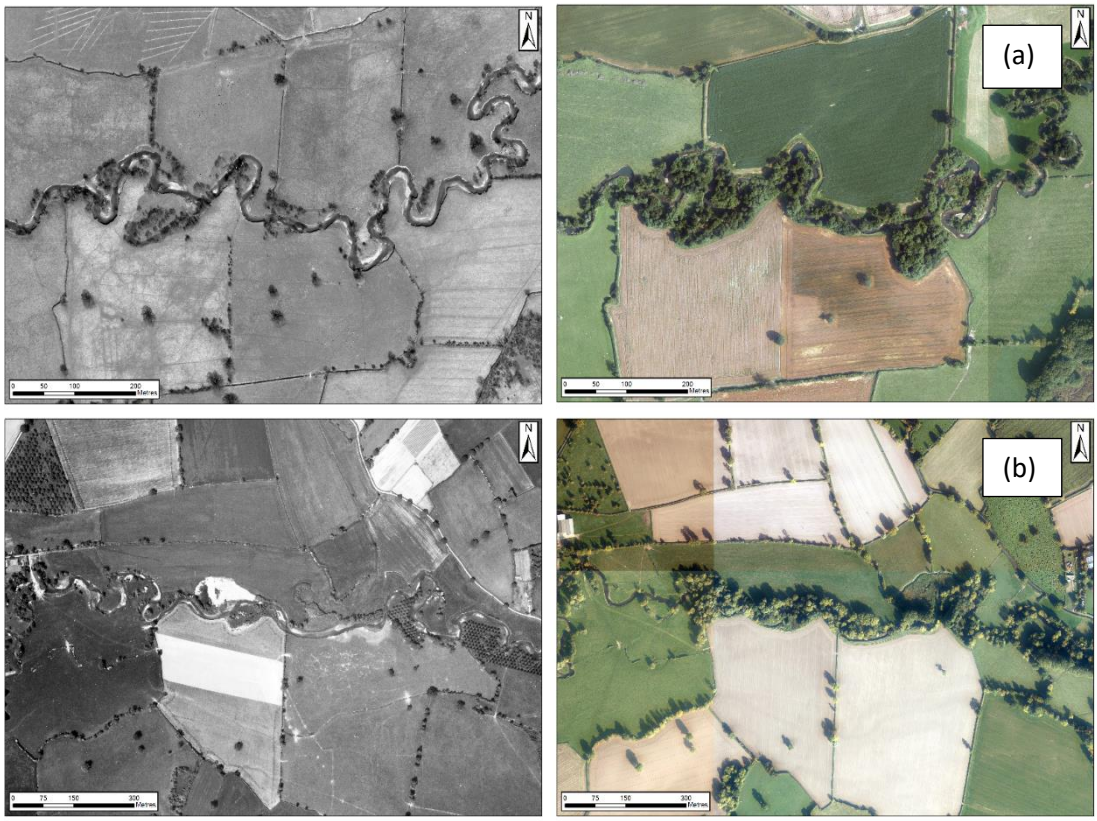

Figure 4.82. Changes in the amount of riparian vegetation coverage on the River Lugg (a) and River Arrow (b).

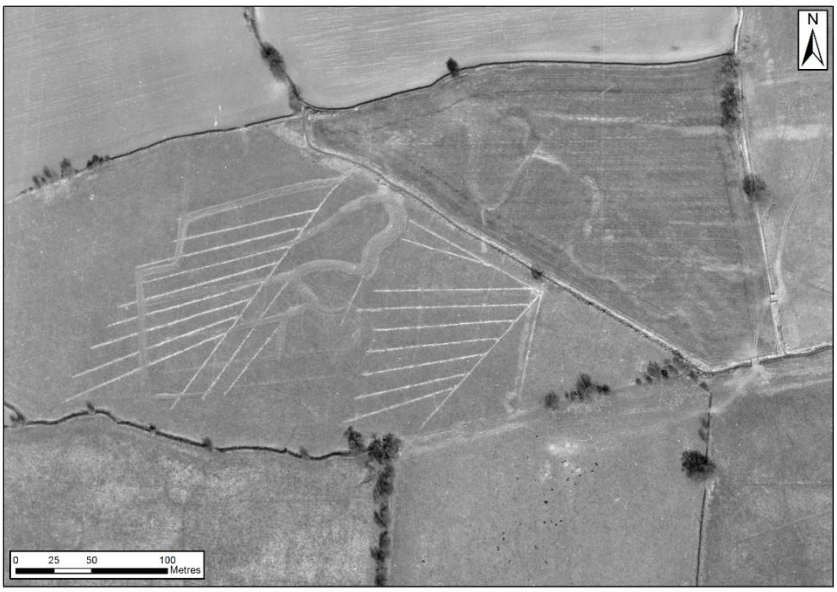

Figure 4.83. Evidence of the installation of drainage ditches in the Lugg catchment. This installation will have increased the rate of runoff entering the main channels

Another possible cause of the increase in erosion is land use changes in the 1950s and 1960s, especially in the River Lugg catchment. Aerial photographs were analysed between 1970 and 2012, which show a large increase in the coverage of riparian vegetation in the River Lugg catchment. The increase in vegetation will have helped stabilise the riverbanks by adding strength through root reinforcement and by deflecting flow away from the riverbank. The River Arrow and the River Lugg showed almost a doubling in the amount of vegetation in the riparian zone, between 1970 and present day, which may account for the decrease in activity seen between the 1960s periods and the later period, despite the presence of higher magnitude and longer duration flow events. Jacobs (2015) suggests that routine maintenance work was performed by Seven-Trent and Welsh Water Authorities along the River Wye and River Severn catchments (including the River Lugg) between 1930 and 1980 that included the removal of pioneer trees along continuous sections of the river channel. Although there is no direct evidence of clearance on the selected reaches in the Lugg catchment, it could explain why the levels of vegetation were so low in the 1970s aerial photographs and why, once the practice was stopped, the riparian zone vegetation has recovered in the later period. Figure 4.84 shows the vegetation changes within the study reaches. The amount of riparian vegetation increased by 1.5 times on the River Lugg, 2.3 times on the River Arrow and 4.2 times on the River Till. Another change that occurred in the 1950s was an increase in the intensity of agricultural production (Internal Drainage Board, 2010), which included the construction of drainage ditches in main fields. Drainage ditches

have been linked with increased channel erosion (Schottler et al., 2014) and incision (Piegay et al., 2005) in the US and the wide scale construction of drainage ditches in the Lugg catchment could have negatively affected the stability of the riverbanks.

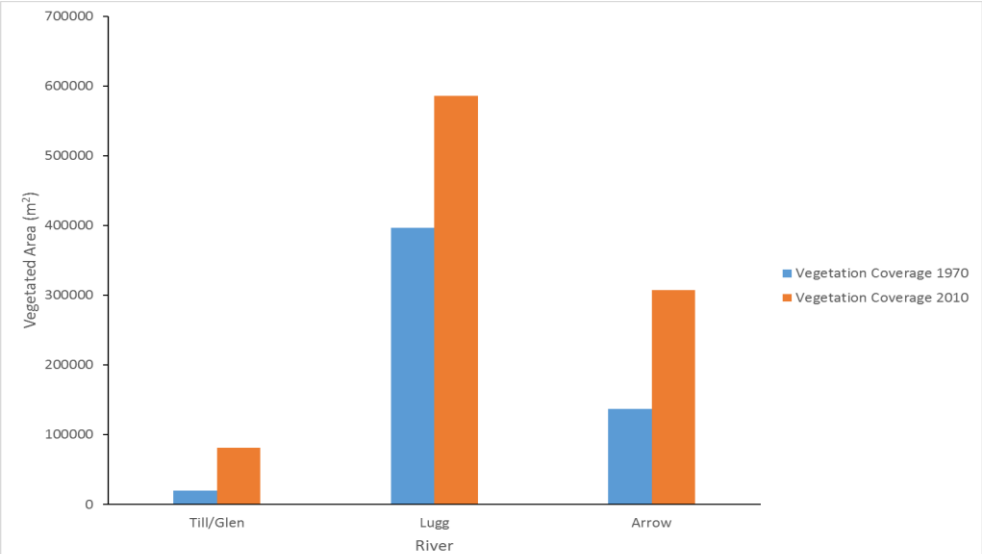

Figure 4.84. Changes in the coverage of riparian vegetation in the Till and Lugg catchments. All reaches showed an increase in the amount of vegetation

4.5.2. Sinuosity Threshold

The high number of cutoffs that occurred in the River Lugg and River Till catchments allowed for a thorough investigation of the relationship between sinuosity and cutoff occurrence for these catchments. Stolum (1996, 1998) suggested that rivers would oscillate between an ordered and chaotic state, with a straight line representing the most ordered state possible for a river channel. Simulations showed the presence of two coexisting domains, one with high sinuosity and one with low sinuosity. The high sinuosity domain represents a supercritical state at which a single cutoff event will generate a cluster of cutoffs throughout the whole system, while the low sinuosity domain represents a subcritical state at which only a single cutoff is likely to occur. In freely migrating rivers, Stolum found that the sinuosity threshold between the two domains was 3.14.

The sinuosity measured before a cutoff for rivers in the River Lugg and River Till catchment were lower than the sinuosity for the simulated rivers used by Stolum. The average sinuosity for a neck cutoff and for a chute cutoff was 1.85 (n=28) and 1.64 (n=43) respectively, which suggests that the rivers are not able to freely migrate. There are a number of reasons why these rivers are not able to freely migrate across the floodplain. The River Till and the River Glen have flood embankments along virtually the entire reach, which have prevented the river from growing across the floodplain, along with certain sections on the River Lugg. The River Lugg in Reach 3 has entered a narrow valley, which has confined the river and led to a low average sinuosity for the whole reach. Rail and road bridges can also act as localised confinement of the river channel, acting as a fixed point through which the river must travel. There is a total of 24 bridges on or between the reaches in the study areas, which will prevent the river from being able to migrate freely and essentially act as an ordered state within the river system.

Many of the cutoffs were only single chute or neck cutoffs without further cutoffs upstream or downstream, suggesting that often the river planform was in a subcritical state when the cutoffs occurred. It is possible to identify some cutoffs that appear to have led to increased erosion on the bends around the cutoff, such as bend 9 on Reach 4, River Lugg where the bends either side of the cutoff were stable before the cutoff occurred between 1928 and 1963, and subsequently became active in the next period. This suggests that the river system is below the supercritical state proposed by Stolum (1998), but that the river system is still sensitive to the cutoff and responds by increasing erosion of the bends surrounding the cutoff. However, a series of cutoffs do occur on a limited number of reaches.

Reach 2 on the River Lugg (see Figure 4.69) had a neck cutoff that was immediately preceded by two chute cutoffs on the bends upstream. The sinuosity through this section was high compared to most cutoffs on the River Lugg, with a mean sinuosity of 2.58. Reach 1 on the River Arrow (see Figure 4.73) had a cluster of neck cutoffs that occurred between 1974 and 2012. The section of the channel had a sinuosity of 2.01 before the cutoffs occurred.

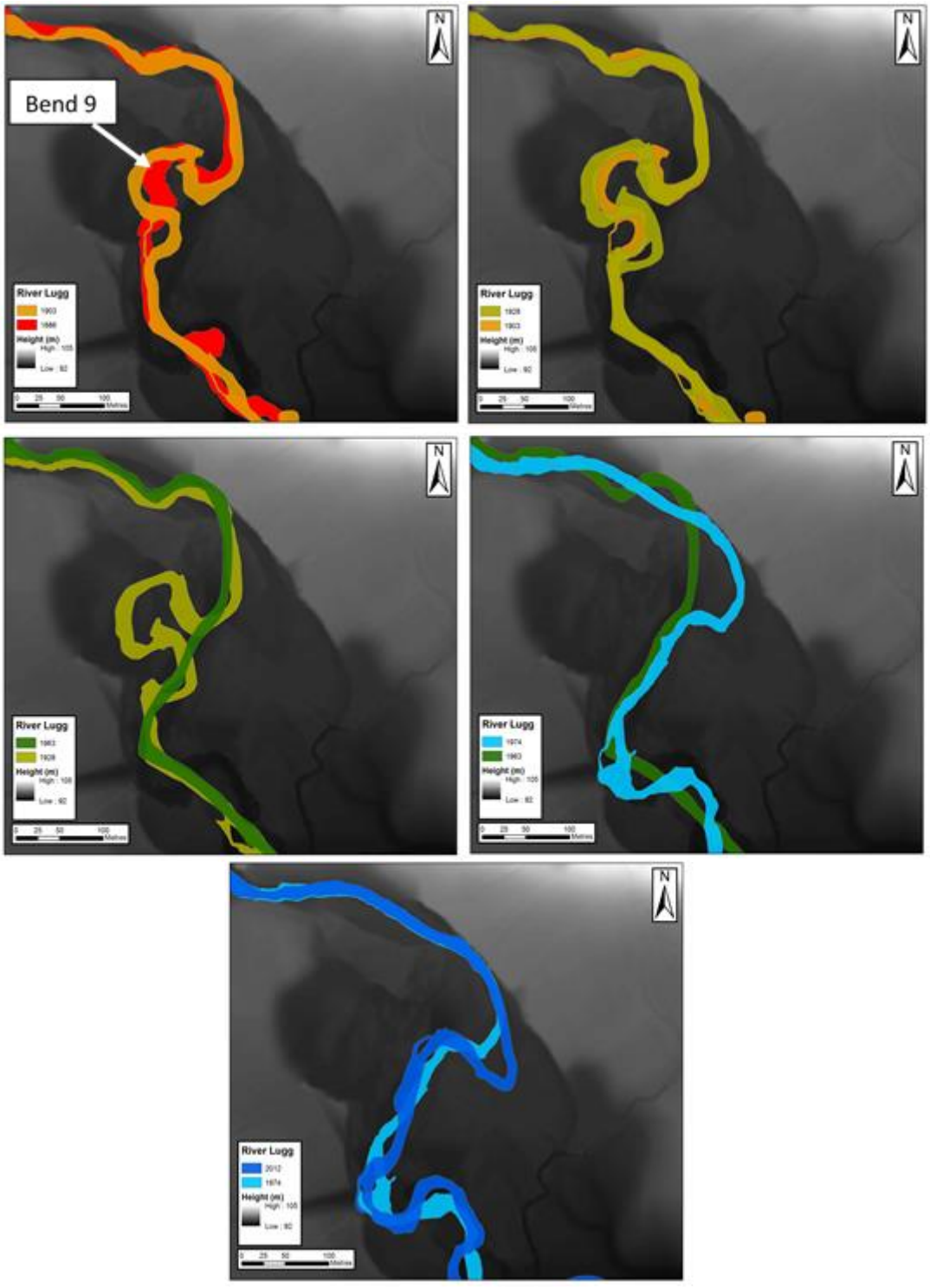

Figure 4.85. Most of the bends around bend 9 are stable prior to the cutoff in the 1928-1963 period, before becoming active and growing across the floodplain after the cutoff occurred

4.6. Conclusion

Historic Ordnance Survey maps from two catchments and six different dates were used to measure the channel change on four actively migrating rivers. The migration rate between different periods was measured every 10m and the mean and maximum rates were calculated for bends (defined as the length of channel between two inflection points). The sinuosity of each channel prior to a cutoff was also measured and compared to the theoretical maxima suggested by Stolum (1996, 1998). The research presented in this chapter has shown that there is a great deal of variability in erosion rates between individual bends on a reach, between different reaches in a catchment and between different time periods.

A notable feature of the migration rates for both catchments was that the highest migration rates were consistently measured for the shortest period between the two map dates (1957-1965/1970 in the Till catchment and 1963-1971/1976 in the Lugg catchment). A log-log plot on the period length against the mean annual migration rate showed an inverse relationship similar to that found by Sadler (1981) in sedimentation rates. This is partially explained by the process of erosion being a threshold driven process where erosion will only occur once a certain threshold in flow magnitude or duration is passed. If the threshold is not passed, then little or no erosion will occur and longer periods between map dates are likely to include more of these periods where no erosion occurred, lowering the net erosion rate for the period. This effect of this process is further increased if the system experiences a change in the threshold for erosion to occur. There is evidence of a large increase in the coverage of riparian vegetation between 1970 and present day, with growth on both the inner and outer bank. This increase in vegetation will add stability to the riverbank through root reinforcement and flow deflection (Abernathy and Rutherfurd, 1998, 2000) and increase the threshold for lateral migration to occur. Changes in flow discharge and duration will also affect the rate of erosion, and an increase in the duration of discharge events was found in the River Lugg catchment, but this coincided with an increase in the riparian vegetation coverage and the effect could be limited. The limited duration of the flow records makes it difficult to examine changes to the flow regime throughout the whole study period.

There are implications for the management approaches such as the erodible corridor (Piegay et al., 2005) and the Freedom Space for Rivers (Biron et al., 2014). These approaches rely on using historic rates of erosion to estimate how much space is required for a river to freely migrate over a period of 50 years. If the estimate migration rates are calculated from short periods of time, the uncertainty in the true long-term migration rate could be very high.

This could lead to an over prediction of the space needed for the river. For this study, there was a large increase in the migration rate once the length of time between the two map dates was ten years. Some of the uncertainty has occurred in this dataset as the scale of the maps changed from 1:10560 to 1:2500. Managers using the approaches above will need to consider the increased impact of the uncertainty in the data sources and appreciate that the impact of any uncertainty will be increased if there is a short length of time between the two data sources.

The high occurrence of cutoffs in the study catchments provided an opportunity to investigate the relationship between channel sinuosity and cutoff occurrence. Stolum (1996, 1998) proposed that there are two opposing processes in meander development: lateral erosion increasing the sinuosity of the channel and cutoffs that decrease the sinuosity. Simulations showed that a stationary mean would be created for two coexisting domains. A high sinuosity domain (~3.5) and a low sinuosity domain (~2.7) at which cutoffs would occur to change the river system from a chaotic state to a more ordered state. The mean sinuosity for neck and chute cutoffs were 1.85 and 1.64 for the Lugg and Till catchments, which is much lower than the values suggested for freely migrating rivers. However, the lower values are more comparable to the results found by Hooke (2004, 2007). This is expected as many of the reaches have some form of confinement through either flood defences or human structures and are not able to freely migrate across the floodplain. The mean sinuosity value of 1.85 for neck cutoffs suggests that once the sinuosity approaches this value then a cutoff is likely to occur.

5. The evolution of meander bends – relating channel curvature to migration rate

5.1. Introduction

The relationship between channel curvature and river channel change has long been studied from the early theoretical work by Bagnold (1960), and Leopold and Wolman (1960) to more recent work by Guneralp and Rhoads (2008, 2009, 2010). Hickin (1974), and Hickin and Nanson (1975) found there was an increase in the migration rate of river bends as the ratio of radius of channel curvature to channel width (r_m/w) reached ~5.0, with the maximum rates of migration found at r_m/w = 3.0 and a rapid decline the migration rate as r_m/w approached 2.0. Hickin and Nanson (1975) found an absence of bends with a ratio between 2.5 and 3.2 and suggested this could be caused by the rapid acceleration in migration rate altering the pattern of the channel quickly. Bagnold (1960) found that the resistance to flow would increase when r_m/w was below 2 as there was a breakdown in the secondary flows on the outside of the bend. Hooke and Harvey (1983) found that the breakdown in the secondary flows occurred at a critical path length and an extra pool and riffle sequence was created, causing a new secondary flow structure in the bend.

A special case for meandering rivers occurs when the meander chain is confined either by natural features, such as bedrock outcrops or valley sides, or by human features, such as bridges or bank protection work. Nicoll and Hickin (2010) studied the planform geometry and migration of confined rivers at 23 locations in Canada. They found that the r_m/w ratio was higher for confined rivers (r_m/w = 4.1) and that the bends appears to migrate downstream, without experiencing cutoffs. The loops are often truncated at the valley sides, producing a distinctive sawtooth pattern.

Nanson and Hickin (1983) proposed that the radius of curvature of a bend should be calculated as the mean of the radius at the apex of the bend and the point of maximum r_m/w (i.e. the point of inflection). This measure would reflect the strong influence at the apex of the bend and the broader sweep of the limbs of the bend. Hooke and Harvey (1983) measured the curvature of the channel every 10m and expressed the curvature in radian/10m, which could be converted to radius of curvature by the equation $r = (L/\theta)$, where r is the radius (m), L is the total length of the bend (m) and θ is the curvature of the channel (radians). Coulthard and Van De Wiel (2006) developed a curvature term for the cellular

model CAESAR based on the number of wet and dry cells of a river bend as defined by the model. The curvature was calibrated to circles with a known number of cells and radius, which produced a strong relationship between the calculated radius and the actual radius. Guneralp and Rhoads (2008) developed a method of defining the curvature of the channel centreline by fitting parametric cubic splines to the centreline and computing analytically the curvature at any location, which overcomes the reliance on average bend curvature values or discrete curvature values.

It was realised that if migration rates were only determined by the local channel curvature, bends would only increase in amplitude and not migrate downstream (Guneralp and Rhoads, 2009) and that the influence of curvature must be extended up and downstream. Many models of meander evolution use a weighted aggregate of local, upstream and downstream curvature to calculate the rates of migration at any point (Ikeda et al., 1981; Howard and Knutson, 1984; Furbish, 1988). These models used a first-order linear model, where the weighting of the curvature effect declines exponentially with distance upstream. More recently higher-order models have been developed (e.g. Campoereale et al., 2007), which were able to reproduce compound meander loops, which was not possible in the first-order models. Guneralp and Rhoads (2009) noted a combination of lateral extension and downstream translation leads to a phase lag between the spatial series for curvature and the migration rate for all of the dates studied on three actively meandering rivers. This was caused by the spatial memory in the system (i.e. the effect of upstream curvature). It was also found that the upstream influence of the spatial memory was longer for simple bends compared to compound bends, with the response distributed further along the river. For compound or multilobe bends, the system will respond over short distances to rapid changes in localised curvature.

Hooke (2003) proposed a framework for the analysis of river meander behaviour and instability. The framework can analyse type of behaviour ranging from stable to chaotic and consider the impact of meander cutoffs on meander evolution. This approach allows the conditions and constraints under which the different types of behaviour occur to be further understood. One of the key tenets of the approach is analysing the behaviour of individual bends in a channel curvature – migration rate phase space. Four different types of common bend behaviour were described and their trajectory plotted within this phase space (figure 1). The most active river bends would follow trajectory A or B, with a rapid increase in migration once the bend curvature reached the critical value described by Hickin (1974). These bends would develop to compound bends once the path length and curvature reached a further threshold, decreasing the overall curvature of the bend. Further development would occur through a cutoff, dramatically reducing the curvature of the bend and the bend development would start again. Chute cutoffs tend to occur at lower curvature and reduce the curvature of the channel less and would follow trajectory B. Some meanders can develop a course with low bend curvature but do not cutoff, actively migrating downstream. These bends would be expected to follow trajectory C. Finally, some bends have developed into tight, sinuous bends, but have since stabilised and are no longer active in the floodplain. This could be caused by the meander bends naturally developing slowly over time, or a change in

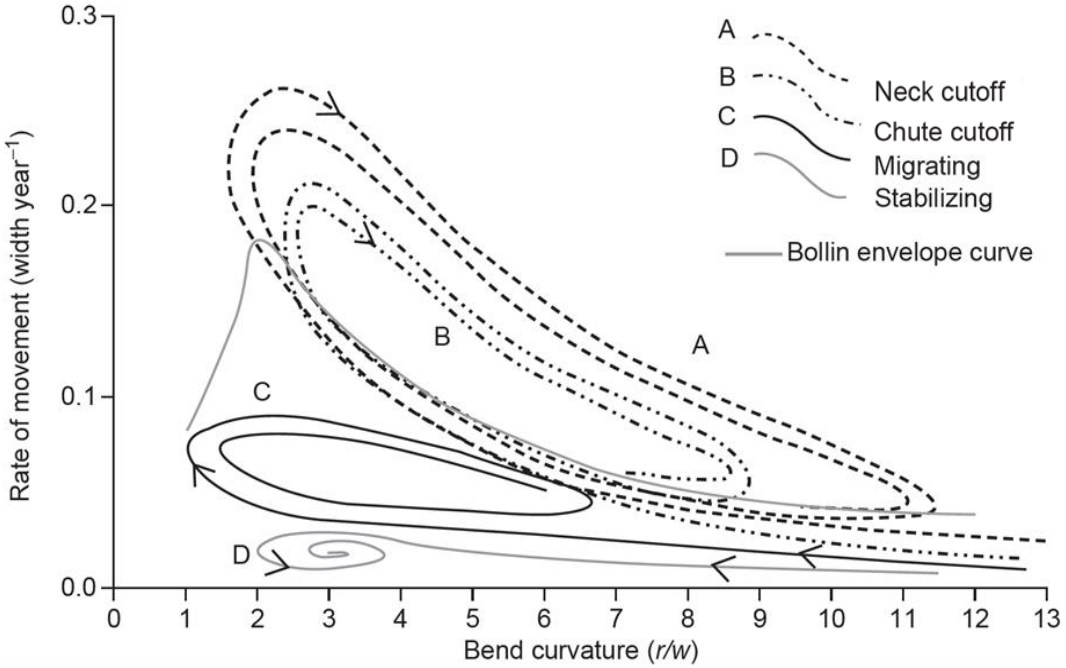

Figure 5.1. Theoretical trajectories of different bend behaviours from Hooke (2003).

the conditions for the meander bends, such as human intervention or climate change. Theoretically, individual bends could loop around the trajectories multiple times during the long-term planform evolution of the channel. However, the process occurs over a long period and there is usually only enough evidence to show a bend completing one loop.

The purpose of this chapter is to introduce several different measurements of curvature for an individual bend using a circle fitting approach, which can characterise the radius of curvature effectively. The approach will be based on the weighted aggregate curvature measurements used in many meander models. The second part of the chapter will use these different measurements of curvature and the migration rates measured in the previous chapter to plot the trajectory of many different bends and test whether the trajectories can be identified.

5.2. Study Area

The analysis in this chapter was completed for bends on the River Lugg, River Arrow, River Glen and River Till, for which the characteristics are described in more detail in Section 4.3.

5.3. Data and Methods

The channel centrelines produced in the previous chapter were the main source of data for this chapter. Channel banklines from historic Ordnance Survey maps were digitised and the channel centreline was used to represent the river channel. The migration rates were calculated as described in the last chapter at 10m intervals along the whole reach length and then sorted into bends based on the inflection point of each individual bend.

The radius of curvature of each of the 10m intervals was measured using a circle fitting tool developing by Gibson (2013), originally for the New Zealand Transport agency to determine the curvature of roads for safety purposes. The code was written using Python 2.7 and ArcGIS 10.1 and calculates the radius of curvature for each triplet of vertices along the centreline. To ensure a consistent measurement of the radius of curvature, points were generated at 10m along the smoothed centreline and a new polyline was created directly connecting each point (see Figure 5.2). These 10m intervals are identical to the 10m intervals used to measure migration rate between consecutive centrelines. The algorithm then extracts the coordinates of three consecutive points along the centreline and calculates the gradient of the two lines. The x,y coordinates of the centre of a circle that intersects with the normal of both lines and passes through all three points is then calculated. Finally, the radius

of the circle is then calculated from the middle coordinate of the triplet of points and the centre of the circle (see Figure 5.3). This process is then repeated for each triplet along the

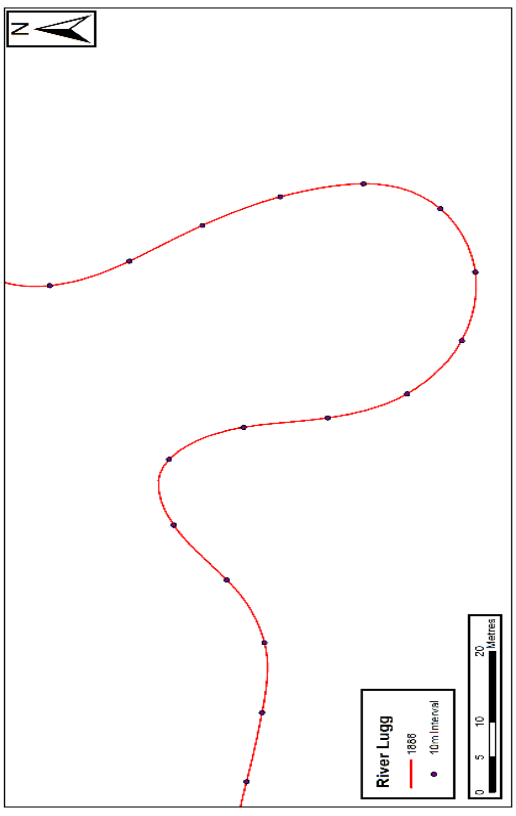

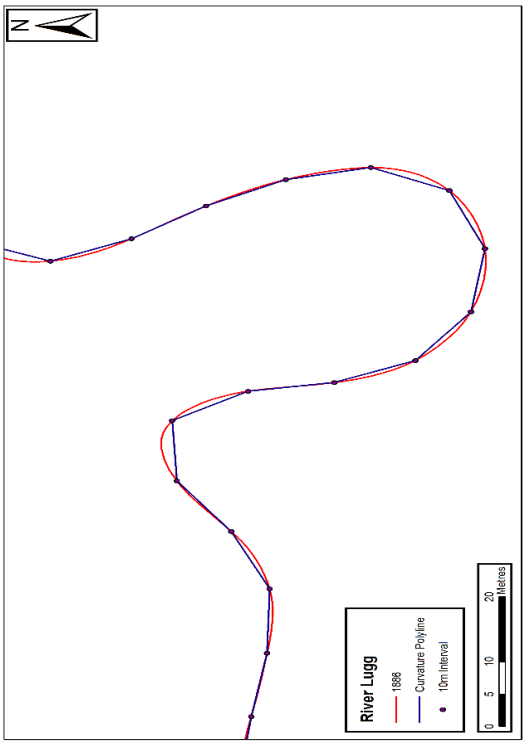

Figure 5.2. The centreline was divided at 10m intervals and polyline was created to allow the measurement of the radius of curvature to be completed at a consistent interval

centreline until all of the radii of curvature have been calculated. The first and last point on the centreline have a zero value for the radius of curvature as they only contain two points. A three-point curvature smoothing method was used to remove oscillations in the curvature measurement as proposed by Crosato (1990) and Motta et al. (2012). The smoothing algorithm takes the form of equation 1:

$$RoC_i = \frac{RoC_{i-1} + 2 \times RoC_i + RoC_{i+1}}{4} \quad (1)$$

where RoC_i is the individual radius of curvature measurement and RoC_{i-1} and RoC_{i+1} are the immediate upstream and downstream radius of curvature measurements.

The centrelines were then divided into bends based on the inflection point generated from the Fluvial Corridor Toolbox (Roux et al., 2013). A minimum bend length of 30m was selected based on Hooke and Harvey (1983). It was possible to calculate some simple statistics such as the mean, median and minimum radius of curvature for each bend.

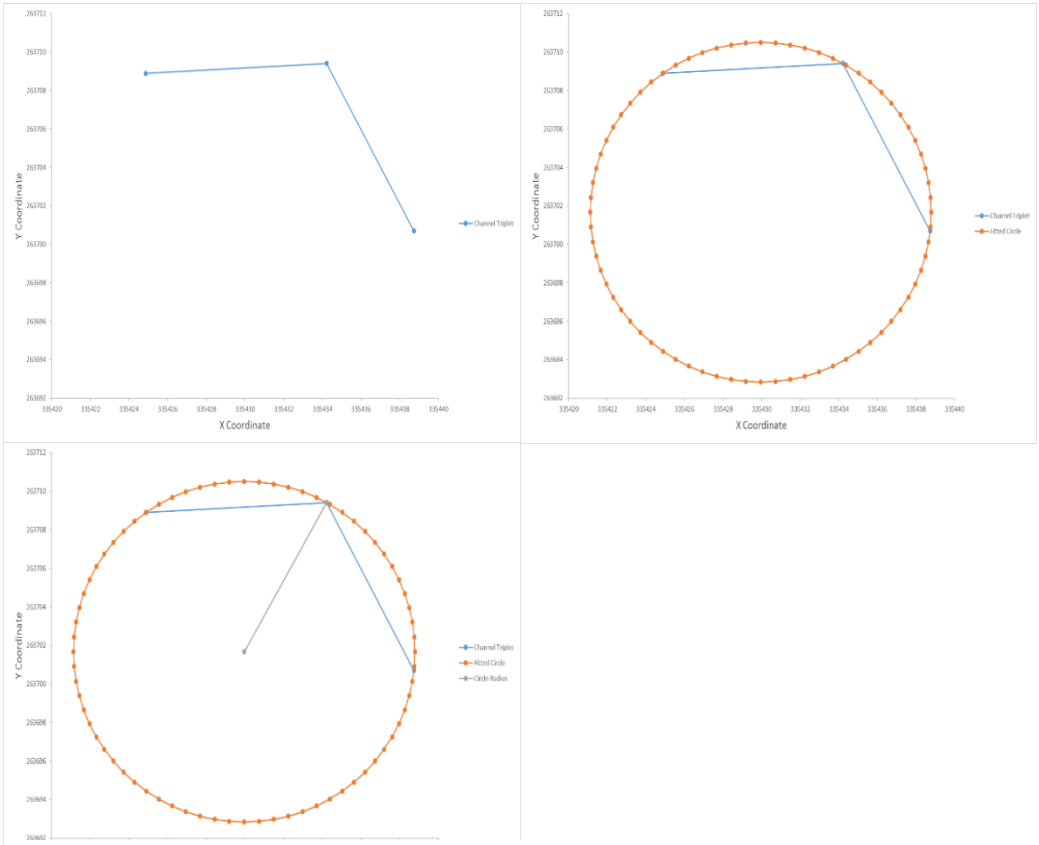

Figure 5.3. The radius of curvature of each 10m interval was measured using a triplet of points, with a circle fitted that would pass through each point and the radius of that circle calculated.

However, as described by Guneralp and Rhoads (2009), there is spatial effect on migration caused by the upstream and downstream curvature. A weighted aggregate of upstream and downstream curvature was used to provide a value for curvature for the whole bend, starting with the point of minimum radius of curvature. Equation 2 formalises the weighted aggregate used in this chapter.

$$RoC_w = MinRoC_{(i)} + \frac{MinRoC_{(i-1)}}{2} + \frac{MinRoC_{(i+1)}}{4} + \ldots + \frac{MinRoC_{(i-n)}}{2n} + \frac{MinRoC_{(i+n)}}{4n} \quad (2)$$

Where RoC_w is the weighted aggregate, $MinRoC_{(i)}$ is the minimum radius of curvature measured for an individual bend, $MinRoC_{(i-1)}$ and $MinRoC_{(i+1)}$ are the radius of curvature measured upstream and downstream of the minimum value respectively. Here both the upstream and downstream curvature are considered in the weighted aggregate, with the upstream component considered having a greater and longer lasting weight compared to the downstream curvature values. A total of five links upstream and two links downstream from the minimum value were used. A number of different combinations were tested, and it was found that the influence of the upstream and downstream links past the number used declined quickly. An advantage of using a weighted aggregate approach compared to the mean or median for each bend is that the measurement will be less sensitive to the location of the inflection points used to define individual bends.

The mean and the maximum migration rate for each bend was calculated allowing the different measures of curvature to be related to the different measures of migration rate for each individual bend, and for the trajectories of individual bends to be followed through time. The bend curvature (r_m/w) was defined as the ratio of the radius of curvature measurement to the mean channel width of the bend as used by Hickin (1974) and Hooke (2003) and is the inverse of the absolute curvature value. To further analyse the relationship between the radius of curvature and the migration rates, the distance between location of the minimum radius of curvature and the maximum migration rate was calculated for each bend.

The final method used in this chapter was to classify each bend based on the shape of the bend from the Brice (1974) classification based on whether the bend was symmetrical or asymmetrical and whether the bend was simple or compound. The total number and total length for each category was calculated. This method is subjective, but it allowed the bends

to be categorised and for bends to be selected randomly in subsequent analysis. The evolution of individual curvature profiles were plotted and analysed for each type of bend.

5.4. Results

5.4.1. Relationship between channel curvature and migration rate

Hickin (1974) and Hickin and Nanson (1975, 1984) predicted that there was a non-linear relationship between channel curvature and migration rate. Once a certain value in the ratio of channel curvature to channel width was passed then curvature would be the main driver of channel change and there would be an acceleration in the rate of migration. Hickin (1974) defined the bend curvature as the ratio of the radius of curvature to channel width, which was also used for this section. Bend curvature term is used to mean radius of curvature to width ratio throughout this chapter, and should not be confused with curvature, which is the inverse of the radius of curvature to width ratio. The data presented in this chapter allow for the relationship between the minimum bend curvature and the maximum width averaged migration rate to be analysed. One of the issues around this analysis is the apparent bias towards a migration rate for shorter periods between two map dates. This meant that the highest migration rates were all measured in the shortest period (1963-1976 in the River Lugg catchment and 1957-1970 in the River Till catchment). Two different domains could be identified, with the shortest period having a different type of behaviour compared to the longer periods. An envelope was drawn around the fastest migrating bends for each of the different reaches and the two different domains (see Figure 5.5 and Figure 5.6). Two of the reaches, Lugg Reach 1 and Lugg Reach 2 both showed only one domain and there was not a large difference between the fastest migrating bends in the 1963-1976 period and the other periods.

When the fastest domain was included it was possible to identify the increase in migration rate once the threshold in bend curvature was reached. Nearly all of the reaches showed an increase in the migration rate once the bend curvature ratio was less than 5.0, and usually reached a maximum between 3.0 and 2.0. When the data from the shortest period were removed and the envelope curves drawn for the remaining data the increase in migration rate was not as obvious. Although most of the reaches did show a slight increase in migration rate, the peak in the envelope curve was not as large. There were also many bends with a bend curvature around the threshold suggested by Hickin, and Hickin and Nanson, which remained stable during the study period and did not show the increase in migration rate. There were some individual bends that had a high migration rate, despite

having a high r_m/w. A good example of this occurred on bend 10 of Reach 4 on the River Lugg. The channel was straight in 1963, before a large amount of erosion occurred between 1963 and 1974 as the river was potentially adjusting to two large cutoffs that had occurred.

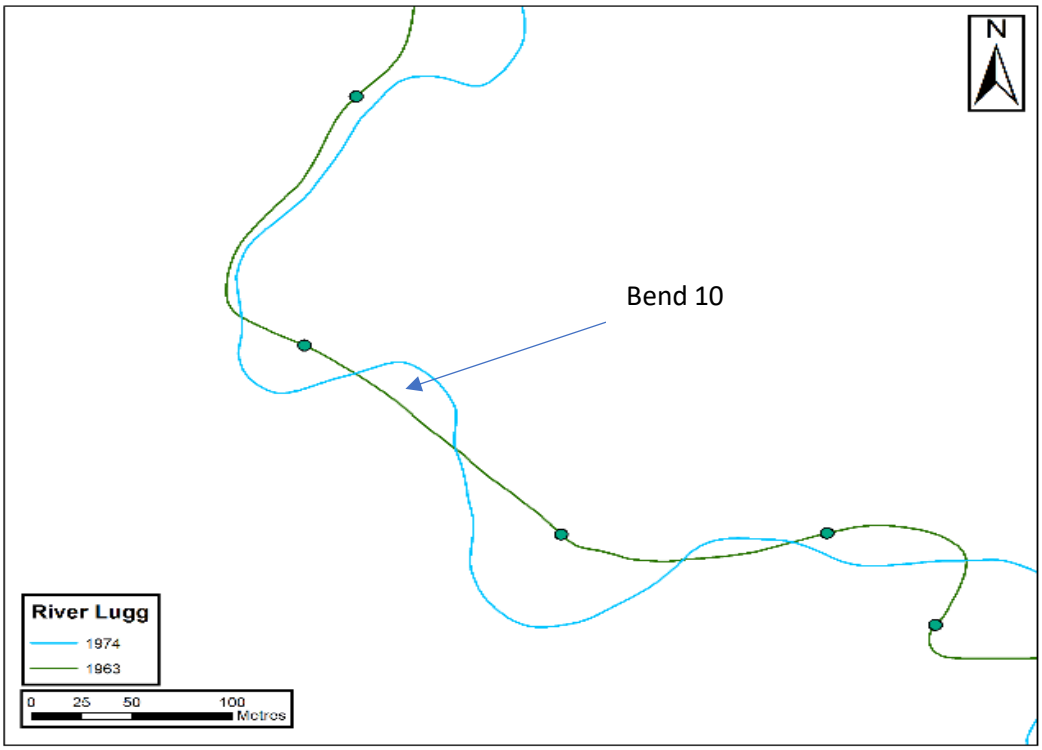

Figure 5.4. Bend 10 was unusual as it had a high r_m/w in 1963, but subsequently eroded rapidly between 1963 and 1974. This appeared to have been caused by erosion upstream, which directed the flow immediately to the bank and caused the initiation of meander bends

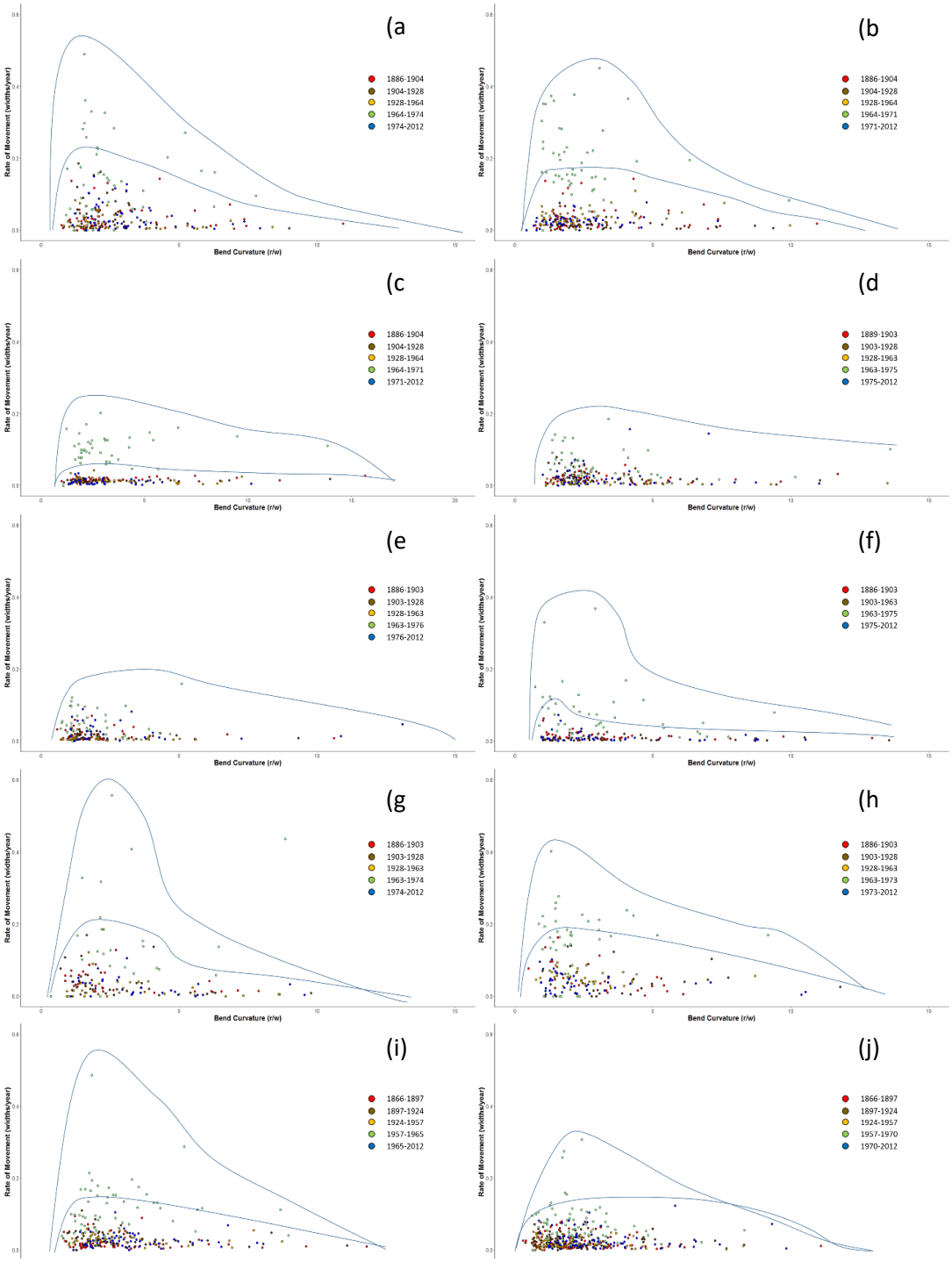

Figure 5.5. The relationship between minimum bend curvature and migration rate for each of the 10 reaches. Where the two different domains existed a second envelope was drawn for the longer periods. The reaches are: a – River Arrow Reach 1, b – River Arrow Reach 2, c – River Arrow Reach 3, d – River Lugg Reach 1, e – River Lugg Reach 2, f – River Lugg Reach 3, g – River Lugg Reach 4, h – River Lugg Reach 5, i – River Glen, j – River Till.

The rates measured in the shortest period were much higher than the maximum rates published by Hickin and Nanson (1984) and subsequently measured by Hooke (1997) on the River Dane and River Bollin in the UK, scaled as widths per year. Figure 5.6a shows the relationship between bend curvature and migration rate for all of the rivers, with the shortest period removed from the data set, while Figure 5.6b shows relationship with the shortest period included. The highest rates of erosion were measured with an r_m/w value between 2 and 3, although the spread of data was greater than that measured by Hickin and Nanson (1984) and Hooke (1997). There was a high amount of variability in the dataset, with many of the bends with a curvature between 2 and 3 showing a low rate of migration.

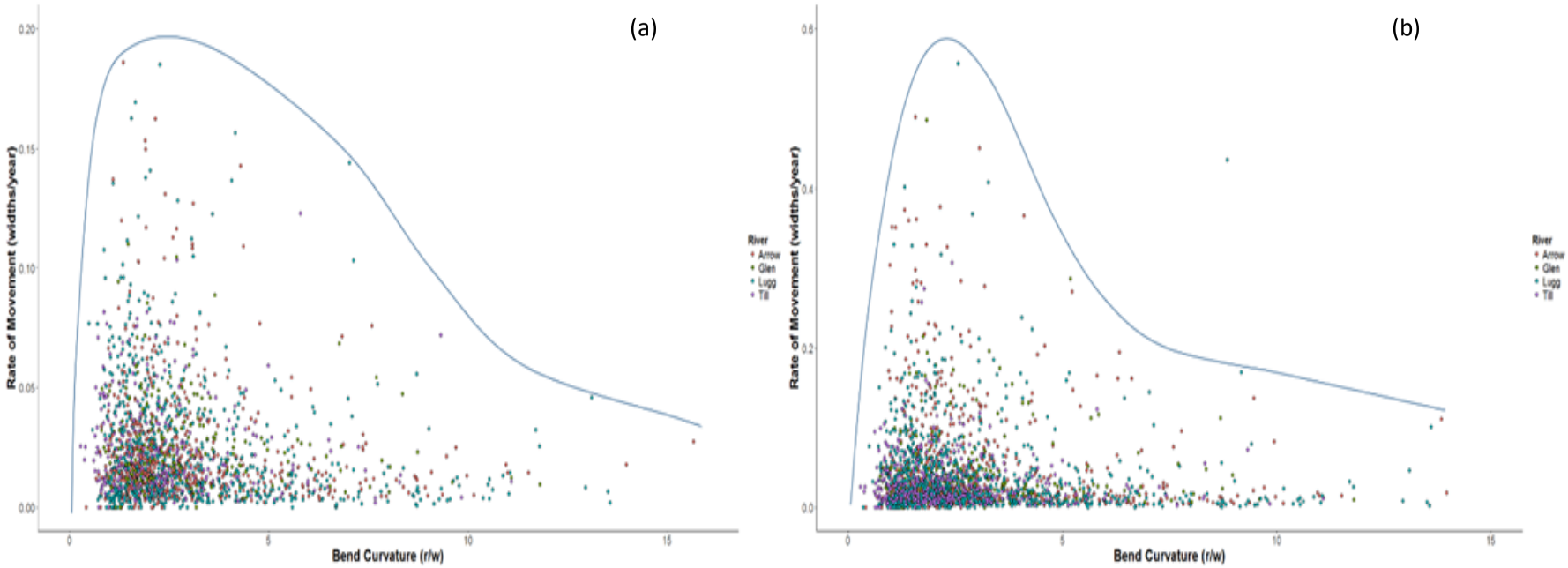

Figure 5.6. The relationship between bend curvature and migration rate. When the migration rates for the shortest period are removed (a), the increase in the migration rate as bend curvature approaches 5.0 is not as obvious

5.4.2. Spatial relationship between the minimum radius of curvature and maximum migration rate

The theoretical work by Ikeda et al. (1981) and subsequent authors (e.g. Furbish, 1988; Seminara et al., 2001) showed a downstream lag in the relationship between the apex of the bend and the fastest migration rate. It is expected that this lag is the cause of downstream migration of bends and prevents bends from simply growing across the floodplain. Sylvester et al. (2019) found the lag was rough constant for each river bend and the migration was shifted downstream by between 2.1 and 4.7 times the channel width. The data collected in this study also allowed for an investigation into the spatial relationship between the location of minimum radius of curvature and the location of maximum migration. For each bend, the transect with the minimum radius of curvature and the transect with the highest migration rate were identified and the distance between the two calculated. For the analysis the bends were split into the different Brice classifications, i.e. simple symmetric (Figure 5.7), simple asymmetric (Figure 5.8), compound symmetric (Figure 5.10) and compound asymmetric (Figure 5.9). The data was also split into bends greater than or equal to 81m and less than 91m, which was the median bend length of the entire dataset. Bends that experienced a cutoff were removed from the analysis, along with the bend at the start and finish of each reach.

In total there were 1710 simple symmetric bends, 273 simple asymmetric bends, 204 compound asymmetric bends and 69 compound symmetric bends. For all the categories, except for the compound symmetric bends, the highest migration rates were measured on the same transect as the lowest radius of curvature measurement. There was then a roughly normal distribution of the location of the highest migration rates upstream and downstream of the minimum radius of curvature. Some of the bends had a distance in excess of 100m either upstream or downstream between the minimum radius of curvature. The compound symmetric bends did not show the same peak at zero distance between the minimum radius of curvature and the maximum radius of curvature. There were peaks around 40m upstream of the minimum radius of curvature and slightly downstream, between 10 and 20m downstream. However, the number of bends in the compound symmetric dataset was much lower than the other three bend types.

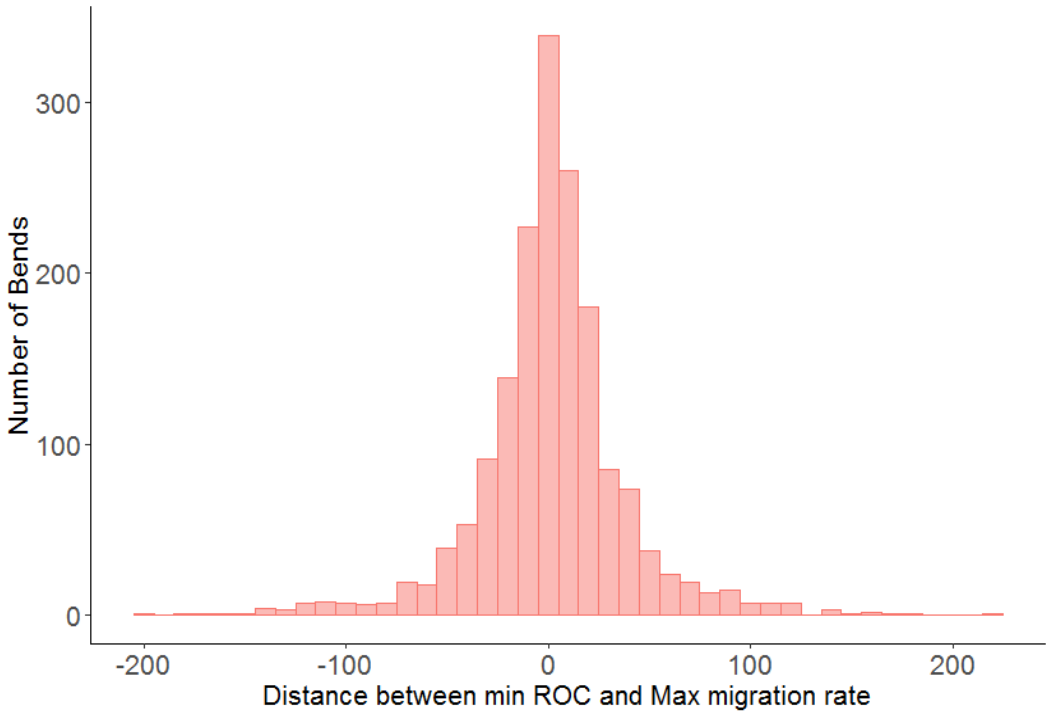

Figure 5.7. Distribution of the distance between the minimum radius of curvature and maximum migration rate location for simple symmetric bends. A positive number is in the downstream direction and a negative number is in the upstream direction.

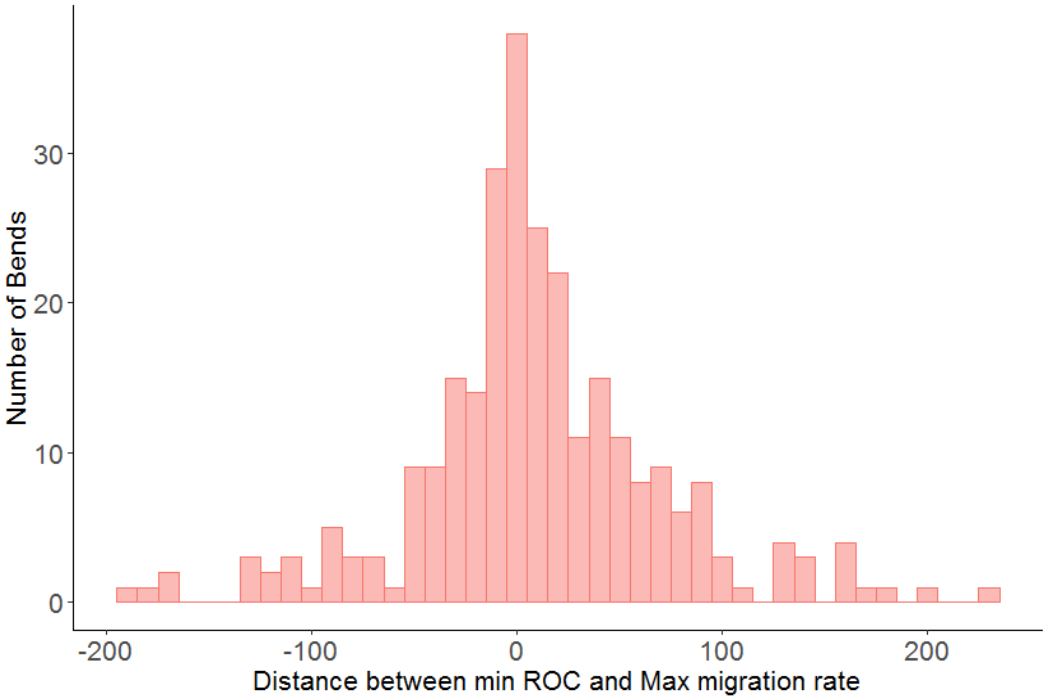

Figure 5.8. Distance between the minimum radius of curvature and maximum migration rate for the simple asymmetric bends

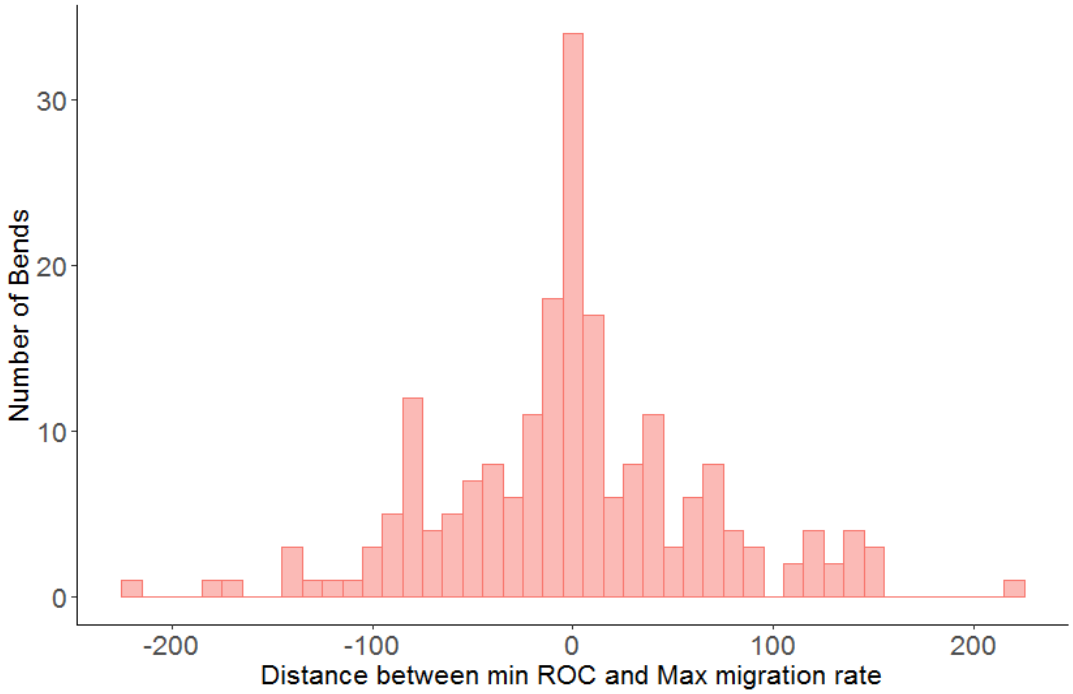

Figure 5.9. Distance between the minimum radius of curvature and maximum migration rate for the compound asymmetric bends

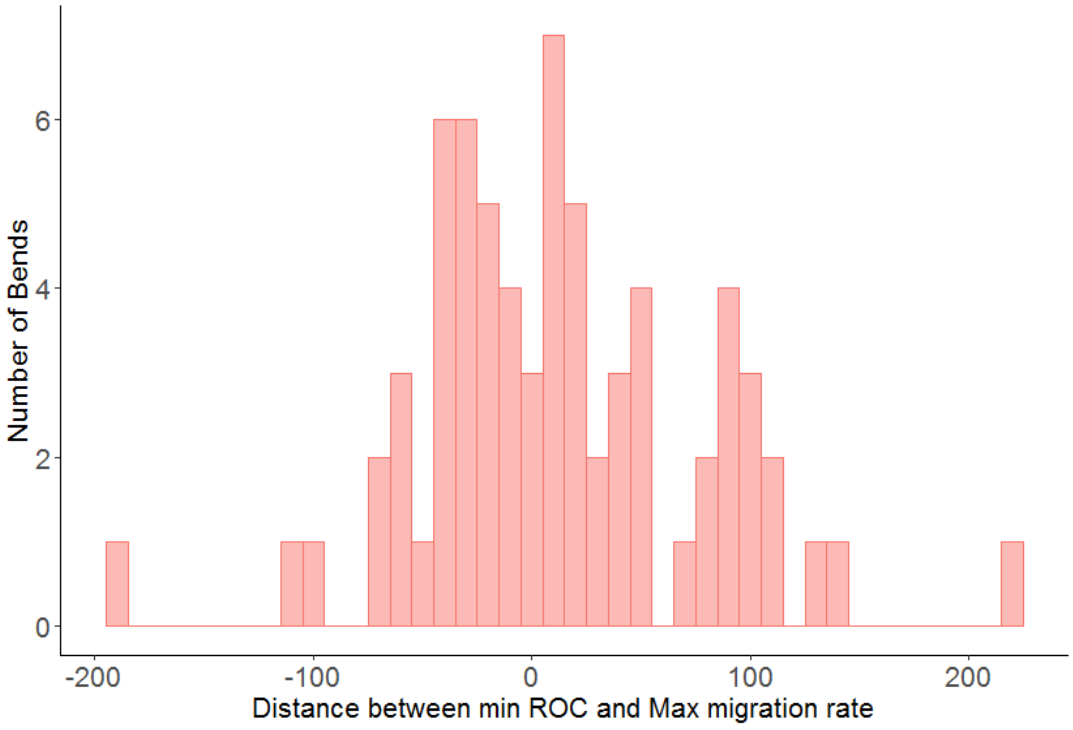

Figure 5.10. Distance between the minimum radius of curvature and the maximum migration rate for compound symmetric bends

When considering the difference between the short bends (<81m) and the long bends (>=81m) there was very little difference in shape of the distribution for the difference between the minimum radius of curvature and the maximum migration rate. The most common distance between the minimum radius of curvature and maximum migration rate was 0m, followed by 10m downstream and 10m downstream. The downstream maximum migration transects tended to have a higher number of bends than the same distance upstream.

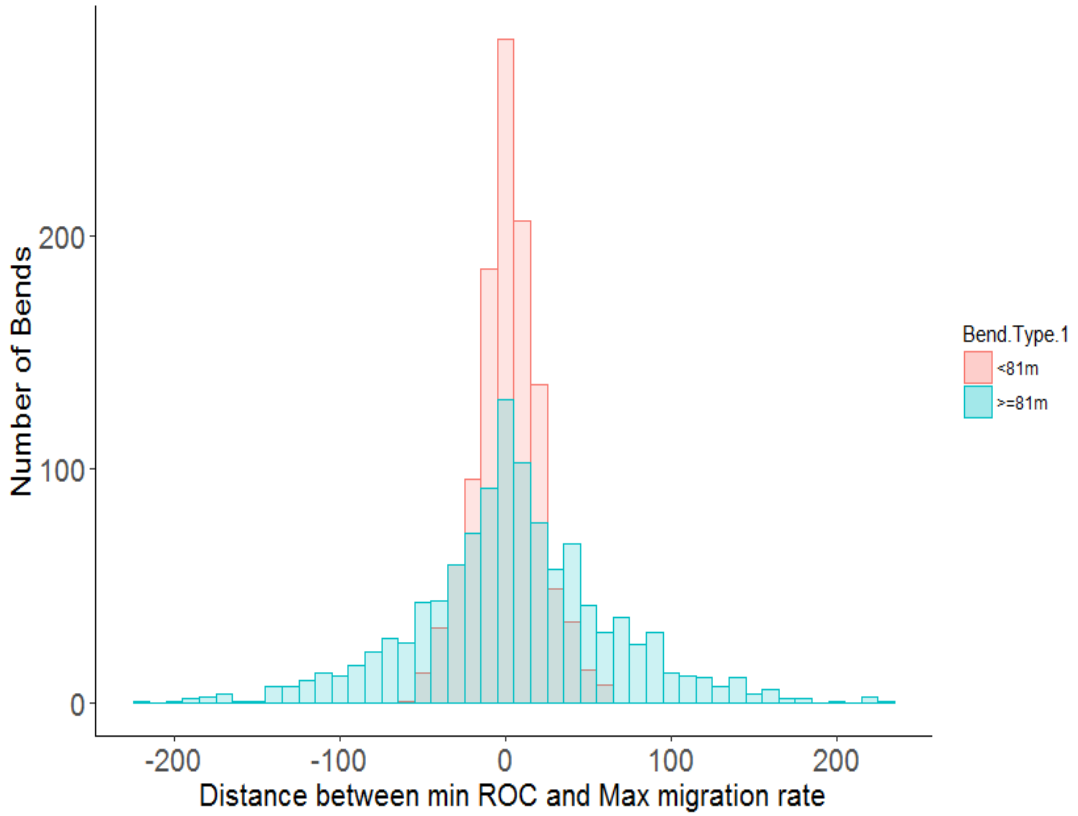

Figure 5.11. The distance between the minimum radius of curvature and maximum migration rate for short and long bends. Both of the datasets had a similar distribution.

5.4.3. Curvature trajectories in the r_m/w – migration rate phase space

It was also possible to track individual bends as they moved through the bend curvature – migration rate phase space. Hooke (2003) proposed that the different behaviour of different types of bends would follow a certain trajectory within the phase space. Four different types of bend behaviour were proposed, with bends being stable, migrating downstream, growing towards a chute cutoff or growing towards a neck cutoff. Before experiencing a neck cutoff, many of the bends would become double-headed or compound. Bends could swap between the different trajectories if the conditions for the reach changed. The process can take a long time, and only the fastest migrating bends will show the different trajectories in the available time frame. The following section shows the behaviour of different bends that would fit into the different trajectories. Four different measurements of curvature were used to describe the bend curvature: the weighted aggregate bend curvature, the minimum bend curvature, the mean bend curvature and the median bend curvature. The changes to the mean channel width are also shown, which displayed high variability through time. Selected bends are shown in this section, with more examples included in the appendix section.

5.4.3.1. Stable Bends

Very few bends were stable throughout the entire study period, with most being active through at least one period. Often the period of activity was associated with the shortest time between two maps dates, which increased the effect of any uncertainty in the position of the channel. Two examples of stable bends are bend 43 on the River Arrow, Reach 1, and bend 15 on the River Arrow, Reach 3. Bend 6 on the River Lugg, Reach 2, is an example of a bend that was stable for the early part of the study period, before becoming active in the later period. All three bends are shown in Figure 5.12.

River Arrow, Reach 1, Bend 43: this bend was stable throughout the entire study period, showing low rates of erosion in all the periods and little change to the different measurements of bend curvature. The bend had developed into a tight bend, with a low r_m/w value, but had subsequently become stable. There is a weir located just downstream of the bend, which may have stabilised the bend due to backwater effects and effectively reduced the gradient of the river at this point.

River Arrow, Reach 3, Bend 15: There was an increase in the migration rate for bend 15 between 1964 and 1971, but this appears caused mainly by uncertainty in the channel position and the short time period the two maps dates (only seven years). The overall shape of the bend remained constant through the study period with only small fluctuations in the r_m/w value.

River Lugg, Reach 2, Bend 6: this bend was stable between 1886 and 1963, with very low migration rates and little change to the shape of the bend. A series of cutoffs occurred downstream, which is likely to have increased the local river gradient and appears to have caused the bend to switch from being stable to migrating downstream between 1963 and 2012. There was a small amount of growth between 1963 and 1976, the same period as the cutoffs, before the bend migrated downstream between 1976 and 2012. The bend maintained a consistent shape as it migrated downstream as there was little change in the bend curvature between the different periods.

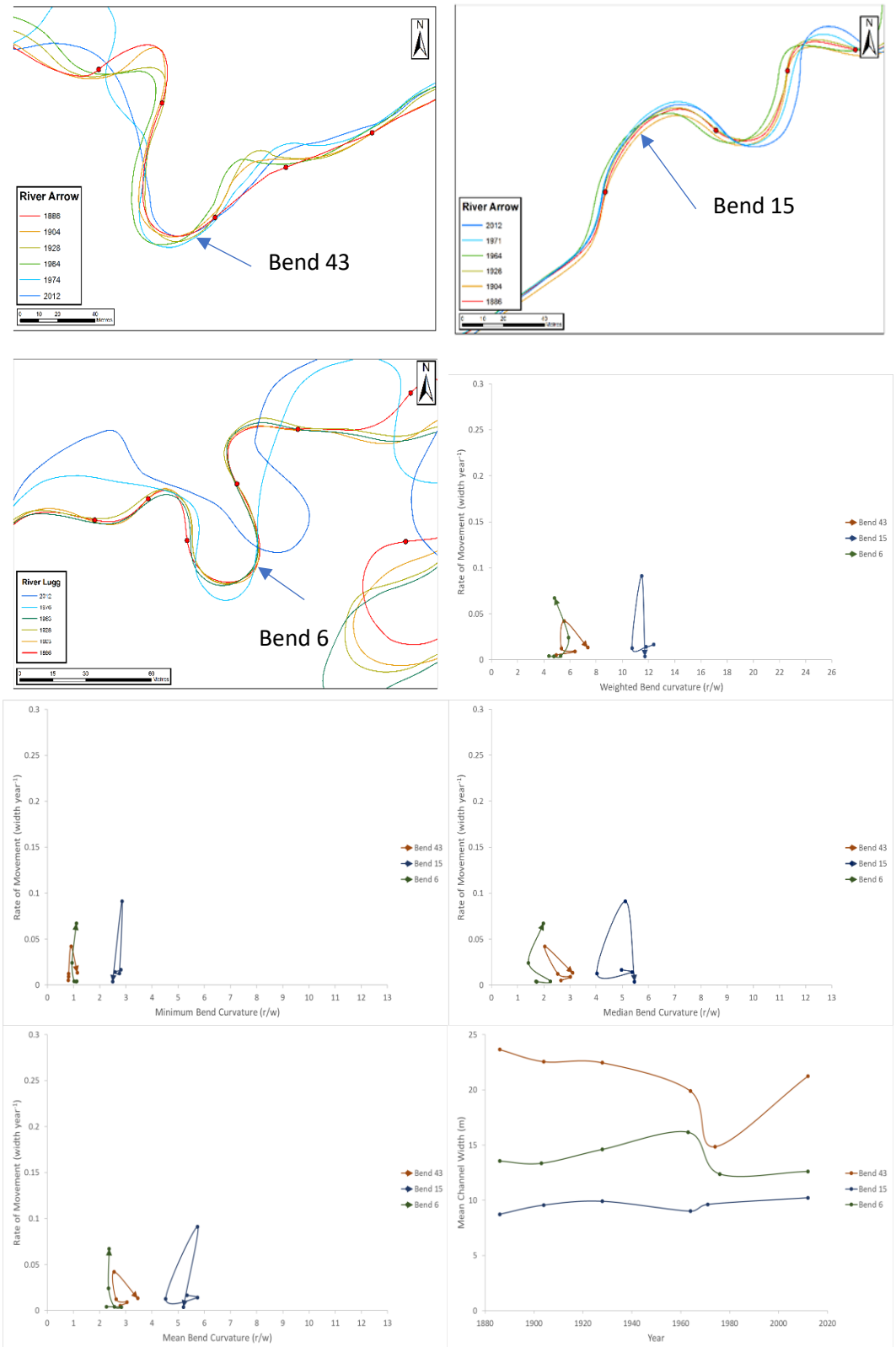

Figure 5.12. The trajectories of stable bends for the different measurements of bend curvature. Bend 6 on the River Lugg was initially stable, before starting to migrate downstream after a cutoff occurred.

5.4.3.2. Downstream Migration

There were numerous bends that were actively migrating downstream in the study reaches. Bends that migrate downstream should show small variations in the bend curvature and migration rate, but not grow across the floodplain and would rarely cutoff. Usually these bends had developed to a sinuous course with low r_m/w values. The rates of migration would often change between the different periods, with the bends remaining stable for some periods before beginning to migrate. The following are examples in Figure 5.13.

River Arrow, Reach 1, Bend 7: Bend 7 had developed into a compound asymmetrical bend by the start of the study period in 1886. The overall shape was maintained throughout the entire study period, with the bend slowly migrating downstream and rotating slightly by 2012. The mean channel width declined between 1886 and 1904 and again between 1964 and 1974 from 18.5m in 1886 to 10.8m in 2012. This could explain the increase in the r_m/w value between 1964 and 1974, even though the radius of curvature remained constant through the study period.

River Glen, Reach 1, Bend 28: This bend was again a well-developed compound asymmetrical bend at the start of the study period in 1866. The bend was stable between 1866 and 1897, before starting to migrate subsequently. The rate of migration remained fairly consistent between the following periods. The mean channel width increased between 1866 and 1924, before declining to 1965, followed by a large increase between 1965 and 2012.

River Glen, Reach 1, Bend 29: Bend 29 was a well-developed simple symmetrical bend in 1866, with a low minimum r_m/w value. The bend was stable in the 1866-1897 and 1924-1957 period, while migrating downstream in the other periods. The bend also started to become double headed towards the end of the study period, which may explain the increase in the r_m/w value towards the end of the study period. The mean channel width showed a steady increase between 1866 and 1957, before declining between 1957 and 1965.

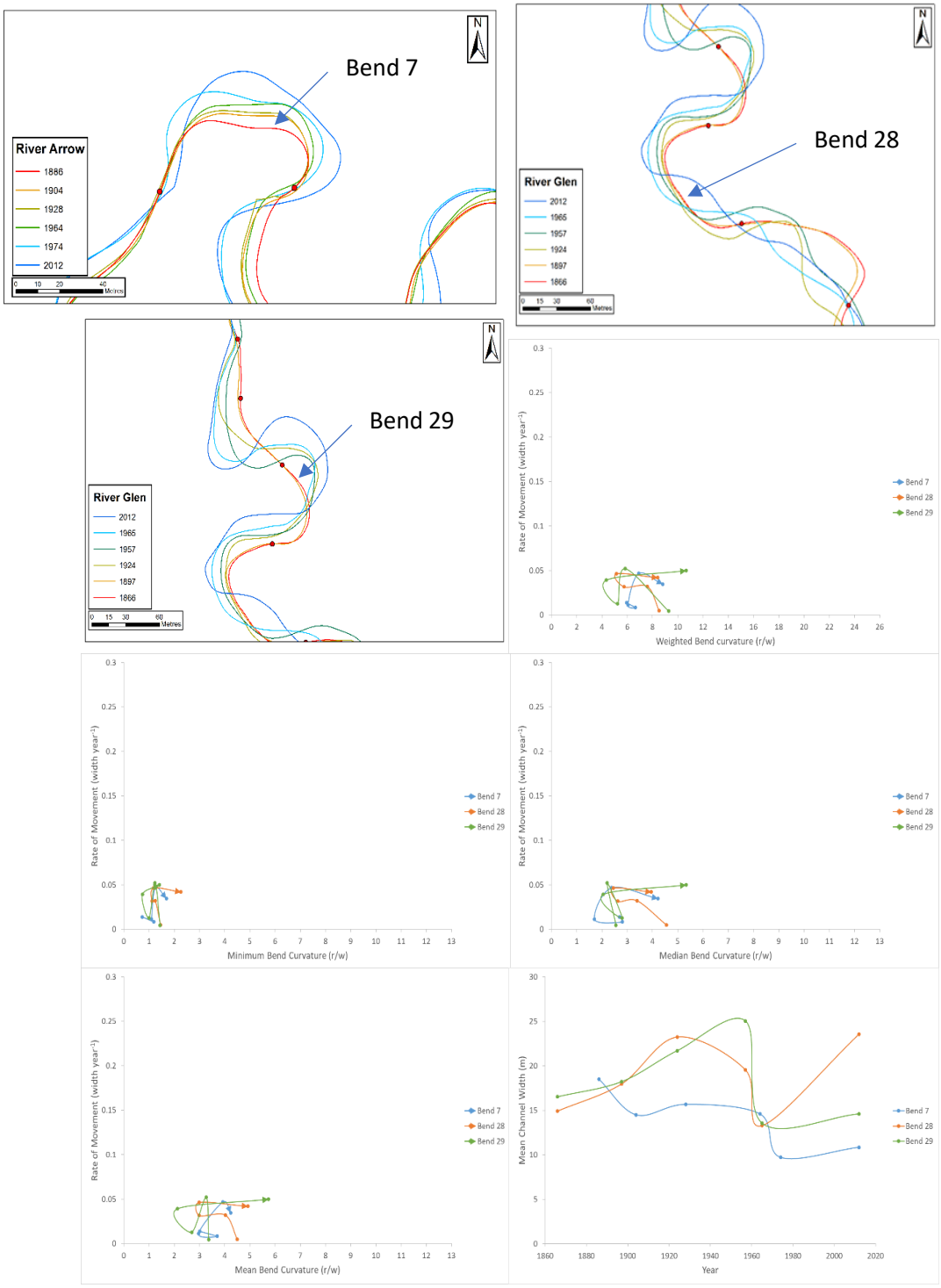

Figure 5.13. The bends that were migrating downstream showed more variation in the migration rate between different periods, and variations in the bend curvature. Each of the bends showed considerable variability in the average channel width.

5.4.3.3. Chute Cutoffs

Chute cutoffs occur when an avulsion causes part of the channel to be removed from the meander chain, but usually at a lower sinuosity and higher bend curvature than neck cutoffs. The bend has been cut off before it has been able to follow the full evolutionary cycle to a compound bend. The bend curvature of the channel would increase once a chute cutoff has occurred, although it would not be expected to become as straight as if a neck cutoff had occurred. Chute cutoffs usually occurred on bends that were shorter than the neck cutoffs. The bend trajectories are shown in Figure 5.14.

River Arrow, Reach 2, Bend 41: Bend 41 was a well-developed simple symmetrical bend at the start of the study period in 1886. The minimum, mean and median bend curvature were all low at the start of the study period. The bend remained stable between 1886 and 1964, with low migration rates and no change to the overall shape of the bend. The chute cutoff occurred between 1964 and 1971, which led to an increase in the minimum and weighted bend curvature although the bend still had a low r_m/w value after the cutoff occurred. The migration rate increased between 1971 and 2012 as the bend grew across the floodplain, potentially reoccupying the downstream limb of the bend, only flowing in the opposite direction! The mean channel width showed a slight increase after the cutoff occurred, before remaining stable in the 1971-2012 period.

River Lugg, Reach 1, Bend 20: Bend 20 was another well-developed simple symmetrical bend with a low minimum bend curvature throughout the study period. The median, mean and weighted r_m/w values showed a slight increase between 1889 and 1903, before decreasing through time to 1975. The chute cutoff occurred between 1975 and 2012, and was related to the neck cutoff that occurred on the next bend downstream. The channel width remained stable between 1889 and 1975, before increasing to 2012, again probably due to the cutoffs that occurred.

River Lugg, Reach 4, Bend 15: Bend 15 was more active through the study period than the previous two bends and showed signs of activity between each of the map dates. The minimum r_m/w value was low at the start of the study period and remained low until the cutoff occurred. However, the bend was growing across the floodplain between 1886 and 1928, with an increase in the mean and median r_m/w values. The chute cutoff occurred between 1928 and 1963, with a corresponding increase in all measures of r_m/w. There was a rapid increase in the migration rate between 1963 and 1974, with the bend growing across

the floodplain at over 0.4 widths per year, and the r_m/w values decreased slightly during this period. The bend continued to grow across the floodplain between 1974 and 2012, although the rate decreased from the 1963-1974 period to erode at a similar rate to the earlier periods. The bend had potentially reoccupied the channel that was abandoned in 1928 by the end of the study period. The mean channel width decreased between 1886 and 1928, before increasing after the cutoff occurred. The mean channel width decreased again between 1963 and 1974, before increasing slightly in 2012.

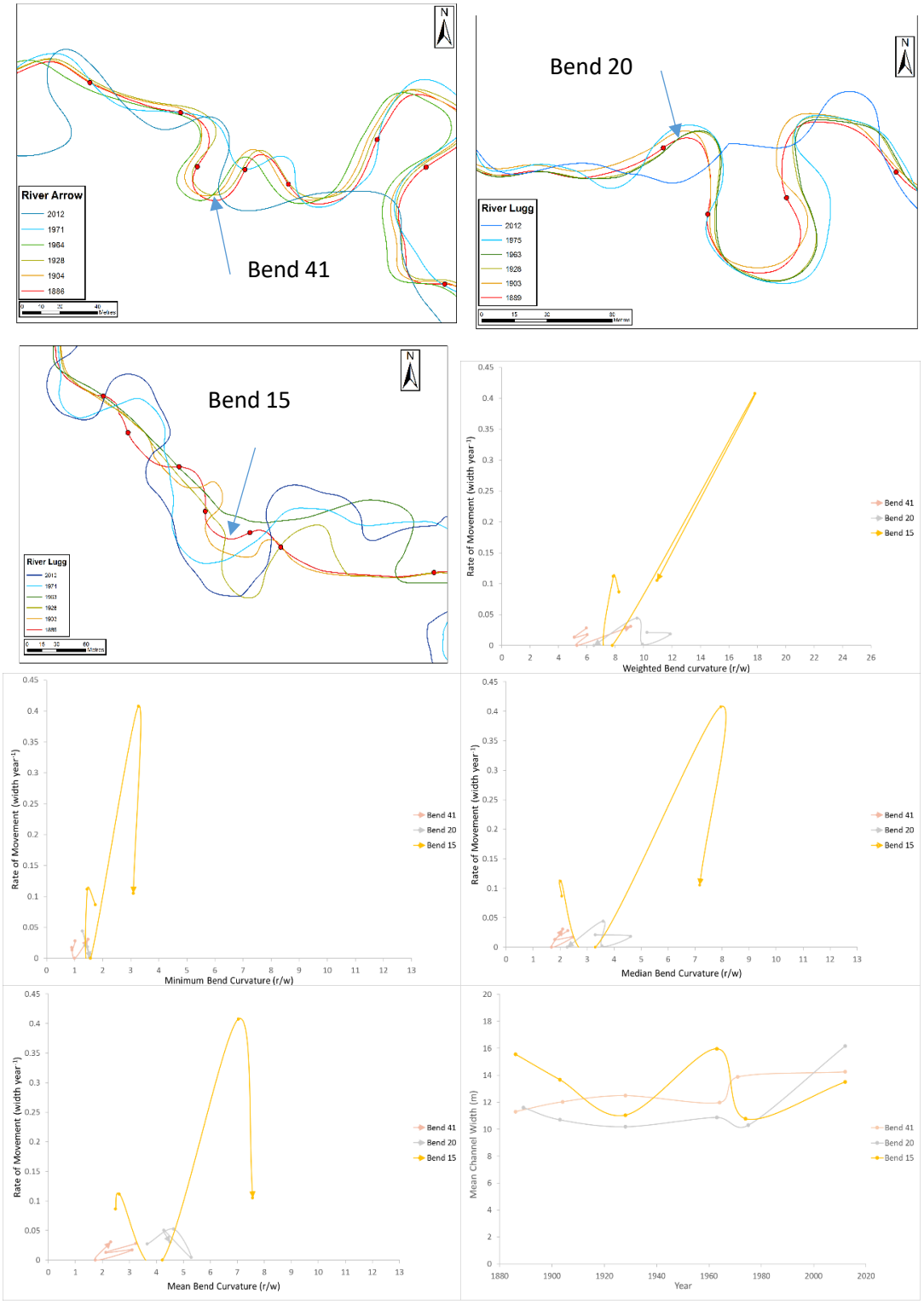

Figure 5.14. The trajectories of bends that eventually cutoff through chute cutoffs. Two of the bends were stable for much of the study period, before eventually cutting off, while bend 15 on the River Lugg was active throughout the study period and showed consistently high migration rates. The bend rapidly adjusted after the cutoff occurred.

5.4.3.4. Neck Cutoffs

The final complete trajectory that Hooke (2003) predicted was for bends that evolve to a neck cutoff. These bends would develop from an initial high r_m/w values and become gradually tighter through time. Once the r_m/w value was below 5.0, the bends would accelerate and grow across the floodplain. When the bend became too long to maintain sediment transport throughout a secondary riffle would form at the apex of the bend and erosion would become concentrated upstream and downstream of the riffle, creating a compound or double-headed bend. This would lead to an increase in the overall bend curvature and sinuosity of the channel and the bend would subsequently cutoff across the neck of the bend. This process can take a long time to complete and it was rare to find a bend that completed the full cycle from initiation to cutoff. However, it was possible to identify bends at different stages of the evolution that subsequently cutoff during the study period. Figure 5.15 shows the trajectories of the examples given below.

River Arrow, Reach 1, Bend 22: Bend 22 was a simple asymmetrical bend at the start of the study period. The bend was stable between 1886 and 1928, with little change to the mean and median r_m/w values during this period. The bend started to become double headed in 1964 as a secondary apex formed on the upstream side of the river bend and there was a large increase in the migration rate between 1964 and 1974 as the downstream apex started to migrate downstream. Using the weighted r_m/w values it was possible to follow the trajectory of the two different apices once they formed, with the upstream apex (22a) migrating at a much lower rate that the downstream apex (22b). The upstream apex, however, became much tighter than the downstream apex as there was a high amount of growth on bend 21, just upstream. The bend was cutoff between 1974 and 2012, leaving a much simpler bend with higher r_m/w values. The mean channel width was constant through the study period.

River Lugg, Reach 2, Bend 10: Bend 10 was already a well-developed simple symmetrical bend at the start of the study period. The bend was slowly growing across the floodplain between 1886 and 1963, with the neck of the bend becoming progressively tighter. The bend is interesting because it did not develop the characteristic double-headed profile as the bend developed, but became tighter at the apex and developing straight channels either side of the apex. This caused the mean and median r_m/w values to increase as the bend developed. The neck cutoff occurred between 1963 and 1976 although the bend maintained a low minimum r_m/w value, and decreased the mean and median r_m/w values as the straight

sections were removed. The bend continued to be active after the cutoff occurred, growing across the floodplain The mean channel width decreased between 1886 and 1903, before remaining stable for the rest of the study period.

River Lugg, Reach 5, Bend 3: Bend 3 developed from a simple symmetrical bend in 1886 to a compound asymmetrical bend by 1963. The rate of migration was high in the three periods before the cutoff occurred as the bend grew across the floodplain in all periods. The neck cutoff occurred between 1963 and 1973 leaving a much simpler bend with a higher r_m/w values for all the measurements. The rate of migration also decreased once the cutoff occurred and the bend had a simpler planform. The mean channel width varied greatly between the different periods, decreasing by nearly half between 1886 and 1903 (21.3m to 11.2m) before fluctuating between 1903 and 2012.

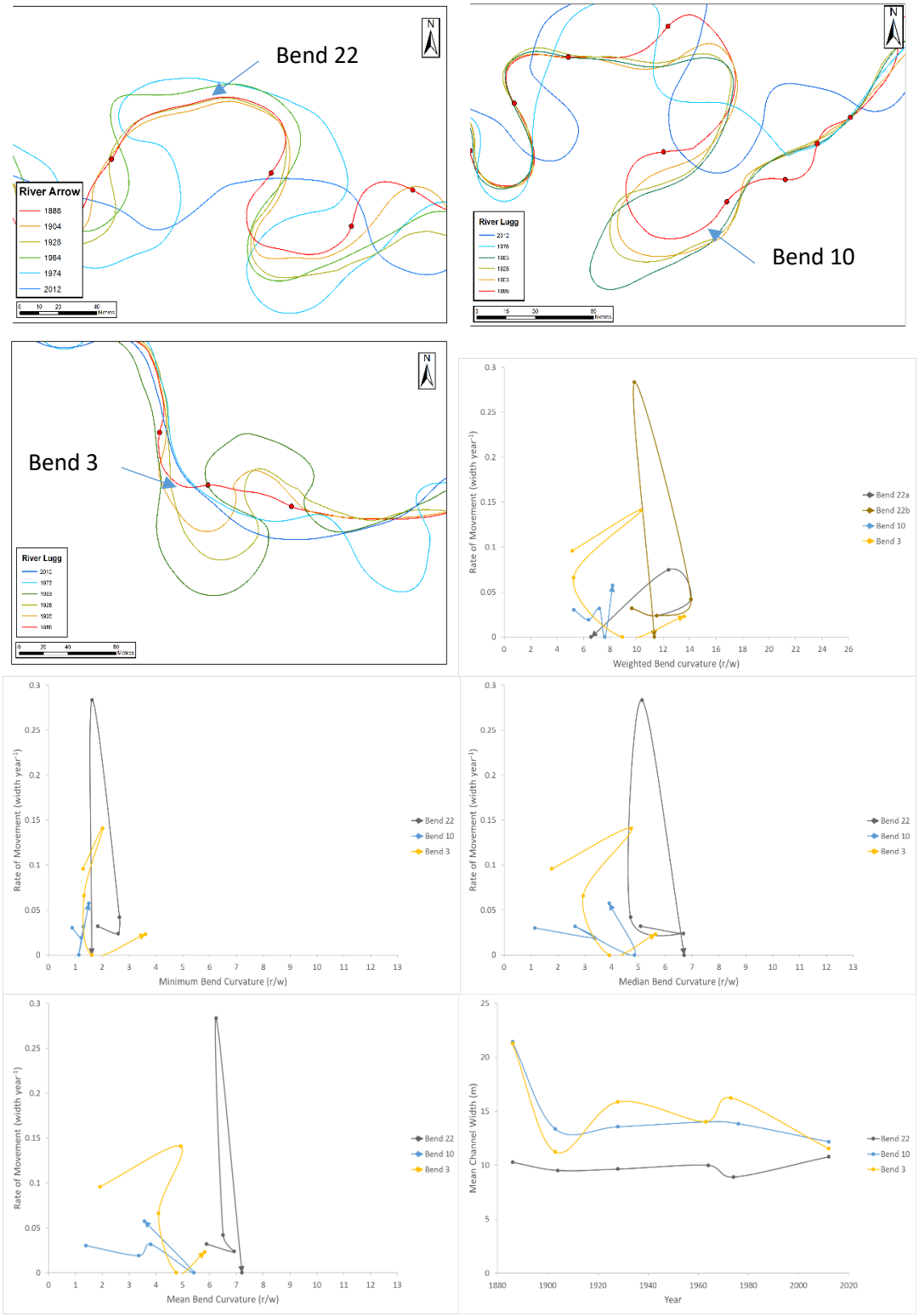

Figure 5.15. The bends that experienced a neck cutoff tended to be in most periods as they evolved. Most of the bends that cutoff in the study period were already well developed at the start and it was not possible to identify the acceleration in growth as the r_m/w values decreased.

5.4.3.5. Double headed or Compound Bends

One of the stages that Hooke and Harvey (1983) and Hooke (1995) suggested that would occur before a cutoff is a double headed or compound profile. This type of bend was also recognised by Brice (1974), who suggested it was a progression of the bends from a simple symmetrical or asymmetrical shape. While the full evolution of the bend would eventually continue towards a cutoff occurring, there were numerous examples of bends that had developed the distinctive compound shape but had not cutoff during the study period. These bends show the earlier part of the behaviour from initially fairly straight channels towards a neck cutoff and will perhaps show a behaviour similar to the previous section in the future. Figure 5.16 shows the evolution of the examples given below.

River Arrow, Reach 3, Bend 27: The bends on reach 3 of the River Arrow tended to be the most stable of the study reaches, with little erosion through most of the study period. Bend 27 remained stable between 1886 and 1964, with low erosion rates and little change in different measurements of curvature. The bend started to grow downstream between 1964 and 1971, and the mean, median and weighted r_m/w values increased. The bend continued to develop between 1971 and 2012, although relatively slowly, into the distinctive double-headed bend with two separate apices. The neck of the bend also narrowed during the study period and will potentially cutoff in the future if erosion occurs on the surrounding bends.

River Glen, Reach 1, Bend 41: Bend 41 on the River Glen developed from a simple symmetrical bend to a compound asymmetrical bend during the study period. The bend was initially stable between 1866 and 1897, with a low amount of migration and little change to the bend curvature. A cutoff occurred upstream between 1897 and 1924, which appears to have caused bend 41 to become active as the river adjusted. The bend started to grow across the floodplain between 1897 and 1924, with an increase in the migration rate and a decrease in all measurements of r_m/w. The migration rate decreased between 1924 and 1957, with the bend starting to migrate downstream rather than growing across the floodplain. The bend then started to grow across the floodplain again between 1957 and 1965 at the fastest rate measured for this bend. There was increase in all of the curvature measurements between 1957 and 1965, although this was related to the decrease in mean channel width (from 14.1m to 7.4m) rather than changes to the radius of curvature measurements (43.6 to 38.0, 20.2 to 19.8, 68.6 to 60.5 and 101.4 to 143.7 for the median, minimum, mean and weighted radius of curvatures respectively). Only the weighted radius of curvature showed an increase when the channel width was not considered. The bend continued to develop between 1965 and

2012 with a high migration rate and a double-headed form. A recent Google Earth aerial photograph from 2018 showed that the neck of the bend was less than 4m and the bend is likely to experience a neck cutoff during the next high flow event.

River Lugg, Reach 5, Bend 16: Bend 16 is part of a series of bends on Reach 5 that developed from simple symmetrical bends with a high r_m/w value to compound asymmetrical bends with a low r_m/w value during the study period. The bend started to grow slowly across the floodplain between 1886 and 1903, with a slight decrease in the r_m/w value. The bend continued to grow across the floodplain between 1903 and 1928, and subsequently became tighter. The bend was mainly stable between 1928 and 1963, before growing again between 1963 and 1973 and producing a clear double headed bend. The migration rate was the highest during this period. The bend then became stable between 1973 and 2012. This was caused by the installation of flood defences and weirs through this section of the channel, which effectively reduced the gradient of the channel to zero. The construction of the flood defences had the effect of shifting the attractor from a neck cutoff trajectory to a stable trajectory and can be accounted for within this type of analysis.

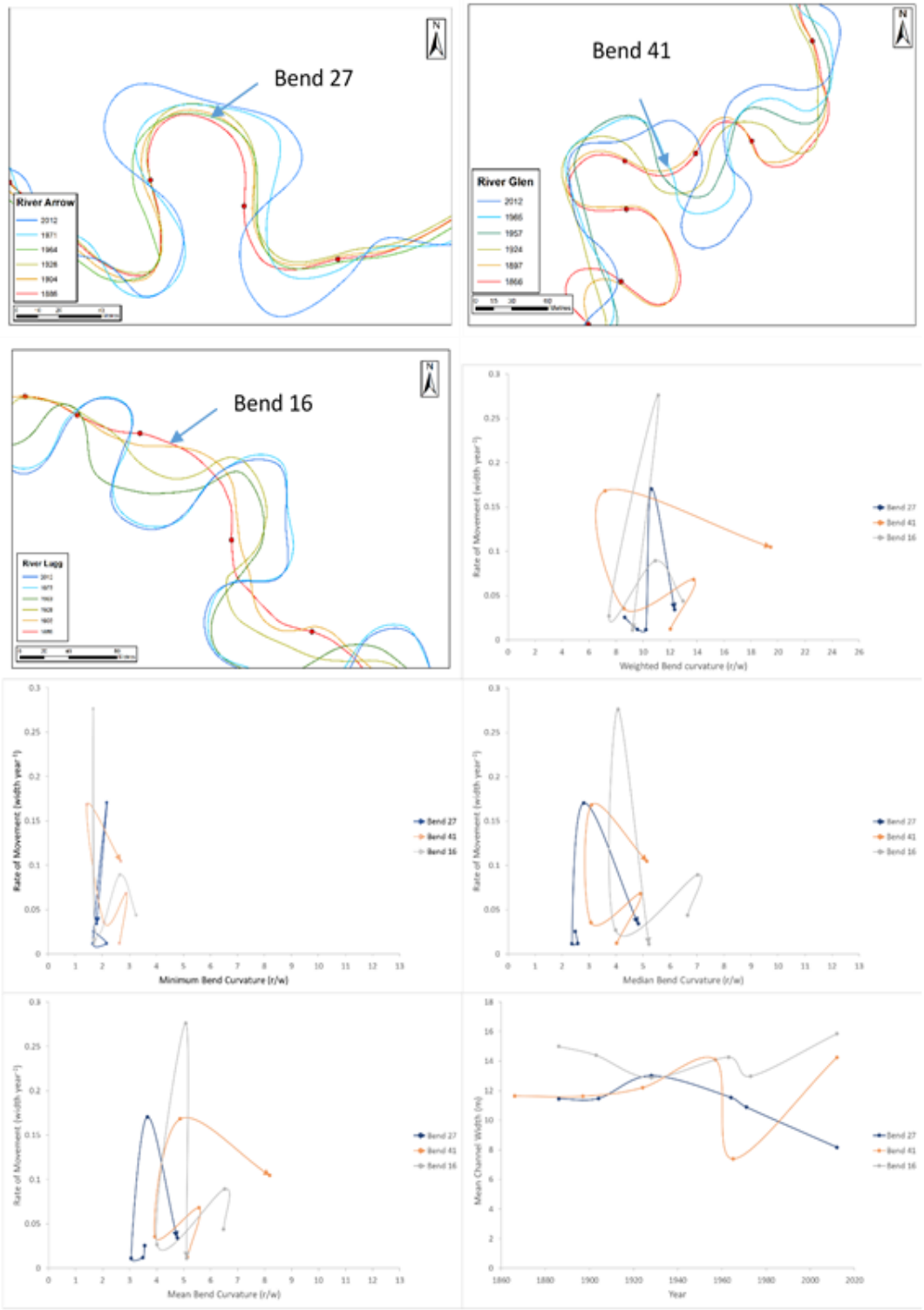

Figure 5.16. Some bends developed from a high r_m/w values towards a lower r_m/w values and potentially saw an increase in the migration rate as the bend curvature tightened. When the bend started to become double-headed, the overall r_m/w values reduced, and the migration rate decreased. It is expected that the bends would cutoff if they continue to erode in the future.

5.4.4. Curvature Profiles

The curvature profiles of individual bends can be plotted from the data. Four different types of bend were identified from the Brice (1974) classification in which bends can be considered simple symmetric, simple asymmetric, compound symmetric and compound asymmetric. Each of the bends will have a different curvature profile: a simple symmetric bends will have one apex (minimum value for the radius of curvature) roughly in the middle of the bend profile; a simple asymmetric bend will have one apex skewed either upstream or downstream from the middle of the profile; a compound symmetric bend will have two apices with a similar shape on the upstream and downstream limbs of the bend; a compound asymmetric bend will have two apices with the radius of curvature being smaller for one of the apices (see Figure 5.17). The curvature profiles of actual bends will not be as easily defined, as the bends are often truncated by the bends upstream or downstream. There is an abundance of short simple symmetric bends (length between 30m and 50m), indicating that these bends are not able to fully develop.

Both the total number of bends and the length of the bends for each category were calculated. Simple symmetric bends were the most numerous in all reaches, but these were often short bends. The average bend length for simple symmetric bends was 75.8 metres, compared to 116.1m, 106.6m and 147.8m for simple asymmetric, compound symmetric and compound asymmetric respectively. The simple symmetric bends tended to be smaller in amplitude suggesting they have not had the time or erosive capability to erode across the floodplain or have been eliminated by the more complex river bends as suggested by

Table 5.1 shows the total number of bends for each category and the percentage of total bend length for each category. Reach two on the River Lugg showed a large increase in the total length of channel classified as compound symmetric or compound asymmetric during the study period. The compound channel length increased from 18.2% of the total channel length in 1886 to 42.1% of the total channel length in 2012.

The curvature profiles of all 2315 bends were analysed for each of the classes to test whether it is possible to identify distinctive profiles for the different types of bend. The changes to the curvature profiles of the most active bends were also tracked through time. The most active bends were chosen as they provide the best opportunity to study the full evolution of the river bend.

Table 5.1. The table shows the total number of bends for each class, the percentage of the total channel length for each class and the average bend length for each class.

Bend Type	Total no. of bends	Total Bend Length (%)	Average Bend Length (m)
Simple Symmetric	1743	63.8	75.8
Simple Asymmetric	248	14.2	116.1
Compound Asymmetric	245	17.7	147.8
Compound Symmetric	79	4.3	106.6

Table 5.2. Brice Classification for individual river bends for each of the different periods

Brice Classification	1st	2nd	3rd	4th	5th	6th	Total
A	14	13	9	7	5	5	53
B	11	7	10	8	9	8	53
C	14	20	17	16	17	20	104
D	11	9	11	16	15	14	76
E	3	3	2	1	3	4	16
F	3	4	5	3	3	2	20
G	1	1	1	2	1	1	7
H	2	2	3	2	5	5	19
I	0	0	0	0	0	2	2
J	0	0	1	1	0	2	4
K	23	19	18	22	13	8	103
L	0	0	0	0	0	0	0
M	11	11	7	6	5	4	44
N	2	4	5	1	5	6	23
O	3	5	9	11	15	15	58
P	2	2	2	3	4	4	17

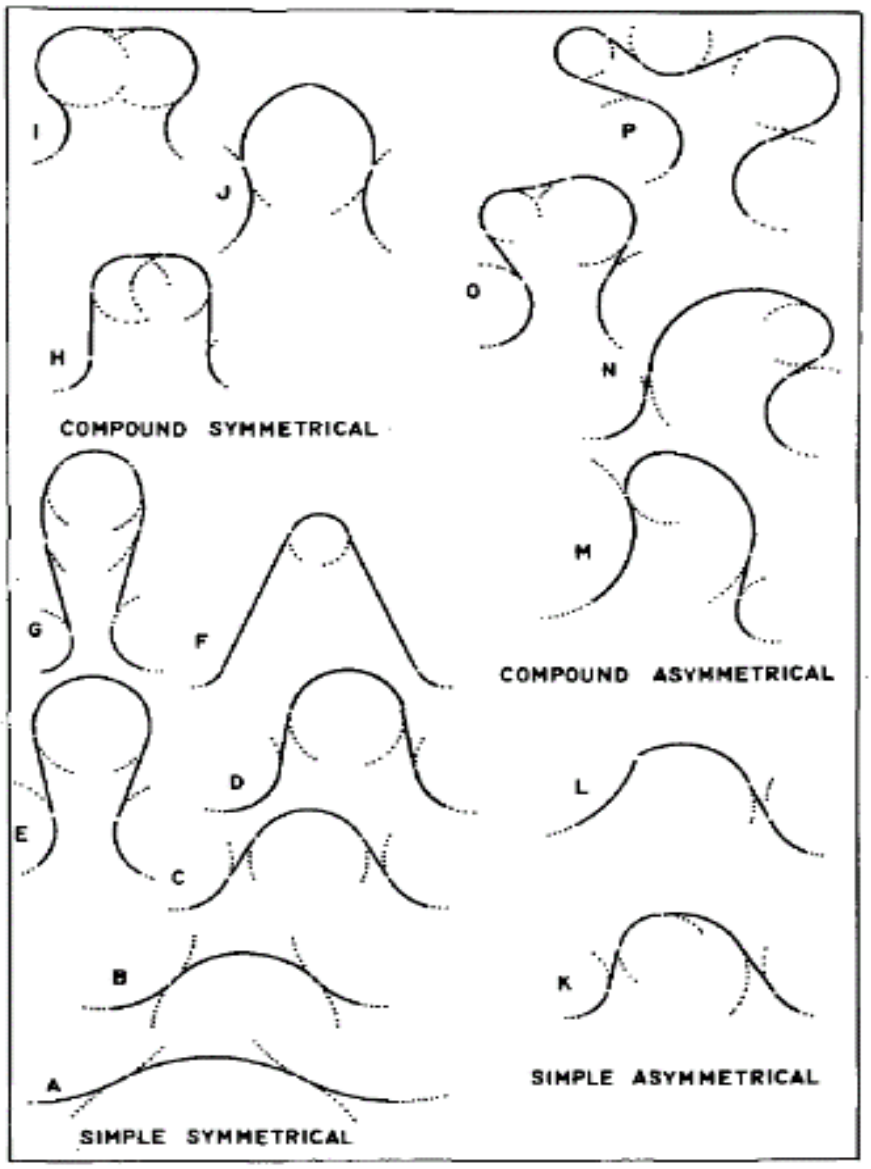

Figure 5.17. The theoretical bend shapes proposed by Brice (1974) ranging from simple symmetric and asymmetric to compound symmetric and asymmetric

5.4.5. Examples of Brice classification bends

A:

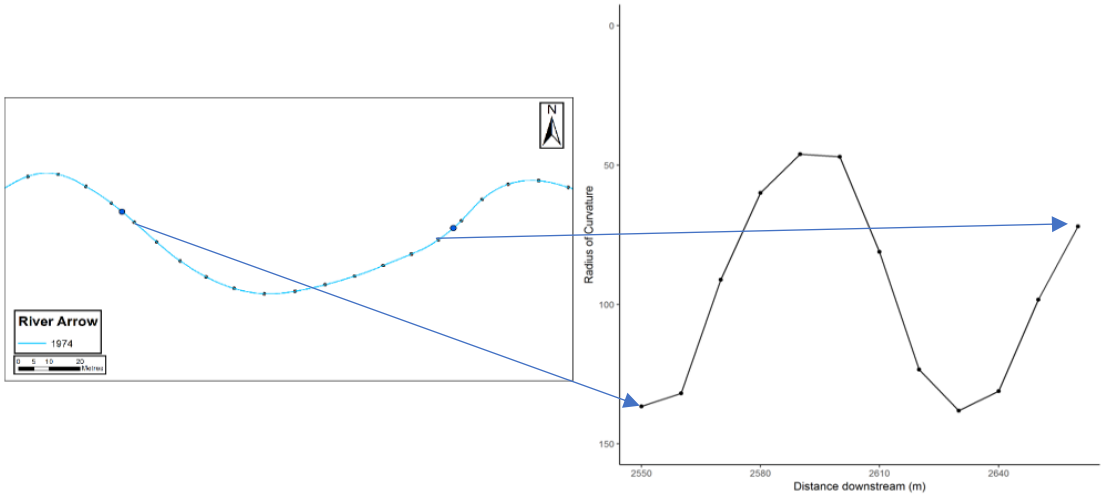

Figure 5.18. A simple symmetrical bend similar to bend type A from Brice (1974) and the variations in the radius of curvature along the bend

B:

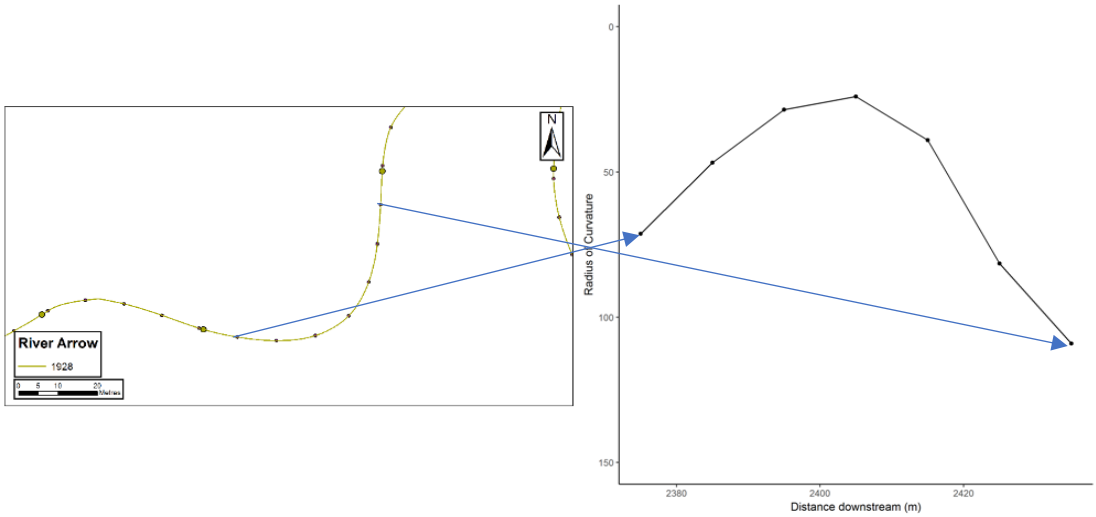

Figure 5.19. Bend type B

C:

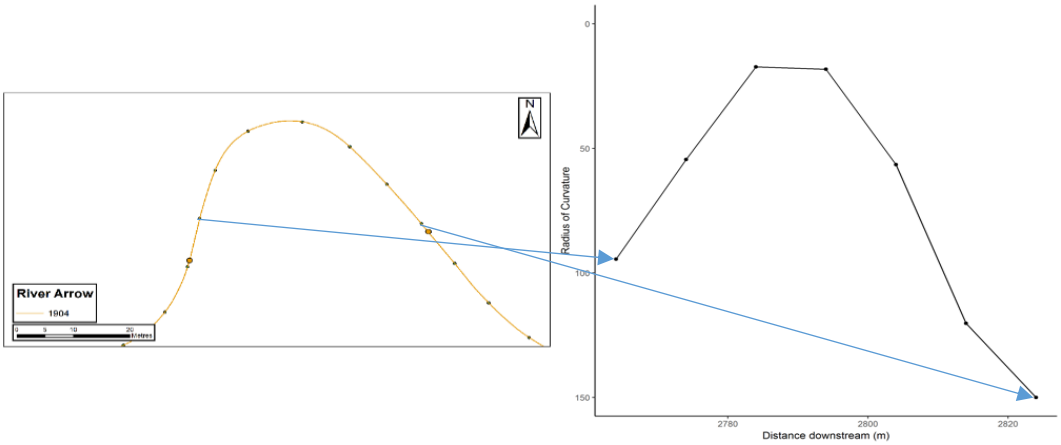

Figure 5.20. Bend type C

D:

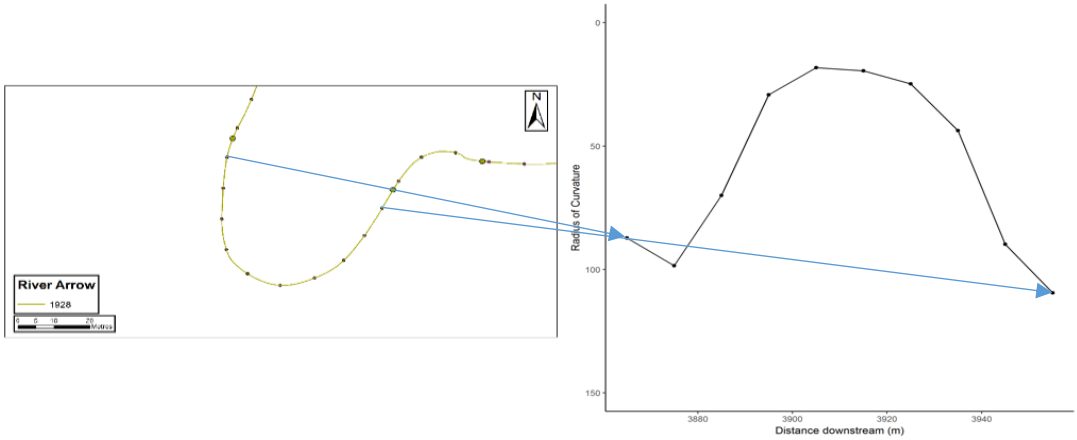

Figure 5.21. Bend type D

E:

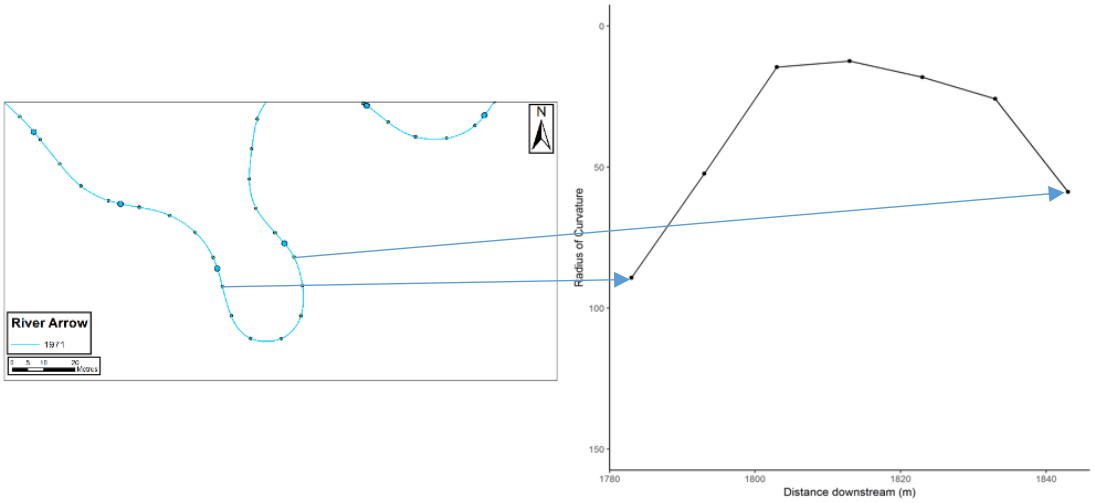

Figure 5.22. Bend type E

F:

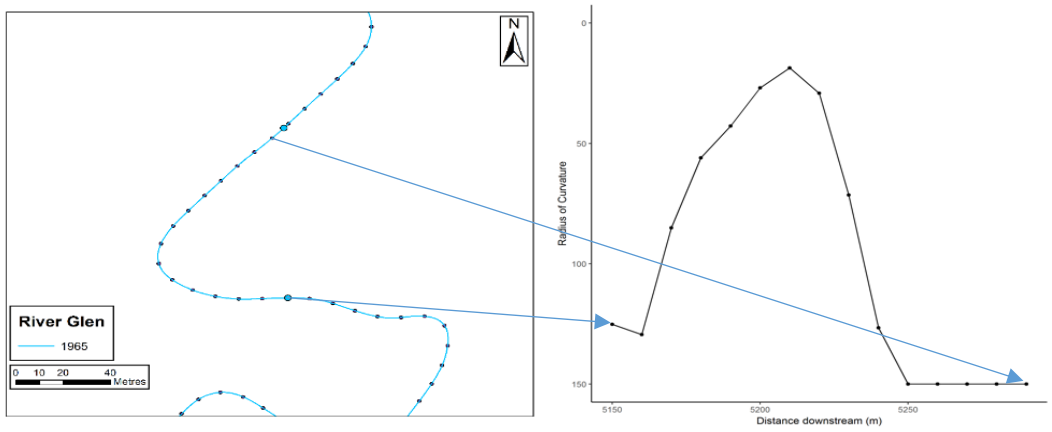

Figure 5.23. Bend type F

G:

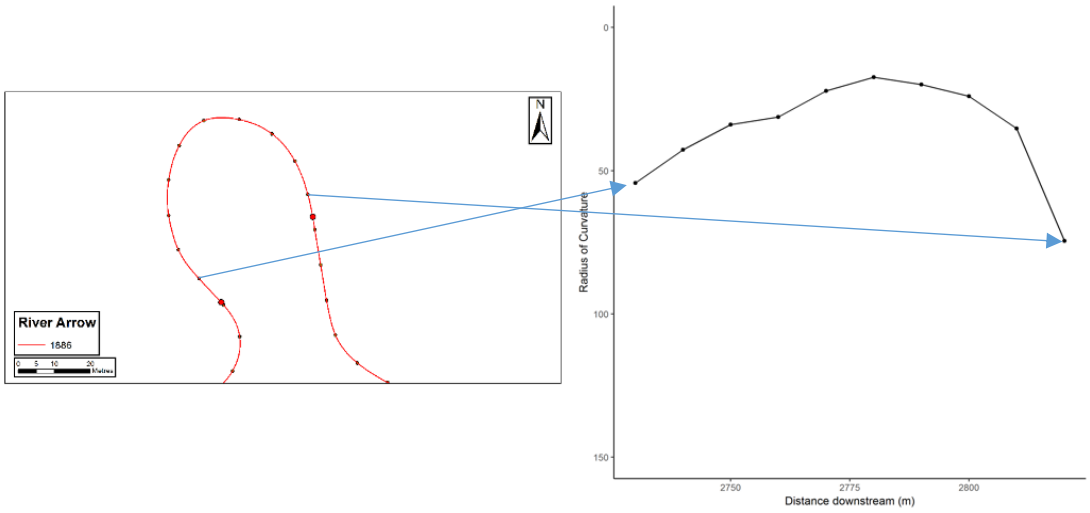

Figure 5.24. Bend type G

H:

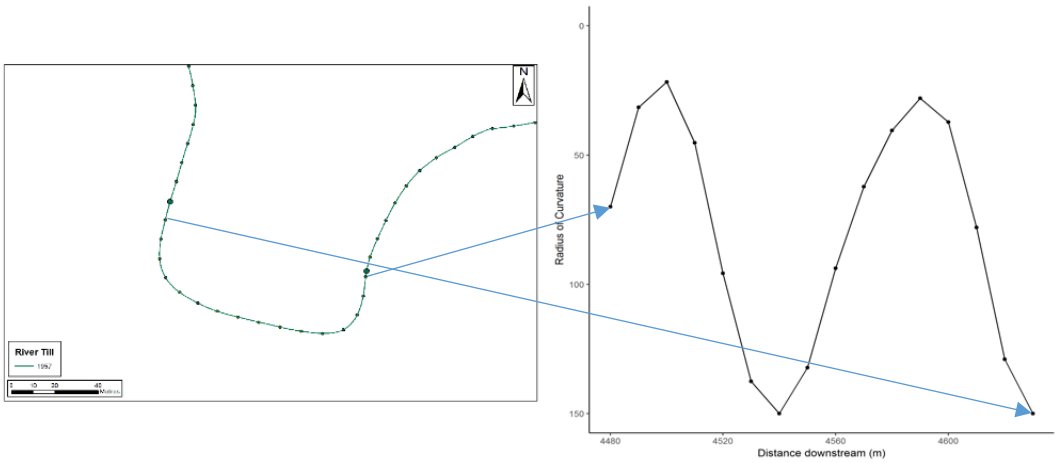

Figure 5.25. Bend type H

I:

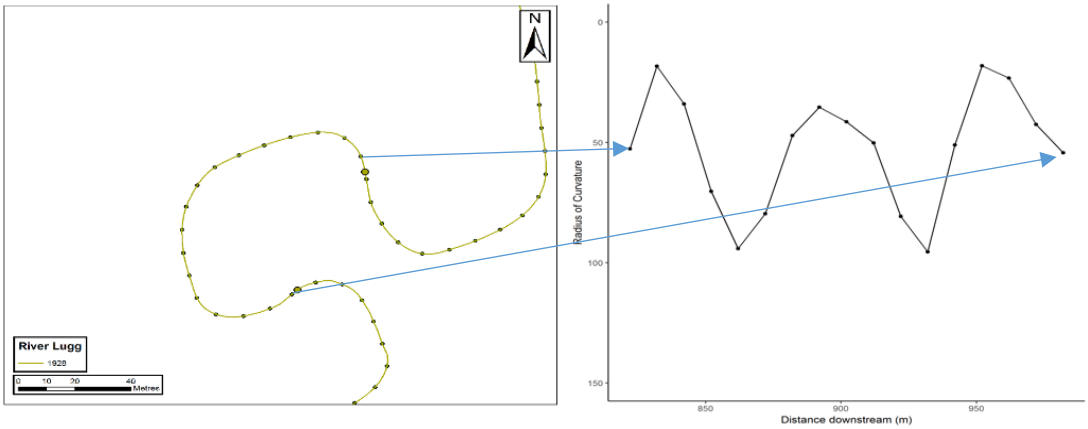

Figure 5.26. Bend type I

J:

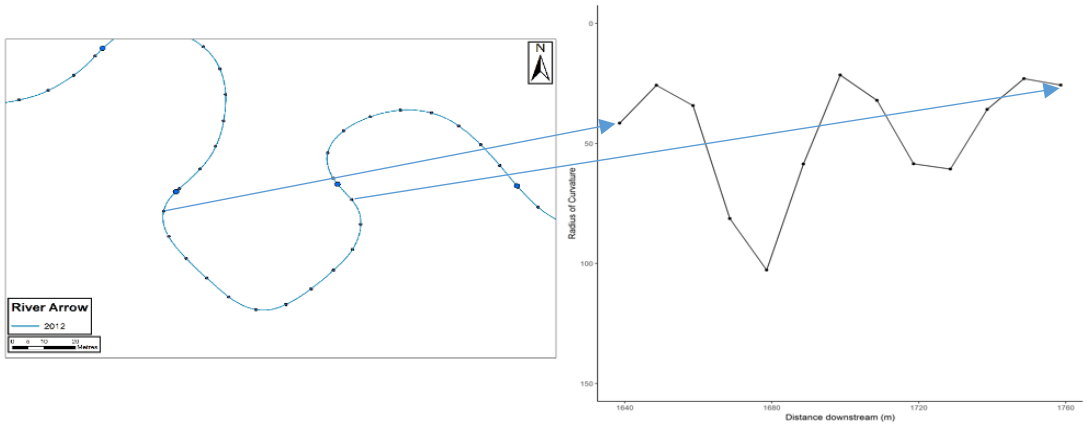

Figure 5.27. Bend type J

:

K (upstream asymmetry):

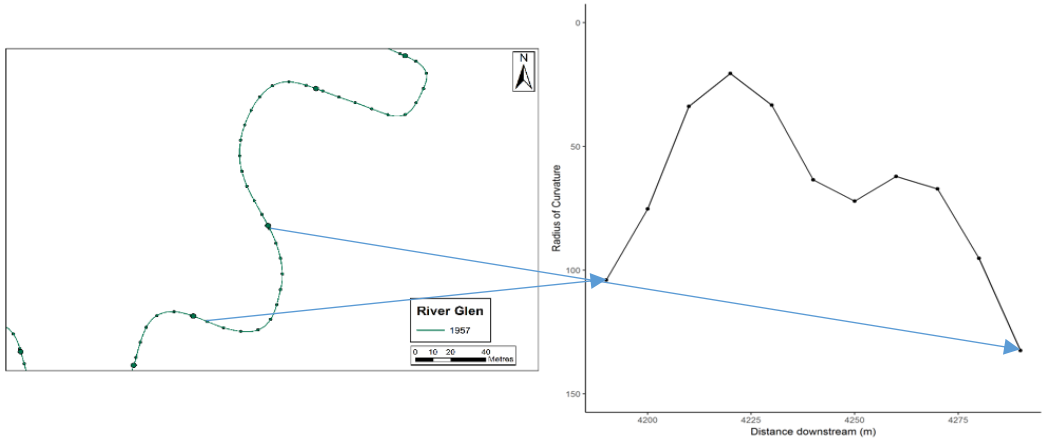

Figure 5.28. Bend type K, with upstream asymmetry

K (downstream asymmetry):

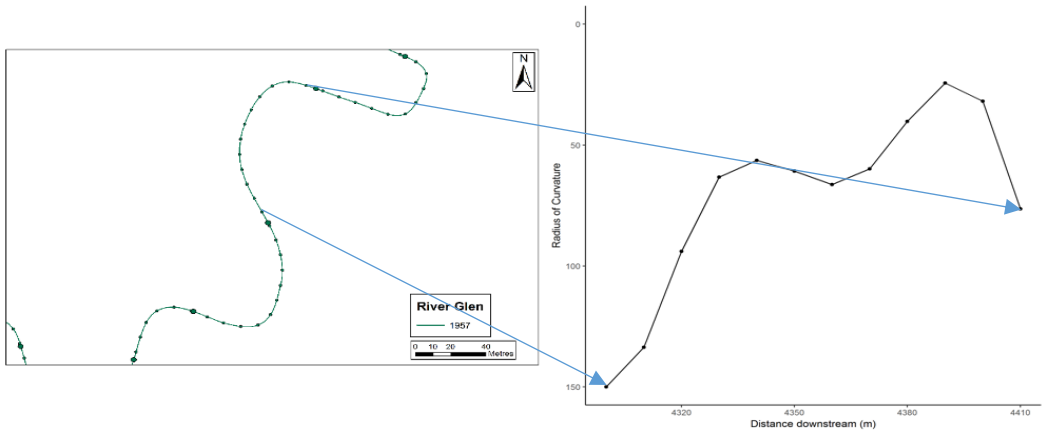

Figure 5.29. Bend type K, with downstream asymmetry

M:

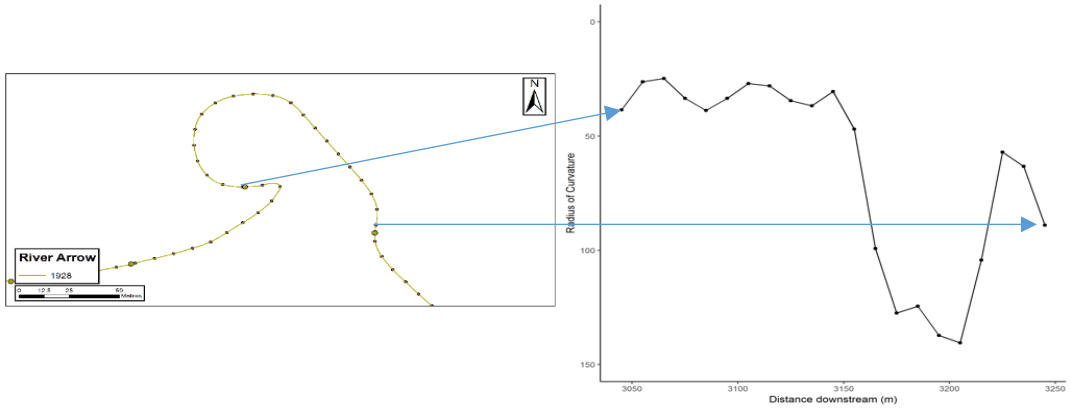

Figure 5.30. Bend type M

N:

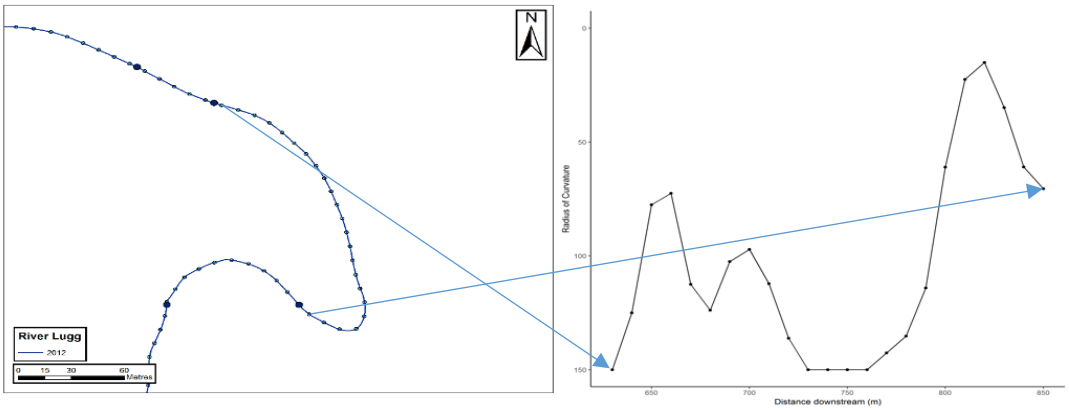

Figure 5.31. Bend type N

O:

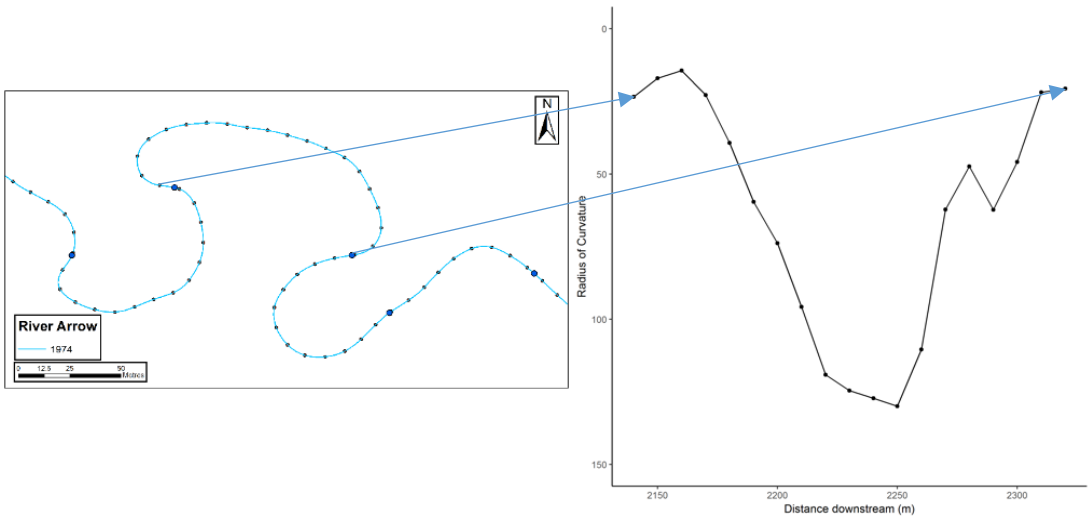

Figure 5.32. Bend type O

The radius of curvature distributions of the different bend types show some distinctive characteristics. The simple symmetric bends tended to have one distinct peak in the radius of curvature, with the tighter bends having a lower measurement for the radius of curvature at the apex. The simple symmetric bends also tended to have a similar profile upstream and downstream of the apex with the radius of curvature decreasing and increasing at a similar rate. As the bends become progressively tighter (bends C-E and G) there are more points with a low radius of curvature at the apex of the bend. Bend F has a low radius of curvature at the apex, but the straight channel at the entrance and exit of the bend means that the radius of curvature increases quickly upstream and downstream of the apex.

The compound symmetric bends had two or more apices, which all have a similar curvature distribution. Three different types of compound symmetrical bends were proposed by Brice (1974), H, I and J and examples are shown in Figure 5.25-22. Bend H shows two distinct minima in the radius of curvature and a section of straight channel connecting the two apices. The radius of curvature of bend type I is lower at the apices of the bend indicating a tighter bend. It was not possible to find any bends that exactly match the example given by Brice for bend type I, with the bends of this type also developing a third apex in the middle of the bend with a higher radius of curvature than the two apices at the start and exit of the bend. The final compound symmetric bend, type J, appeared to have three distinct apices, all with a similar minimum radius of curvature and curvature profiles. Overall, compound symmetric bends were rare for rivers in the Lugg and Till catchment, representing 4.3% of the total bend length and 3.4% of the total number of bends.

Brice suggested that are two types of simple asymmetrical bends, type K and L. Both bends have a very similar curvature profile and it was not possible to distinguish them from the bends in the study. However, the bends have been identified with both an upstream and a downstream asymmetry, which are both common within the dataset. The bends with a simple asymmetrical form tend to have one apex with the curvature distribution skewed either upstream or downstream and a long “tail” depending on the direction of the skew. Two examples of this were shown for the River Glen, one with an upstream skew and one with a downstream skew. The curvature profiles were remarkably similar for the two bends only reversed.

The final bend type proposed by Brice was compound asymmetrical bends. Bend type P would be considered as three separate bends in this study as the length of the bends

would cross the threshold of 30m. One example of this did occur on reach 5 of the River Lugg, which will be described later in this chapter in the section focussing on the changes to the curvature profiles as they evolve. Bends with a profile similar to type M, N and O were identified in the dataset and presented. Bends M and N are similar with one main apex with an apex with a much larger radius of curvature on the upstream or downstream limb. Bends with the planform suggested for bend O would have two apices but they would be asymmetrical in either the minimum value of the radius of curvature or the profile. This can be seen in Figure 5.32 with a much tighter apex at the start of the bend compared to the exit.

There were also variations in the mean, median, minimum and weighted radius of curvature between the different types of bend. Bend type A had the highest values for all four different types of measurement for radius of curvature. The minimum value for the radius of curvature decreased through the progression from A to G as the bends tended to get tighter around the apex as they developed. The median and mean radius of curvature also tended to decrease along the progression from A to G, with the exception of bend type F. Bend type F is characterised by a sharp apex (minimum radius of curvature of 18.7m) for the example given, but also with straight channels leading up to and away from the apex. This meant that despite the low radius of curvature at the apex the over mean and median radius of curvature was higher than then other bends, including bend type A.

The compound symmetrical bends also showed a decrease in the mean and median radius of curvature from bends H to J; however, there is less variation in the minimum radius of curvature. This suggests that the compound symmetric bends have well developed apices. Bend type H is formed of two well-developed apices, connected by a straight section of channel, which led to a high mean and median radius of curvature. Bends I and J were more rounded and although the minimum radius of curvature did not decrease greatly, the parts of the channel connecting the apices had a lower radius of curvature and the mean and median radius of curvature decreased for both bend types.

The simple asymmetrical bends tended to have one tight apex with a low radius of curvature, either at the start or at the end of the bend, with a section of the channel having a higher radius of curvature. The minimum radius of curvature was low for the two examples given, however due to the long “tail” with higher radius of curvature the mean and median radius of curvature was higher than the simple symmetrical bends with a similar shape at the apex. The compound asymmetrical bends all showed variations in minimum, mean and median radius of curvature. Bend types M and N tended to be characterised by one half of

the bend, with a low radius of curvature, especially around the minimum point, with a second apex formed with a higher radius of curvature. The mean and median radius of curvature tended to be higher in examples of these types of bends. The example provided here is an extreme form of the compound asymmetrical bend with eleven points with a radius of curvature less than 50m. Finally, bend type O had two separate apices, both of which with a low radius of curvature, connected by a section of channel with a high radius of curvature. This meant that the mean and median radius of curvature was high compared to the more rounded symmetrical bends despite the low value for the minimum radius of curvature.

Figure 5.33 and Table 5.3 show how the different measurements of radius of curvature varied for the example bends show above. The minimum radius of curvature was the least sensitive of the measurements, with a range of 33.7m between the largest and smallest measurement. The weighted radius of curvature measured, RoC_w, had the highest range. The mean and median RoC had similar mean values for all the bends, but the median RoC measurement had a greater range of measurements.

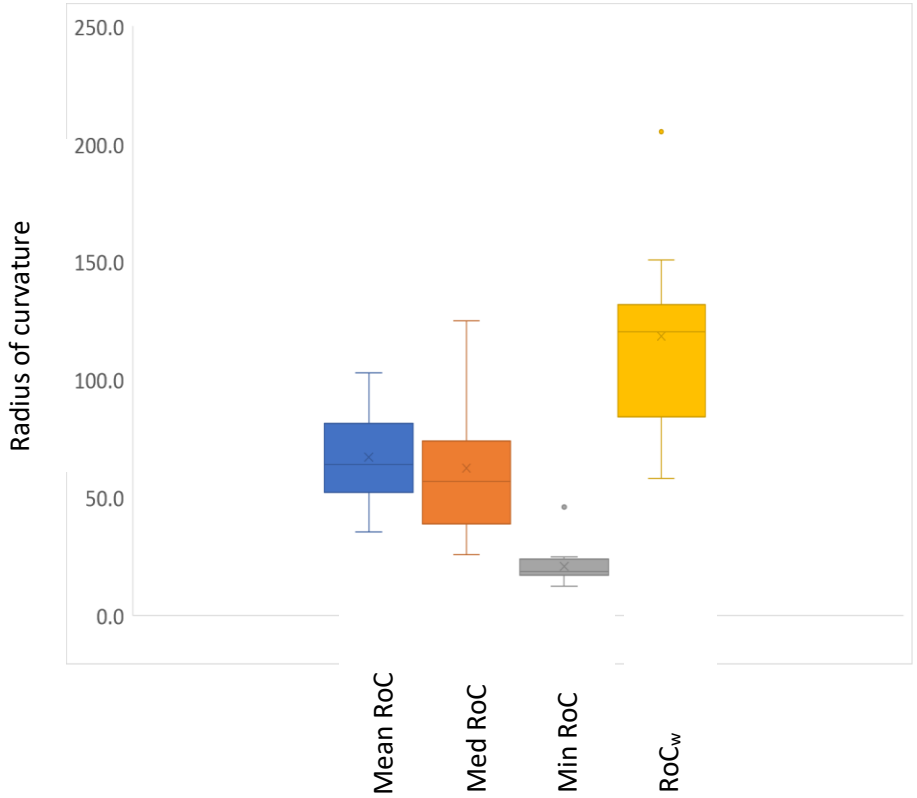

Figure 5.33. The distribution of the different radius of curvature measurements for the Brice classification example bends. The minimum radius of curvature was the least sensitive of the four different types of measurement

Table 5.3. Summary table of the different measurements of radius of curvature for each of the different types of bend proposed by Brice (1974)

Bend Type	Mean RoC	Median RoC	Minimum RoC	RoC_w
A	96.4	94.7	46.1	205.2
B	57.1	46.8	24.0	131.0
C	73.0	56.5	17.3	114.7
D	59.1	56.9	18.3	120.4
E	38.8	25.8	12.4	84.3
F	97.4	125.1	18.7	115.2
G	35.5	32.6	17.4	72.9
H	81.4	74.0	21.8	150.9
I	52.3	50.2	18.1	123.8
J	46.3	35.9	21.5	131.9
K (Up)	69.1	67.2	20.5	123.6
K (Down)	71.4	62.0	24.3	120.0
M	63.9	38.8	24.8	84.0
N	102.9	112.6	15.0	142.3
O	64.1	59.6	14.4	58.3

5.4.6. Evolution of the curvature profiles of individual bends

Brice suggested that the individual bends would follow a certain evolutionary trajectory based on the initial shape of the river bend. Bends A to C represent the evolution of a simple bend with a high radius of curvature, with the radius of curvature gradually decreasing and forming the U-shaped bend identified as bend D. If there are straight sections of channel either side of the loop then they may develop towards bend type E-G. Asymmetry in bends is produced when a second arc is created on the same loop and further exaggerated by encroachment by another adjacent loop, usually on the upstream side of the bend. Bends gradually develop towards compound if a separate arc grows on the same side of a simple loop. Brice found that most compound loops were asymmetrical, which was also the case for the rivers in this study (17.7% of the total channel length, compared to 4.3% for the compound symmetrical bends). Brice suggested that the development from simple to compound is a gradual process occurring over a long period for the rivers studied. This section of the chapter will focus on the evolution of individual bends and how the curvature profiles changed as the bend developed.

River Arrow, Reach 1, Bend 11. (Figure 5.34 to Figure 5.36)

The following figures show the evolution of different types of bends in the River Lugg and River Till catchment. Bend 11 on the River Arrow starts as a simple symmetric bend with a low minimum radius of curvature with a bend type similar to bend C in the Brice classification. The bend is stable between 1886 and 1964 with low levels of migration on the bend. Between 1964 and 1974 there is some small growth on the bend and the bend developed towards bend type D. Erosion on the preceding bend and further growth means the bend developed to bend type E between 1974 and 2012. Overall, the total migration was low on this simple symmetric bend and it remained simple symmetric throughout the study period.

Date	Brice Classification
1886	C
1904	C
1928	C
1964	C
1974	D
2012	E

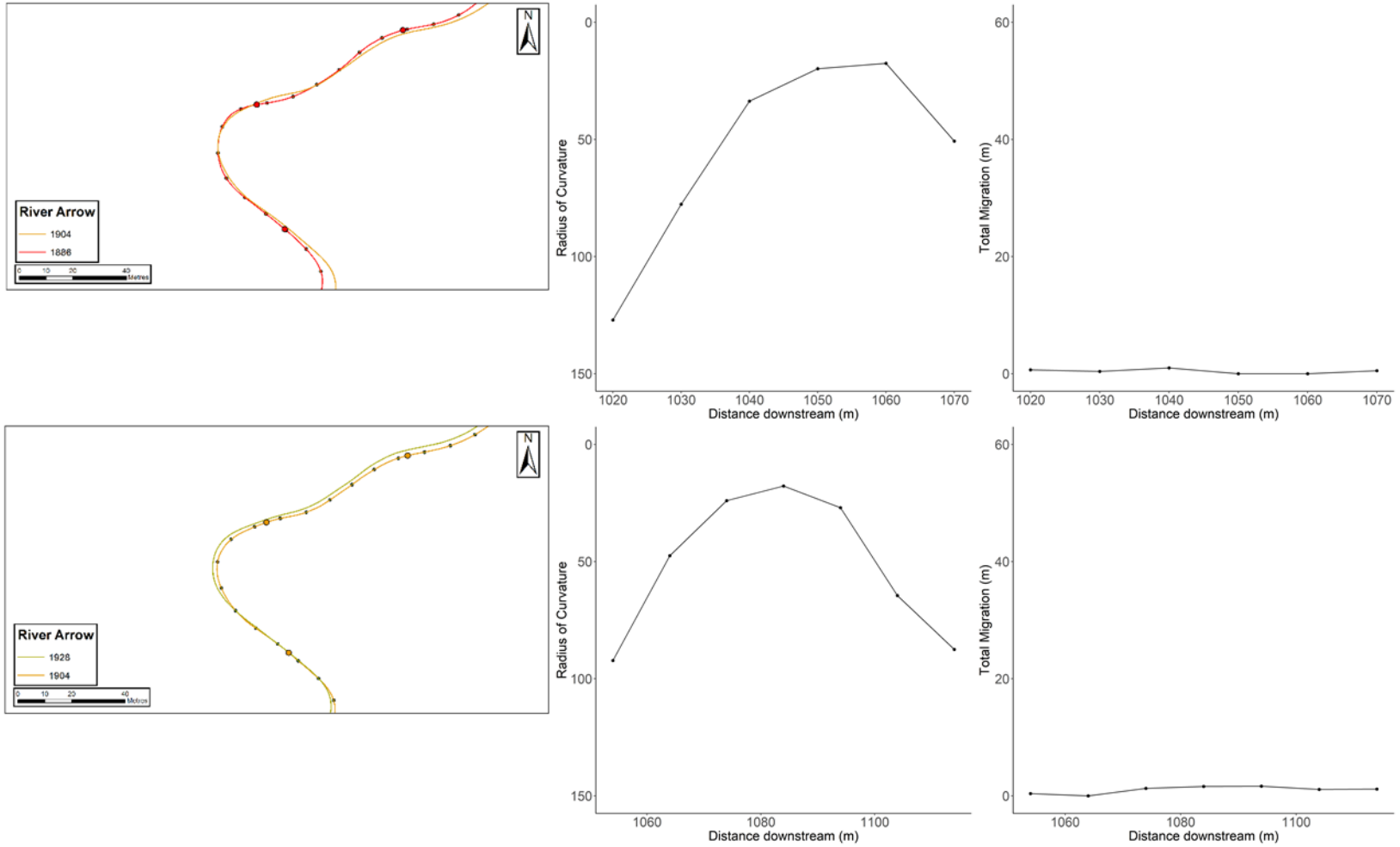

Figure 5.34. Changes to the curvature for Bend 11, Reach 1, River Arrow, between 1886 and 1928

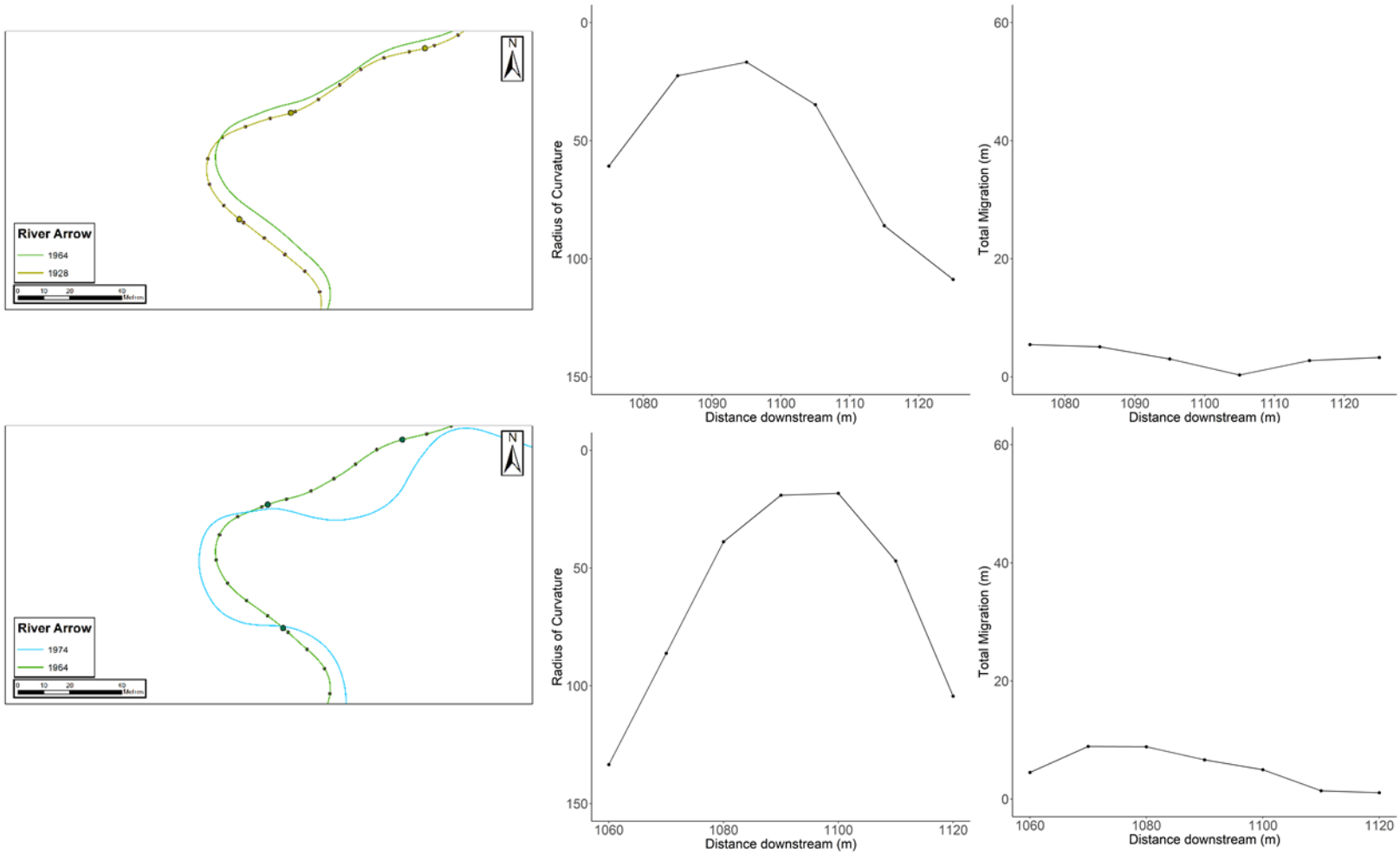

Figure 5.35. Changes to the curvature of Bend 11, Reach 1, River Arrow between 1928 and 1974

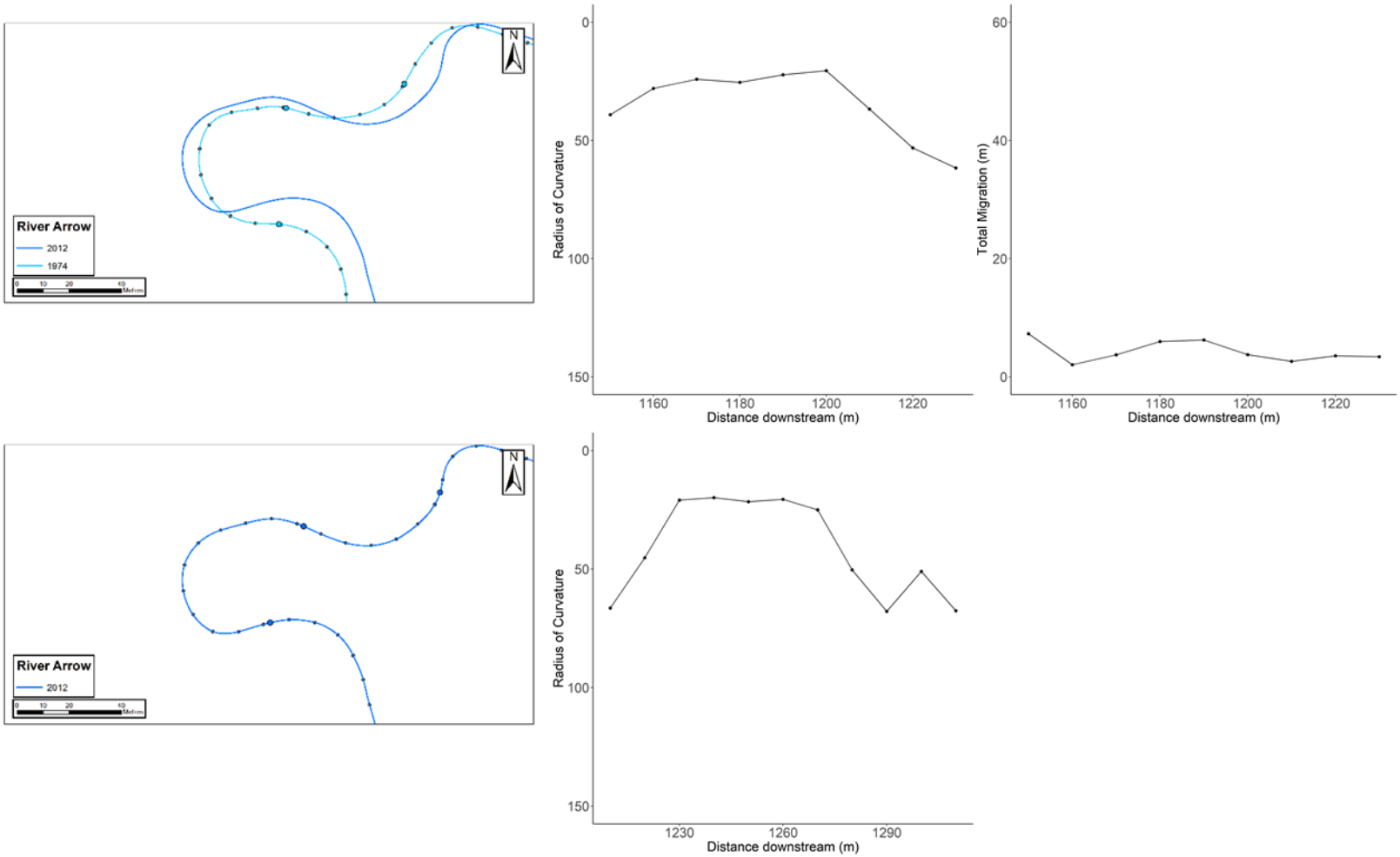

Figure 5.36. Changes to the curvature of Bend 11, Reach 1, River Arrow between 1974 and 2012

River Arrow, Reach 1, Bend 21 (Figure 5.37 to Figure 5.39)

Bend 21 starts as a simple symmetric bend in 1886 with a slight skew on the downstream limb of the bend. The radius of curvature is low through most of the bend and the bend type is similar to C/D from the Brice classification. There were low amounts of erosion between 1886 and 1964 with some downstream migration between 1904 and 1928. Between 1964 and 1974 the bend developed two well defined apices and the bend was defined as compound asymmetrical, with the highest amount of erosion occurring on the downstream side of the bend. Between 1974 and 2012 the bend experienced a cutoff and a new simple symmetric bend was created.

Date	Brice Classification
1886	C/D
1904	C/D
1928	C/D
1964	C/D
1974	O
2012	B

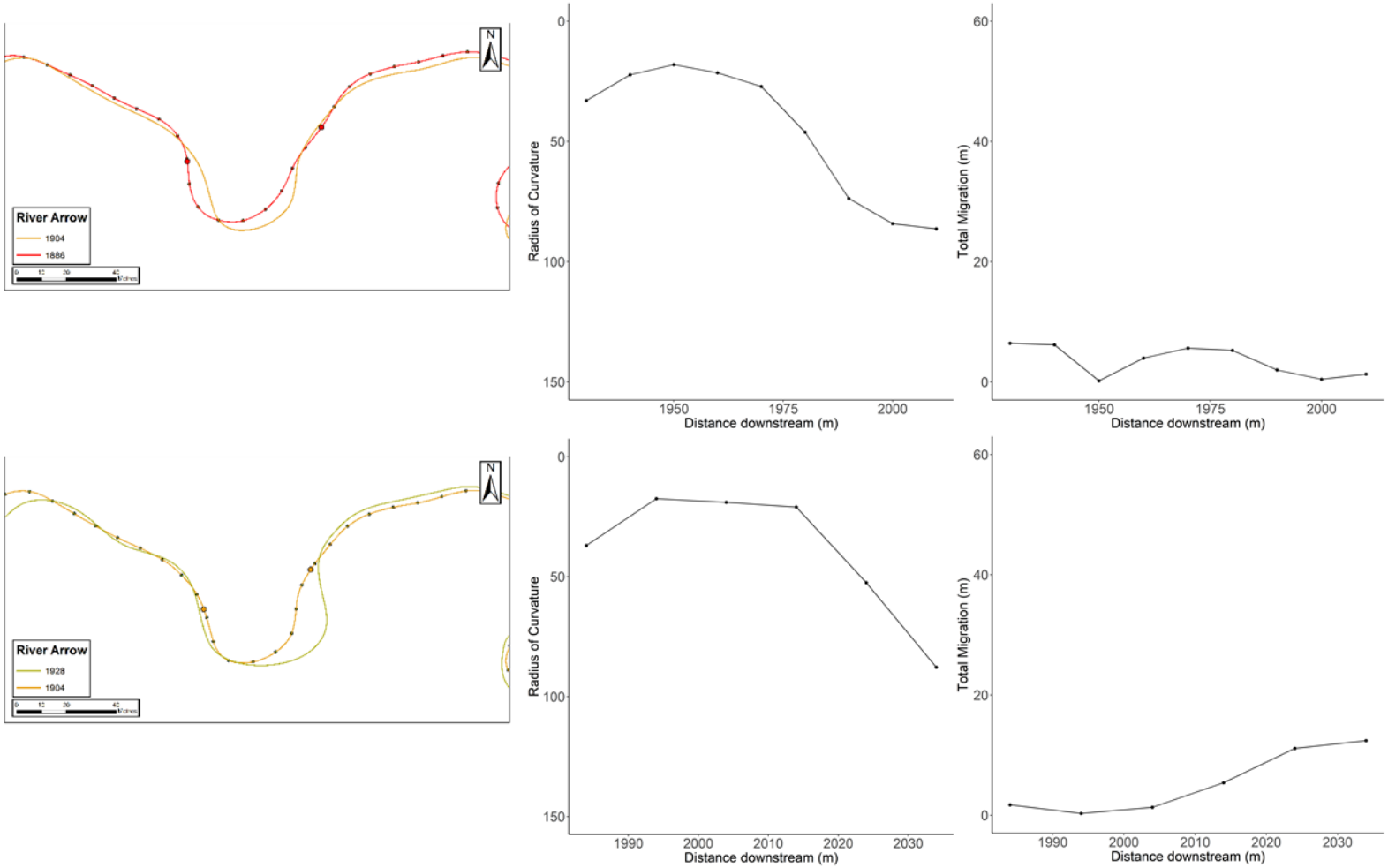

Figure 5.37. Changes to the curvature for Bend 21, Reach 1, River Arrow, between 1886 and 1928

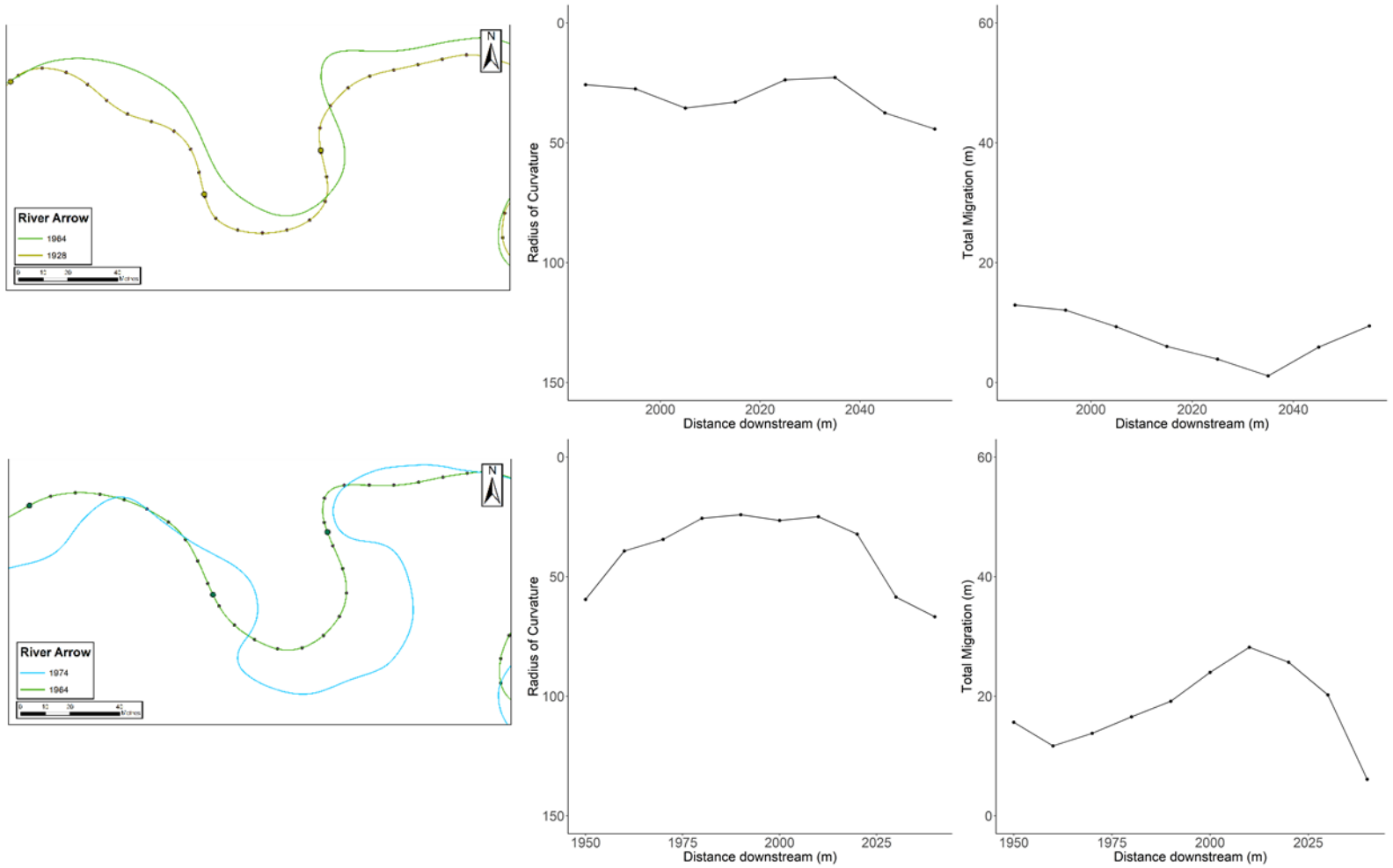

Figure 5.38. Changes to the curvature of Bend 21, Reach 1, River Arrow, between 1928 and 1974

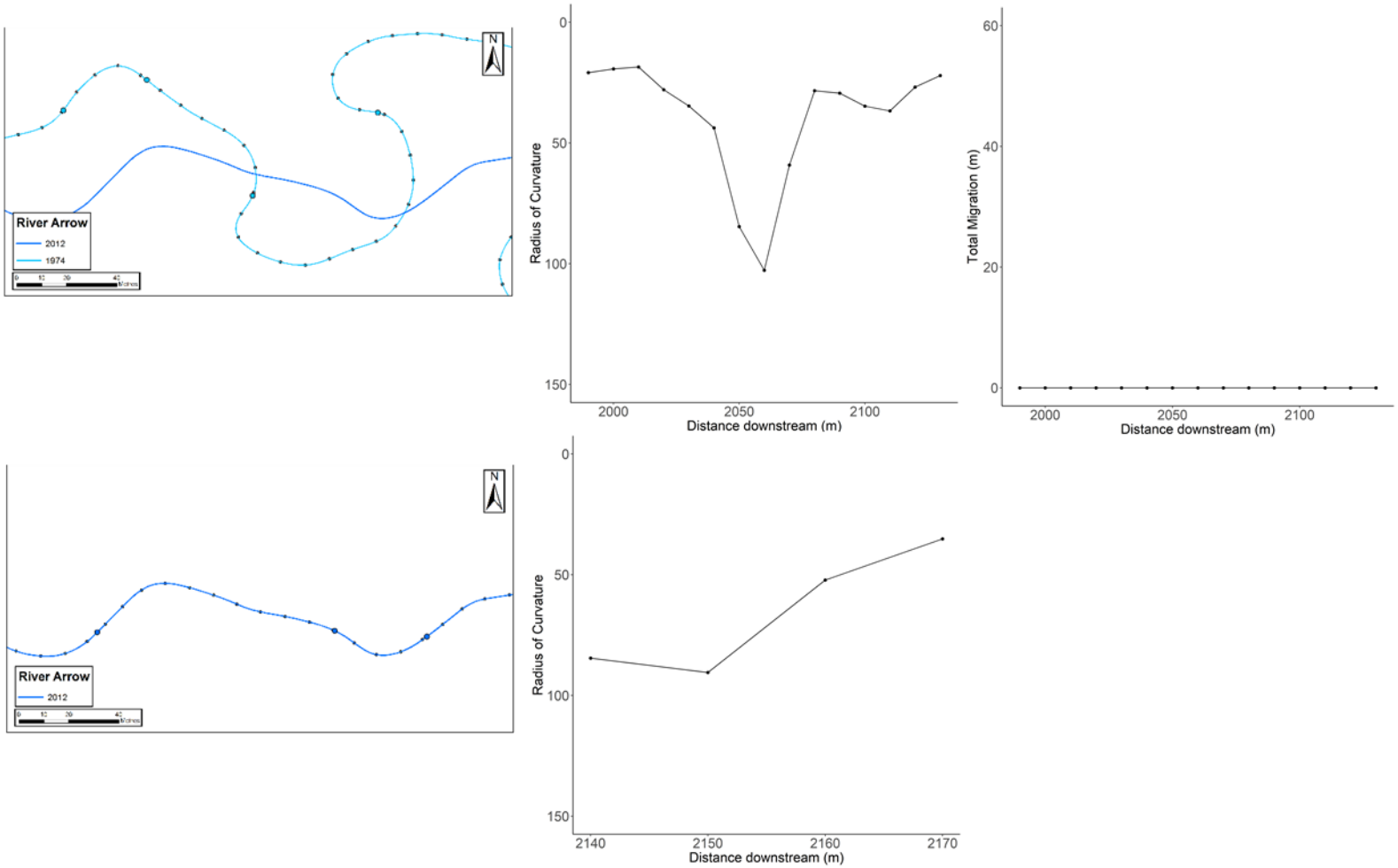

Figure 5.39. Changes to the curvature of Bend 21, Reach 1, River Arrow between 1974 and 2012

River Arrow, Reach 1, Bend 22 (Figure 5.40 to Figure 5.42)

Bend 22 could be considered as either a simple asymmetrical or compound asymmetrical bend. There are two apices on the bend, with the apex at the start of the bend having a much higher radius of curvature compared to the apex at the end of the bend. The length of the apex is also shorter at the start of the bend compared to the apex at the end of the bend. The bend could be considered as either bend K or bend N. The bend shape remains constant between 1886 and 1928, with a small increase in the radius of curvature on the upstream apex between 1904 and 1928. Between 1928 and 1964, there is a small amount of growth across the floodplain and the upstream apex because much tighter and sharper and two distinct apices have formed. The highest amount of erosion also occurred for this part of the bend. Erosion between 1964 and 1974 on both this bend and the preceding bend caused the two very tight apices to form. The bend did not grow across the floodplain, so all of the erosion occurred at the downstream end of the bend which migrated downstream. The bend form is best described by bend type O in the Brice classification, although the bend could have potentially produced a bend type similar to P if the cutoff had not occurred. The bend was cutoff between 1974 and 2012 and subsequently developed into a simple asymmetrical bend, which was recorded in 2012.

Date	Brice Classification
1886	K/N
1904	K/N
1928	K/N
1964	O
1974	O
2012	K

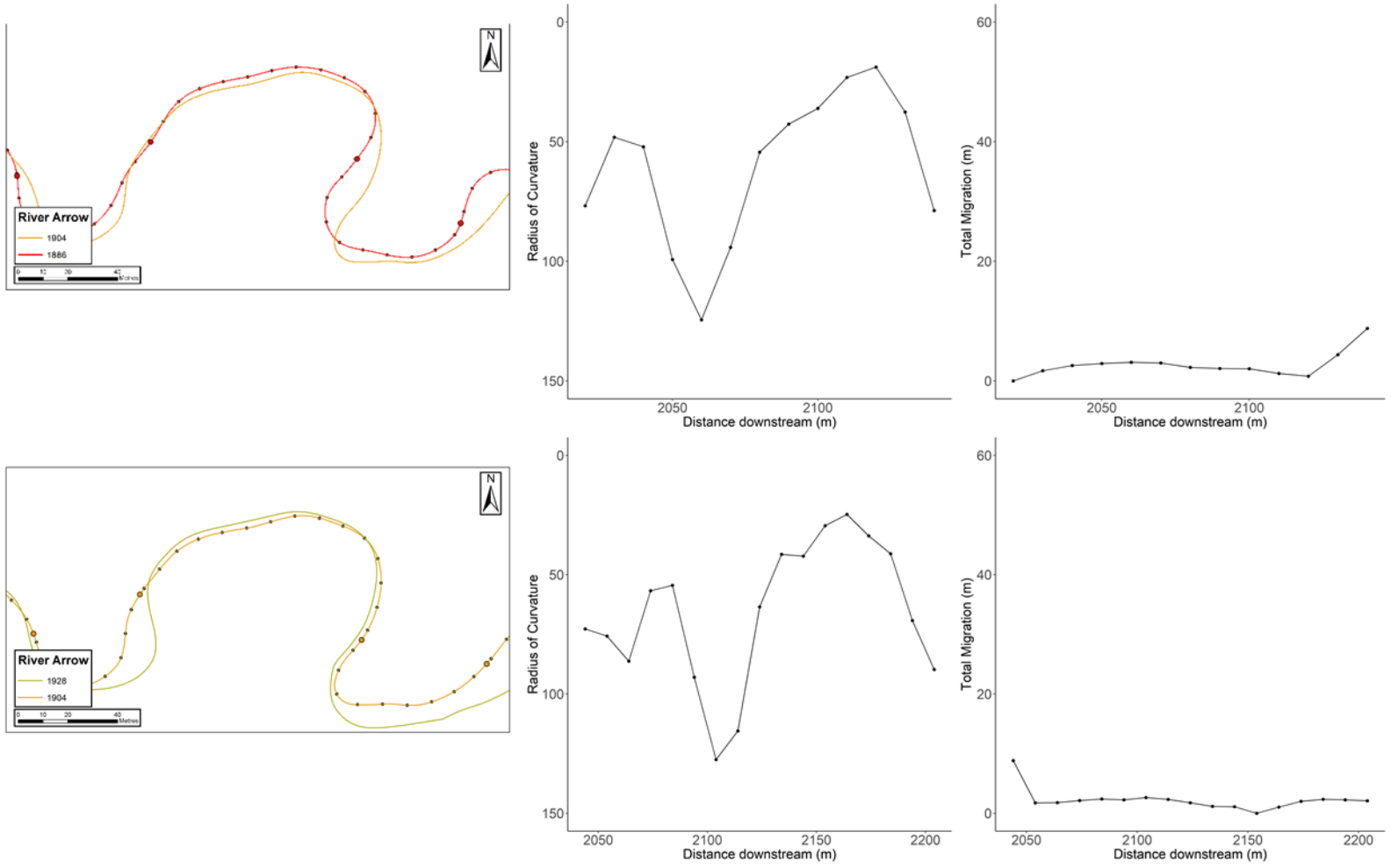

Figure 5.40. Evolution of the curvature for Bend 22, Reach 1, River Arrow, between 1886 and 1928

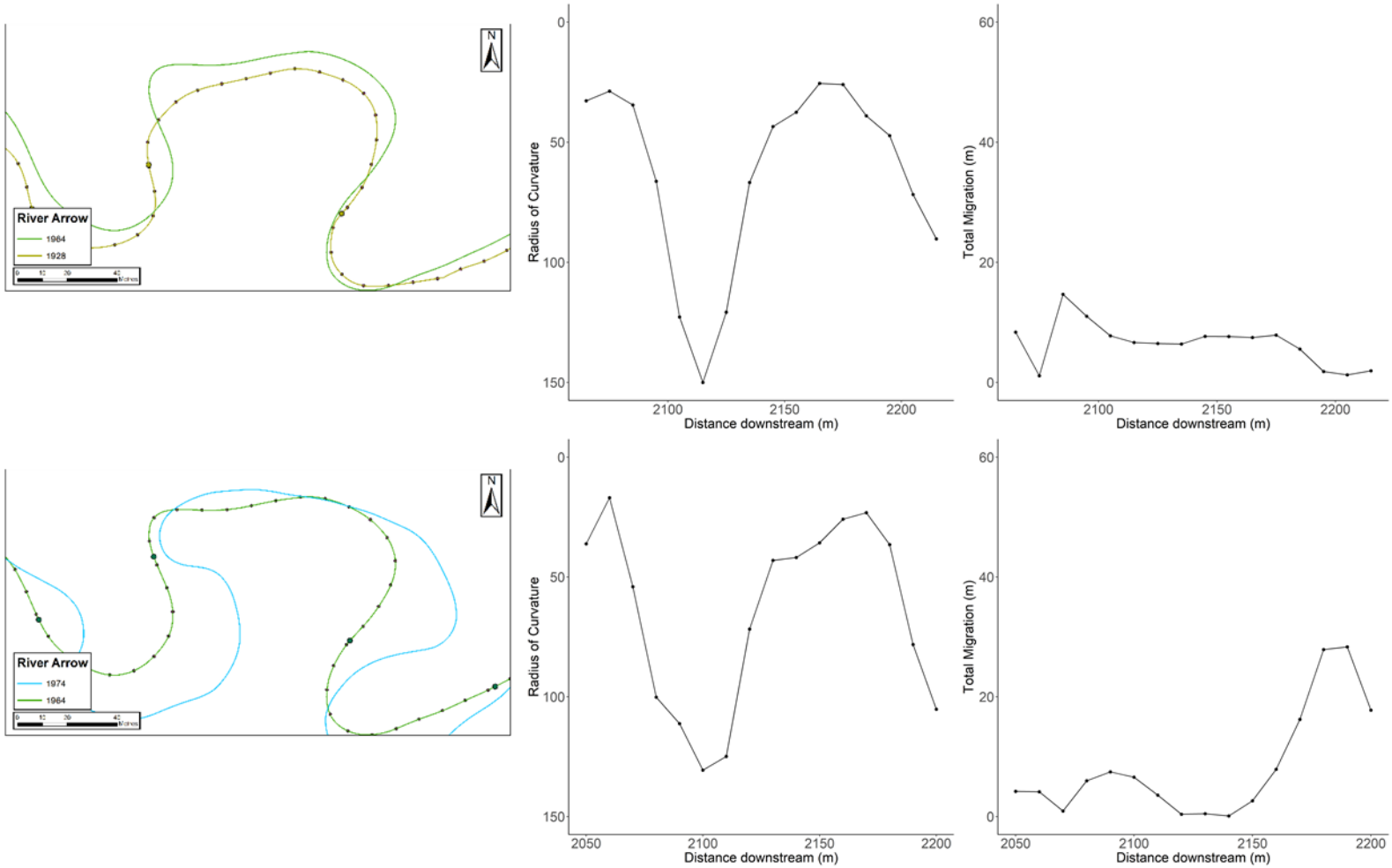

Figure 5.41. Evolution of the curvature for Bend 22, Reach 1, River Arrow, between 1928 and 1974

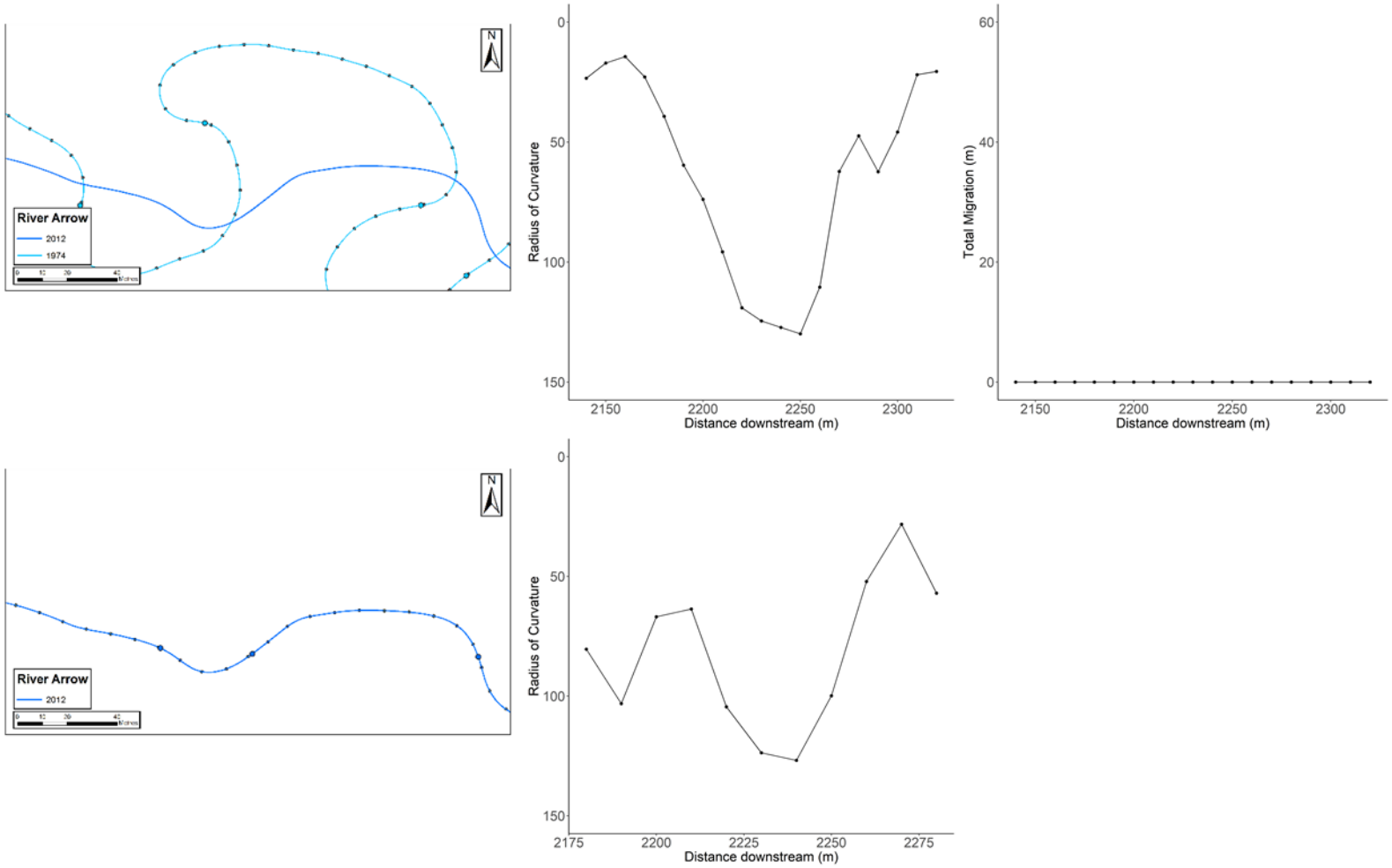

Figure 5.42. Evolution of the curvature for Bend 22, Reach 1, River Arrow, between 1974 and 2012

River Arrow, Reach 1, Bend 26 (Figure 5.43 to Figure 5.45)

Bend 26 starts as a simple asymmetrical bend with a skew in the downstream direction. The bend is stable between 1886 and 1904, before experiencing a high amount of erosion on the upstream side between 1904 and 1928. This led to the development of a compound symmetrical bend in 1928 with two similar apices in the shape and minimum radius of curvature. The erosion is low between 1928 and 1964 and the bend maintained the compound symmetrical shape, as bend H in the Brice classification. The bend is cutoff between 1964 and 1974 and the river started to develop to the other side of the valley. A simple symmetrical bend is formed, similar to bend type A. There is a decrease in the radius of curvature towards the end of the bend, suggesting a second apex could form, but the inflection point is found here, and the next bend starts before the apex can be fully developed. Between 1974 and 2012 the bend continued to grow across the floodplain and the radius of curvature began to decrease and the length of the apex increased.

Date	Brice Classification
1886	K
1904	K
1928	H
1964	H
1974	A
2012	B

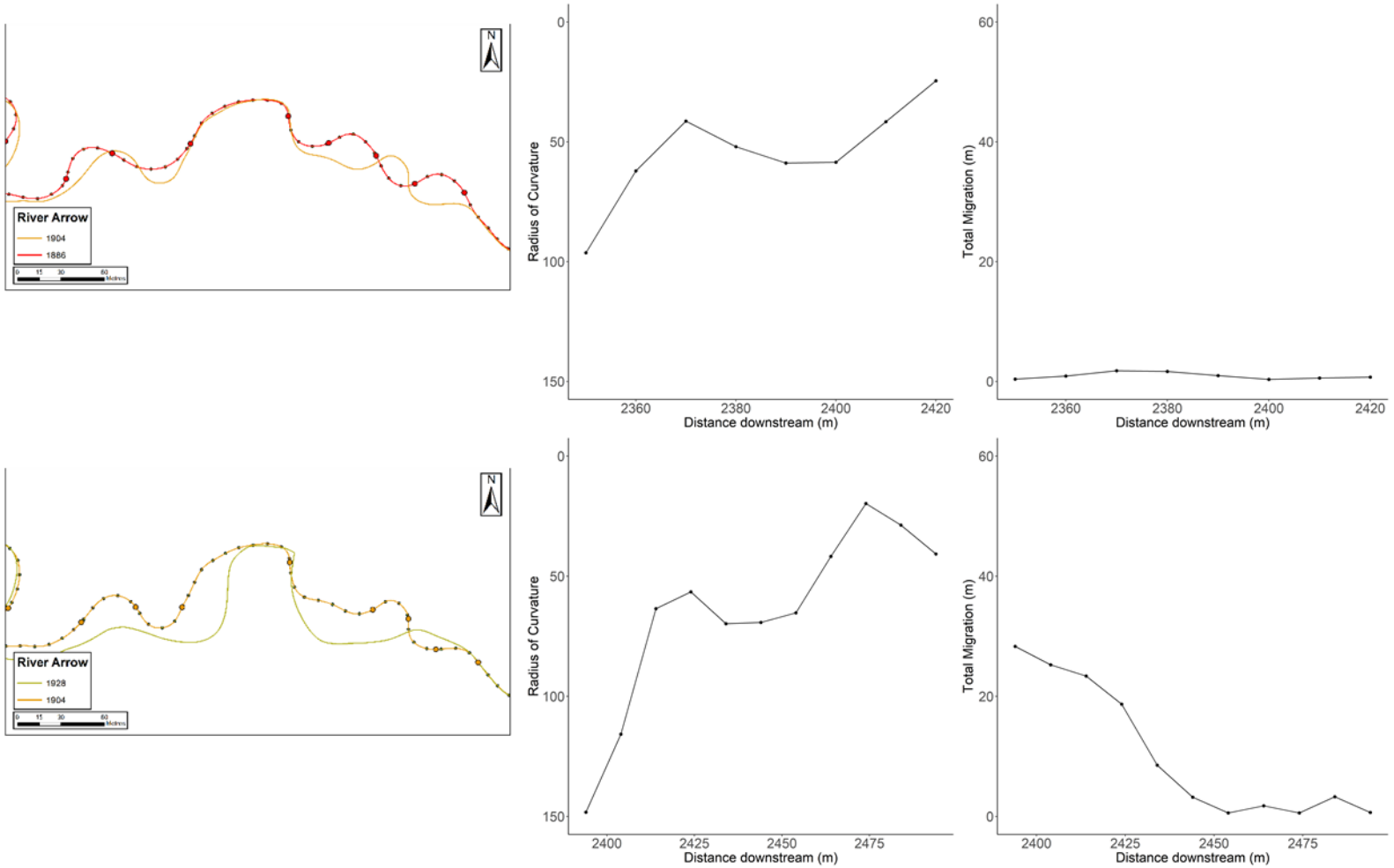

Figure 5.43. Changes to the curvature profile for Bend 26, Reach 1, River Arrow, between 1886 and 1928

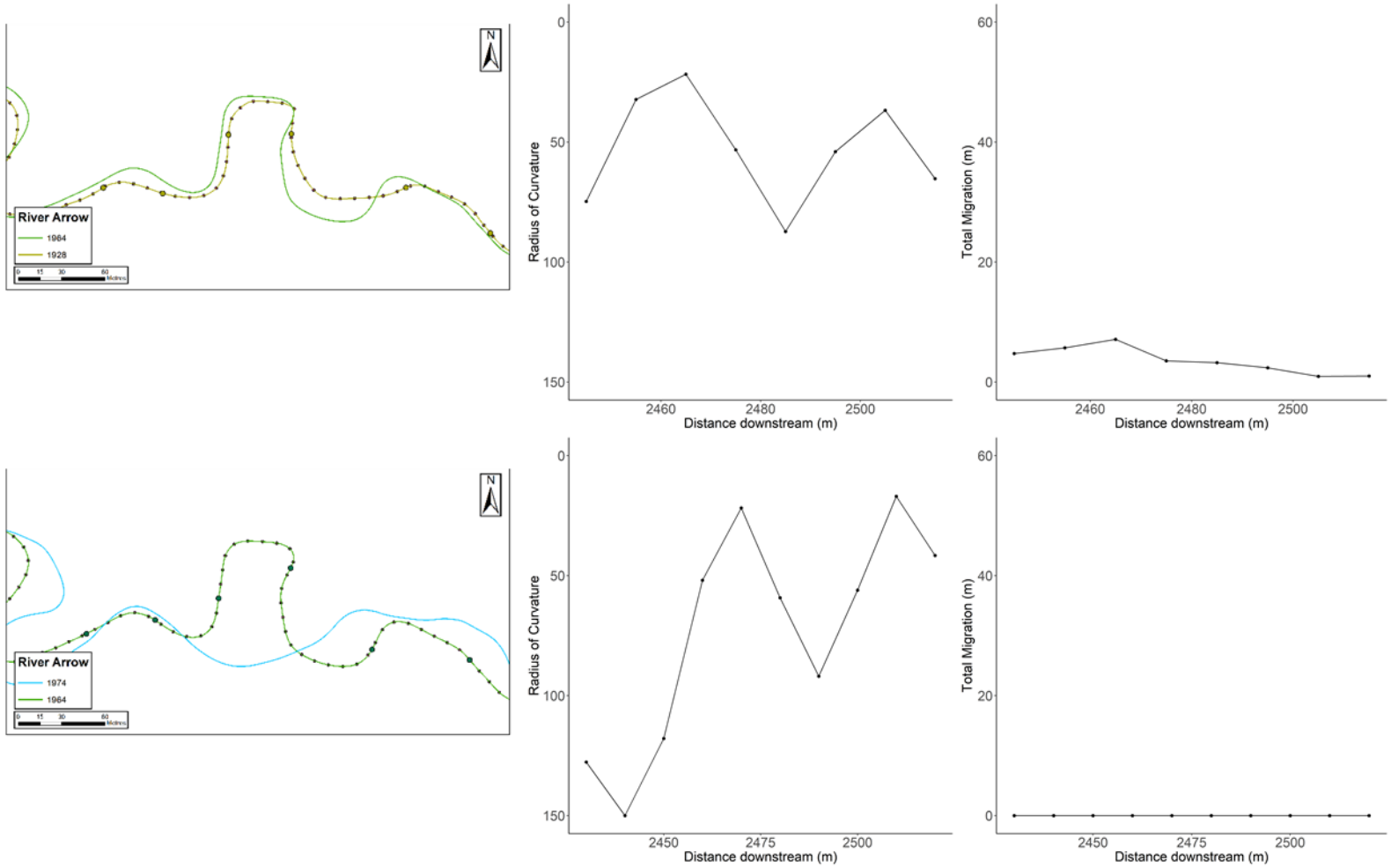

Figure 5.44. Changes to the curvature profile for Bend 26, Reach 1, River Arrow, between 1928 and 1974

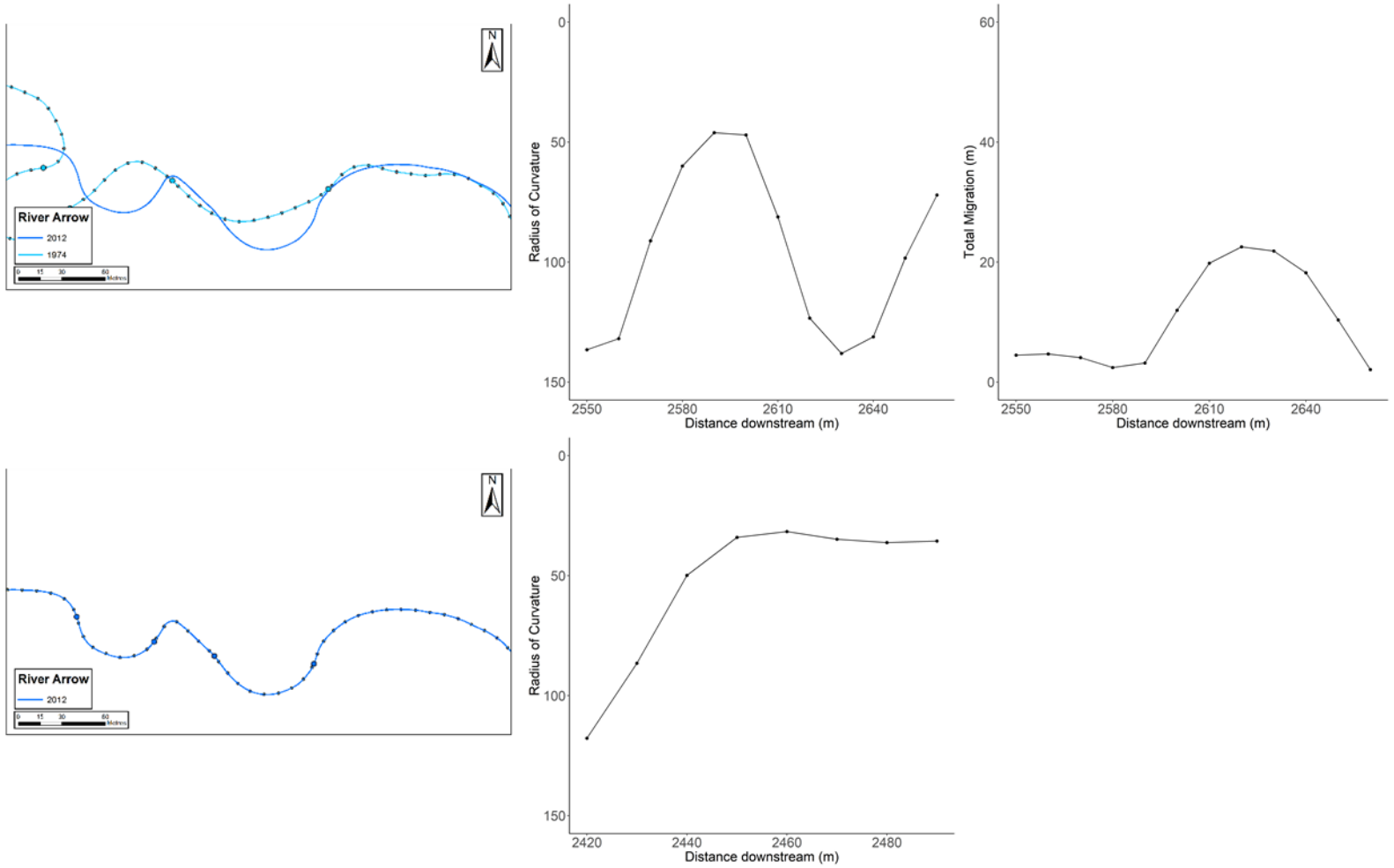

Figure 5.45. Changes to the curvature profile for Bend 26, Reach 1, River Arrow, between 1974 and 2012

River Arrow, Reach 1, Bend 34 (Figure 5.46 to Figure 5.48)

Bend 34 is one of the most active bends throughout the entire study period, constantly changing its planform and shape in each period. The bend started in 1886 as a simple asymmetrical bend with an upstream skew. There was a high amount of erosion on the upstream bend between 1886 and 1904, which produced a very sharp apex on the upstream limb and a secondary apex at the end of the bend. The bend became compound asymmetric, with a similar bend form to bend M. During the period 1904 to 1928 most of the erosion was concentrated just downstream of the apex creating a very long apex with constant radius of curvature, which was further exaggerated by erosion on the preceding bend upstream. A cutoff occurred between 1928 and 1964 that created a simple symmetric bend and removed the upstream asymmetrical part of the bend. The bend had become similar to bend type F. The bend then evolved to two simple symmetric bends and one compound symmetric bend between 1964 and 1974, with most of the erosion occurring on the apex of the bend, also with the straight section leading into the bend imitating new meanders. The separate bends continue to develop between 1974 and 2012, with the third compound symmetrical bend migrating downstream and becoming a simple symmetrical bend.

Date	Brice Classification
1886	K
1904	M
1928	M
1964	F
1974	C-C-H
2012	C-A-E

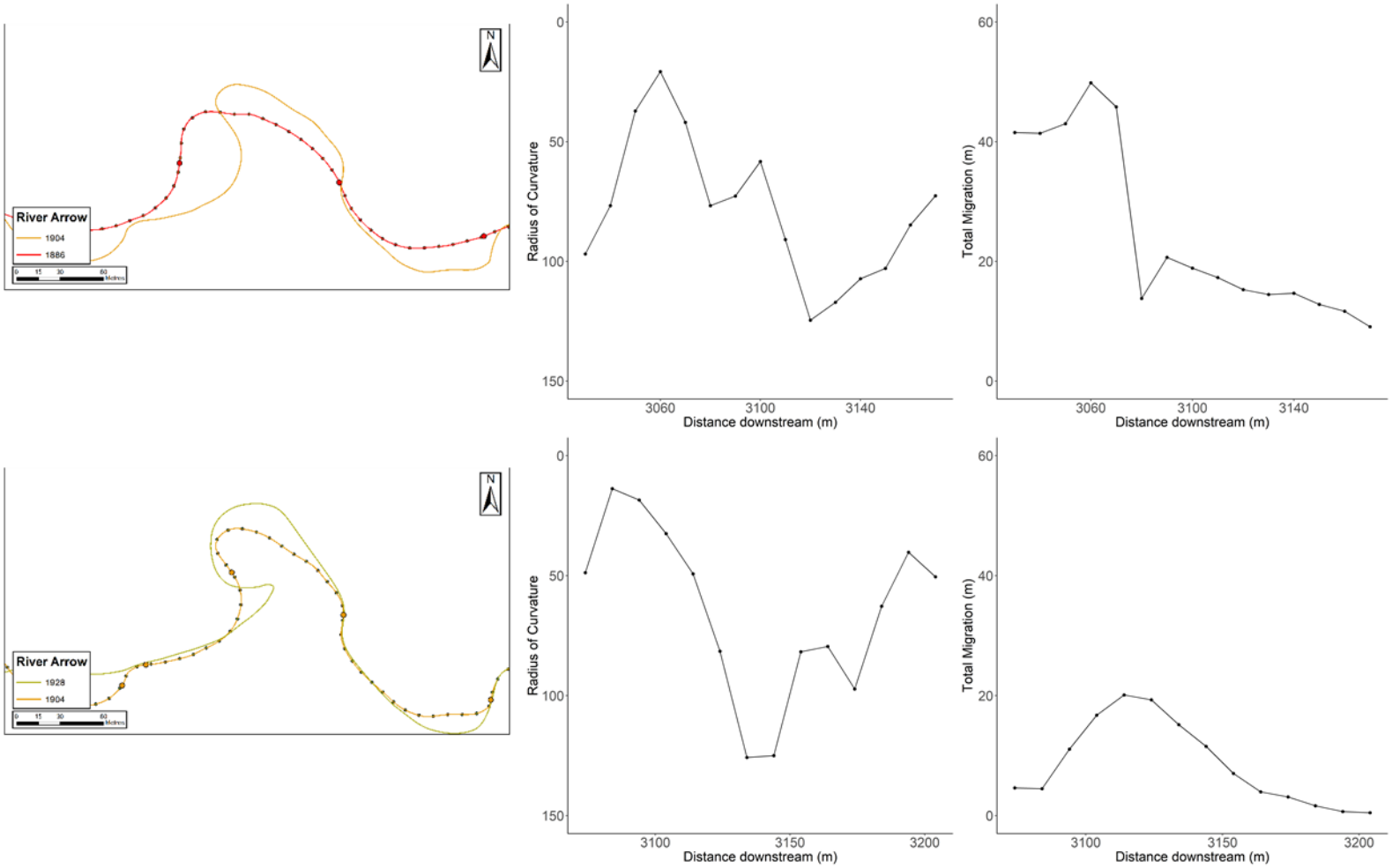

Figure 5.46. Changes to the curvature profile, Bend 34, Reach 1, River Arrow, between 1886 and 1928

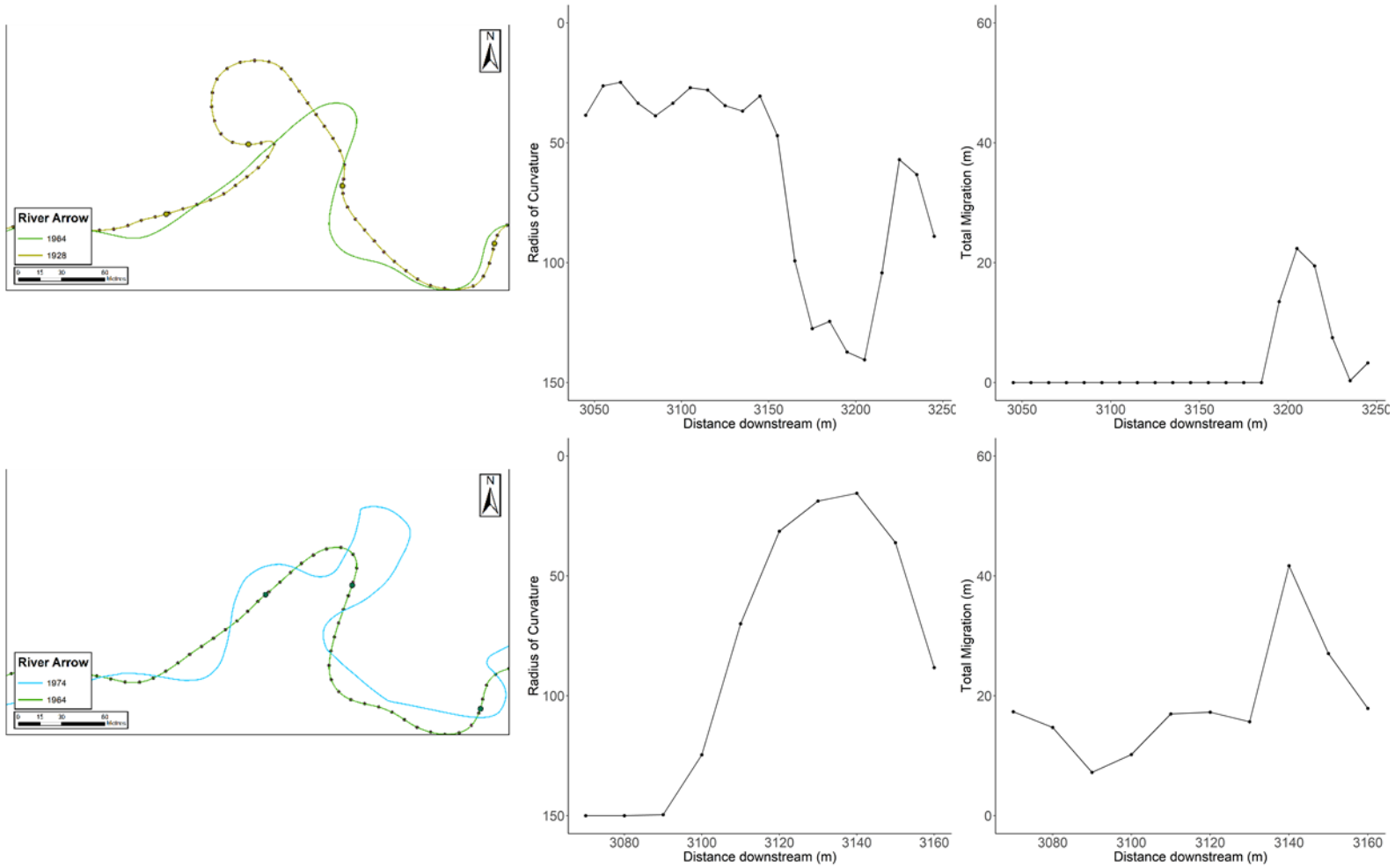

Figure 5.47. Changes to the curvature profile for Bend 34, Reach 1, River Arrow between 1928 and 1974

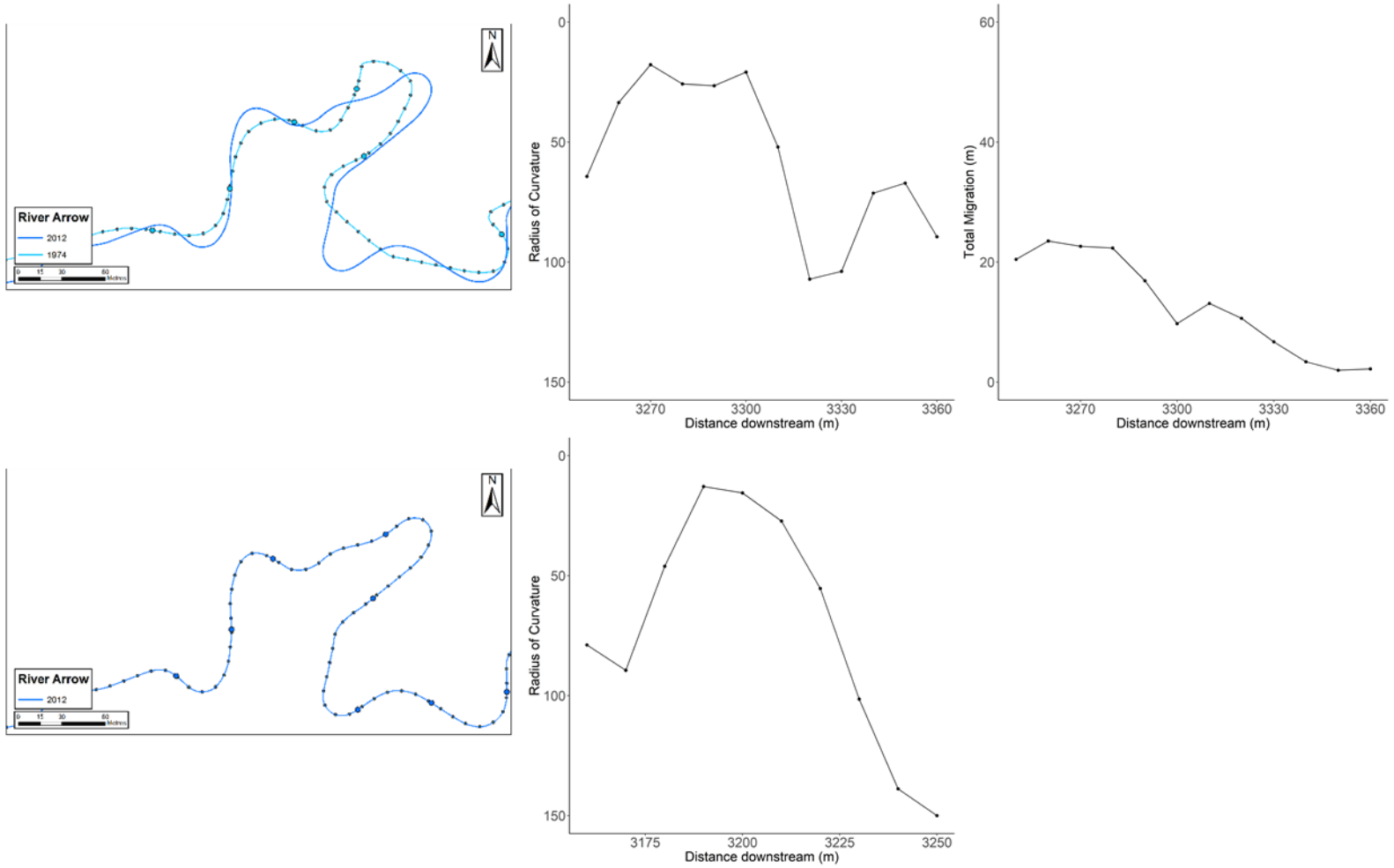

Figure 5.48. Changes to the curvature profile for Bend 34, Reach 1, River Arrow, betwen 1974 and 2012

River Arrow, Reach 2, Bend 23 (Figure 5.49 to Figure 5.51)

Bend 23 started in 1886 as a simple asymmetrical bend. There is a second apex at the start of the bend, but this is truncated by the preceding bend. The bend is stable between 1886 and 1928 with very little movement or change to the overall shape of the bend. The bend in 1904 appears sensitive to the position of the inflection point, which explains why the radius of curvature does not decrease as seen in 1886 and 1928. The apex of the bend became longer between 1928 and 1964, and there were high amounts of erosion downstream of the apex. By 1974, the bend had developed to a compound asymmetrical form, with a tighter and longer apex found on the downstream side of the river bend. Erosion downstream of the apex again caused three separate apices to form by 2012, with each peak in the radius of curvature having a similar minimum and shape. The Brice classification bend that best represents this bend is bend type J.

Date	**Brice Classification**
1886	K
1904	K
1928	K
1964	D
1971	N
2012	J

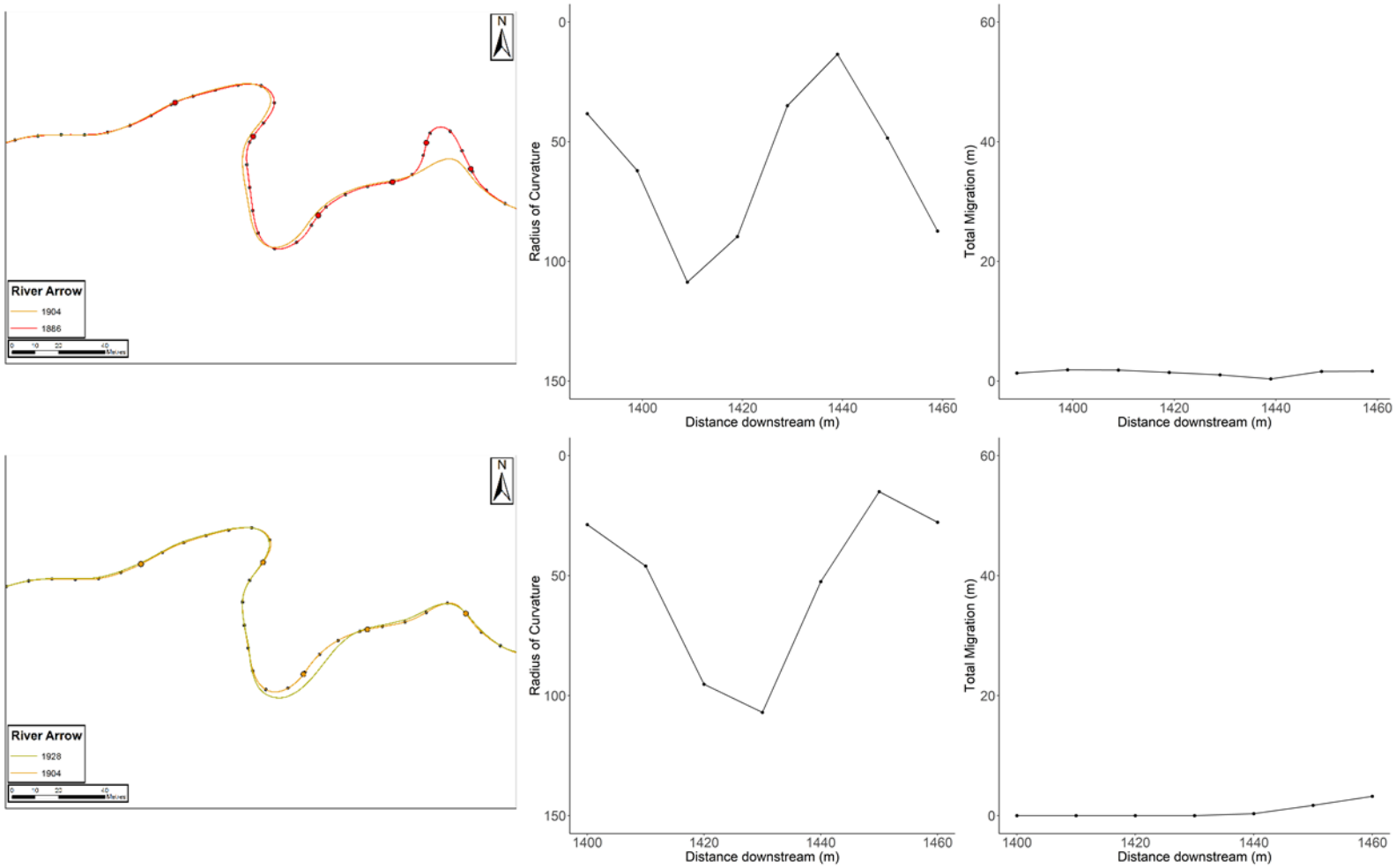

Figure 5.49. Changes to the curvature profile of Bend 23, Reach 2, River Arrow

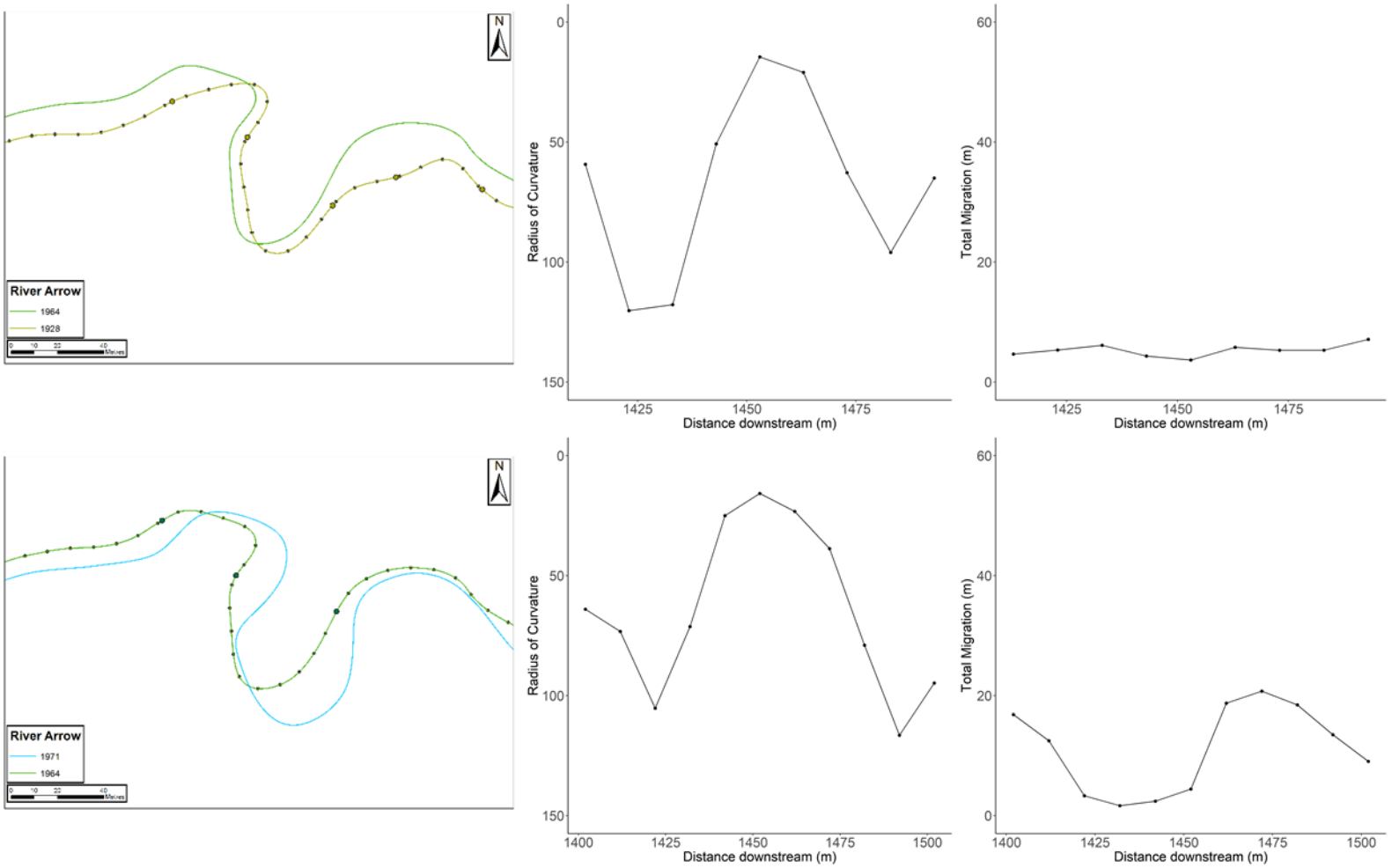

Figure 5.50. Changes to the curvature profile of Bend 23, Reach 2, River Arrow

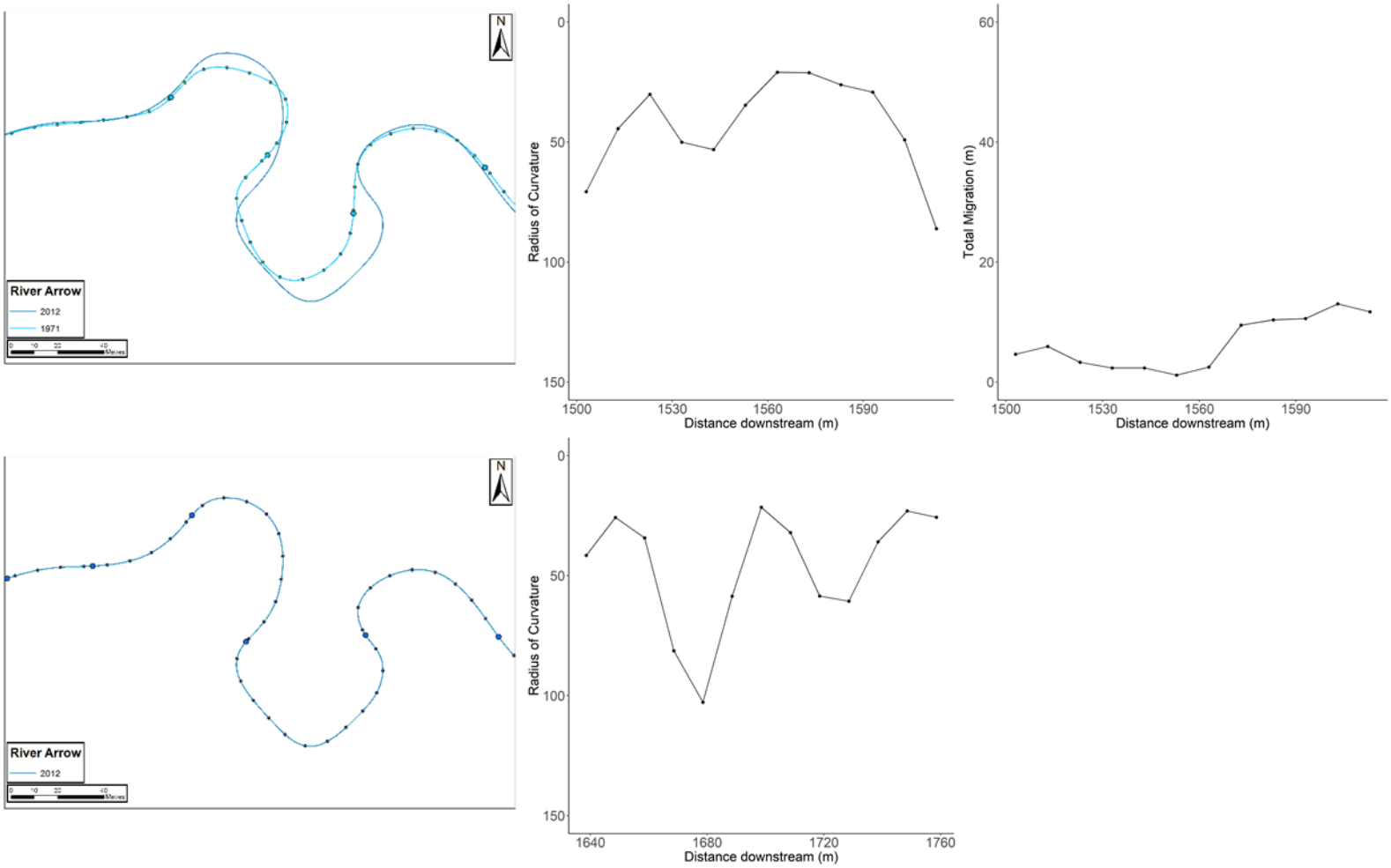

Figure 5.51. Changes to the curvature profile of Bend 23, Reach 2, River Arrow

River Arrow, Reach 2, Bend 29 (Figure 5.52 to Figure 5.54)

Bend 29 started as a simple symmetrical bend, with low amounts of erosion occurring between 1886 and 1928. The shape of the curvature profile changes between 1886 and 1928, but this is mainly due to sensitivity with the location of the inflection points. The shape of the bend around the apex does not change with at least three points with a low radius of curvature. The bend is most similar to bend type D in the Brice classification. The bend appeared to retract between 1928 and 1964 while maintaining a consistent shape. This change was potentially caused by an error in the map data for the 1964 period. This means that the amount of movement measured for the bend is probably an over estimation, but the measurement of the actual shape of the bend is correct. The bend tightened between 1964 and 1971 and started to migrate downstream. The bend developed to bend type E or G during this period. Between 1971 and 2012, there was further migration on the downstream side of the bend, while the upstream side remained stable. The bend started to show signs of becoming compound in 2012 with two possible minima in the radius of curvature.

Date	**Brice Classification**
1886	D
1904	D
1928	D
1964	D
1971	E/G
2012	E/G

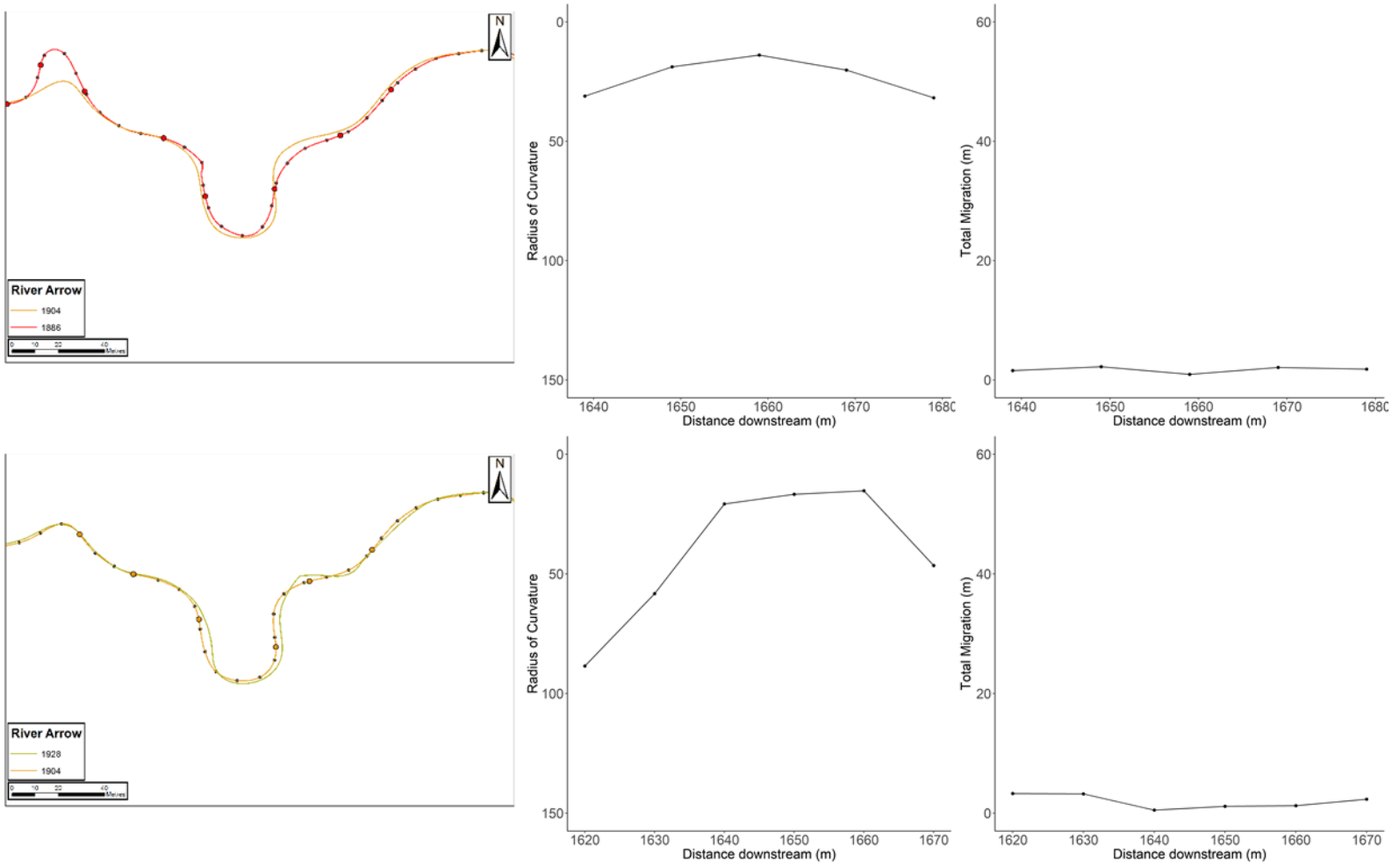

Figure 5.52. Changes to the curvature profile of Bend 29, Reach 2, River Arrow

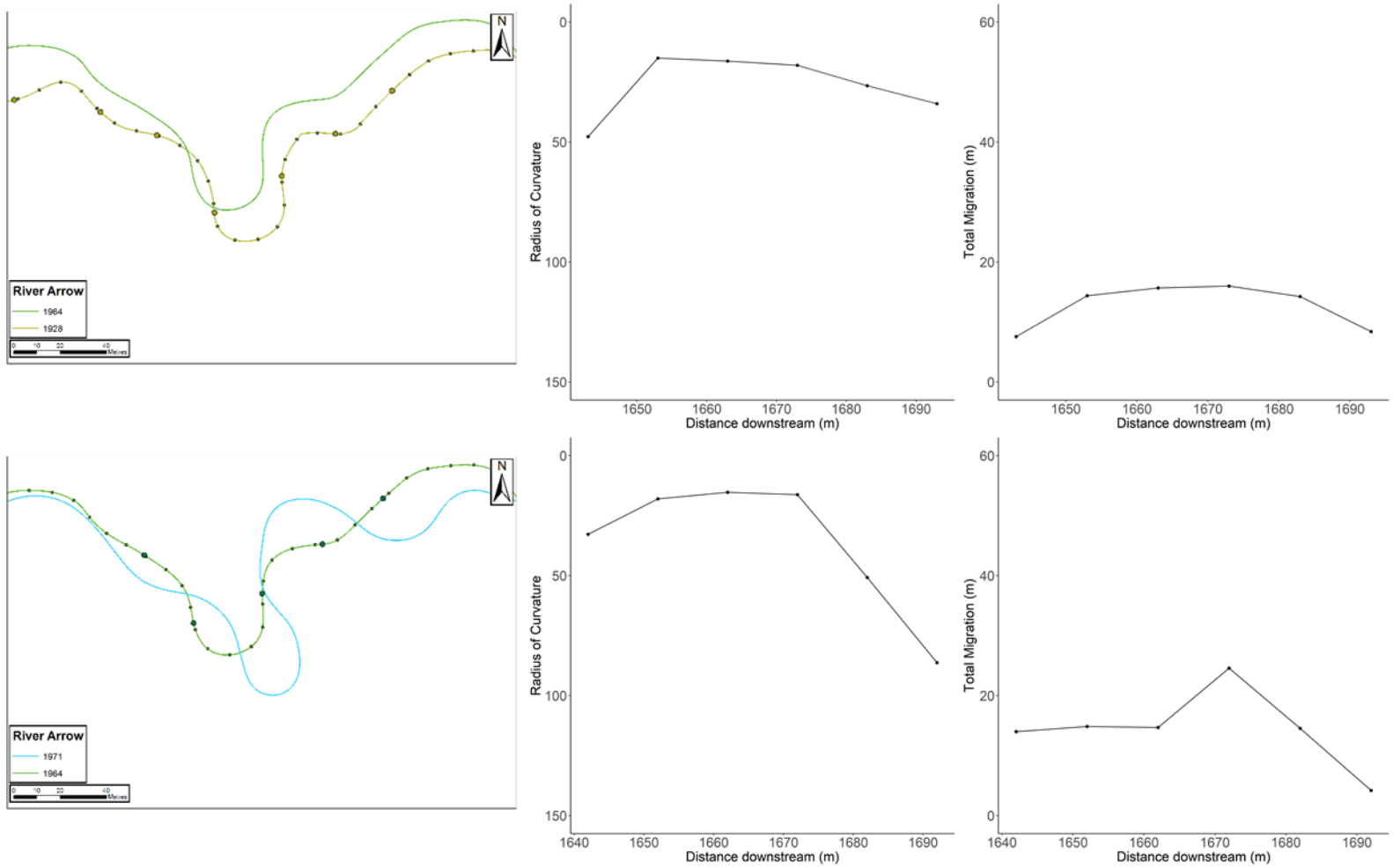

Figure 5.53. Changes to the curvature profile of Bend 29, Reach 2, River Arrow

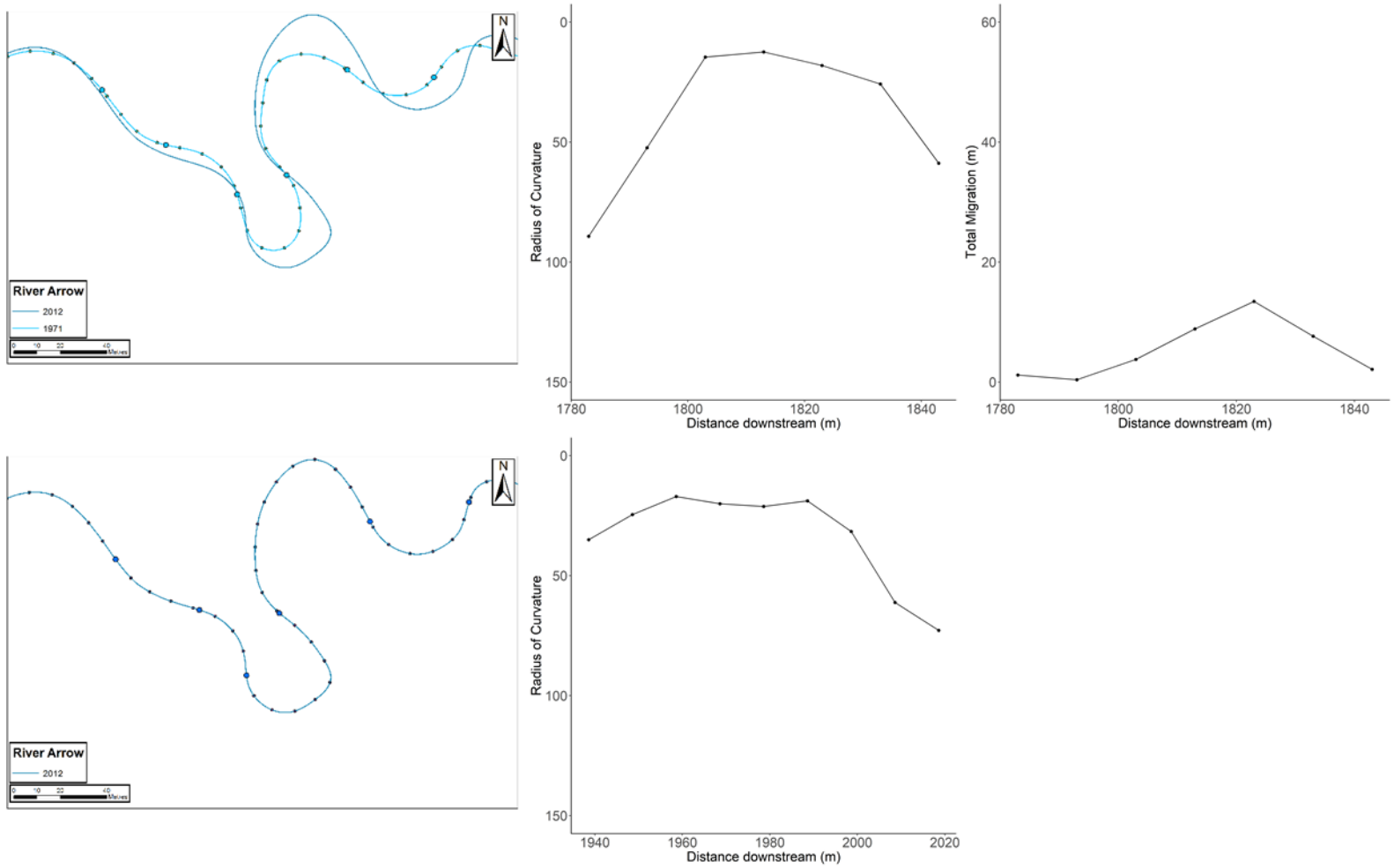

Figure 5.54. Changes to the curvature profile of Bend 29, Reach 2, River Arrow

River Arrow, Reach 2, Bend 30 (Figure 5.55 to Figure 5.57)

Bend 30 started as a short simple symmetrical bend, similar to type A or B in the Brice classification. The bend was stable between 1886 and 1904. Although the erosion rate was low between 1904 and 1928, the bend became tighter as the inflection points migrated downstream. The bend apparently migrated across the floodplain between 1928 and 1964, but the amount of movement is probably overestimated again due to the error in the mapping for this particular period. The overall radius of curvature for the bend appeared to become higher between the two dates as well. The length of the bend increased between 1964 and 1971, from four links to nine links and it was possible to identify two minima in the radius of curvature. Most of the erosion occurred downstream of the apex for the bend. The bend was a compound asymmetrical bend in 1971, similar to bend N in the Brice classification. The bend continued to migrate downstream, with the erosion mainly occurring downstream of the second, tighter apex. The bend developed two separate apices, with the first apex near the start of the bend having a large radius of curvature compared to the second apex, giving the bend a downstream skew.

Date	Brice Classification
1886	A/B
1904	A/B
1928	A/B
1964	B
1971	N
2012	N

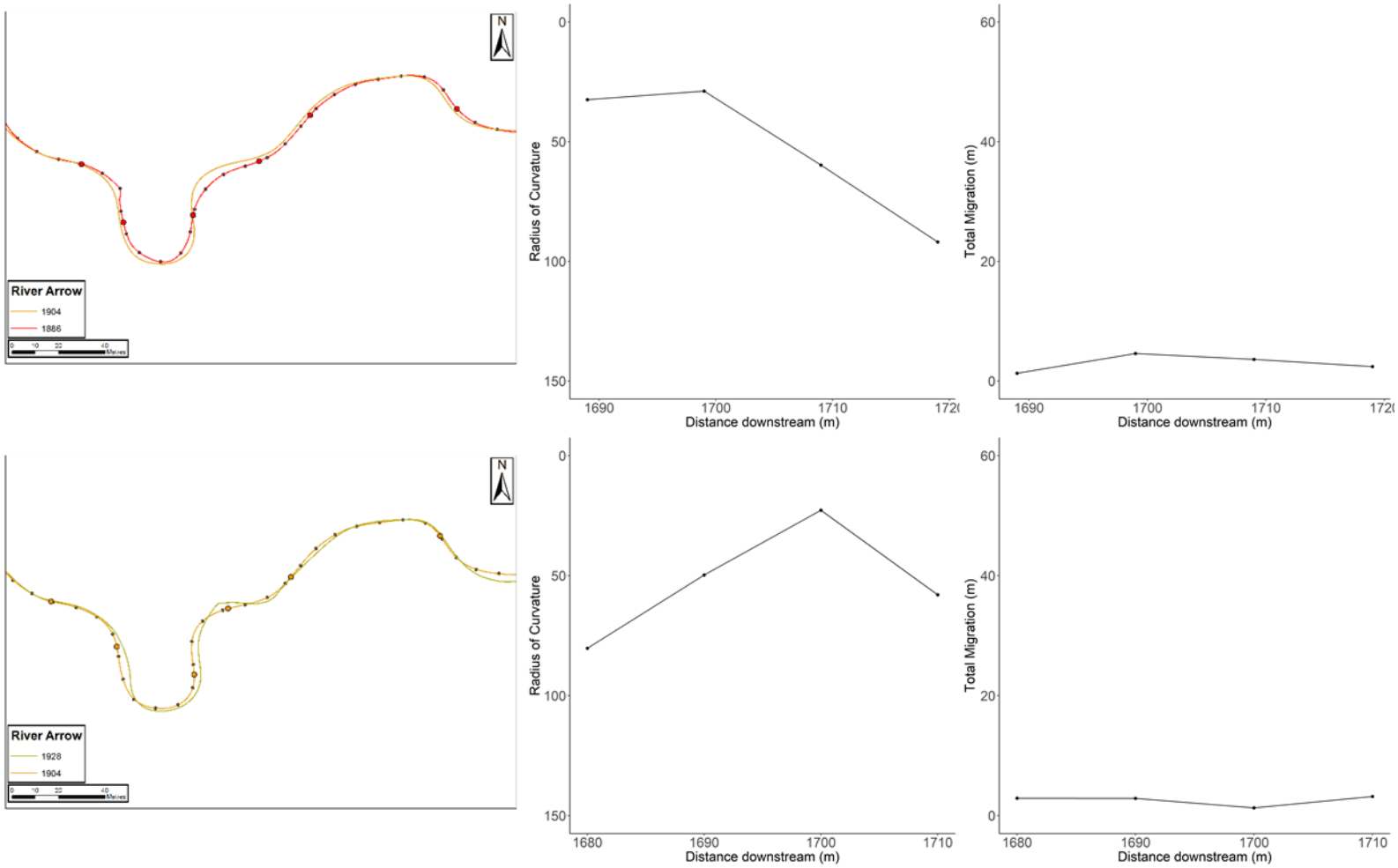

Figure 5.55. Changes to the curvature profile of Bend 30, Reach 2, River Arrow

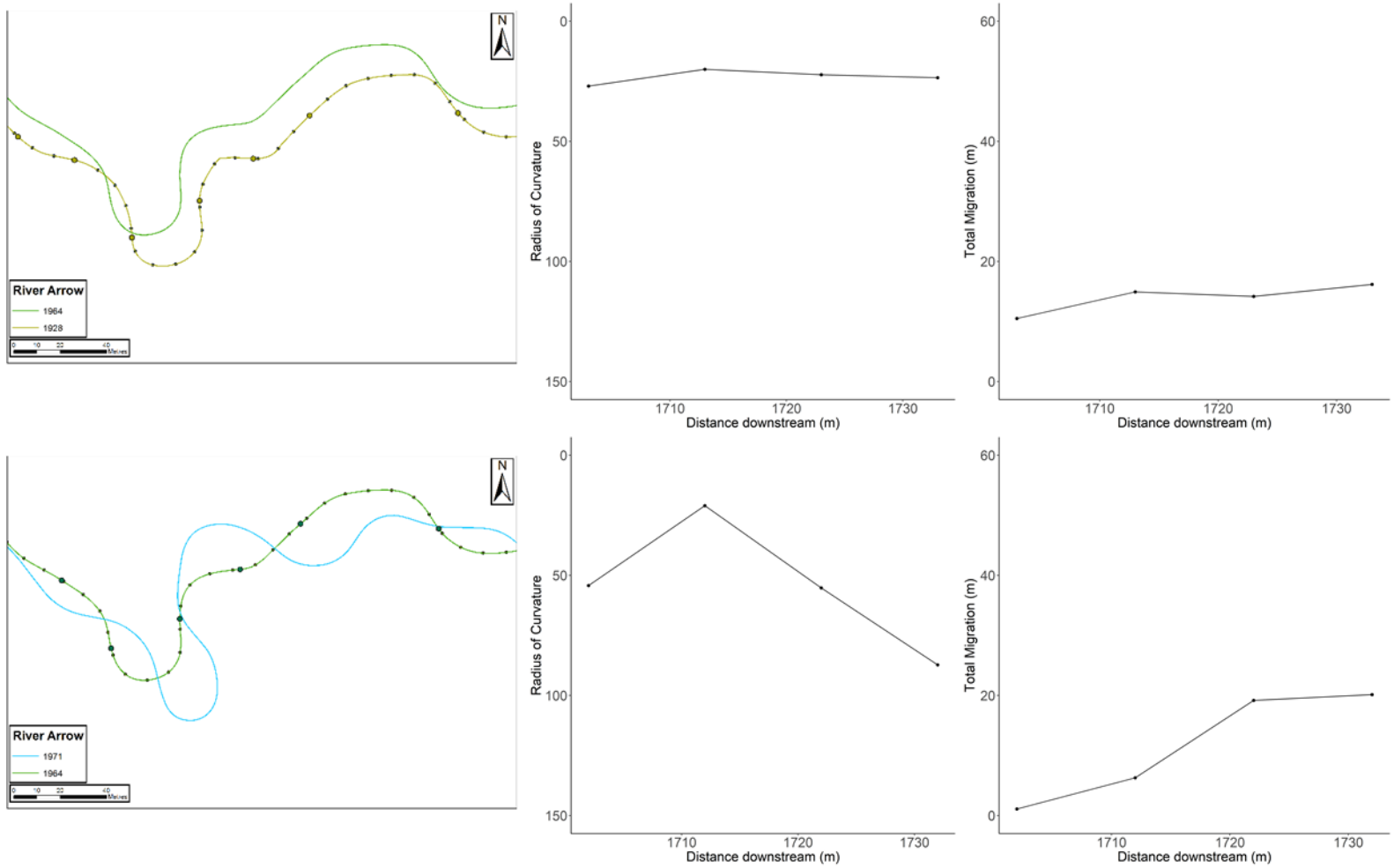

Figure 5.56. Changes to the curvature profile of Bend 30, Reach 2, River Arrow

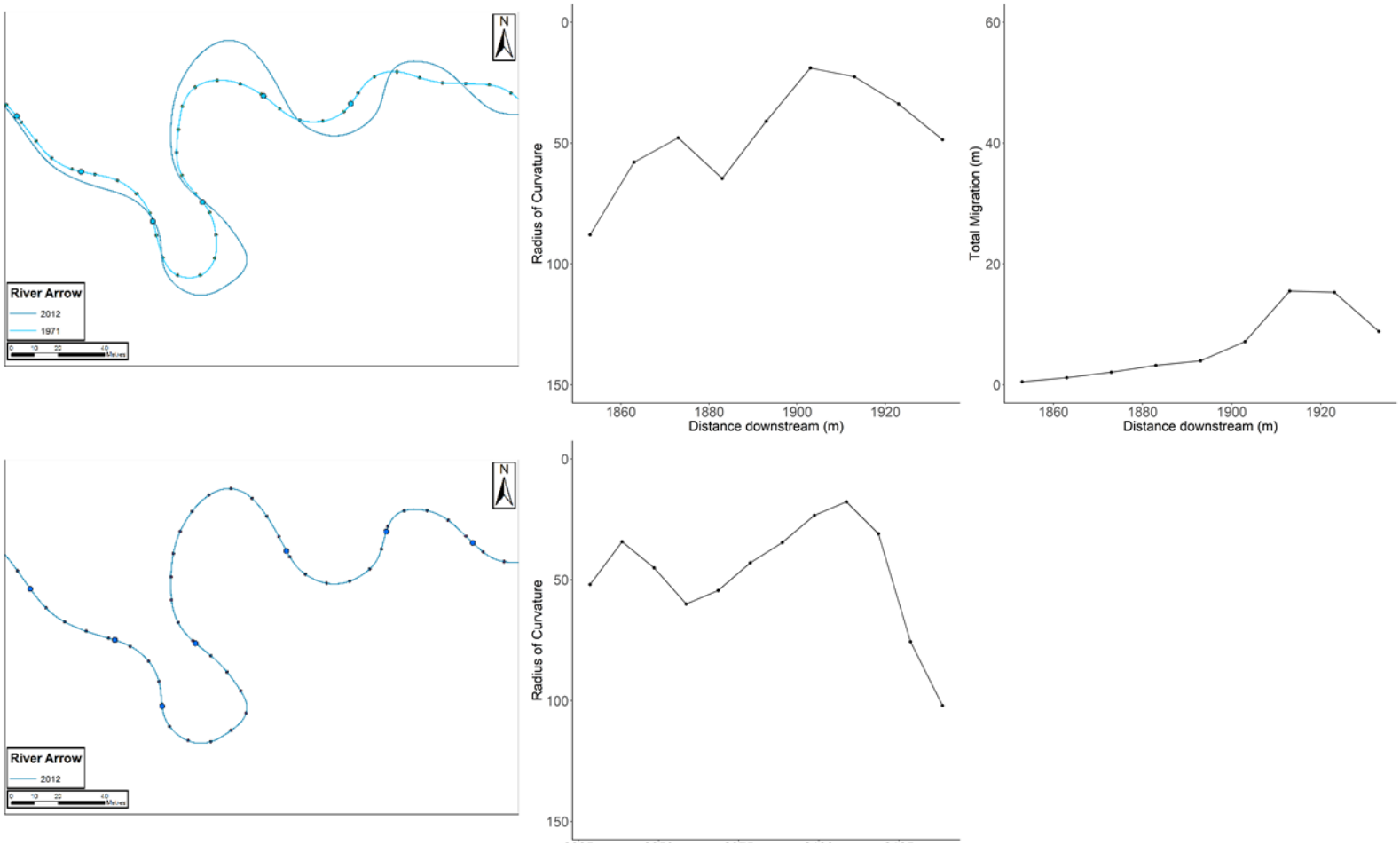

Figure 5.57. Changes to the curvature profile of Bend 30, Reach 2, River Arrow

River Arrow, Reach 3, Bend 27 (Figure 5.58 to Figure 5.60)

Bend 27 was a well-developed simple symmetrical bend in 1886, with a constant radius of curvature around the apex of the bend. The bend could be described as either bend D or bend E from the Brice classification. The erosion rate is low between 1886 and 1964, with the bend remaining stable throughout this whole period. There is little change to the overall curvature profile of the bend. The bend started to migrate between 1964 and 1971, with most of the erosion occurring at the downstream end of the bend. The bend subsequently became compound in 1971, with two distinctive apices formed. The upstream apex was longer and had a slightly lower minimum radius of curvature. Between 1971 and 2012, erosion was concentrated on this upstream side of the bend, with lower erosion occurring on the downstream side. The bend continued to develop two distinctive apices and formed a bend similar to type O in the Brice classification. The upstream apex remained longer, although the minimum radius of curvature for the two apices was similar.

Date	**Brice Classification**
1886	D/E
1904	D/E
1928	D/E
1964	D/E
1971	O
2012	O

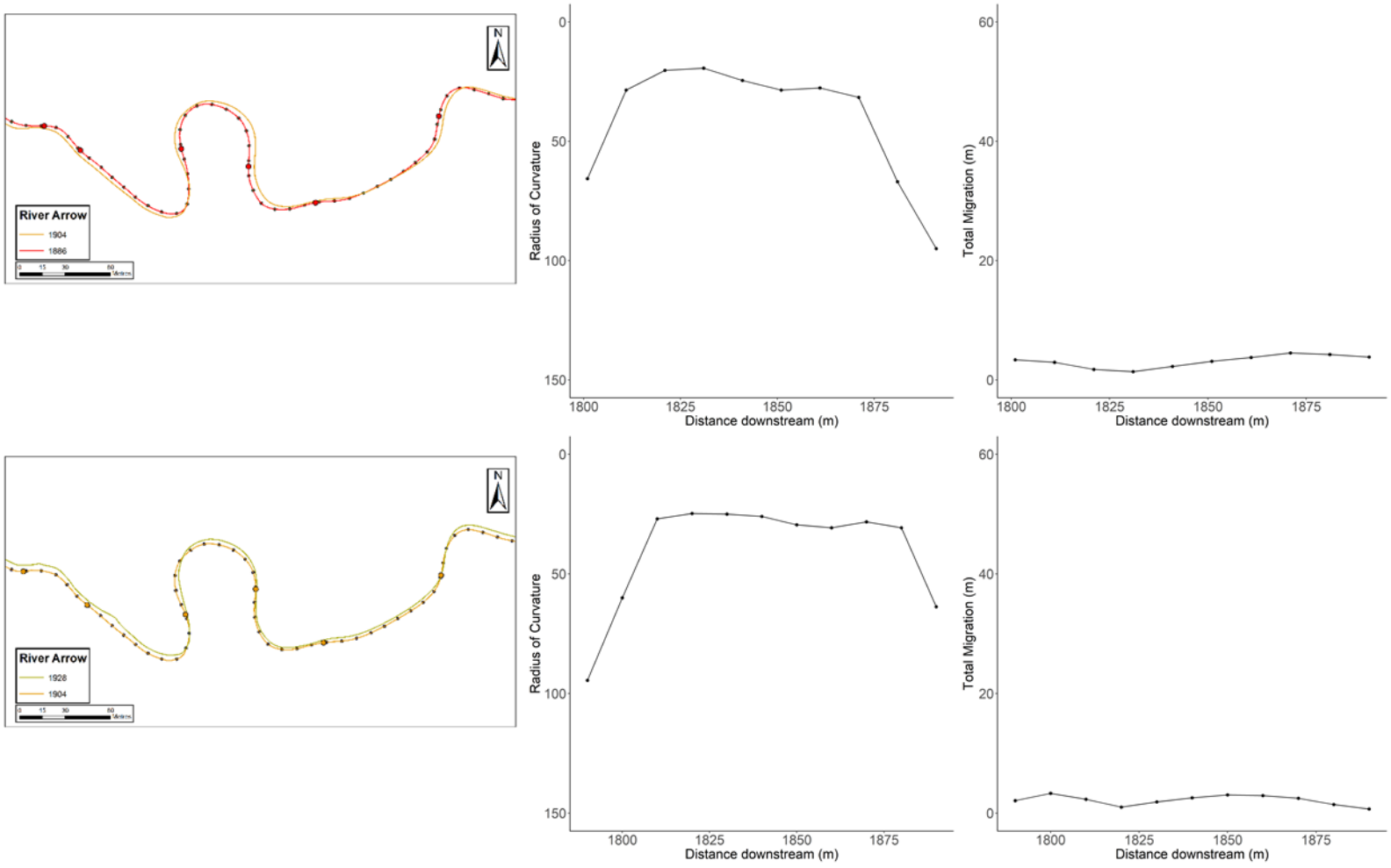

Figure 5.58. Changes to the curvature profile of Bend 27, Reach 3, River Arrow

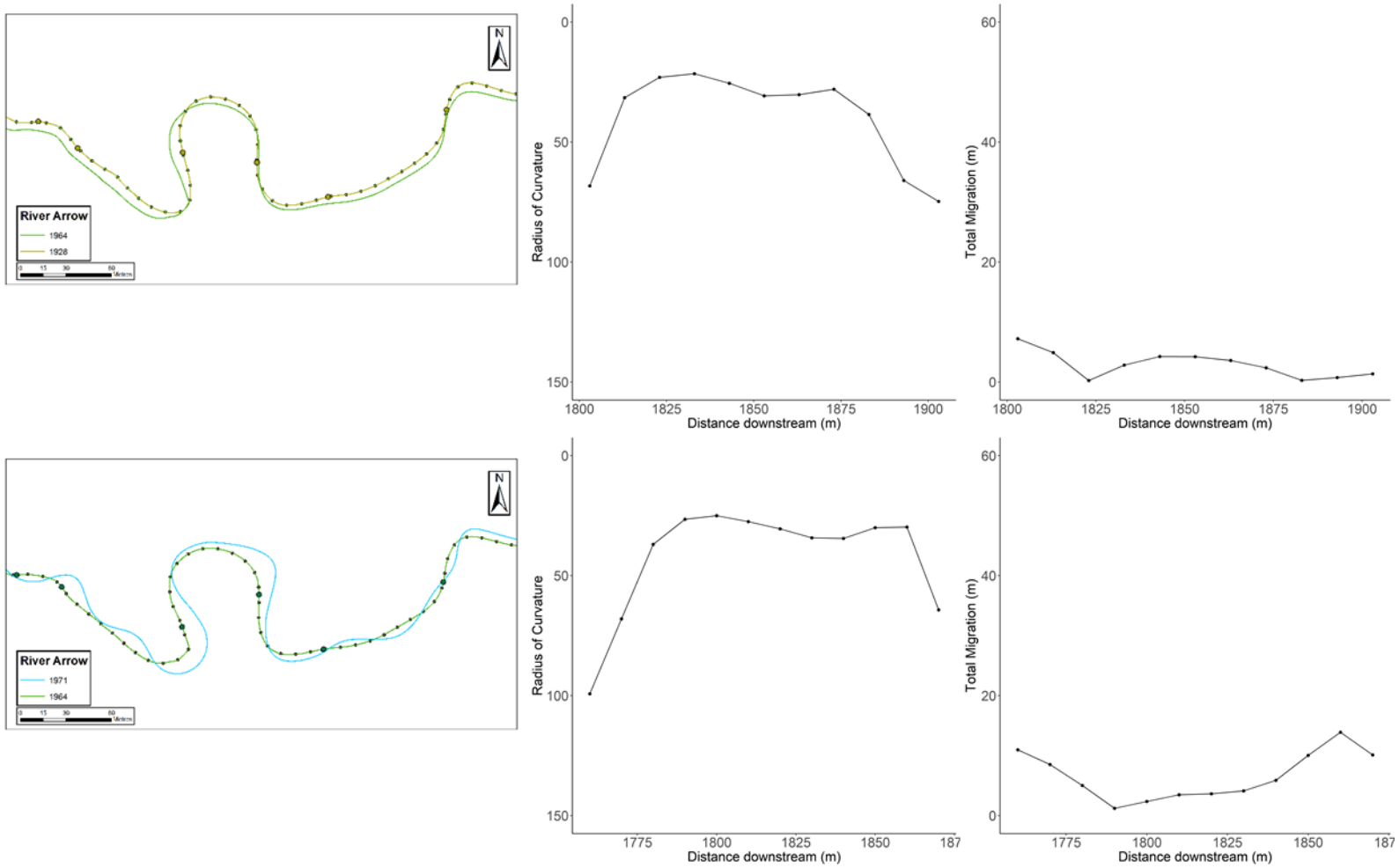

Figure 5.59, Changes to the curvature profile of Bend 27, Reach 3, River Arrow

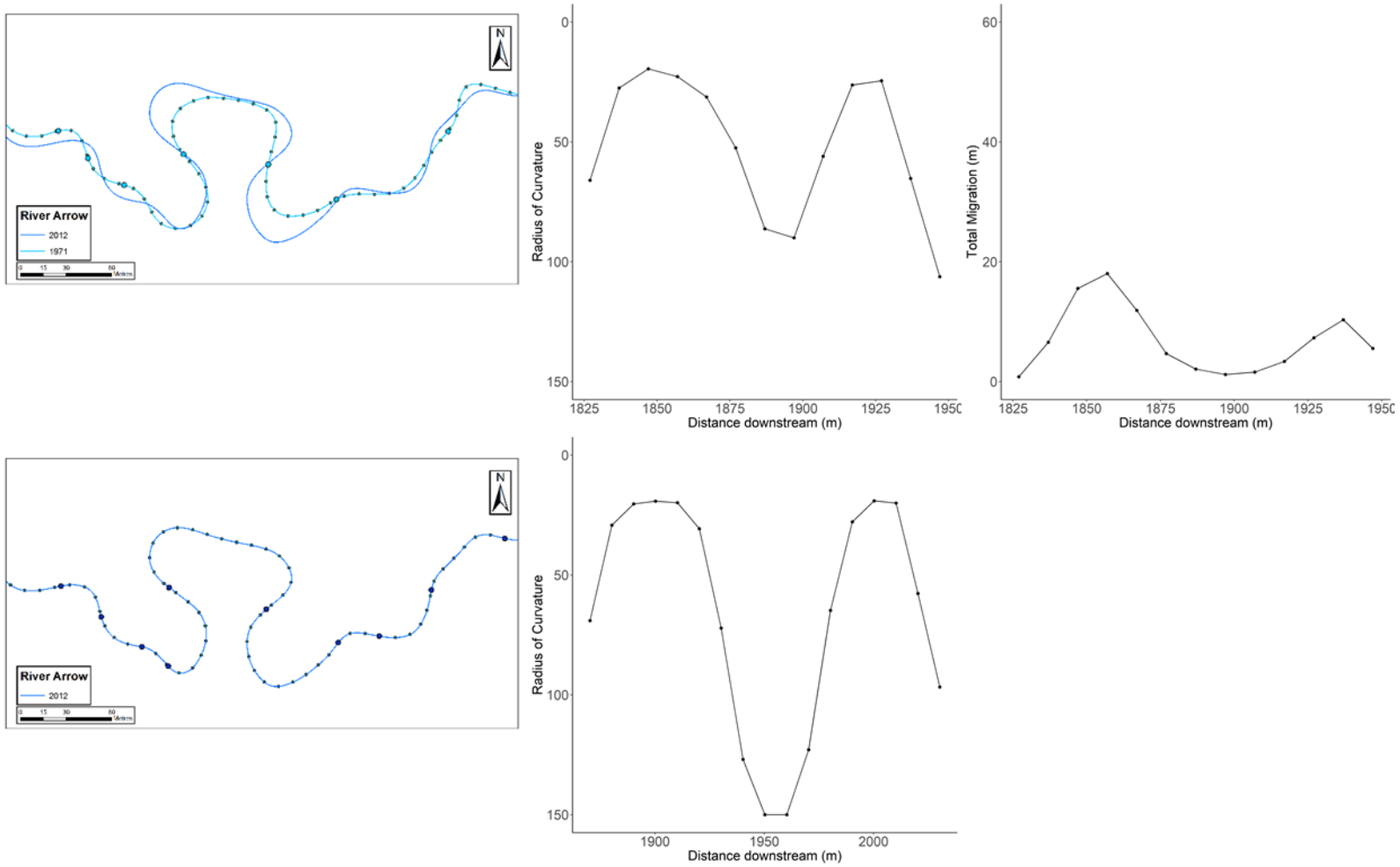

Figure 5.60. Changes to the curvature profile of Bend 27, Reach 3, River Arrow

River Lugg, Reach 1, Bend 4 (Figure 5.61 to Figure 5.63)

The bend starts as a simple symmetrical bend with a low radius of curvature. The bend type is similar to bend type D in the Brice classification. The bend is essentially stable between 1889 and 1963, with small amounts of erosion occurring just downstream of the apex. There was a sudden acceleration in the amount of migration between 1963 and 1975 as the bend grew across the floodplain and became tighter at the apex and the bend transitioned from a simple symmetrical to a compound asymmetrical bend. The bend type was then similar to type N in the Brice classification. There was some erosion on the upstream side of the bend and just downstream of the main apex between 1975 and 2012.

Date	Brice Classification
1886	D
1903	D
1928	D
1963	D
1975	N
2012	N

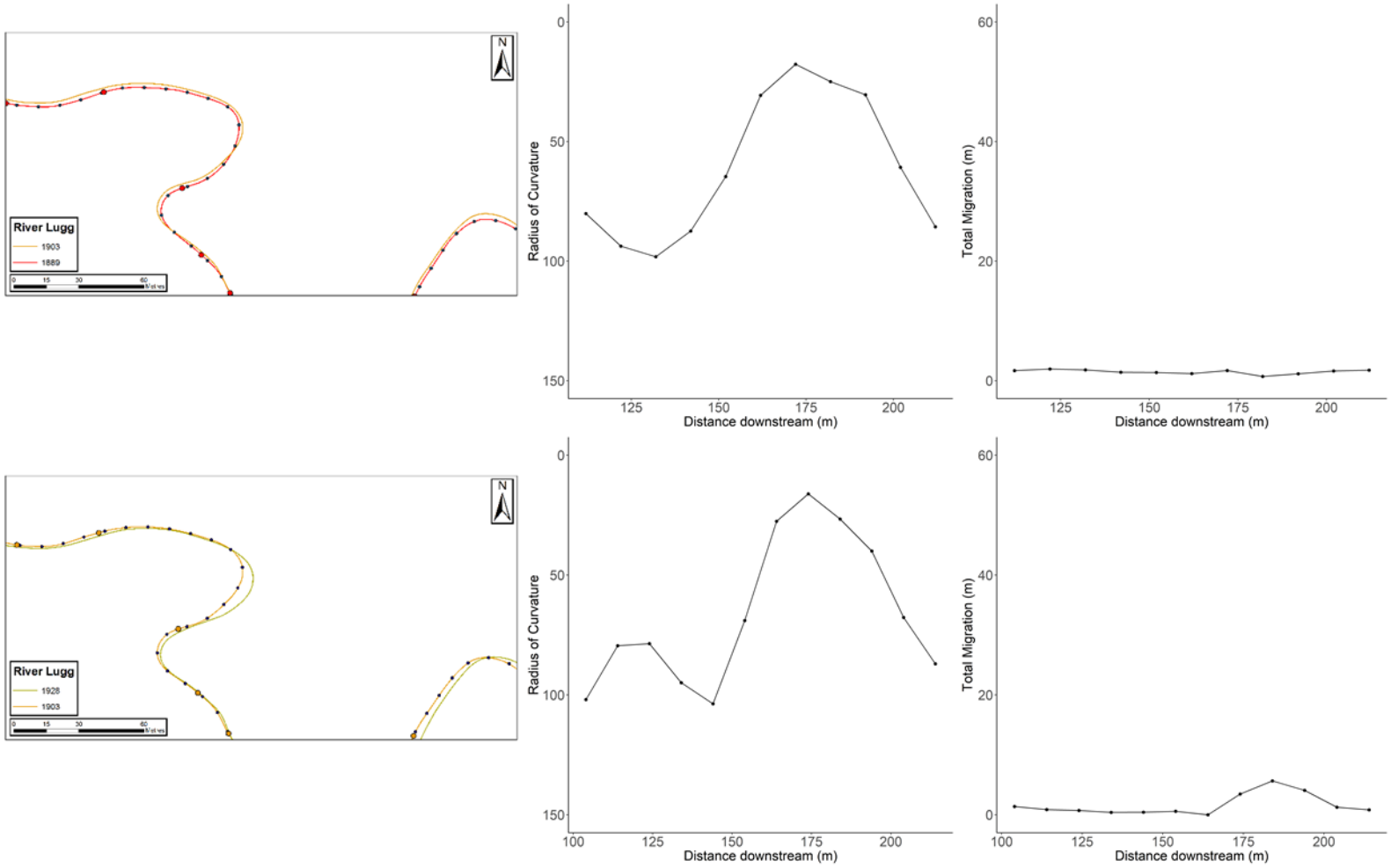

Figure 5.61. Changes to the curvature profile for Bend 4, Reach 1, River Lugg

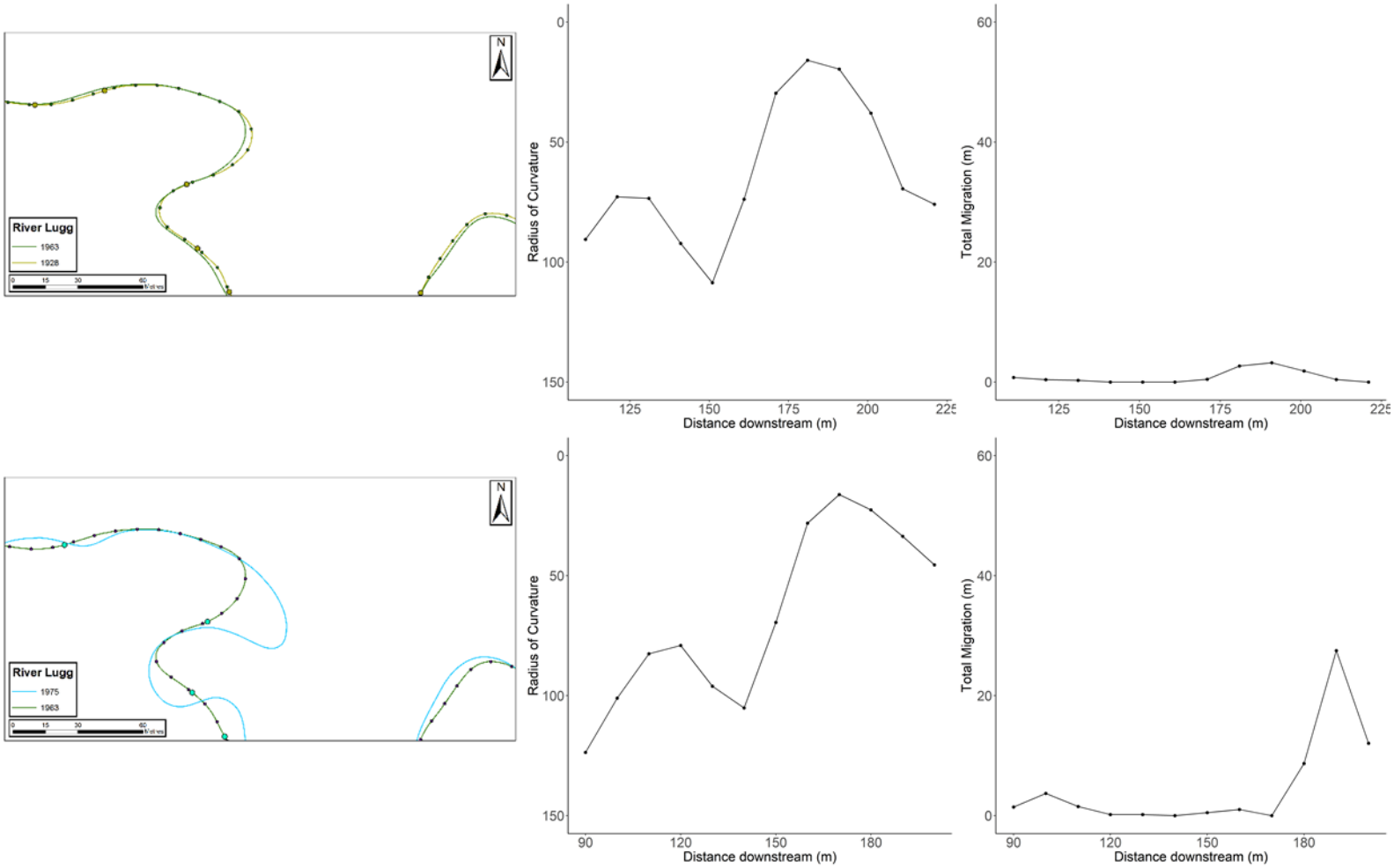

Figure 5.62. Changes to the curvature profile for Bend 4, Reach 1, River Lugg

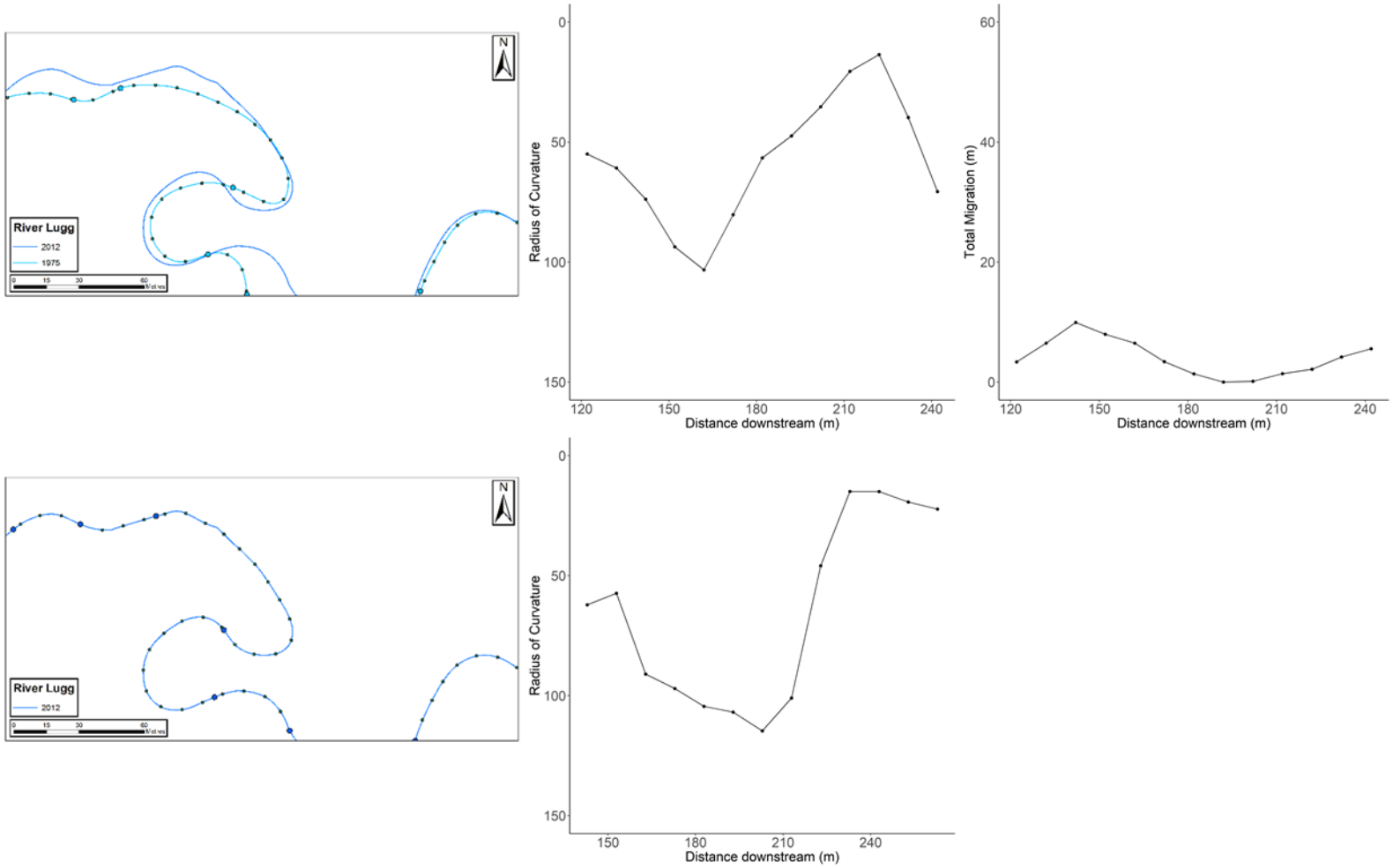

Figure 5.63. Changes to the curvature profile for Bend 4, Reach 1, River Lugg

River Lugg, Reach 1, Bend 5 (Figure 5.64 to Figure 5.66)

Bend 5 started as a simple symmetrical bend in 1889 with a low minimum radius of curvature value. The bend is stable between 1889 and 1963 with the shape remaining constant and very little erosion occurring at any point on the bend. Erosion did occur between 1963 and 1975 and was concentrated downstream of the apex. The curvature profile changed as well, from having one single point as the minimum radius of curvature to having multiple consecutive points with a similar low radius of curvature. The bend was on the boundary between simple symmetrical and compound asymmetrical due to the slight downstream skew in the curvature values. The bend continues to grow slowly between 1975 and 2012 with erosion occurring at almost every point along the bend. The bend has started to produce a compound shape, similar to bend I from the Brice classification, although the radius of curvature is fairly constant throughout the whole bend, with only a small increase between the two apices.

Date	Brice Classification
1886	C
1903	C
1928	C
1963	C
1975	E
2012	I

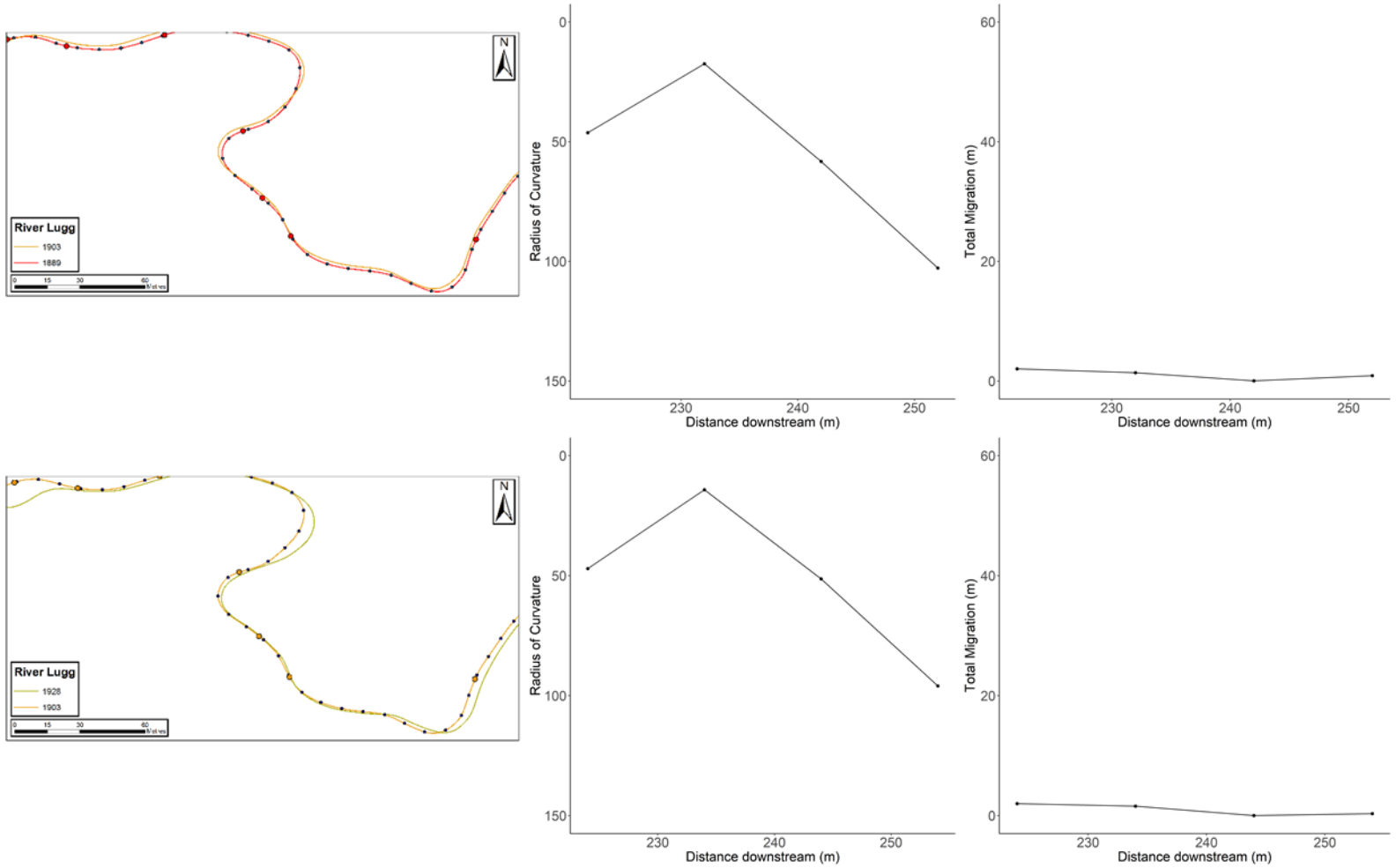

Figure 5.64. Changes to the curvature profile of Bend 5, Reach 1, River Lugg

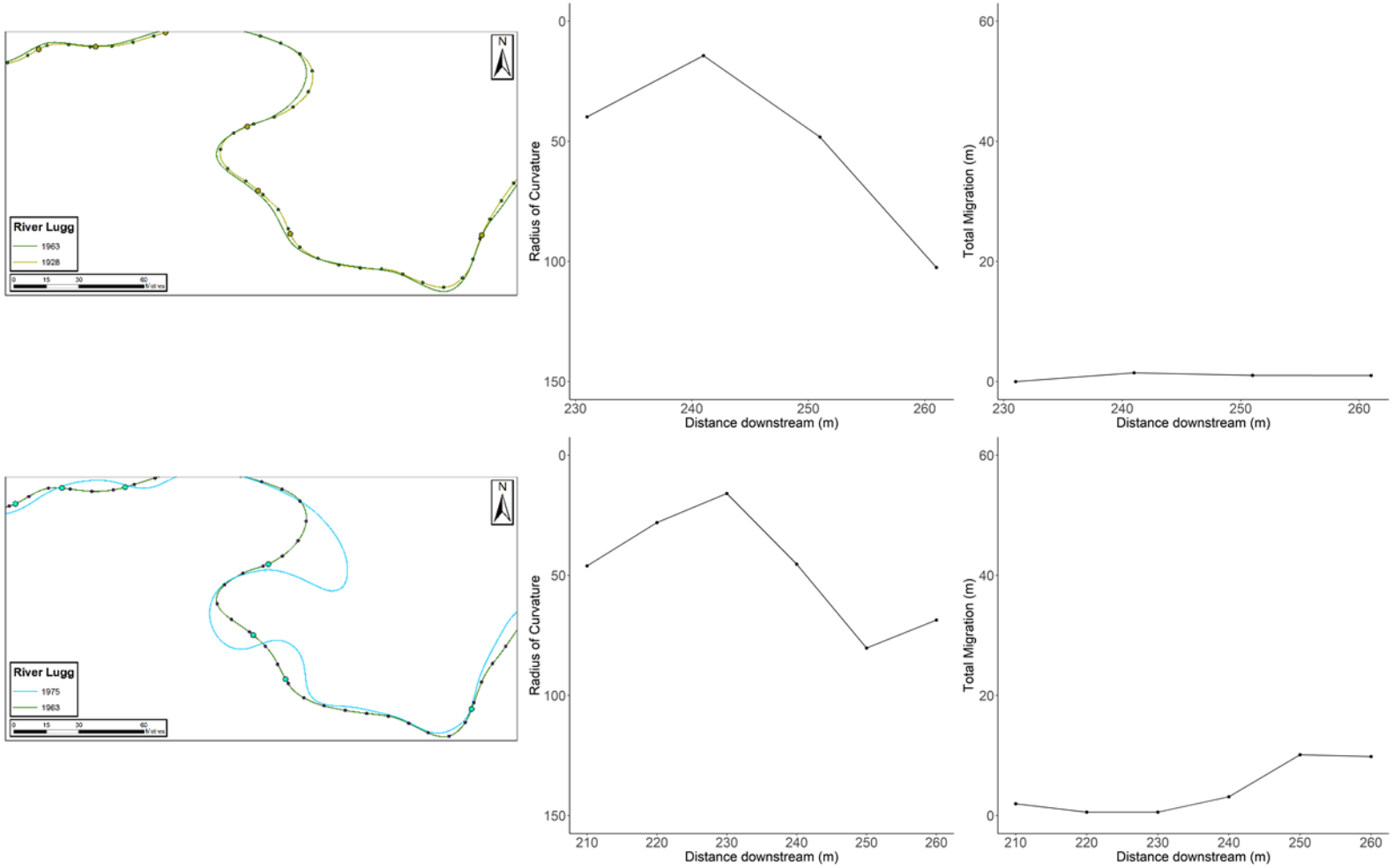

Figure 5.65. Changes to the curvature profile of Bend 5, Reach 1, River Lugg

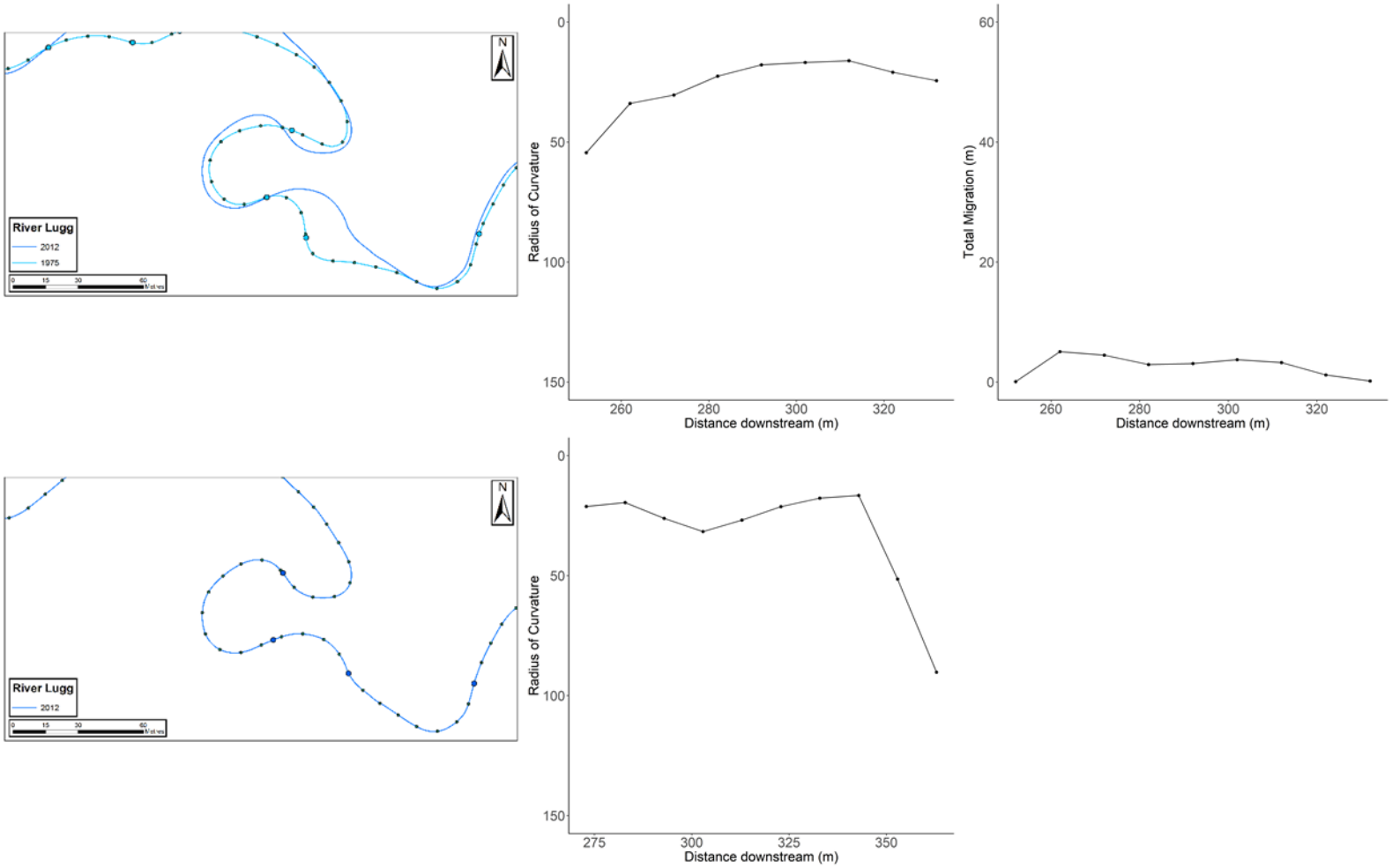

Figure 5.66. Changes to the curvature profile of Bend 5, Reach 1, River Lugg

River Lugg, Reach 2, Bend 10 (Figure 5.67 to Figure 5.69)

Bend 10 was a simple symmetrical bend in 1886 with a consistent low radius of curvature throughout, similar to bend type E in the Brice classification. There was erosion on most points between 1886 and 1903, and the bend developed two apices although the second apex had less points and a higher radius of curvature. The bend was stable between 1903 and 1928, with little change to the shape of the bend and low amounts of erosion. There was further growth at the apex of the bend between 1928 and 1963, with the main apex becoming tighter and overall bend shape becoming more elongated. The bend is most like bend type G from the Brice classification, although there is some asymmetry in the bend form. The bend subsequently cutoff between 1963 and 1976, leaving a short simple symmetric bend. There were high amounts of erosion between 1976 and 2012, which produced a much longer simple symmetric bend, similar to type D. The bend had a constant radius of curvature around the apex of the bend.

Date	**Brice Classification**
1886	E
1903	E
1928	E
1963	G
1976	B
2012	D

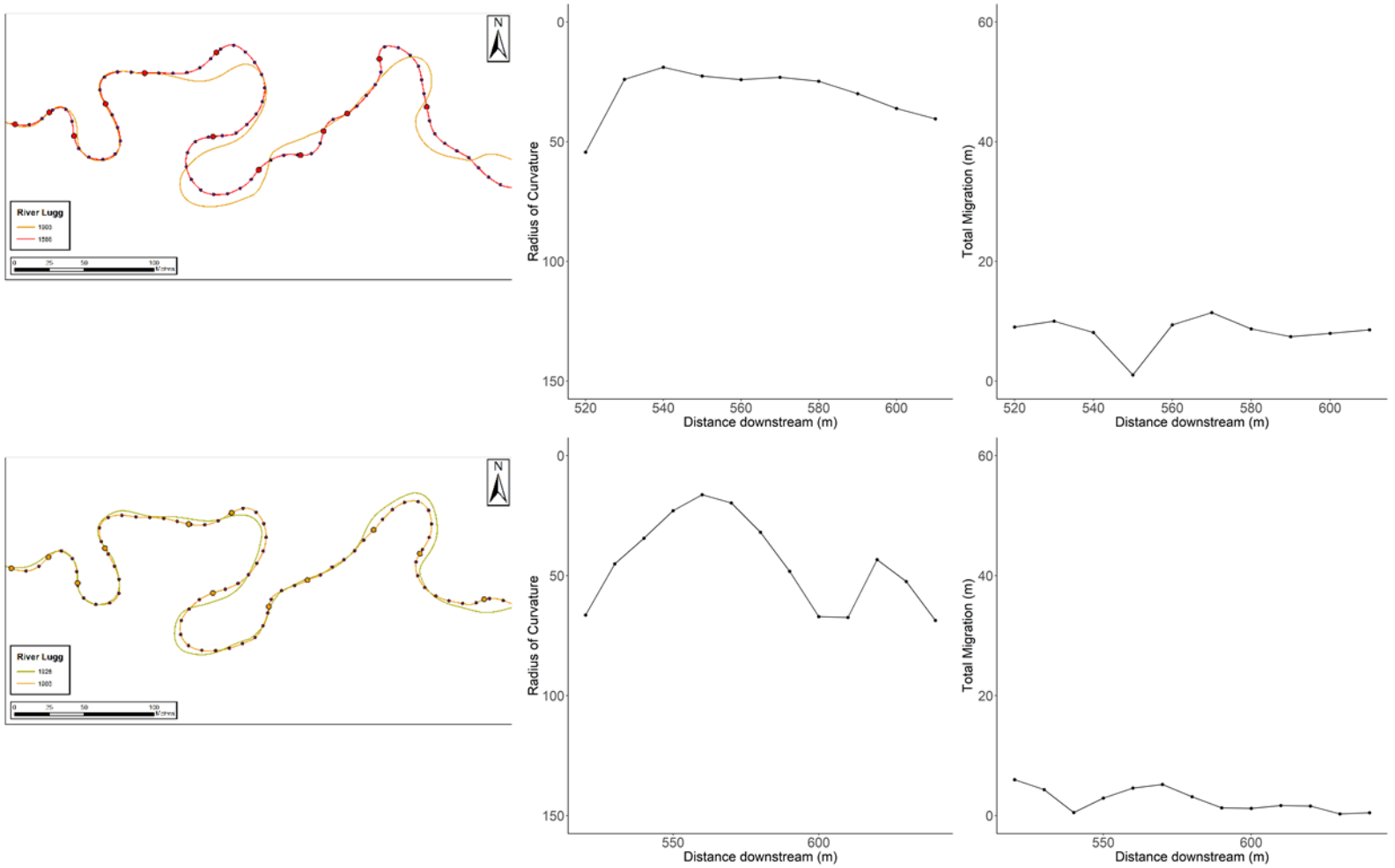

Figure 5.67. Changes to the curvature profile of Bend 10, Reach 2, River Lugg

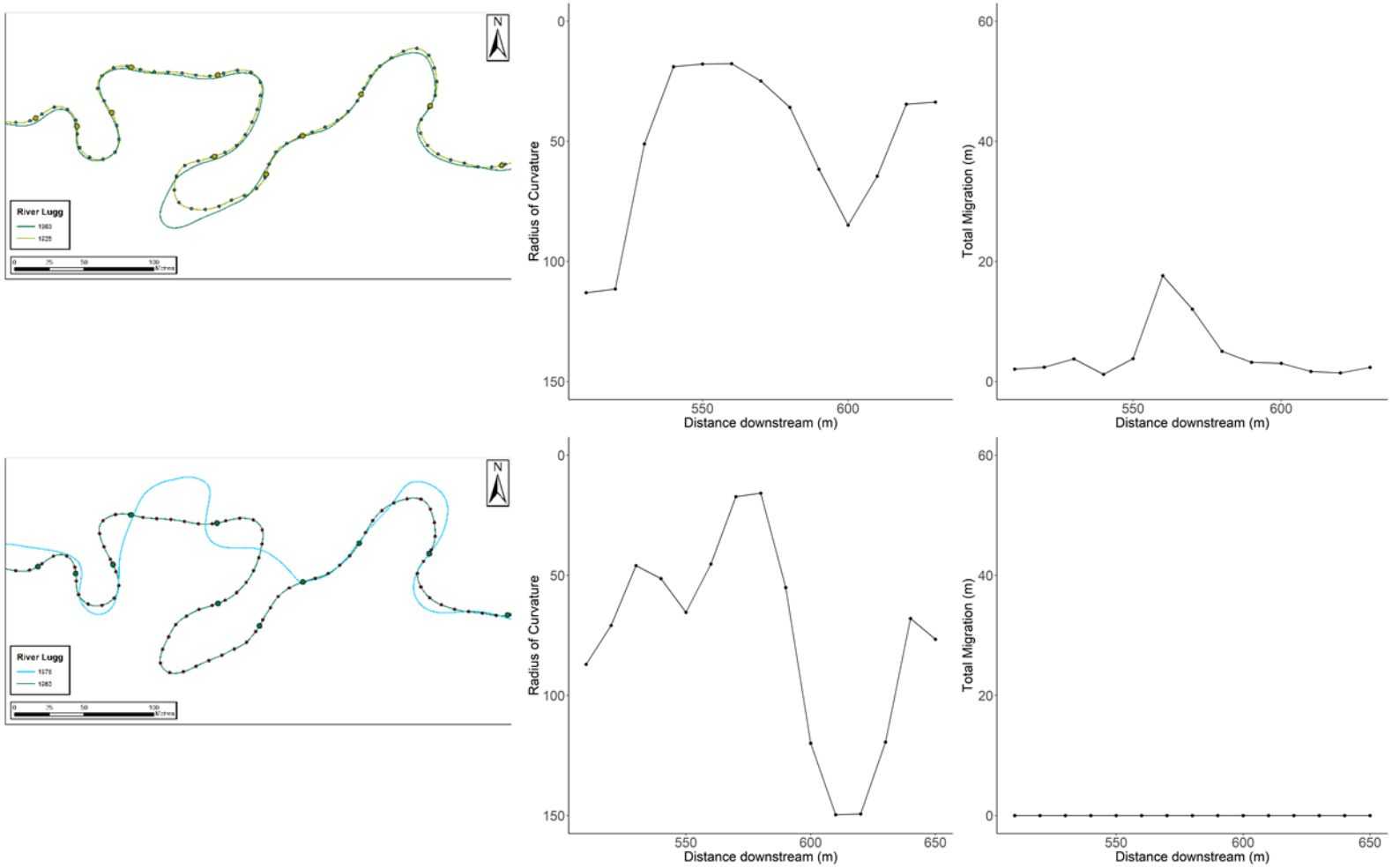

Figure 5.68. Changes to the curvature profile of Bend 10, Reach 2, River Lugg

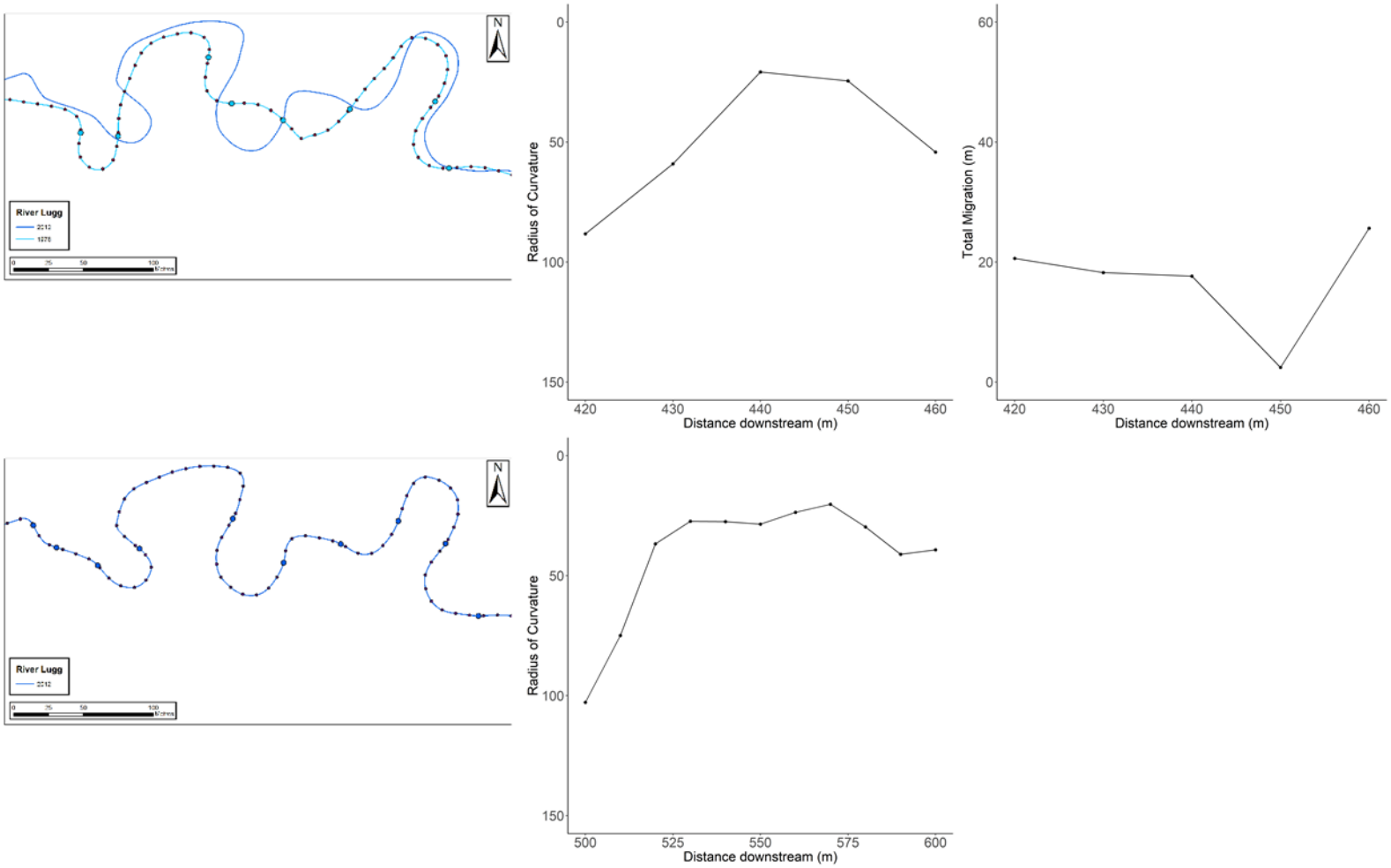

Figure 5.69. Changes to the curvature profile of Bend 10, Reach 2, River Lugg

River Lugg, Reach 2, Bend 21 (Figure 5.70 to Figure 5.72)

Bend 21 started as a simple symmetrical bend, similar to bend type D. The bend was stable between 1886 and 1963, with low amounts of erosion during this period. The shape of the bend and the curvature profile remained consistent through this period. The bend started to grow across the floodplain between 1963 and 1976, with most of the growth concentrated downstream of the apex. The bend maintained the simple symmetric form in 1976, before becoming compound asymmetrical in 2012 as the erosion continued downstream of the apex. The bend eventually formed three distinct apices, at the start and end of the bend and in the middle of the bend. The bend type in 2012 does not fit to any of the bends in the Brice classification.

Date	Brice Classification
1886	D
1903	D
1928	D
1963	D
1976	D
2012	NA

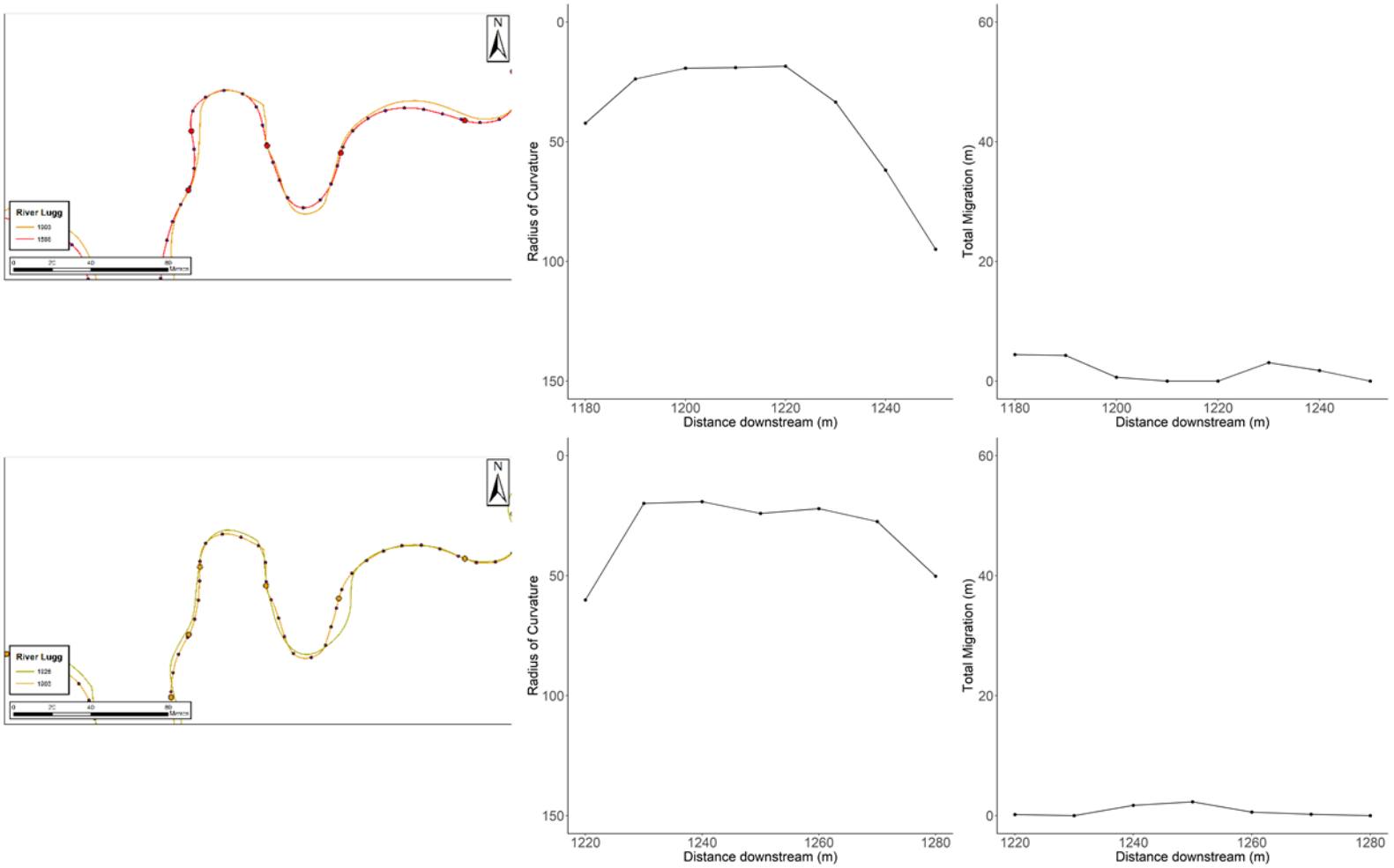

Figure 5.70. Changes to the curvature profile of Bend 21, Reach 2, River Lugg

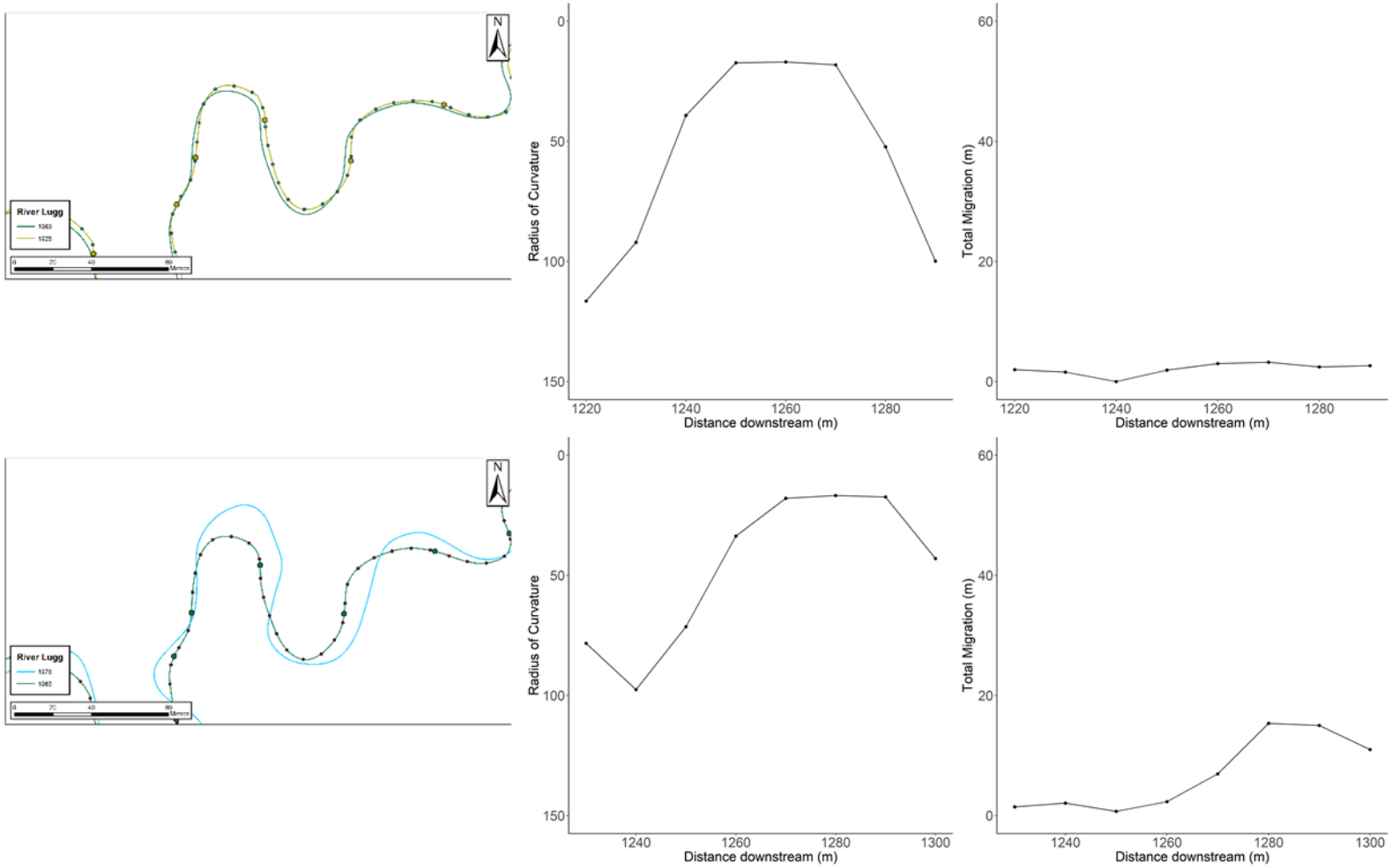

Figure 5.71. Changes to the curvature profile of Bend 21, Reach 2, River Lugg

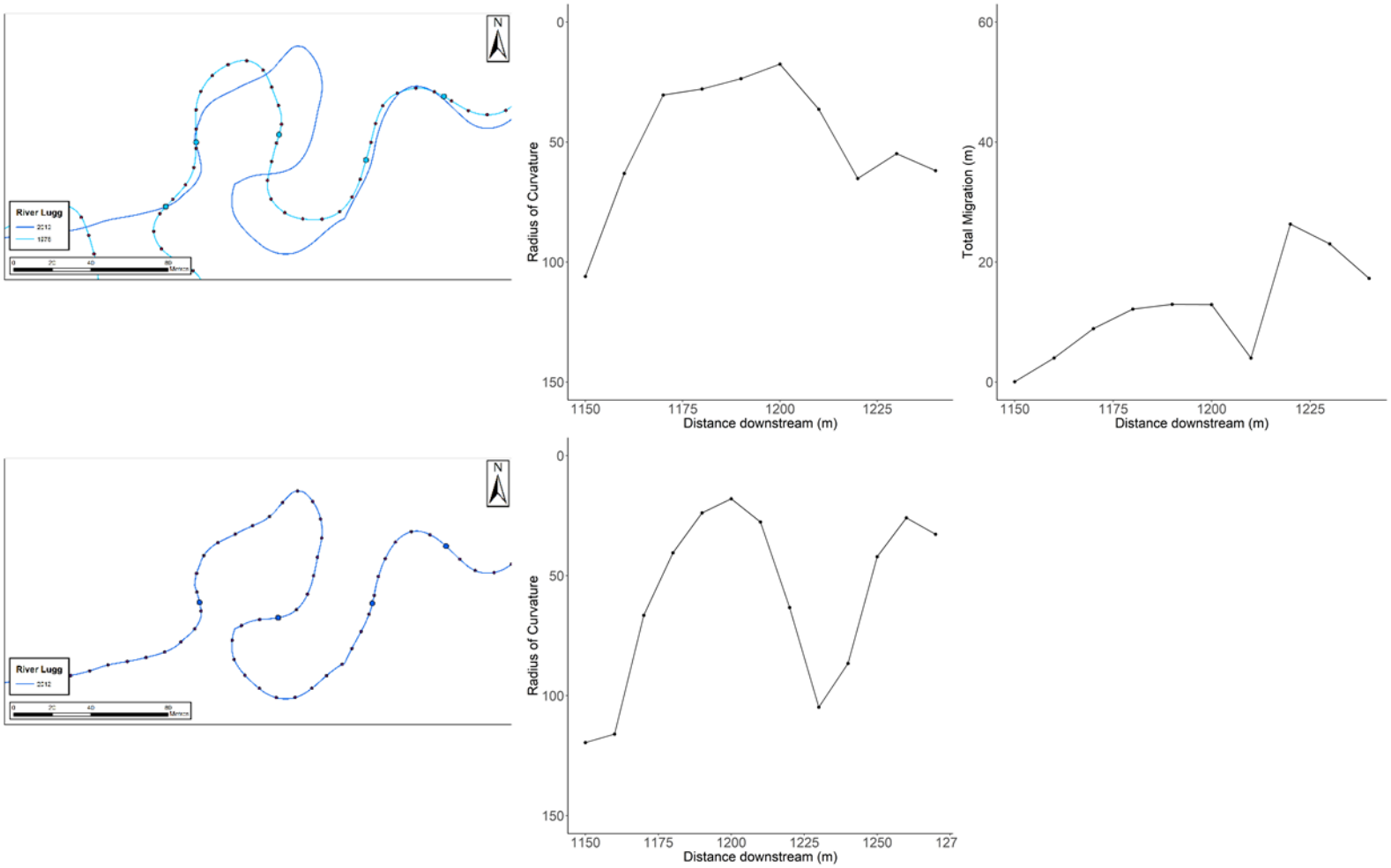

Figure 5.72. Changes to the curvature profile of Bend 21, Reach 2, River Lugg

River Lugg, Reach 2, Bend 22 (Figure 5.73 to Figure 5.75)

Bend 22 was a simple symmetrical bend, with a low radius of curvature at the apex of the bend. There was little change in the bend shape between 1886 and 1903, with some slight erosion at the apex of the bend. The two limbs of the bend were straight and had a high radius of curvature. The bend was best described as bend type F in the Brice classification. Between 1903 and 1928, there was a small amount of erosion on the downstream limb of the bend, which decreased the radius of curvature for these points and led to a more rounded channel planform downstream of the apex. The bend profile remained consistent between 1928 and 1963, with low amounts of erosion and little change to the overall shape of the bend. Between 1963 and 1976, there was erosion at the start of the bend, mainly driven by migration on the preceding bend, and erosion downstream of the apex, which led to a more rounded apex, with five points with a similar radius of curvature measurement. The bend has become like bend type D. There were high levels of erosion between 1976 and 2012 at start of the bend, which may have been exacerbated by the downstream migration of the preceding bend and two distinct apices were formed on the bend, with a long downstream stream limb with a high radius of curvature. The bend has become compound and is probably asymmetrical due to the slight difference in the radius of curvature at the two apices. Bend type O is the best example from the Brice classification.

Date	Brice Classification
1886	F
1903	F
1928	D
1963	D
1976	D
2012	O

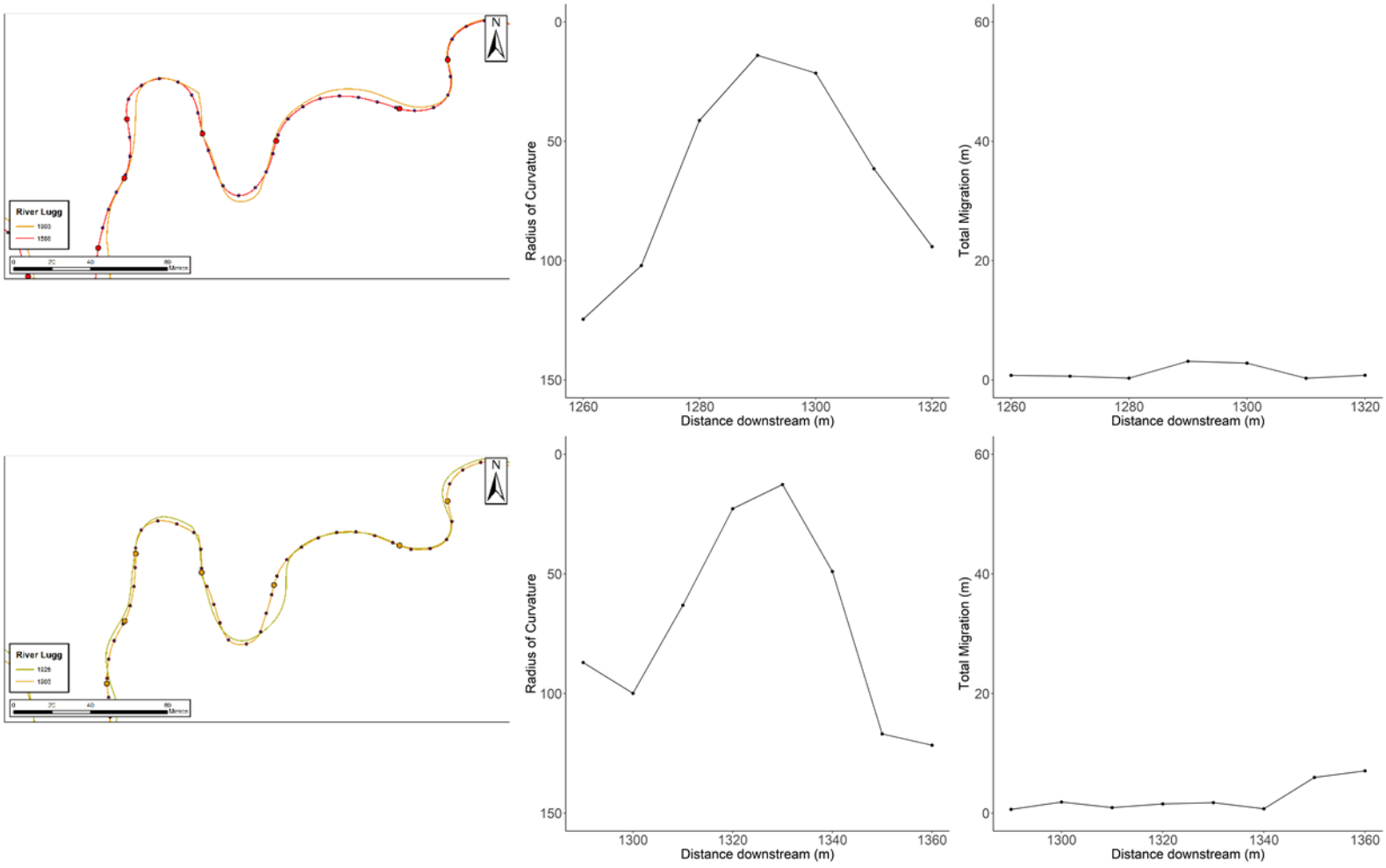

Figure 5.73. Changes to the curvature profile of Bend 22, Reach 2, River Lugg

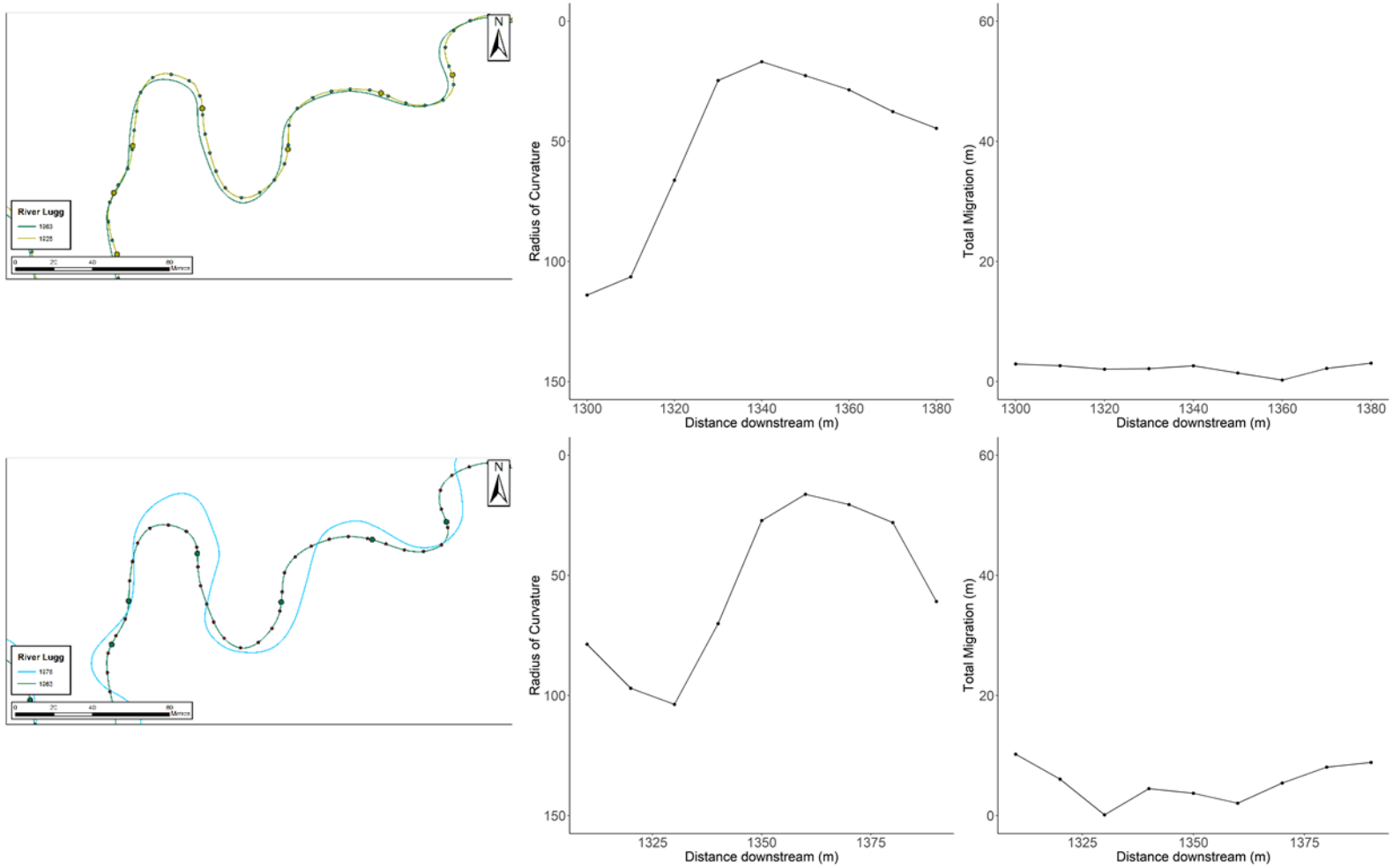

Figure 5.74. Changes to the curvature profile of Bend 22, Reach 2, River Lugg

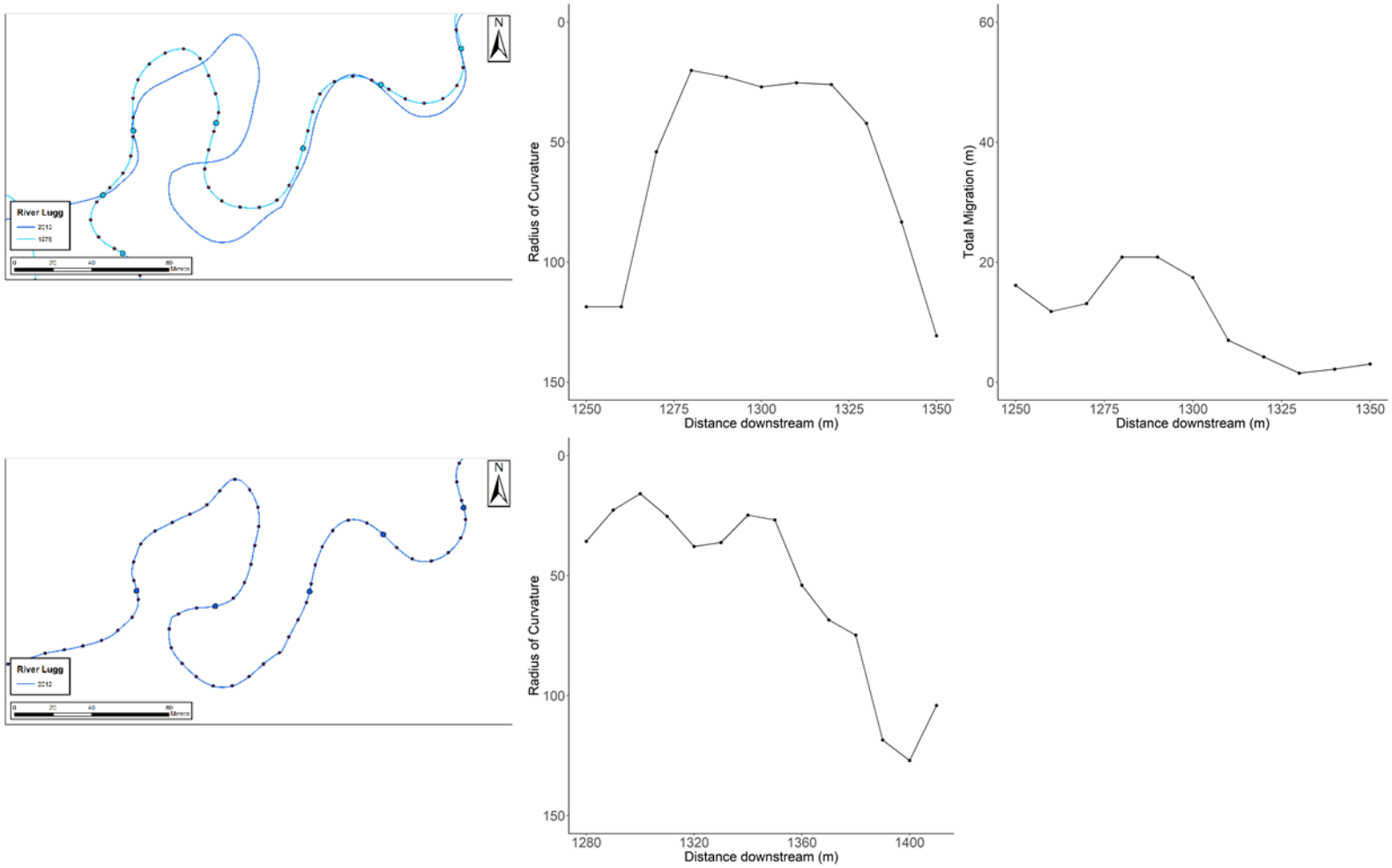

Figure 5.75. Changes to the curvature profile of Bend 22, Reach 2, River Lugg

River Lugg, Reach 3, Bend 11 (Figure 5.76 to Figure 5.78)

The River Lugg passes through a narrow valley for Reach 3 and the amount of change is limited on the bends through this section. However, there was some substantial change that occurred on bend 11. Bend 11 started in 1886 as a compound asymmetrical bend with a tighter apex on the downstream side of the bend and the bend type was type O. Between 1886 and 1903, there was erosion on the upstream apex, with some erosion driven by the preceding bend upstream and some erosion downstream of the first apex. This created a tighter apex at the start of the bend, although the bend type remained the same. The bend was stable between 1903 and 1963, with no erosion occurring and no changes to the bend shape. The curvature profile remained similar between the two different periods. The first apex of the bend started to migrate downstream between 1963 and 1975, with over 20m of erosion occurring downstream of the apex. The second apex became less tight as erosion occurred on the bend downstream and led to the channel becoming straighter at the downstream inflection point. There was a slight retraction at the first apex between 1975 and 2012, which led to a straighter channel between the two apices and a higher radius of curvature. The bend finished as bend type O from the Brice classification, although the first apex was now the tighter apex.

Date	Brice Classification
1886	O
1903	O
1928	O
1963	O
1975	O
2012	O

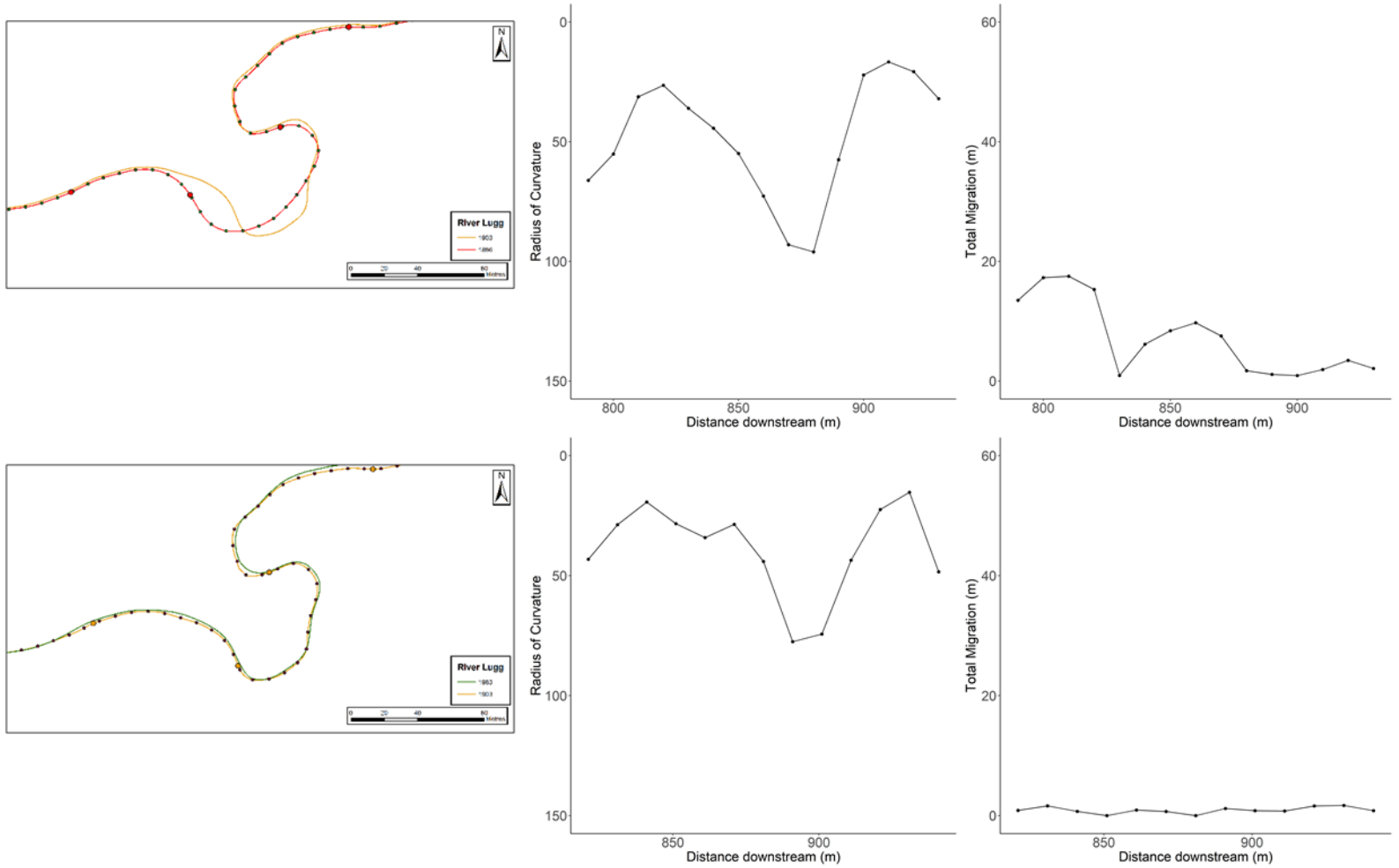

Figure 5.76. Changes to the curvature profile of Bend 11, Reach 3, River Lugg

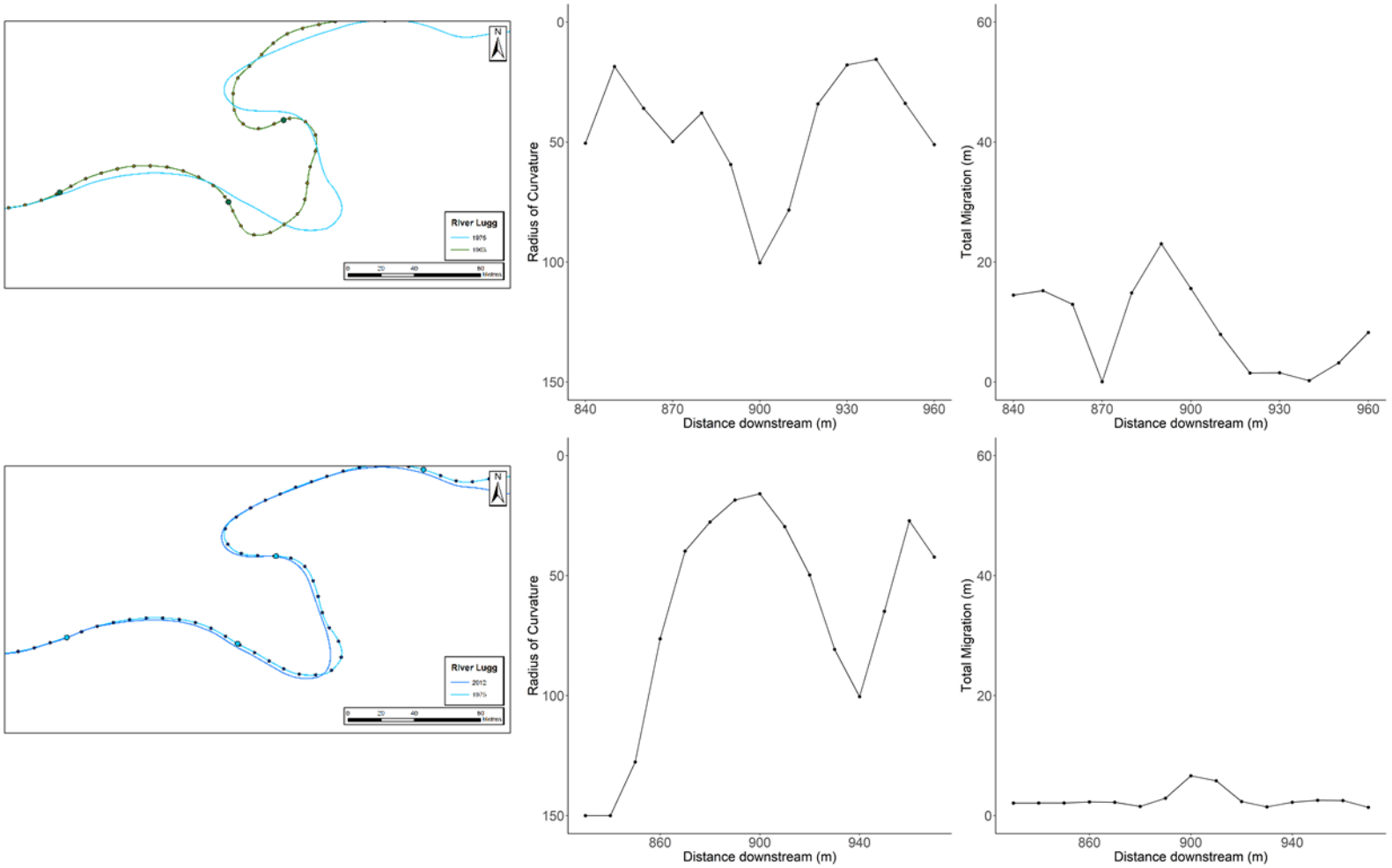

Figure 5.77. Changes to the curvature profile of Bend 11, Reach 3, River Lugg

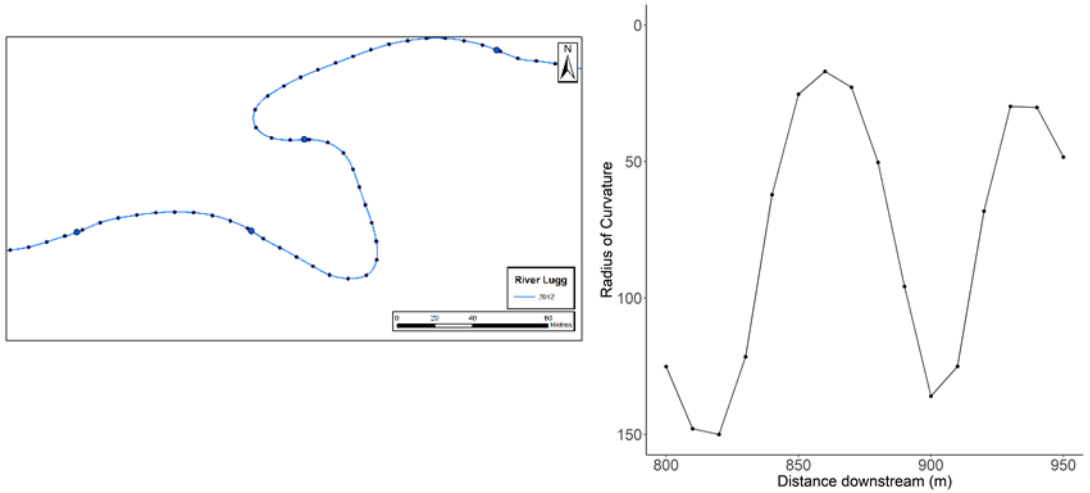

Figure 5.78. Changes to the curvature profile of Bend 11, Reach 3, River Lugg

River Lugg, Reach 4, Bend 8 (Figure 5.79 to Figure 5.81)

Bend 8 was a compound asymmetrical bend in 1886, similar to bend type N, with a tighter and longer apex on the downstream side of the bend. Most of the erosion is concentrated on the downstream apex between 1886 and 1903, with the downstream apex also becoming double-headed. The bend remained stable between 1903 and 1928, with only a small amount of erosion occurring for the last few points on the bend. The bend retained a similar curvature profile between 1903 and 1928. A neck cutoff occurred between 1928 and 1963, which cutoff the third apex on this bend and lead to a more simple curvature profile, with a lower radius of curvature at the start of the bend compared to the finish. The bend was most like bend type M from the Brice classification. There was a large amount of erosion that occurred between 1963 and 1974, with the river retracting directly at the first apex and growing across the floodplain just downstream of the apex. The radius of curvature at the downstream end of the bend increased. The erosion between 1974 and 2012 was concentrated at this downstream end of the bend. The apex continued to develop and created a tight apex with a low radius of curvature. The bend finished as bend type N.

Date	Brice Classification
1886	N
1903	N
1928	N
1963	M
1974	N
2012	N

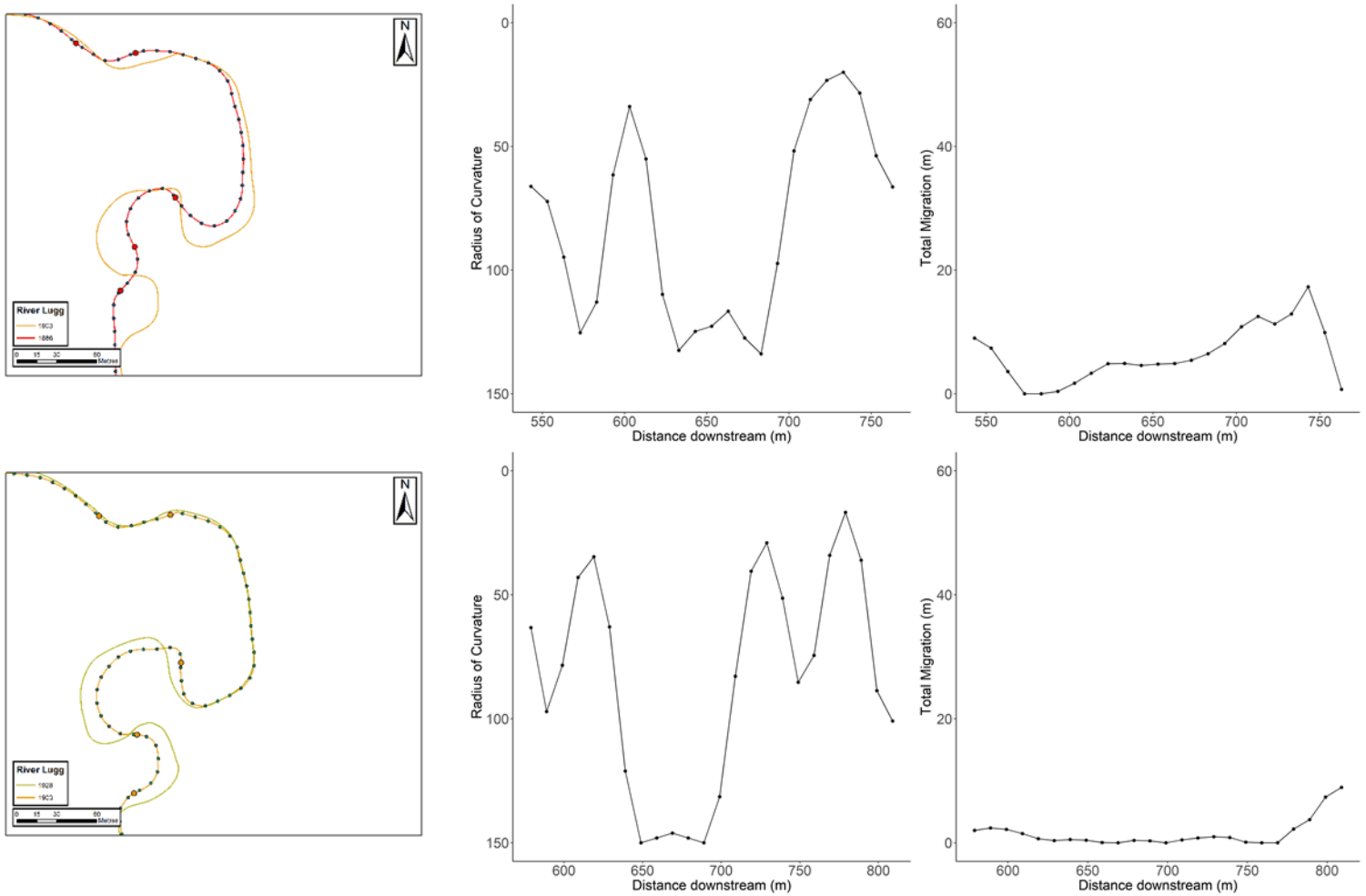

Figure 5.79. Changes to the curvature profile of Bend 8, Reach 4, River Lugg

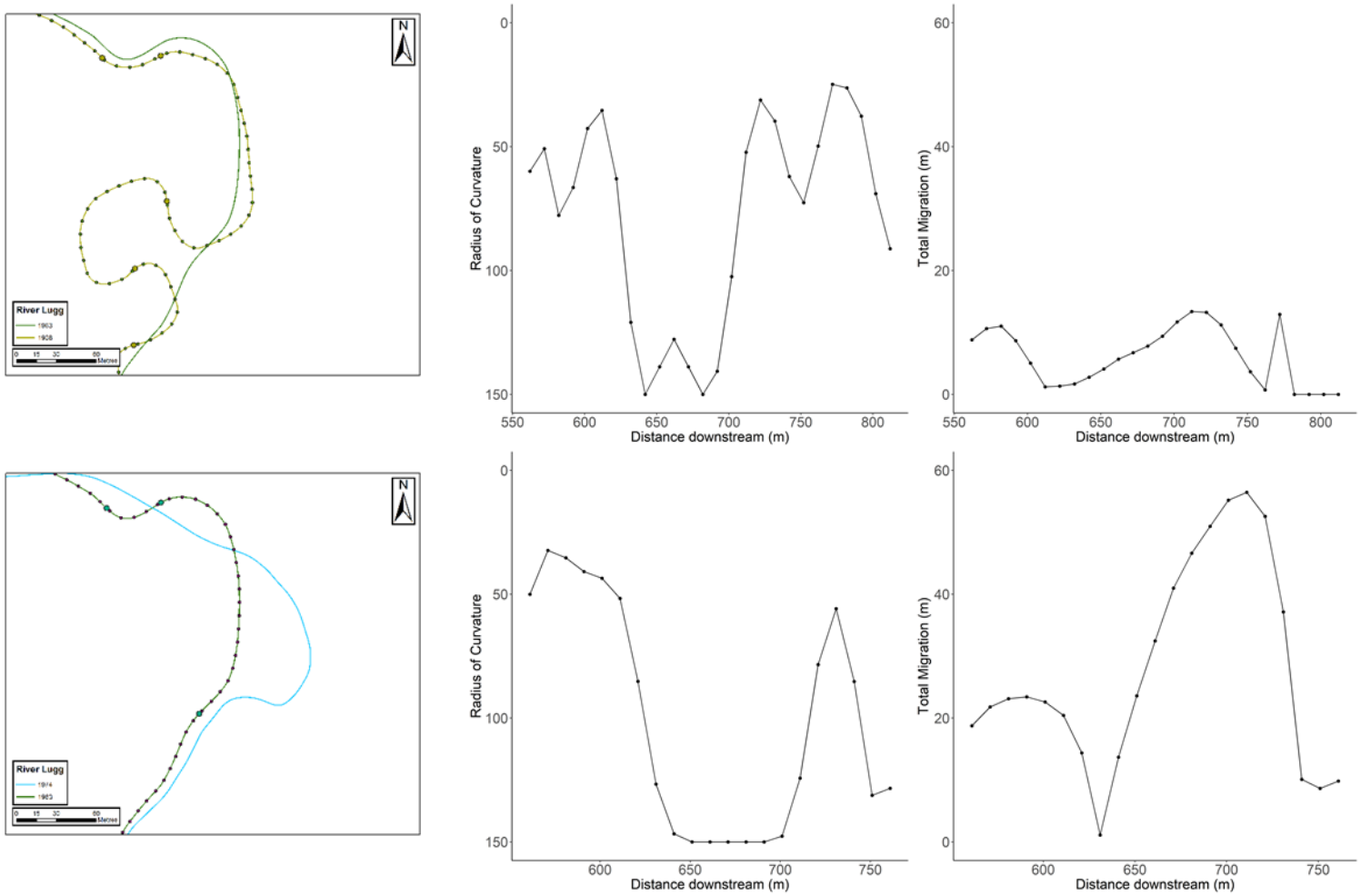

Figure 5.80. Changes to the curvature profile of Bend 8, Reach 4, River Lugg

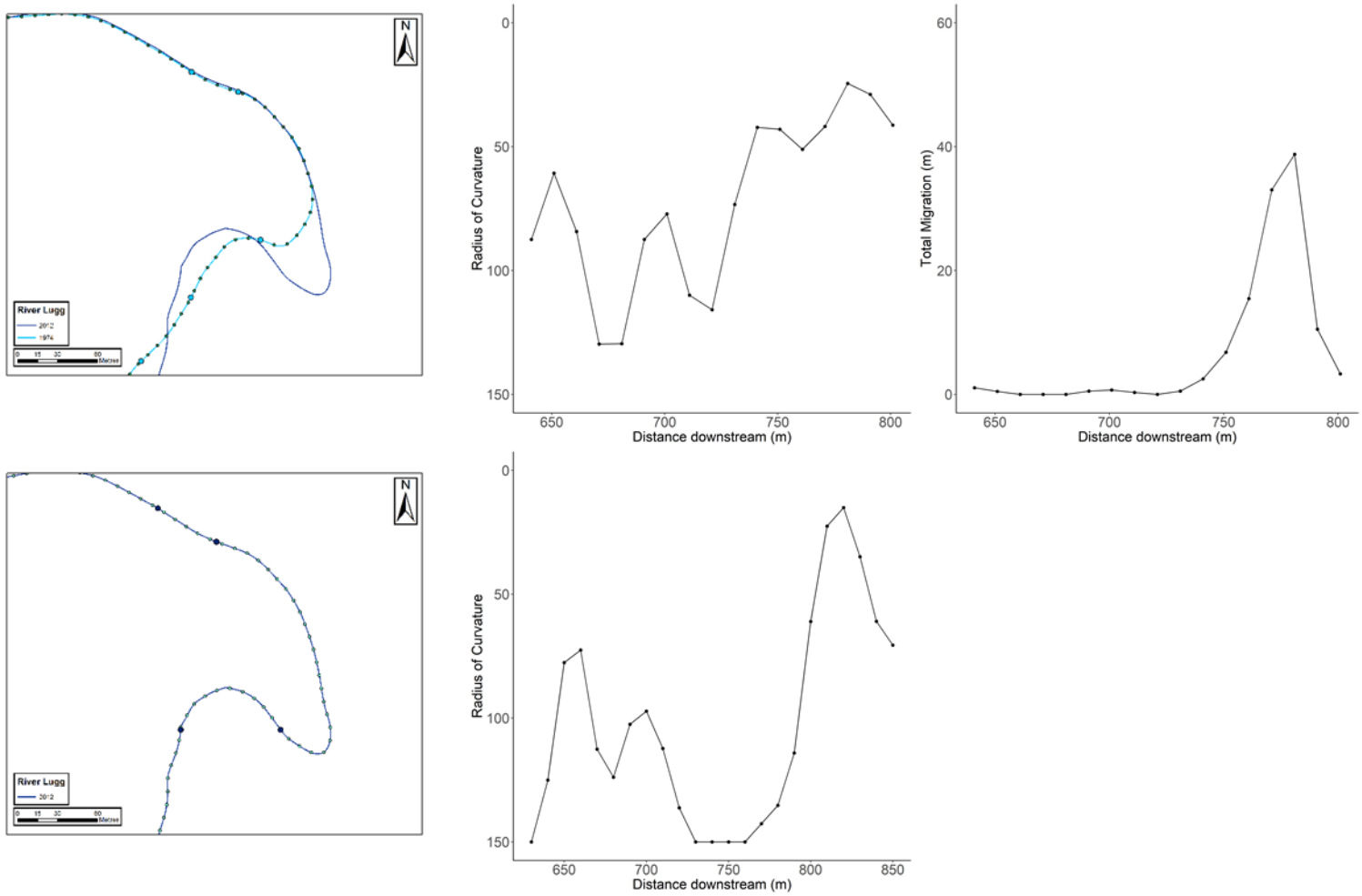

Figure 5.81. Changes to the curvature profile of Bend 8, Reach 4, River Lugg

River Lugg, Reach 4, Bend 9 (Figure 5.82 to Figure 5.84)

Bend 9 was a simple symmetrical bend in 1886 with a low average radius of curvature, which indicated that the bend was tight overall. The bend eroded on the downstream side of the bend between 1886 and 1903, with the upstream side remaining stable. This created a compound asymmetrical bend, with a small apex at the start of the bend and a much longer apex at the end of the bend. The bend type was O. The bend continued to migrate downstream and extend across the floodplain between 1903 and 1928, with three individual apices created. The bend developed towards a compound symmetrical bend, with the apices at the start and finish of the bend having a similar curvature profile. A cutoff occurred between 1928 and 1963 leaving behind a straight channel and no definitive bend in the same position in 1963. The bend only developed again in 1974 as a simple asymmetrical bend, which started to erode towards the bend that was cutoff between 1928 and 1963. Erosion occurred at each point on the bend in 1974 and the bend developed into a simple symmetrical bend by 2012.

Date	Brice Classification
1886	D
1903	O
1928	O
1974	B
2012	C

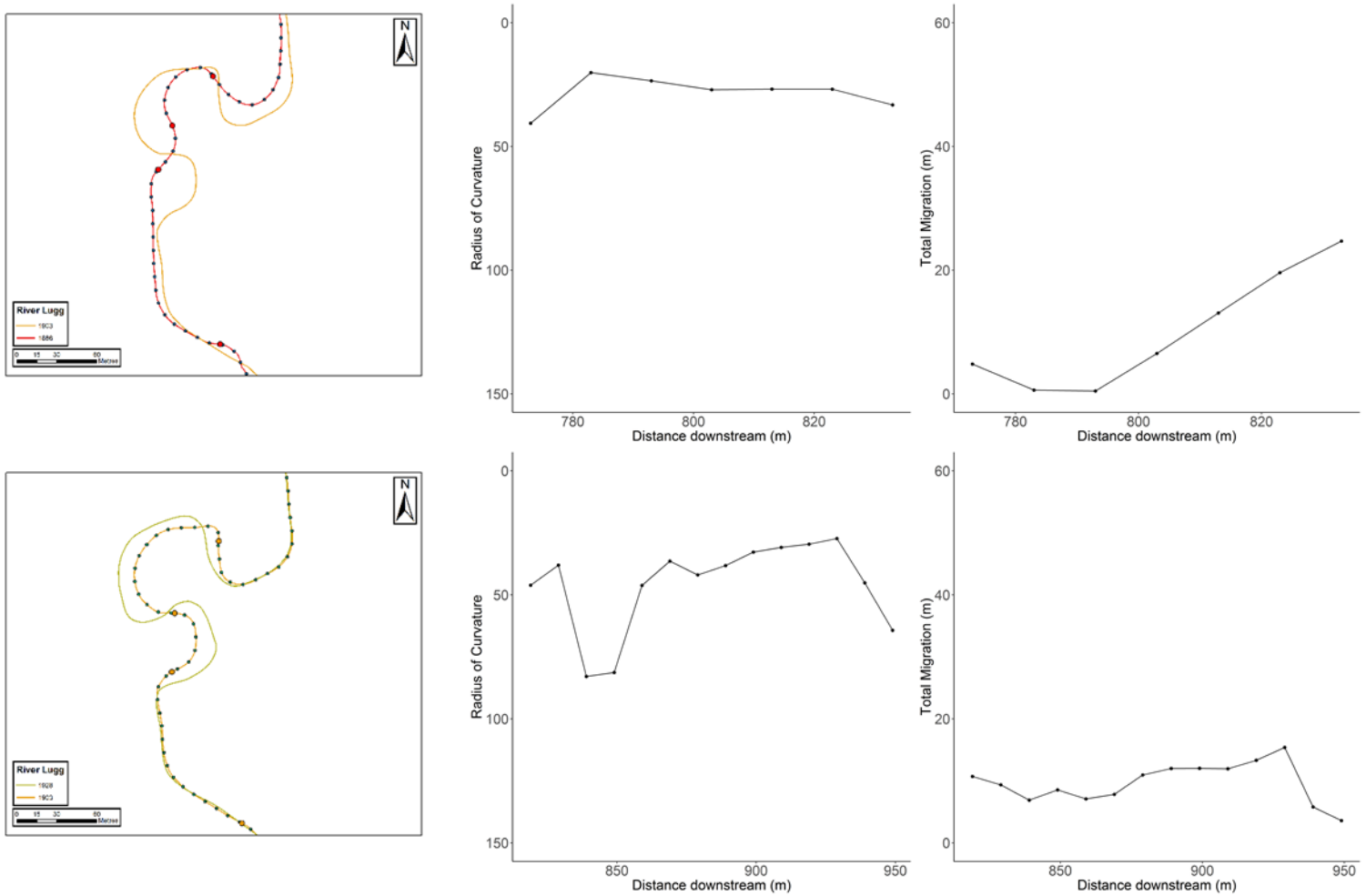

Figure 5.82. Changes to the curvature profile of Bend 9, Reach 4, River Lugg

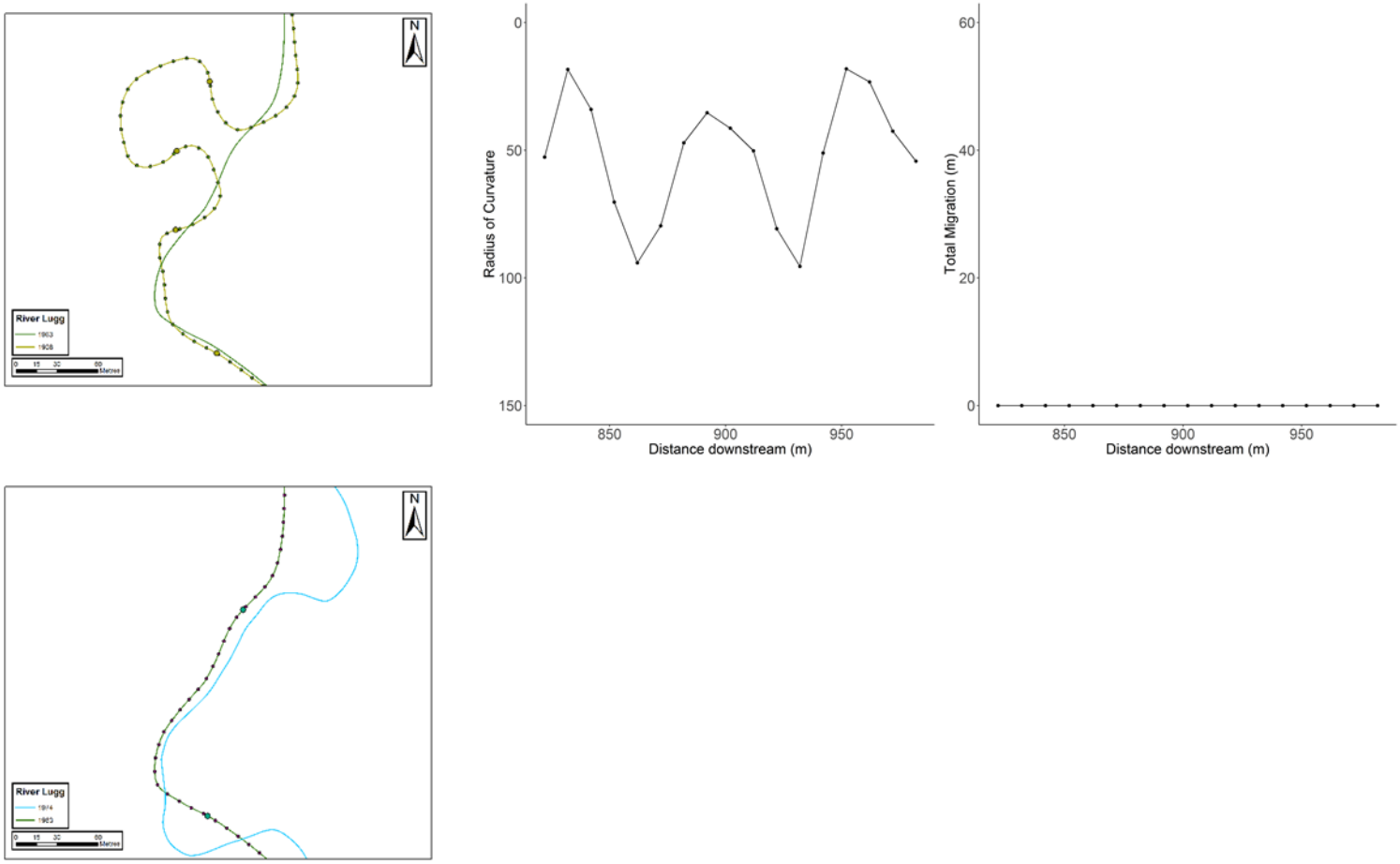

Figure 5.83. Changes to the curvature profile of Bend 9, Reach 4, River Lugg. Note there was no bend include for 1963 as was not long enough to be considered an individual bend

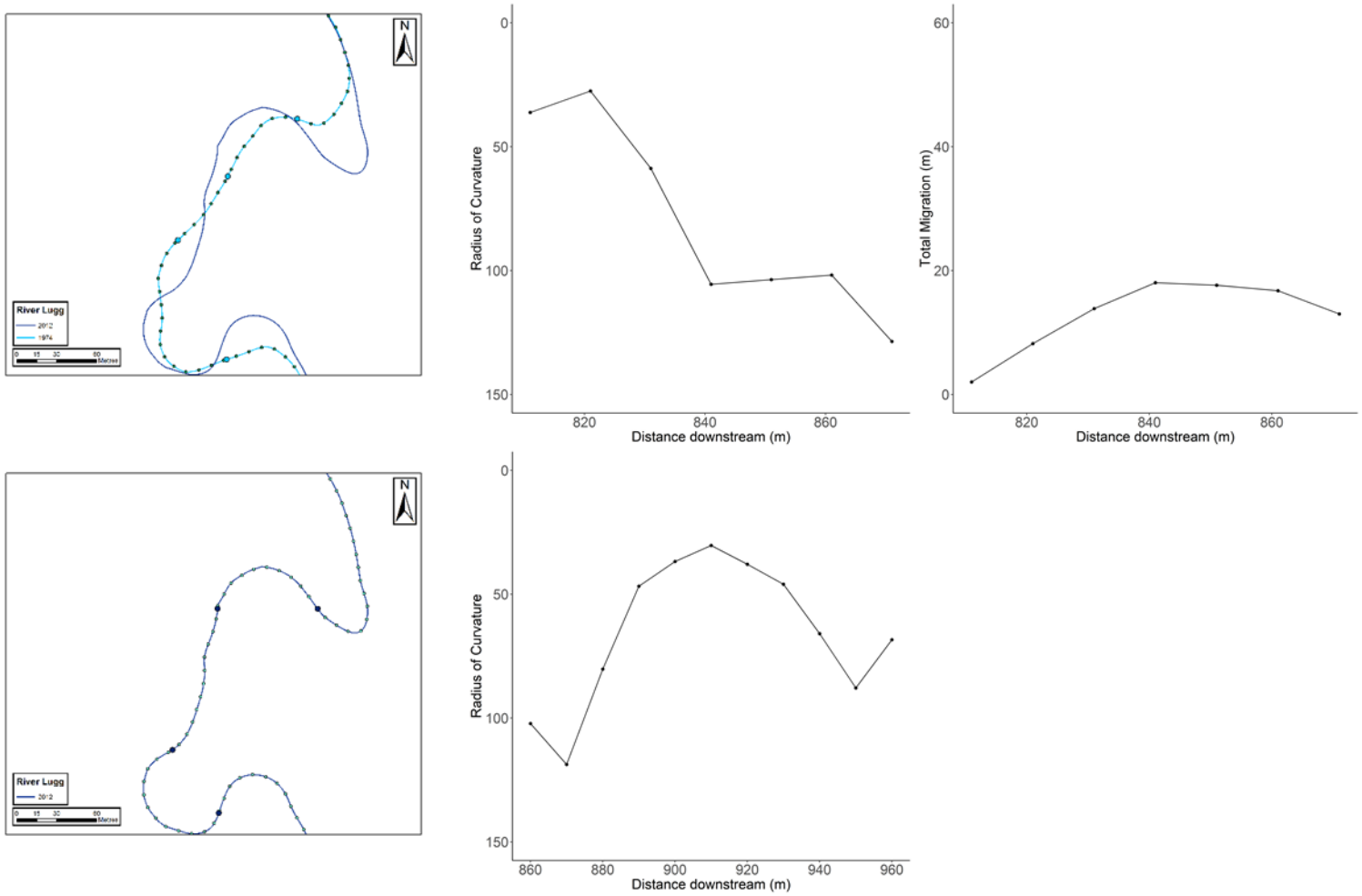

Figure 5.84. Changes to the curvature profile of Bend 9, Reach 4, River Lugg

River Lugg, Reach 5, Bend 14 (Figure 5.85 to Figure 5.87)

Bend 14 was initially a simple symmetrical bend, with a high average and minimum radius of curvature. The bend was best described as bend type A from the Brice classification. There was initially little erosion between 1886 and 1903 and the bend remained stable during this period. Between 1903 and 1928, there was little erosion on bend 14, but high amounts of erosion both upstream and downstream of the bend. This changed the position of the inflection points for the bend and it became a longer bend, with the average radius of curvature remaining high. Further erosion occurred between 1928 and 1963 on both the preceding bend upstream and the following bend downstream, and this created a much tighter simple symmetrical bend, similar to bend type C. The bend continued to grow between 1963 and 1973, with the highest erosion rates found downstream of the apex. The bend remained as a simple symmetrical bend however, developing towards bend type D. The series of flood protection and weirs that were constructed in the 1970s prevented the river channel from migrating further between 1973 and 2012 and the change in the curvature profile was caused by sensitivity to the location of the inflection points.

Date	**Brice Classification**
1886	A
1903	A
1928	A
1963	C
1973	D
2012	D

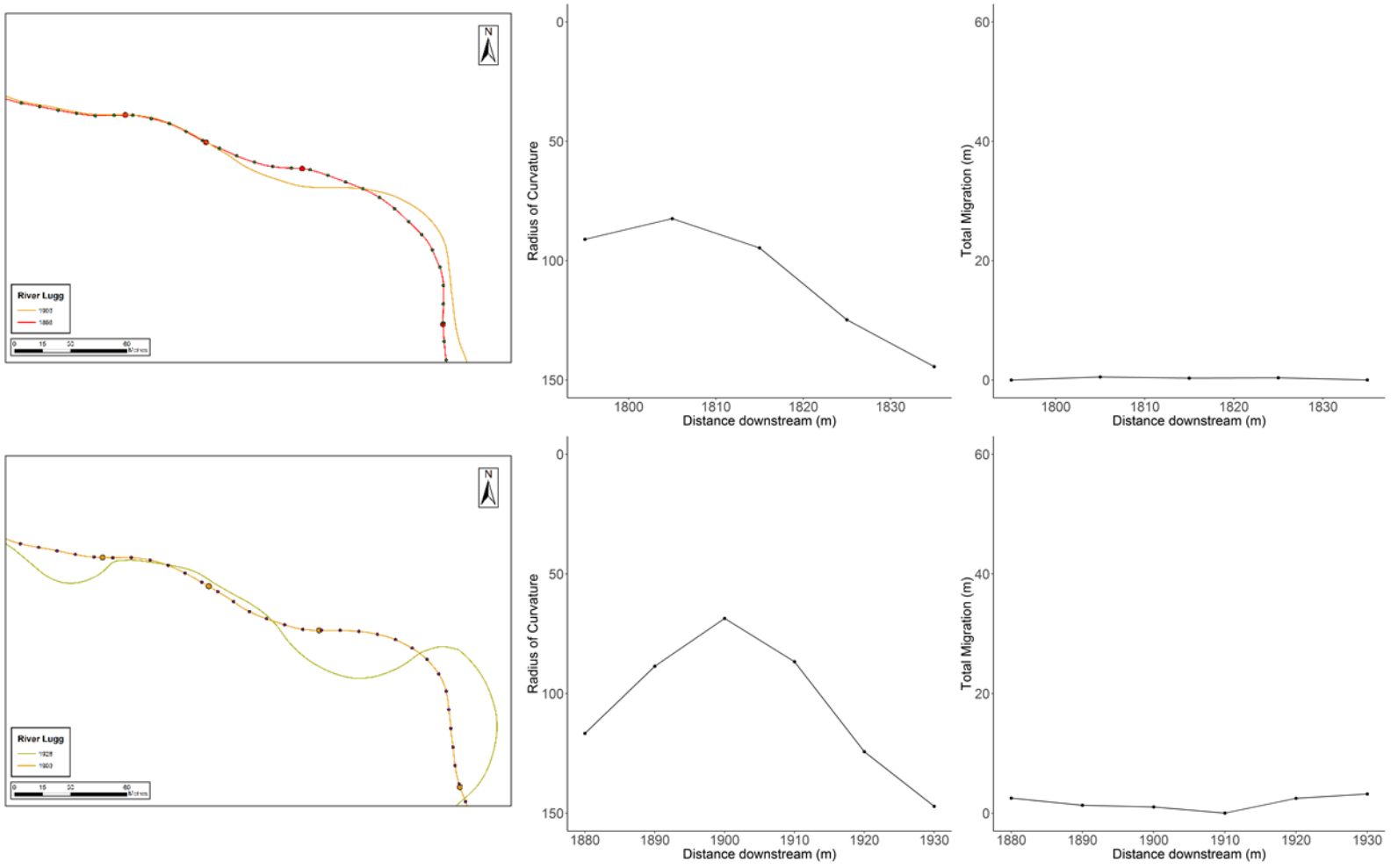

Figure 5.85. Changes to the curvature profile of Bend 14, Reach 5, River Lugg

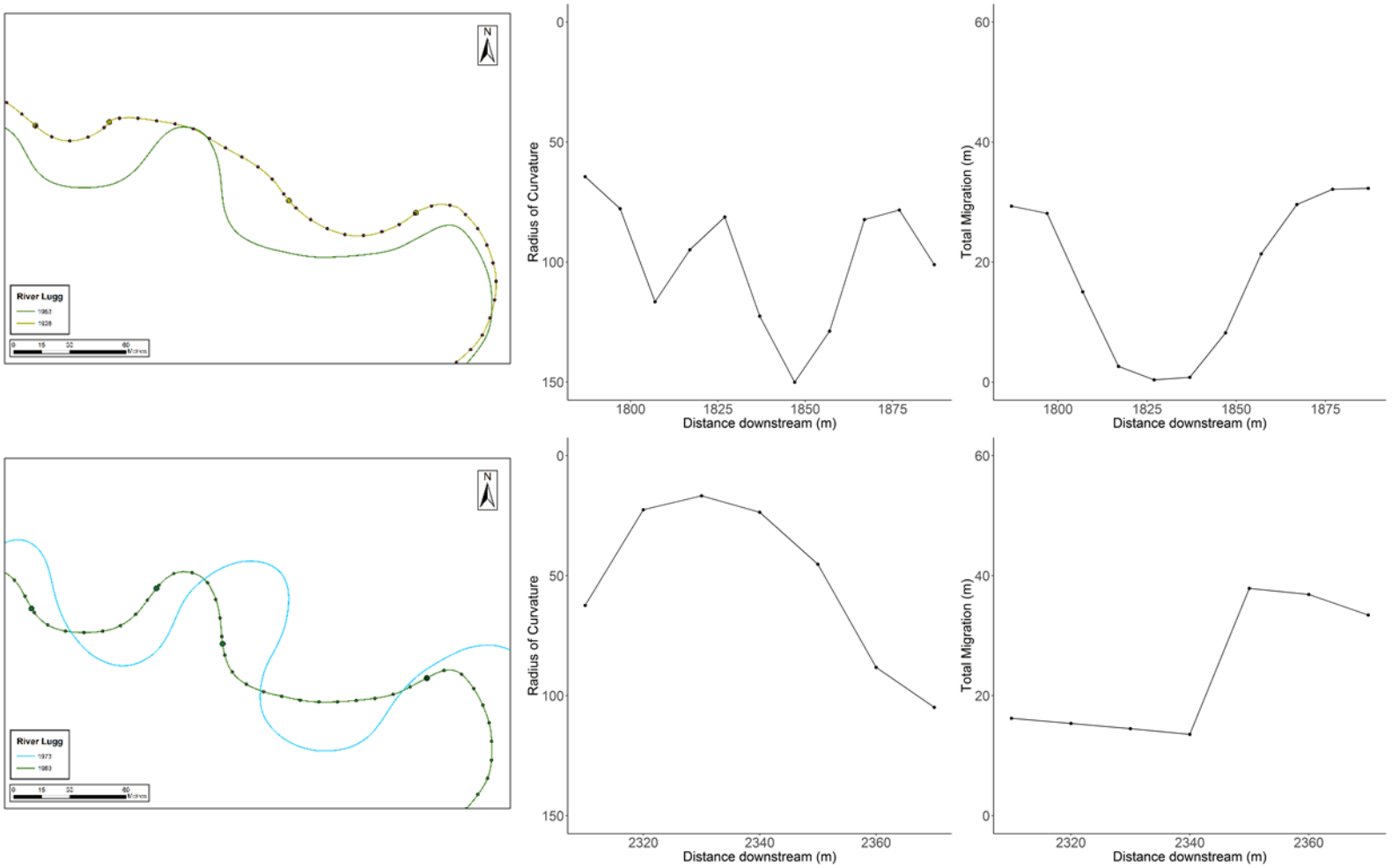

Figure 5.86. Changes to the curvature profile of Bend 14, Reach 5, River Lugg

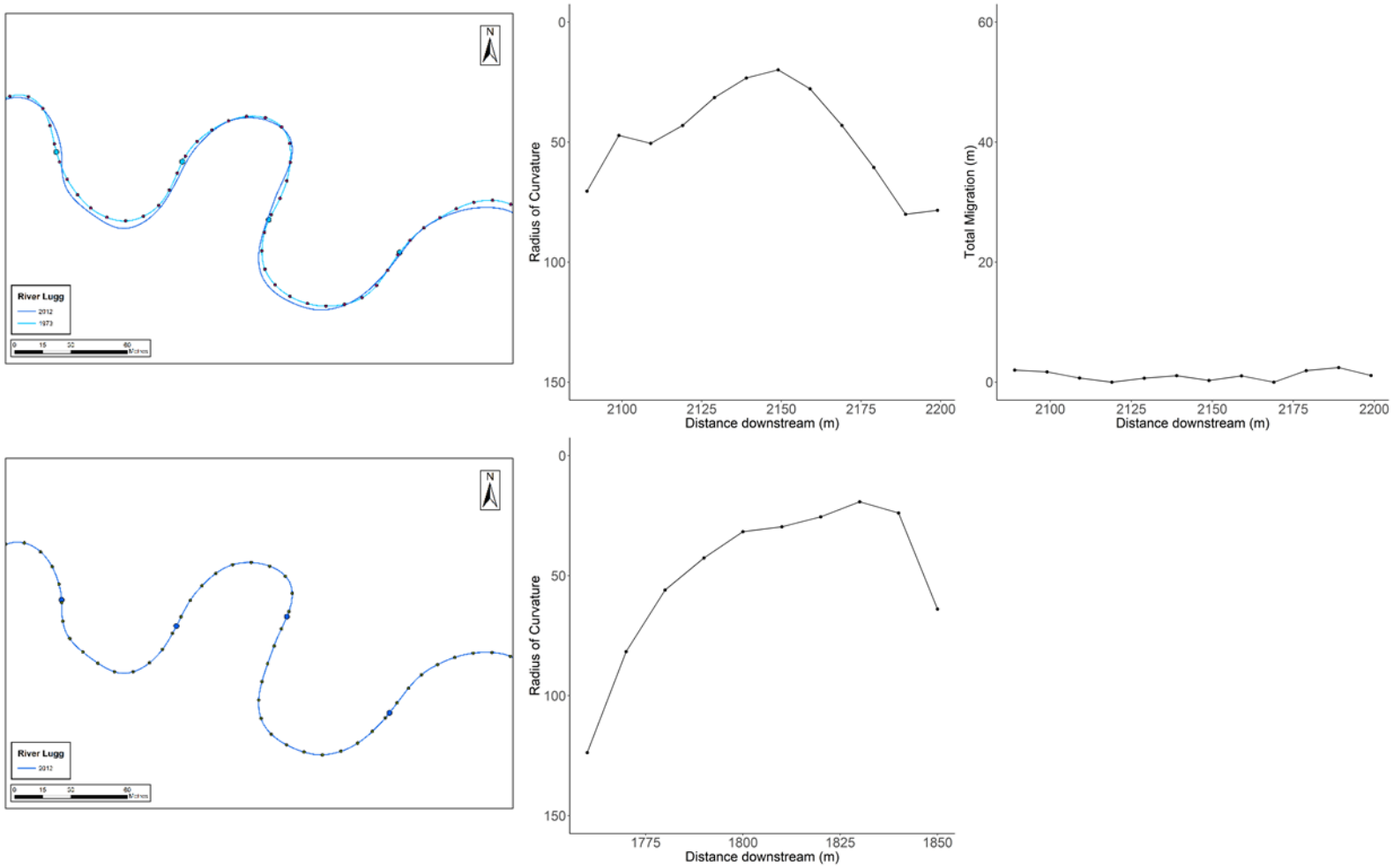

Figure 5.87. Changes to the curvature profile of Bend 14, Reach 5, River Lugg

River Lugg, Reach 5, Bend 16 (Figure 5.88 to Figure 5.90)

Bend 16 started as a simple symmetrical bend in 1886, with a high minimum radius of curvature. There was a slight skew in the downstream direction on the bend. A small amount of erosion occurred throughout the bend, and the inflection points of the bend shifted slightly downstream. The minimum radius of curvature decreased between 1886 and 1903 and the curvature profile showed one well-defined peak. There was erosion upstream and downstream of the apex between 1903 and 1928, and the minimum radius of curvature decreased again during this period. Overall, the mean radius of curvature also decreased during this period and the bend changed from being simple symmetrical to simple asymmetrical. The total amount of erosion decreased between 1928 and 1963, but some erosion still occurred at the start of the bend. The apex at the start of the bend became tighter again, and a second apex could be identified in the curvature profile. The total amount of erosion increased between 1963 and 1973, with the bend growing across the floodplain. The bend became compound during this period, with two well-defined minima in the radius of curvature. The radius of curvature minima was similar for both apices along with the curvature profile. The bend was similar to bend O in the Brice classification at this point. There was limited amounts of erosion between 1973 and 2012 and the curvature profile remained similar during this period.

Date	Brice Classification
1886	B
1903	B
1928	K
1963	K
1973	O
2012	O

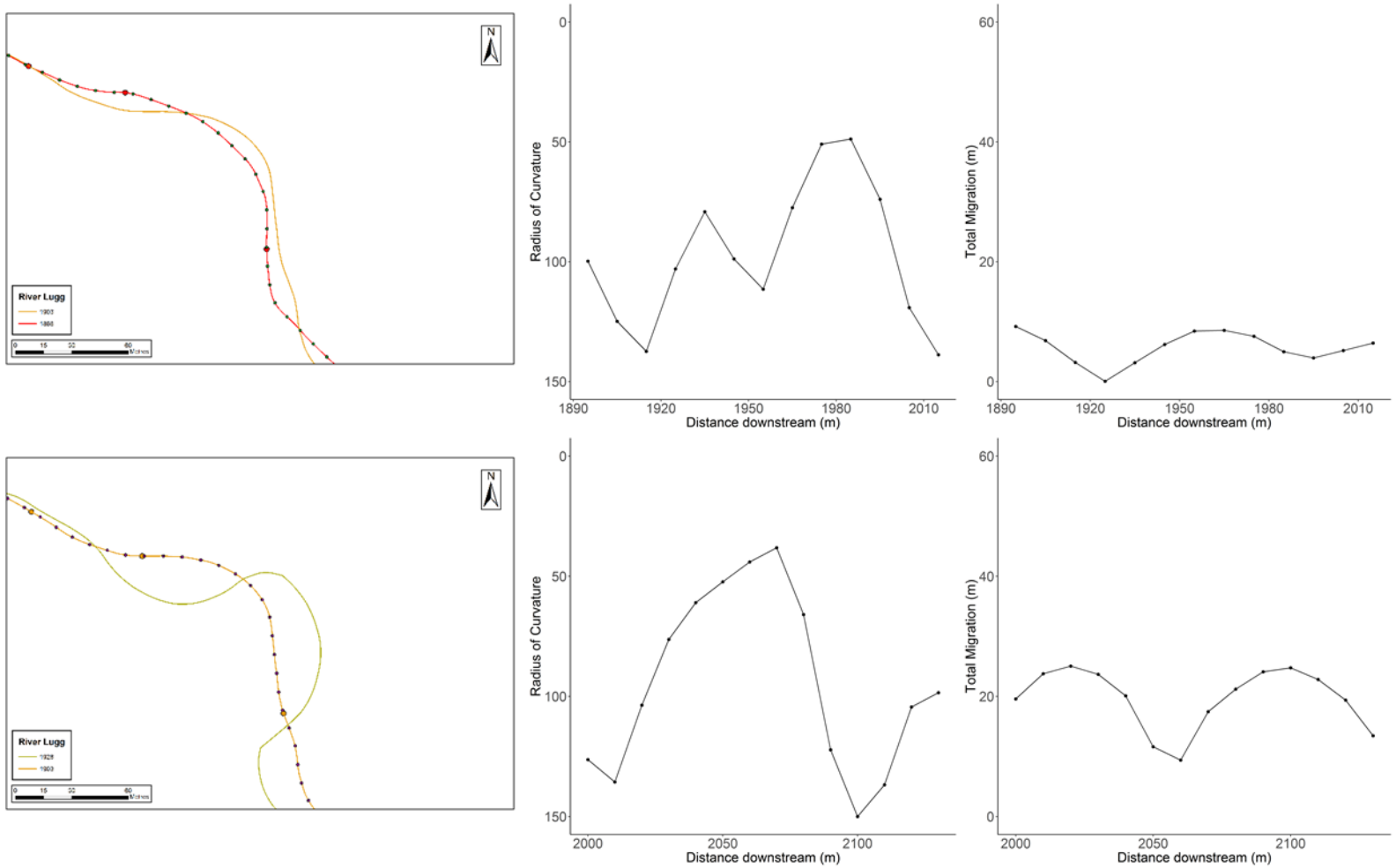

Figure 5.88. Changes to the curvature profile of Bend 16, Reach 5, River Lugg

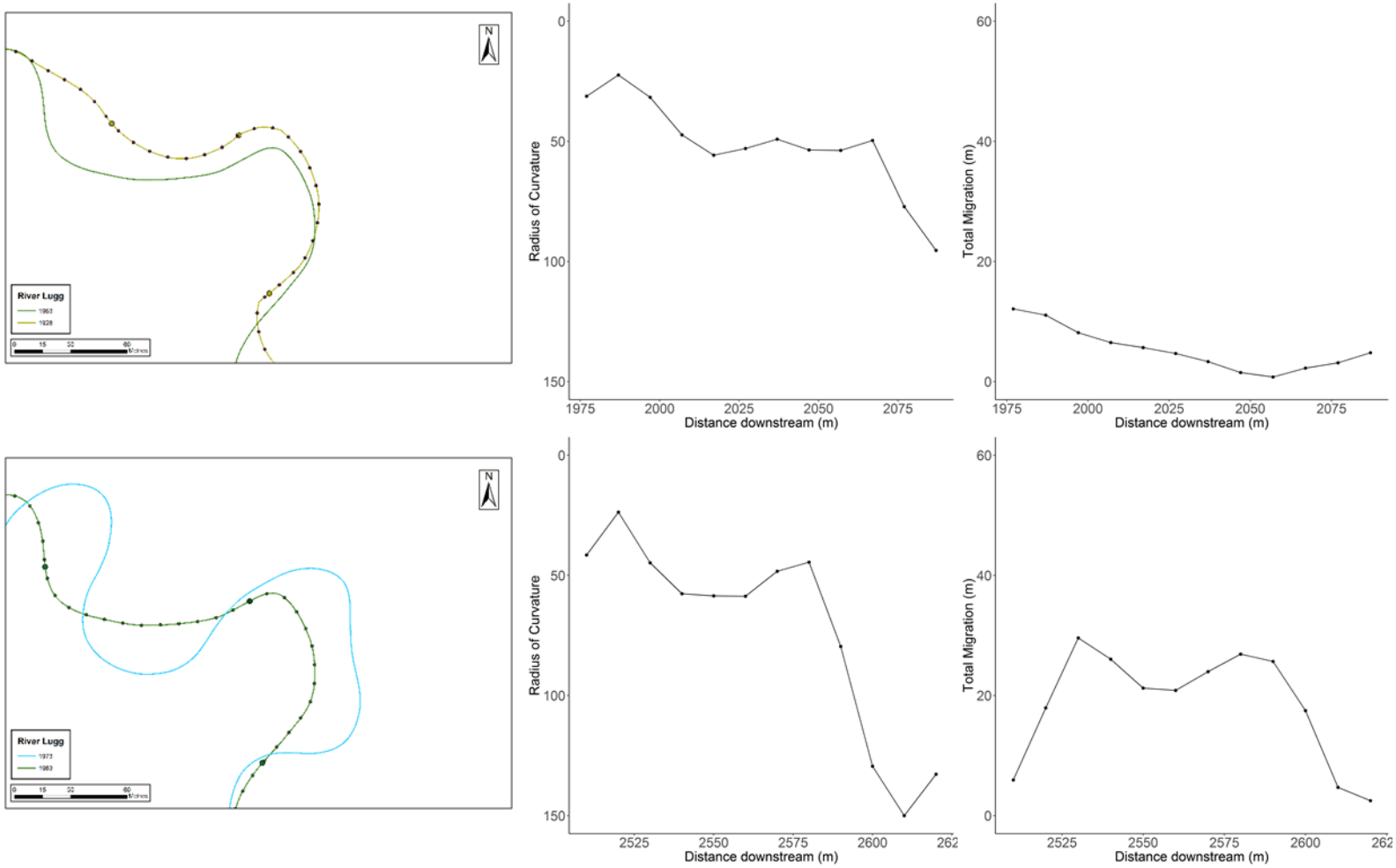

Figure 5.89. Changes to the curvature profile of Bend 16, Reach 5, River Lugg

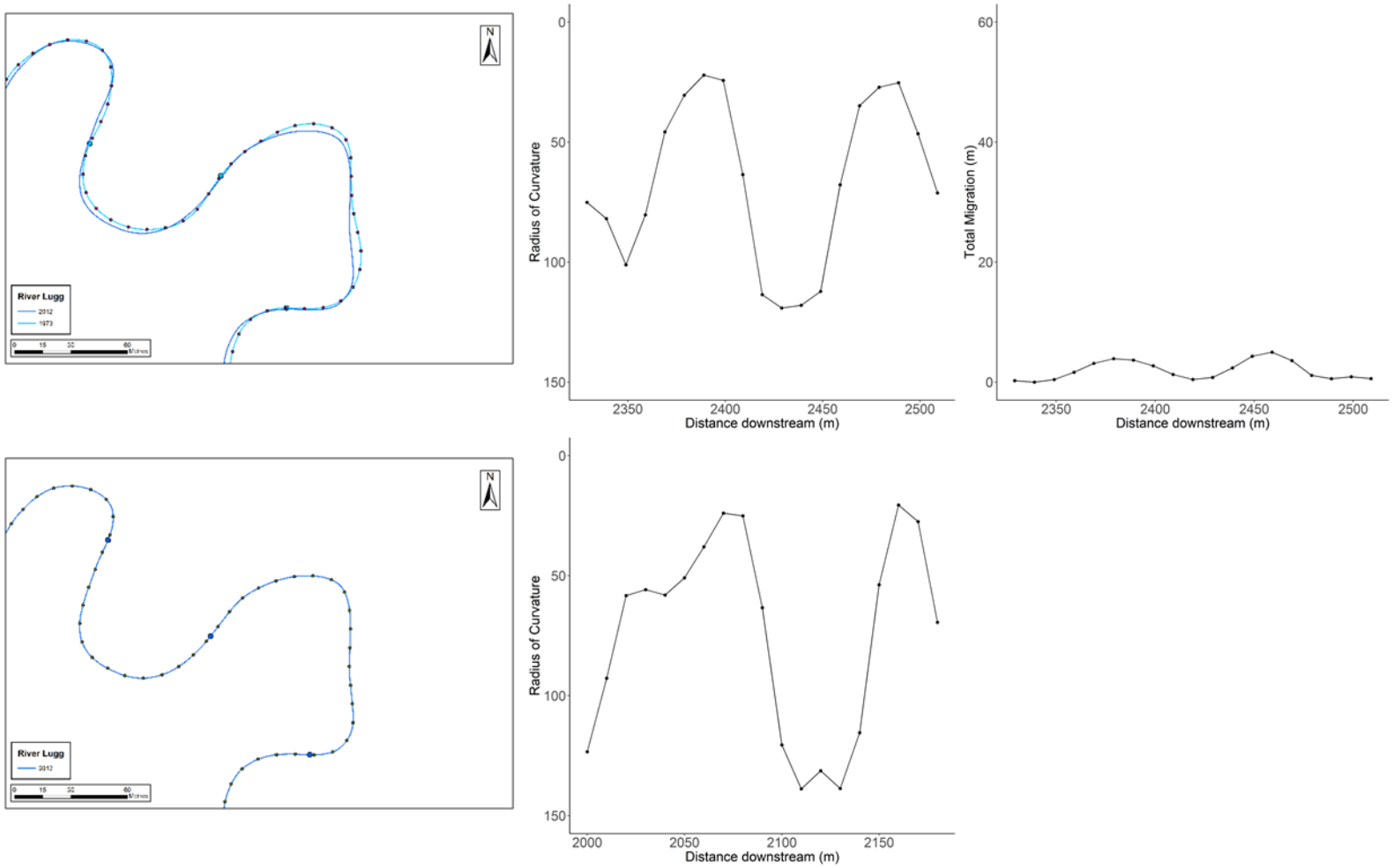

Figure 5.90. Changes to the curvature profile of Bend 16, Reach 5, River Lugg

River Lugg, Reach 5, Bend 22 (Figure 5.91 to Figure 5.93)

Bend 22 started as a simple asymmetrical bend in 1886, skewed in the upstream direction. The radius of curvature at the apex was low, with a long straight limb downstream of the apex. This limb subsequently eroded between 1886 and 1903 and formed a new bend, leaving bend 22 shorter and created a simple symmetrical bend. Between 1903 and 1928, erosion occurred downstream of the apex as the bend started to grow across the floodplain. This growth created a simple symmetrical bend with straight channels before and after the apex, similar to bend type F. The bend continued to be active between 1928 and 1963, with the bend retracting from the apex. Growth on the previous bend also created a second apex on bend 22, which had become compound asymmetrical, similar to bend type O. The two apices started to develop separately between 1963 and 1973 and became three separate bends using the methodology used here to define individual bends. If all three bends were considered together then the bend had developed to bend type P, with two apices growing in independent directions across the floodplain. The radius of curvature of the upstream bend became tighter than the downstream bend and the channel migrated at a faster rate on the upstream bend. The downstream bend retracted between 1973 and 2012, becoming shorter and having a lower average radius of curvature.

Date	**Brice Classification**
1886	K
1903	C
1928	F
1963	O
1973	P
2012	P

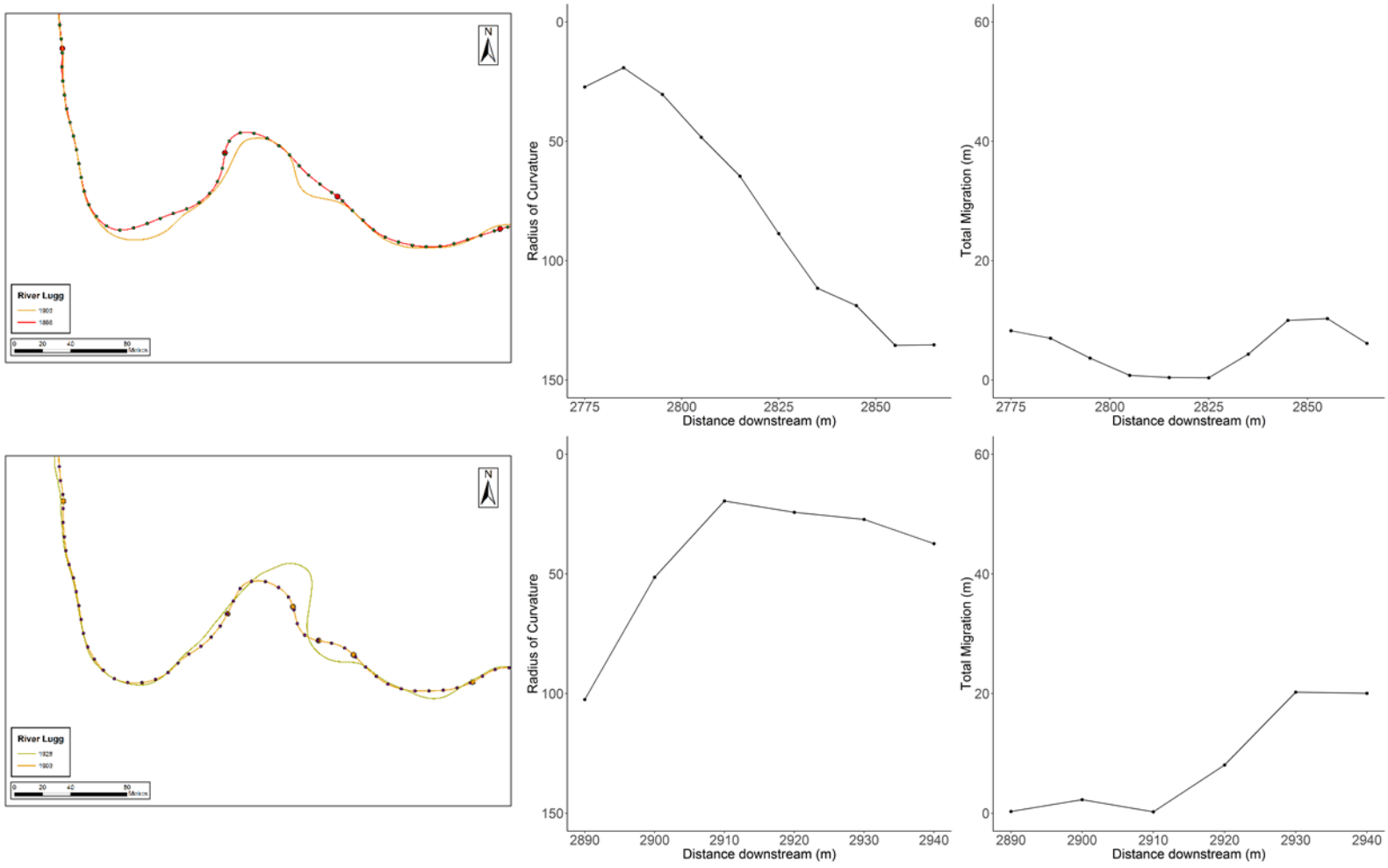

Figure 5.91. Changes to the curvature profile of Bend 22, Reach 5, River Lugg

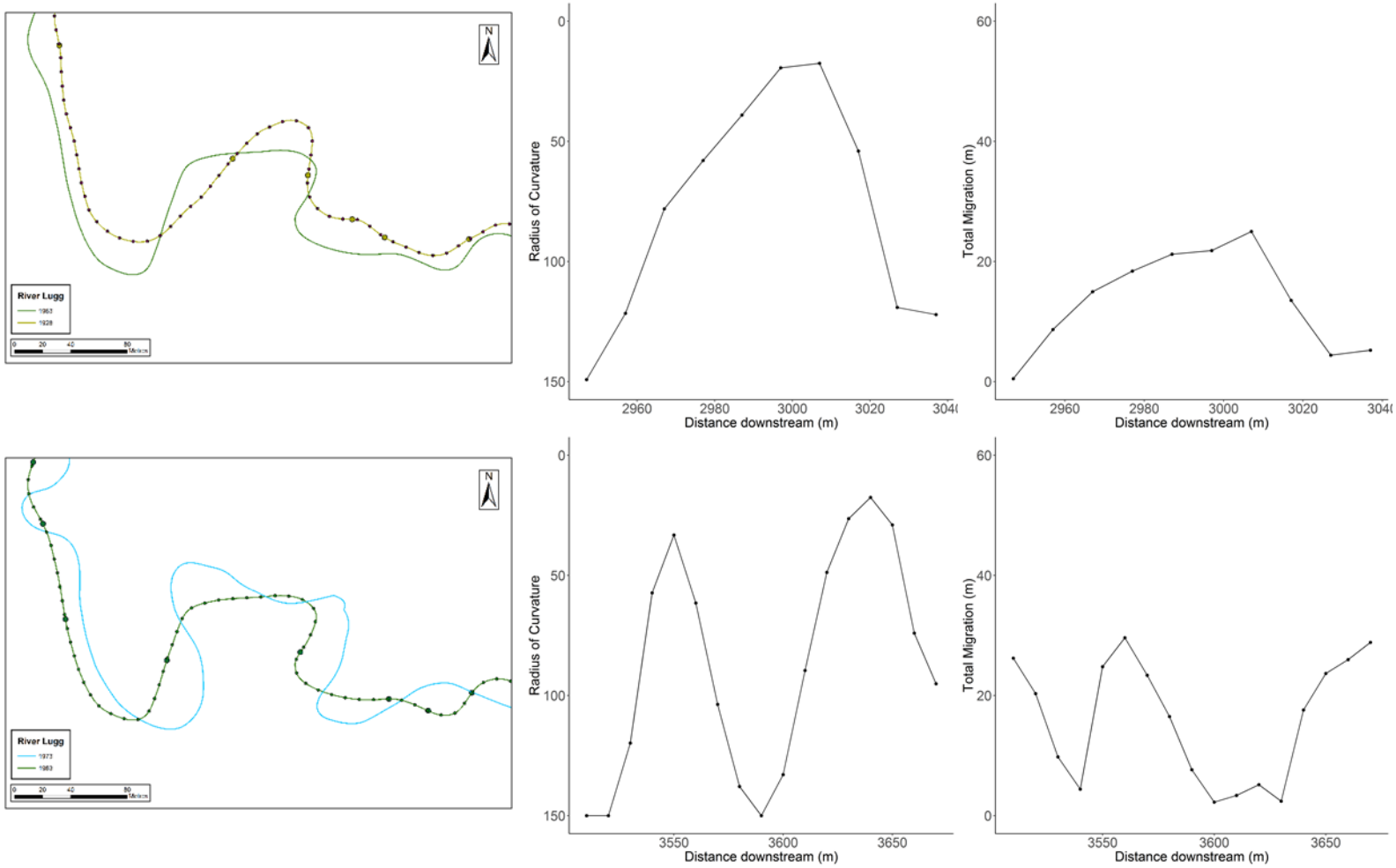

Figure 5.92. Changes to the curvature profile of Bend 22, Reach 5, River Lugg

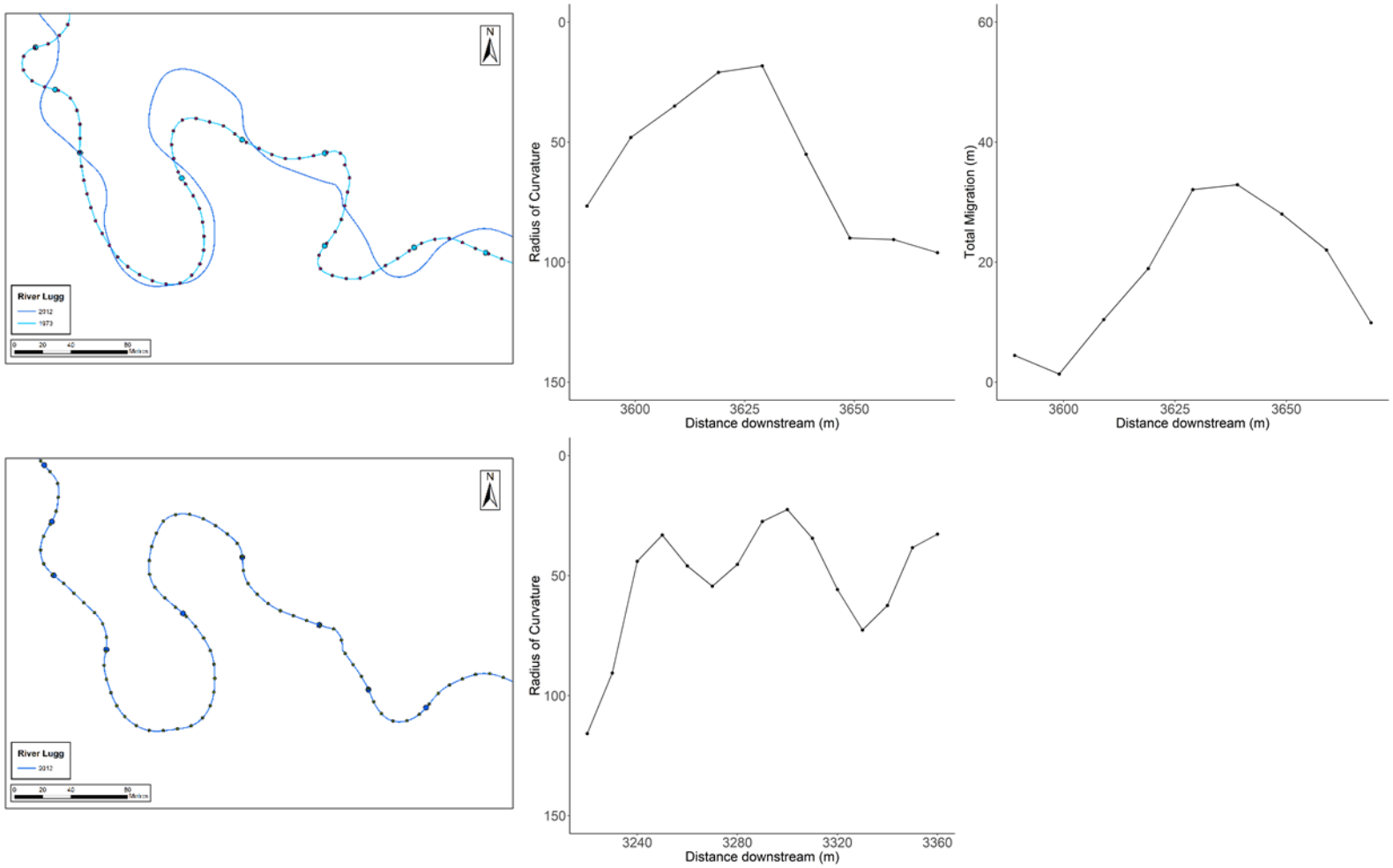

Figure 5.93. Changes to the curvature profile of Bend 22, Reach 5, River Lugg

River Glen, Reach 1, Bend 29 (Figure 5.94 to Figure 5.96)

Bend 29 started as a simple symmetrical bend in 1866, most similar to bend type C from the Brice classification. The curvature profile has five points all with a similar radius of curvature. The bend remained stable between 1866 and 1897, with low amounts of erosion and little change to the curvature profile. The bend became active between 1897 and 1924, with the highest amount of erosion occurring downstream of the apex and the bend started to migrate downstream. The tightest part of the bend shifted downstream during this period and a second apex with a larger radius of curvature was created at the upstream end of the bend. The bend had become compound asymmetric, most like bend type N in the Brice classification. Erosion was limited between 1924 and 1957, however the first apex on the bend continued to develop and became tighter and longer. This made the first apex more distinctive than it had been in 1924. The bend continued to migrate downstream between 1957 and 1965 and the two apices in the bend became more distinct in the curvature profile. Between 1965 and 2012, the highest amount of erosion occurred downstream of second apex. The bend became more rounded during this period and the two distinctive apices were lost from the curvature profile. The best fit for the bend in 2012 was bend type J from the Brice classification.

Date	Brice Classification
1866	C
1897	C
1924	N
1957	N
1965	O
2012	J

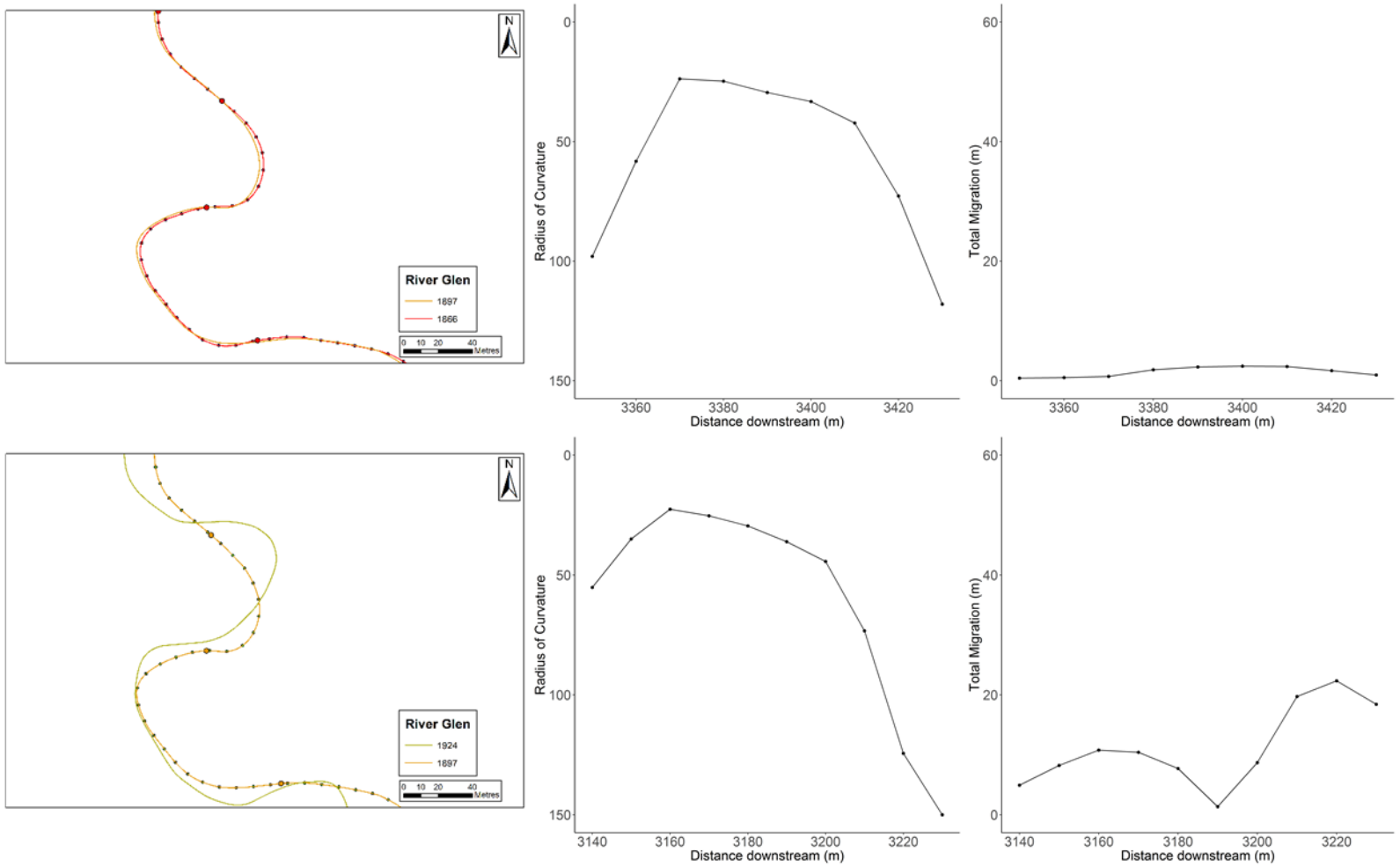

Figure 5.94. Changes to the curvature profile of Bend 29, River Glen

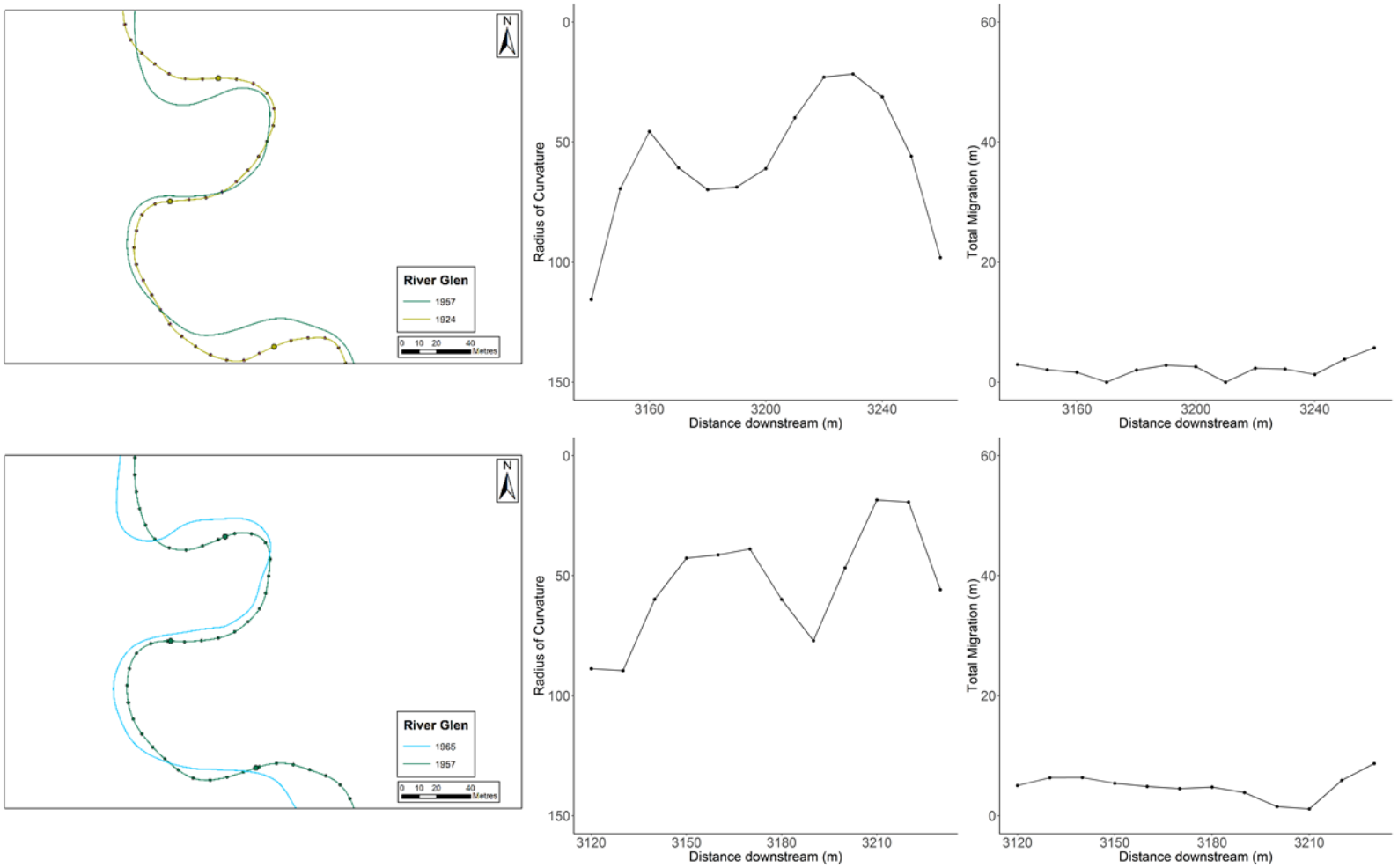

Figure 5.95. Changes to the curvature profile of Bend 29, River Glen

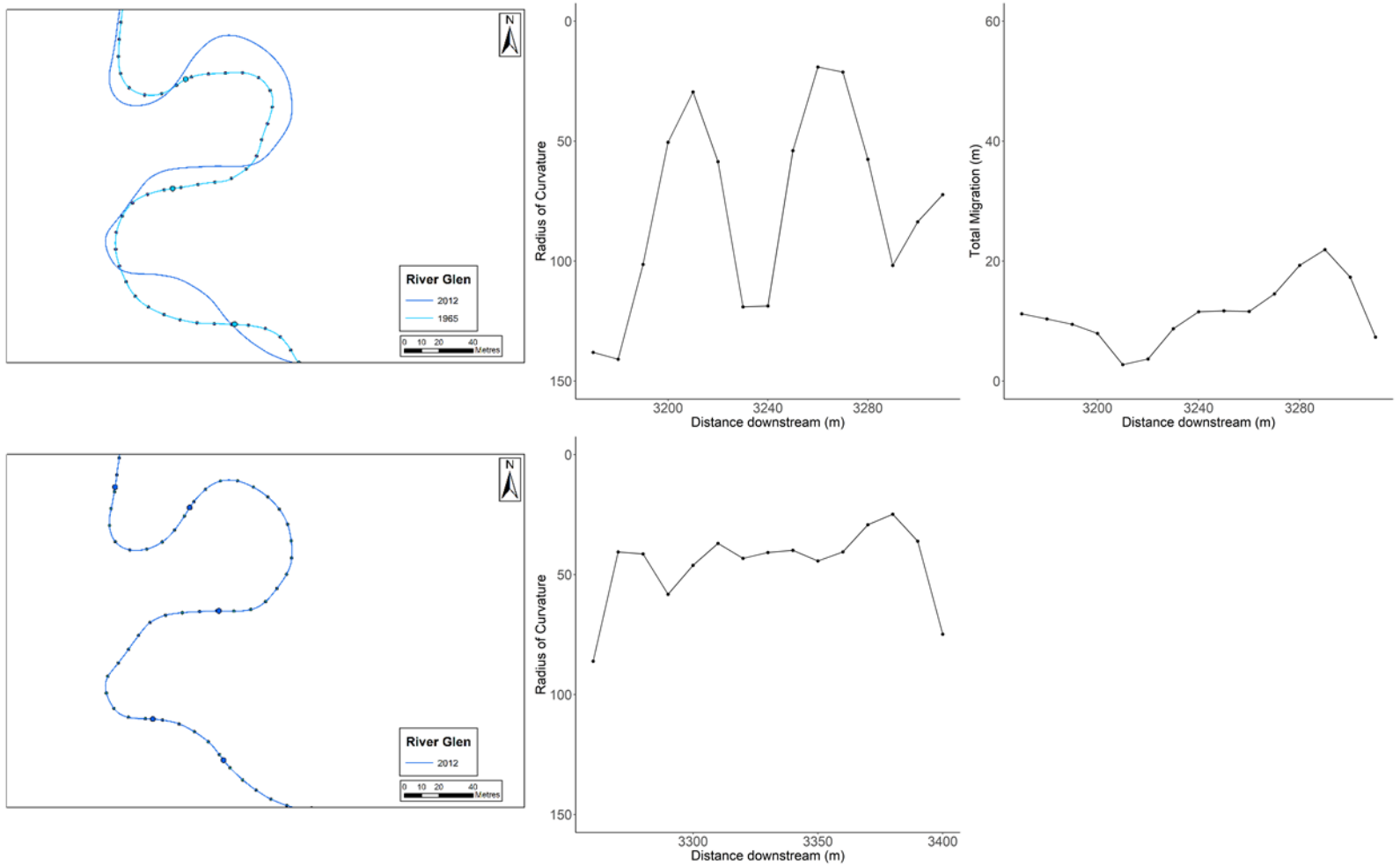

Figure 5.96. Changes to the curvature profile of Bend 29, River Glen

River Glen, Reach 1, Bend 40 (Figure 5.97 to Figure 5.99)

Bend 40 on the River Glen started in 1866 as a simple symmetrical bend, similar to type E in the Brice classification. The curvature profile shows a minimum in the radius of curvature towards the start of the bend, which remained low through most of the bend. The bend was stable between 1866 and 1897 with very low amounts of erosion and no change to the curvature profile during this period. Between 1897 and 1924, the preceding bend experienced a neck cutoff, which also affected part of bend 40. The minimum radius of curvature increased during this period and the start of the bend became much straighter. The bend started to grow across the floodplain as the river channel was readjusting to the cutoff. The bend type changed to bend type D after the cutoff occurred. The bend migrated downstream between 1924 and 1957, although the erosion was higher towards the end of the bend and two apices began to develop in the curvature profile. Although the total amount of erosion was low between 1957 and 1965, the two apices continued to develop and created a compound symmetrical bend, similar to bend type H. The bend continued to migrate downstream between 1965 and 2012, which led to a more complicated curvature profile in 2012, with potentially three separate apices identified. The bend was most similar to bend type O in 2012.

Date	Brice Classification
1866	E
1897	E
1924	D
1957	D
1965	H
2012	O

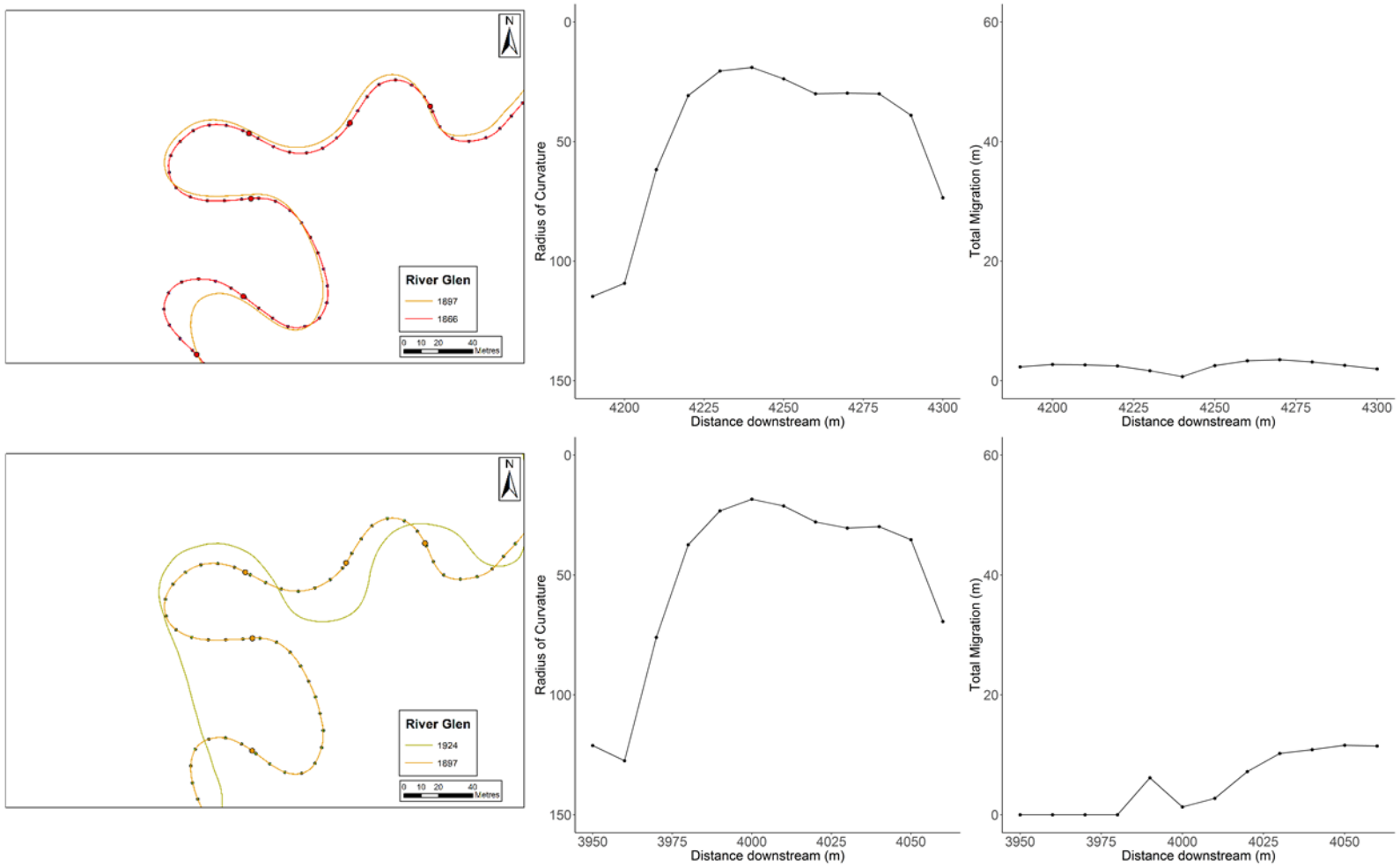

Figure 5.97. Changes to the curvature profile of Bend 40, River Glen

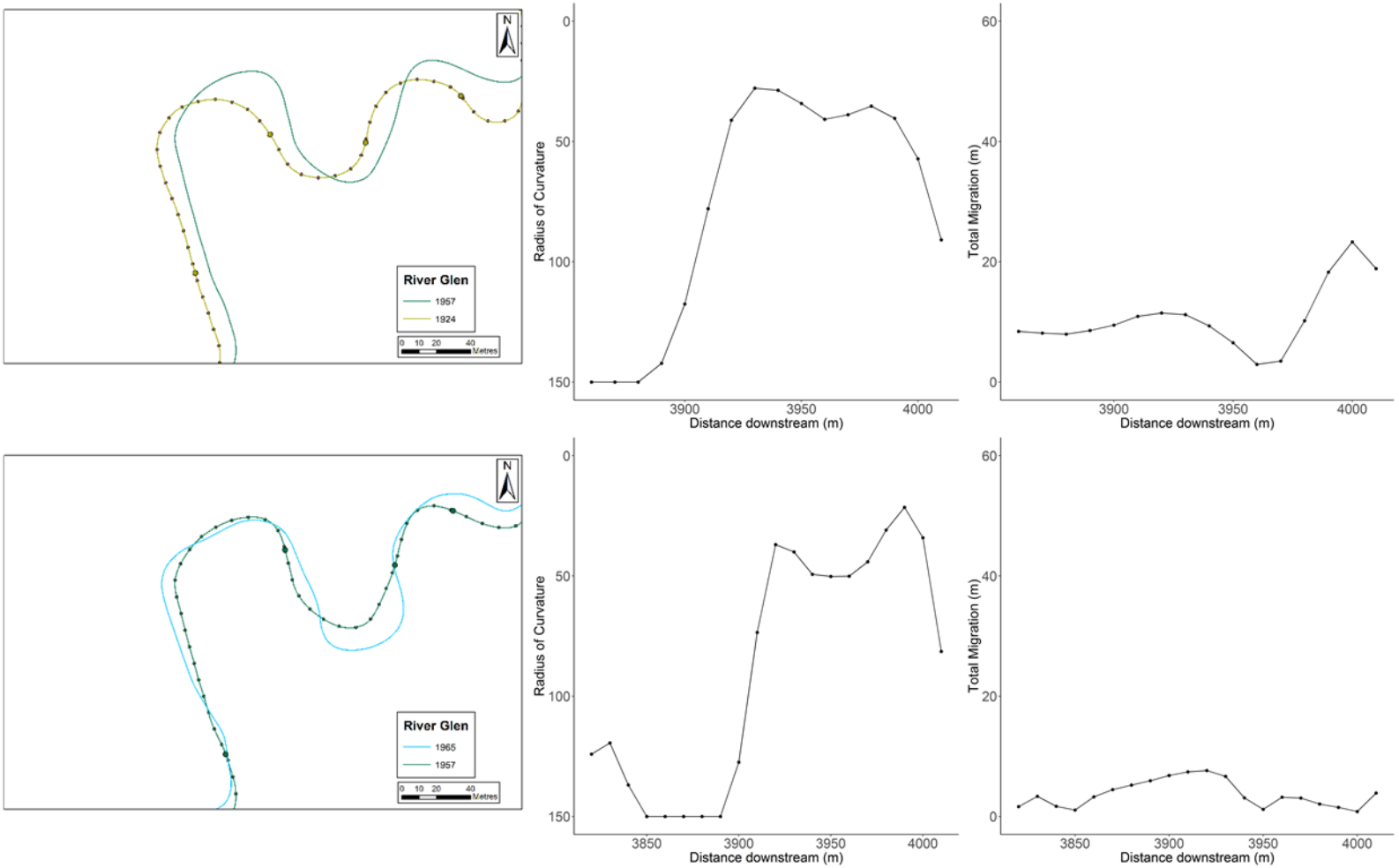

Figure 5.98. Changes to the curvature profile of Bend 40, River Glen

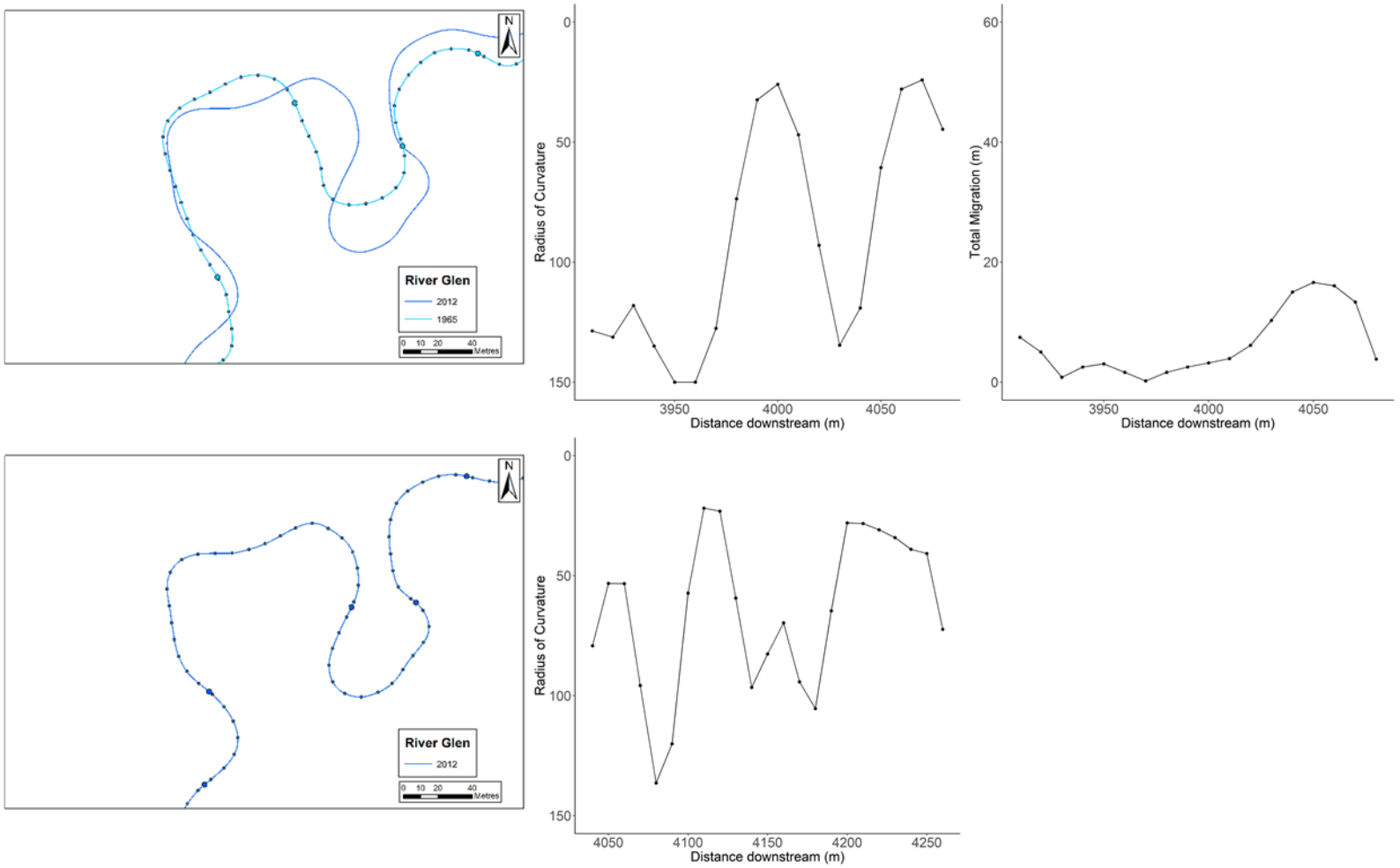

Figure 5.99. Changes to the curvature profile of Bend 40, River Glen

River Glen, Reach 1, Bend 41 (Figure 5.100 to Figure 5.102)

Bend 41 started as a simple symmetrical bend, similar to bend type A or B in the Brice classification. The bend remained stable between 1866 and 1897 and there was very little change to the curvature profile during this period. As with the previous bend, the cutoff seemed to initiate erosion on this bend, with the bend starting to grow across the floodplain between 1897 and 1924. The minimum radius of curvature decreased slightly during this period. The bend type changed from type A or B to type C or D during this period. The bend migrated downstream during the next period, between 1924 and 1957, and the radius of curvature increased both before and after the apex. The bend then switched back to a growth phase between 1957 and 1965 and two apices began to form in the curvature profile. The bend started to become similar to bend type H in the Brice classification. Finally, downstream migration on the previous bend, and growth on this bend produced a compound asymmetrical bend with two distinctive apices in the curvature profile in 2012. The first apex was longer, with five points with a radius of curvature less than 50m, compared to only a single point on the second apex, although the actual minimum value for the radius of curvature was similar for both apices.

Date	**Brice Classification**
1866	A/B
1897	A/B
1924	C/D
1957	C/D
1965	H
2012	O

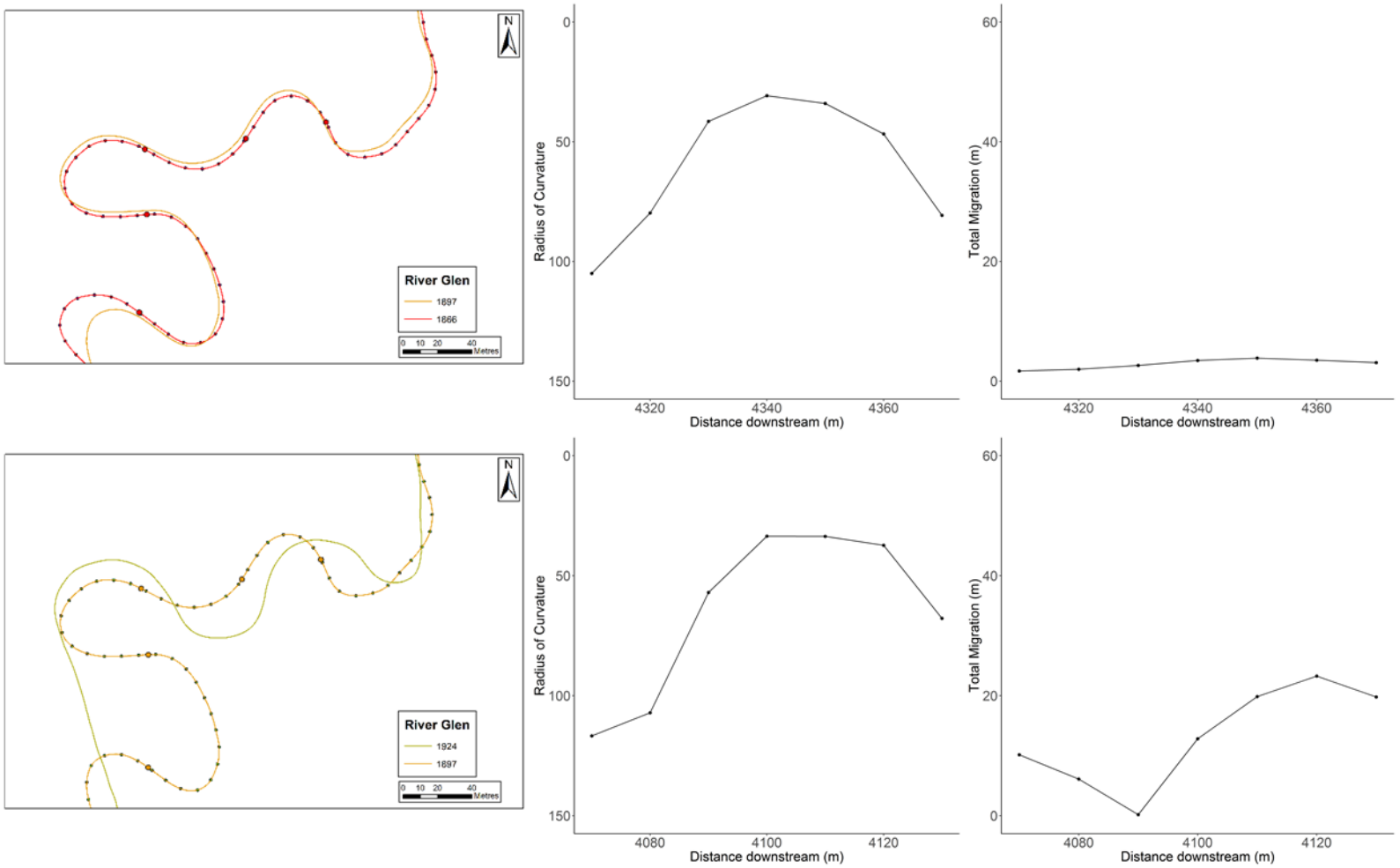

Figure 5.100. Changes to the curvature profile of Bend 41, River Glen

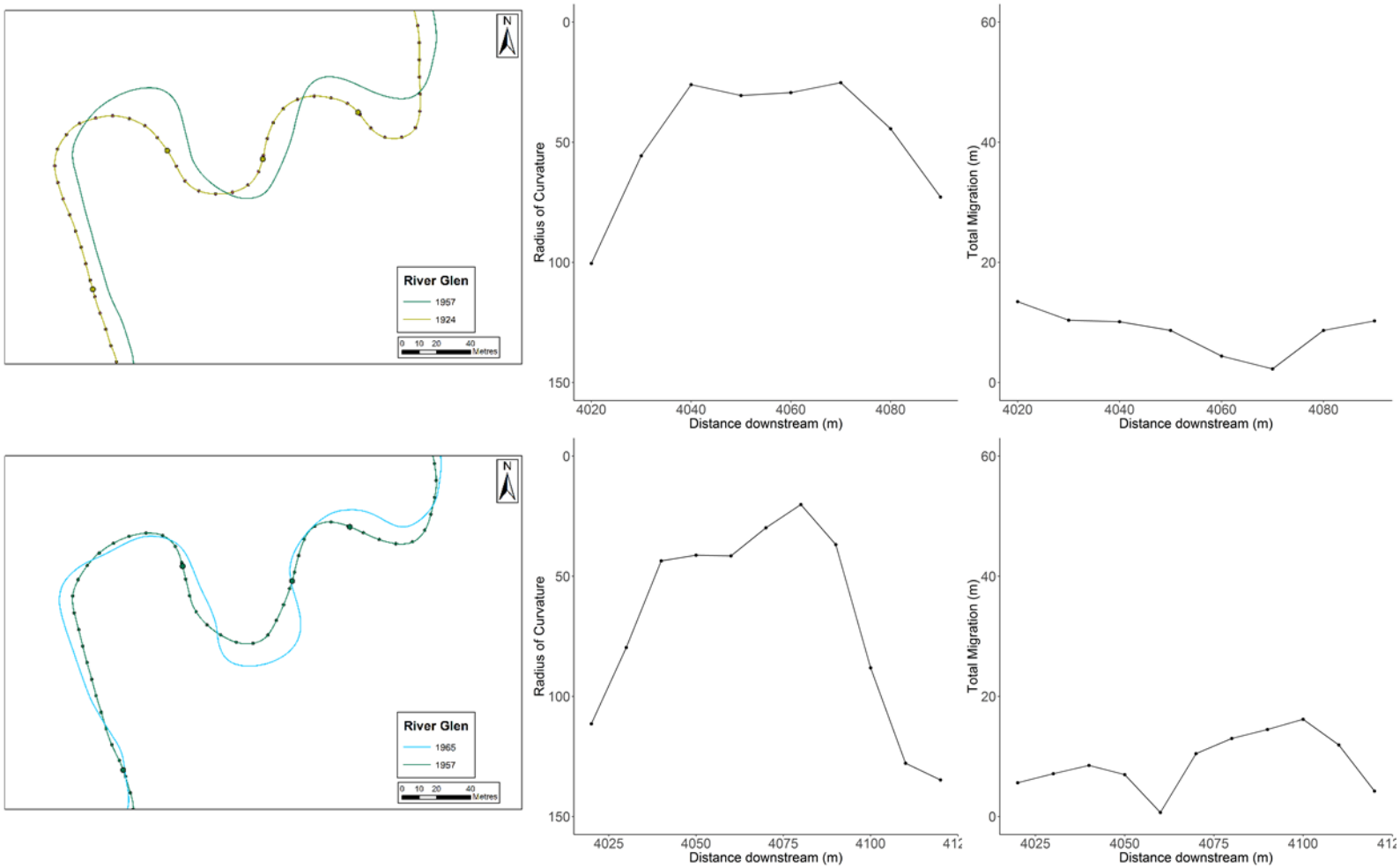

Figure 5.101. Changes to the curvature profile of Bend 41, River Glen

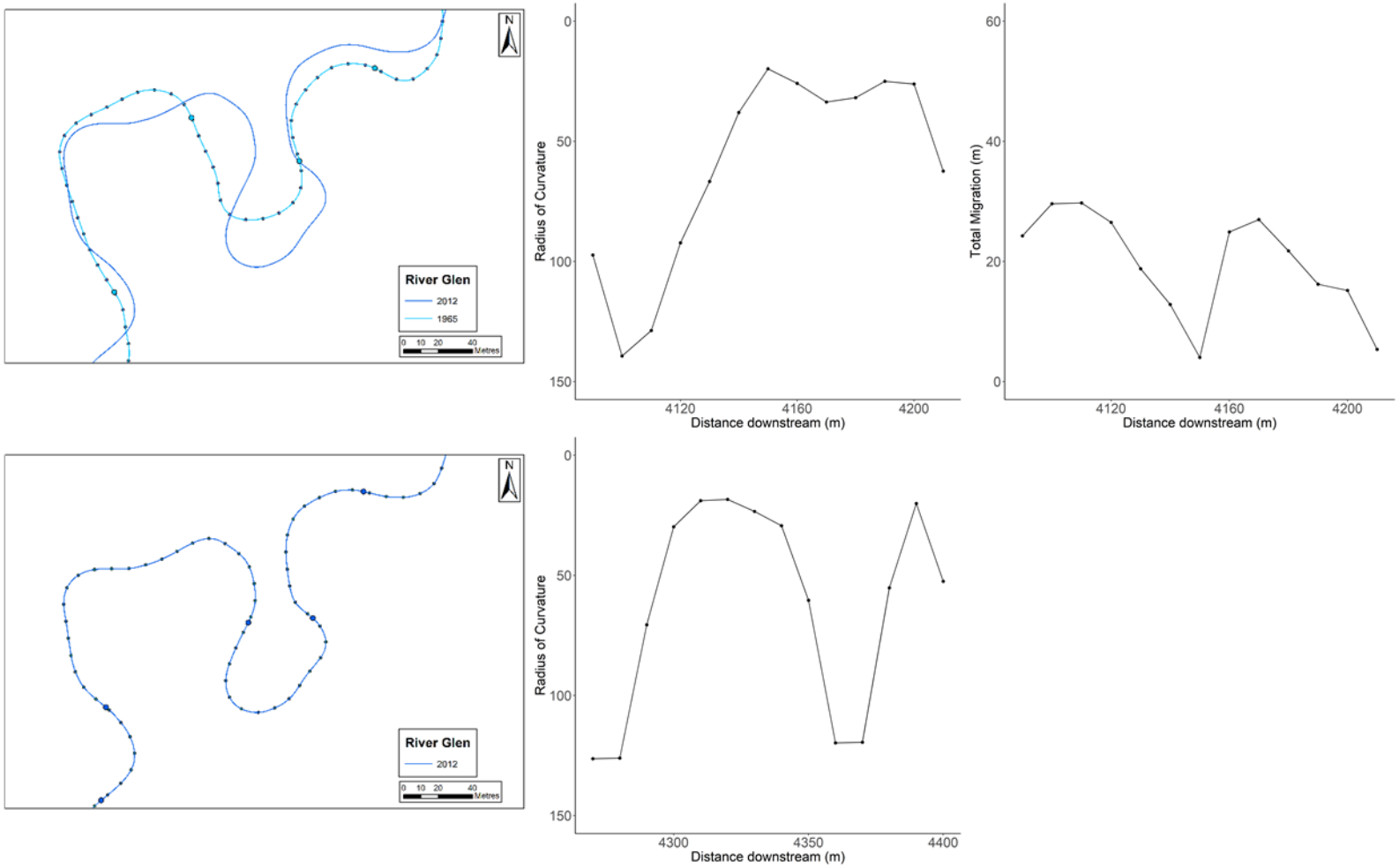

Figure 5.102. Changes to the curvature profile of Bend 41, River Glen

5.4.7. River Bend Evolution through the Brice Classification

Examples of the evolution of individual bends were given above, but the general trends can also be explored within the dataset. Brice (1974) recognised that many bends evolve over long time scales and are unlikely to show changes in the timescales used for this study. However, as shown above some bends did show rapid change in a relatively short period. The ten most active bends from each reach were chosen and the changes in classification from A to P were measured and collated. The totals for each bend classification and the period in which they occurred are shown in Table 5.4. Bend types A and K showed a general reduction through time while bend type O increased from the first period to the last. The bends selected here were biased towards the most active bends that have developed through time from simple symmetric to more complex shapes.

The most common bend type for the bends selected were C and K, both of which had a similar shape, with type C being symmetrical and type K being asymmetrical. Types C, D and K appeared to be the critical point at which the evolution of the bends is determined. Most of the simple of bends with a low amplitude (A and B) tended to develop slowly towards bend types C/D/K through growth at the at the apex of the bend. Once the bends reached this critical point, they tended to follow three different paths. The most common path was to develop towards becoming compound asymmetric. The next most common development path was to develop towards bend types E, F and G. The least common evolutionary

Table 5.4. The total number of bends in each Brice Classification for the different periods.

Brice	1st	2nd	3rd	4th	5th	6th	Total
A	14	13	9	7	5	5	53
B	11	7	10	8	9	8	53
C	14	20	17	16	17	20	104
D	11	9	11	16	15	14	76
E	3	3	2	1	3	4	16
F	3	4	5	3	3	2	20
G	1	1	1	2	1	1	7
H	2	2	3	2	5	5	19
I	0	0	0	0	0	2	2
J	0	0	1	1	0	2	4
K	23	19	18	22	13	8	103
L	0	0	0	0	0	0	0
M	11	11	7	6	5	4	44
N	2	4	5	1	5	6	23
O	3	5	9	11	15	15	58
P	2	2	2	3	4	4	17

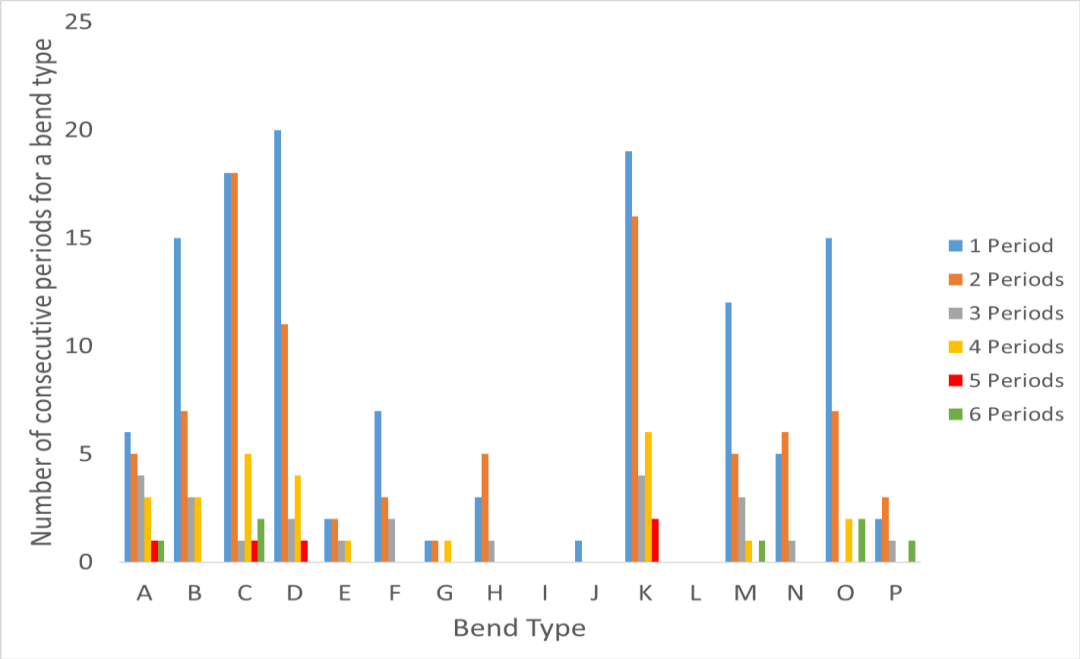

Figure 5.103. The number of consecutive periods that each bend type remained as the same type before developing, indicating the level of stability of the different bend types

development was towards compound symmetrical. The compound symmetrical bends accounted for less than 5% of the total bend types measured. Some of the bends that became compound symmetrical developed later to become compound asymmetrical, usually caused by differing rates of erosion for the two different apices.

The evolutionary cycle of the bends tended to terminate at different points depending on which path was followed after reaching the critical point at C/D/K. The bends that followed the path F→E→G tends to terminate at G and not become compound symmetrical or compound asymmetrical. The bends that were type G terminated through neck cutoffs usually. However, this type of evolution of path was not common for these rivers. The most common compound symmetrical bend was bend type H, which was often the end point for bends that developed along this path. The bends would become simpler through cutoffs or with higher erosion on one of the apices to become bend type K. In two instances the bends became compound asymmetric due to uneven migration on the limbs of the bend (see Figure 5.102 for an example of the transition from bend type H to bend type O). These bends also seemed to be influenced by migration occurring on the bends upstream and downstream of the individual bend. Once the bends became compound asymmetric (bends types M to P) they tended to cutoff and become simple symmetric bends.

It was also possible to preliminarily investigate how long a bend type remained in that shape as they developed. It was not possible to express the length of time in years, but it was possible to look at the number of consecutive map dates with the same bend type. The most stable bend type was type A (mean consecutive periods = 2.63, n = 19), while the least stable bend type (with more than five occurrences) was type F (mean consecutive periods = 1.58, n = 12). The compound asymmetric bends M, N and O all lasted for less than two consecutive periods on average (1.86, n = 22; 1.67, n = 12; 1.88, n = 26 respectively), but bend type P was more stable with an mean consecutive period length of 2.25 (n = 8). Figure 5.103 shows the total numbers for each bend and how long they remained as they same bend type. The majority of bends remained as the same bend type for only one or two periods before adjusting. It should be noted that the bends used in this study represent some of the most active bends in England and therefore the transitions between the different bends types are likely to occur more rapidly than for most bends for similar size rivers.

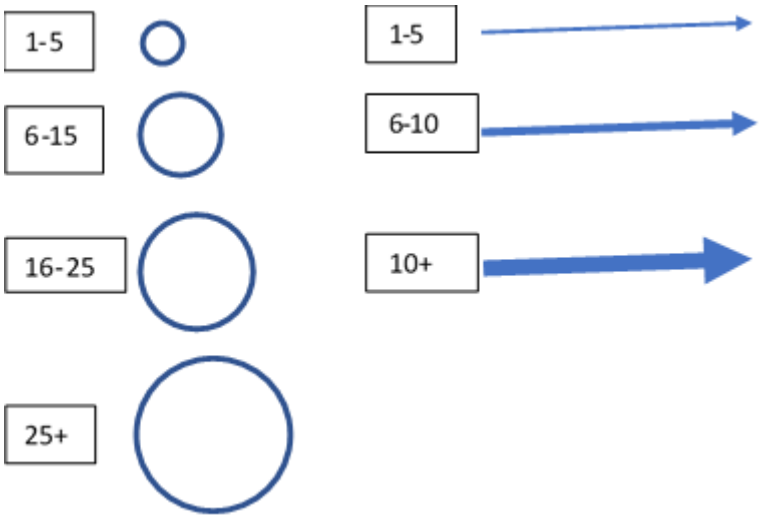

Figure 5.104. Scale circles and arrows used to indicate the number of bends that remained as the same Brice classification from one period to the next (circles) and the number of bends that changed to a new classification and which classification they became (arrows)

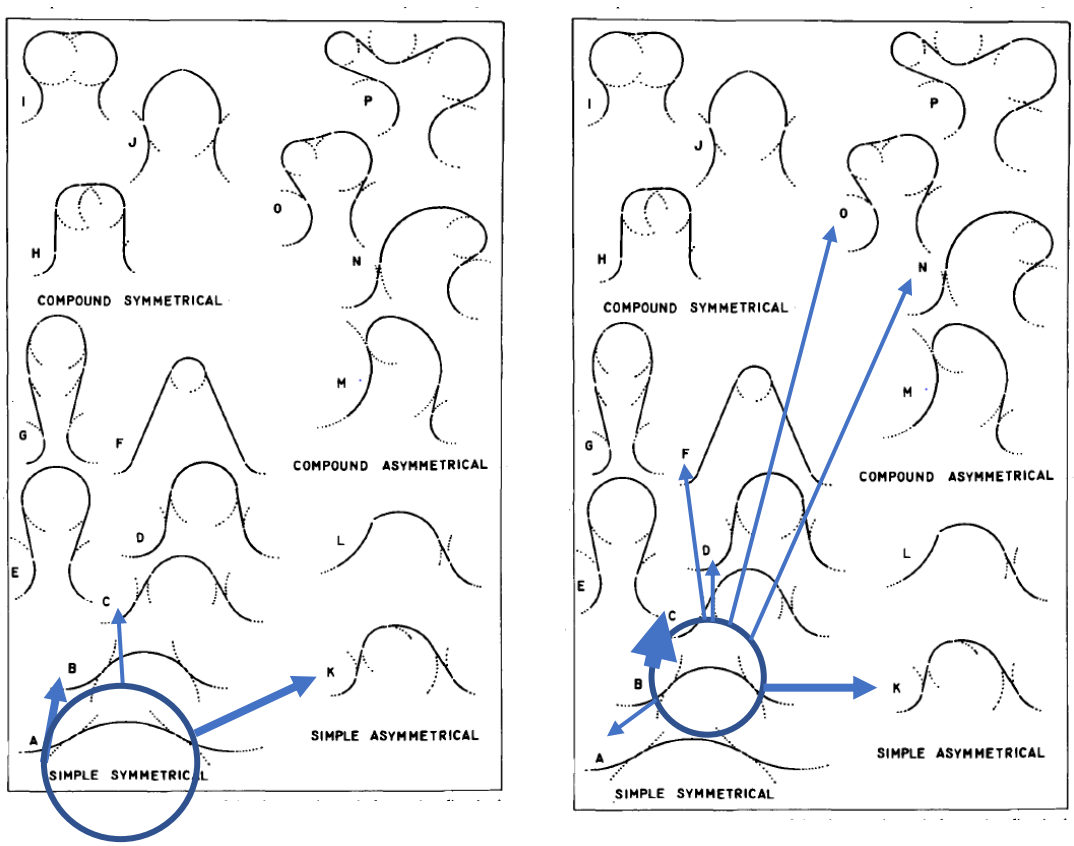

Figure 5.105. The transition path for bend types A and B. Many of the bends remained as the same bend type for at least one period. The simple bends tended to move to the next bend type along the evoluvtionary cycle, with some bends becoming asymmetric as they altered through time.

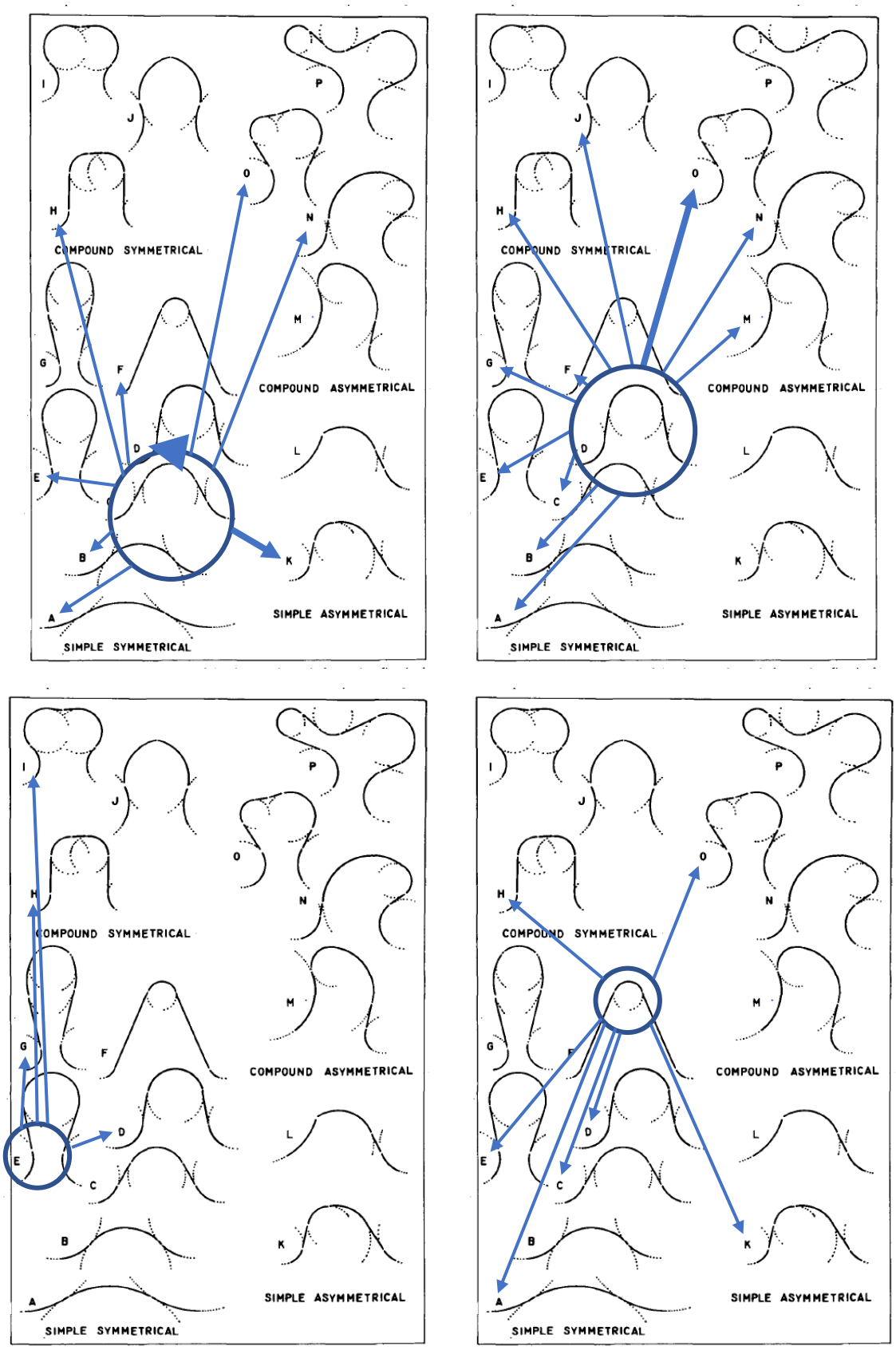

Figure 5.106. The general trends for bend types C, D, E and F. Bends C and D appear to be key points in the evolution of a channel, at which the bends can follow multiple different paths. Bends E and F were less common, although bend F did develop in a variety of ways. These tended to be single bends following that route.

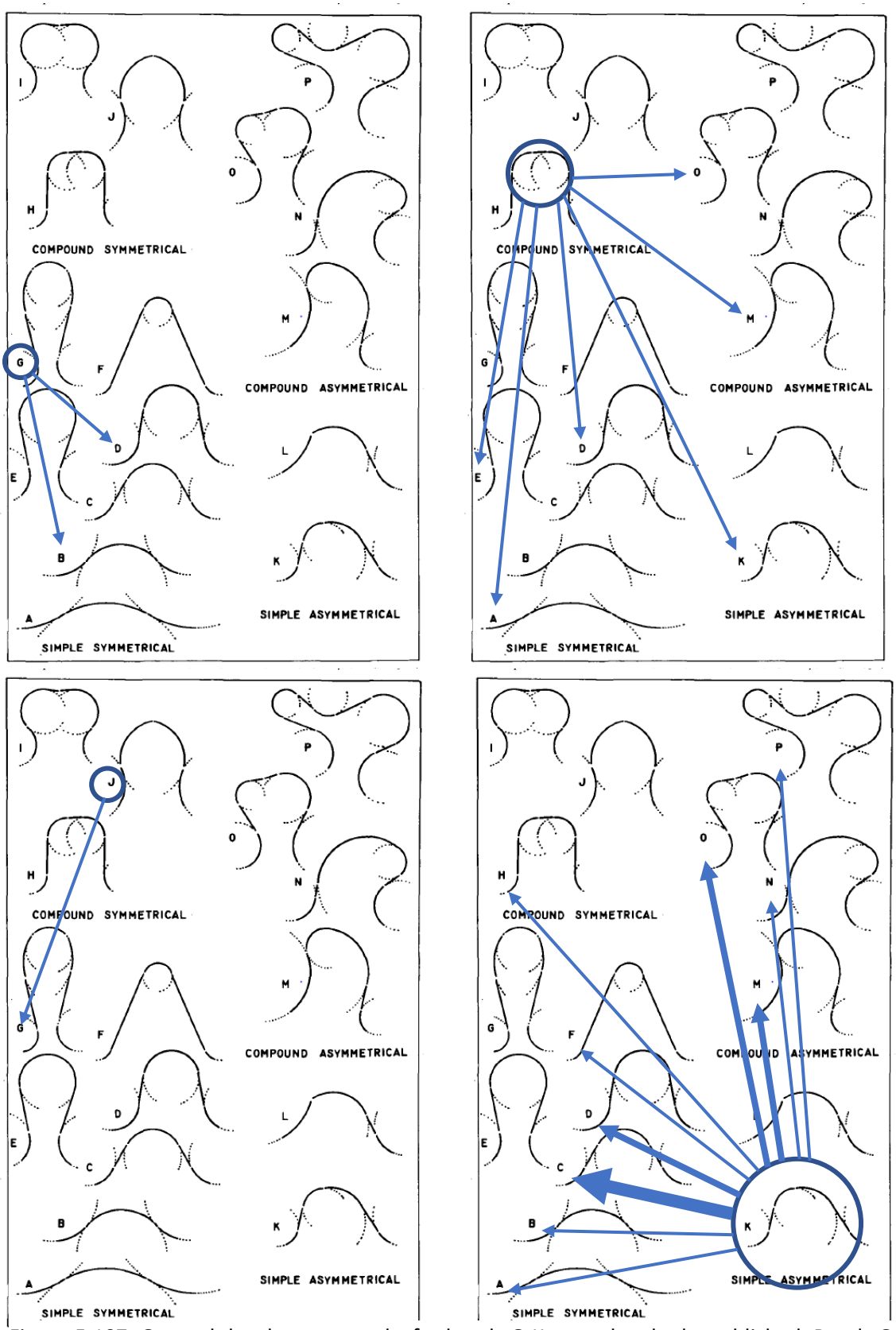

Figure 5.107. General development paths for bends G-K once they had established. Bends G and J were uncommon, and generally became simpler when they evolved. Bend H could either become compound asymmetrical or return to simple symmetric. Bend K was another key bend in the evolution development. It was the asymmetrical form for bend C and D but tended to evolve towards compound asymmetry.

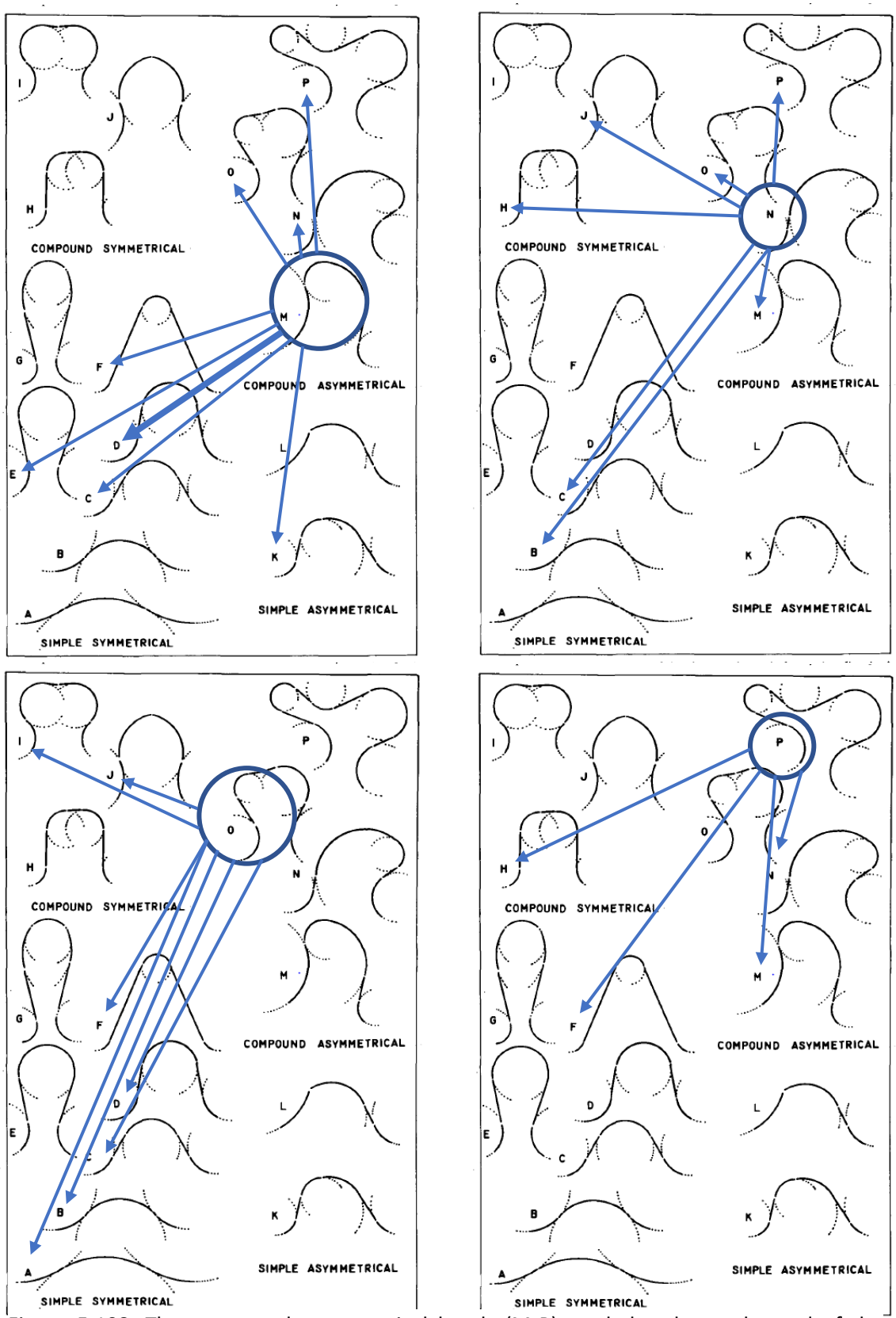

Figure 5.108. The compound asymmetrical bends (M-P) tended to be at the end of the evolutionary development of the bends and subsequently cutoff and became simpler. Bends M and N could develop towards O and P as the bends developed two distinct apices or become simpler through cutoffs. Once the bends reach O or P they tend to cutoff and become simple symmetric bends.

5.5. Discussion

5.5.1. Relationship between channel curvature and migration rate

The relationship between channel curvature and migration is complex. Hickin (1978) suggested that there is a non-linear relationship between channel curvature and migration rate, with a growth phase in the migration rate once a certain threshold in bend curvature is reached. Envelope curves were produced by Hooke (1997) for rivers in the United Kingdom and United States, which showed an acceleration in the migration rate of bends as the r_m/w values became less than 5.0, reaching a maximum at 3.0. The previous chapter discussed issues around calculating the migration rate from maps dates with a different length of time between the dates and the tendency for the shorter periods to have a higher erosion rate. There appear to be two separate domains created due to this effect, with the shortest period having much higher migration rates. Only on Reach 1 and 2 for the River Lugg this effect does not seem apparent. The rates of movement measured for the shortest period are up to 0.5 widths per year, which is much higher than any of the rates measured by Hickin and Nanson, or Hooke. When the shortest period is removed from the dataset the maximum rate is around 0.2 widths per year, which is more similar to the rates presented by the previous authors.

Leopold and Wolman (1960) found that a large proportion of the bends measured on 50 different rivers had a bend curvature between 1.5 and 4.3. In this study, bends with a minimum bend curvature of 4.3 or less accounted for 84.5% of all bends in the study reaches. This suggests that it is rare for river bends to maintain a straight channel and that there is an equilibrium value for bend curvature in natural channels. Hickin (1974) suggested that bends with a high bend curvature experience a super-elevation of the water surface and a deepening of the channel at the outer bank, increasing the flow velocity and leading to erosion. Once the r_m/w value has decreased to 5.0 this process dominates the erosion dynamics of the river until a threshold is passed at $r_m/w = 2.0$. Once this threshold has been passed, Bagnold (1960) argued that a strong separation zone is created, which effectively reduces that channel width and increase the resistance to flow throughout the bend. These patterns appear present in the study reaches with an increase in the migration rate once the minimum bend curvature is below 5.0, before reaching a peak between 2.0 and 3.0 and declining as the bend became tighter past this point.

The theoretical work that developed during the 1980s from Ikeda et al. (1981), Howard and Knutson (1984) and Furbish (1988) suggested that migration rate was an

integration of the upstream curvatures and there should be a phase lag between the minimum radius of curvature and the maximum migration rate. The spatial distance between the transect with the minimum radius of curvature and the transect with the maximum migration rate was measured for all of the bends in the study and subsequently sorted into the four Brice classifications of simple symmetric, simple asymmetric, compound symmetric and compound asymmetric. There was no lag apparent between the minimum radius of curvature and the maximum migration rate for three of the classifications, simple symmetric, simple asymmetric and compound asymmetric. The maximum migration rate was usually located either at the minimum radius of curvature or close to the minimum radius of curvature, either one transect upstream or downstream of the apex of the bend. For the compound symmetric bends there is a slight lag between the minimum radius of curvature and the maximum migration rate in the upstream direction, however there are only a limited number of bends used in this study that are simple symmetric and it is difficult to compare with the other classifications. The lag did not exist for either the short or the long bends in the dataset.

The results in this study suggest the most common type of meander bend change would be through growth of the bend at the apex and that upstream or downstream migration is less common on these rivers. However, there are some other potential factors that could influence the location of the maximum migration that have not been considered in this chapter. The influence of bank material and riparian vegetation was not considered for this chapter but can have an important role in meander dynamics (e.g. Abernathy and Rutherfurd, 1999; Guneralp and Rhoads, 2012). In a homogeneous floodplain the resistance of the bank would be constant, and curvature would have the highest influence on erosion rates in individual bends. However, in heterogeneous floodplains the resistance of the bank material will potentially lead to a change in the location of the maximum migration. Many of the simple symmetric bends were short and they would not be able to migrate much further downstream from the apex of the bend. However, even for the longer bends and the more complex bends there was little evidence of the lag between the minimum radius of curvature and the maximum migration rate.

5.5.2. Channel curvature and migration rate for individual bends

Hooke in her seminal 2003 paper - River meander behaviour and instability: a framework for analysis - proposed a method of analysis using the relationship between

channel curvature and migration rate. Earlier work by Hooke and Harvey (1983) showed that the fastest evolving bends could follow an evolutionary path from their initiation on a straight channel to downstream migration, growth and eventually becoming double headed or compound and finally cutting off. The trajectories proposed were considered as autogenic processes, occurring without any alteration in the conditions on the river system. Different types of evolution could be analysed including stable bends, bends migrating downstream and bends experiencing a cutoff. It is possible for bends to change between these different types of evolution due to a number of factors including land use changes, climate change, human intervention or a major flood event causing a metamorphosis. This change can be accounted for using this method of analysis, as the trajectory would switch to a different attractor. The theoretical trajectories shown in figure 1 were smooth, but it is expected that the actual rates of change will be jerky as erosion is episodic and only occurs when there are competent events.

The bends presented in this study show all the different behaviours suggested by Hooke (2003), including bends that appeared to swap between the different attractors. Bend 6, from Reach 2 on the River Lugg is an example of a bend that changed from being initially stable between 1886 and 1963 before growing across the floodplain between 1963 and 1976 and finally migrating downstream in the final period. The cause of this change in the attractors (from stable to downstream stream migration) was potentially a series of neck and chute cutoffs that occurred downstream of the bend. A large loop at bend 10 was cutoff at the neck and two chute cutoffs occurred. This would have increased in the local stream gradient and this knickpoint would migrate upstream, causing instability and the river to become unstable. The bends that were actively migrating downstream throughout the whole study period showed only small variations in both the migration rate and the bend curvatures and tended to migrate at a slower rate than the bends that experienced cutoffs or grew to become double-headed. The trajectory of bends experiencing a neck cutoff were shown in Figure 5.15. Two of the bends were fairly well developed and stable before the neck cutoff occurred and then subsequently adjusted slowly after the cutoff. Bend 15 from Reach 4 on the River Lugg was active in all of the periods and showed dramatic change, especially after the neck cutoff occurred. Between 1963 and 1974, the channel migrated at over 0.4 widths per year and rapidly grew across the floodplain, eroding into the material deposited between 1886 and 1963. This material could be potentially unconsolidated and could explain why the migration rates were so high after the cutoff occurred.

Despite the length of the study period, it was rare to find bends that had completed the full evolutionary cycle of a neck cutoff bend. This suggests that the full development from initiation on a straight channel to a compound bend and finally a neck cutoff is longer than 150 years, even on the most active bends in the study reaches. Most of the bends that experienced a neck cutoff were already well developed at the start of the study period. Bend 3, from Reach 5 on the River Lugg probably showed the fastest development, developing from a simple channel initially to becoming double headed by 1963 and eventually cutting off between 1963 and 1973. Subsequently the bend curvature became higher and the rate of migration decreased after the cutoff occurred. There were a number of bends that did evolve from a fairly straight initial channel to become compound but had not cutoff at the point of data collection. These bends showed the decrease in bend curvature as the bend developed though the growth and compound phase and an acceleration in the migration rate as the bend developed. Bend 16 from Reach 5 on the River Lugg is a classic example of the evolution from a simple symmetric bend through migration and growth to become compound. The bend became stable between 1973 and 2012 after a series of flood defences and weirs were built in this section of channel and the trajectory switch from trajectory A to trajectory D in the bend curvature – migration rate phase space.

One issue complicating this analysis is the variations in individual channel width between different dates. It was more common for a bend to vary its width during the study period than to remain stable. The variations were large in some cases, with the mean channel width halving between consecutive periods. The bend curvature measurement is dimensionless as the ratio of radius of curvature to channel width, so that rivers of different sizes can be analysed. This, however, means that if the radius of curvature remains stable, but the channel width increases or decreases significantly, the bend curvature will be affected, even if the shape of the bend has not altered. Ikeda et al. (1981) assumed that channel width remained constant in their classical 2D model of meander channels, with erosion on the outer bank balanced by deposition on the inner bank, but the variations in channel width shown in this chapter suggest this is not necessarily true and individual bends can alter their channel width greatly between different periods.

5.5.3. Curvature profiles

Each of the different bends proposed by Brice (1974) had distinctive curvature profiles when the individual radius of curvature measurements were plotted against distance downstream. Bends A to D tended to have one or two points of low curvature around the

apex of the bend, with the radius of curvature increasingly steadily away from the minimum value. As the bends progressed from A to D the mean and minimum radius of curvature tended to decrease as the bend developed. Bends E to G occur when there is an elongation of the simple symmetrical loop. Bends E and G tended to have a very low mean and minimum radius of curvature as the radius of curvature was low for most points in the bend and the peak in the radius of curvature was not as distinctive as for the other simple symmetrical bends. Bend type F tended to evolve with a low minimum radius of curvature at the apex, but straight channel leading up to the bend apex, which led to a high mean radius of curvature.

The compound symmetrical bends (H to J in the Brice classification) showed two or three peaks in the radius of curvature, with a profile that tended to be symmetrical for each of the peaks. Overall, the compound symmetrical bends were rare in the study reaches, accounting for 3.4% of the total number and 4.3% of the total bend length. The relative lack of compound symmetrical bends suggests that either evolving bends do not often produce this shape, or that the shape produced are often unstable and quickly develop into compound asymmetrical bends or the bends experience a cutoff as the bends tended to have a high sinuosity.

The simple asymmetrical bends tended to have one clear peak in the radius of curvature, with one limb of the bend being longer and a lower slope to the radius of curvature profile. The bends were identified that were skewed in either the upstream or the downstream direction. The compound asymmetrical bends also showed asymmetry in the curvature profiles, often with two distinctive minima in the radius of the curvature and a different shape to the profile around the minima. The compound asymmetrical bends tended to have a low minimum radius of curvature but a higher mean radius of curvature as the two apices were connected by a straighter section of channel.

By studying the evolution of individual bends, it was possible to see how the curvature profile of different types of bends changed through time. Brice (1974) suggested that bends would follow a sequence as they developed. In the original paper, Brice thought that the evolution of the bends would occur over long periods, but the evolution was completed within the study period for the fastest migration bends. Many of the fastest migrating bends evolved from simple symmetric through to compound symmetric or compound asymmetric during the study period. The curvature profiles tended to show a similar pattern developing from a single point with a low radius of curvature, to multiple

points with low curvature but still as a single peak. Two minima of the radius of curvature with a small increase in the radius of curvature between the two peaks would develop. It is possible that at this point the extra riffle identified by Hooke and Harvey (1983) has developed on the apex of the bend. It is not possible from this study to know whether the extra riffle developed first, and the two apices develop subsequently, or whether the two apices begin to develop, and this is followed by deposition of a new riffle at the first apex. A more detailed record would be required to determine which process occurs first but could be completed with an annual record of the curvature profile and the location of riffles in the river channel. The two peaks would then start to develop independently, eroding across the floodplain in different directions. If the shape of the bend or the rate of erosion were different between the two apices then the bend would become asymmetrical, while if the shape and rate of erosion remained similar then the bend would produce a symmetrical compound bend. They would remain connected by a section of straight channel, which could eventually form into a new separate bend. Figure 5.111 shows the theoretical development of a river bend from simple symmetrical to compound symmetrical or asymmetrical.

5.5.4. Brice Evolutionary Paths

The bends in this study were used to investigate whether any general patterns of change exist within the Brice classification. The data used in this section of the study is biased towards the fastest moving and most active bends as they were the bends that showed enough change in the relatively short time available from historic mapping. It is also limited by the number of data points available, meaning that some of the bend type changes may not be recorded. Despite these limitations it was possible to some general trends from the rivers presented in this study.

Initial bend stages: Bends that started as type A tended to remain stable for the highest number of consecutive periods. All the bends only developed towards bend type B, C or K. This indicates that bends with high radii of curvatures are unlikely to adjust rapidly, and the overall change in shape will be limited when they do. Once a bend has progressed to bend type B, there was an increase in the number of paths that the bends followed. The majority of bends progressed to either bend type C or type K, but some bends did start to show more rapid change. The bends that transitioned from bend type B to bend type N and O were not adjusting to a cutoff upstream or downstream but were located on rapidly migrating river bends. On the River Arrow, the bends upstream and downstream were all rapidly adjusting

and the change from type B to type N occurred within ten years. It is clear the shape of the bend is also affected by changes occurring on the surrounding bends.

The critical point for the initial stages of the bend development appeared to be bend types C and K. They were the most common bend type recorded for the bends and accounted for more than 30% of the total number of bend types recorded. The bend shapes are very similar, and bends would often transition from symmetric (C) to asymmetric (K) or vice versa. This would be caused by small variations in the bend profile. Once the bends reached this point, they appeared to follow three different development paths.

Complex bend development: The three different paths seemed to develop towards different termination points in river bend development. Some of the bends stayed as simple symmetric throughout and followed the path D→E/F→G. These bends accounted for 7% of the total number of bends, indicating that for the river systems studied here it is a relatively uncommon path.

Some of the bends developed towards becoming compound symmetric from simple symmetric following either D→H, D→F→H or D→E→H/I or became compound symmetric from compound asymmetric N/O/P→H/I/J. However, this was the least common route as the compound symmetric bends represented less than 4% of the total bend numbers. Three of the bends that were classified as type H developed to type M and O due to uneven erosion rates on the downstream side of the bend.

The most common path was to develop from simple symmetric/asymmetric bends D/K to M/N/O/P. The compound asymmetric bends accounted for 24% of the total number of bends in the study. The bends could develop straight from type D or type K to any of the compound asymmetrical bends, but the most common path was to develop to type M and type O. Some of the bends would develop further once they became bend type M or N towards bend type O and P, but there were no bends that developed from bend type O to P, which suggests these bends were terminating before the two apices can fully develop into separate bends.

Termination of the bends: There were numerous different termination points for the evolution of the bends at which the complex simplified back to become simple bends. The most common reason for a bend becoming simpler was through cutoffs. Once a bend had become compound, the neck continued to become narrower and a neck cutoff tended to

occur before the compound bends could become two independent bends. This indicates the bends are migrating downstream at a higher rate than growth across the floodplain.

On the confined sections of river (Lugg reach 3, Glen and Till) cutoffs still occurred, but the main termination process for the bends was through retraction as the bends were not able to grow across the floodplain, but were able to still adjust in the downstream direction. The bends could become compound when space allowed in the floodplain, but once they were constrained erosion would start to occur on the upstream limb of the bend and the apex of the bend in question would start to retreat from the confinement. These bends would become simpler as this process continued. Bend 16 (see **Error! Reference source not found.**) on the River Till shows an example of this process occurring, before eventually cutting off between 1957 and 1970 after retracting between 1866 and 1957.

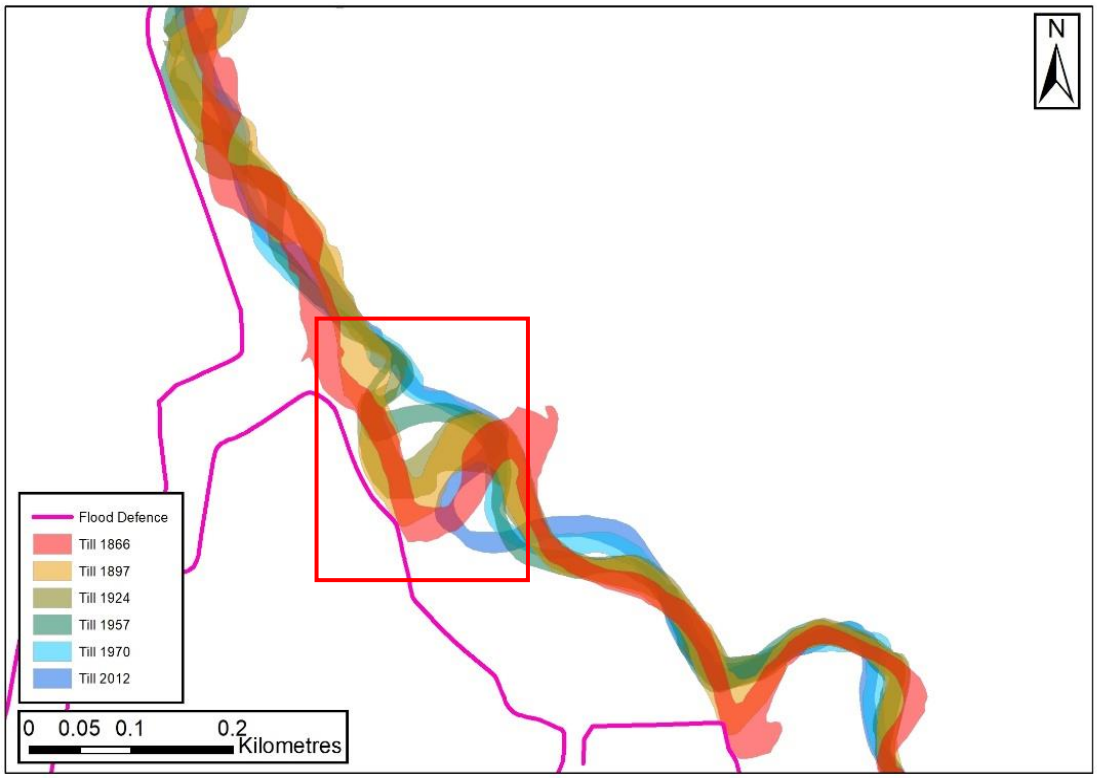

Figure 5.109. Evolution of bend 16 (highlighted) on the River Till. The bend had become confined by flood defences and was no longer able to grow across the floodplain. The focus of the erosion then switched to the upstream limb of the bend and the apex retracted from the position of confinement.

There are several potential reasons for the different evolutionary paths seen on these river bends. One of the most important controls appeared to be whether a bend was confined or not. Bends that were confined were rarely able to form compound asymmetrical bends and the bends were more likely to retract from the apex. On the River Till and River Glen, where the flood defences were constructed prior to 1866 and the confinement was artificial, the compound bends gradually cutoff through the study period, while most of the simple bends did not become compound. For the less confined reaches on the River Lugg and River Arrow there was a wider variety in the forms of bend encountered. Bends that followed the path D→E→G tended to occur when the bends upstream and downstream were stable and the bend was able to grow across the floodplain without the neck becoming too narrow and a cutoff occurring. It was rare for bend type G to develop in sections of river with several consecutive active bends. Where several bends were active the evolutionary path would usually follow D/K→M/N→O/P. This is potentially caused by changes in the flow patterns meaning that the location of the fastest flows is constantly changing, and location of the highest erosion adjust in response. The cross-over point, where the fastest flows switch from one bank to the other would occur early in the bend and erosion would occur on the upstream limb, rather than at the apex. The relative erodibility of the banks will also play an

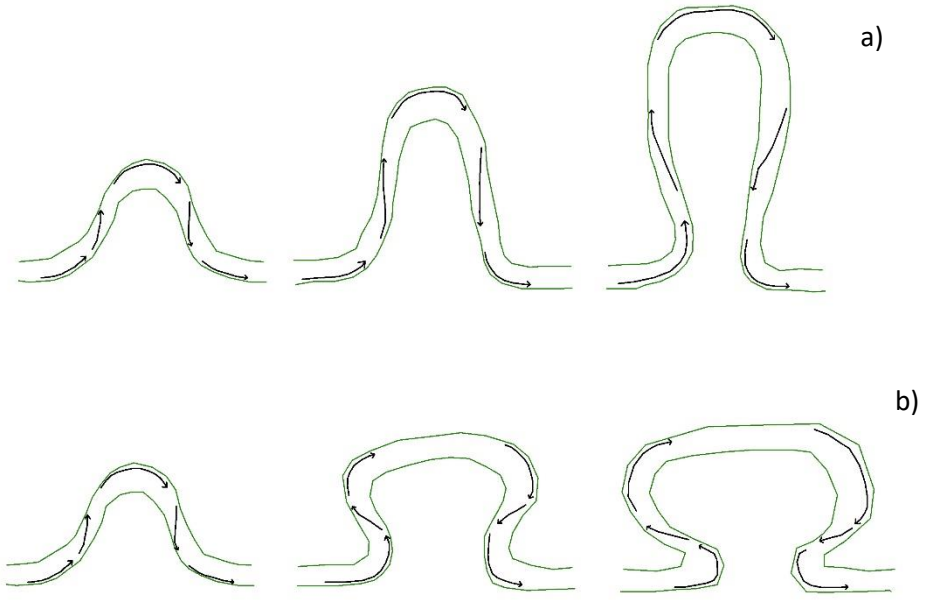

Figure 5.110. a) When the surrounding bends were stable, most of the erosion occurred at or just downstream of the apex of the bend, causing the bend to grow across the floodplain and produce bend type G. b) when consecutive bends were active, the fastest flow velocities would adjust to the migrating bends and become focused upstream and downstream of the apex, causing the bend to become compound. For the rivers studied here the high rate of erosion at the neck of bends meant they cutoff before the bends could become bend type P.

important control on location and rate of erosion and will help explain why for some reaches several consecutive bends are active and why for some reaches only single bends are active.

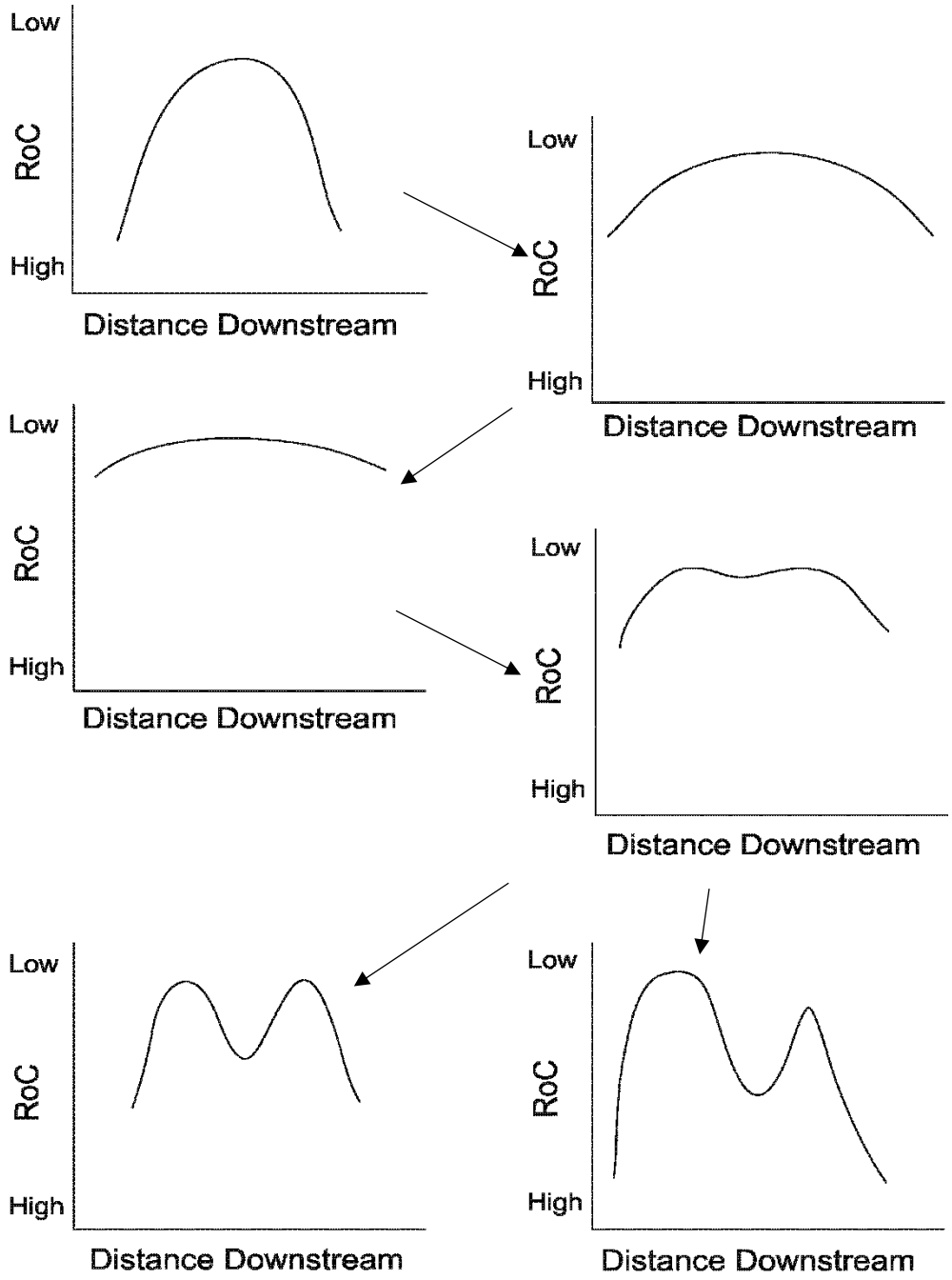

Figure 5.111. The theoretical evolution of curvature profiles as a bend develops from a simple symmetrical bend, to become tighter before two separate apices develop. Once the separate apices have developed, they can behave independently. If they continue to erode at a similar rate then the bend will become symmetrical, or if the erosion rate differs between the two apices then the bend will become asymmetrical

5.6. Conclusion

The results presented in this chapter show that the relationship between channel curvature and migration rate is complex and varies between individual bends, reaches and different time periods. Hooke (2003) showed that a range of different behaviours would be apparent in meandering systems, which is further confirmed by the results in this study. The results also showed bends that could change between different types of behaviour due to a number of different reasons. The change can be caused by human intervention, as occurred on Reach 5 of the River Lugg when the river changed from actively migrating and following the path to a neck cutoff to become stable; or as response to cutoffs and adjustments in the channel slope, as occurred on Reach 2 of the River Lugg when a previous stable bend appeared to become active because of a cutoff that occurred just downstream. Hickin (1974) proposed that there would be an acceleration in the migration rate of bends once the r_m/w values reached 5.0 and reach a maximum at 3.0, if the bends were migrating through a homogeneous floodplain material and not confined by the valley edge. The trend does appear within this dataset, although the acceleration is not as clear as measured by Hickin (1974) and Hickin and Nanson (1978, 1984). There was no evidence of the lag between the location of the minimum radius of curvature and the location of the maximum migration in the large dataset, most of the maximum migration transects occurring on or close to the minimum radius of curvature.

It was possible to see a general pattern in the curvature profile of the fastest developing bends in the study reaches, as they developed from simple symmetric to become compound asymmetrical or symmetrical. Bends would develop from having a simple short apex towards a much longer and tighter apex. Small variations in the curvature would develop, creating two separate minima in the radius of curvature that would then start to act independently. As two apices continue to develop, they would produce that distinctive compound or doubled-headed form that is seen for many rivers across the world.

6. Multivariate modelling of riverbank erosion rates using Boosted Regression Trees

6.1. Introduction

Boosted regression trees (BRT) are an ensemble, machine-learning technique, combining the boosting methods with a conventional regression tree. Breiman et al. (1984) and Hastie et al. (2001) describe regression trees statistically. The approach iteratively partitions the data into two subsets, determined by a threshold in the explanatory variable. The split that generates the most homogeneous subsample is selected. For continuous variables, the deviance is used to measure the homogeneity of the subsample (Crisci et al., 2012). The number of splits or interactions determine the complexity of the individual tree. A weak point of regression trees is the sensitivity to changes in the training dataset. Small changes in the dataset can change the model structure substantially (Crisci et al., 2012). Figure 1 shows the conceptual schematic of a regression tree, with two predictor variables X_1 and X_2, used to determine a response variable, Y. The threshold at each split, S, determines the direction of a subset of the data. In *Figure 6.1*, there are four splits, with predictor X_1 appearing in three of the splits and X_2 appearing at one node.

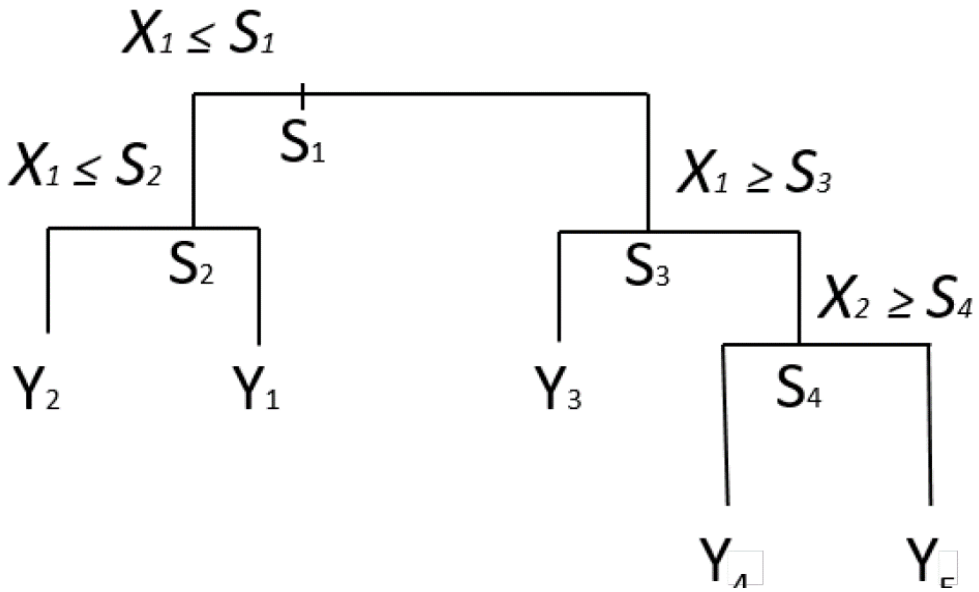

Figure 6.1. Schematic representation of a regression tree with two predictors (X_1 and X_2), which determine the response variable (Y). The thresholds are denoted by S. The TC for this example is 4. From Evans (2018).

To overcome this limitation, boosting methods have been applied to regression tree analysis to improve the predictive performance of the models. It is based on the idea that it is easier to find and average many rough predictions, rather than finding a single, highly accurate predictive rule (Elith et al., 2008). Boosting is an iterative, stagewise procedure that attempts to minimise a measure of the loss of predictive performance. The first boosting algorithm was called "Adaboost.M1" by Freund and Schapire (1997). The loss function is a measure of the loss predictive performance due to a suboptimal model. In this chapter, the deviance is used as the measure for the loss function. The first regression tree is the one that reduces the loss function by the maximum amount. The following trees focus on reducing the residuals, i.e. the variation not yet explained in the model. The residuals are calculated by subtracting the expected value from the actual value. The new tree can have different variables and structure from the previous tree and the model is updated to include the two trees. The residuals from this new two tree model are calculated and then loss function is minimised again in the third tree. The existing trees are left unaltered as the model is enlarged, hence the stagewise procedure. The final model is a linear combination of many trees. The best performance is achieved if the model moves slowly down the loss function gradient, controlling by a learning rate (LR) that is substantially less than one (Elith et al., 2008). The learning rate controls how quickly the model tries to correct the error in the model. Since the purpose of boosting is to create a sequence of many weak classifiers (regression tree models in this case), a low learning rate is used (Hastie et al., 2009). A variety of response types can be used in BRT models; in this chapter both a Gaussian type response variable and a binomial response (i.e. an indication of a stable or active bank) variable will be used. The mathematical details for the different distributions used are provided by Ridgeway (2006), including the calculation for deviance.

Elith et al. (2008) described some of the important features of BRT models. The process is stochastic, meaning that only a random subset of the data is used to fit each tree (Friedman, 2002). The proportion of the subset is user defined, usually between 0.5 and 0.75 and is known as the bag fraction in the code. This means that the models are subtly different each time they are run, and predictive performance is improved. The second feature relates to the stagewise procedure used, with the process building on the previously fitted trees. This means the model focuses on the hardest observations to predict. In the code provided by Elith et al. (2008) and Elith and Leathwick (2017), there are two important parameters controlled by the user: The learning rate (LR) or the shrinkage parameter controls the

contribution of each tree to reducing the deviance of the model. The tree complexity (TC) controls the number of interactions allowed in each tree. A TC value of one means there is a single decision stump and two terminal nodes, a TC value of two allows for a two-way interaction. These two factors then control the optimal number of trees for the best prediction. BRTs can cope with missing data, do not require scaling for real variables and are able to use a mixture of categorical, discontinuous and continuous data.

BRT models have been used in ecological studies over the last ten years since first described by Leathwick et al. (2006) and Elith et al. (2008). Often the researchers would explore the distribution of fish species and understand the importance of different factors in controlling the distribution and abundance. Pittman et al. (2009) used LiDAR bathymetry to model the distribution of fish and corals in the coastal zone of Puerto Rico. Buston and Elith (2011) used BRT analysis to determine the reproductive success of clownfish pairs. Carslow and Taylor (2009) used BRT to explore the sources of nitrogen oxides at an international airport and found that good explanatory models could be developed. Youssef et al. (2016) and Park and Kim (2019) used BRT models to produce landslide susceptibility maps and compared the approach with different machine learning and statistical approaches. Both found high levels of predictive accuracy using the BRT approach (over 85% correctly classified landslide locations). Finally, Evans (2018) used BRT, alongside other machine learning techniques, to explore internal and external saltmarsh dynamics on the east coast of England.

This chapter attempts to use the statistical modelling approach, BRT, to predict the location and rates of migration for bends in the Lugg, Ribble and Till catchments. The model is developed using historic migration rate between the 1970s and present day based on the data developed in Chapter 4. Multiple datasets were created for potential explanatory variables and used to evaluate the predictive performance of the BRT approach. The purpose of this chapter is to develop a model that uses factors that are easily measured from remote data sources and could be applied across a large spatial area, with the aim of helping river managers to determine how to target resources efficiently.

6.2. Methods

Fourteen potential predictor variables were selected as likely to provide information on the distribution and rates of river bend migration based on the literature reviewed at the start of this thesis. All of the variables had to be available from remote data sources without the requirement for field collection so the approach could be applied at a catchment scale. Three response variables were to represent the location and rate of bend migration. The first two represent the mean and maximum migration rates of individual bends, calculated using the approach applied in the previous two chapters. The width-averaged rate was used so there was no issue of scale between different size rivers used in this study. A $\log_{10}$ transformation was performed on the migration rates, so that the response variables represented a normal distribution. The third response variable was used to classify whether a river bend was active or stable. Using the width-averaged maximum migration rate, a threshold of 0.046 (which corresponds to 4.6% of the channel width per year) was applied. This threshold represents the top 10% fastest migrating bends in the dataset. Any bend that was above this threshold was classified as active and any bend below the threshold was classified as stable.

In total there were 1081 bends across three catchments and eight rivers. The study reaches included all of the sections used in the previous chapters, and included extra sections on the River Lugg, River Arrow and River Till. Four rivers were included from the River Ribble catchment, the River Calder, River Loud, Skirden Beck and Holden Beck, which had been identified as being laterally active after discussion with the River Ribble Trust. The first bend was removed from each dataset as they did not contain a complete record of the bend, and any bend that experienced an avulsion through a chute or neck cutoff was removed from the dataset. This left a total of 1015 bends. From within this remaining dataset, 200 bends were selected as the evaluation dataset using a uniform random distribution, leaving 815 bends in the training dataset.

The study period was between the 1970s and 2010s. The map data available from the 1970s had the best spatial coverage and had the highest resolution. There was also a wide coverage of aerial photographs available from this period from the Ordnance Survey, meaning the map data and aerial photography data were taken from similar times. Although there are aerial photographs from later periods, the uncertainty in the migration rate, as discussed in Chapter 4, meant that a longer-term approach was taken. The period covers around 40 years. Biron et al. (2014) defined a mobility space called M_{50}, which represents the

predicted rate of erosion over a 50 year period based on the extrapolation of past migration rates. The 40 year period used in this study represents a similar length of time and could be used to define the space required for the rivers to freely migrate in the future.

6.2.1. Existing data sources

The intention of this chapter was to apply to remotely sensed data at a large reach to catchment scale, without the need for extensive fieldwork, to predict riverbank erosion rates and distributions. The aim was to use data that is either freely available or widely available at a low cost. The main data sources are:

- current and historic Ordnance Survey maps, available from Digimap.
- historic aerial photographs for the study reaches, available from Historic England.
- current aerial photographs, available from Digimap
- 1m and 2m LiDAR derived digital elevation model (DEM), available from Environment Agency
- 5m DEM, available from Digimap. The LiDAR DEM was used for most of the study reaches as it provides higher accuracy data but was not available for the River Loud.
- Drift material and bedrock geology, available from British Geological Survey.
- Buildings, flood defences and roads shapefiles, available from Digimap.
- Location of bridges and weirs, from historic Ordnance Survey maps.

6.2.2. Channel centreline

The channel location was digitised from the 1970s Ordnance Survey maps and the 2010s Ordnance Survey maps. The resolution was 1:2500 for the 1970s maps and 1:2000 for the 2010s maps. The bank lines were digitised in ArcMap 10.6 (ESRI UK) at a maximum scale of 1:800 and with at least one point per 5m. A centreline was produced using the Collapse Dual Line to Centreline tool, and any errors manually corrected. The centreline was then smoothed using the Smooth Line tool, using the PAEK smoothing option and a tolerance of 25.

6.2.3. Channel Migration Rate

The channel centreline migration rate was calculated using the River Migration Toolbox (Legg et al., 2014). The distance between the two centrelines was measured at 10m intervals. The mean and the maximum migration rates were calculated for each individual bend. The width-averaged rates were then calculated so there was no issue of scale between the different size rivers. A $\log_{10}$ transformation was performed so the data represented a normal distribution for analysis in the model.

6.2.4. Channel Width

The channel width was also measured at the same location as the channel migration transects and the mean channel width was calculated for each individual bend. Although the channel width was not used directly in the model, it was used to calculate the width-averaged migration rates and width-averaged radius of curvature (RoC/w) so that scale was not an issue between the different rivers. The mean channel width ranged from 5.42m on the River Loud to 24.92m on the River Calder.

6.2.5. Radius of curvature

The radius of curvature was measured using python code from Gibson (2013). The radius of curvature was measured at 10m intervals along the centreline for the 1970s. The mean, median and minimum radius of curvature for each bend was calculated. The radius of curvature was then divided by the mean channel width for each individual bend to calculate the RoC/w value used by Hickin and Nanson (1984) and Hooke (2003).

6.2.6. Riparian Vegetation

Aerial photographs were obtained from Historic England for the 1970s and from Digimap for the 2010s. The 2010s photographs are already available geo-rectified. The 1970s photographs were geo-rectified in ArcMap 10.6, using a 1st order polynomial transformation and a minimum of ten ground control points, using fixed objects from the 2010s aerial photographs. A 30m buffer was delineated around the channel bank lines for the 1970s and 2010s and any riparian vegetation was digitised. It was not possible to distinguish between different types of vegetation in this study due to the quality of the aerial photographs so only an absence or presence of vegetation was used. The percentage of each bend with vegetation on the outer bank, within the 30m buffer, was then calculated. This was completed for the 1970s aerial photographs and the 2010s aerial photographs. The change in the percentage of vegetation coverage between the two periods was also calculated for each individual bend.

6.2.7. Slope

The valley slope was calculated using the LiDAR generated DEM and the 1970s channel position. The elevation of the valley was calculated at 500m intervals along the 1970s channel, using undisturbed sections of the valley floodplain. The elevation difference between two consecutive points was calculated and divided by the length of the channel between the two points to give a measure of the slope in m/m.

6.2.8. Valley Confinement

Valley confinement can reduce the rate of erosion by restricting the space for the river to migrate across the floodplain. The confinement can be due to natural features, such as valley sides or bedrock outcrops, or just due to human intervention such as flood defences or bank protection work. The location of valley side was calculated using the valley bottom tool in the Fluvial Corridor Toolbox and the LiDAR DEMs were available. A secondary check was made using the slope function in the image analysis tool in ArcMap to ensure that significant breaks in the floodplain slope were not missed. The location of roads, flood defences and buildings were available in a shapefile from Digimap. An assumption was made that human infrastructure located close to the river channel would have some type of bank protection to reduce erosion close to the infrastructure. The distance from the apex of each individual bend to the confinement was then measured. The distance was measured from the outer bank towards the confinement and therefore only considered one side of the floodplain for each bend. A confinement factor was calculated, based on the ratios developed by Rapp and Abbe (2003), which considered a river confined if the ratio between valley width and channel width was less than two, semi-confined if the ratio was between two and four, and unconfined if the ratio was greater than four. Each bend was classified as one of these factors. The type of confinement was also recorded for each bend, such as road, buildings, valley edge.

6.2.9. Bank Material and Drift Geology

The floodplain material and drift geology shapefiles were downloaded from the British Geological Survey. The type of material and the geology was classified for each individual bend. If the bend was located next to bedrock, then the drift geology was classified as bedrock and the material category was left as missing data. Most of the rivers were classified as alluvium for the drift geology as they are located within their own floodplain.

6.2.10. Upstream catchment area

The upstream catchment area was calculated for each reach, based on the watershed function in ArcMap and the end point of each reach. The upstream area ranged from 11.2km^2 for Holden Beck to 581.5km^2 for the lower section of the River Till, reach 3b.

6.2.11. Distance to in-channel structures

Two types of in-channel structures were identified that may affect the rate of lateral channel migration. The location of bridges and weirs were identified from the historic

Ordnance survey maps, and the distance of each bend from the structures was measured. It was assumed that these structures will have some form of hard engineering in place to prevent the channel from migrating at this location. The bends with a structured location within them had a distance set to 0. For weirs the distance was calculated in the upstream direction as the back-water effect is likely to reduce the effective channel slope and lower the energy of the river. The distance upstream and downstream to a bridge was calculated for each bend. Bridges act as fixed constriction point, at which the bend is unable to lateral migrate. The distance was measured to bridges and weirs at the start and finish of each of the reaches. If there were no bridges or weirs present within 5km of the reach, no value for was entered for the individual bends in the reach.

6.2.12. Model setup

In total fourteen potential explanatory variables were used to try to predict the lateral migration rates, shown in Table 6.1. A range of tree complexities (TC) and learning rates (LR) were used to find the optimal model configuration by reducing the error within the model. TC refers to the number of different interactions that a single tree can contain, i.e. a TC of one has a single split and two terminal nodes and a TC of two produces a tree with a two-way interaction. The learning rate controls the contribution of each tree to the overall model and determines how quickly the model reduces the prediction error. Elith et al. (2008) suggest that at least 1000 trees are needed to have stability in the model. As the tree complexity increases, the learning rate needs to decrease to ensure the model does not fit the data too quickly. Six different values for TC were tested (2, 3, 4, 5, 8 and 10) to explore the effect of differing model complexities on model performance. The learning rate was adjusted to ensure the number of trees was between 1000 and 10000. In total, there were 36 combinations of TC, migration rate and RoC/w.

Table 6.1. Predictor values used to for the BRT modelling, with a description of each variable

No.	Label	Description
1	bend.veg.1974	Proportion of the outer bank vegetation coverage from 1970s aerial photographs
2	bend.veg.2012	Proportion of the outer bank vegetation coverage from 2010s aerial photographs
3	change.bend.veg	The change in the riparian vegetation coverage for individual bends
4	Slope	The floodplain slope, calculate every 500m along the 1970s channel position
5	RoC/w	The mean, median and minimum radius of curvature, divided by the average channel width
6	Upstream.Area	The upstream area, calculated from the last bend on the reach
7	Distance_valley_edge	The distance from the apex of the bend to a natural or artificial confinement point.
8	conf_type	The type of confinement, whether valley edge, flood defence or transport infrastructure
9	Confinement.Factor	Bends were classified as confined, semi-confined or unconfined based on the ratio between the distance to valley edge and channel width.
10	Drift.Geology	The drift geology based on the British Geological Survey data for each bend, with bedrock assigned if drift geology was empty
11	Material	The type of material for the floodplain, available from the BGS drift geology data. If bedrock was present the data was left blank.
12	Dist_weir	The distance from a bend to a weir in the upstream direction
13	Dist_bridge_up	The distance from a bend to a bridge in the upstream direction
14	Dist_bridge_down	The distance from a bend to a bridge in the downstream direction

The boosted regression tree analysis was performed in R (R Core Team, 2013) using the two packages 'gbm' and 'dismo' provided by Elith at al. (2008) and Ridgeway (2019) respectively. The 'gbm.step' function, with a 'Gaussian' distribution, available from Elith et al. (2008) was used to identify the optimum number of trees for a given combination of TC and LR by calculating the 10-fold cross-validation (CV) deviance. The CV deviance is automatically calculated by randomly splitting the training dataset into ten separate groups and validating the model built on nine of the groups on the remaining group. This process is then repeated until all of the groups have been validated against each other. Trees are added to the model, reducing the CV deviance until the model begins to over fit the data, and the

CV deviance begins to increase. The model with the lowest CV deviance is then used to determine the optimal number of trees. The best performing models from each TC value were selected to be tested using the evaluation dataset.

A limitation of the 'gbm.step' function is that the minimum number of observations needed for a terminal node is set to ten. This is to reduce the impact of outliers on the overall model. However, in this case there is particular interest in the extremes of the data distribution as this will contain the fastest migrating bends, which will have the most impact on the surrounding floodplain and potentially require sustainable strategies to reduce the impact of the migration. The dataset used in this chapter is also small for a machine learning technique and there are a limited number of bends in the training dataset with high migration rates. The 'gbm.fit' function available from Ridgeway (2019) allows the modeller to control the minimum number of observations. A limitation of this function is that the CV deviance is no longer calculated, and the number of trees has to be set, and the optimal number of trees might not be found. For this chapter, the number of minimum observations was set to one for terminal nodes. The variables used in the model were:

- TC values - 2, 3, 4, 5, 8, and 10;
- LR values - 0.001. 0.002, 0.005, 0.0075 and 0.01;
- Number of trees was set to 1000 and 2000.

The 'predict.gbm' and 'predict' functions were used from the 'gbm' and 'dismo' packages to model the results for the validation dataset. The best model from each tree complexity was tested and the deviance between the modelled results and the expected results was calculated using the 'calc.deviance' function. The RMSE and R^2 performance metrics were used to evaluate the performance of the models.

The active/stable bends modelling was performed using the 'Bernoulli' distribution option from 'gbm.step'. The models calculated the likelihood of a bend being active or stable. The models were evaluated using a Receiver Operator Characteristic (ROC) curve. A series of thresholds are tested for whether a bend is classified as active or stable and a confusion matrix was produced to include the total number of true positive, false negative, false positive and true negative results. The ROC curve is plotted using the True Positivity Rate (TPR) and the False Positive Rate (FPR), and the area under the curve (AUC) is calculated as a measure of the performance of the model. An AUC value of 0.5 means the model is not performing better than a random guess, while a value close to 0 or 1 means the model is correctly classifying most of the bends. The best performing threshold was calculated using

the distance to corner method. This calculates the distance of each point on the ROC curve to the top left corner of the figure. The closer to the corner, the better the performance of the threshold. The best performing threshold was applied to data to investigate which bends were incorrectly classified as active and incorrectly classified as stable and are potential causes of the misclassification.

6.3. Results

The results of the 'gbm.step' function from Elith et al. (2008) will be presented in the first part of the results chapter. The cross-validated (CV) deviance was lower for the log maximum width-averaged migration in all cases and the minimum RoC/w had the lowest average CV deviance (0.117). The following results will focus on the minimum RoC/w and the maximum migration rate as the models gave the best performance. Table 6.2 shows the models with the best CV deviance, along with the associated LR and the number of trees used to fit the model. The deviance in the model reduced as the tree complexity increased although the reduction in error was low. Table 6.2 also shows the performance of the models on the evaluation dataset. The deviance and RMSE decreased slightly as the TC increased and the R^2 between the predicted and actual values increased, although the performance of the models was poor. The mean RMSE of all the model runs was 0.353, with a minimum of 0.351 and a maximum of 0.359. The mean R^2 of all the model runs was 0.380, with a minimum of 0.358 and a maximum of 0.389. The performance improved as the tree complexity increased, and the number of interactions modelled increased.

Table 6.2. The best performing model for each of the TC values. The CV deviance is the cross validated deviance in the training dataset. The deviance, RMSE and R^2 values are the performance metrics for the evaluation dataset

Model Name	TC	LR	CV Deviance	nTrees	Deviance	RMSE	R^2
TC2_LR01	2	0.01	0.120	3100	0.126	0.355	0.373
TC3_LR005	3	0.005	0.121	3000	0.125	0.354	0.377
TC4_LR005	4	0.005	0.118	2200	0.124	0.352	0.384
TC5_LR002	5	0.002	0.117	4300	0.124	0.353	0.383
TC8_LR002	8	0.002	0.114	4250	0.123	0.351	0.388
TC10_LR0075	10	0.0075	0.117	900	0.123	0.351	0.388

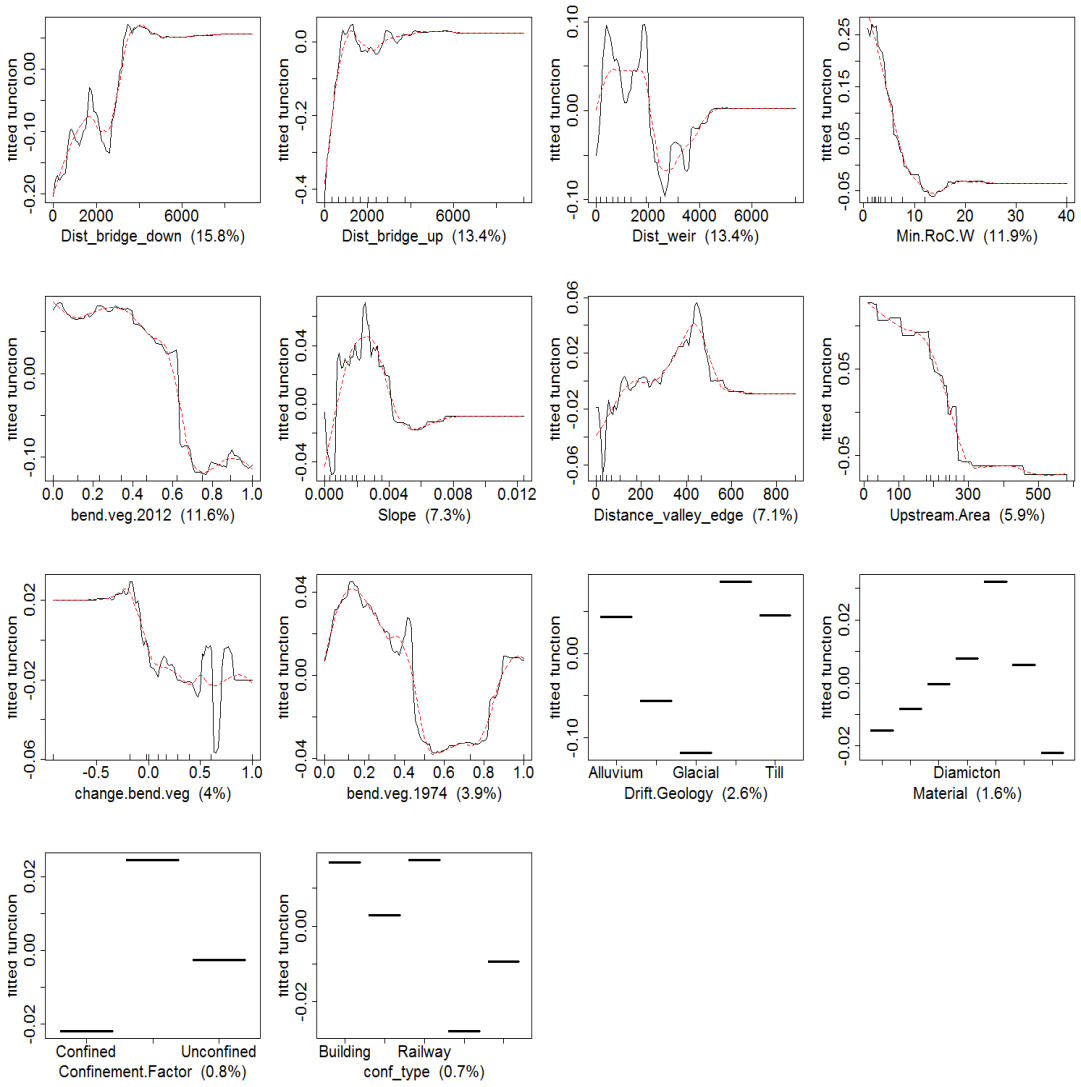

Figure 6.2. Partial dependence plots for all of the variables in the TC8_LR002 model of maximum migration. The fitted function represents the impact on the predicted migration rate and value in parenthesis represents the number of trees in which each variable appears, weighted by the improvement to model performance. The rug plots (the tick marks on the x-axis for continuous variables) indicate the distribution of the data in deciles, and the red line is the smoothed impact of the different variables.

The contribution of each of the variables to the overall model is shown in Figure 6.2. Human infrastructure had a high influence on the migration rate of river bends. River bends that were located close to the bridges reduced the rate of migration both upstream (Dist_bridge_down) and downstream (Dist_bridge_up) of the bridge. The impact of bridges on upstream migration rates had a lower impact than the impact on downstream migration rates but appeared to last for a longer distance. The minimum RoC/w showed an increase in migration rate as the curvature decreased and did not show the decrease expected as RoC/w was less than 3.0.

The bend vegetation was digitised for both the 1970s and 2010s, as there were large changes between the coverage of riparian vegetation between the two periods, especially in the River Lugg catchment. Where vegetation was able to establish on the outer bank, there was a large reduction in the amount of erosion when the proportion of bend vegetation was 0.6. A similar effect occurred for the proportion of bend vegetation coverage in the 1970s; however, the impact was lower than the bend vegetation in 2012 and occurred in less trees. The type of material and drift geology had a low impact on the overall model performance, but the spatial resolution of material data was very low and most of the bends in a single reach had similar material type and drift geology. It was not possible to show the variation in bank material that has been reported by other authors (such as Guneralp and Rhoads (2012) and Konsoer et al. (2016)).

In the multiple model runs, no single variable emerged as the most important predictor. The distance from a bridge upstream to a bend was highest contributor for five of the six different tree complexity, although never appearing in more than 16% of the total number of trees in the model. The confinement factor and the conf_type were the least useful predictors, only occurring in 0.8% and 0.7% of the trees across all the models, suggesting they are having little impact on the overall prediction of the migration rate. However, many of the river bends used in this study were freely migrating bends as the research was focussed on the evolution of the fastest moving bends. The influence of these predictor variables may be higher if more confined sections of river were included in the future.

The models were able to predict the median migration rates for the whole dataset but struggled to predict the extreme values. Figure 6.3 shows the distribution of the actual migration rates, compared to the predicted migration rates of the best model for each TC value. The predicted mean log maximum width-averaged migration rate was -1.88, which corresponds to 1.3% of the channel width per year. The mean actual migration rate was -1.84 or 1.4% of the channel width per year. Figure 6.4 shows the results of the model predictions against the actual migration rates for the six different tree complexities used. Generally, the model was able to predict the general trend as the actual migration rate increased with the predicted migration rate. However, the models consistently under predicted the most active bends and over predicted the least active bends. The actual minimum migration rate was 0.03% of the channel width per year, while the model predicted 0.1% of channel width per year. The maximum measured rate of migration was 15.9% of channel width per year, while the highest predicted migration rates were 5.1% of channel width per year. Figure 6.5 shows the predicted migration rates minus the actual migration rates, where a negative value

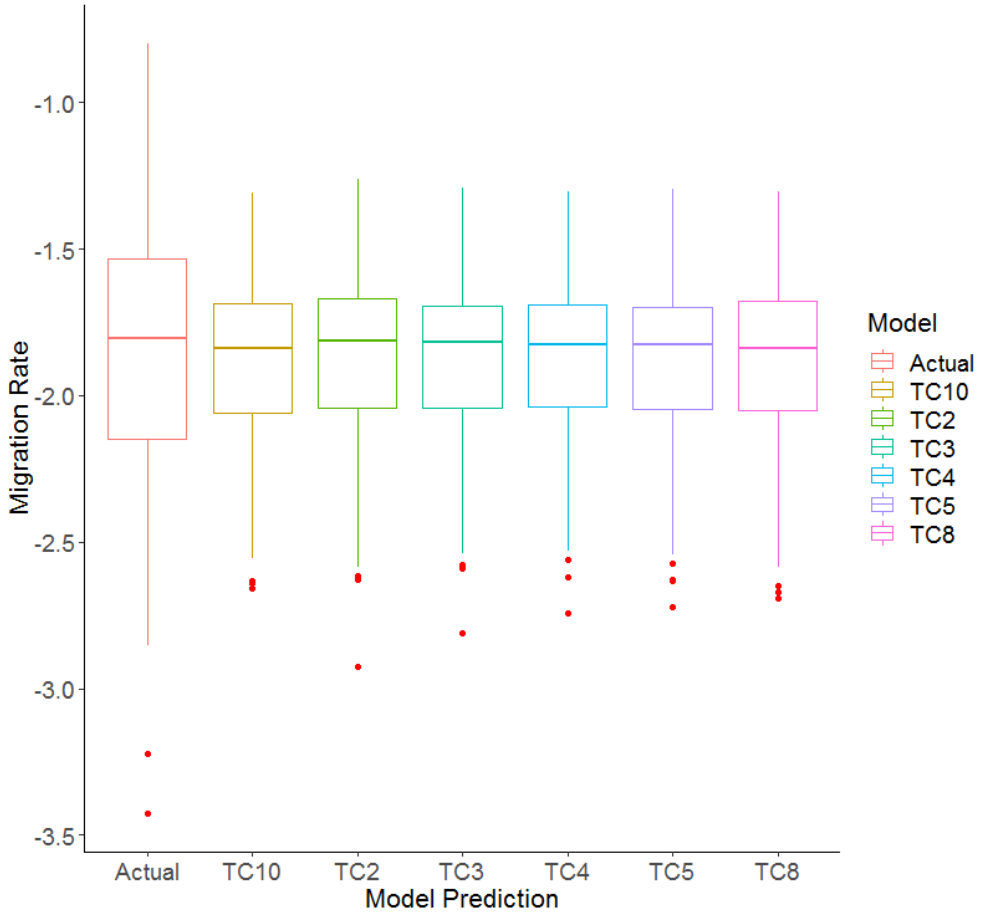

Figure 6.3. Boxplots of the predicted migration rate for the best models for each of the TC values used, compared to the actual dataset

indicates an under prediction and a positive value indicates an over prediction. A clear bias is apparent in the model, where the model is not able to predict the highest and lowest migration rates.

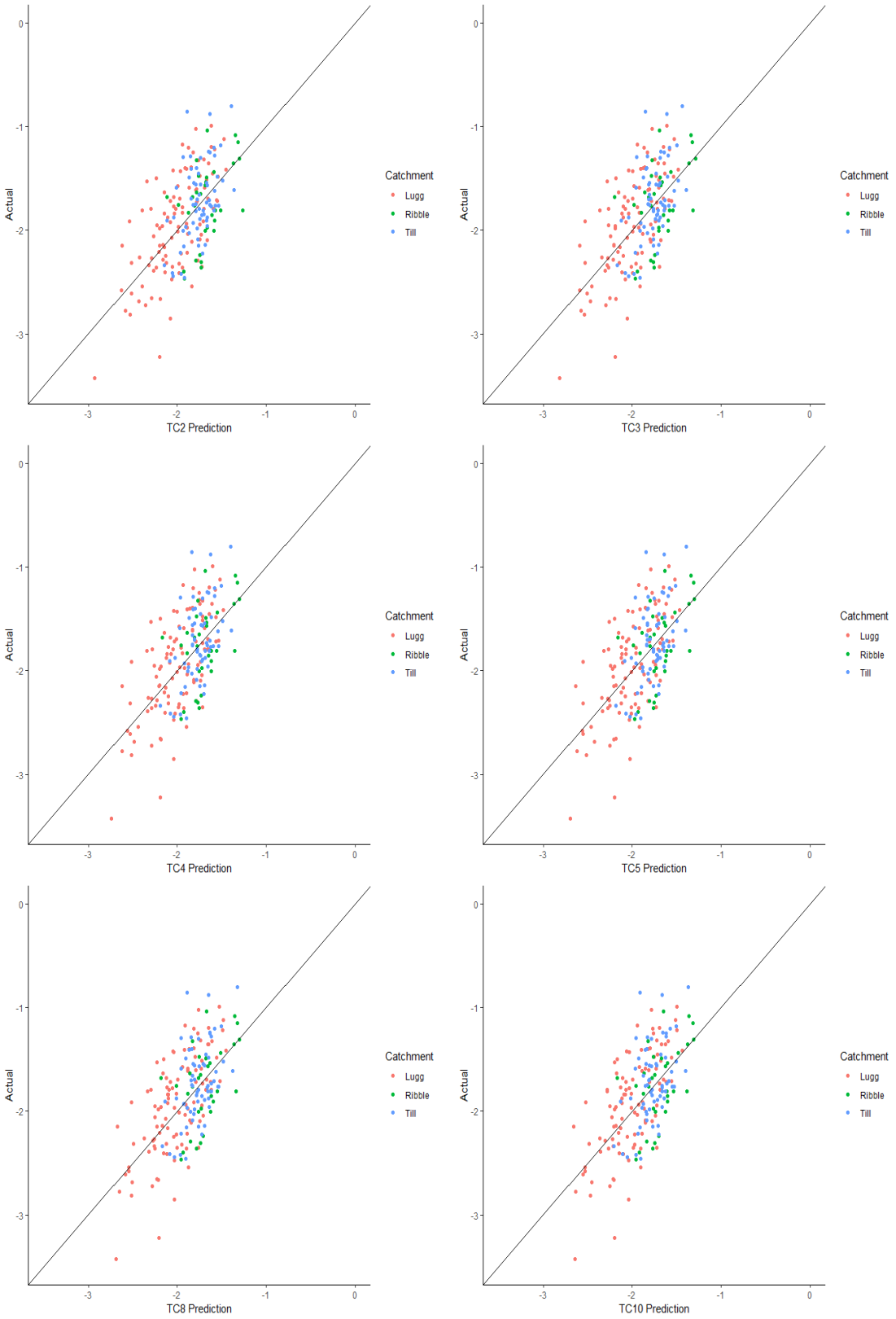

Figure 6.4. Comparing the model prediction migration rates to the actual migration rates for the best performing models

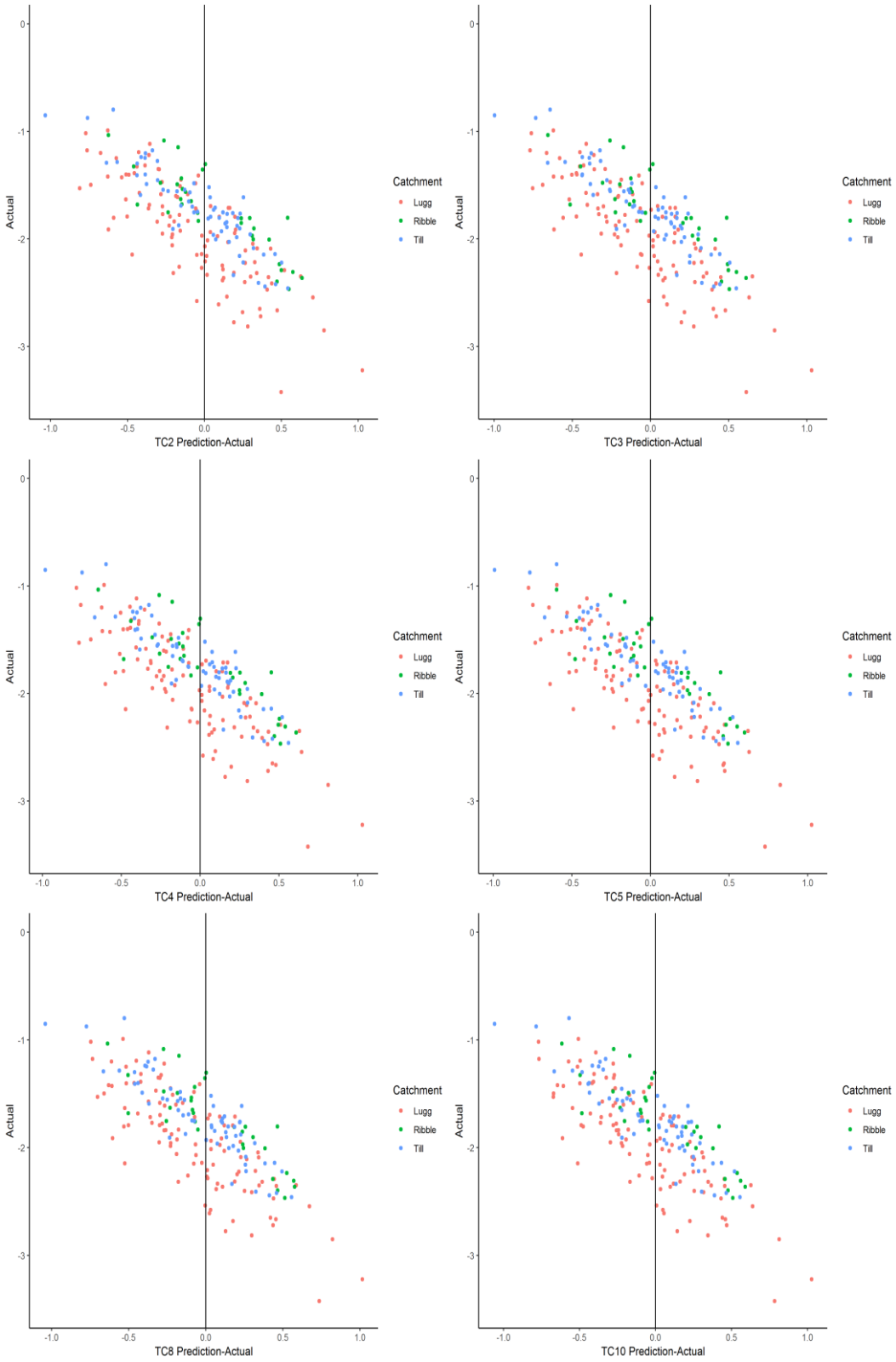

Figure 6.5. The predicted - actual migration rates for each of the different TC values. There was a clear bias evident with over prediction of the lowest migration rates and under prediction of the most active bends

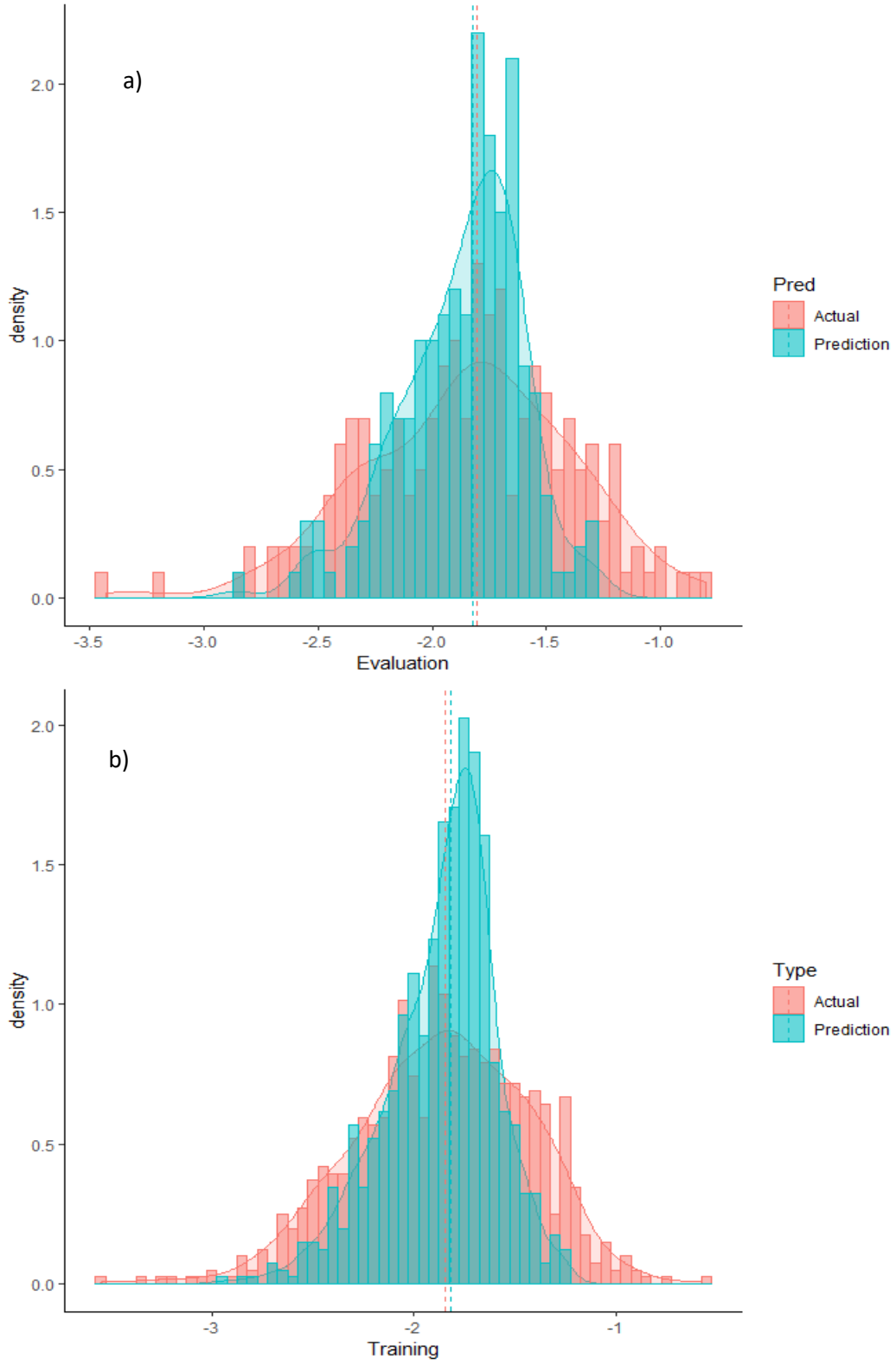

Figure 6.6. Density plots of the migration rates for the evaluation dataset and the training dataset. In both a) the evaluation dataset and b) the training dataset the results are not able to reproduce the results at the high and low end of the distribution

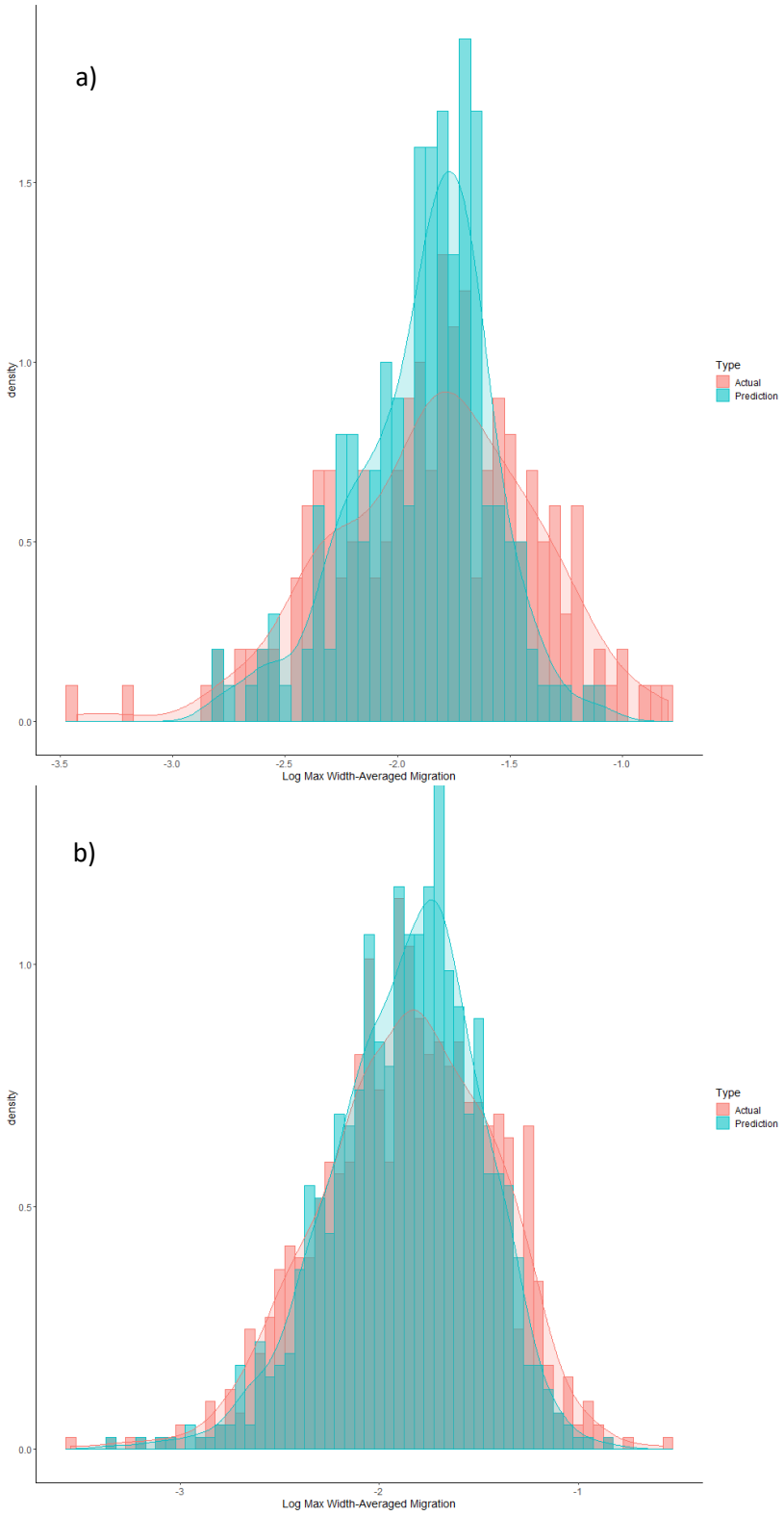

Figure 6.7. Density plot for the best performing model once the minimum number of observations in a terminal node was set to 1. a) shows the distribution of results in the evaluation dataset using the 'gbm.fit' function and b) shows the distribution of results when the training dataset is run back through the model

The density plot shown in Figure 6.6a shows the range of migration rates predicted using the TC8 model and the actual migration rates for the evaluation dataset. The model was then rerun using the training dataset, to determine how well the model could predict using the data it was trained with. The performance was poor again for the values furthest away from the mean (Figure 6.6b). Although the dataset is large for this type of study (over 1000 river bends), it is relatively small for use in machine learning. The number of observations in the training dataset at the extreme values are limited, meaning they are having a small impact on the overall model performance. It was also noted that in the general gbm.step code the default number of minimum observations to be considered in an end node is 10, while in the training dataset the number of observations at the high and low ends of the distribution is generally less than this.

Using the gbm.fit function available in the dismo package (Ridgeway, 2019), it was possible to alter the minimum number of observations used to be the model in a terminal node. New models were produced using the gbm.fit function and n.minobsinnode = 1 to try and make full use of the dataset. TC values of 2, 3, 4, 5, 8 and 10 were used and LR values of 0.01, 0.02, 0.05, 0.075 and 0.01. In gbm.fit the number of trees must be selected, so models with 1000 and 2000 trees were tested. There was no difference in performance using the gbm.fit function compared to the gbm.step function on the evaluation dataset. The results of the gbm.fit function are shown in Table 6.3. The mean RMSE was 0.352 and 0.353 using the two different functions and the mean R^2 value was 0.384 and 0.382. There was, however, an improvement when the model was used on the training dataset variables compared to the gbm.step function.

Table 6.4 shows the performance of the model using the training dataset. Figure 6.7 shows the distribution of the evaluation data and the training data for the best performing model TC10_LR01, with 2000 trees. The model could predict the general trend well, but there was a large spread for the evaluation dataset. The model perfomed very well for the training dataset with low deviance (0.013), RMSE (0.109) and high R^2 (0.943). As the number of interactions in the model increased, the performance improved for the evaluation and training datasets, although the increase in performance was small for the evaluation dataset.

Table 6.3. Results for the best performing models using the gbm.fit package on the evaluation dataset. There was little improvement over the gbm.step function for the evaluation dataset.

Model	Migration	TC	LR	Deviance	RMSE	R^2
TC2_LR01	Maxmigw	2	0.01	0.124	0.352	0.379
TC3_LR01	Maxmigw	3	0.01	0.126	0.355	0.372
TC4_LR01	Maxmigw	4	0.01	0.123	0.350	0.391
TC5_LR01	Maxmigw	5	0.01	0.125	0.353	0.382
TC8_LR01	Maxmigw	8	0.01	0.125	0.354	0.382
TC10_LR01	Maxmigw	10	0.01	0.127	0.356	0.375

Table 6.4. The performance of the models on the training dataset was much better when the number of minimum observations was set to 1 and improved as the number of interactions within the model were increased.

Model #	Migration	TC	LR	# Trees	Deviance	RMSE	R^2
TC2_LR01	Maxmigw	2	0.01	2000	0.077	0.273	0.564
TC3_LR01	Maxmigw	3	0.01	2000	0.059	0.235	0.691
TC4_LR01	Maxmigw	4	0.01	2000	0.045	0.206	0.768
TC5_LR01	Maxmigw	5	0.01	2000	0.036	0.185	0.819
TC8_LR01	Maxmigw	8	0.01	2000	0.019	0.132	0.915
TC10_LR01	Maxmigw	10	0.01	2000	0.013	0.109	0.943

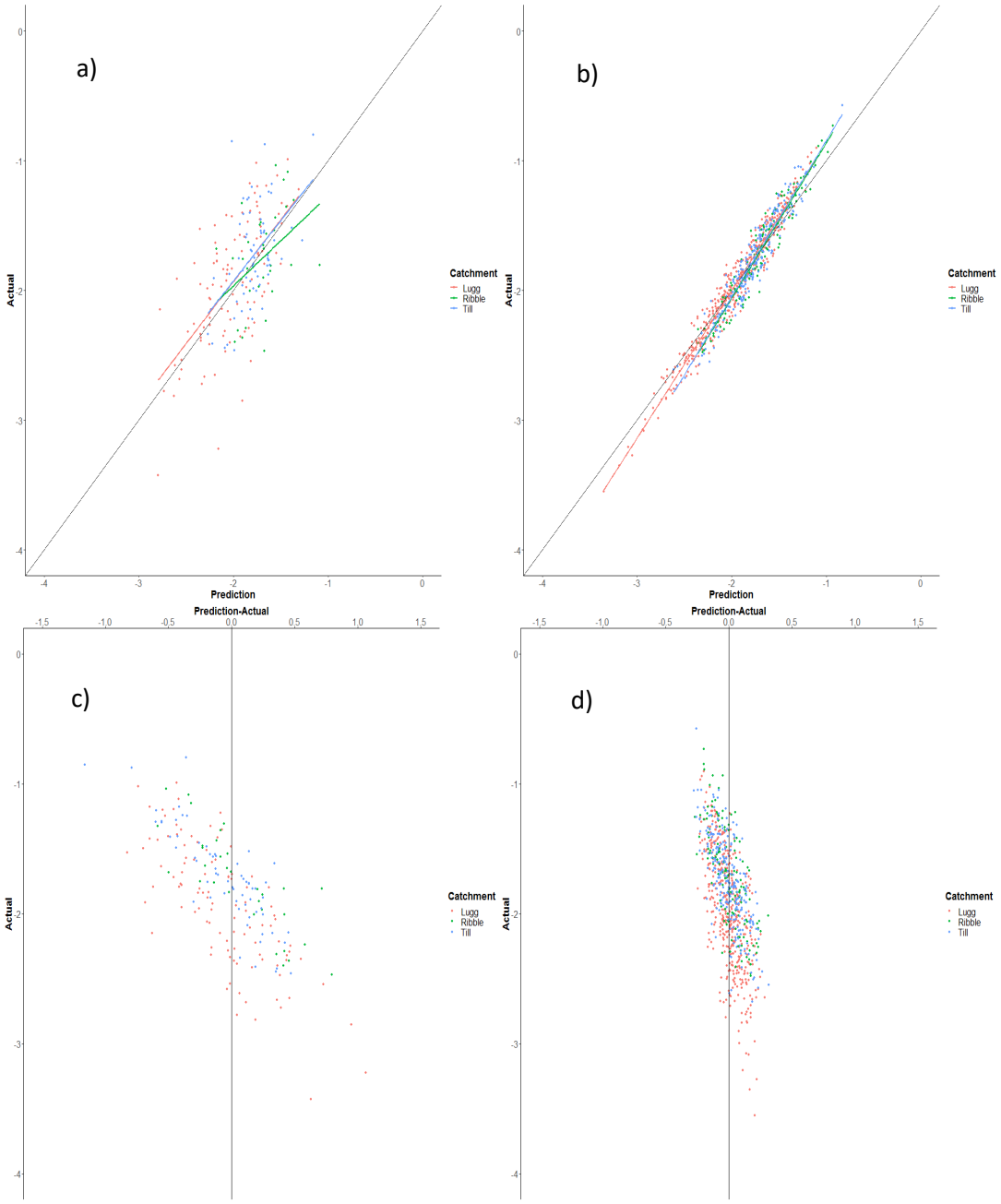

Figure 6.8. The performance of the evaluation (a) and the training dataset (b) for the predicted migration rates against the actual measured migration rates for model TC8_LR002. c) and d) show the over- and under-prediction of the model results for the evaluation and training datasets.

6.3.1. Active/Stable River Bends

Another potential approach for using BRT models is to use the Bernoulli distribution, which attempts to predict the absence or presence of an outcome variable. This has been used frequently in ecological studies (e.g. Elith et al., 2008; Buston and Elith, 2011; Cheong et al., 2014) and to predict the occurrence of landslides or frost (Youssef et al., 2016; Park and Kim, 2019; Pouteau et al., 2011). The threshold selected here was where bends with >4.6% channel width per year migration rates were considered active, and below this threshold were considered stable. The 4.6% threshold represents the top decile of migration rates in the training dataset. The models were run using the Bernoulli distribution (absence or presence data) using the same TC and LR values and Receiver Operator Characteristic (ROC) curves were created for each model and the Area Under the Curve (AUC) was calculated for each model. The model predicts the likelihood of a river bend being considered stable or active and then tests a series of thresholds to determine the number of true positive, false positive, true negative or false negative results for each model. The false positive rate is then plotted against the true positive rate and the AUC is calculated. A value of 0.5 indicates a random chance of successfully classifying a bend, while a value of 1.0 indicates a perfect model. The range of AUC values for the different models is shown in Figure 6.9. The best performing model was TC8LR002_NT1000 with AUC = 0.790. The ROC curve is shown in Figure 6.10. The threshold used to determine whether a bend is active or stable depends on the nature of the management approach. If the approach is to reduce erosion on as many of the active bends as possible then a low threshold could be used, which would capture the most active bends, but also many bends that would be stable and not need intervention. If a high threshold is set, then it is possible that some active bends will not be properly classified, and erosion could occur in unexpected locations. For the purpose of this study, the distance to the corner was used to determine the best threshold and was then tested on the model with the highest AUC.

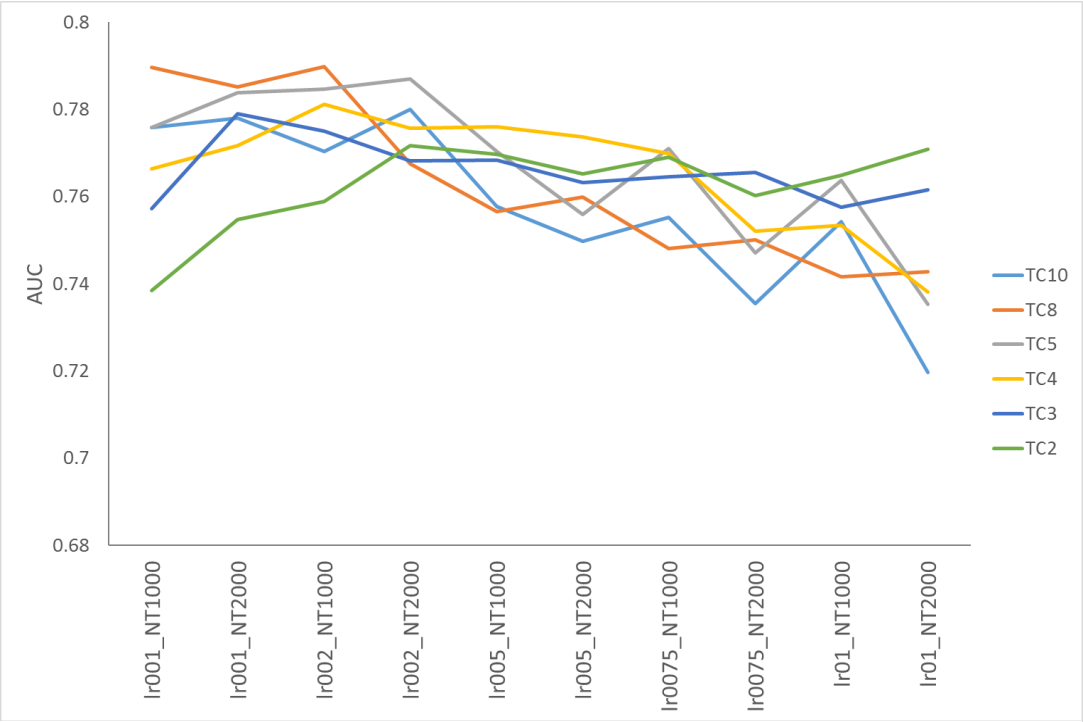

Figure 6.9. The AUC performance of the different models, when applied to the active/stable dataset

In the evaluation dataset, 26 bends were considered active and 174 were considered stable, based on the >4.6% channel width threshold. Using the lowest distance to corner from Figure 6.10 the total number of bends classified as active was 59 and 141 were classified as stable. The total number of correctly classified bends was 147. Of the 53 incorrectly classified bends, 42 were predicted to be active, while being stable in the actual dataset and eleven bends were predicted as stable while being classified as active in the evaluation dataset.

All eleven bends were analysed to discover whether any unexpected behaviour was occurring that could potentially explain the failure of the model to correctly classify the bend activity. One of the main reasons for the failure has been due to high erosion rates occurring on the preceding bend, which has then caused high migration rates on the bend in question. This occurred on four of the eleven bends on the River Arrow, River Glen and River Till (see Figure 6.11a for an example). For bend 21, Reach 3 on the River Lugg (Figure 6.11b) the bend was confined tightly against the valley side (28m from the channel centreline to edge of the valley) and confined by bedrock. However, the bend was able to shift its position downstream leading to high erosion rates. One other potential cause of the misclassification is the occurrence of a cutoff just downstream of the bend. For bend 13, Reach 3 on the River Arrow a chute cutoff occurred between the 1970s and present day (Figure 6.11c). The local increase in channel slope can cause erosion upstream and the bend has become active despite the

relatively high minimum RoC/w and vegetation coverage. On the River Loud (Figure 6.11d), the river bend that was misclassified eroded through retraction, rather than downstream migration or growth and it appears the model is unable to correctly predict this type of behaviour.

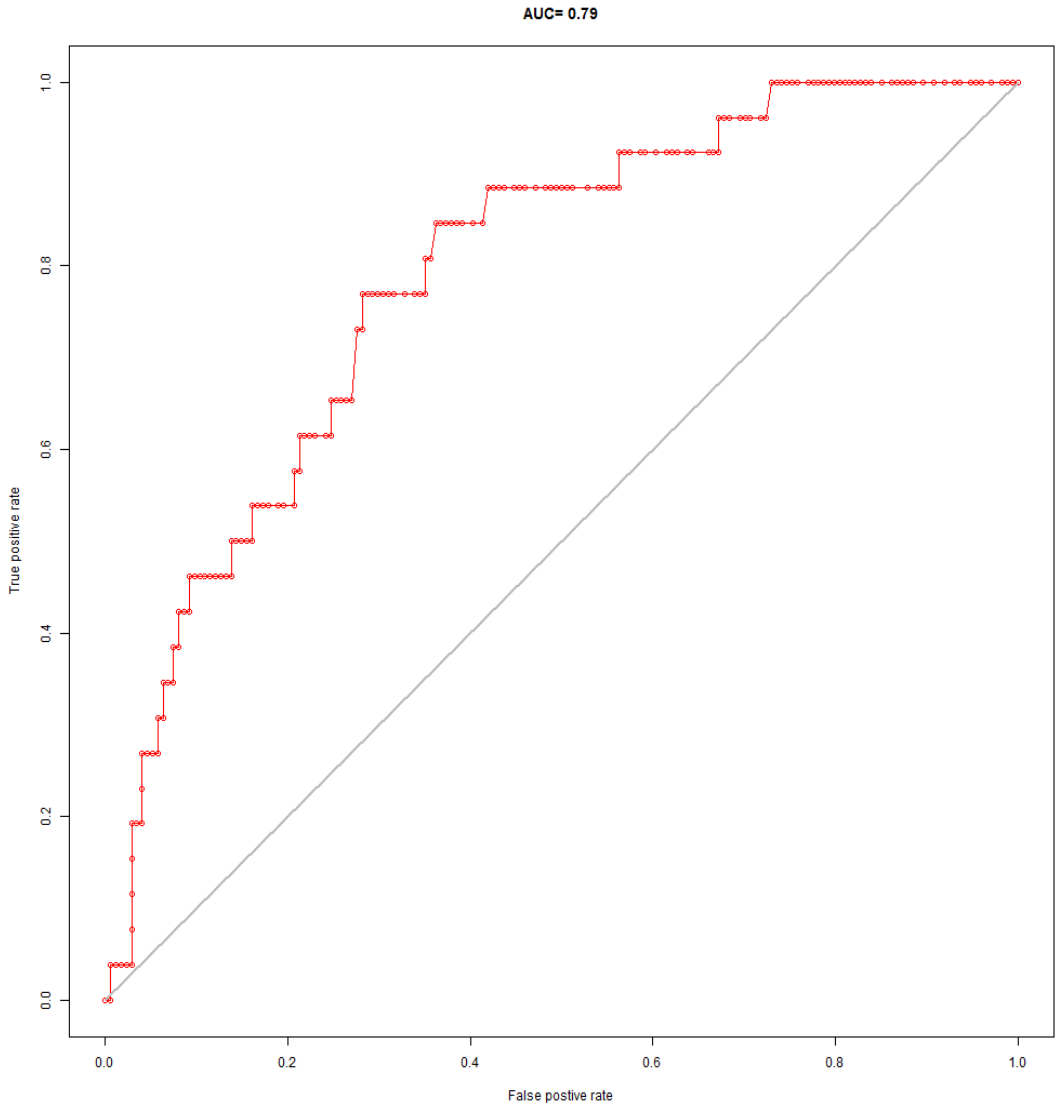

Figure 6.10. The ROC curve for the best performing model, TC8_LR002 with 1000 trees. Each point represents a threshold tested to classify whether a bend is active or stable.

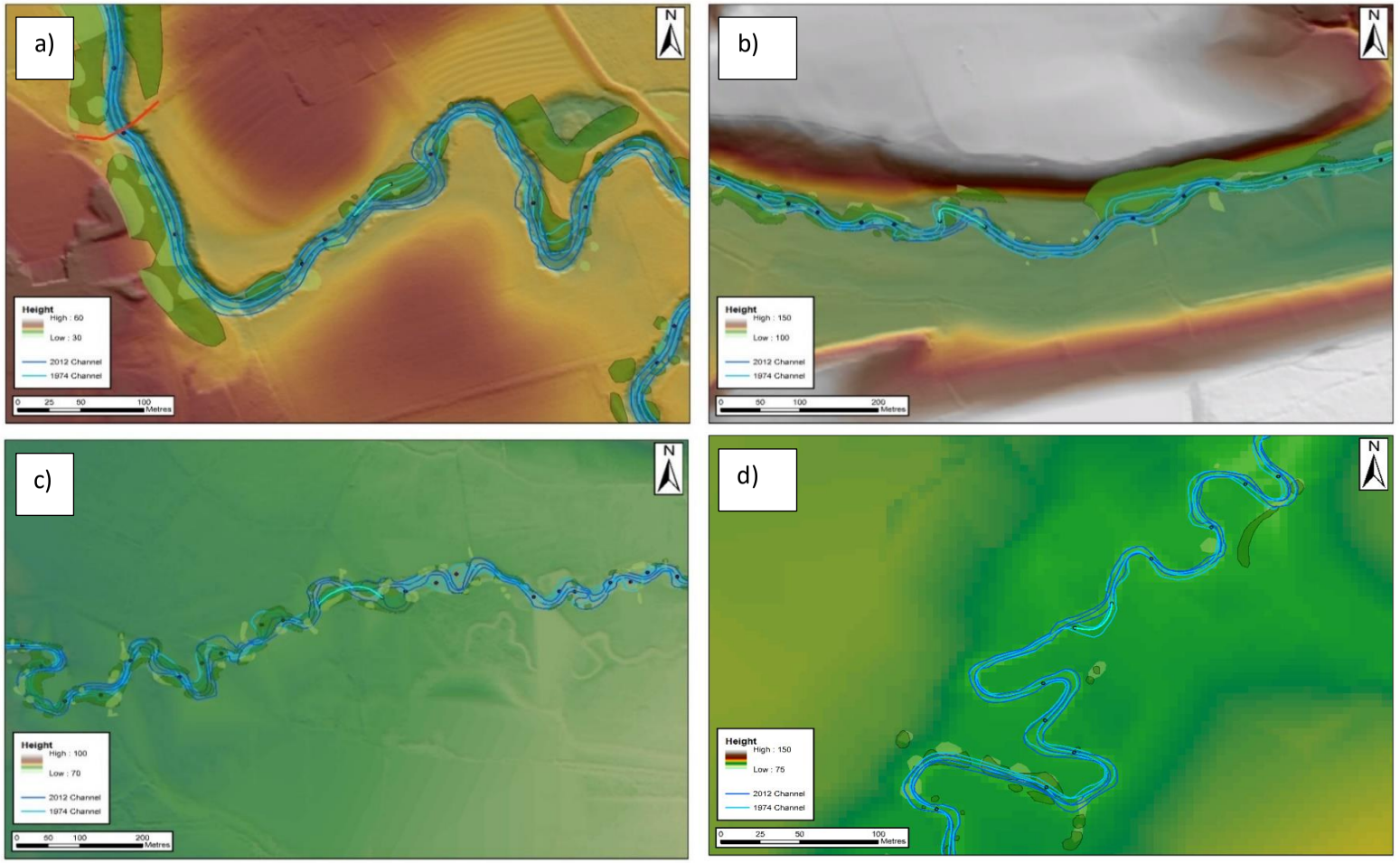

Figure 6.11. Examples of the bends which were classified as stable but were active in the evaluation dataset. The misclassified bend is highlighted. a) Migration on the preceding bend upstream on the River Till. b) The bend was pinned against the side of the valley in the 1970s but migrated downstream during the study period on the River Lugg. c) The bend was just downstream of a cutoff between the 1970s and 2010s and appears to increase the erosion rate on the bend despite a high minimum radius of curvature on the River Arrow. d) On the River Loud the planform changed through retraction, rather than downstream migration or growth and the model was not able to account for the process.

6.4. Discussion

The results in this chapter show the potential applicability of BRT models to predict riverbank erosion rates. The models were able to reproduce the general trend in the log width-averaged maximum migration, although the best R^2 value was 0.388, indicating only a weak relationship between the predicted and actual values. The original models were built using the 'gbm.step' function in the GBM package and were able to predict the mean and median values of the evaluation dataset well, but the models were not able to predict the migration rates at the ends of the distribution. It was noted that 'gbm.step' function uses a minimum number of observations in the terminal node of a tree of 10. Although over 1000 river bends that were analysed in this study represent many data points for geomorphological analysis, it is a relatively small amount for machine learning techniques. Therefore, the BRT models were not fully utilising the fastest and slowest migration bends when developing the model from the training dataset. The 'gbm.fit' function available in the 'dismo' library (Ridgeway, 2019) allows for the minimum number of observations in a terminal node to be adjusted, allowing the extreme values to be built into the model. The 'gbm.fit' function did not improve the performance of the model on the evaluation dataset, but when the training dataset was rerun through the model the performance improved dramatically, with the best model producing a R^2 value of 0.943.

The bends with the largest under prediction and over prediction were analysed and several reasons for the failure of the model could be identified. The bends with the highest over prediction tended to be very stable bends with essentially no change between the two map dates. The predicted log width-averaged migration rates are an order of magnitude higher than the actual log width-averaged migration rates, but this represents a difference between 0.7% and 0.06% of the average channel width per year. The high over prediction is due to the nature of the $\log_{10}$ transformation performed on the dataset. When considering the width-averaged migration rates, the largest over prediction represents 2.7% of the channel width per year. An over prediction on a bend could mean that management practices are put in place to prevent erosion that are unnecessary and reduce the natural processes on the river. However, the over predictions tend to be low compared to the bends with an under prediction of the width-averaged migration rate. The three bends with the greatest under prediction were all located on Reach 1 of the River Till and have an under prediction of 11-12% of the average channel width. The training data for section of the river only contains 30 bends and it is located on the transition between a wandering gravel bed river

and a single thread meandering channel meaning the channel is liable to being highly active. The high migration rate on bend 10, Reach 1, River Till was caused by the large amount of erosion that occurred on the preceding bend. Bend 21, Reach 3, River Lugg was originally pinned against the side of the valley in the 1970s, but subsequently migrated downstream and, once the constriction was removed, grew across the floodplain. The under-estimation of erosion at bends is a more important issue for management purposes, especially if infrastructure in the floodplain is at risk.

The absence/presence approach was also used in this chapter using the "Bernoulli" fitting function in the GBM model and a threshold of 4.6% width-averaged migration rate to define whether a bend is active or stable. Using this approach, it was possible to achieve an AUC = 0.79 for the best performing model and with 147 out of 200 bends correctly classified. Of the 53 incorrectly classified bends, 42 were classified as active when they were considered stable in the evaluation dataset. The average width-averaged migration rate of the 42 bends was 0.016. Eleven of the bends were incorrectly classified as stable, which is a greater concern for management practices as bends with high migration rates and potentially causing risk to infrastructure could be left unmanaged. There are a number of potential causes for the misclassification. A number of the misclassified bends have high erosion rates on the preceding bends, causing an adjustment on a straighter/more confined section of the channel. One of the bends was also confined against the valley side preventing the river from growing further across the floodplain. Most of the confined bends along this section of the River Lugg were stable during the study period, however, the misclassified bend was able to migrate downstream and had a high migration rate in the evaluation dataset.

The relative influence of the different predictor variables showed that no one single factor was dominating the response in the model. The top three most influential predictor variables were all human infrastructure either in the floodplain or in the river channel itself. The top three were Dist_bridge_down, Dist_bridge_up and Dist_weir. The distance to a bridge, both upstream and downstream showed a strong negative impact on the rate of erosion close to the bend, before approaching zero further away from the bend. Downstream of the bridge (Dist_bridge_up) showed a strong influence to around 1000m downstream of the bridge, before having little impact on the migration rate further away than this. The distance upstream of a bend (Dist_bridge_down) affected the river further upstream (to around 3000m) but had a lower influence on the migration rate. The distance downstream to a weir also impacts on the migration rate, with an increase of the migration rate close to

the bend, before decreasing further away from the weir. It would be expected that the migration rate would decrease immediately upstream of a weir due to the backwater effect, however this does not appear to occur for the selected reaches.

The next most influential variables were Min.RoC.W and bend.veg.2012. The minimum radius of curvature had a slight negative impact on the migration rate, until the RoC/w became less than ten. Below ten there was a steady increase in the migration rate as the radius of curvature decreased. There was a slight decrease when the radius of curvature was less than two, although the decrease was not as large as expected by Hickin and Nanson (1984), but otherwise fitted well with the increase in migration rate once the r_m/w value was less than 5.0. The riparian vegetation in 2012 as had a strong control on the migration rate, with a large decrease in the migration rate when the proportion of vegetation was over 0.6. There is a question as to whether the banks were stabilised due to the presence of vegetation, or whether the bends were stable and allowed the riparian vegetation to become established. There was a large increase in the amount of vegetation coverage between the two periods, with over 60% of the bends showing at least some increase between the 1970s and 2010s (as seen in the change.bend.veg variable). A combination of both factors probably led to the establishment of riparian vegetation on many bends, with a period of stability allowing the vegetation to establish. Once the vegetation had established, the strength of the bank tends to be increased through root reinforcement (Abernathy and Rutherfurd, 2000), allowing vegetation to further establish. The bend vegetation from the 1970s shows a similar influence, with a decrease once the proportion of vegetation coverage is greater than 0.5, but the overall influence on the model is lower.

The next three most influential variables were Slope, Distance_valley_edge and Upstream.Area. There was an increase in the migration rate as the slope increased from 0 to 0.004, before decreasing between 0.004 and 0.012. This is somewhat surprising, as it would be expected that higher slope rivers would have more energy and more ability to erode the bank. However, the higher slope values only account for 10% of the total dataset, and more of these smaller high energy rivers would need to be included to further examine the impact of slope on migration rates. The rivers with the high slope also tended in smaller upstream catchments (Holden Beck and Skirden Beck), which have smaller valleys and can be confined by the valley sides. The distance to the valley side had an influence on migration rate. At distances less than 200m the impact on migration rate was negative, before increasing between 200m and 400m to have a positive influence. Once the distance to the valley edge

was over 400m there was little impact on the overall model. The upstream area showed a decreasing influence as the area increased. Hooke (1979) showed that migration rates increased as catchment area increased, however in this study the width-averaged migration rate was used meaning that each bend was scaled by the average channel width, so while the total distance eroded by the bank will have increased, it was lower as a proportion of the channel width.

The four categorical factors were the predictor variables with the lowest influence on the overall model build. The drift geology and the type of material on the bend only had 2.6% and 1.6% relative influence on the overall model. This is potentially due to the homogeneity of the data source in the study reaches. Many of the reaches were located in alluvial floodplains and there was little difference between the individual bends and the reaches. Both the confinement factor and the confinement type had very little influence on the model and could potentially be removed from the final model. However, many of the reaches were selected to study freely migrating meander bends and the number of confined bends was limited. The addition of more rivers, especially urbanised rivers, would potentially increase the importance of these two variables.

There are several limitations with the data/approach used in this method. One of the major data limitations is in the soils/geology data. The spatial resolution of the data is very low and only changes at major boundaries in soil type. Guneralp and Rhoads (2012) and Konsoer et al. (2016) showed that riverbank material can vary at a bend scale and has a major control on the rates of erosion. The bank material data only varied at reach scale for this study and was only represented in a low number of the model trees. The slope data was also calculated over five bends, rather than for each individual bend, and used the valley slope, rather than the channel slope. The channel can vary more than the valley slope, especially around channel cutoffs. In this study, each bend is considered independent of the surrounding bends but there is ample evidence of bends being affected by the migration rate of the bends on either side. The hydrology of the system was also not considered as part of the study and the responsiveness of different catchments could have a significant impact on the migration rates, although will not impact on the spatial variability within the individual reaches. One final limitation is the relatively low number of bends and catchments used in this study for machine learning techniques. Although the number of river bends studied, over 1000, is high for geomorphological studies it is at the low number of data points for machine learning methods. There are also only three catchments used and eight different rivers,

which represent some of the most active rivers in England. If this approach was to be used on a national scale then more rivers would need to be included, representing a wider range of conditions in the UK. The boosted regression tree approach also attempts to limit the impact of outliers on the overall model development, with the default of ten observations needed in a terminal tree node. In geomorphological studies, these values at the extreme end of the distribution are of high interest, especially the highly active river bends. There are only a small number of very active bends in the training and evaluation dataset, but these are the bends that are most likely to threaten infrastructure in the floodplain and produce high amount of sediment to enter the river channel. There could also be some hidden factors that were not identifiable from remotely sensed data. There could be hidden bank protection or previous channel management that are not evident in the remote data sources and would require more local knowledge to identify these features. The approach also used a single centreline to represent the channel position, whereas features such as mid-channel bars can be a major component of the dynamics of meandering rivers (Hooke and Yorke, 2011).

The machine learning approach shows potential for attempting to predict areas of high riverbank erosion on large catchment scales, despite the limitations of the dataset used in this study. The model was able to predict the location of active bends and gave some indication of the magnitude of the change as well. The aim was to use readily available remotely data sources to predict riverbank erosion without the need for large fieldwork studies to sample the riverbank material and measure the channel slope. This initial study shows that Boosted Regression Trees could be used to predict areas of high erosion, with the accuracy improved with more data added to the training dataset. Once the model has been constructed, the most up to date information on riverbank material, vegetation and slope could be used to predict the location and the magnitude of migration on large catchment scales. This could allow catchment managers to identify the location of erosion hotspots, which can be assessed, and appropriate sustainable management practices put into place.

6.5. Conclusions

In this chapter a statistical modelling approach, Boosted Regression Trees (BRT), was used to explore lateral riverbank migration. The models were developed using readily available remotely sensed data sources, without the need for large scale field sampling. The BRT models showed a strong ability to predict the location of laterally active river bends between the 1970s and present day but struggled to predict the magnitude of the changes

in an evaluation dataset. Two different BRT approaches were used and the 'gbm.fit' function performed much better than the 'gbm.step' function when the training data was rerun through the model, but there was little difference in performance between to the two functions for the evaluation dataset. The influence of the predictor variables showed that not one factor was dominant in controlling the lateral migration rate, although human infrastructure in or close to the channel (bridges and weirs) accounted for 42.6% of the lateral migration rate. The minimum radius of curvature and the riparian vegetation coverage also had a strong control on the migration rate.

The model could be improved with a better representation of the riverbank material, a larger training dataset with more variation in the type of river and the ability to consider the river bends as not independent units, but part of a system where the erosion rate on one bend affects the bends both upstream and downstream. The model could be reapplied using the most recent channel position and vegetation coverage to inform catchment managers about parts of the river that may have an erosion hotspot or provide managers with information about the potential lateral migration rates on rivers where artificial confinement (such as flood defences) is removed. The study investigates erosion at a bend scale, meaning that sustainable management approaches could be used to help manage at a local scale and use resources efficiently.

7. Synthesis

7.1. Introduction

The purpose of this chapter is to provide a summary of the observations and insights arising from this thesis, relating to the hypotheses, research questions and objectives proposed in Chapter 1, sections 1.2 and 1.3. The overall purpose of this research was to investigate the dynamics and evolution of actively meandering rivers in the United Kingdom. To achieve this a long-term perspective is required as many rivers appear to be stable over short periods and require a long time to complete their evolutionary cycle. Limitations of the methods used in this research are discussed and opportunities for future work are suggested.

Where, why and how meandering rivers develop over time have been important questions investigated by many researchers over the last 100 years using a variety of approaches. Researchers have used field-based methods, remotely sensed data and computer modelling to investigate the dynamics of meandering rivers and this thesis has used a combination of remotely sensed data and statistical modelling to investigate the location, magnitude and dynamics of rivers in three catchments in the United Kingdom. This research was performed at a bend scale, and so the dynamics of individual bends could be investigated. Archive data sources were used to record the changes in channel position. A semi-automated approach was used to measure the location and magnitude of river bend migration which allowed the study of over 400 bends in chapters four and five, and the use of over 1000 bends in the machine learning modelling approach used in chapter six. The methods developed to measure the migration rate of individual bends in chapter four were used in chapters five and six to explore the dynamics of meander bend evolution and try to predict channel migration rates given a set of variables. Chapter six represents the first attempt to use a machine learning approach to try to predict the location and magnitude of river bend migration rates.

7.2. Are there any measurable differences in channel migration rate between different channel reaches and dissimilar time periods?

Research question one focused on the variations in migration rate on actively migrating sections of river in the River Lugg catchment and River Till catchment. The first objective for this chapter was to identify actively migrating river channels that have not been previously researched to provide a novel dataset. The next objective was to develop a new,

automated method of measuring individual bend migration rates, which would allow a large dataset of bends to be collated. The third objective was to investigate whether the "Sadler" effect could be identified within the dataset, were annualise rates from dissimilar time periods would be biased towards higher rates when the length of time between data points is shorter. Other potential reasons for the differences in measured rates are also explored. The final objective was to explore the influence of cutoffs on the migration rate of the surrounding bends and determine whether a sinuosity threshold existed.

To achieve the long-term perspective, historical Ordnance Survey maps were used to map the position of the river channel as far back as the 1880s in the River Lugg catchment and 1860s in the River Till catchment. There are some limitations with this approach:

- There is uncertainty on the actual date of survey for each map.
- The scale of the map can change between consecutive dates.
- The position of the bank line can be subjective, depending on the interpretation of the surveyor. To counter-act this issue, the normal winter level is usually used to define the position of the channel.
- The length of time between different maps can vary by a large amount. In this study the shortest period between consecutive maps was seven years on the River Arrow, while the longest period was 60 years on the River Lugg. The impact of any uncertainty using this approach to calculate annual migration rates is magnified in the shorter periods compared the longer periods. The length of time between the dates means that effect of individual events is averaged out over the study period.
- In very active sections of the river, it can be difficult to follow the changes to river bends when the river channel has migrated across large sections of the floodplain or behaved in a complex manner.

Despite these limitations, using historical maps is the only approach able to record actual changes to large sections of a river catchment over long periods of time and capture the full evolutionary cycle of meandering river bends.

The sections of river studied represent some of the most active rivers in England and Wales (see Table 7.1 for comparison). The rates maximum rates for individual measured for this study ranged from 3.6ma^{-1} on the River Till to 5.1ma^{-1} on the River Lugg, which equates to the channel migrating its entire channel width every three to five years, if these were

Table 7.1. Published rates of channel migration from similar size rivers in England and Wales

River	Maximum Annual Migration Rate (ma^{-1})	Channel Width (if known) (m)	Source
Severn	0.46	30	Bull (1997)
Severn	0.6	30	Thorne and Lewin (1979)
Arrow (Warwickshire)	0.18		Couper and Maddock (2001)
Devon Rivers	2.58		Hooke (1980)
Pen-y-cwm	0.12	2.5-5.0	Henshaw et al. (2012)
Ilston	0.35		Lawler (1986)
Swale-Ouse	0.44		Lawler et al. (1999)
Dane	3.08	15-20	Hooke (2007), Hooke and Yorke (2010)
Bollin	2.11	10 to 15	Hooke (1995)
Afon Trannon	0.96	17-18	Leeks et al. (1988)
Lugg	5.1	13	Regan (This thesis)
Arrow	4.2	9.75	Regan (This thesis)
Glen	4.1	11.3	Regan (This thesis)
Till	3.6	16	Regan (This thesis)

constant through time. The average rates were lower for the two catchments (see Table 7.2), but still high when compared to most rivers in England and Wales.

The second aim of the chapter was to develop methods that could measure the migration rate of individual bends using an automated or semi-automated approach allowing many bends to be measured rapidly and accurately. Using this approach, it was possible to develop a large database of individual river bend migration rates and investigate how the rates varied between different periods and sections of the rivers. A total of 465 bends was studied across ten individual reaches and six time periods. Measuring the migration rate at 10m intervals and then collating the data for individual bends means the location of highly active sections can be readily identified.

Table 7.2 The mean migration rates of all bends in the River Lugg and River Till catchments, compared to the length of time between the two maps.

River Lugg Average Migration Rate (ma^{-1})	Period Length	River Till Average Migration Rate (ma^{-1})	Period Length
0.20	17	0.20	31
0.14	29	0.26	27
0.15	38.5	0.23	33
0.82	10.25	0.84	10.5
0.15	38.375	0.18	44.5

The measurement at bend scale was used in subsequent chapters to investigate the impact of different factors on channel migration rate and to attempt to predict migration rates. The methods developed in this chapter could be applied readily and widely to rivers of any size to measure the migration rate of many bends rapidly. The ability to measure the erosion rates of individual bends means that better spatial information can be collected compared to the more traditional methods of calculating erosion rate.

There were large variations measured in the migration rates between individual bends in reaches and on a reach scale between the different time periods. The most active periods for the River Lugg catchment were measured in the 1963-1976 period and in the 1957-1970 period for the River Till catchment. The mean erosion rates for all the bends were $0.82ma^{-1}$ for the River Lugg catchment and $0.84ma^{-1}$ for the River Till catchments. Table 7.2 shows the mean migration rate for each of the periods, which showed the migration rate during the 1963-1976 period and the 1957-1970 period was up to four times higher than all the other periods. There are several potential causes of this apparent increase in the shorter period in the 1960s. The "Sadler" effect, which suggests the calculation of annualised rates will have a bias when dissimilar time periods are used. The bias will mean that shorter time periods will generally have higher erosion rates and there should be an obvious logarithmic trend when length of period is plotted against erosion rates. For this study a negative linear trend emerged, with a R^2 value of 0.503 (see Figure 4.80). This was first identified by Sadler (1981) and applied to riverbank erosion by Kessler et al. (2013). The results showed a marked increase in calculated migration rates when the length of time between time periods was less than fifteen years. This has important implications for future studies on the migration of active channels, especially when different types of data sources are used, for example field studies and archive sources. The bias evident for shorter periods could lead to an over-estimation of the true long-term average migration rates. It is suggested that at least fifteen years are needed to gain the most accurate measurement of average channel migration rates.

Another potential cause of the increased erosion rates calculated the 1960s period was the occurrence of a number of high flow events. There was some difficulty in ascertaining whether there was an especially high flow during the period, or the number of flow events during these periods as the flow records in the catchments started in the 1966 and 1969 for the Lugg catchment and 1966 in the Till catchment, which only covered the last two map periods available. There was an increase in the number and length of peak over threshold

events and the maximum discharge measured in the River Lugg catchment since the 1960s to present day. However, many of the bends appear to have become more stable during this later period and vegetation was able to establish in the riparian zone on the River Lugg and River Till. A technical report compiled by Jacobs (2015) for the River Lugg suggested there was a practice of clearing vegetation from the riparian zone for management purposes between the 1930s and 1980s. This would leave the riverbanks exposed and more vulnerable to erosion during this period and potentially combined with a series of high flow events that occurred in the winter of 1968 and 1969 to cause the high erosion rates measured in the 1960s period.

The short period between the maps dates also increases the impact of any uncertainty in the channel position when calculating an average migration rate. If the uncertainty in any given channel position is 1m, then the uncertainty in a 10-year period will equate to $0.1ma^{-1}$, but over a 30-year period the uncertainty would represent $0.03ma^{-1}$. The map available for 1963 on the River Lugg and for 1957 on the River Till had the lowest spatial resolution of the maps used in this study, 1:10560, which will have increased the uncertainty in the channel position for the periods using these maps.

The ability to accurately measure past river channel change over large sections of river channel would be very useful for management approaches such as the Erodible River Corridor concept by Piegay et al. (2005) or the Freedom Space for Rivers concept by Biron et al. (2014), which use past erosion rates to define an amount of space that should be allowed for rivers to function within. With an accurate measurement of past migration rates within a catchment, estimates could be provided for future channel migration and appropriate planning measures put in place. However, the presence of the "Sadler Effect" means that estimates should not be created from short periods as they can overestimate the true long-term migration rates.

Channel cutoffs are another process that will affect the meander dynamics and need to be considered when managing floodplain infrastructure. Stolum (1996, 1998) predicted there would be a high sinuosity domain and a low sinuosity domain, which would have different responses to a cutoff occurring. In the high sinuosity domain, a single cutoff could cause a cluster cutoffs as the meander chain responds to the cutoff. In the low sinuosity domain, a cutoff would tend to be isolated and have limited impact of the rest of the surrounding channel. Stolum predicted that the threshold between the two domains would be 3.14 on freely migrating rivers, although this was found to be lower when chute cutoffs

were included and if the floodplain was restricted. The average sinuosity for cutoffs was lower on the reaches used in this study, with an average of 1.85 for neck cutoffs and 1.64 for chute cutoffs. There are some potential reasons for the lower sinuosities measured here than suggested by Stolum. The meander belts used in this study are not completely free to migrate and chute cutoffs were more common that neck cutoffs, which tend to occur at a lower sinuosity. There were 43 chute cutoffs compared to 28 neck cutoffs. The measurement of sinuosity was also taken at a local scale, three bends up and downstream of the bend that was cutoff.

The impact of the cutoffs appeared to be limited for most of the reaches and only two sections of river channel appeared to have a cluster of cutoffs. Bend 10 on Reach two on the River Lugg cutoff between 1963 and 1976, along with two chute cutoffs at bend 7 and 9. Bends 27-29 from Reach one, River Arrow also all cutoff in the period 1974 to 2012. The bend sinuosity was 2.01, 1.91 and 1.75 for the three-consecutive bends. It was not possible to know whether the bends all cutoff during one winter as occurred on the River Bollin (Hooke, 2004). There was little change further upstream or downstream of the three bends, indicating that the river channel was in the subcritical state. There were two neck cutoffs that did not involve a cluster of cutoffs but did seem to affect the channel in the local vicinity. On Reach four of the River Lugg, bend 9 was cutoff in 1928. The bend had been growing across the floodplain and becoming more sinuous, but the sinuosity was only 1.69 when the cutoff occurred. The cutoff appears to have triggered an increase in the migration rates of the bends both upstream and downstream of the bend, with the bends that were previously stable becoming active in the subsequent periods (see Figure 4.27 and Figure 4.85). The migration rate reached a maximum of 2.5ma^{-1} on the bend immediately upstream and 2.0ma^{-1} two bends downstream as the river channel adjusted to the cutoff. The bends in this section were located in a mainly agricultural floodplain and there was little impact on any floodplain infrastructure. However, on the River Till, a neck cutoff occurred downstream of Doddington Bridge and has potentially caused instability that damaged the bridge. Bend 27 cutoff in two stages between 1924 and 1970, with a large loop cutoff between 1924 and 1957 and the remaining bend cutoff between 1957 and 1970. The aerial photograph from the 1970s (Figure 4.75) showed damage to the bridge and a replacement temporary bridge installed. The sinuosity reached a maximum of 2.07 before the cutoff occurred. The large increase in the channel slope caused by the cutoff could have travelled upstream and helped caused the instability around the bridge.

The results in this chapter showed that the sections of river channel studied here are amongst the most active in the England and Wales, with rates comparable to other actively migrating river channels previously studied. Methods were developed to accurately measure the rates of migration for individual bends for long reaches, which could easily be scaled up to calculate rates of erosion at a catchment scale. The results also confirm the existence of thresholds for which channels can rapidly readjust after a cutoff. The threshold was lower than in other published studies (Stolum, 1996; Hooke, 2004), which suggests these systems could rapidly adjust despite having a low sinuosity value. Although the impact of the cutoffs were spatial limited to the immediately bends upstream and downstream, it indicates that similar systems could rapidly adjust during cutoff events.

7.3. How well do models of bend evolution fit the observed changes on the rivers in the River Lugg and River Till catchment?

The second hypotheses concerned the long-term evolution of meander bends and aimed to test the applicability of three related models of evolution (Brice, 1974; Hickin, 1974; Hickin and Nanson, 1975; Hooke and Harvey, 1983; Hooke, 2003). Using the methods developed in the previous chapter, relationship between channel curvature and migration rate were explored and the trajectories of different bends were plotted in a curvature-migration rate phase space. The study also represented the first time that changes relating to the Brice classification were quantified for individual bends developed during the study period.

The relationship between channel curvature and migration rate has been explored extensively in the literature, both from a practical perspective with field studies (e.g. Hickin, 1974; Hickin and Nanson, 1975, 1984; Hooke, 2003, 2007; Guneralp and Rhoads, 2008, 2009. 2010; Sylvester et al., 2019) and a theoretical perspective through modelling approaches (e.g. Ikeda et al., 1981; Howard, 1984; Parker and Andrews, 1986; Seminara et a., 2001; Camporeale et al., 2007). The results from this study add further evidence of the importance channel curvature in controlling the rate and location of channel migration. There was an increase in the channel migration rate as r_m/w reached 5.0 before achieving a maximum somewhere between 2.0 and 3.0. However, there were many bends that remained stable despite having a low r_m/w value, which suggests there are further controls on the migration rate that are having a greater impact than the channel curvature.

An interesting finding from the research was the lack of an obvious lag between the location of minimum radius of curvature and maximum migration rate. Research has suggested there should be a lag between the minimum radius of curvature and the maximum migration rate, roughly equivalent to one channel width downstream (Furbish, 1988; Guneralp and Rhoads, 2009; Sylvester et al., 2019), which helps explain why there is a usually a downstream migration in the channel shape. However, for this study it was found that the highest rates of erosion for an individual bend were most often located at the tightest part of the bend. This suggests that for the majority of bends there was little downstream translation and they would normally grow across the floodplain.

This chapter also explored the evolution of meander bends, from two different frameworks. The first framework was proposed by Hooke (2003) and considered the changes to individual bends in a curvature-migration rate phase space. The idea was to be able to follow the trajectories of the bends as they develop from a straight channel or simple bend through to cutoff. Different types of bend evolution would follow different trajectories and it would be possible to determine if the geomorphic thresholds changed for the river, through, for example, climate change or human intervention. For this section, four measurements of the radius of curvature were used. The minimum, mean, and median radius of curvature was calculated for each bend, and a weighted radius of curvature value was developed that would consider both the upstream and downstream curvature values around the minimum radius of curvature for each bend. This aggregate measure is similar to that used by Ikeda et al. (1981) in their seminal paper on meandering modelling, and similar versions have been developed since to produce the complex structures seen in actual meandering rivers.

It was possible to follow the trajectory of many of the bends across the two catchments and determine whether the suggested behaviours occurred. A long-term perspective was used to fully capture the evolutionary cycle of meander bends, from the initiation through to compound or double-headed behaviour and eventually cutoff, as predicted by Hooke and Harvey (1983) and Hooke (1995). Even though a record of channel position was available for the last ~130 years, none of the bends completed the full evolutionary cycle from initiation to cutoff. However, it was possible to identify bends at different stages of the development and plot the trajectory as they developed through time.

The bends that were either stable, or migrating downstream tended to have little change in the bend curvature value or the migration rate and plotted around path C or D

from Figure 5.1. The study period was not long enough to know whether the bends had slowly migrated to the current position or whether the bends had rapidly developed a complex channel planform and then become stable. The bends that experienced chute and neck cutoffs were much more active during the study period, adjusting both the curvature and the migration rate between the different periods as they adjusted. The chute cutoffs tended to show small changes in the curvature-migration rate phase space, before more rapidly adjusting after a cutoff occurred, while the neck cutoffs had the most rapid adjustment before the cutoff occurred, before more slowly readjusting afterwards due to the high r_m/w values. It was possible to follow the trajectory of some of the bends that developed from a high r_m/w and a simple bend to a compound or double-headed bend. Although these bends did not complete the full evolutionary cycle, they were close to cutoff and would potentially cutoff in the future. There were variations in the curvature values, but the bends tended to develop lower r_m/w as the bend became tighter, before increasing as the bends became doubled headed.

The second conceptual framework used in this chapter was based on the work by Brice (1974). The bends were classified as one of four categories, simple symmetric, simple asymmetric, compound symmetric and compound asymmetric. It was found that simple symmetric bends were the most common bends, accounting for over 70% of the total number of bends and over 63% of the total bend length. The simple symmetric bends tended to be shorter than the other types of bend and were often stable. The least common bend type was compound symmetric bends, which only accounted for 3% of the total number of bends and 4% of the total bend length. This suggests that it is either uncommon for the bends to form into these shapes initially, or that once in the compound symmetric form the bends are unstable and rapidly become asymmetric, develop into two separate bends or experience a neck cutoff.

The evolution of some of the most active bends in the reaches was studied, considering the changes to the bends in the Brice classification and how the curvature profiles developed as the bends developed. An attempt was made to determine any general trends for the bends as they developed from simple symmetric bends (Type A) through to termination. Two critical points were identified, which appeared to determine the future evolutionary route of the bends. Once a bend reached Type C (for symmetric bends) or Type K for asymmetric bends, there were three different evolutionary paths the bends tended to follow. The most common path was for the bends to develop towards compound asymmetric

bends, starting at Type M and N, but eventually finishing at Type O or P, before a cutoff occurred. The next most common path was to develop towards bend type G, via types D, E and F. The least common evolutionary path was towards the compound symmetric bends, which represented less than 5% of all bends within the study. The results shown in this study could help river managers understand the likely changes in bend shape along their rivers, even if exact location and rate cannot be determined.

This chapter adds to the overall body of research focusing on the long-term evolution of river meander bends. The relationship between channel curvature and channel migration is shown to be complex, with individual bends adjust rapidly through time. Some general trends are identified in the changes to bend shape, based on the Brice (1974) bend type classification and a critical point in bend evolution is identified at which the future bend evolution appears to be determined.

7.4. Can we predict the location and rates of channel migration using a machine learning technique?

The final chapter in this thesis represents the first attempt using a machine learning technique, Boosted Regression Trees, to predict the location and rates of channel migration across three catchments in the United Kingdom. The semi-automated method developed the previous chapters in this thesis meant the migration rate and radius of curvature values of many bends could be measured and calculated rapidly and a large database could be developed. Over 1000 bends were used in this chapter and the period from the 1970s to present day was used to validate the performance of the model. This represents one of the largest datasets used to investigate channel migration. Fourteen potential explanatory variables were produced, based on the literature reviewed at the start of this thesis, and used to determine which of the variables had the highest impact on channel migration rate and to validate the performance of the model on a subset of the data.

Five variables tended to have the highest influence of the migration rate predicted by the model. The distance upstream from a bridge, the distance downstream from a bridge, the distance to a weir, the minimum width averaged radius of curvature and the percentage of riparian vegetation on the outside of the bend at the end of the study period. The slope, distance to the valley edge and upstream area were the next most important factors. The local geology, floodplain material and confinement type were the least important factors.

This will partially be due to the homogeneous nature of many of the floodplains in which the study reaches were located, and the low number of confined bends used in the study.

The model performed well when predicting the location of active or stable bends. An active bend was defined if the channel had migrated at 4.6% of its channel width per year or higher, which represented the top 10% of the migrating channel bends. The model was able to correctly predict whether a bend was stable or active for around 75% of the bends, using the best performing model and only 11 of the 200 bends were classified as stable but were active over the last 40 years. Some potential reasons for the failure were given. Some of the bends migrated downstream rapidly, despite being pinned tightly against a confining valley wall or changed their shape through retraction, rather than growing across the floodplain or migrating downstream. For some of the other bends that were incorrectly classified, the high migration on the bend was either caused by a large change in position of the bend immediately upstream or downstream of the bend, or the bend had become active after a cutoff just downstream.

The model did not perform as well when attempting to predict the magnitude of the channel migration for individual bends. The R^2 values for performance on the validation dataset was low and only reached a maximum of 0.388. The model had difficulty predicting the rates of migration for the highest migrating bends in the validation dataset and performed poorly when the training data was test in the model. The initial function used in the study was the 'gbm.step' function produced by Elith and Leathwick (2017). In this function, the minimum number of observations allowed in a terminal node of a tree was ten. However, in this study, there was only a small number of bends at the high and low end of the distribution and the model was not able to represent these data points. Often models want to reduce the impact of outliers on the overall model performance; however, for the purpose of channel migration we are actually often interested in the fastest migrating bends. A second function was used 'gbm.fit' from Ridgeway (2019) and the number of minimum observations in a terminal node was set to one. The performance in the validation dataset did not improve greatly, but there was a large improvement in the performance when the training data was retested in the model. The highest R^2 value was 0.943 and the model was able to predict accurately the magnitude of the channel change for the dataset.

There were some limitations of the approach used in this chapter. The first limitation is the low number of bends in the overall dataset. Although the number of bends is large for a geomorphic study, it is low for a machine learning approach. Similar studies have datasets

with over 10000 data points to provide information for the model (e.g. Evans, 2018). More bends would need to be included in the study to better predict the changes to the fastest migrating bends and more rivers in different types of environment should be included, such as confined rivers in an urban setting that will have a faster response time to rainfall events. Another limitation of this approach was that each bend was considered as independent from the other bends in the meander chain. This problem became apparent when bends were adjusting after a cutoff had occurred or where there was high migration on a neighbouring bend causing a bend that would otherwise be stable to shift across the floodplain. A final limitation of the study was the homogenous nature of the data sources for floodplain material and drift geology. There was little change between individual bends within a reach, whereas previous research has shown that bank material can change over a bend scale (e.g. Konsoer et al., 2016). A more detailed survey of bank material may help explain some of the discrepancy between the erosion rates measured on bends with similar curvature and vegetation levels.

This novel approach represents the first attempt to apply a machine learning approach to estimate channel migration rates. The results were mixed, the model was good at determining the which of the bends would be the most active but struggling at predicting the rate of migration. Some of the possible reasons for the failure are mentioned above. Despite the poor results for predicting the rate of erosion the method shows promise for attempting the predict the long-term migration rate of river bends and could be used to help identify areas vulnerable to change for future management. It is noted that there are some limitations with the approach that could be improve by collecting more data and adding additional parameters to improve the accuracy of the model. The results are now only applicable to active meandering rivers in the middle reaches of the watercourse, that are generally free to migrate across the floodplain. More urban and lowland rivers should be included to give a wider perspective for UK rivers and to help inform river managers in a wider variety of environments.

7.5. Directions for Future Work

There are two potential directions for future work that have emerged from this thesis. The methods developed in this thesis would allow for the rapid analysis of the relationship between channel curvature and channel migration rate using a data source with a consistent length of time between dates. A data source with a good annual record is

available using satellite imagery. Although the total amount of time available (the first satellite imagery is available from the 1972 from Landsat 1) is unlikely to capture the full evolution of individual bends, it should be possible to identify bends at different stages of the evolutionary cycle and follow the trajectory of the bend as develop. Large scale rivers would be required so the position of the channel can be accurately measured. For example, rivers in the Amazonian Basin would provide an ideal study area as they are large enough to be captured in the imagery and mobile enough that changes can be detected within the available data sources. There are additional advantages that the amount of human intervention will be limited, and much longer uninterrupted sections of the channel can be studied. It would also be possible to compare the records of annual discharge with the annual record of channel migration. Using the annual record will reduce the uncertainty associated with the "Sadler effect" and allow for a better comparison of the migration rates between the different periods.

The second area of potential future work would be to further investigate the applicability of machine learning approaches to predicting the location and magnitude of river channel migration. Additional rivers would be required to ensure that all river types are included within the study. It would be important to include more lowland, stable rivers and rivers located in or close to urban centres. More detailed information about the bank material could be collected to further explore the impact it has on channel migration rate, although this would require large field surveys to collect the data required to provide information for each individual bend. There would also need to be a method incorporated within the model to consider bends as a series of related units, where the erosion rates on one bend will influence the erosion rates on the surrounding bends. Once a large dataset had been collected and validated, the models could be used to predict the location and magnitude of channel migration at a catchment scale, using the most recent spatial data. This could identify the location of erosion hotspots that would allow catchment managers to use sustainable management approaches to manage the erosion hotspots. It could also be used to predict the location and magnitude of erosion if hard defences are removed from the floodplain and rivers are allowed to migrate more freely.

References

Abad, J.D., Garcia, M.H., 2006. RVR Meander: A toolbox for re-meandering of channelized streams. *Comput. Geosci.* 32, 92–101. https://doi.org/10.1016/j.cageo.2005.05.006

Abernethy, B., 2001. The distribution and strength of riparian tree roots in relation to riverbank reinforcement. *Hydrol. Process*. 79, 63–79.

Abernethy, B.,Rutherfurd, I.D., 2000. The effect of riparian tree roots on riverbank stability. *Earth Surf. Process. Landf*. 25, 921–937.

Abernethy, B., Rutherfurd, I.D., 2000b. Does the weight of riparian trees destabilize riverbanks? *Regul. Rivers Res. Manag.* 16, 565–576. https://doi.org/10.1002/1099-1646(200011/12)16:6<565::aid-rrr585>3.0.co;2-1

Abernethy, B., Rutherfurd, I.D., 1998. Where along a river's length will vegetation most effectively stabilise stream banks? *Geomorphology* 23, 55–75. https://doi.org/10.1016/S0169-555X(97)00089-5

Ahmed, J., Constantine, J.A., Dunne, T., 2019. The role of sediment supply in the adjustment of channel sinuosity across the Amazon Basin. *Geology* 47, 1–4. https://doi.org/10.1130/g46319.1

Anderson, D., Moggridge, H., Warren, P., Shucksmith, J., 2015. The impacts of "run-of-river" hydropower on the physical and ecological condition of rivers. *Water Environ. J*. 29, 268–276. https://doi.org/10.1111/wej.12101

Arulanandan, K., Gillogley, E., Tully, R., 1980. Development of a quantitative method to predict critical shear stress and rate of erosion of natural undisturbed cohesive soils. Report GL-80-5, US Army Engineers,Waterways Experiment Station, Vicksburg, MS.

Bagnold, R. A. 1960. Some aspects of river meanders. United States, Geological Survey, Professional Paper 282-E, 10 p.

Bak, P. and Chen, K., 1991. Self-organised criticality. *Scientific American* 264, 26–33

Bak, P. and Tang, C., 1989. Earthquakes as a Self-Organized Critical Phenomenon. *Journal of Geophysical Research* 94, 15635-15637

Bak, P., Tang, C. and Wiesenfeld, K., 1987. Self-organised criticality: an explanation of 1/f noise. *Physical Review Letters* 59, 381–4

Bathurst, J.C., Thorne, C.R., Hey, R.D., 1977. Direct measurements of secondary currents in river bends. *Nature* 269, 504–506. https://doi.org/10.1038/269504a0

Bathurst, J. C., Thorne, C. R., and Hey, R. D. ,1979. Secondary flow and shear stress at river bends. *J. Hydr. Div.,* 105, 1277–1295.

Beeson C. E., Doyle P. F., 1995. Comparison of bank erosion at vegetated and non-vegetated channel bends. *American Water Resources Bulletin* 31(6): 983–990.

Biron, P. M., Buffin-Bélanger, T., Larocque, M., Choné, G., Cloutier, C. A., Ouellet, M. A., Demers, S., Olsen, T., Desjarlais, C., Eyquem, J., 2014. Freedom space for rivers: a sustainable management approach to enhance river resilience. *Environmental Management* 54: 1056–1073.

Bizzi, S. and Lerner, D.N., 2015. The use of stream power as an indicator of channel sensitivity to erosion and deposition processes. *River Res. Appl.* 31 (1), 16–27.

Blondeaux, P., and Seminara G., 1985. A unified bar-bend theory of river meanders. *J. Fluid Mech.*, 157, 449–470.

Breiman, L., Friedman, J. H., Olshen, R. A. and Stone, C. J., 1984. Classification and Regression Trees. Wadsworth International Group, Belmont, CA, USA.

Brewer, P. and Lewin, J., 1998. Planform cyclicity in an unstable reach: complex fluvial response to environmental change. *Earth Surface Processes and Landforms* 23, 989–1008

Brice, J.C., 1974. Evolution of meander loops. *Bulletin of Geological Society of America* 85, 581–586
Brice, J.C., 1977. Lateral migration of the middle Sacramento River, California. *USGS Water Resources Investigation* 77-43, 51 pp
Buston, P. M. and Elith, J., 2011. Determinants of reproductive success in dominant pairs of clownfish: a boosted regression tree analysis. *Journal of Animal Ecology*, 80: 528-538.
Camporeale, C., Perona, P., Porporato, A., Ridolfi, L., 2005. On the long-term behaviour of meandering rivers. *Water Resources Research* 41(12).
Camporeale, C., Perona, P., Porporato, A., Ridolfi, L., 2007. Hierarchy of models for meandering rivers and related morphodynamic processes. *Reviews of Geophysics* 45(1)
Camporeale, C., Perucca, E., Ridolfi, L., 2008. Significance of cutoff in meandering river dynamics. *Journal of Geophysical Research-Earth Surface* 113
Candel, J.H.J., Kleinhans, M.G., Makaske, B., Hoek, W.Z., Quik, C., Wallinga, J., 2018. Late holocene channel pattern change from laterally stable to meandering - A palaeohydrological reconstruction. *Earth Surf. Dyn*. 6, 723–741. https://doi.org/10.5194/esurf-6-723-2018
Carslaw, D.C., Taylor, P.J., 2009. Analysis of air pollution data at a mixed source location using boosted regression trees. *Atmos. Environ*. 43, 3563–3570. https://doi.org/10.1016/j.atmosenv.2009.04.001
Cheong, Y.L., Leitão, P.J., Lakes, T., 2014. Assessment of land use factors associated with dengue cases in Malaysia using boosted regression trees. *Spat. Spatiotemporal. Epidemiol*. 10, 75–84. https://doi.org/10.1016/j.sste.2014.05.002
Chiverrell RC, Forster GC, Thomas GSP, Marshall P. 2010. Sediment transmission and storage: the implications for reconstructing landform development. *Earth Surface Processes and Landforms* 35: 4–15
Choné G., and Biron P. 2015. Assessing the relationship between river mobility and habitat. *River Research and Applications* 32(4): 528–539.
Church, M., and Rice, S.P., 2009. Form and growth of bars in a wandering gravel-bed river. *Earth Surface Processes and Landforms* 34(10), 1422–1432
Church M. and Ferguson RI. 2015. Morphodynamics: rivers beyond steady state. *Water Resources Research* 51(4): 1883–1897. https://doi.org/10.1002/2014WR016862.
Constantine, J.A., Dunne, T., 2008. Meander cutoff and the controls on the production of oxbow lakes. *Geology* 36, 23–26. https://doi.org/10.1130/G24130A.1
Cook, K.L., 2017. An evaluation of the effectiveness of low-cost UAVs and structure from motion for geomorphic change detection. *Geomorphology* 278, 195–208. https://doi.org/10.1016/j.geomorph.2016.11.009
Coulthard, T.J., Van De Wiel, M.J., 2006. A cellular model of river meandering. *Earth Surf. Process. Landforms* 31, 123–132. https://doi.org/10.1002/esp.1315
Coulthard, T.J., Van De Wiel, M.J., 2012. Modelling river history and evolution. *Philos. Trans. R. Soc. A Math. Phys. Eng. Sci*. 370, 2123–2142. https://doi.org/10.1098/rsta.2011.0597
Coulthard, T.J., Hicks, D.M., Van De Wiel, M.J., 2007. Cellular modelling of river catchments and reaches: Advantages, limitations and prospects. *Geomorphology* 90, 192–207. https://doi.org/10.1016/j.geomorph.2006.10.030
Couper, P.R., 2004. Space and time in river bank erosion research: A review. *Area* 36, 387–403. https://doi.org/10.1111/j.0004-0894.2004.00239.x
Couper, P.R., Maddock, I.P., 2001. Subaerial river bank erosion processes and their interaction with other bank erosion mechanisms on the River Arrow, Warwickshire, UK. *Earth Surf. Process. Landforms* 26, 631–646. https://doi.org/10.1002/esp.212
Crisci, C., Ghattas, B., Perera, G., 2012. A review of supervised machine learning algorithms and their applications to ecological data. *Ecol. Modell*. 240, 113–122. https://doi.org/10.1016/j.ecolmodel.2012.03.001

Croke, J., Denham, R., Thompson, C., Grove, J., 2015. Evidence of Self-Organized Criticality in riverbank mass failures: A matter of perspective? *Earth Surf. Process. Landforms* 40, 953–964. https://doi.org/10.1002/esp.3688
Crosato, A., 1990. Simulation of meandering river processes. Communications on Hydraulic and Geotechnical Engineering Report. Delft University of Technology, Delft, Netherlands, pp. 90–93.
Czuba, J.A., Foufoula-Georgiou, E., 2015. Dynamic connectivity in a fluvial network for identifying hotspots of geomorphic change. *Water Resour. Res*. 51, 1401–1421. https://doi.org/10.1002/2014WR016139
Daly, E.R., Miller, R.B., Fox, G.A., 2015. Modeling streambank erosion and failure along protected and unprotected composite streambanks. *Adv. Water Resour*. 81, 114–127. https://doi.org/10.1016/j.advwatres.2015.01.004
Darby, S. E., D. Gessler, and C. R. Thorne, Computer program for stability analysis of steep, cohesive riverbanks, *Earth Surf. Processes Landforms*, 25, 175– 190, 2000.
Darby, S.E., Alabyan, A.M., Van de Wiel, M.J., 2002. Numerical simulation of bank erosion and channel migration in meandering rivers. *Water Resour. Res*. 38, 2-1-2–21. https://doi.org/10.1029/2001wr000602
Darby, S.E., Rinaldi, M., Dapporto, S., 2007. Coupled simulations of fluvial erosion and mass wasting for cohesive river banks. *J. Geophys. Res. Earth Surf*. 112, 1–15. https://doi.org/10.1029/2006JF000722
Darby, S.E., Trieu, H.Q., Carling, P.A., Sarkkula, J., Koponen, J., Kummu, M., Conlan, I., Leyland, J., 2010. A physically based model to predict hydraulic erosion of fine-grained riverbanks: The role of form roughness in limiting erosion. *J. Geophys. Res. Earth Surf*. 115, 1–20. https://doi.org/10.1029/2010JF001708
De Rose, R.C., Basher, L.R., 2011. Measurement of river bank and cliff erosion from sequential LIDAR and historical aerial photography. *Geomorphology* 126, 132–147. https://doi.org/10.1016/j.geomorph.2010.10.037
Deb, M., Ferreira, C., 2015. Planform channel dynamics and bank migration hazard assessment of a highly sinuous river in the north-eastern zone of Bangladesh. *Environ. Earth Sci*. 73, 6613–6623. https://doi.org/10.1007/s12665-014-3884-3
Dépret, T., Gautier, E., Hooke, J., Grancher, D., Virmoux, C., Brunstein, D., 2017. Causes of planform stability of a low-energy meandering gravel-bed river (Cher River, France). *Geomorphology* 285, 58–81. https://doi.org/10.1016/j.geomorph.2017.01.035
Dewan, A., Corner, R., Saleem, A., Rahman, Md Masudur, Haider, M.R., Rahman, Md Mostafizur, Sarker, M.H., 2017. Assessing channel changes of the Ganges-Padma River system in Bangladesh using Landsat and hydrological data. *Geomorphology* 276, 257–279. https://doi.org/10.1016/j.geomorph.2016.10.017
Dietrich, W.E., Smith, J.D., Dunne, T., 1979. Flow and sediment transport in a sand bedded meander. *Journal of Geology* 87(3), 305–315.
Dixon, S.J., Sambrook Smith, G.H., Best, J.L., Nicholas, A.P., Bull, J.M., Vardy, M.E., Sarker, M.H., Goodbred, S., 2018. The planform mobility of river channel confluences: Insights from analysis of remotely sensed imagery. *Earth-Science Rev*. 176, 1–18. https://doi.org/10.1016/j.earscirev.2017.09.009
Downs, P. & Kondolf, G., 2002. Post-Project appraisals in adaptive management of river channel restoration. *Environmental Management* 29: 477. https://doi.org/10.1007/s00267-001-0035-X
Eaton, B.C., Millar, R.G., Davidson, S., 2010. Channel patterns: Braided, anabranching, and single-thread. *Geomorphology* 120, 353–364. https://doi.org/10.1016/j.geomorph.2010.04.010

Eke, E., G. Parker, Y. Shimizu., 2014. Numerical modelling of erosional and depositional bank processes in migrating river bends with self-formed width: Morphodynamics of bar push and bank pull, *J. Geophys. Res. Earth Surf*., 119, 1455–1483, doi:10.1002/2013JF003020.
Elith, J., Leathwick, J., 2015. Boosted Regression Trees for ecological modeling 1–22.
Elith, J., Leathwick, J.R., Hastie, T., 2008. A working guide to boosted regression trees. *J. Anim. Ecol*. 77, 802–813. https://doi.org/10.1111/j.1365-2656.2008.01390.x
Erskine, W. D., 1992. Channel response to large ‐ scale river training works: hunter river, Australia. *Regul. Rivers: Res. Mgmt*., 7: 261-278. doi:10.1002/rrr.3450070305
Evans, B. R., 2018. Data-driven prediction of saltmarsh morphodynamics (Doctoral thesis). https://doi.org/10.17863/CAM.24102
Fisk, H.N., 1944. Geological Investigation of the Alluvial Valley of the Lower Mississippi River. Mississippi River Commission, Vicksburg, MI.
Fonstad, M., Marcus, W.A., 2003. Self-organized criticality in riverbank systems. *Ann. Assoc. Am. Geogr*. 93, 281–296. https://doi.org/10.1111/1467-8306.9302002
Foster, G.C., Chiverrell, R.C., Thomas, G.S.P., Marshall, P., Hamilton, D., 2009. Fluvial development and the sediment regime of the lower Calder, Ribble catchment, northwest England. *Catena* 77, 81–95. https://doi.org/10.1016/j.catena.2008.09.006
Frascati, A., Lanzoni, S., 2010. Long-term river meandering as a part of chaotic dynamics? A contribution from mathematical modelling. *Earth Surf. Process. Landforms* 35, 791–802. https://doi.org/10.1002/esp.1974
Freund, Y. and Schapire, R., 1997. A decision-theoretic generalization of online learning and an application to boosting, *Journal of Computer and System Sciences* 55: 119–139.
Friedkin, J.F., 1945. A Laboratory Study of the Meandering of Alluvial Rivers. US Waterways Experiment Station, Vicksburg, Mississippi.
Friedman, J.H. (2002) Stochastic gradient boosting. *Computational Statistics and Data Analysis*, 38, 367–378.
Furbish, D.J., 1988. River-bend curvature and migration: how are they related? *Geology* 16, 752–755. https://doi.org/10.1130/0091-7613(1988)016<0752:RBCAMH>2.3.CO;2
Furbish, D.J., 1991. Spatial autoregressive structure in meander evolution. *Geol. Soc. Am. Bull*. 103, 1576–1589. https://doi.org/10.1130/0016-7606(1991)103<1576:SASIME>2.3.CO;2
Gay, G.R., Meade, R.H., Moody, J.A., Gay, H.H., Gay, W.H., Martinson, H.A., 1998. Evolution of cutoffs across meander necks in Powder River, Montana, USA. *Earth Surf. Process. Landforms* 23, 651–662.
Gibson, J., (2013). Python scripts for ArcGIS Desktop 10.1, which provide measures of polyline curvature. Available: https://www.arcgis.com/home/item.html?id=b9a2e709d9c143469c8aa62a6efbe412. Last accessed 22/09/2019.
Gilvear D.J., 1999. Fluvial geomorphology and river engineering: future roles utilizing a fluvial hydrosystems framework. *Geomorphology* 31, 229–245.
Gilvear, D.J., 2004. Patterns of channel adjustment to impoundment of the upper River Spey, Scotland (1942-2000). *River Res. Appl*. 20, 151–165. https://doi.org/10.1002/rra.741
Gilvear, D., Winterbottom, S., Sichingabula, H., 2000. Character of channel planform change and meander development: Luangwa River, Zambia. *Earth Surf. Process. Landforms* 25, 421–436. https://doi.org/10.1002/(SICI)1096-9837(200004)25:4<421::AID-ESP65>3.0.CO;2-Q
Gilvear, D.J., Casas, R., Spray, C., 2011. Trends and issues in delivery of integrated catchment scale river restoration: lessons from a national restoration survey within Scotland. *River. Res. App.* 27, 111e121.
Gilvear, D.J., Spray, C.J., Casas-Mulet, R., 2013. River rehabilitation for the delivery of multiple ecosystem services at the river network scale. *J. Environ. Manage*. 126, 30–43. https://doi.org/10.1016/j.jenvman.2013.03.026

Greenwood P, Kuhn N. 2013. Does the invasive plant, Impatiens glandulifera, promote soil erosion along the riparian zone? An investigation on a small watercourse in northwest Switzerland. *Journal of Soils and Sediments*. DOI: 10.1007/s11368-013-0825-9
Greenwood, P., Kuhn, N.J., 2015. Earth Surface Exchanges (ESEX) Commentary on "Plants as river system engineers" by A. Gurnell. Earth Surface Processes and Landforms 39: 4-25, 2014. DOI 10.1002/esp.3397. *Earth Surf. Process. Landforms* 40, 131–134. https://doi.org/10.1002/esp.3672
Gregory, K.J., 2006. The human role in changing river channels. *Geomorphology* 79, 172–191. https://doi.org/10.1016/j.geomorph.2006.06.018
Grove, J.R., Croke, J., Thompson, C., 2013. Quantifying different riverbank erosion processes during an extreme flood event. *Earth Surf. Process. Landforms* 38, 1393–1406. https://doi.org/10.1002/esp.3386
Güneralp, I., Marston, R.A., 2012. Process-form linkages in meander morphodynamics: Bridging theoretical modelling and real world complexity. *Prog. Phys. Geogr*. 36, 718–746. https://doi.org/10.1177/0309133312451989
Güneralp, I., Rhoads, B.L., 2008. Continuous characterization of the planform geometry and curvature of meandering rivers. *Geogr. Anal*. 40, 1–25. https://doi.org/10.1111/j.0016-7363.2007.00711.x
Güneralp, I., Rhoads, B.L., 2009. Empirical analysis of the planform curvature-migration elation of meandering rivers. *Water Resour. Res*. 45, 1–15. https://doi.org/10.1029/2008WR007533
Güneralp, I., Rhoads, B.L., 2010. Spatial autoregressive structure of meander evolution revisited. *Geomorphology* 120, 91–106. https://doi.org/10.1016/j.geomorph.2010.02.010
Güneralp, Í., Rhoads, B.L., 2011. Influence of floodplain erosional heterogeneity on planform complexity of meandering rivers. *Geophys. Res. Lett*. 38, 2–7. https://doi.org/10.1029/2011GL048134
Gurnell, A., 2014. Plants as river system engineers. *Earth Surf. Process. Landforms* 39, 4–25. https://doi.org/10.1002/esp.3397
Gurnell, A.M., Rinaldi, M., Belletti, B., Bizzi, S., Blamauer, B., Braca, G., Buijse, A.D., Bussettini, M., Camenen, B., Comiti, F., Demarchi, L., García de Jalón, D., González del Tánago, M., Grabowski, R.C., Gunn, I.D.M., Habersack, H., Hendriks, D., Henshaw, A.J., Klösch, M., Lastoria, B., Latapie, A., Marcinkowski, P., Martínez-Fernández, V., Mosselman, E., Mountford, J.O., Nardi, L., Okruszko, T., O'Hare, M.T., Palma, M., Percopo, C., Surian, N., van de Bund, W., Weissteiner, C., Ziliani, L., 2016. A multi-scale hierarchical framework for developing understanding of river behaviour to support river management. *Aquat. Sci*. 78, 1–16. https://doi.org/10.1007/s00027-015-0424-5
Hall, J.E., Holzer, D.M., Beechie, T.J., 2007. Predicting river floodplain and lateral channel migration for salmon habitat conservation. *J. Am. Water Resour. Assoc*. 43, 786–797. https://doi.org/10.1111/j.1752-1688.2007.00063.x
Harley, J., 1965. The Re-Mapping of England, 1750-1800. *Imago Mundi*, 19, 56-67. Retrieved from http://www.jstor.org/stable/1150330
Harrison, L.R., Dunne, T., Fisher, G.B., 2015. Hydraulic and geomorphic processes in an overbank flood along a meandering, gravel-bed river: Implications for chute formation. *Earth Surf. Process. Landforms* 40, 1239–1253. https://doi.org/10.1002/esp.3717
Harvey, A.M.,1985. The river systems of north–west England. In: Johnson, R.H. (Ed.), The Geomorphology of north–west England. Manchester University Press, Manchester, pp. 122–142.
Harvey, A.M., 1997. Coupling between hillslope gully systems and stream channels in the Howgill Fells, northwest England: temporal implications. *Geomorphologie: Relief, Processus, Environnement* 1, 3–20.

Harvey A.M., Alexander R.W., James P.A., 1984. Lichens, Soil Development and the Age of Holocene Valley Floor Landforms: Howgill Fells, Cumbria, *Geografiska Annaler: Series A, Physical Geography*, 66:4, 353-366, DOI: 10.1080/04353676.1984.11880121
Hasegawa, K. 1977. Computer simulation of the gradual migration of meandering channels [in Japanese], Proceedings of the Hokkaido Branch, Japan Society of Civil Engineering, pp. 197–202.
Hasegawa, K. 1989. Studies on qualitative and quantitative prediction of meander channel shift. In: Ikeda, S., Parker, G. (Eds.), River Meandering. AGU Water Resources Monograph 12, pp. 215–236.
Hastie, T., Tibshirani, R. & Friedman, J.H. (2001) The Elements of Statistical Learning: Data Mining, Inference, and Prediction. Springer-Verlag, New York.
Hastie, T., Tibshirani, R., Friedman, J., 2009. The elements of statistical learning. Elements (Vol. 1), New York City, NY.
Henderson, F.M., 1963. Stability of alluvial channels. Transactions of the ASCE 128, 657–686.
Henshaw, A.J., Thorne, C.R., Clifford, N.J., 2013. Identifying causes and controls of river bank erosion in a British upland catchment. *Catena* 100, 107–119. https://doi.org/10.1016/j.catena.2012.07.015
Hickin, E.J., 1974. Development of meanders in natural river-channels. *American Journal of Science* 274(4), 414–442.
Hickin, E.J., 1978. Mean flow structure in meanders of Squamish River, British-Columbia. *Canadian Journal of Earth Sciences* 15(11), 1833–1849.
Hickin, E.J., 1978. Hydraulic factors controlling channel migration. In: Davidson-Arnott, R., Nickling, W. (Eds.), Research in Fluvial Geomorphology, Proceedings Fifth Guelph Symposium on Geomorphology, pp. 59–66.
Hickin EJ. 1984. Vegetation and river channel dynamics. *The Canadian Geographer* 28(2): 111±126.
Hickin, E.J., Nanson, G.C., 1975. The character of channel migration on the Beaton River, Northeast British Columbia, Canada. *Geological Society of America Bulletin* 86, 487–494.
Hickin, E.J., Nanson, G.C., 1984. Lateral migration rates of river bends. *Journal of Hydraulic Engineering, ASCE* 110(11), 1557–1567.
Hofmann, A., 1929. Loss in 90-degree pipe bends of constant circular cross-section. Univ. Munich Tech. Hydraulic Inst. Bull. 3, (English translation of the original, pub. 1935 by Am. Soc. Mech. Engineers, New York), 45p.
Hooke, R. LeB., 1975, Distribution of sediment transport and shear stress in a meander bend: *Journal of Geology*, v. 83, p. 543-565.
Hooke, J.M., 1977. The distribution and nature of changes in river channel pattern. In: Gregory, K.J. (Ed.), River Channel Changes. John Wiley, Chichester, pp. 265–280.
Hooke, J.M., 1979. Analysis of the processes of river bank erosion. *Journal of Hydrology* 42(1–2), 39–62.
Hooke, J.M., 1980. Magnitude and distribution of rates of river bank erosion. *Earth Surface Processes* 5(2), 143–157.
Hooke J.M., 1995a. River channel adjustment to meander cutoffs on the River Bollin and River Dane, northwest England. *Geomorphology* 14: 235–253.
Hooke, J.M., 1995b. Processes of channel planform change on meandering channels in the UK. In: Gurnell, A., Petts, G.E. (Eds.), Changing River Channels. Wiley, Chichester, pp. 87–116.
Hooke, J.M., 1997. Styles of channel change. In: Thorne, C., Hey, R., Newson, M. (Eds.), Applied Fluvial Geomorphology for River Engineering and Management. Wiley, Chichester, pp. 237–268.
Hooke, J.M., 2003. River meander behaviour and instability; a framework for analysis. *Transactions of Institute of British Geographers* 28, 238–253.

Hooke, J.M., 2004. Cutoffs galore!: occurrence and causes of multiple cutoffs on a meandering river. *Geomorphology* 61(3–4), 225–238.
Hooke, J.M., 2007a. Complexity, self-organisation and variation in behaviour in meandering Rivers. *Geomorphology* 91, 236–258.
Hooke, J.M., 2007b. Spatial variability, mechanisms and propagation of change in an active meandering river. *Geomorphology* 84, 277–296.
Hooke, J.M., 2013. River meandering. In: Shroder, J. (Editor in Chief), Wohl, E. (Ed.), Treatise on Geomorphology. Academic Press, San Diego, CA, vol. 9, Fluvial Geomorphology, pp. 260–288.
Hooke, J.M., 2015. Variations in flood magnitude-effect relations and the implications for flood risk assessment and river management. *Geomorphology* 251, 91–107. https://doi.org/10.1016/j.geomorph.2015.05.014
Hooke, J.M., Harvey, A.M., 1983. Meander changes in relation to bend morphology and secondary flows. In: Collinson, J., Lewin, J. (Eds.), Modern and Ancient Fluvial Systems. International Association of Sedimentologists Special Publications, Vol. 6, pp. 121–132.
Hooke, J.M., Kain, R.J.P., 1982. Historical Change in the Physical Environment: A Guide to Sources and Techniques. Butterworths, London.
Hooke, J.M., Redmond, C.E., 1989. Use of cartographic sources for analysis of river channel change in Britain. In: Petts, G.E. (Ed.), Historical Changes on Large Alluvial European Rivers. Wiley, Chichester, pp. 79–93.
Hooke, J.M., Redmond, C.E., 1992. Causes and nature of river planform change. In: Billi, P., Hey, R.D., Thorne, C.R., Tacconi, P. (Eds.), Dynamics of Gravel-Bed Rivers. Wiley, Chichester, pp. 549–563.
Hooke, J.M., Yorke, L., 2010. Rates, distributions and mechanisms of change in meander morphology over decadal timescales, River Dane, UK. *Earth Surface Processes and Landforms* 35(13), 1601–1614.
Hooke, J.M., Yorke, L., 2011. Channel bar dynamics on multi-decadal timescales in an active meandering river. *Earth Surface Processes and Landforms* 36, 1910–1928.
Howard, A. D., 1984, Simulation model of meandering, in Elliott, C. M., ed., River meandering: New York, American Society of Civil Engineers, p. 952–963.
Howard, A.D., Knutson, T.R., 1984. Sufficient conditions for river meandering: a simulation approach. *Water Resources Research* 20, 1659–1667.
Hudson, P.F., Kesel, R.H., 2000. Channel migration and meander-bend curvature in the lower Mississippi River prior to major human modification. *Geology* 28(6), 531–534.
Hurst, H. E., 1951. Long-term storage capacity of reservoirs, *Trans. Am. Soc. Civil Eng*., 116, 770,
Ikeda, S., Parker, G., Sawai, K., 1981. Bend theory of river meanders 1. Linear development. *Journal of Fluid Mechanics* 112(Nov), 363–377.
Javernick, L., Brasington, J., Caruso, B., 2014. Modeling the topography of shallow braided rivers using structure-from-motion photogrammetry. *Geomorphology* 213:166–182. http://dx.doi.org/10.1016/j.geomorph.2014.01.006.
Johannesson, H., Parker, G., 1989. Velocity redistribution in meandering rivers. *Journal of Hydraulic Engineering-ASCE* 115(8), 1019–1039.
Julian, J.P., Torres, R., 2006. Hydraulic erosion of cohesive riverbanks. *Geomorphology* 76, 193–206.
Kasvi, E., Alho, P., Lotsari, E., Wang, Y., Kukko, A., Hyyppä, H., Hyyppä, J., 2015. Two-dimensional and three-dimensional computational models in hydrodynamic and morphodynamic reconstructions of a river bend: Sensitivity and functionality. *Hydrol. Process.* 29, 1604–1629. https://doi.org/10.1002/hyp.10277
Kemble, K., 2015. River Lugg SSSI Restoration Technical Report. Jacobs Project No: B228B001

Kessler, A.C., Gupta, S.C., Dolliver, H.A.S., Thoma, D.P., 2012. Lidar quantification of bank erosion in Blue Earth County, Minnesota. *J. Environ. Qual*. 41, 197–207. https://doi.org/10.2134/jeq2011.0181
Kessler, A.C., Gupta, S.C., Brown, M.K., 2013. Assessment of river bank erosion in Southern Minnesota rivers post European settlement. *Geomorphology* 201, 312–322. https://doi.org/10.1016/j.geomorph.2013.07.006
Kiss, T., Blanka, V., 2012. River channel response to climate- and human-induced hydrological changes: Case study on the meandering Hernád River, Hungary. *Geomorphology* 175–176, 115–125. https://doi.org/10.1016/j.geomorph.2012.07.003
Kiss, T., Fiala, K., Sipos, G., 2008. Alterations of channel parameters in response to river regulation works since 1840 on the Lower Tisza River (Hungary). *Geomorphology* 98, 96–110.
Knighton, A.D., 1973. Riverbank erosion in relation to streamflow conditions, River Bollin-Dean, Cheshire. *East Midland Geographer* 5, 416–426.
Knighton, A.D., 1999. Downstream variation in stream power. *Geomorphology* 29, 293–306. https://doi.org/10.1016/S0169-555X(99)00015-X
Knighton, A. D. and Nanson, G. C. 1993. Anastomosis and the continuum of channel pattern, *Earth Surface Processes and Landforms*, 18, 613–625.
Kondolf, G.M., 1997. Hungry water: Effects of dams and gravel mining on river channels. *Environ. Manage*. 21, 533–551. https://doi.org/10.1007/s002679900048
Kondolf, G.M., 2006. River restoration and meanders. *Ecol. Soc*. 11. https://doi.org/10.5751/ES-01795-110242
Konsoer, K.M., Rhoads, B.L., Langendoen, E.J., Best, J.L., Ursic, M.E., Abad, J.D., Garcia, M.H., 2016. Spatial variability in bank resistance to erosion on a large meandering, mixed bedrock-alluvial river. *Geomorphology* 252, 80–97. https://doi.org/10.1016/j.geomorph.2015.08.002
Kummu, M., Lu, X.X., Rasphone, A., Sarkkula, J., Koponen, J., 2008. Riverbank changes along the Mekong River: Remote sensing detection in the Vientiane-Nong Khai area. *Quat. Int*. 186, 100–112. https://doi.org/10.1016/j.quaint.2007.10.015
Lane, E.W., 1955. The importance of fluvial morphology in hydraulic engineering. *Proceedings of the American Society of Civil Engineers* 81, 1–17.
Langbein, W., Leopold, L.B., 1966. River meanders – theory of minimum variance. US Geological Survey Professional Paper 422-H.
Langendoen, E.J., Alonso, C. V., 2008. Modeling the evolution of incised streams: I. model formulation and validation of flow and streambed evolution components. *J. Hydraul. Eng*. 134, 749–762. https://doi.org/10.1061/(ASCE)0733-9429(2008)134:6(749)
Langendoen, E.J., Simon, A., 2008. Modeling the evolution of incised streams. II: Streambank erosion. *J. Hydraul. Eng*. 134, 905–915. https://doi.org/10.1061/(ASCE)0733-9429(2008)134:7(905)
Lawler, D.M., 1992. Process dominance in bank erosion systems. In: Carling, P.A., Petts, G.E. (Eds.), Lowland Floodplain Rivers: Geomorphological Perspectives. Wiley, Chichester, pp. 117e143.
Lawler, D.M., 1993. The measurement of river bank erosion and lateral channel change – a review. *Earth Surface Processes and Landforms* 18(9), 777–821.
Lawler DM. 1994. Temporal variability in streambank response to individual flow events: the River Arrow, Warwickshire, UK. In Variability in Stream Erosion and Sediment Transport (Proceedings of the Canberra Symposium, December 1994). IAHS Publication No. 224: 171–180.
Lawler DM. 1995. The impact of scale on the processes of channel-side sediment supply: a conceptual model. In Effects of Scale on Interpretation and Management of Sediment and Water Quality (Proceedings of a Boulder Symposium, July 1995). International Association of Hydrological Sciences Publication 226: 175–184.

Lawler, D.M., Thorne, C.R., Hooke, J.M., 1997. Bank erosion, stability and retreat. Chapter 7. In: Thorne, C., Hey, R., Newson, M. (Eds.), Applied Fluvial Geomorphology for River Engineering and Management. Wiley, Chichester, pp. 137–172.
Lazar, A.N., Butterfield, D., Futter, M.N., Rankinen, K., Thouvenot-Korppoo, M., Jarritt, N., Lawrence, D.S.L., Wade, A.J., Whitehead, P.G., 2010. An assessment of the fine sediment dynamics in an upland river system: INCA-Sed modifications and implications for fisheries. *Sci. Total Environ*. 408, 2555–2566. https://doi.org/10.1016/j.scitotenv.2010.02.030
Leathwick, J.R., Elith, J., Francis, M.P., Taylor, P., 2006. Variation in demersal fish species richness in the oceans surrounding New Zealand. *Mar. Ecol. Prog. Ser*. 321, 267–281. https://doi.org/10.3354/meps321267
Legg, N., Heimburg, C., Collins., B., Olson, P., 2014. The Channel Migration Toolbox. ArcGIS Tools for Measuring Stream Channel Migration. Department of Ecology, State of Washington. Available at: https://fortress.wa.gov/ecy/publications/SummaryPages/1406032.html
Leliavsky, S., 1955, 1966. An Introduction to Fluvial Hydraulics. Dover Publications, New York, 257 pp.
Leopold, L.B., Wolman, M.G., 1957. River Channel Patterns: Braided, Meandering and Straight. US Geological Survey Professional Paper 282B, 85p.
Leopold, L.B., Wolman, M.G., 1960. River meanders. Geological Society of America Bulletin 71, 769–794.
Lewin, J., 1972. Late-stage meander growth. Nature Physical Science 240, 116.
Lewin, J., 1976. Initiation of bed forms and meanders in coarse-grained sediment. Geological Society of America, Bulletin 87, 281–285.
Lewin, J., 1978. Meander development and floodplain sedimentation: a case study from mid-Wales. Geological Journal 13, 25–36.
Lewin, J. 1987. 'Historical channel changes', in Gregory, K. J., Lewin, J. and Thornes, J. B. (Eds), Palaeohydrology in Practice, Wiley, Chichester, 161–175.
Lewin, J., Brindle, B.J., 1977. Confined meanders. In: Gregory, K.J. (Ed.), River Channel Changes: Chichester, UK. John Wiley & Sons, pp. 221–233.
Lewin, J. and Macklin, M. G., 2010. Floodplain catastrophes in the UK Holocene: messages for managing climate change, Hydrol. Process., 24, 2900–2911.
Lewis, G.W., Lewin, J., 1983. Alluvial cutoffs in Wales and the Borderlands. In: Collinson, J.D., Lewin, J. (Eds.), Modern and Ancient Fluvial Systems: International Association of Sedimentologists. Special Publication, 6, pp. 145–154.
Luppi L, Rinaldi M, Teruggi LB, Darby SE, Nardi L. 2009. Monitoring and numerical modelling of riverbank erosion processes: a case study along the Cecina River (central Italy). Earth Surface Processes and Landforms 34: 530-546. DOI. 10.1002/esp.175
Markham, A.J., Thorne, C.R., 1992. Geomorphology of gravel-bed rivers. In: Billi, P., Hey, R.D., Thorne, C.R., Tacconi, P. (Eds.), Dynamics of Gravel – Bed Rivers. Wiley and Sons, Chichester, pp. 433–456.
Matsuoka N. 1996. Soil moisture variability in relation to diurnal frost heaving on Japanese high mountain slopes. Permafrost and Periglacial Processes 7: 139–151.
Micheli, E., Kirchner, J., 2002. Effects of wet meadow riparian vegetation on streambank erosion. 1. Remote sensing measurements of streambank migration and erodibility. Earth Surface Processes and Landforms 27, 627–639.
Micheli, E.R., Kirchner, J.W., Larsen, E.W., 2004. Quantifying the effect of riparian forest versus agricultural vegetation on river meander migration rates, central Sacramento River, California, USA. River Res. Appl. 20, 537–548. https://doi.org/10.1002/rra.756
Mosley, M. (1975), Meander cutoffs on the River Bollin, Cheshire, in July 1973, Rev. Geomorphol. Dyn., 24, 21–32.

Mosselman, E. (1991), Modelling of river morphology with nonorthogonal horizontal coordinates, Commun. Hydraul. Geotech. Eng. 91-1, Delft Univ. of Technol., Delft, Netherlands.
Mosselman, E. (1998), Morphological modelling of rivers with erodible banks, Hydrol. Processes, 12, 1357–1370.
Mosselman, E., Mathematical modelling of morphological processes in rivers with erodible cohesive banks, Commun. Hydraul. Geotech. Eng. 92-3, Delft Univ. of Technol., Netherlands, 1992.
Motta, Davide, Abad, J.D., Langendoen, E.J., Garcia, M.H., 2012. A simplified 2D model for meander migration with physically-based bank evolution. Geomorphology 163–164, 10–25. https://doi.org/10.1016/j.geomorph.2011.06.036
Motta, D., Abad, J.D., Langendoen, E.J., García, M.H., 2012. The effects of floodplain soil heterogeneity on meander planform shape. Water Resour. Res. 48, 1–17. https://doi.org/10.1029/2011WR011601
Nanson, G.C., Hickin, E.J., 1983. Channel migration and incision on the Beatton river. Journal of Hydraulic Engineering – ASCE 109(3), 327–337.
Nanson, G.C., Hickin, E.J., 1986. A statistical analysis of bank erosion and channel migration in western Canada. Geol. Soc. Am. Bull. 97, 497–504. https://doi.org/10.1130/0016-7606(1986)97<497:ASAOBE>2.0.CO;2
Nanson, G.C., Huang, H.Q., 2018. A philosophy of rivers: Equilibrium states, channel evolution, teleomatic change and least action principle. Geomorphology 302, 3–19. https://doi.org/10.1016/j.geomorph.2016.07.024
Nicoll, T.J., Hickin, E.J., 2010. Planform geometry and channel migration of confined meandering rivers on the Canadian prairies. Geomorphology 116, 37–47. https://doi.org/10.1016/j.geomorph.2009.10.005
O'Neal, M.A., Pizzuto, J.E., 2011. The rates and spatial patterns of annual riverbank erosion revealed through terrestrial laser-scanner surveys of the South River, Virginia. Earth Surf. Process. Landforms 36, 695–701. https://doi.org/10.1002/esp.2098
Osman, A.M., Thorne, C.R., 1988. Riverbank stability analysis I: Theory. Journal of Hydraulic Engineering. 114, 134-150
Micheli, E.R., Kirchner, J.W., Larsen, E.W., 2004. Quantifying the effect of riparian forest versus agricultural vegetation on river meander migration rates, central Sacramento River, California, USA. River Res. Appl. 20, 537–548. https://doi.org/10.1002/rra.756
Motta, Davide, Abad, J.D., Langendoen, E.J., Garcia, M.H., 2012. A simplified 2D model for meander migration with physically-based bank evolution. Geomorphology 163–164, 10–25. https://doi.org/10.1016/j.geomorph.2011.06.036
Motta, D., Abad, J.D., Langendoen, E.J., García, M.H., 2012. The effects of floodplain soil heterogeneity on meander planform shape. Water Resour. Res. 48, 1–17. https://doi.org/10.1029/2011WR011601
Nanson, B.G.C., Hickin, E.J., 1983. CHANNEL MIGRATION AND INCISION bend curvature (radius of bend curvature / channel width , r m / w). This relationship is in the form of a complex curve reproduced again in Fig . 2 (a). Although the fit of the curve to the data points appears justified 109, 327–337.
Nanson, G.C., Hickin, E.J., 1986. A statistical analysis of bank erosion and channel migration in western Canada. Geol. Soc. Am. Bull. 97, 497–504. https://doi.org/10.1130/0016-7606(1986)97<497:ASAOBE>2.0.CO;2
Nanson, G.C., Huang, H.Q., 2018. A philosophy of rivers: Equilibrium states, channel evolution, teleomatic change and least action principle. Geomorphology 302, 3–19. https://doi.org/10.1016/j.geomorph.2016.07.024

Nicoll, T.J., Hickin, E.J., 2010. Planform geometry and channel migration of confined meandering rivers on the Canadian prairies. Geomorphology 116, 37–47. https://doi.org/10.1016/j.geomorph.2009.10.005
O'Neal, M.A., Pizzuto, J.E., 2011. The rates and spatial patterns of annual riverbank erosion revealed through terrestrial laser-scanner surveys of the South River, Virginia. Earth Surf. Process. Landforms 36, 695–701. https://doi.org/10.1002/esp.2098
Owens, P.N., Batalla, R.J., Collins, A.J., Gomez, B., Hicks, D.M., Horowitz, A.J., Kondolf, G.M., Marden, M., Page, M.J., Peacock, D.H., Petticrew, E.L., Salomons, W., Trustrum, N.A., 2005. Fine-grained sediment in river systems: Environmental significance and management issues. River Res. Appl. 21, 693–717. https://doi.org/10.1002/rra.878
Park, S., Kim, J., 2019. Landslide susceptibility mapping based on random forest and boosted regression tree models, and a comparison of their performance. Appl. Sci. 9. https://doi.org/10.3390/app9050942
Parker, G., Andrews, E.D., 1986. On the time development of meander bends. Journal of Fluid Mechanics 162, 139–156.
Parker, G., Sawai, K., Ikeda, S., 1982. Bend theory of river meanders. Part 2. Nonlinear deformation of finite-amplitude bends. J. Fluid Mech. 115, 303–314. https://doi.org/10.1017/S0022112082000767
Parker, C., Simon, A., Thorne, C.R., 2008. The effects of variability in bank material properties on riverbank stability: Goodwin Creek, Mississippi. Geomorphology 101, 533–543. https://doi.org/10.1016/j.geomorph.2008.02.007
Parker, G., Shimizu, Y., Wilkerson, G. V., Eke, E.C., Abad, J.D., Lauer, J.W., Paola, C., Dietrich, W.E., Voller, V.R., 2011. A new framework for modeling the migration of meandering rivers. Earth Surf. Process. Landforms 36, 70–86. https://doi.org/10.1002/esp.2113
Passmore, D., Waddington, C., Van Der Schriek, T., 2006. Enhancing the evaluation and management of river valley archaeology; geoarchaerology in the Till-Tweed catchment, Northern England. Arcaeol. Prospect. 13, 269-281.
Perucca, E., Camporeale, C., Ridolfi, L., 2005. Nonlinear analysis of the geometry of meandering rivers. Geophys. Res. Lett. 32, 1–4. https://doi.org/10.1029/2004GL021966
Piégay, H., Darby, S.E., Mosselman, E., Surian, N., 2005. A review of techniques available for delimiting the erodible river corridor: A sustainable approach to managing bank erosion. River Res. Appl. 21, 773–789. https://doi.org/10.1002/rra.881
Pittman, S.J., Costa, B.M., Battista, T.A., 2009. Using Lidar Bathymetry and Boosted Regression Trees to Predict the Diversity and Abundance of Fish and Corals. J. Coast. Res. 10053, 27–38. https://doi.org/10.2112/si53-004.1
Pizzuto, J., O'Neal, M., Stotts, S., 2010. On the retreat of forested, cohesive riverbanks. Geomorphology 116, 341–352. https://doi.org/10.1016/j.geomorph.2009.11.008
Polvi, L.E., Wohl, E., Merritt, D.M., 2014. Modeling the functional influence of vegetation type on streambank cohesion. Earth Surf. Process. Landforms 39, 1245–1258. https://doi.org/10.1002/esp.3577
Pouteau, R., Rambal, S., Ratte, J.P., Gogé, F., Joffre, R., Winkel, T., 2011. Downscaling MODIS-derived maps using GIS and boosted regression trees: The case of frost occurrence over the arid Andean highlands of Bolivia. Remote Sens. Environ. 115, 117–129. https://doi.org/10.1016/j.rse.2010.08.011
Pugh, J. H. 1975. Surveying for Field Scientists, Methuen, 230 p.
Quik, C., Wallinga, J., 2018. Reconstructing lateral migration rates in meandering systems - A novel Bayesian approach combining optically stimulated luminescence (OSL) dating and historical maps. Earth Surf. Dyn. 6, 705–721. https://doi.org/10.5194/esurf-6-705-2018
Rapp, C., Abbe, T., 2003. A framework for delineating channel migration zones.

Rhoades, E.L., O'Neal, M.A., Pizzuto, J.E., 2009. Quantifying bank erosion on the South River from 1937 to 2005, and its importance in assessing Hg contamination. Appl. Geogr. 29, 125–134. https://doi.org/10.1016/j.apgeog.2008.08.005
Rhoads, B.L., Lewis, Q.W., Andresen, W., 2016. Historical changes in channel network extent and channel planform in an intensively managed landscape: Natural versus human-induced effects. Geomorphology 252, 17–31. https://doi.org/10.1016/j.geomorph.2015.04.021
Richards, K. 1982: Rivers: form and process in alluvial channels. London: Methuen.
Ridgeway, G., 2019. Generalized Boosted Models: A guide to the gbm package. Compute 1, 1–12. https://doi.org/10.1111/j.1467-9752.1996.tb00390.x Accessed 2019.
Rinaldi, M., Nardi, L., 2013. Modeling Interactions between Riverbank Hydrology and Mass Failures. J. Hydrol. Eng. 18, 1231–1240. https://doi.org/10.1061/(ASCE)HE.1943-5584.0000716
Rinaldi, M., Mengoni, B., Luppi, L., Darby, S.E., Mosselman, E., 2008. Numerical simulation of hydrodynamics and bank erosion in a river bend. Water Resour. Res. 44, 1–17. https://doi.org/10.1029/2008WR007008
Roux, C., Alber, A., Piégay, H., 2013. Polyline disaggregation guideline for the FluvialCorridor toolbox, a new ArcGIS toolbox package for exploring multiscale riverscape at a network scale. Sedalp (Sediment Management in Alpin Basins) and CNRS (UMR5600).
Sadler, P.M., 1981. Sediment accumulation rates and the completeness of stratigraphic sections. J. Geol. 89, 569–584. https://doi.org/10.1086/628623
Salo, J., R. Kalliola, I. Hakkinen, Y. Makinen, P. Niemela, M. Puhakka, and P. Coley (1986), River dynamics and the diversity of Amazon lowland forest, Nature, 322, 254– 258.
Schottler, S.P., Ulrich, J., Belmont, P., Moore, R., Lauer, J.W., Engstrom, D.R., Almendinger, J.E., 2014. Twentieth century agricultural drainage creates more erosive rivers. Hydrol. Process. 28, 1951–1961. https://doi.org/10.1002/hyp.9738
Schumm, S.A., 1960. The shape of alluvial channels in relation to sediment type. US Geological Survey Professional Paper 352-B.
Schumm, S.A., 1963. Sinuosity of alluvial rivers on the Great Plains. Geological Society of America Bulletin 74, 1089–1100.
Schumm, S.A., 1977. The Fluvial System. John Wiley and Sons, New York, 338 pp.
Seminara, G., 2006. Meanders. Journal of Fluid Mechanics 554, 271–297.
Seminara, G., Zolezzi, G., Tubino, M., Zardi, D., 2001. Downstream and upstream influence in river meandering. Part 2. Planimetric development. Journal of Fluid Mechanics 438, 213–230.
Shields, I.A., 1936. Application of similarity principles and turbulence research to bed-load movement. In: Ott, W.P., van Uchelen, J.C. (Eds.), (Translators), Hydrodynamics Laboratory Publication, vol. 167. California Institute of Technology, Pasadena
Simon, A., Collison, A.J.C., 2001. Pore-water pressure effects on the detachment of cohesive streambeds: seepage forces and matric suction. Earth Surface Processes and Landforms 26, 1421– 1442.
Simon, A., Darby, S.E., 1997b. Bank erosion processes in two incised meander bends: Goodwin Creek, Mississippi. In: Wang, S.S.Y., Langendoen, E.J., Shields Jr., F.D. (Eds.), Management of Landscapes Disturbed by Channel Incision. University of Mississippi, Oxford, MS, pp. 256– 261.
Simon, A., Curini, A., Darby, S.E., Langendoen, E.J., 1999. Streambank mechanics and the role of bank and near-bank processes in incised channels. In: Darby, S.E., Simon, A. (Eds.), Incised River Channels. Wiley, Chichester, UK, pp. 123– 152.
Simon, A., Curini, A., Darby, S.E., Langendoen, E.J., 2000. Bank and near-bank processes in an incised channel. Geomorphology 35, 193–217.
Stolum, H.H., 1996. River meandering as a self-organization process. Science 271(5256), 1710–1713.

Stolum, H.H., 1998. Planform geometry and dynamics of meandering rivers. Geological Society of America Bulletin 110(11), 1485–1498.
Stott, T., 1997. A comparison of stream bank erosion processes on forested and moorland streams in the Balquhidder Catchments, central Scotland. Earth Surf. Process. Landforms 22, 383–399. https://doi.org/10.1002/(SICI)1096-9837(199704)22:4<383::AID-ESP695>3.0.CO;2-4
Sun, T., Meakin, P., Jøssang, T., Schwarz, K., 1996. A simulation model for meandering rivers. Water Resour. Res. 32, 2937–2954. https://doi.org/10.1029/96WR00998
Sun, T., Meakin, P., Jøssang, T., 2001. A computer model for meandering rivers with multiple bed load sediment sizes 1. Theory. Water Resour. Res. 37, 2243–2258. https://doi.org/10.1029/2000WR900397
Sun, T., Meakin, P., Jøssang, T., 2001. A computer model for meandering rivers with multiple bed load sediment sizes 2. Computer simulations. Water Resour. Res. 37, 2243–2258. https://doi.org/10.1029/2000WR900397
Surian, A., 1999. Channel changes due to river regulation: the case of the Piave River, Italy. Earth Surface Processes and Landforms 24, 1135–1151.
Sylvester, Z., Durkin, P., Covault, J.A., 2019. High curvatures drive river meandering. Geology 47, 263–266. https://doi.org/10.1130/G45608.1
Thomas, R. J., Constantine, J. A., Gough, P., Fussell, B., 2015 Rapid Channel Widening Following Weir Removal due to Bed-Material Wave Dispersion on the River Monnow, Wales. River Res. Applic., 31: 1017-1027. doi: 10.1002/rra.2803.
Thompson, A., 1986. Secondary flows and the pool-riffle unit: A case study of the processes of meander development. Earth Surf. Process. Landforms 11, 631-641. https://doi.org/10.1002/esp.3290110606
Thorne, C.R., 1981. Field measurements of rates of bank erosion and bank material strength. Eros. sediment Transp. Meas. Proc. Florence Symp. June 1981, (International Assoc. Hydrol. Sci. IAHS-AISH Publ. 512) 503–512.
Thorne, C.R., 1990. Effects of vegetation on riverbank erosion and stability. In: Thornes, J.B. (Ed), Vegetation and Erosion. Wiley, Chichester, UK. 125-144
Thorne, C.R., Hey, R.D., 1979. Direct measurements of secondary currents at a river inflection point. Nature 280(5719), 226–228.
Thorne, C.R., Lewin, J., 1979. Bank processes, bed material movement and planform development in a meandering river. In: Rhodes, D.D., Williams, G.P. (Eds.), Adjustments of the Fluvial System. George Allen and Unwin, London, pp. 117–137.
Thorne, C.R., Tovey, N.K., 1981. Stability of composite river banks. Earth Surface Processes and Landforms 6(5), 469–484.
Thorne, C.R., Murphey, J.B., Little, W.C., 1981. Stream channel stability appendix D: Bank stability and bank material properties in the bluffline streams of northwest Mississippi, Report to U.S. Army Corps of Engineers, Vicksburg District, Vicksburg, Mississippi.
Tooth, S., McCarthy, T.S., Brandt, D., Hancox, P.J., Morris, R., 2002. Geological controls on the formation of alluvial meanders and floodplain wetlands: The example of the Klip River, eastern Free State, South Africa. Earth Surf. Process. Landforms 27, 797–815. https://doi.org/10.1002/esp.353
Wiel, M. J. and Darby, S. E., 2007. A new model to analyse the impact of woody riparian vegetation on the geotechnical stability of riverbanks. Earth Surf. Process. Landforms, 32: 2185-2198. doi:10.1002/esp.1522
Van den Berg, J. H.: Prediction of alluvial channel pattern of perennial rivers, Geomorphology, 12, 259–279, 1995.

Wade, A.J., Butterfield, D., Griffiths, T., Whitehead, P.G., 2007. Eutrophication control in river-systems: An application of INCA-P to the River Lugg. Hydrol. Earth Syst. Sci. 11, 584–600. https://doi.org/10.5194/hess-11-584-2007
Walling, D.E., 2005. Tracing suspended sediment sources in catchments and river systems. Science of the Total Environment 344, 159–184.
Werritty, A., Leys, K.F., 2001. The sensitivity of Scottish rivers and upland valley floors to recent environmental change. Catena 42, 251–273. https://doi.org/10.1016/S0341-8162(00)00140-5
Wharton, G., Gilvear, D.J., 2007. River restoration in the UK: Meeting the dual needs of the European union water framework directive and flood defence? Int. J. River Basin Manag. 5, 143–154. https://doi.org/10.1080/15715124.2007.9635314
Wolman MG. 1959. Factors influencing erosion of a cohesive river bank. American Journal of Science 257: 204-216.
Wolman, M., Miller, J., 1960. Magnitude and Frequency of Forces in Geomorphic Processes. The Journal of Geology 68, 54–74.
Youssef, A.M., Pourghasemi, H.R., Pourtaghi, Z.S., Al-Katheeri, M.M., 2016b. Landslide susceptibility mapping using random forest, boosted regression tree, classification and regression tree, and general linear models and comparison of their performance at Wadi Tayyah Basin, Asir Region, Saudi Arabia. Landslides 13, 839–856. https://doi.org/10.1007/s10346-015-0614-1
Zhou, M., Xia, J., Lu, J., Deng, S., Lin, F., 2017. Morphological adjustments in a meandering reach of the middle Yangtze River caused by severe human activities. Geomorphology 285, 325–332. https://doi.org/10.1016/j.geomorph.2017.02.022
Ziliani, L., Surian, N., 2016. Reconstructing temporal changes and prediction of channel evolution in a large Alpine river: the Tagliamento river, Italy. Aquat. Sci. 78, 83–94. https://doi.org/10.1007/s00027-015-0431-6
Zolezzi, G., Seminara, G., 2001. Downstream and upstream influence in river meandering. Part 1. General theory and application overdeepening. J. Fluid Mech. 438, 183–211. https://doi.org/10.1017/S002211200100427X